A NEW THEORY FOR MODELLING THE MASS-EFFICIENCY OF MATERIAL, SHAPE AND FORM

Damiano Pasini

A thesis submitted to the University of Bristol

in accordance with the requirements

of the degree of Doctor of Philosophy

in the Faculty of Engineering,

Department of Mechanical Engineering

December 2002

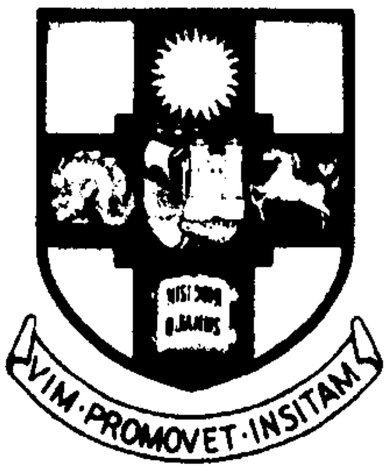

Department of Mechanical Engineering, University of Bristol, Bristol BS8 1TR, UK

Word count: 48785

ABSTRACT

Performance factors and design charts can be used to quickly model and compare the mass-efficiency of different materials, shapes and structural forms.

This thesis presents a new theory of shape transformers for modelling the mass-efficiency of structures at the conceptual stage of design. A shape transformer, S, is a dimensionless parameter which relates a geometric quantity, G, of a cross-section, such as the area, to the geometric quantity, G_D, such as the area, of the envelope which surrounds a cross-section. Shape transformers describe the shape properties of a cross-section and are used to define classes of shapes in a way which is similar to the way in which materials are classified.

The advantage of shape transformers is that the contribution of the shape can be specified separately to the contribution of the sizes of a cross-section. A geometric quantity G of a cross-section can be expressed by the product of the shape properties, S, and the geometric quantity of the envelope, G_D, i.e. $G=SxG_D$. This allows the fundamental equations of mechanics to be expressed in terms of material properties, M, shape properties, S, and geometric quantity of the envelope, G_D, i.e. $MxSxG_D$..

Shape transformers are used to produce analytical solutions to the mass-efficiency of cross-sections. A general solution has been produced for performance indices for arbitrarily scaled cross-sections. Shape transformers are also employed to examine structured layered systems with different material and shape properties. Plastic shape transformers are defined also for the case of plastic bending design.

Shape transformers are used to produce selection charts and design maps for materials, shapes and forms. The interaction between the selection of a cross-section and the selection of a structural form is explored when buckling is included. Shape transformers are applied to man-made and natural structures and have been used to tackle an industrial case study. The theory of the shape transformers provides insight for designers, students and educators.

AUTHOR'S DECLARATION

I declare that the work in this dissertation was carried out in accordance with the Regulations of the University of Bristol. The work is original except where indicated by special reference in the text.

Any views expressed in the dissertation are those of the author and not represent those of the University of Bristol. The dissertation has not been presented to any other University for examination either in the United Kingdom or overseas.

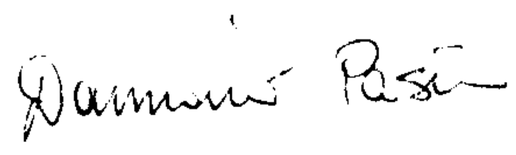

Damiano Pasini

December 2002

to

my mum, Sandra

my dad, Luigi

my brother, Giovanni

S.D.G.

ACKNOWLEDGEMENTS

I would particularly like to thank my supervisors, Dr. S.C. Burgess and Prof. D.J. Smith, for giving me the opportunity to come to Bristol in autumn 2000. I express to them my gratitude for their support and guidance throughout this research.

The Engineering and Physical Sciences Research Council is gratefully acknowledged for financing this work. The research grant (GR/No 3648) was entitled: "Modelling the efficiency of geometrically constrained structures".

I also wish to thank all my friends of room 1.58 for sharing with me the every day life in a very cordial and multicultural environment.

Lastly, I thank my family for their support and encouragement during these years.

PUBLICATIONS ARISING FROM THIS RESEARCH

Journals papers

1. Pasini, D., Burgess, S. C., Smith D.J, (2002) Performance indices for arbitrarily scaled rectangular cross-sections in bending stiffness design. *Proc. Instn Mech. Engrs, Part L, Journal of Design and application,* vol. 216, pp. 101-113
2. Pasini, D., Smith D.J, Burgess, S. C., Selection of arbitrarily scaled cross-sections in bending stiffness design. *Proc. Instn Mech. Engrs, Part L, Journal of Design and application,* (in press).
3. Pasini, D., Smith D.J, Burgess, S. C., Structural efficiency maps for beams subjected to bending, *Proc. Instn Mech. Engrs, Part L, Journal of Design and application,* (in press).
4. Pasini, D., Burgess S. C., Analysis of the structural features of trees and comparison with the structural features used in engineering, *Journal of engineering design,* (accepted).
5. Burgess S. C. and Pasini D., Improved visualisation of performance trends using nested performance charts, *Journal of engineering design,* (accepted)

Conferences papers

6. Burgess S.C., Pasini D., Smith D.J., (2001) Form factors: a design method to support the selection of structural concepts, *ICED 01*, Glasgow, 21-23, pp. 179-186
7. Pasini, D., Burgess S. C., (2002) Optimal structural features in trees and their application in engineering, *Design & Nature 2002 conference*, Udine
8. Pasini, D., Burgess, S. C., Smith D.J, (2002) A method of selection for large-scale structures. *ASME 2002, Design theory and methodology conference*, Montreal, Canada

Chapter book

9. Burgess S. C. and D. Pasini, The structural efficiency of trees, in "*Nature and Design*" edited by M. W. Collins, J. A. Bryant and M. A. Atherton, WTI press. Forthcoming 2003

CONTENTS

LIST OF FIGURES

LIST OF TABLES

LIST OF NOTATIONS

A, A_e	Cross sectional area (m^2)
A_D	Area of the envelope, D.
A_f	Frontal area (m^2)
A_p	area of the plastic part of the section, $D_{e\text{-}p}$
B	Width of a cross-section (m)
b	Internal width of a cross-section (m)
B_o	Width of the reference cross-section (m)
b_o	Internal width of an equiaxed rectangular cross-section (m)
c_1	Constant for stiffness depending on boundary conditions and load
C_d	Drag coefficient
d	Number of discrete levels for each variable
D, D_e	Envelope of a cross-section in the elastic region
$D_{e\text{-}p}$	Envelope of a cross-section in the elastic-plastic region
D_p	Fully plastic envelope of a cross-section
E	Young's modulus (GPa)
F	Functional requirements
F_w	Wind loading (N)
G	Geometric quantity of a cross-section
G_D	Geometric quantity of the envelope of a cross-section
h	Internal height of a cross-section (m)
H	Height (m)
h_o	Internal height of an equiaxed rectangular cross-section (m)
H_o	Height of the reference cross-section (m)
h_p	Internal height of the plastic envelope (m)
I	Second moment of area (m^4)
I_D	Second moment of area of the envelope (m^4)
k	Linear stiffness requirement (N/m)
K_1	Shanley shape parameter
L	Length (m)
L_i^c	Length of a compressive member i (m)
m	Mass (Mg)
M	Material parameters
M_y	Bending moment requirement for yield design
n	Number of design variables
N	Number of charts for the design space
p	Performance index

P	Load (N)
P_{crit}	Euler critic load
P_i^c	Compressive internal force in an i member (N)
P_i^t	Tensile internal force in an i member (N)
q	Power of the performance index
R	Reaction (N)
r_g	Radius of gyration (m)
r_{gD}	Radius of gyration of the envelope, *D*. (m)
r_o	Radius of the support of a Michell cantilever (m)
S	Shape of the cross section
u	Scaling factor of the widths
v	Scaling factor of the heights
v_w	Wind velocity (m/sec^2)
W	Structure weight (N)
y_m	Maximum distance outer fibres from the neutral axis of the section
z	Constant for the second moment of area
Z, Z_e	Section modulus of the cross-section in the elastic region
Z_D	Section modulus of the envelope
Z_p	Section modulus of the plastic part of a cross-section
ε	Strain in the horizontal direction at the furthest point of the envelope
δ	Deflection (m)
ε_o	Strain of the yield fibre nearest to the neutral axis
ϕ	Ashby shape factor
ϕ_H	Ashby shape factor for height constraint
ϕ_H	Ashby shape factor for width constraint
λ_I	Envelope efficiency parameter for section modulus
λ_Z	Envelope efficiency parameter for second moment of area
μ	Material parameter in the Rankine-Gordon formula [$\mu = \sigma_y/(\pi^2 E)$]
θ	Angle of a slope constraint
ρ	Material density (Mg/m^3)
σ_B	Tensile pre-stress (MPa)
σ_f	Compressive failure stress (MPa)
σ_y	Yield stress (MPa)
σ_y^c	Yield compressive stress (MPa)
σ_y^t	Yield tensile stress (MPa)
ψ_A	Shape transformer of the area
ψ_I	Shape transformer of the second moment of area
ψ_A^P	Plastic shape transformer of the area
ψ_Z	Shape transformer of the section modulus
ψ_Z^P	Plastic shape transformer of the section modulus

CHAPTER 1

INTRODUCTION

1.1 THE FUNDAMENTAL CHARACTERISTICS OF STRUCTURAL SYSTEMS

Basic function. Structures are generally systems of elements which span a design space to carry loads. The function of a structure is to transmit forces through its body. There may be a multiplicity of forces which load a structure in different directions. Self-weight, wind, seismic loading, thermal expansion are some examples. A structure can be a single linear element, such as a bar in tension, or a surface, such as a plate, or a spatial arrangement of more elements connected together by joints, such as a truss or a more complex framework.

Attributes. A set of physical attributes describes a single component. These attributes are material, dimensions and shape of the cross-section and of the longitudinal profile. The material has a variety of properties and has no geometry. The material and geometric attributes are complementary because the material is shaped to make a structure. In general the material attributes remain constant for given conditions. However, temperature and pressure variations as well as pre-stressed action can be applied to change the properties of a shaped material. In the case of a more complex structure, which contains an assembly of separate

elements, there is another feature of the structural system: the overall form or topology. The form can be described as the macro geometry of a structure. Sub-features of the form include: the structural joints (such as pinned, roller or rigid nodes), and their mutual geometric relations (such as planar and spatial angles between elements).

Structural hierarchy. The members of a structure can be arranged at different levels of hierarchy. At the highest order, there is the form which is the topology or structural type of the system. At the next level, the constituent members can have a different form along their length and certain shapes of cross-section. Below this level, the members can have a further order of structural hierarchy as they can contain stiffeners and other elements with different shapes. At the lowest level, there is the material which can have an internal microstructure of reinforcing elements. Therefore, the physical attributes of the elements at each hierarchical level and the arrangement of the members within a form characterise a structural system.

Design Space. The design space is vital to a structure since without space there can be no structure. A structure is generally located in a three-dimensional space defined by different planes. For example, the span of a single component is bounded by two vertical planes, while three or four limit planes can border the cross-section along the length of the element. The design space can also be prescribed for complex structures. In this case, all the constituent elements are wholly housed inside.

1.2 STRUCTURAL DESIGN

Functional requirement. Structural design involves conceiving a structural system which will properly perform the function of transferring external forces in certain directions through a space. Since a structure is described by a set of physical attributes, the attainment of an effective set of physical attributes of a structural system is the essence of structural design. The selection of these design variables has the purpose of providing the structure with the necessary attributes to perform a function and to achieve a certain level of quality. When the structure does not satisfy the functional requirements, there is potential for failure. This is the case when, for example, the prescribed level of strength, or a certain deflection or a specified

energy content are not achieved. The factors involved when designing a structure are illustrated in Figure 1.1. Some examples of possible functional requirements are shown.

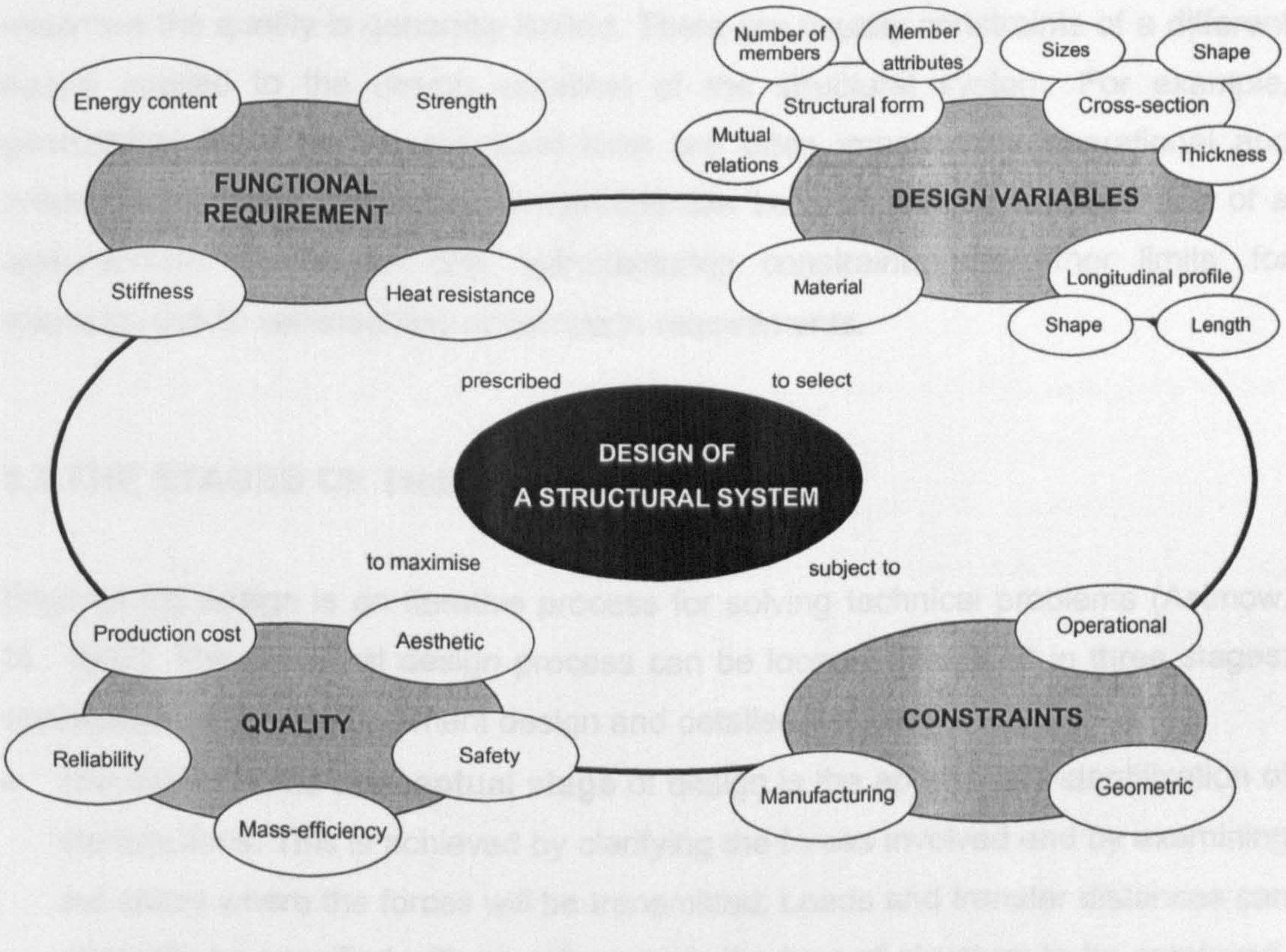

Figure 1.1 The context of structural design

Design variables. The attributes of a structure are the variables which describe the geometry and the material of a structure. In general, some attributes are variables whilst others are fixed. For example, when designing a beam, the length is often fixed whilst the shape and sizes of the cross-section are free variables. The design goal, or objective function, of structural design is to select an optimal combination of the variables which maximise the quality of a structure.

Quality. The measure of quality defines a means whereby competing structures are compared. The quality is established relative to one or more design/selection criteria. There are several different ways of measuring the quality of a structural design. Some examples are shown in Figure 1.1. Minimising the weight of a structure is one of the most common goals because it involves the saving of the cost of material. The minimisation of production and maintenance costs can also be a criterion of selection. An appropriate level of reliability or safety can also be chosen

for evaluating the quality of a structure during its life. Aesthetic rules can be also specified for the selection of the best structural design.

Constraints. During the process of selection, the choice of the variables which maximise the quality is generally limited. There are usually constraints of a different nature applied to the design variables of the structural system. For example, geometrical limits on the structural form are often imposed by operational and production reasons. Geometric constraints can be also applied to the shape of a cross-section. There are also manufacturing constraints and other limits, for example, due to serviceability or corrosion requirements.

1.3 THE STAGES OF THE DESIGN PROCESS

Engineering design is an iterative process for solving technical problems (Asimow, M., 1962). The structural design process can be loosely described in three stages: conceptual design, embodiment design and detailed design.

- The outset of the **conceptual stage** of design is the appropriate identification of the functions. This is achieved by clarifying the forces involved and by examining the space where the forces will be transmitted. Loads and transfer distances can generally be specified with no reference to the type of structure to be employed. However, if the functions of the structure are well-defined and understood, then the form of the structure will be easier to conceive because form generally follows the function. Alternative ideas are explored and evaluated. The experience and creativity of designers play an important role in generating and exploring alternative structural concepts. The best concepts, which maximise the design goal, are selected and developed in the other stages.
- In the **embodiment stage**, the promising structural options which meet the functional requirements are analysed and optimised to maximise the performance. This stage ends with the selection of the most promising solutions.
- The **detailed stage** deals with the definition of all the details of the design which are required to manufacture and assemble the structure. The specifications are prepared and drawings are finalised.

1.4 THE AIM OF THE THESIS

The aim of this research is to model the **mass-efficiency** of structural systems at the **conceptual stage** of design. This is illustrated in the upper part of Figure 1.2 together with the methodological approach in the lower part. The mass-efficiency is generally the main design criterion for the selection of the variables of the structural systems. The mass-efficiency is modelled for man-made and natural systems and it is examined in relation to the **design space** which the structures occupy. For this reason, the minimisation of space is also considered. Two design conditions are considered in this thesis:

- Unconstrained design. There are no spatial restrictions on the design variables. Unconstrained structures utilises freely the design space to carry loads.
- Constrained design. Geometric constraints are applied to the variables of a structure: material, shape and form. The design space for constrained structures is limited.

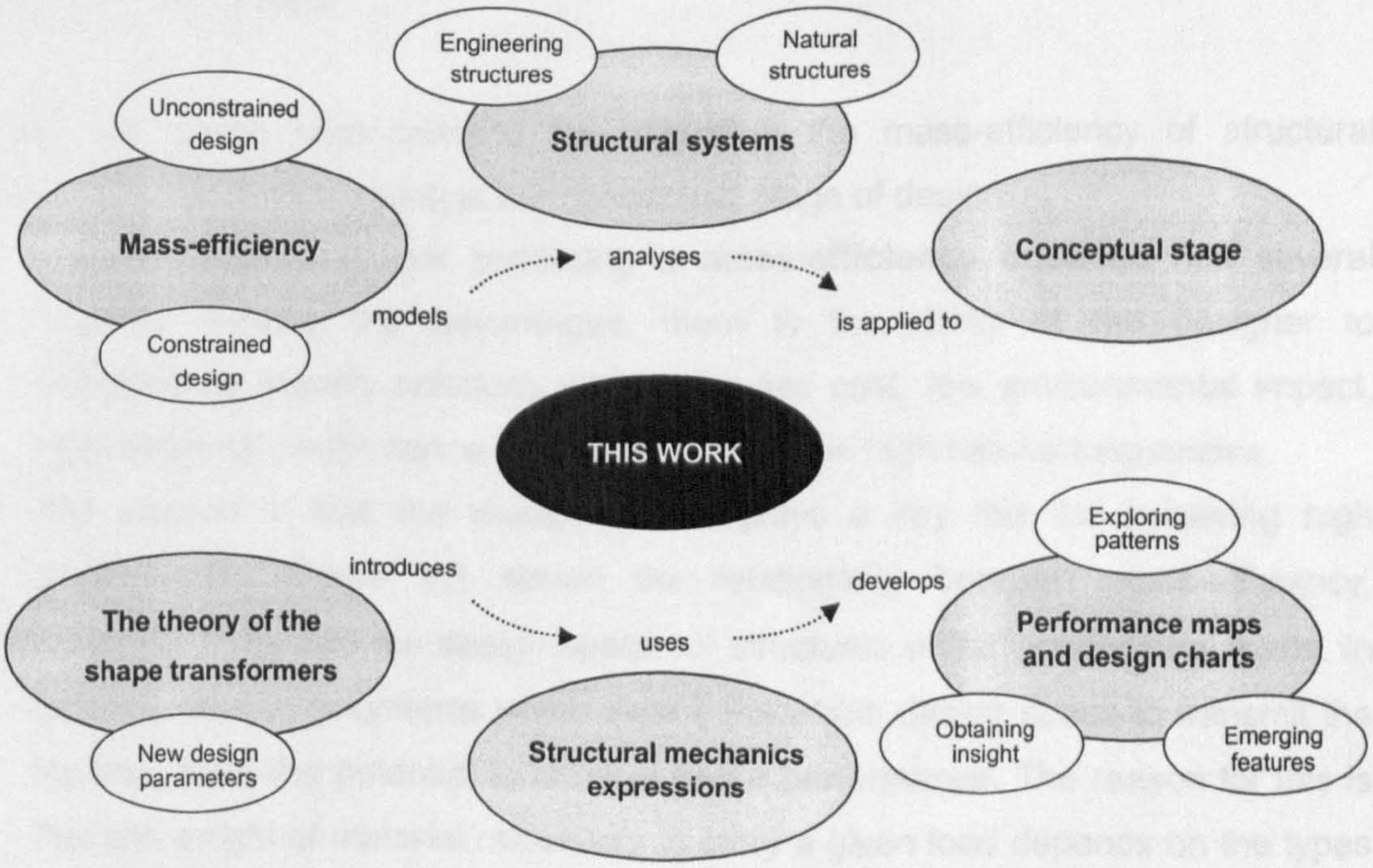

Figure 1.1 Upper part: the aim of the thesis. Lower part: the methodological approach

1.5 THE METHODOLOGIC AL APPROACH

This thesis presents a theory using the concept of shape transformers to model the mass-efficiency of structural systems. The shape transformers are dimensionless design parameters which describe the geometric properties of a cross-section. These parameters are used in the equations of structural mechanics to model the functional requirements and the mass-efficiency criterion, as summarised in the lower part of Figure 1.2.

The visualisation of the structural performance is also a key point in the new method described in this thesis. Therefore, performance maps and design charts are developed for helping designers in the selection of promising structural concepts. These charts are an aid to reasoning because they directly map the design variables and factors that penalise or benefit the performance. In addition, design maps allow patterns of performance and emerging features to be explored at an early stage.

1.6 MOTIVATIONS

There are three main reasons for modelling the mass-efficiency of structural systems in the design space at the conceptual stage of design.

1. The first reason is that producing a **mass-efficiency criterion** has several benefits. Among the advantages, there is the ability of the designer to conveniently identify solutions which give low cost, low environmental impact, high technical performance, low inertial loads and high natural frequencies.
2. The second is that the **design space** plays a key role for achieving high performance. Figure 1.3 shows the relationship between mass-efficiency, structural form, and the design space for structures under gravitational loads. In general, structural systems which exploit the whole design space to transmit the loading, have the potential to achieve better performance. The reason for this is that the weight of material necessary to carry a given load depends on the types and magnitude of internal forces generated throughout the body of a structure. These internal forces are determined by the relation between the pattern of the applied load and the form of the longitudinal axis of a structure.

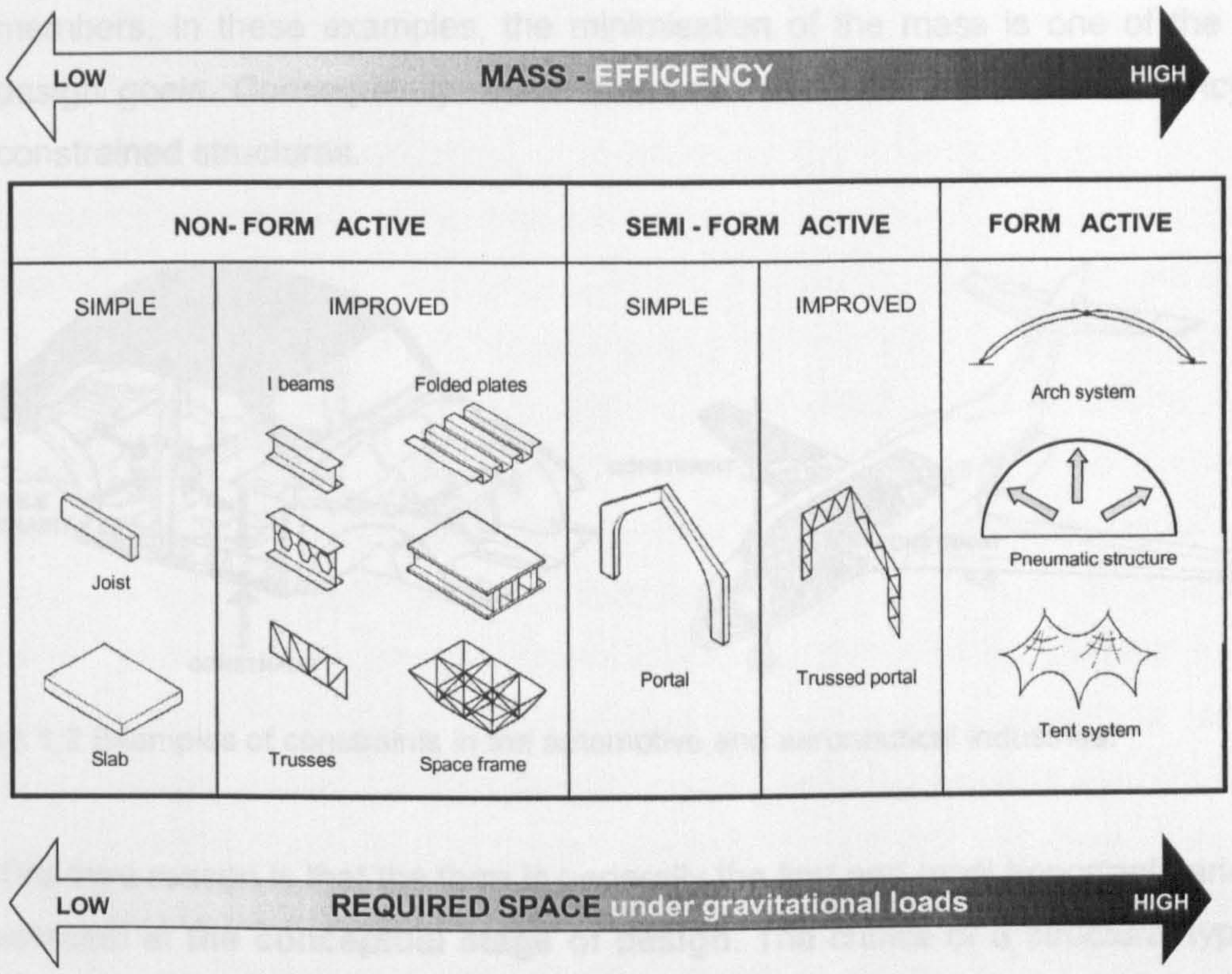

Figure 1.1 Relation between structural form, mass efficiency and design space. (Modified from Structure & Architecture A. J. Macdonald - Architectural Press 2001)

This relation between pattern of load and form of the longitudinal axis can be used to classify structures into three categories: form-active, semi-form active and non-form active (Engel, H., 1967). Improvement of the cross-sections is also used for a further classification within each category. In a form-active structure, the internal force generated in the structure is only axial and the material is used efficiently because each part of the cross-section can be stressed to its limit. For semi-form active, the elements are subjected to bending and axial loading. For non-form active, bending dominates. When bending is involved, the material is used inefficiently because bending stress varies from a minimum at the neutral axis to a maximum at the extreme fibres and, therefore, the middle of the cross-section is not stressed. For structures subjected mainly to gravitational loads, form-active and semi-form active structures generally require more space, as shown in Figure 1.3. There are many cases where the layout of these forms is impractical and the only feasible structures are the non-form active. For example, in automotive and aircraft design as shown in Figure 1.4, the aerodynamic priorities and the minimisation of the space impose tight restrictions on the design space and constrain the depth and width of structural

members. In these examples, the minimisation of the mass is one of the key design goals. Consequently, there is a need to model the mass-efficiency of constrained structures.

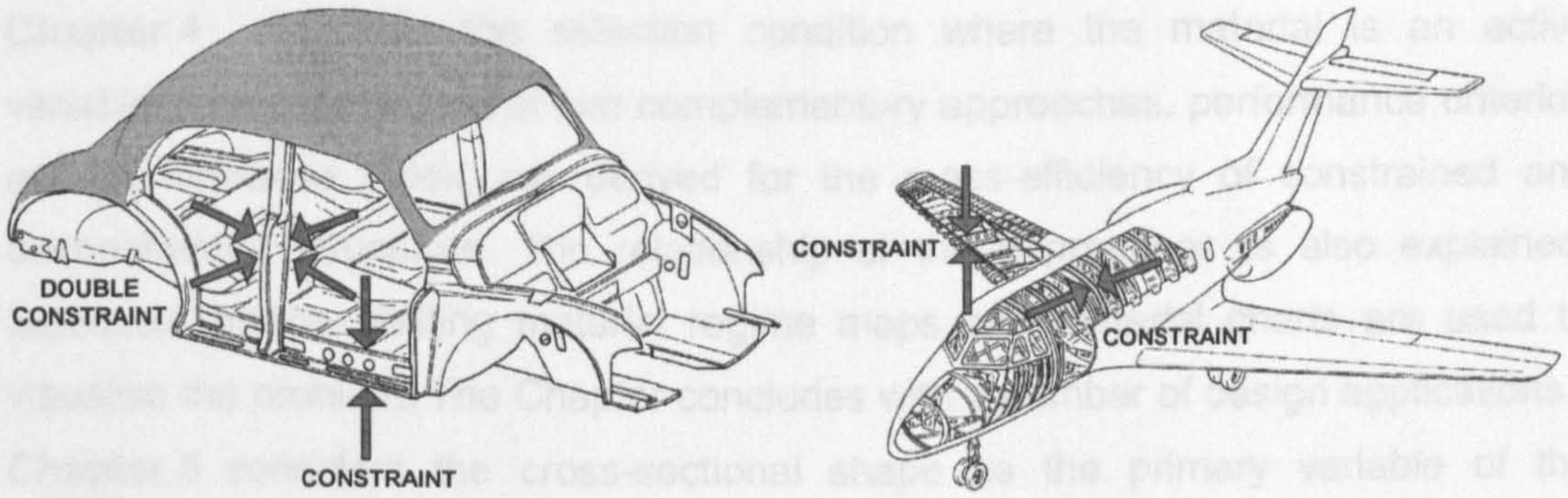

Figure 1.2 Examples of constraints in the automotive and aeronautical industries.

3. The third reason is that the form is generally the first and most important variable selected at **the conceptual stage of design**. The choice of a structural type is decisive for achieving high mass-efficiency as illustrated in Figure 1.3. It has also been demonstrated [Caldwell, J.B. and Woodhead, R.G., 1973] that when optimisation algorithms are applied to a structural concept which is inefficient, the concept cannot generally be changed into a new concept which is efficient. Therefore, there is need to develop a methodology which enables different structural concepts to be explored at the early stage of design.

1.7 THESIS STRUCTURE

The thesis consists of 10 Chapters:

Chapter 1 explains the scope of the research in the context of the design of structural systems. The methodology developed to accomplish the goal of the work is described.

Chapter 2 describes previous methods for the selection of structural concepts and computational algorithms for the optimisation of engineering structures. The applicability of these methods to the early stages of design is explained. The key features of each method including the main equations and the techniques for visualisation of performance are summarised.

Chapter 3 analyses the functional requirements and the objective function in order to identify the relevant structural parameters. A new concept for conceiving a cross-

section is used to introduce the theory of the shape transformers. New design parameters are defined to describe the geometric attributes of a cross-section and are used to model the equations characterising the mass-efficiency. Different conditions for the selection of the variables are specified.

Chapter 4 discusses the selection condition where the material is an active variable. The expressions of two complementary approaches, performance criterion and performance index, are derived for the mass-efficiency of constrained and unconstrained structures. The relationship of the approaches is also explained. Selection graphs, limiting material regime maps and material charts are used to visualise the problem. The Chapter concludes with a number of design applications.

Chapter 5 considers the cross-sectional shape as the primary variable of the selection process. The shape transformers are used in the expressions for the performance criterion and the performance index. These parameters are also used to produce shape charts, limiting shape regimes graphs and envelope efficiency maps for the selection of optimal shapes in any constrained condition. A number of applications are described to show the use of the charts.

Chapter 6 investigates the co-selection of material and shape. The shape transformers are used to introduce a condition to interchange material and shape proprieties. The envelope efficiency map is superimposed on the material chart to provide the co-selection of both variables. The envelope efficiency map is used to explore the limits to the shape transformers due to manufacturing constraints. The case of compression failure is analysed. The shape transformers are used to derive the limits to the height of cross-sections due to mechanical instability.

Chapter 7 examines structuring and layering as two features of shaping a material. The shape transformers are used to give general expressions of the properties of layered structured systems. The performance of these systems is illustrated using an envelope efficiency map and material chart. The case of plastic bending is also analysed and an analogy is used to extend the definition of the shape transformers to the plastic case. Two and three dimensional maps are produced for the visualisation of the plastic case.

Chapter 8 is about the effect of the structural form on mass-efficiency. Performance functions are derived for a non-prismatic component and for pin-jointed frames. A new concept of a performance chart is used in an industrial case study to visualise the performance of structures with more than three variables. The interaction between form selection and cross-section selection for pin-jointed structures which can fail for buckling loads is explored using the shape transformers.

Chapter 9 examines the mass-efficiency of a natural system: a tree branch. The shape transformers and the performance index are used to investigate the structural efficiency of branches and performance maps compare the efficiency with man-made structures. (Note that this Chapter is complemented by the appendix E. In appendix E, the optimal structural features of trees and the analogies with engineering systems are studied to promote novel technical solutions in engineering design).

Chapter 10 summarises the key contributions and the concluding remarks of this work within the context of analysis and visualisation of structural performance. Features for future research are addressed.

1.8 SUMMARY

Structures are systems which span a space to carry loads. Structures are described by material and geometric attributes. Some of these attributes are the variables which a designer selects when designing a structure. The form is generally the first variable to be selected at the conceptual stage of design and has the most marked effect on the mass-efficiency. In general, low mass structures require more space to fulfil the benefits of the form (simple tension is an obvious exception to this rule). Geometric constraints restrict the space where a structure operates and often restricts the choice of efficient structural forms. Therefore, there is need to investigate the effect of geometric constraints on the mass-efficiency. This work models the mass-efficiency at the early stage of design for unconstrained and constrained structures. The theory of the shape transformers is based on a new concept for understanding a cross-section and is used to model the efficiency of material, shape and form. Performance maps and design charts are provided to help in the process of selecting variables and to obtain insight for designers.

CHAPTER 2

LITERATURE REVIEW

2.1 INTRODUCTION

This Chapter reviews the methods that are available for optimising the mass-efficiency of structures at the early stage of design. The methods can be categorised into two types. The first makes use of computer generated algorithms. The second is based on an analytical method to derive selection criteria which allow different structural systems to be selected on design charts. The Chapter consists of three main parts:

1. The first section considers approaches based on optimisation routines which are implemented with computer technology. The aim is not to examine the details and the features of these numerical algorithms but rather to understand their role and effectiveness when applied to the conceptual stage of structural design.
2. The second part describes methods for the selection of material, shape and form. The selection of these variables is discussed in relation to the design space, which can be unconstrained or constrained. The main features of the methods, such as analysis, assumptions and selection charts, are summarised in tables.
3. Remarks on the methods of selection are given in the third section. Gaps in the literature and unclear points which need more understanding are outlined. The Chapter concludes by explaining how this thesis contributes to the area.

2.2 COMPUTATIONAL ROUTINES OF OPTIMISATION

The iterative nature of computational routines of optimisation means that many calculations need to be carried out. Several trial structures are repeatedly analysed before a feasible and finally optimum design is accepted. The procedure for searching an optimum solution can be very time consuming and requires a great deal of computing resources. However, computational routines of optimisation can be effective. In general, an optimisation procedure consists in finding a combination of parameters which optimise a given quantity often called the objective function. The parameters of the problem are the design variables which can be subjected to some restrictions termed constraints. The procedure of optimisation combines the numerical analysis and a mathematical algorithm. The numerical analysis is firstly used to compute the performance of an initial system through a finite element code. Then a mathematical algorithm, i.e. an optimisation routine, gradually modified the design variables of the system in order to optimise the performance. The iterative process continues before an acceptable solution is obtained.

There are several techniques of optimisation. These methods use linear or non linear-programming depending on the relationship among the variables of the problem (Dieter, G.E., 2000). Deterministic algorithms are mathematical techniques used to optimise systems whose structural behaviour is specified without probabilities and predictable without uncertainties (Meiser, V., 1995). Deterministic algorithms are systematically used for unconstrained optimisation, i.e. when there are no restrictions to the variables of a system. The basic structure of local methods (such as descent directions, line search), gradient methods (such as derivative programming, steepest descent, conjugate gradient), Newton methods (discrete Newton, quasi Newton, truncated Newton) are some examples (Meiser, V., 1995). In general deterministic algorithms are also used for constrained non-linear problems, i.e. when there are restrictions on the values of the variables of a system (Arora, J.S., 1989). The basic approach is to simplify the problem so it can be reformulated by a sequence of related problems, solvable by the methods for the unconstrained case (Hafka, R.I.T.1992).

When deterministic algorithms fail in solving some common optimization problems, non-systematic procedures, i.e. stochastic methods, are employed (Meiser, V., 1995). Generally stochastic routines are used to tackle problem of high complexity.

A stochastic algorithm is a procedure of calculation which uses some random mechanism to optimise the variables. These algorithms using some forms of stochastic search include simulated annealing (Kirkpatrick, S., et al, 1984), genetic algorithms (Holland, J.H., 1975), and evolutionary strategies (Schwefel, H.P. (1995).

2.2.1 Application of computational optimisations in structural design

The mathematical routines can be used in structural design to optimise different variables of a structure such as sizes, cross-sectional shape and form. For this reason, structural optimisation can be generally applied to optimise the dimensions, the shape of a cross-section and the topology of a structure (Dieter, G.E., 2000).

- **Size optimisation** deals with parameters that do not alter the location of the nodal points of the numerical model describing the structural system. It consists in optimising the variables relating, for example, to the thickness of a structure (Dieter, G.E., 2000).
- **Shape optimisation** involves systematically removing material from under-utilised regions or adding material to over-utilised regions, so that the resulting structure evolves towards an optimum (Xie Y.M. and Steven G.P. 1993, Qing Li et al 1999). The method consists in setting a threshold value of stress at when material will be removed or added. In contrast to size optimisation, the boundary nodes which describe the shape of the cross-section are altered and, hence, the model has to be continually re-meshed (Dieter, G.E., 2000).
- **Topology optimisation** is usually applied to the form of a structure. Different approaches are used to evolve the topology of a structure. For example, some approaches are similar to shape optimisation (Sigmund, O and Pederson, P. 1996, Chu, N. D. et al, 1997, Steven, G.P. et al. 2000, 2001) and allow the removal not only of material but also entire under-stressed elements, thus causing a topology modification. Other random approaches (Chapman, C. et al. 1993, Shea, K. et al, 1997, Shea, K., 2001, Suppapitnarm A., 2001), employ a shape grammar, which is made up of rules for modifying the topology to optimise the structural form. These procedures adopt stochastic algorithms such as the genetic algorithm (Holland, J. H. 1975) or shape annealing (Kirkpatrick S et al, 1983).

2.2.2 Benefits and limits of computational methods of optimisation

Computational optimisation procedures can be effective techniques to apply to design problems in view of the benefits and limits they can provide.

- **Size optimisation** provides excellent results when the overall form of the structural system is already decided and therefore fixed. It is the simplest and most common type of optimisation (Dieter, G.E., 2000).
- **Shape optimisation** can lead to significant weight benefits. However, it can provide uncommon cross-sectional shapes that are difficult, expensive and, sometimes, impossible to manufacture (Dieter, G.E., 2000).
- **Topology optimisation** can give useful information about the number and position of the holes to place in a structure. However, when stochastic approaches are used to generate structural topologies for the early stage, there are some disadvantages. Based on the review of earlier works (Shea, K. *et al.*, 1997; Suppapitnarm A., 2001; Starling, A.C. and Shea, K., 2002) which used stochastic methods of optimisation, the following observations can be drawn:
  i. *Random nature of the optimisation technique.* Stochastic searches involve a partially random exploration of the space. There is the possibility of being trapped in local minima without guaranteeing the identification of the global minimum.
  ii. *Sensitivity of the solutions to the grammar rules.* The grammar rules are set in advance by the designers to allow an alternative topology to be generated. The explored solutions, therefore, are highly sensitive to the topology modification laws. Although these procedures generate several solutions which can help designer in the selection, they are unable generally to jump from one structural form to an alternative form. This is because a structure is generated from the previous one by changing the values of the variables. However, the different nature of some structural forms require changing not the values of the variables but rather the variables themselves.
  iii. *Confusing solutions.* A large number of structures are explored. However, many solutions are not practical and, therefore, an accurate screening is required. If the experience of the designer is poor, the high number of solutions can entrap rather than enhance the creativity.
  iv. *No visualisation of performance trends.* The random nature of these routines does not permit the representation of performance trends. Therefore, these

methods do not provide much insight and do not facilitate communication within a design team.

2.3 SELECTION METHODS

In general optimisation procedures are not able to move from one structural concept to another. For example, a truss structure cannot evolve into an I beam and a hollow triangular cross-section cannot evolve into a T section. The reason why designers are able to change from one concept to another is that designers themselves take the initiative to intervene and change the forms. When creative talent and experience are used to explore a wide range of alternative structural concepts (both forms and cross-sectional shapes), then the process of **design** could be **reduced** from an iterative analysis procedure **to** a single stage of **selection**. In such a case, the designer can simply choose the best solution among structures where the selectable variables are either material, or cross-sectional shape or form, or a combination of these. Once an optimum structural concept has been selected, then optimisation procedures can be used to improve the performance.

In the last century, methods of selection for the early stages of design have been developed by several authors in various disciplines such as aircraft, ship, civil and mechanical engineering. The aim of these activities was to provide quick and accessible procedures which could be used to produce design charts for the selection of an optimum structural concept. The studies focused on the relationship between mass efficiency and the main variables of a structural system: material, cross-sectional shape and form.

A summary of these studies has been organised chronologically in Table 2.1 and 2.2. In Table 2.1, there are methods which deal mainly with the selection of structures in an unconstrained design space. In contrast, Table 2.2 lists procedures which permit the selection of structures subjected to some geometrical constraints. In the columns of Tables 2.1 and 2.2, the main variables of a structure used to model the mass-efficiency are reported, while in the rows, for each author the following features have been considered:

- Design/Loading cases examined.
- Analytical approach and assumptions adopted.
- Novelties and/or main features introduced.
- Graphical representation used.

Author	Research features	MATERIAL	CROSS SECTION SHAPE	STRUCTURAL FORM
MICHELL (1904) Civil engineering	Design cases			Two dimensions: 1. Cantilever beam under point end load 2. Centrally loaded beam in a whole plane 3. Centrally loaded beam in half plane 4. Three forces directed to one point Three dimensions: 5. Couples applied at two points of a straight line
	Analysis			The optimal layout theory is derived using a lemma by J. C. Maxwell (1869) and the principle of virtual work.
	Assumptions			▪ No buckling, i.e. tension and compressive members designed for yield failure ▪ No weight of joints
	Novelties & main peculiarities			1. Features of optimum structures: ▪ Virtual deformation of the region with strains along the members = $\pm\varepsilon$ ▪ Uniform stresses in all members = $\pm\sigma$ 2. Optimum structures: ties and struts, catenaries, triangular frames and orthogonal curves, where tension and compression members meeting at a node are orthogonal. Among orthogonal curves there are: ▪ System of tangents and involute derived from evolute ▪ Equiangular spirals ▪ Networks of straight lines ▪ Concentric circles and radii
	Graphical visualisation			Optimum layouts for the five loading cases are provided
	Comment			Optimum structures require the design space to be unconstrained.
CHAN A.S.L. (1960) & **CHAN H.S.Y.** (*) (1963) Aeronautical engineering	Design cases			1. Cantilever under tip shear force 2. Beam under uniform bending moment 3. Three parallel asymmetric forces (*)
	Analysis			Based on Michell theory and analogy with perfect plastic flow
	Assumptions			▪ No buckling ▪ No weight of joints
	Novelty			
	Graphical visualisation			Graphical construction of two dimensional structural layouts
	Comment			Comparison with conventional alternative structural forms

Table 2.1 Methods of selection for unconstrained design

Author	Research features	MATERIAL	CROSS SECTION SHAPE	STRUCTURAL FORM
COX (1923-65) Aeronautical engineering	Design cases	Compression, bending		Compression, bending
	Analysis	The mass-efficiency is given by the material breaking length, f/ρ. Example for round section $\frac{f}{\rho} = \underbrace{0.886}_{Shape} \quad \underbrace{\frac{E^{0.5}}{\rho}}_{Material} \quad \underbrace{\left(\frac{P}{L^2}\right)^{0.5}}_{Str.Index}$		Exploration of Michell's orthogonal curves
	Assumptions	Unrestricted cross-section. All dimensional proportions must be preserved Uniform cross-section along structure length		Two dimensional structures No buckling No weight of joints
	Main peculiarities	A solid circle is introduced as reference section.		
	Graphical visualisation	Plot of structures for different materials and shapes (Figure 2.1)		
	Comment	In the mass-efficiency criterion, 0.866 includes a shape coefficient and an empirical parameter for local buckling.		Michell's theory is applied to practical design to show that neither the effect of joint weight nor the influence of instability invalidates the optimal layout theory.
SHANLEY (1952-60) Aeronautical engineering	Design cases	Compression		
	Analysis	Mass-efficiency criterion $\frac{W}{L^3} = \frac{\rho A}{L^2} = \frac{1}{\pi}\underbrace{\frac{1}{K_1^{0.5}}}_{Shape}\underbrace{\frac{\rho}{E_t^{0.5}}}_{Material}\underbrace{\left(\frac{P}{L^2}\right)^{0.5}}_{Str.Index}$		
	Assumptions	Unrestricted cross-section. All dimensional proportions must be preserved when different material and/or shape are selected.		
	Novelties	Shape parameter : $K_1 = r_g^{\,2} / A$ K_1=1 for the solid reference section. (r_g radius of gyration) The limits to K_1 for tubes are derived		
	Graphical visualisation	Plot of structures for different materials (Figure 2.2)		
	Comment	Expression of K_1 can be derived for any cross-sectional shape		

Table 2.1 Methods of selection for unconstrained design

Author	Research features	MATERIAL	CROSS SECTION SHAPE	STRUCTURAL FORM
CALDWELL (1960-65) Naval engineering	Design cases	Bending, compression		
	Analysis	The volume index V/L^3 is the selection criterion used to compare different cross-sections and alternative forms: $\frac{V}{L^3} \propto \left(\left(\frac{P}{\sigma_y L^2} \right), \left(\frac{\sigma_y}{E} \right)^{0.5}, \ldots \right)$		
	Assumptions	Prismatic beam Unrestricted cross-section		For trusses: Pinned joints so that internal forces derived by statics Fixed topology (truss bays are equilateral)
	Novelty	The design index $\mu = P/(L^2 f_L)$ is plotted against the volume index $\nu = V/L^3$		
	Graphical visualisation	Plot of different forms and simple shapes for different materials		Plot of different structural types (truss vs. beam) for one material: steel (Figure 2.7)
	Comment	The structural form is the first variable to select because the most crucial in low-mass design.		
PARKHOUSE (1984-93) Civil Engineering	Design cases	Compression and bending		
	Analysis	The flexural and axial stiffnesses of a generic structure, *s*, can be replaced by the properties of an equivalent structure, *e*, when: $E_s A_s = E_e A_e$ Axial $E_s I_s = E_e I_e$ Flexural $\therefore I_s / A_s = I_e / A_e \longrightarrow r_{gs}^{\ 2} = r_{ge}^{\ 2}$		
	Novelty	$i = E/E' = A'/A$ is the dilution factor or sparsity		
	Graphical visualisation			
	Comment	The elliptical equivalent section has $r_{gs} = r_{ge}$ The sparsity is given only for some simple equiaxed sections. (The method is used to model the efficiency of alternative structural forms by Birmingham).		

Table 2.1 Methods of selection for unconstrained design

Author	Research features	MATERIAL	CROSS SECTION SHAPE	STRUCTURAL FORM
ASHBY (1989-99) Mechanical/ Materials engineering	Design Cases	Bending, compression, twisting, tension for stiffness and strength requirements		
	Analysis	Material index for material selection in bending $M = \frac{E^{0.5}}{\rho}$	Index for material and shape co-selection in bending $M = \frac{(E\phi_B)^{0.5}}{\rho}$	
	Assumptions	Unrestrained section		
	Novelties and main peculiarities		Shape factors given for the design cases. Example for stiff light beam: $\phi_B = \frac{4\pi I}{A^2} = 4\pi \frac{r_g^{\ 2}}{A}$ Solid circular reference with $\phi = 1$ Micro shape factors given for the design cases.	
	Graphical visualisation	Materials charts for selecting the best material and co-selecting shape and material		
	Comment	The shape has to be prescribed.	Approximate formulae are given for geometric quantities of shapes, such as *I* and *A*.	
BIRMINGHAM (1994) Naval engineering	Design Cases	Bending, twisting, shear, compression, tension		
	Analysis	Parkhouse's method is used to model the efficiency of different trusses		
	Novel visualisation	A chart of four linked quadrants (Figure 2.8)		
	Comment	The topologies of the structures are fixed. The mutual geometric relations among the constituent elements are constant.		
WEAVER and ASHBY (1996-97) Materials engineering	Design Cases	Compression, bending, torsion for tubes and box section Compression and bending for I section		
	Analysis	Study of interaction among failure modes: yield, general and local buckling		
	Assumptions	Empirical factor to describe local buckling		
	Main features	Empirical limits to the shape factors for standard structures. Material limits to the shape factors Minimum mass relationship derived for the optimal ϕ		
	Graphical visualisation	Plot of the stiffness, EI, and unit mass, $A\rho$, for existing structural sections Plot of contours of mass as function of the shape factor ϕ		
	Comment	The interaction between failure modes is explored.		

Table 2.1 Methods of selection for unconstrained design

Author	Research features	MATERIAL	CROSS SECTION SHAPE	STRUCTURAL FORM
CRANE J.A. CHARLES F.A. (1984) Mechanical / Materials engineering	Design Cases	Bending and compression for stiffness requirement		
	Analysis	Mass index $M = \frac{\rho}{E^{1/3}}$ width constraint		
	Assumptions			
	Comments	The shape has to be prescribed.		
ASHBY (1992) Mechanical / Materials engineering	Design cases	Bending for stiffness and strength requirement		
	Analysis	Performance indices $M = \frac{E\phi_B{}^h}{\rho}$ for height constrained beam $M = \frac{\left(E\phi_B{}^b\right)^{1/3}}{\rho}$ for width constrained beam		
	Novelties	Shape factors: $\phi_B{}^h = 16\frac{r_g{}^2}{h^2}$ $\phi_B{}^b = \pi^2\frac{Ib^2}{A^3}$		
	Graphical visualisation	Guide lines for material selection chart (Figure 2.3)		
	Assumptions	Reference section: $\phi_B{}^h = \phi_B{}^b = 1$		
	Comments	Ranges of the shape factor $\phi_B{}^h$ are given		
BURGESS (1999-2000) Mechanical engineering	Design cases	Bending and torsion for stiffness and strength requirements	Simply supported and centrally loaded beam	
	Analysis	Ashby's method is used to examine height constrained design	Form factor method	
	Assumptions	Solid circular reference section	No buckling. No joints weight	
	Novelty		λ dimensionless factor depending on the form	
	Graphical visualisation		Comparison among trusses with variable and uniform section, and beams with tapered width and height	
	Comment	Circle is not an appropriate reference section for constrained design (Figure 2.6)	Description of aspects affecting the performance	

Table 2.2 Methods of selection for constrained design

Author	Research features	MATERIAL	CROSS SECTION SHAPE	STRUCTURAL FORM
This thesis (2000-02)	Design cases	Tension, bending, compression for stiffness and strength requirement, plastic bending		Tension, bending and compression for non prismatic element and pin-jointed frames.
	Novelties	The theory of the shape transformer is based on the concept that the main sizes of a cross-section describe the rectangular envelope enclosing the shape. The shape transformers are the shape properties of a cross-section ▪ ψ_I , ψ_Z , ψ_A shape transformers for elastic case ▪ ψ_I^p , $\psi_A{}^p$ shape transformers for plastic case ▪ λ_I, λ_Z envelope efficiency parameters ▪ $q = f(u,v)$ scaling parameter (where u and v are envelope sizes multiplicators) for arbitrary scaling		Buckling considered in form selection
	Analysis. (some examples are reported here)	Performance criterion and performance index for arbitrarily scaled sections. Examples for material and shape co-selection Performance criterion $p = v^2 \frac{E}{\rho} \frac{\psi_I}{\psi_A}$ Performance index $p = \frac{(E\psi_I)^q}{\rho\psi_A}$ Structured layered systems: mass, stiffness and performance: $\frac{m}{A_D} = \sum_{i=1}^{n} \rho_i x \prod_{j=1}^{t} \psi_{Ai}^j$ $\frac{k}{I_D} = \sum_{i=1}^{n} E_i x \prod_{j=1}^{t} \psi_{Ii}^j$ $p = \sum_{i=1}^{n} \frac{E_i}{\rho_i} x \prod_{j=1}^{t} \lambda_{Ii}^j$		A parametric expression of the cross-sectional area is derived to prevent buckling of struts. The design parameters are included in order to pre-select the cross-sectional shape and to verify the effect on the mass-efficiency of different structural forms.
	Assumptions	Reference section: square with $\psi_I = \psi_A = \lambda_I = \lambda_Z = 1$		No joint weight Shear negligible Determinate pin jointed frameworks
	Graphical representation	Limiting material and shape regimes graphs Combined graph for material and shape selection Envelope efficiency map for shape selection. The envelope efficiency map is a selection chart of the shape properties as the material chart is for the material properties. Envelope efficiency map for structured layered systems. Two dimensional and three dimensional maps for the plastic case.		Charts for different structural concepts. Nested performance charts for multivariable structural systems.
	Comments	The method has been applied to man made and natural systems		The shape transformers are used to explore the interaction among material, cross-sectional shape and form selection.

Table 2.3 Main features of this research.

2.3.1 Material and shape selection-methods for unconstrained design

At the beginning of the twentieth century in branches of engineering where the mass efficiency is a major factor, such as aircraft and naval design, both material and shape were considered the variables to be selected to optimise the performance of a structure. For this reason, the selection criterion reported in this Section includes terms containing material and shape attributes. Only recently (Crane, F.A.A. and Charles, J.A., 1984, Ashby, M.F., 1989), the separability of material and shape has become more significant in areas such as material selection.

Since these methods of selection are used to design a structural system, it is important to specify the background of the **design analysis**. This design approach uses the **principle of dimensional similarities** to discover the optimum proportions which can be applied to another structure of a different scale and/or different attributes without any additional calculations. In the past, the principle of geometrical similarities was widely adopted to design a structure. For example, Galileo (1638) elucidated the importance of determining the design proportions of a cantilever under a given load before building it. In general, design analysis is the reverse of stress analysis. The aim of the stress analysis is to find the allowable stress of a structure assuming that the size, shape and material are already known.

In order to achieve the beneficial effects of geometrical similarities in the design of optimum structures, Wagner (1929) first introduced a measure of the magnitude of the load, P, and the distance, L, over which the load is transmitted. This measure is called the structural index, P/L^2, and has units of stress. Provided that the structural index is the same, the optimum proportions of a structure can be applied to any other with no additional stress analysis and on the conditions that all the dimensional ratios of the structure remain unchanged.

Several authors, such as Cox and Smith (1943), Shanley (1960) and Cox (1965), have used the structural index to derive a selection criterion. One advantage for this is that if P/L^2 is the same, the mass efficiency of structures with different materials and cross-sectional shapes can be quickly compared without the main sizes of the cross-sections being calculated. It is necessary that the design space is

unconstrained so that the proportions and the main sizes of a cross-section can be preserved when different material and shape attributes are selected.

The structural index, P/L^2, has been given different names by different authors. Cox and Smith (1943), for example, referred to it as the structural loading coefficient. Shanley (1960) used the original name of structural index, which, for this reason, is adopted also in this Chapter. In the following, a number of studies for unconstrained design by various researchers are reviewed. Table 2.1 summarises the main features of these selection methods.

(i) Cox

In Cox's analysis (1965) for compression and bending cases, the structural performance is expressed in terms of the structural index (Cox, H.L. and Smith, H.E., 1943) and the material-breaking length f/ρ, i.e. stress, f, divided by material density, ρ. This factor represents the length of a freely hung rod which would break under its own self-weight. The selection criterion was derived using the Euler's formula for primary buckling failure and for a predetermined shape of the cross-section. For example, Cox (1965) provided the following criterion for a solid round strut with Young's Modulus, E, density, ρ, and yield stress, f,:

$$\frac{f}{\rho} = \underbrace{(0.886)}_{Shape} \underbrace{\left(\frac{E^{0.5}}{\rho}\right)}_{Material} \underbrace{\left(\frac{P}{L^2}\right)^{0.5}}_{\substack{Structural \\ Index}} \tag{2.1}$$

The second member of expression (2.1) has been purposefully split here into three factors to identify the role of the design variables: shape, material and load requirement. E and ρ are the material attributes, P and L are the functional requirements, 0.886 is the shape parameter. This constant includes information about the shape and could also contain a specific ratio of the thickness of hollow cross-sections to take into account the effect of local buckling. The criterion (2.1) was derived assuming that the structures are unconstrained to meet the design requirement, P/L^2, and that the sections are uniform along their length (Cox, H.L., 1965).

The selection criterion (2.1) was used by Cox (1965) to produce design charts for simple elements. An example is shown in Figure 2.1 for different struts where the selectable variables are material and shape. For a given requirement P/L^2, the design charts permit the selection of the best combination of material and shape for unconstrained cross-sections.

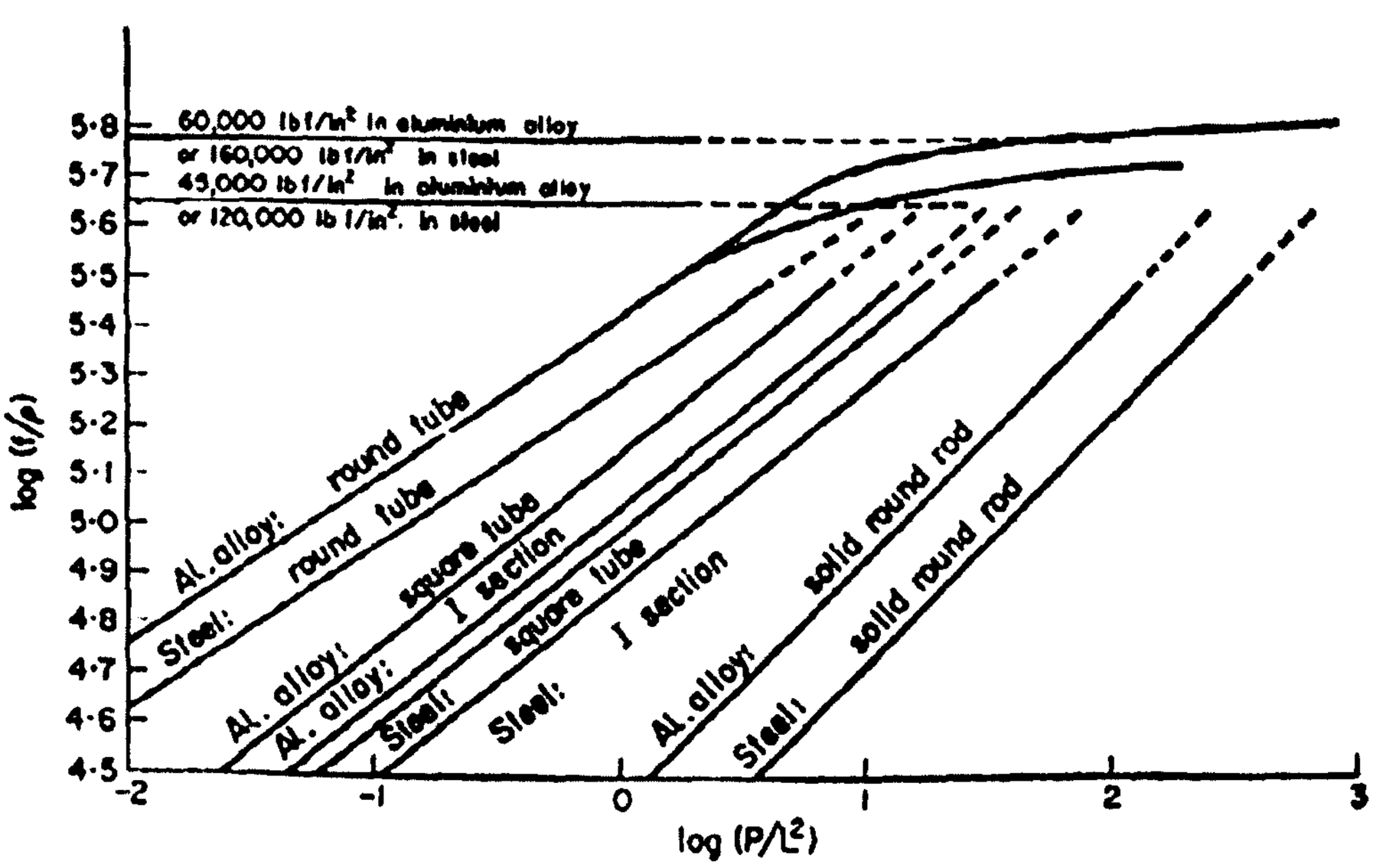

Figure 2.1 An example of a chart produced by Cox (1965): comparative weights of struts for different cross-sectional shapes and materials.

(ii) Shanley

During the 1960's, Shanley (1960), who was professor of aeronautical engineering at the University of California, analysed the principles of optimum design for aircraft structures. The method, related to Cox's theory, presents a novel term, the shape parameter, K_1, to model systematically the shape of a cross-section (Shanley, 1960). Under the control of the designer, the shape parameter is dimensionless because it is derived by normalising the radius of gyration, r_g (where $r_g = \sqrt{I/A}$ is a function of the second moment of area, I, and the area, A), of a cross-section by its area, A, so that $K_1 = r_g^2/A$. Cross-sections with a prescribed shape, whose dimensions are relatively proportionally scaled, have the same K_1. In contrast to Cox (1965), the selection criterion, W/L^3, is, here, related to the mass, $W=\rho AL$, and includes primary buckling. Shanley suggested that the effect of local buckling can be considered with adequate accuracy if the tangent modulus E_t (Engesser, F., 1889) is substituted by

the reduced modulus (Jasinski, F., 1895). For the simple case of pin-ended column the minimum-mass is given by

$$\frac{W}{L^3} = \frac{1}{\pi}\underbrace{\left(\frac{1}{K_1^{0.5}}\right)}_{Shape}\underbrace{\left(\frac{\rho}{E_t^{0.5}}\right)}_{Material}\underbrace{\left(\frac{P}{L^2}\right)}_{Structural\ index}^{0.5} \tag{2.2}$$

Expression (2.2) presents the same groups highlighted in Cox's analysis (1965): the structural index, the ratio of the material properties which is inverted but with the same exponents for E and ρ, and the shape parameter, K_1, elevated to the same exponent as for E, i.e. 0.5. The criterion allows alternative structures to be compared provided that all the dimensions (length, width and thickness) remain proportional (Shanley, 1960).

Two important features emerge from this analysis. Firstly, to facilitate the mass comparison, Shanley (1960) suggested reducing the mass criterion to a common reference section by considering a standard material and a solid circular shape, whose shape parameter is unity. Secondly, the shape parameter was used to derive the optimum structural proportions for round tubes when general and local instability were considered. It was found that the optimum limits to the shape parameter are determined by the material properties.

Although expressions of the shape parameter could be derived for any given section, equation (2.2) was mainly used to produce graphs which compare the mass of a single cross-section made from different materials. An example is shown in Figure 2.1 where L_o is the effective column length and c is the coefficient of fixity dependent on the end restraint conditions so that $L=cL_o$. The shape of the cross-section is predetermined. However, the mass penalties, involved in using a 'non-optimum' type of structure, can be determined when both the variables, material and shape, are active.

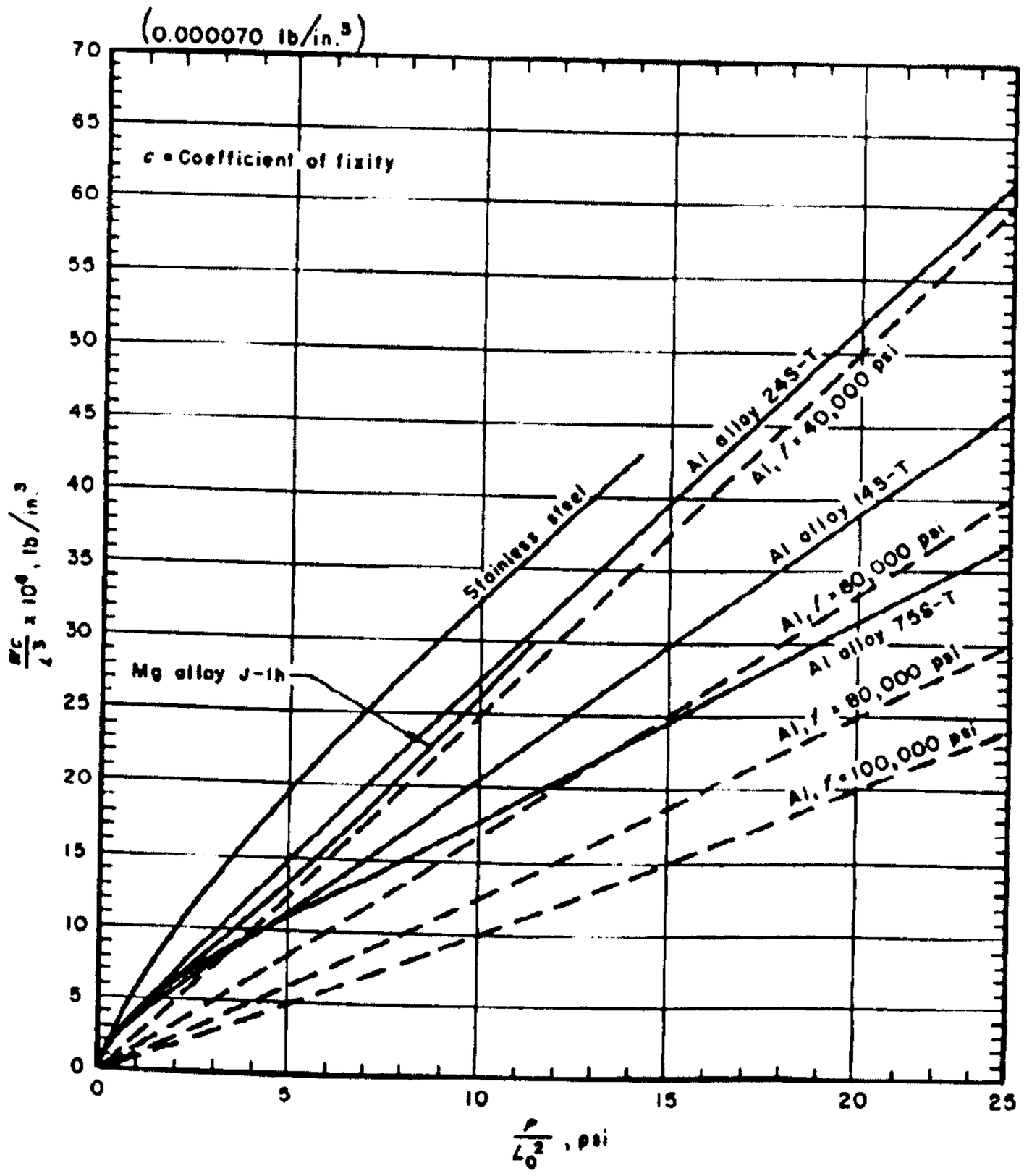

Figure 2.1 An example of chart produced by Shanley (1960): minimum weights for round compressive tubes of different materials.

(iii) Parkhouse

Parkhouse (1984, 1989, 1993) also recognised shape and material to be relevant to structural performance in the 1980's and 1990's. He introduced the concept of structuring which describes how a material is shaped into a structure. This concept indicates that the variables, material and shape, are complementarity in making a structure (Parkhouse, 1984). He used the terms "material dilution" or "sparsity" to describe how material was spread in a cross-section. He showed that there is no clear divide between structure and material because a shaped material is a structure, which can be called a macro-material (Parkhouse, 1993).

In order to specify the properties of a macro-material subjected to bending in one direction, the axial and flexural properties in the direction bending of bending were

modelled to show that a generic cross-sectional shape, *s*, is equivalent to a solid elliptical shape, *e*, for the following conditions:

$$E_s A_s = E_e A_e \tag{2.3}$$

$$E_s I_s = E_e I_e \tag{2.4}$$

Therefore:

$$I_s/A_s = I_e/A_e \quad \text{so that} \quad r_{gs}{}^2 = r_{ge}{}^2 \tag{2.5}$$

Expressions (2.3) and (2.4) show that the geometric properties of a generic cross-sectional shape can be seen as the material properties of an equivalent solid ellipse. Consequently, the cross-sectional shape can be treated as a transformed material with equivalent property: $E_s = E_e\, I_e/I_s$ and $E_s = E_e\, A_e/A_s$. However, it should be noted that since a cross-section has two axis, it is of primary importance to consider according to the axial and bending loadings which of the two radii of gyrations the equivalent material is referred to. The resulting expression (2.5) indicates that if the ellipse and a generic cross-section have the same radius of gyration about one axis and if a dilution factor or sparsity is defined as $i = A_s/A_e$, then the material property E_s of the shaped material is $E_s = E_e/i$. The sparsity is set to be unity for the elliptical cross-section and values of i greater than 1 are given for some simple shapes such as square and circular tubes.

The concept of macro-material can be used to model not only different shapes but also different structural forms. Although Parkhouse does not produce any design charts for form selection, the theory was used in the 1990's (Birmingham, 1994) to produce such charts. This will be reported later in the Section related to form selection.

(iv) Ashby

Cox and Shanley, who were structural engineers, developed analytical methods which allow different structures to be selected on charts which directly display the selection criterion against the structural index. Ashby, who is material scientist, adopted a material-based approach to selection. His approach identifies the best material for a given design requirement. In contrast to Cox (1943, 1965) and

Shanley (1960), Ashby (1989, 1991) considered separately the material selection, as it was done previously by Crane and Charles (1984), and the co-selection of material and shape. The fundamental equations of mechanics were used to derive a performance expression, p, in terms of functional requirements, F, geometry, G, and material properties, M. If F is a design input to be satisfied, G and M are the selectable variables to optimise p, which can be written as:

$$p = f(F, G, M) \tag{2.6}$$

Ashby's rationale was to assume that the groups of parameters in (2.6) are separable. If the function, f, in equation (2.6), can be expressed by a product, i.e. $p = F \times G \times M$, then the groups are separable and the geometry and material can be selected independently (Ashby, 1991, 1992). For example, the selection criterion for a beam designed to minimise the mass, m, and to meet a stiffness requirement, is given by (see Appendix A for derivation)

$$m = \underbrace{\left(\frac{P}{\delta}\right)^{0.5}}_{F,\text{Requirement}} \underbrace{\left(\frac{L^5}{zc}\right)^{0.5}}_{G,\text{Geometry}} \underbrace{\left(\frac{\rho}{E^{0.5}}\right)}_{M,\text{Material}} \tag{2.7}$$

where δ is the prescribed deflection under the load P, c represents a number depending on the boundary conditions, L and z are the length and a constant, peculiar to the particular shape, respectively.

The following observations can be drawn when comparing Cox's equation (2.1), and Shanley's equation (2.2), with Ashby's criterion (2.7). The material group, $\rho/E^{0.5}$, is the same although inverted in Cox's criterion. The functional requirement in equation (2.7) plays a similar role to the structural index in equation (2.1) and (2.2) since they are all design inputs. However, while the requirement F contains only load details and the length is placed in the geometry group, G, together with the shape details, P/L^2 includes both the load requirement and the geometric length of the element.

In the following aspects of Ashby's work, different features are here considered: material selection, material and shape selection, microstructured materials, limits to the efficiency of shaped materials.

a) Material selection

Ashby (1989, 1992) resorts to the separability of the variables to isolate the material properties group, *M*, from *G*. When the cross-sectional shape and length are prescribed, the geometry group is constant and the material is the only selectable variable. Therefore, for a given requirement, the mass-efficiency of a structure is minimised when the inverse of the material group in equation (2.7) is maximised. This group, *M*, is a combination of material properties and is given by:

$$M = \frac{E^{0.5}}{\rho} \tag{2.8}$$

The relation (2.8) is called the material index, *M*, because only material properties are apparently included. However, in this thesis it will be explained that the exponent of *E* is an outcome of a geometric assumption about the sizes which define the area of a section (see Appendix A). Since the shape is fixed, the sizes of the cross-sectional area, necessary to meet the functional requirement *F*, is determined by the material attributes. This means that the proportions of the cross-sections remain constant and the sizes of the candidate sections are proportionally scaled. In some cases, a designer may wish that a section is proportionally scaled. However, this is not always the case. An example where proportional scaling is appropriate, is for a structural component which is subjected to bending from any direction, e.g. a lamp post subjected to multidirectional wind. However, when bending is only in one direction, then proportional scaling is generally not appropriate.

Although expression (2.8) provides a model for one design condition, Ashby (1989) shows that indices of performance can be derived for a number of different design cases and they can be mainly described by a combination of material properties. Ashby (1991) plotted one material attribute against another on log-log charts so that the material property space can be visualised in a concise and accessible format. In addition, the material properties charts can be used for material selection for different requirements, such as stiffness and strength. In contrast, the charts of Cox and Shanley considered only a single loading case. Ashby (1991) produced his charts by rearranging the expressions of the performance indices to superimpose lines of constant performance on logarithmic scale charts. An example of a **design chart** of Young's modulus against density is shown in Figure 2.4. Contours of equal performance are displayed so as to act as guidelines for the selection of the best

material which maximises the stiffness while minimising the mass of a structure. The exponent of E in the performance index is the slope of these selection lines. The choice of an index, or slope, has the effect of introducing geometric information on the material domain. For a given index, structures of equal performance lie on the same line while the selection of materials above or below the line gives structures with better or worse mass-efficiency respectively.

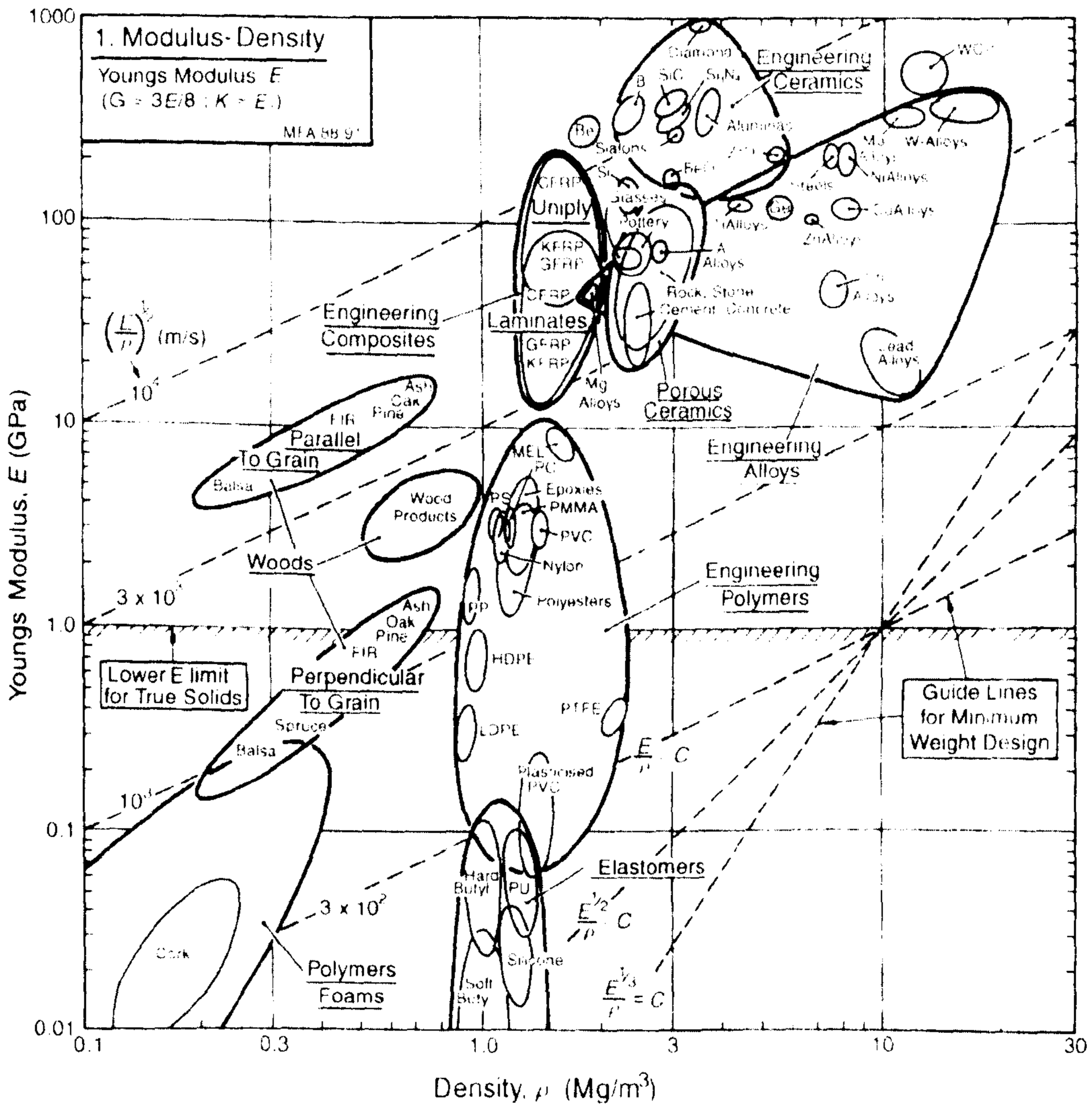

Figure 2.1 An example of Ashby's selection chart (1999), E against ρ.

b) Material and shape selection

The studies by Cox (1965) and Shanley (1960) considered material and shape together as a design variable. Cox did not define a factor to systematically include the effect of shape. However, Shanley conceived an innovative way to include the shape variable for compression and bending cases and to enable the comparison of different shapes on a reference basis. In Parkhouse's analysis (1984), the dilution

factor was introduced to measure the effect of the shape of a generic section compared to an ellipse with the same radius of gyration. Since a cross-section has two radii of gyration about the axis of symmetry, only the radius of gyration about the axis of symmetry which is the axis of bending loading is considered for the definition of the dilution factor. Ashby's approach (1989) to the shape variable is related to these previous works. The concept of a shape parameter and reference section were adopted by Ashby (1991) and extended (Ashby, M.F., 1992) to different loading conditions, such as torsion, and functional requirements, such strength and stiffness.

Ashby (1991) introduced a shape factor to characterise the efficiency of a cross-sectional shape. This factor is a dimensionless number which is given for a mode of loading regardless of the scale, i.e. it remains constant for sections which have the same shape and are proportionally scaled. For example, a centrally loaded beam of a given length must meet a prescribed value of stiffness, called a bending stiffness requirement, k, to avoid a certain deflection under the load. In this case, the shape factor, ϕ, of a particular section is defined as the ratio of the stiffness of that generic cross-sectional shape, k, and a reference circular section, k_o. The ratio ϕ for structures made out of the same material is given by.

$$\phi = \frac{k}{k_o} = \frac{I}{I_o} = \frac{I}{\pi r^4/4} = \frac{I}{A_o\, r^2/4} \tag{2.9}$$

where I is the second moment of area of the generic section and I_o, A_o and r are second moment of area, area and radius of the circular reference section.

If it is assumed that the area of the reference circular section A_o is the same of the area of the generic cross-sectional shape, A, then $A=A_o$ and ϕ takes the form:

$$\phi = \frac{I}{A r^2/4} = 4\pi \underbrace{\frac{r_g^{\,2}}{A}}_{\substack{\textit{Shanley's}\\ \textit{parameter}}} \tag{2.10}$$

The equality of the areas is an important assumption because it enables ϕ to specify the stiffness improvement of a cross-sectional shape compared to a reference circular section of the same mass. However, there are two aspects to consider for this assumption. Firstly, $A=A_o$ has the same effect of normalising the radius of

gyration of the generic section by its own area. Therefore, the shape factor, ϕ, expresses Shanley's (1965) shape parameter, K_1, in a different form. Secondly, since the value of the area A is considered variable and since 4π is only a constant of the second moment of area of the circular reference cross-section, any geometrical information about the sizes of the reference section is lost.

Adding the shape factor to the material index, $E^{0.5}/\rho$, which was derived assuming that the sections are proportionally scaled, gives

$$M = \underbrace{\left(\phi^{0.5}\right)}_{Shape} \quad \underbrace{\left(\frac{E^{0.5}}{\rho}\right)}_{Material} \tag{2.11}$$

Ashby's (2.11) and Shanley's (2.2) criteria have the same groups for shape and material. The only difference is that the groups are inverted since Shanley's criterion is a direct measure of the mass. Whereas Shanley (1965) does not derive any expression for K_1, Ashby (1992) provides approximate formulas of ϕ for practical cross-sectional shapes.

Ashby (1991) also uses material selection charts for the selection of shaped materials. The shape factor is used to display the properties of a shaped material. For example, in the co-selection of shape and material for a light beam, the effect of giving a shape, ϕ, to a material, (E, ρ), on performance can be shown by considering an equivalent material (E_e, ρ_e) with the following properties:

$$\begin{cases} E_e = \dfrac{E}{\phi} \\ \rho_e = \dfrac{\rho}{\phi} \end{cases} \tag{2.12}$$

Figure 2.4 shows that shaping a material with properties (E, ρ) through ϕ increases the structural performance. The shaped material has transformed properties which are displayed on the chart at a point with co-ordinates (E_e, ρ_e). This chart can be used for the selection of the best combination of material and shape for a given stiffness requirement.

c) Microstructured materials

The approach to modelling the mass-efficiency of macroscopic cross-sectional shapes can be extended to a microscopic level. Ashby's theory (1991) on micro-structuring runs in parallel to Parkhouse's theory (1984) on macro-materials. While Parkhouse examined large-scale structures such as frames and bridges, Ashby looked at materials which have a micro-structure (Gibson, L.G. *et al* 1995) such as wood and foam.

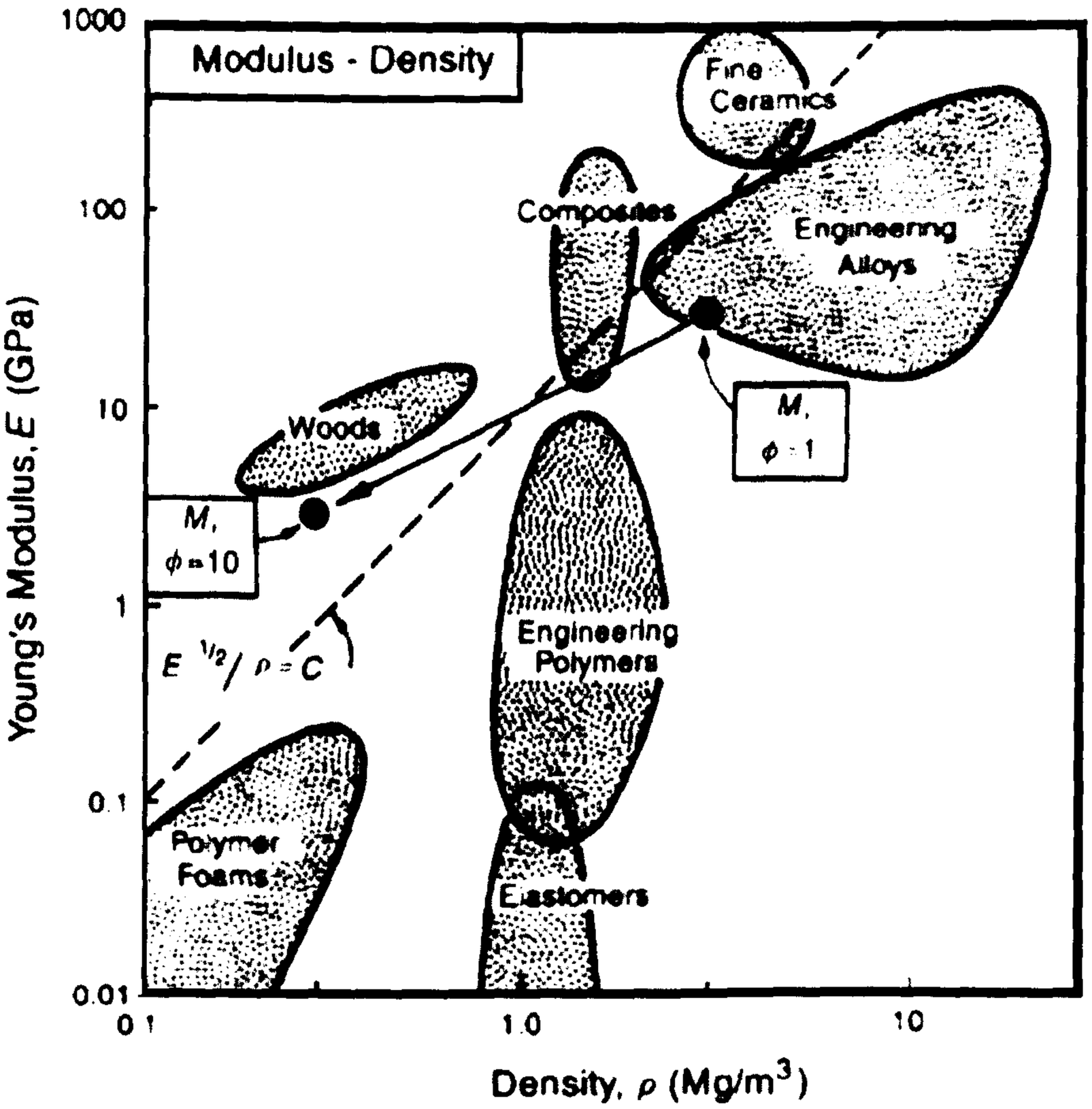

Figure 2.1 An example of Ashby's chart for the co-selection of material and shape (1991).

Ashby (1991, 1992) defined a micro-shape factor for bending and torsion for stiffness and strength requirements, which is analogous to ϕ. Provided that the material properties are not dependent on the size of the cell, the micro-shape factor allows the performance of materials with different types of micro-structure to be compared. The performance of a shaped material with micro-structure, i.e. a shaped micro-structured material, is given by the products of the micro-shape and macro-shape factors. As with the co-selection of material and shape, material charts can be used for selecting shaped micro-structured materials.

d) Limits to the efficiency of shaped materials

Shape factors can help in the design of an efficient cross-sectional shape. The higher the value of ϕ, the better is the design. However, there are limits to the extent to which a material can be shaped. For example, there are limits to how thin the wall can be made in a thin-walled tube. Ashby and Weaver (1996, 1997) investigated the limits to the attainable efficiency of sections. They identified two sources: the manufacturing constraints and the material limits.

- **Manufacturing constraints.** The process used to manufacture a cross section determines the practical limits to the shape factor. Extrusion, rolling, pultrusion are some processes for shaping materials into cross-sections which can be solid or hollow. When the geometric quantities, such as second moment of area or section modulus, of standard cross-sections available in the market are plotted against the area than it is possible to record the maximum ϕ attainable at present. These limits are empirical and have been investigated for stiffness and strength requirements for bending and torsion loading.
- **Material limits**. In addition to the techniques for shaping material, another factor has been recognised as playing an important role in reducing the structural efficiency: the properties of a material. This is because the material properties determine the failure mechanisms of a cross-section. There are three main failure mechanisms, namely plastic collapse, primary and local buckling (Shanley 1960). Shanley used the shape parameter to derive relations of the optimum thickness for axial loaded tubes and to elucidate that the material properties determine the limits to the optimum shape. In a similar way, Weaver and Ashby (1997) employed the shape factor (Ashby, M.F., 1991) to investigate the relationship between the three failure modes and to derive the limits to the shape factor for tubes, box and I sections under compression, bending and torsion loading. In their work, expressions for the mass for each failure mode were rearranged in terms of the shape factor and the structural index to yield stress ratio. These relations were plotted as three boundary curves which identify regions for each failure mechanism. The efficiency of shapes is close to the limit when two or more failure modes interact and occur at nearly the same load. The limits to the shape factor have been derived by imposing the condition that failure should occur when yield interacts with local buckling rather than with general buckling. The reason for this is that primary buckling causes abrupt failure which is undesirable. Therefore, the limits to the shape factors have been

derived to select ductile structures which have large deformations to warn about the potential failure.

2.3.2 Material and shape selection-methods for constrained design

Table 2.2 summarises the main features of the selection methods for constrained design.

(i) Ashby

In the following aspects of Ashby's work for constrained design, material selection and material and shape selection are considered.

a) Material selection

The material index $E^{0.5}/\rho$ relies upon the assumption that the second moment of area of a cross-section can be expressed as a function only of the area. For example as explained in Appendix A, for equiaxed sections the area can be written as $A=zI^{0.5}$ with z constant for the shape and, consequently, the exponent 0.5 becomes the exponent for E in the selection index. This is valid also for two sections, S1 and S2, which are not equiaxed but whose dimensions are relatively proportionally scaled. In this case, it is the height to depth ratio that remains constant since $A_{S1}/A_{S2} = (I_{S1}/I_{S2})^{0.5}$.

Although $E^{0.5}/\rho$ may seem to include only the material properties E and ρ, information about the geometry, i.e. the sizes, of a cross-sectional shape is contained in the index. This is evident if one of the main dimensions, height or width of a cross-section, are prescribed to be constant. In this case, the material, which maximises the performance, follows the indices (Crane, F.A.A and Charles, J.A., 1984):

$$M = \frac{E^{1/3}}{\rho} \qquad \text{for constrained width} \qquad (2.13)$$

$$M = \frac{E}{\rho} \qquad \text{for constrained height} \qquad (2.14)$$

Expression (2.13) and (2.14) have the same material properties, E and ρ. However, constraining one of the main dimensions of a cross-section gives different exponents to Young' Modulus. The exponents, 1/3 and 1, can be displayed on the material charts as guide lines to select the best material in the constrained cases of width and height (Ashby, M.F., 1992). When the exponent is 0.5 this means that a constraint of proportional scaling has been made. As mentioned before this constraint is reasonable for loading in two planes. However, this is not the case for a load in one plane.

b) Material and shape selection

A shape factor is a dimensionless number which characterises the efficiency of a cross-sectional shape regardless of the scale. The **constancy of the shape factor for a given scaling** is an important feature because it permits the scale effect to be removed. This means that designers can compare the efficiency of different cross-sections without taking into account the exact sizes of the structure. Figure 2.5 shows that cross-sections with the same generic shape have generally the same ϕ if their dimensions are relatively proportionally scaled, although they occupy a different space. The value of the reference section area is determined by the material properties for a given requirement. Therefore, these different values of A in the expression (2,10) have the effect of constraining, i.e. maintaining constant, the ratio of the sizes of the cross-sections. If the space is unconstrained, the reference and generic sections are proportionally scaled to meet the requirement.

In constrained design, the cross-sections are not proportionally scaled. If two cross-sectional shapes are horizontally constrained, the fixed parameter is not the area but the height and, consequently, the shape factor, given by expression (2.10) cannot be constant. There is a need to define other expressions of ϕ so that the shape factor can remain constant for a scaling that is not proportional.

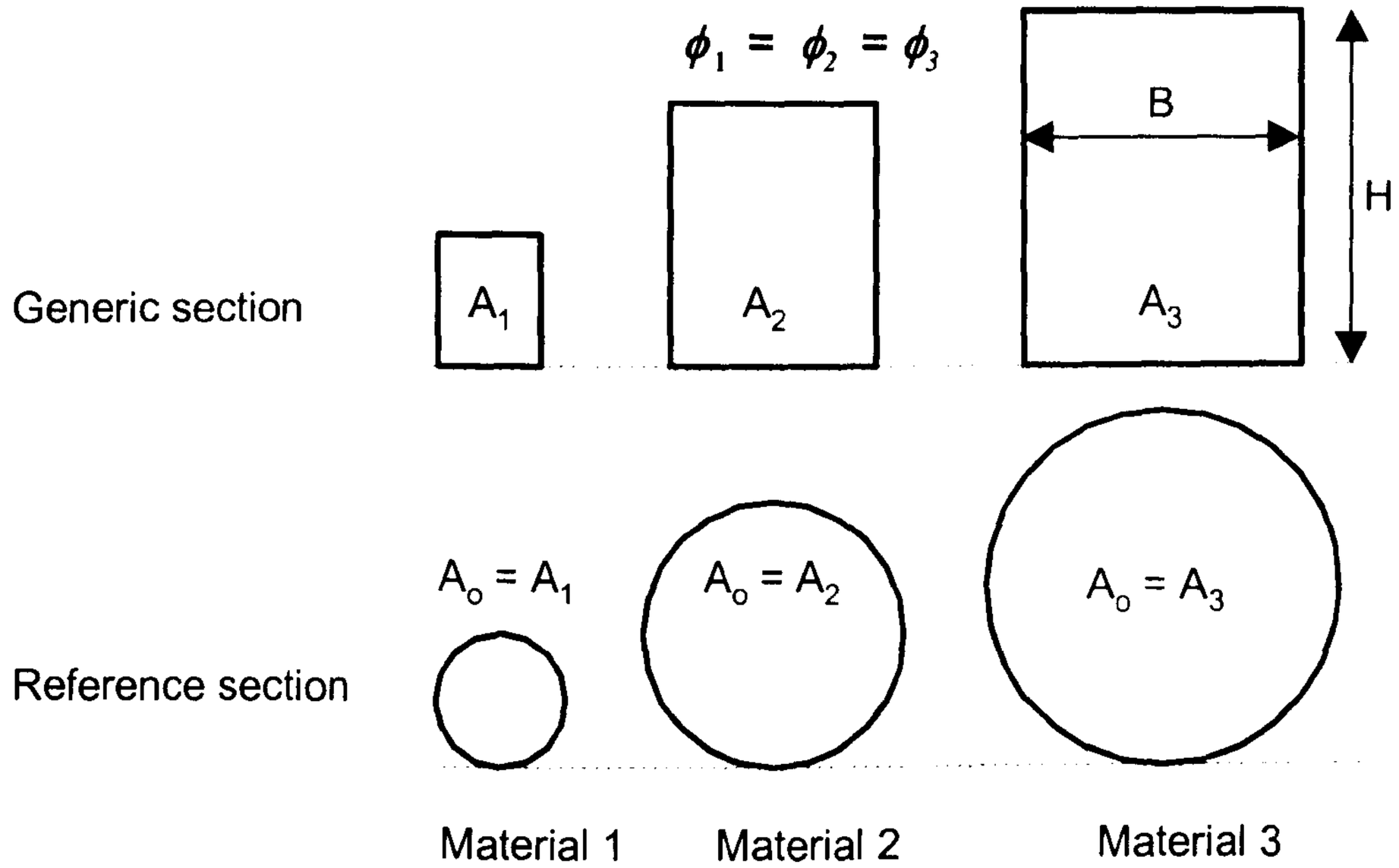

Figure 2.1 Constancy of ϕ for proportionally scaling in an unconstrained space.

In bending stiffness design, two expressions of the shape factors, ϕ_H and ϕ_B, were introduced (Ashby,M.F., 1992) for two scaling conditions as:

$$\phi_H = 16\frac{r_g^{\,2}}{H^2} \qquad \text{for horizontal scaling} \qquad (2.15)$$

$$\phi_B = \pi^2 \frac{IB^2}{A^3} \qquad \text{for vertical scaling} \qquad (2.16)$$

where *B* and *H* are the width and the height of the cross-sections shown in Figure 2.1.

Then, Ashby (1992) included ϕ_H and ϕ_B in equations (2.13) and (2.14) to give the performance index for height and width constrained structures.

$$M = \frac{\phi_H E}{\rho} \qquad \text{for constrained height} \qquad (2.17)$$

$$M = \frac{(\phi_B E)^{1/3}}{\rho} \qquad \text{for constrained width} \qquad (2.18)$$

Expressions (2.17) and (2.18) cannot be used for other constraints which impose, for example, a sloped scaling to the cross-sections. Although theoretical ranges of

ϕ_H are given for a height constraint (Ashby, 1992), the approximate formulae for standard cross-sectional shapes have been more recently provided (Burgess, S.C., 2000a).

(ii) Burgess

Burgess (2000a) used the factor ϕ_H to discuss the effect of a height constraint on the mass-efficiency. Ashby's methodology for constrained design (1992) was extended to the torsion loading for stiffness and strength design (Burgess, S.C., 2000a, 2000b). In his works, the performance of different cross-sectional shapes was compared to a solid circular reference assuming that the shape factors, ϕ_H and ϕ_B, remain constant. It was shown that dimensional constraints can have a severe effect on the mass-efficiency. However, it is important to note that the circle is not an appropriate shape for non-proportionally scaling. The reason for this is that the circle cannot be scaled as shown in Figure 2.6 and, consequently, the shape factor cannot remain constant. For example, when there is a height constraint, all the horizontal dimensions are scaled in the free direction, whereas the vertical dimensions are fixed. Therefore, ϕ_H cannot remain constant because the area of the reference cannot be increased unless the shape of the circle is altered.

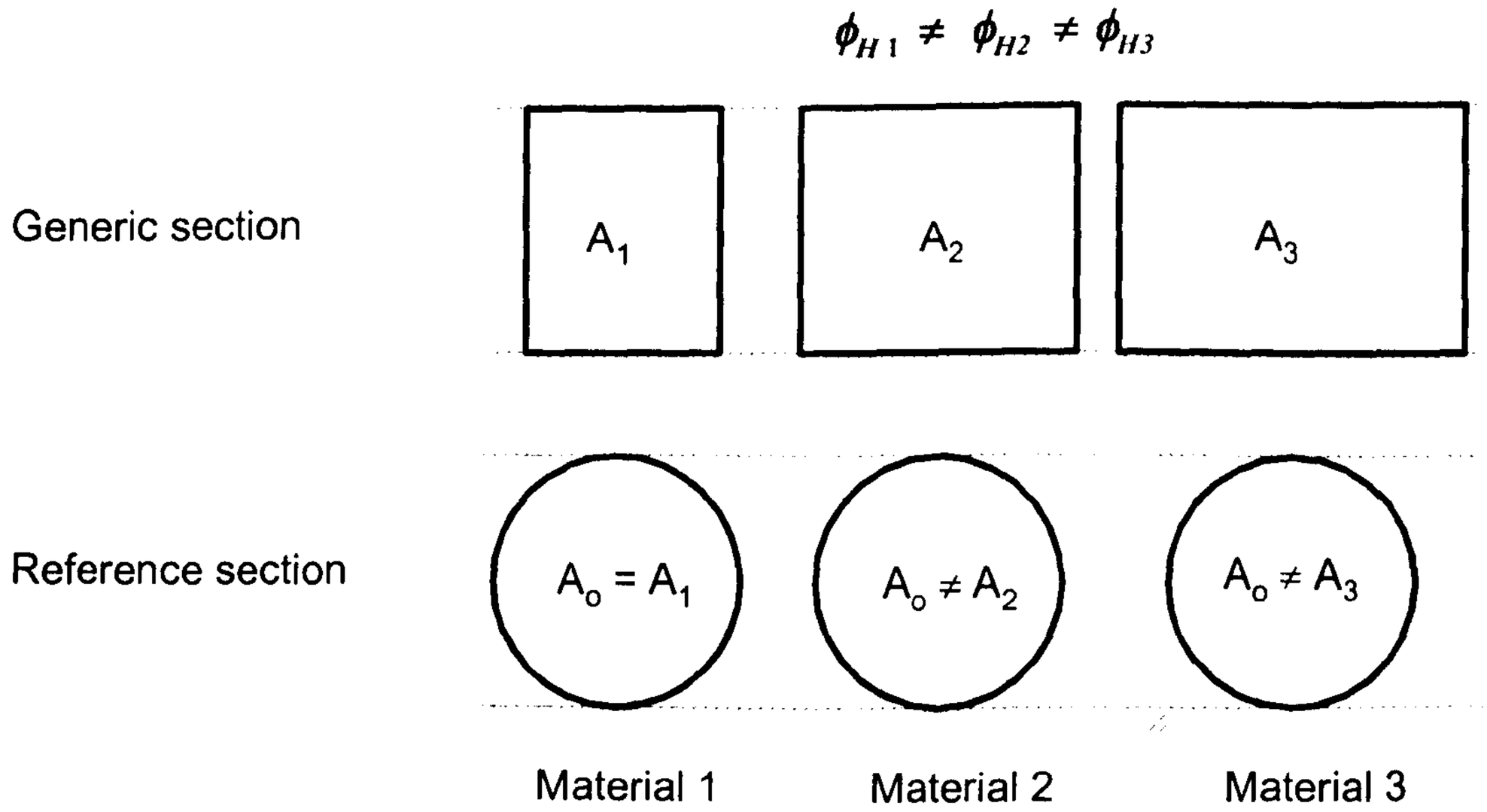

Figure 2.1 An example of height constraint: the circle is not an appropriate reference shape because during the horizontal scaling ϕ_H cannot remain constant.

2.3.3 Form selection methods

This Section presents methods for selecting alternative structural forms at the early stage of design. Since there is no specific distinction among the methods for constrained and unconstrained form as for the case of material and shape selection, the methods developed by the authors are discussed separately. The following classification is by author.

(i) Michell

At the beginning of the twentieth century, A.G.M. Michell (1904), who was an engineer at the civil engineering department of Melbourne University, published a seminal theorem about optimum structural form. The theory starts from a lemma developed by J. Clerk Maxwell (1869), to provide theoretical lower limits to the quantity of material necessary to sustain a given system of forces. Michell's theory is for frameworks and permits the discovery of the forms of frames which use the least amount of material. Both the results given by Maxwell and Michell ignore buckling and were developed using the principle of virtual work.

Maxwell's lemma states that the virtual work, L_o, of a given system of external forces for a uniform dilatation ε, is given by:

$$V_t\sigma_t - V_c\sigma_c = L_o/\varepsilon \tag{2.19}$$

where V_t and V_c are the volumes of ties and struts in a structure and σ_t and σ_c are the stresses in tension and compression members. External forces and their points of application determine the virtual work, L_o. This is a constant which is independent from the structural form, i.e. it is the same for any framework whatever its extent. Among the class of all competing frameworks which satisfy conditions (2.19), Michell (1904) showed that the volume of a pin-jointed structure is a minimum if all the constitutive members experience a uniform dilatation of space with the same linear strain, $+\varepsilon$ or $-\varepsilon$. This condition can be achieved only if any member is stressed to its allowable limit, $+\sigma$ or $-\sigma$.

One immediate consequence of this principle is that the simplest minimum volume frames are those whose elements are in tension, or compression only, since this enables them to give uniform dilatation of space. Minimum volume structures include ties and struts subjected to equal and opposite forces, triangular and tetrahedral frames under forces applied at their joints, and catenaries in general.

The second important consequence is that the kinematic condition of Michell's theorem is satisfied also by frameworks whose elements form an orthogonal system before and after the deformation. Classes of structural systems, where tension and compression members meeting at a node are orthogonal, include: rectangular networks, tangents and involutes derived from any evolute curve including concentric circles and their radii, equiangular spirals and any combination of orthogonal curves. In general, the characteristics of the geometrical property of these orthogonal systems were found to be analogous to slip lines in a two-dimensional perfect flow (Hemp, W.S. 1958, Prager, W., 1958). The members of a Michell's structure can be considered as lying along lines which have the same form as the slip-lines in a plastic continuum. The knowledge of slip-line field can help the discovery of Michell structures. The techniques for calculating and constructing their geometry were investigated by Hill in the case of rigid-plastic material under conditions of plane strain (Hill, R. 1998).

A peculiar feature of minimum volume layouts is that they require the whole design space to fulfil absolute optima. The reason for this is that only an unlimited design space allows the virtual deformation to be applied to each member extending to infinity in all the directions. Such examples of unconstrained forms were studied by Michell (1904) for four loading cases, three of them for structures in two dimensions, the fourth developed for a three dimensional case. These cases are: 1) a cantilever with an end point load, 2) a centrally loaded beam, 3) three equal forces directed to a point on the line of action of the third, and finally 4) two equal and opposite torques.

If the design space is constrained, then the optimum layout may be different to the structures for the unconstrained case and there is an increase of the material volume for the structure. Michell showed that constraints can affect the minimum material volume for the load case of a centrally loaded beam. Michell demonstrated that a restriction of the design space to a half plane causes a volume increase for

the optimum layout. In general, for a given load case, limitations of the space imposed by assigned boundaries, i.e. constraints, can have a double effect: firstly, a Michell structure may not be possible, secondly, if a Michell's solution is feasible, rearrangement of the structural form causes a weight penalty.

(ii) Chan A.S.L (1960) and Chan H.S.Y. (1963)

Most progress in developing Michell's field was concerned with two dimensional structures. A method of graphical construction was investigated at the college of Aeronautics in Cranfield during the 1960's. Chan A.S.L (1960), first, analysed two-dimensional structures, such as cantilevers under tip shear force and beams under uniform bending moments, and Chan H.S.Y. (1963) considered the case of three parallel asymmetric forces. They used the analogy with the theory of plane plastic flow to determine the slip-lines of structural layouts. They then set Michell's frames as an ultimate standard, whereby the merit of other alternative structural concepts, such as a Warren girder, a webbed beam and a simple triangle, could be judged comparatively under the same loading conditions.

(iii) Cox

The design of real structures involves also other issues which are not limited only to buckling. For example, Cox (1965), whose background was in structural engineering, examined Michell's structures and attempted to apply the outcome of the theory to practical cases. He was concerned that a structure has to be designed not only for a single load but for a set of loads. He proved that for a given load, the lightest structure is not simply a stiff framework, but rather a mechanism to any other loading. He discussed also the problem of buckling and joints weight and made the following conclusion:

"... neither the effect of joint weight nor the influence of instability invalidates the theory of optimally layout (i.e. Michell's theorem) completely. In some few cases the general theory could remain perfectly valid and although in most practical cases some allowance for instability will have to be made, the necessary changes leave the general tenor of the theory still applicable."

Therefore, Michell's theorem can still be a useful guide to the choice of the best structural concept despite the fact that there can be the problem of instability and a large number of joints (this principle will be demonstrated in Chapter 8). With respect to joints, it is clearly advantageous to reduce the number of joints. However, when there are many members, this may decrease the stress at the junctions, thus requiring lighter joints. Furthermore, as far as stability in the loading plane is concerned, for a specified external load, the internal forces in any compressive element is proportional to the spaces between bars. Therefore, an adequate distance between orthogonal slip-lines can be adopted to preclude buckling.

(iv) Caldwell

From Michell's work it is clear that optimal forms often require a large amount of space and therefore the effect of geometrical constraints in a design problem is a key issue. Caldwell, professor of ship structures at Newcastle University, explored the crucial influence of the form on the efficiency of a structure (Caldwell, Y.B. and Woodhead, R.G., 1973). To show that form is important, the minimum mass criterion was measured by the structure volume, $\nu=V/L^3$, and was expressed as a function of a design index, $\mu= P/(L^2 f_L)$, with f_L the allowable stress. The design index, μ, is dimensionless because it is obtained by dividing the structural index P/L^2 (Wagner, H., 1929) by the allowable stress of the structure, f_L.

Caldwell (1973) realised that the structural performance is reduced by the presence of spatial restrictions. In order to show this, he adopted the span, L, to depth, D, ratio of a structure to compare the mass-efficiency of alternative structures, such as I beams and trusses. Among the charts produced, Figure 2.7 shows an example where the volume index, $\nu=V/L^3$, measures the mass-efficiency as a function of the design index, $\mu= P/(L^2 f_L)$, for different values of L/D. The efficiency of different structural types, constructed from the same material and designed also for buckling, is compared. Among the findings pointed out by Caldwell (1973), three are relevant here. The first finding confirmed that efficient forms tend to require more space. The second finding revealed that the presence of spatial restrictions, in terms of a height constraint, reduces the structural performance severely. The last point is that the gains in efficiency provided by the choice of optimised thicknesses of a cross-section, do not make it possible to obtain the same performance as can be achieved

by the selection of an efficient structural form. Therefore, only once the general form is decided, optimisation techniques become useful.

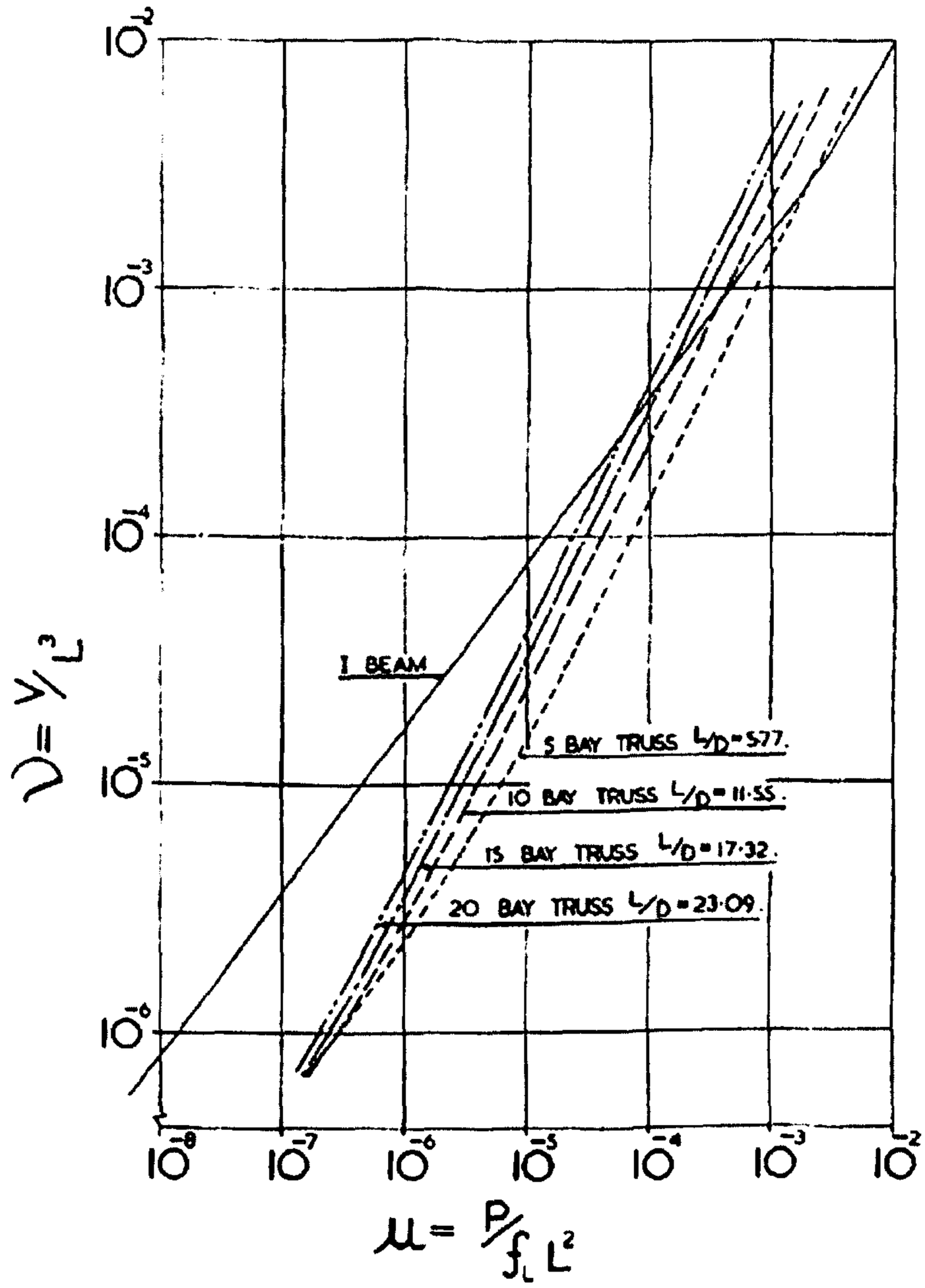

Figure 2.1 Example of Caldwell design charts in logarithmic scale: *L* is the span while *D* is the height of the beam (1973).

(v) Birmingham

Research on efficient structural forms, such as those by Chan and Caldwell, has shown that selection charts can be of great help at the early stage of design. Exploring alternative concepts with selection charts allows the designer to identify an optimum design for a particular application. More recently, a graphical procedure to present different structural forms has been introduced for different load cases

(Birmingham, R.W., 1994). The performance of alternative forms, such as simple, double, triple Warren trusses, and standard beams, such as I beam, are displayed on a diagram comprised of four-linked quadrants with common adjacent axes. An example for the case of a light stiff beam is shown in Figure 2.8.

Birmingham employed the method of describing a structure as a macro material, developed by Parkhouse (1984) and reported in Section 2.3.1. The structures are treated as macro-material, i.e. as simple solid rods made of an equivalent material. The properties which model the mass efficiency of standard structural topologies are displayed as points on the charts. Although the charts are successfully populated by alternative concepts, each point refers to the properties of a structural topology which has a fixed arrangement of its elements. The effect of a variation of the mutual geometric relations among the constituent elements within the same topology is not considered.

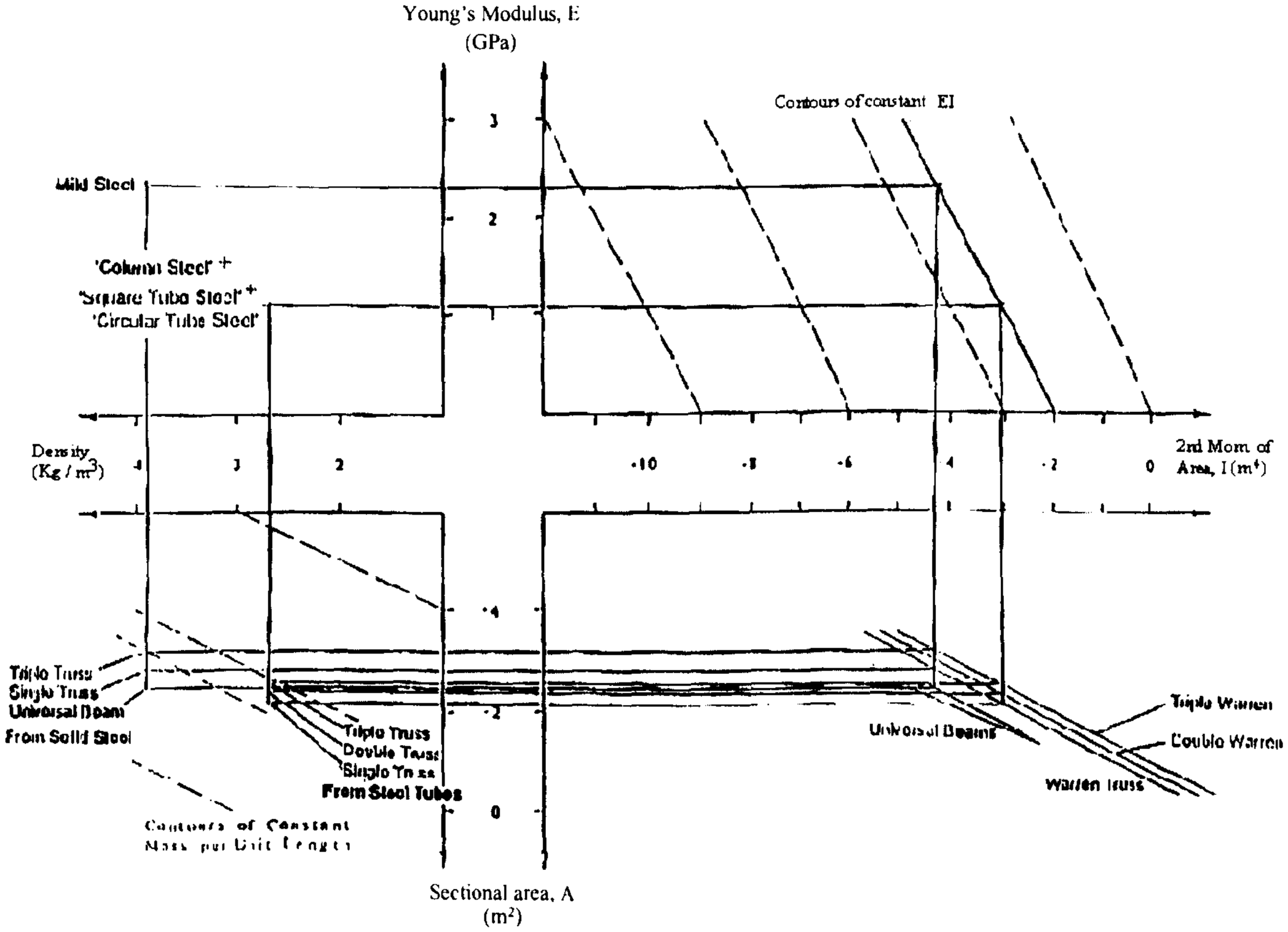

Figure 2.1 An example of a selection chart by Birmingham (1994)

(vi) Burgess

A method to support the selection of structural layouts at the early stage of design has been presented recently by Burgess (1998a, 1998b). The mass efficiency of a structural form is described by a form factor which permits the structural performance of different structural concepts to be ranked. The form factor is dimensionless and is a function only of the geometrical parameters defining the form for a given scale. The method is applied to the load case of a simply supported centrally loaded structure. Form factors are derived for trusses of variable and uniform sizes and beams with different types of taper and cross-sections, for a given stiffness and strength requirement. However, the effect of buckling is not considered.

As with Caldwell (1973), the height to span ratio of the structures is adopted as a design variable. This enables the structural efficiency to be assessed for different levels of height constraints. Although the method confirms the results of previous investigations (Caldwell, Y.B. and Woodhead, R.G., 1973) about the severity and utilisation of the height, other design features such as uniformity of stress and principle of load transfer are recognised as factors affecting the structural efficiency.

2.4 REMARKS

2.4.1 Previous research

The following features can be summarised concerning previous research related to the conceptual design.

a) Material selection methods

- The selection of a material has an effect on the geometry of a cross-section, i.e. its sizes.
- The indices for selecting the material which maximises the performance have been derived assuming that material and geometry are independent. However, a

geometric assumption has been speculated on the sizes of a cross-section with a prescribed shape.

- The indices of selection provide the best material when *H/B*, *H* or *B* are considered constant. Therefore, they are relevant for proportionally, horizontally, and vertically scaled cross-sections. However, the effect of a constraint at an inclined angle which imposes scaling at an arbitrary angle is not examined.
- The index $E^{0.5}/\rho$ is not related to any geometrical constraint. It has been derived by considering area as a variable. As a result, the height to depth ratio, *H/B*, is kept constant and the cross-sections are proportionally scaled. Consequently, although $E^{0.5}/\rho$ is an index of mass minimisation, it is not generally the best index for unconstrained design.
- It has generally been assumed that $E^{0.5}/\rho$ is the appropriate index for all bending stiffness design cases apart from height and width constraints. However, the only design scenario where proportional scaling is relevant is for cross-sections where the bending moment is multidirectional. For example, an equiaxed cross-section subjected to bending from two directions, x-x and y-y, such as a vertical tube under multidirectional wind forces, experiences the peak stress all around the periphery of its cross-section. Therefore in such a case, a proportional increase in the dimensions of the section maximises the stiffness while minimising the use of material.

b) Material-shape selection methods

- The sizes of the cross-sectional shapes are not determined only by the material attributes, such as E and σ_y, but also by the geometric attributes concerned with the shape of the cross-section. Consequently, since the constraints are applied generally to the main dimensions of a cross-section, the relation between shape and main sizes of a cross-section needs more investigation.
- Whereas the material properties are displayed successfully in selection charts, there is not a similar map for the geometric properties of the shapes.
- A circular section is not suitable as the reference for constrained design.
- The shape factors derived for height and width constraints are not appropriate for other kinds of constraints which impose different scaling to the cross-sections.

- The co-selection of material and shape on material charts requires more understanding.

c) Form selection methods

- Michell's theory (1904) and the majority of earlier work ignores mechanical instability. Therefore there is need to establish a method to consider buckling at the early stage of design.
- Buckling acts generally on a secondary hierarchical level of a structure which is represented by the constituent elements. Therefore, shape and material properties have to be considered in relation to the variable form. The interaction between form selection and shape selection needs to be explored .
- Each topology has been assumed fixed. This means that the mutual geometric relations, such as angles between elements, are not permitted to vary. However, spatial constraints often require geometric changes of the mutual relation among elements.
- When changes in the topology are considered, several geometric variables are introduced in the structure. These variables are used to model the mass-efficiency of the system. Since traditional charts can display no more than three variables, there is a need to develop charts which permit performance trends with more than three variables.

2.4.2 This research

Although from earlier published work it emerges that the mass-efficiency of a structure is severely affected by spatial restrictions, there is no systematic method for the selection of material, shape and form in any constrained condition. One of the main aims of this work is to have a better understanding of the role of the design variables of a structural system in relation to the design space. In a similar way to Tables 2.1 and 2.2, the main features of this work are summarised in Table 2.3.

In highly integrated structures, such as aircraft and cars, spatial restrictions are usually applied to the sizes of a cross-section. In order to explore the mass-efficiency of constrained structures, the theory of shape transformers is introduced. The theory is based on the concept that the main dimensions of the cross-section

identify the rectangular envelope which encloses the shape. Dimensionless properties of the shape of a cross-section, called shape transformers, are defined for the geometric quantities, such as area and second moment of area, relevant for modelling the mass-efficiency. This permits the contribution to the mass-efficiency of the shape of a cross-section to be separated with respect to the contribution of the sizes of the cross-section. One of the advantages of this is that the rectangular envelope can be easily related to geometric constraints which impose any kind of scaling to the cross-sections.

2.5 SUMMARY

Computational algorithms and selection procedures are methods used to optimise the mass-efficiency of a structural system at the early stage of design. Whereas mathematical routines of optimisation cannot evolve from one structural concept to another, methods of selection permit the designer to chose the best candidate among alternative concepts. Methods for selecting material, shape and form have been examined. A number of detailed points and the issues, which need to be addressed, have been reported. The Chapter concluded with the concept which will be used in the following Chapter to tackle the unsolved problems.

CHAPTER 3

THE THEORY OF SHAPE TRANSFORMERS

3.1 INTRODUCTION

This Chapter presents the basis of a theory for modelling the mass-efficiency of skeletal structures which will be used later in the thesis to tackle the problems and limits of the methods reported in the literature survey. Deflections due to axial deformation are not included. The Chapter comprises three main parts:

- It starts with a **classification of engineering structures** according to the type of loading transferred across a span and the response of the structure to the load. The purpose is to establish a common language used throughout this work which identifies different design contexts. The classical equations of mechanics are used to describe each **design context** and to model the mass-efficiency of structures. The parameters under the control of the designer, material attributes and geometrical quantities, are specified for the design context.
- With the design background established, a **concept of understanding a cross-section** in the design space is introduced. This concept is used to define **the shape transformers**. The fundamentals of the theory of the shape transformers provides a means of identifying the components which make up a cross-section. An **analogy between material and shape** is used to define new design parameters which describe the geometrical properties of a cross-section
- In the third part, the **shape transformers** are substituted **in the equations of mechanics** describing the design contexts and are identified as variables under the control of the designer. These equations are then used in the following Chapters for modelling the mass-efficiency in different selection conditions.

3.2 FUNCTIONAL REQUIREMENTS AND OBJECTIVE FUNCTION

The function of a structural component is to carry a load. External loads are usually transferred across a span by internal forces generated throughout the interior of an element. The types of the internal forces, or mode of actions, define the mechanism of load transfer. Bending, axial, or shear, are examples of internal actions. The nature of these forces depends on the relationship between the directions of the longitudinal axis of a structural member and the load which is applied to it. If a force, for example, acts parallel to the longitudinal axis of the element, axial internal forces are generated. Any load which is not applied along the neutral axis creates a bending moment. A combination of axial forces and bending is produced, for example, for loads applied obliquely to the longitudinal axis. It is quite common that engineering structures are subjected to external forces that can create a combination of internal forces. However, when one action mode dominates, the element can be identified directly by the name of the prevalent mechanism of load transfer. The mechanisms of load transfer defining different types of structural element are

- Compression acting in "Struts".
- Tension carried by "Ties".
- Bending supported by "Beams".
- Torsion which occurs in "Shafts".

When failure is prevented, a structure carries the load successfully. Failure is a structural response to the applied load. There are different modes causing the failure of a component. Three failure modes are:

- Deflection.
- Yield.
- Collapse.

If a beam is designed to meet a given stiffness, failure occurs as a result of excessive deflection. Other modes of structural failure are yield and collapse. A structure performs properly the function of avoiding failure when it is designed to meet a "functional requirement".

Provided that the functional, or design, requirement, *F*, is satisfied, the designer selects the structure which maximises the performance. The criterion of selection is,

therefore, the objective function to optimise. Cost and mass are some common selection criteria. However, others, such as safety and reliability, can be adopted.

In this work, the transfer load mechanisms considered are tension, bending and compression. The functional requirements are yield and deflection for beams, yield for ties and collapse failure for struts. Deflection due to axial deformation is not included. The objective function is to minimise the mass.

3.3 THE RELEVANT EQUATIONS OF THE DESIGN CASES

Equations from structural mechanics are used to describe failure of elements under specific internal actions. The transfer load mechanism and the design requirement are, therefore, two conditions to be established in order to identify the appropriate equations. This section examines the equations used to describe (i) deflection and yield for beams, (ii) collapse for struts, (iii) the objective function, and reports the design parameters involved. The conventional form of these equations is rearranged in order to separate the variables under the control of the designer (on the right hand side of the equation) from the parameters of the problem which remain constant (on the left hand side).

3.3.1 Objective function

The expression for the mass *m* of a structure is given by

$$\frac{m}{L} = \rho A \tag{3.1}$$

where ρ is the specific density and *A* the cross-sectional area.

The variables are:

Material: ρ Geometry: A

3.3.2 Tie, yield

A tie must support a tensile load, *P*, without failure. Since the design requirement is the load, *P*, which causes failure, this design context is called "*tensile load design*". The requirement, *P*, is given by:

$$P = A\sigma_y^t \tag{3.2}$$

where σ_y^t is the yield tensile stress.

The variables are:

Material: σ_y^t, ρ Geometry: A

3.3.3 Beam, deflection

In the design of a beam, failure must not occur for deflection more than δ, under a load P. Since bending is the transfer load mechanism and the stiffness, P/δ, of the element is the structural attribute which satisfies the requirement, this design context is called "*bending stiffness design*". An expression for the bending stiffness k is:

$$\frac{kL^3}{c_1} = EI \tag{3.3}$$

where c_1 is a constant depending on the boundary and loading conditions, E is the Young's Modulus, L is the span, I is the second moment of area of the cross-section.

The variables are:

Material: E Geometry: I

3.3.4 Beam, yield

The beam is designed to support the load before reaching yield failure. Since the yield strength is the relevant property, this context is called "*strength design*", The bending moment, M_y, which causes yielding in the cross-section of the beam is given by:

$$M_y = \sigma_y \frac{I}{y_m} = \sigma_y Z \tag{3.4}$$

where σ_y is the yield strength at the furthest point, y_m, from the neutral axis of the section, I the second moment of area and Z the section modulus. It is assumed that yield in tension, σ_y^t, and yield in compression, σ_y^c, are the same, i.e. $\sigma_y^t=\sigma_y^c=\sigma_y$.
The variables are:

Material: σ_y Geometry: Z

3.3.5 Struts, collapse

Yielding and buckling are two modes of interacting failures for a strut. Thick and short columns experience plastic collapse whereas long and thin struts become unstable, i.e. buckle, under critical loads. In general, "*compression load design*" is used throughout this work to refer to the design of struts.

Short thick strut. A short and thick column is designed to prevent failure by yielding. The failure load *P* is given by:

$$P = \sigma_y{}^c A \tag{3.5}$$

where σ_y^c is the yield strength in compression
The variables are:

Material: σ_y^c Geometry: A

Slender column. A long and slender strut with very small imperfections is designed to avoid buckling. The Euler critical load, P_{crit}, which induces elastic buckling in a slender column, is:

$$\frac{P_{crit}}{n^2\pi^2}L^2 = EI_{\min} \tag{3.6}$$

where the constant *n* depends on the end conditions.
Since L is considered constant, the variables are:

Material: E Geometry: I

Struts of any slenderness. Experimental results have shown that equations (3.5) and (3.6) do not model correctly the failure of engineering struts. Work to establish the correct prediction of strut failure in the inelastic regime was done over the last centuries. Engesser (1889) suggested using in the Euler's formula given by equation

(3.6) the tangent modulus, E_t, which depends on the stress-strain distribution. However, E_t was recognised to be deficient and was replaced by the reduced modulus E_r (Karman, T., 1910), whose values is more difficult to estimate because it depends not only on the magnitude of the stress but also on the convex and concave sides of the strut. Only at the middle of the last century, Shanley (1946) explained the discrepancy between E_t and E_r. He developed the theory of inelastic buckling to explain that buckling starts at E_t and, then, the load increases and reaches E_r only for very large deformation. Although Shanley's approach is now accepted for real columns, it has the drawback that it is cumbersome to use because E_t is derived from the stress-strain curves and, therefore, is a function of the stress. For this reason, in this work a semi-empirical formula, which contains only material properties not dependent on the stress-distribution, is adopted for the design of struts of variable length. This formula, developed by Rankine and Gordon (Case, J. *et al.*, 1999), has been shown to give a safe estimate of failure for real struts with geometrical imperfections. The failure stress which models collapse in a member subjected to compressive load, P, is given by:

$$\sigma_f = \frac{P}{A} = \frac{\sigma_y^c}{1 + \mu\left(\frac{L}{r_g}\right)^2} \tag{3.7}$$

where $\mu = \frac{\sigma_y^c}{\pi^2 E}$ depends only on the material properties and the radius of gyration, $r_g = \sqrt{I/A}$, depends on the geometry of the section.

Equation (3.7) can be used as a "design line" for dimensioning compression struts of any slenderness. It will be adopted to model the mass-efficiency of structural forms in Chapter 8. In such a case the length, L, of any compressive member can vary, and therefore the variables are:

Material: E, σ_y^c Geometry: r_g, L

Equations from (3.1) to (3.7) show that the variables which exercise choice in the design of ties, beams and struts are the material properties and the geometric quantities of the cross-section.

3.4 A NEW CONCEPT FOR UNDERSTANDING A CROSS-SECTION: THE ENVELOPE AND THE SHAPE

Structures occupy space. Any material moulded in a shape fills a space. The main sizes of a steel box section, for example, specify the space occupied by a hollow rectangle filled by steel. Material and shape are contained in a definite space. The ***spatial container*** which can enclose any shape is defined as the ***envelope***. The most intuitive and suitable for engineering purposes is the rectangular envelope, which occupies a rectangular space. Inside this space, any shape can be inserted. A 'cross-section' is, therefore, defined as a 'shape' which fits within a rectangular 'envelope'. The **material**, ***M***, and the **shape**, ***S***, complement the **envelope**, ***D,*** to make the **cross-section**. Figure 3.1 shows two examples of cross-sections where *D* specifies the main sizes of the shape enclosed in the envelope. While in Figure 3.1(a) shape and envelope are different, in Figure 3.1(b) the shape completely fills the envelope.

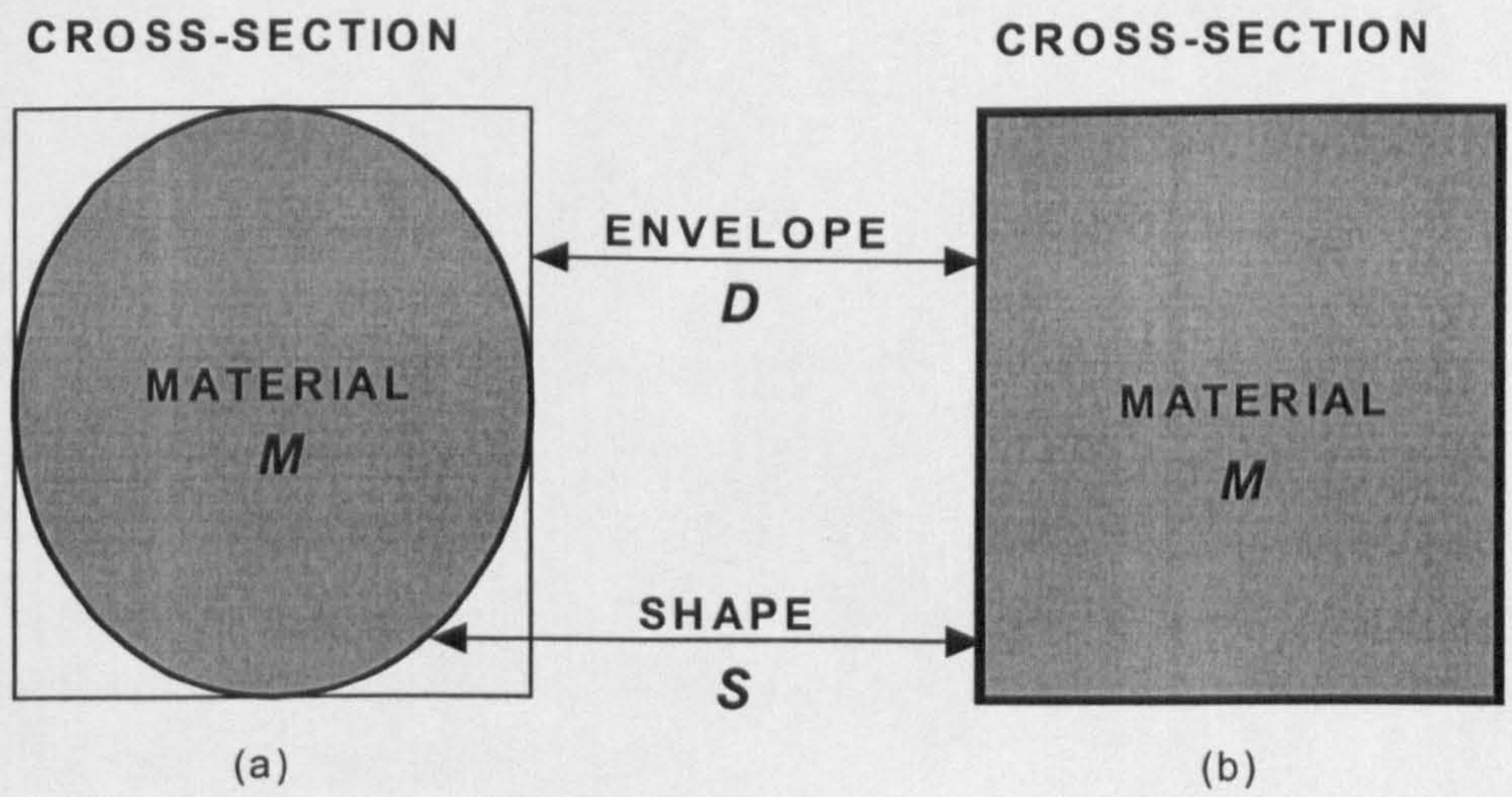

Figure 3.1 The constituents of a cross-section: shape and envelope

3.4.1 Material classes and Shape classes

A set of attributes identifies a material. The properties of a material are usually measured experimentally. Expressing the properties as numbers per unit area or volume enables designers to make a proper comparison among materials. Tensile

Young's modulus, yield stress and density, are force, or mass, related to a unit area or volume. This is because a material must be contained in a space volume. From another perspective, an empty volume or an empty envelope, *D*, can possess a number of properties if a material fills it. In such a case, the profile of properties of a material characterises the envelope, *D*. Steel, for example, gives different properties to a space, *D*, than aluminium. However, the range of the attributes of steel and aluminium are similar because the materials belong to the same class. For example, the Young's modulus of metals ranges approximately from 60 to 400 GPa, whereas polymers ranges from 0.1 to 5 GPa and composites from 10 to 250 GPa. Metals, polymers, composite are examples of material classes as shown at the top of Figure 3.1. Each class shows a characteristic range of properties as shown on the top of Figure 3.1 for a given space envelope, *D*.

Rectangles, ellipses, lozenges (diamonds) are classes of shapes. Boxes, tubes and any hollow or open shape derived from the respective solid shapes belong to a class. Examples of shape classes are shown on the bottom of Figure 3.1. The space envelope *D* of these geometric shapes occupies a rectangular space. From another point of view, a given space *D* possesses a number of geometric properties if a shape occupies it. Therefore, "shape properties" can be defined in an analogous way to the material properties. As the Young's Modulus is expressed by a force, *N*, normalised with respect to a unit area, **shape properties, called shape transformers, *S*,** can describe the geometric quantities, *G*, such as *I*, *Z*, *A*, of a cross-section per given space envelope *D*. In such a case, dimensionless shape properties characterise a space envelope just as the material properties do. The reason for the name shape transformers is that if a shape transformer S_1 is applied to the geometric quantity G_o of a rectangular cross-section C_o with material M_o and S_o=1, then G_o is transformed in $G_o x S_1$.

Therefore, as shown in Figure 3.1, a cross-section can be considered to be an envelope which contains a set of numbers which are the material and the shape properties. As the material properties allow a designer to make a comparison among materials contained in the same envelope, *D*, so the shape transformers provide a means for comparing shapes within the same envelope. In the next section, the shape transformers are defined and the ranges of properties, similar to the range of material properties, are presented for each class of shape, as shown in Figure 3.1.

Material classes	**METALS**	**POLYMERS**	**COMPOSITES**	**CERAMICS**
Sub classes	Aluminium alloys Steels Titanium alloys Copper alloys	Polycarbonate Polyesters Polypropylene Epoxys	Woods GFRP CFRP Foams	Sialons Diamond Alumina Silicon carbide
N.B. Tonalities of a colour describe material properties of a class	Aluminium Steel Titanium Copper	Polycarb. Polyprop Polyester Epoxies	Oak Gfrp Cfrp Cork	Sialons Diamond Alumina Sil. Car.
Ranges of **M**aterial properties	$60 < E < 400$ GPa $2 < \rho < 25$ Mg/m^3	$0.1 < E < 5$ GPa $0.8 < \rho < 2$ Mg/m^3	$10 < E < 250$ GPa $0.1 < \rho < 1.8$Mg/m^3	$60 < E < 400$GPa $2 < \rho < 5$ Mg/m^3

Material properties, *M*

SPACE ENVELOPE, ***D***

Shape properties, *S*

Shape classes Sub classes	**Rectangles** Derived and hollow rectangles	**Ellipses** Derived and hollow Ellipse	**Triangles** Derived and hollow triangles	**Lozenges** Derived and hollow Lozenge
Ranges of **S**hape properties	$0 < \psi_A < 1$ $0 < \psi_I < 1$	$0 < \psi_A < \pi/4$ $0 < \psi_I < 3\pi/16$	$0 < \psi_A < 1/2$ $0 < \psi_I < 1/3$	$0 < \psi_A < 1/2$ $0 < \psi_I < 1/4$

Figure 3.1 Examples of material and shape classes.

3.4.2 The definition of shape transformers to describe shape properties

As shown in Section 3.3, area, *A*, second moment of area, *I*, and section modulus, *Z*, are geometric quantities, G, relevant to modelling the mass efficiency of structures for a given design requirement. For common cross-sections, *A, I, Z* are reported in Table 3.1, where *B* and *H* are the width and depth of the space envelope *D*, *b* and *h* are the internal width and height. The expressions of the geometric quantities of *A* and *I* are not approximate, while *Z* is approximate but suitable for the early stage of design. They have been derived assuming that the shape is extracted by removing material from a solid envelope.

In order to define shape properties, *S*, the geometric quantities, *G*, must be related to the geometric quantities, G_D, of a fixed rectangular envelope, *D*. The following symbols are used to distinguish the envelope from the shape:

For a generic cross-section the geometric quantities, *G*, are:

$$G \begin{cases} A & = \text{area of shape} \\ I & = \text{second moment of area about the axis x-x of bending} \\ Z & = \text{section modulus} \\ r_g & = \text{radius of gyration} \end{cases}$$

For the rectangular envelope, *D*, with width *B*, and height *H*, enclosing the shape, the geometric quantities, G_D, are:

$$G_D \begin{cases} A_D & = \text{area of space envelope} \\ I_D & = \text{second moment of area of the envelope about bending axis x-x} \\ Z_D & = \text{section modulus of space envelope} \\ r_{g\,D} & = \text{radius of gyration of space envelope} \end{cases}$$

For any rectangle or square, the envelope and the shape coincide, therefore:

$$G=G_D \begin{cases} A = A_D \\ I = I_D \\ Z = Z_D \\ r_g = r_{g\,D} \end{cases}$$

CROSS-SECTIONAL SHAPE	A	I	Z	$r_g^2 = \frac{I}{A}$
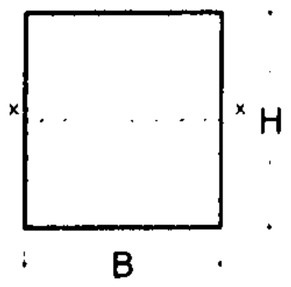	BH	$\frac{BH^3}{12}$	$\frac{BH^2}{6}$	$\frac{H^2}{12}$
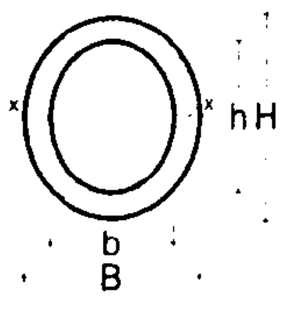	$\frac{\pi}{4}(BH - bh)$	$\frac{\pi}{64}(BH^3 - bh^3)$	$\frac{\pi}{32}(BH^2 - bh^2)$	$\frac{1}{16}\left(\frac{BH^3 - bh^3}{BH - bh}\right)$
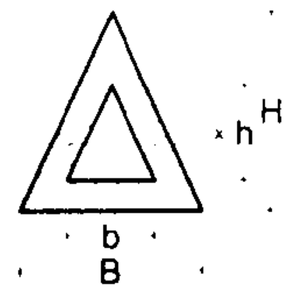	$\frac{1}{2}(BH - bh)$	$\frac{(BH^3 - bh^3)}{36}$	$\frac{(BH^2 - bh^2)}{18}$	$\frac{1}{18}\left(\frac{BH^3 - bh^3}{BH - bh}\right)$
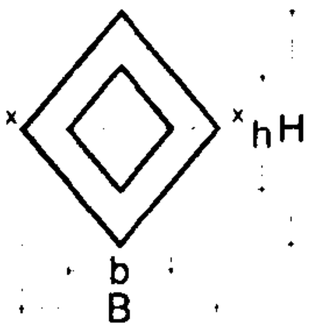	$\frac{1}{2}(BH - bh)$	$\frac{(BH^3 - bh^3)}{48}$	$\frac{(BH^2 - bh^2)}{24}$	$\frac{1}{24}\left(\frac{BH^3 - bh^3}{BH - bh}\right)$
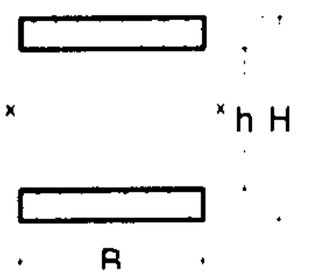	$B(H - h)$	$\frac{B(H^3 - h^3)}{12}$	$\frac{B(H^2 - h^2)}{6}$	$\frac{H^2}{12}\left(1 + \frac{h}{H} + \frac{h^2}{H^2}\right)$
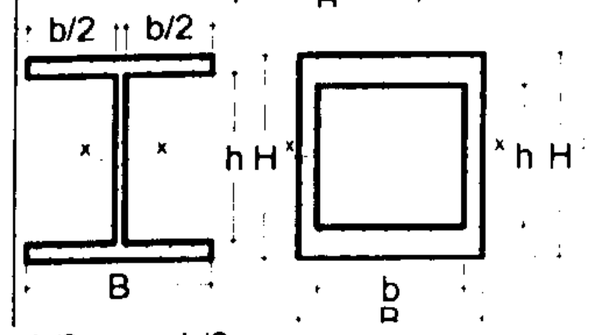	$BH - bh$	$\frac{BH^3 - bh^3}{12}$	$\frac{BH^2 - bh^2}{6}$	$\frac{1}{12}\left(\frac{BH^3 - bh^3}{BH - bh}\right)$
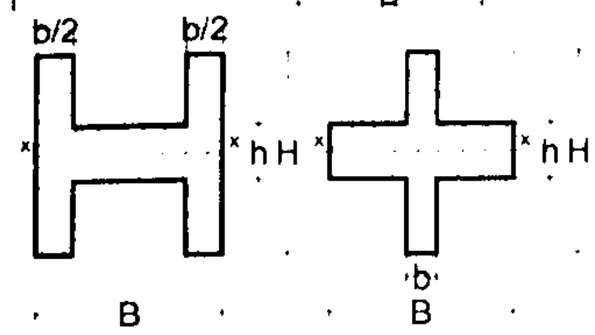	$bH + h(B - b)$	$\frac{bH^3}{12} + \frac{(B - b)h^3}{12}$	$\frac{bH^2}{6} + \frac{(B - b)h^2}{6}$	$\frac{1}{12}\left(\frac{bH^3 + (B - b)h^3}{bH + (B - b)h}\right)$
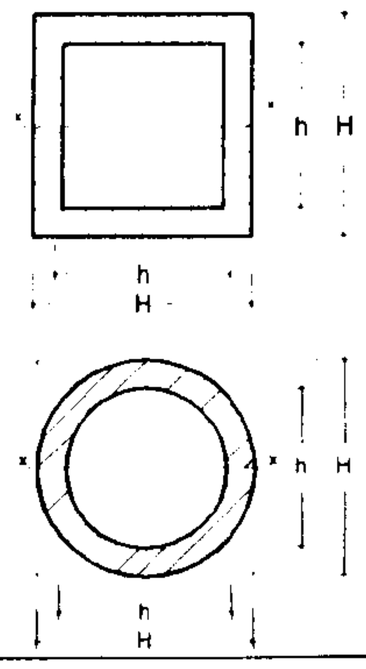	$H^2 - h^2$	$\frac{H^4 - h^4}{12}$	$\frac{H^3 - h^3}{6}$	$\frac{H^2 + h^2}{12}$
	$\frac{\pi}{4}(H^2 - h^2)$	$\frac{\pi}{64}(H^4 - h^4)$	$\frac{\pi}{32}(H^3 - h^3)$	$\frac{H^2 + h^2}{16}$

Table 3.1 Area, second moment of area and radius of gyration of the most common sections. For solid sections b=h=0. (I and r_g are given about the axis x-x of bending).

The shape transformers are dimensionless numbers which describe the shape properties, *S*, of a cross-section. They are defined for the following geometric quantities, *G*, as:

$$S = \frac{G}{G_D} \qquad \begin{cases} \psi_A = \dfrac{A}{A_D} \\ \psi_I = \dfrac{I}{I_D} \\ \psi_Z = \dfrac{Z}{Z_D} \end{cases} \tag{3.8}$$

ψ_A, ψ_I, ψ_Z are called **"shape transformers"** because they characterise and, hence, transform the geometric quantities, *G*, of a rectangular space. They are also used to derive the **envelope efficiency parameters**, λ_I and λ_Z. These factors describe how efficiently the shape fills the envelope for a given requirement. They are given by:

$$\begin{cases} \lambda_I = \dfrac{\psi_I}{\psi_A} \\ \lambda_Z = \dfrac{\psi_Z}{\psi_A} \end{cases} \tag{3.9}$$

Note that λ_I is also equal to the ratio of the radius of gyration of the shape to its envelope, $\lambda_I = r_g^2 / r_{gD}^2$.

Figure 3.1 illustrates the analogy of material and shape. The shape transformers ψ_A, ψ_I, ψ_Z, are the shape properties of a rectangular envelope, *D*, as the attributes of a material ρ, *E*, σ_y are the material properties. This means that when structures are designed to meet a given functional requirement, then the shape transformers determine the sizes of a cross-sections as do the material properties.

The shape properties enable the designer to express the product of geometry, ***G***, and material, ***M***, i.e. ***MxG***, for a **cross-section** as a product $MxSxG_D$ of three contributions: material, *M*, shape, *S*, and envelope, *D*. For example, using the definition of shape transformers in (3.8), the mass per unit length of a component, $m/L = \rho A$, can be expressed as $m/L = \underbrace{\rho}_{MATERIAL}\ \underbrace{\psi_A}_{SHAPE}\ \underbrace{BH}_{ENVELOPE}$. This will be shown in detail in Section 3.5 where the shape transformers are used to rewrite the equations of mechanics given in Section 3.3.

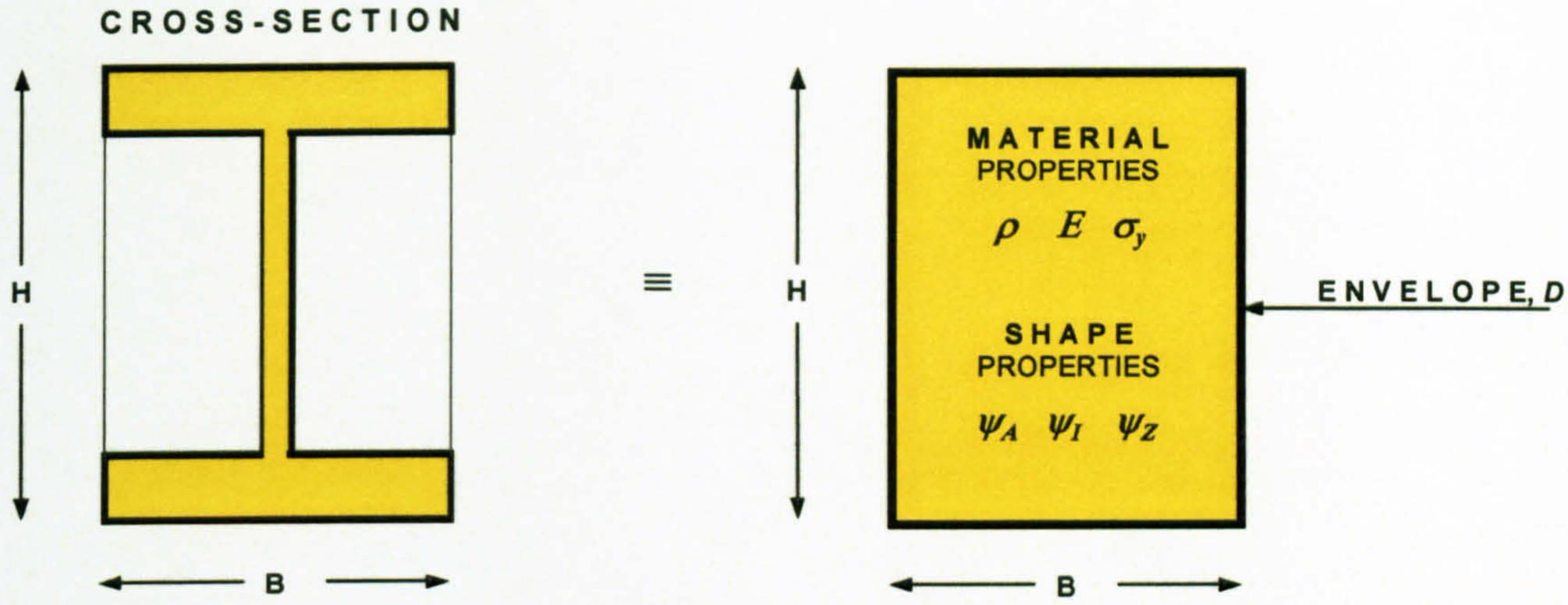

Figure 3.1 is the material described by the material properties.
is the shape described by the shape properties.
is container of the properties of material and shape.

The material properties, ρ, E, σ_y of some common materials are given in Table 3.2, the shape transformers ψ_A, ψ_I and ψ_Z are provided in Table 3.3, and λ_I, λ_Z in Table 3.4. (Note that ψ_I and λ_I are respectively different from ψ_Z and λ_Z because expressions of Z given in Table 3.1 are approximate). Whereas the shape properties ψ_A, ψ_I and ψ_Z of solid shapes are specific values for a given envelope BxH, for hollow belonging to a class of shape, there is a specific range. For any rectangle/square, they are unity as:

$A = A_D \rightarrow \psi_A = 1$ and $A_o = A_{Do} \rightarrow \psi_A = 1$

$I = I_D \rightarrow \psi_I = 1$ and $I_o = I_{Do} \rightarrow \psi_I = 1$

$Z = Z_D \rightarrow \psi_Z = 1$ and $Z_o = Z_{Do} \rightarrow \psi_Z = 1$

$\lambda_I = \lambda_{I,D} \rightarrow \lambda_I = 1$ and $\lambda_{Io} = \lambda_{I,Do} \rightarrow \lambda_I = 1$

$\lambda_Z = \lambda_{Z,D} \rightarrow \lambda_Z = 1$ and $\lambda_{Zo} = \lambda_{Z,Do} \rightarrow \lambda_Z = 1$

The parameters ψ_A, ψ_I, ψ_Z and λ_I, λ_Z are dimensionless design parameters which model the geometric quantities, G, such as A, I and Z, and will be used in Chapter 5 to model the mass-efficiency of a generic shape in relation to its envelope. They can be used in a design task to quickly identify and distinguish the contribution to the structural efficiency of the shape from its envelope. For a given class of cross-sectional shape within an envelope there is a theoretical range of values for the parameters ψ_I, ψ_A and λ. For example, in the case of a hollow elliptical cross-section, Table 3.3 shows that the lowest value of ψ_A is zero and this corresponds to

an infinitesimally thin wall thickness for the cross-section. The largest value of ψ_A is $\pi/4$ and occurs when the elliptical cross-section is solid.

Theoretical ranges for the parameters ψ_A, ψ_I, ψ_Z for other different cross-sections are shown in Table 3.3. ψ_A, ψ_I, ψ_Z **give information about the space** a cross-section must occupy to meet a functional requirement. As far as the space is concerned, they act like the material properties in determining the sizes of a cross-section which satisfy a given design requirement. For this reason they can be particularly useful for any type of constraint applied to the sizes of a cross-section. For example, for a given requirement, a value of ψ_I close to unity indicates a section which minimises the space better because it tends to fill the envelope. On the contrary, shapes with low values of ψ, close to zero, claim more space to satisfy the functional requirement. On the other hand, the range of the envelope efficiency parameters, λ, shown in Table 3.4 gives a direct indication of the mass saving which a shape can provide. This is because λ describes how efficiently the area of a cross-sectional shape is placed in its envelope. For example for a given stiffness requirement, a shape with λ_I=1.5 provides a saving of 1.5 times in the mass of a solid rectangular section. It is worth noting that the ranges of λ_I or λ_Z are not large because they refer only to the contribution of the shape and not the contribution of the envelope sizes. The physical meaning of shape transformers and efficiency parameters will be explained in more detali in Chapter 5.

Material	**Density** Mg/m^3	**Elastic Modulus** GPa	**Yield Stress** MPa
Aluminium	2.71	70	20
Brass	8.4 - 8.75	96 - 110	70 - 550
Bronze	7.8 - 8.8	96 - 120	82 - 690
Copper	8.94	110 - 120	55 - 330
GFRP	1.8	30	
Iron	7.87	83 - 170	120 - 290
Magnesium	1.74	41	20 - 70
Nickel	8.89	210	140 - 620
Steel	7.85	190 - 210	280 - 1600
Titanium	4.54	110	300-1000
Wood; Ash (Bending)	0.56 - 0.64	10	40 - 70
Wood; Oak (Bending)	0.64 - 0.72	11	40 - 60

Table 3.2 Approximate material properties of common materials.

CROSS-SECTIONAL SHAPE for a given envelope BxH	$\psi_A = \frac{A}{A_D}$	RANGE ψ_A	$\psi_I = \frac{I}{I_D}$	RANGE ψ_I	$\psi_Z = \frac{Z}{Z_D}$	RANGE ψ_Z
Envelope A_D, I_D 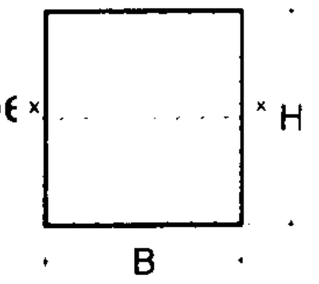	1	No range	1	No range	1	No range
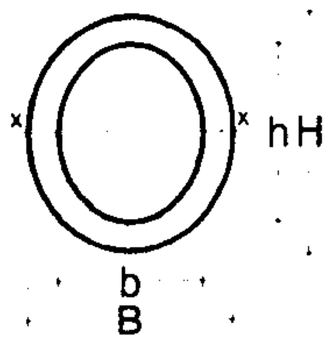	$\frac{\pi}{4}\left(1-\frac{bh}{BH}\right)$	0 to π/4	$\frac{3\pi}{16}\left(1-\frac{bh^3}{BH^3}\right)$	0 to 3π/16	$\frac{3\pi}{16}\left(1-\frac{bh^2}{BH^2}\right)$	0 to 3π/16
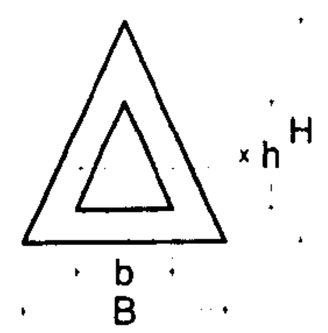	$\frac{1}{2}\left(1-\frac{bh}{BH}\right)$	0 to 1/2	$\frac{1}{3}\left(1-\frac{bh^3}{BH^3}\right)$	0 to 1/3	$\frac{1}{3}\left(1-\frac{bh^2}{BH^2}\right)$	0 to 1/3
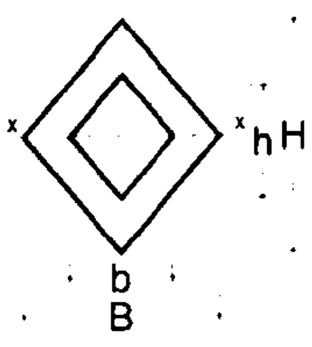	$\frac{1}{2}\left(1-\frac{bh}{BH}\right)$	0 to 1/2	$\frac{1}{4}\left(1-\frac{bh^3}{BH^3}\right)$	0 to 1/4	$\frac{1}{4}\left(1-\frac{bh^2}{BH^2}\right)$	0 to 1/4
	$1-\frac{h}{H}$	0 to 1	$1-\frac{h^3}{H^3}$	0 to 1	$1-\frac{h^2}{H^2}$	0 to 1
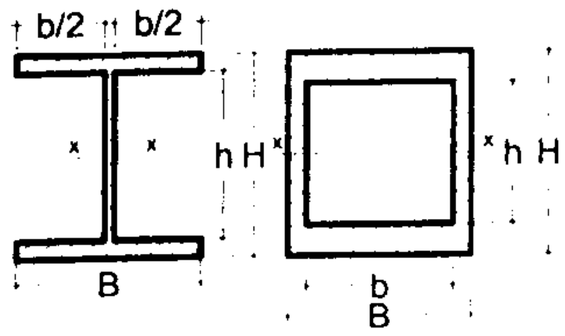	$1-\frac{bh}{BH}$	0 to 1	$1-\frac{bh^3}{BH^3}$	0 to 1	$1-\frac{bh^2}{BH^2}$	0 to 1
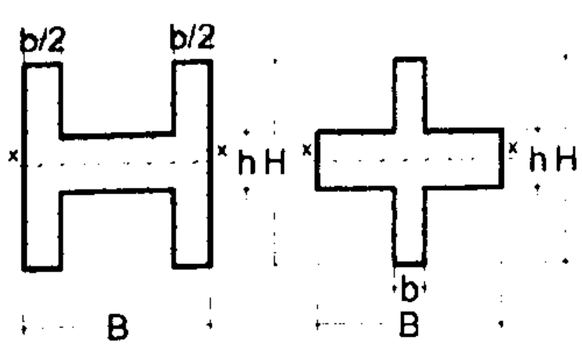	$\frac{b}{B}+\frac{h}{H}-\frac{bh}{BH}$	0 to 1	$\frac{b}{B}+\frac{h^3}{H^3}-\frac{bh^3}{BH^3}$	0 to 1	$\frac{b}{B}+\frac{h^2}{H^2}-\frac{bh^2}{BH^2}$	0 to 1
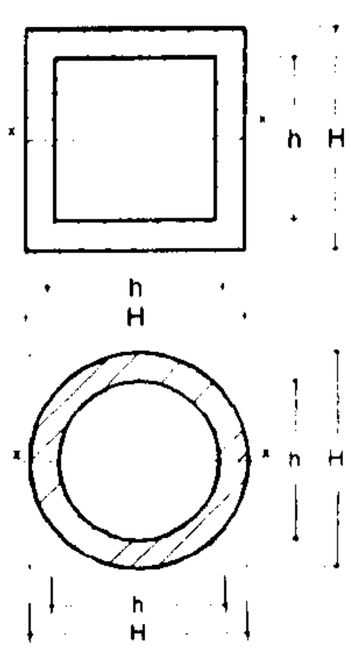	$1-\frac{h^2}{H^2}$	0 to 1	$1-\frac{h^4}{H^4}$	0 to 1	$1-\frac{h^3}{H^3}$	0 to 1
	$\frac{\pi}{4}\left(1-\frac{h^2}{H^2}\right)$	0 to π/4	$\frac{3\pi}{16}\left(1-\frac{h^4}{H^4}\right)$	0 to 3π/16	$\frac{3\pi}{16}\left(1-\frac{h^3}{H^3}\right)$	0 to 3π/16

Table 3.3 Shape properties, ψ, of sections. For solid sections b=h=0 and ψ_A, ψ_I, ψ_Z = upper values of the range. (The envelope for boxes and tubes has B=H and b=h).

CROSS-SECTIONAL SHAPE for a given envelope BxH	$\lambda_I = \frac{\psi_I}{\psi_A}$	RANGE λ_I	$\lambda_Z = \frac{\psi_Z}{\psi_A}$	RANGE λ_Z
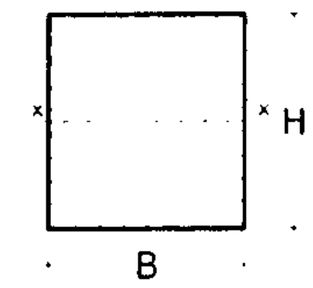	1	No range	1	No range
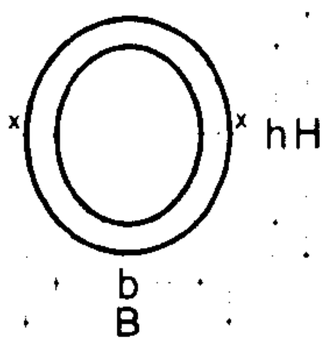	$\frac{3}{4}\left(\frac{1-\frac{bh^3}{BH^3}}{1-\frac{bh}{BH}}\right)$	3/4 to 9/4	$\frac{3}{4}\left(\frac{1-\frac{bh^2}{BH^2}}{1-\frac{bh}{BH}}\right)$	3/4 to 3/2
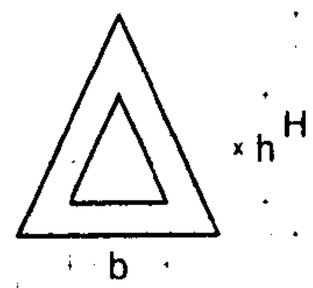	$\frac{2}{3}\left(\frac{1-\frac{bh^3}{BH^3}}{1-\frac{bh}{BH}}\right)$	2/3 to 2	$\frac{2}{3}\left(\frac{1-\frac{bh^2}{BH^2}}{1-\frac{bh}{BH}}\right)$	2/3 to 4/3
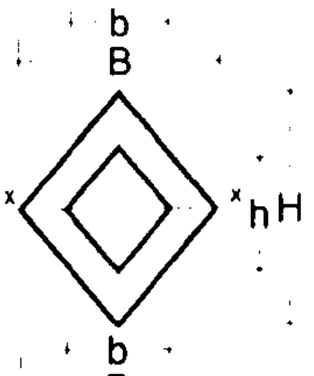	$\frac{1}{2}\left(\frac{1-\frac{bh^3}{BH^3}}{1-\frac{bh}{BH}}\right)$	1/2 to 3/2	$\frac{1}{2}\left(\frac{1-\frac{bh^2}{BH^2}}{1-\frac{bh}{BH}}\right)$	1/2 to 1
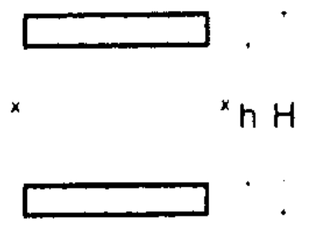	$1+\frac{h}{H}+\frac{h^2}{H^2}$	1 to 3	$1+\frac{h}{H}$	1 to 2
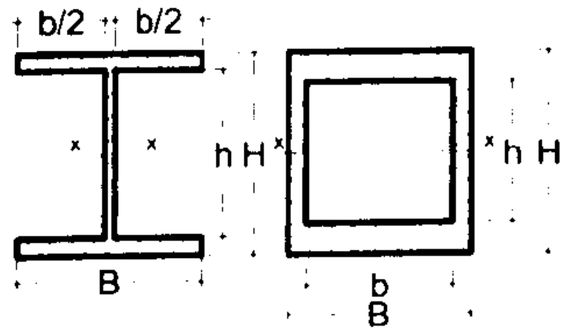	$\frac{1-\frac{bh^3}{BH^3}}{1-\frac{bh}{BH}}$	1 to 3	$\frac{1-\frac{bh^2}{BH^2}}{1-\frac{bh}{BH}}$	1 to 2
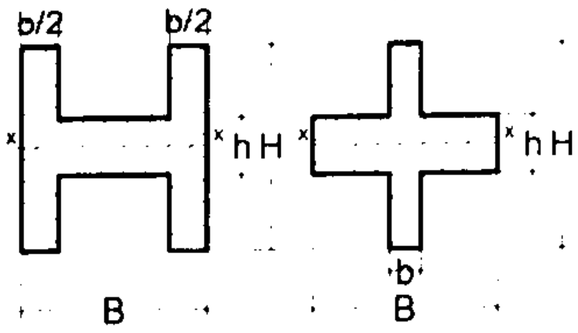	$\frac{\frac{b}{B}+\frac{h^3}{H^3}-\frac{bh^3}{BH^3}}{\frac{b}{B}+\frac{h}{H}-\frac{bh}{BH}}$	0 to 1	$\frac{\frac{b}{B}+\frac{h^2}{H^2}-\frac{bh^2}{BH^2}}{\frac{b}{B}+\frac{h}{H}-\frac{bh}{BH}}$	0 to 1
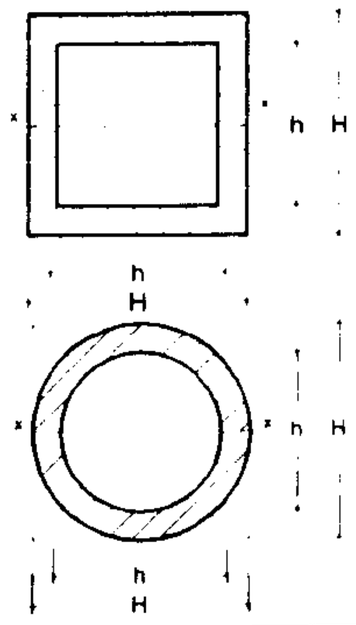	$1+\frac{h^2}{H^2}$	1 to 2	$\frac{1+\frac{h}{H}+\frac{h^2}{H^2}}{1+\frac{h}{H}}$	1 to 3/2
	$\frac{3}{4}\left(1+\frac{h^2}{H^2}\right)$	3/4 to 3/2	$\frac{3}{4}\left(\frac{1+\frac{h}{H}+\frac{h^2}{H^2}}{1+\frac{h}{H}}\right)$	3/4 to 9/8

Table 3.4 Envelope efficiency parameters, λ, of sections. For solid sections b=h=0 and λ_I, λ_Z = lower values of the range. (The envelope for boxes and tubes has B=H).

3.4.3 Envelope multiplicators

The shape properties defined in the previous Section characterise sections which are enclosed in the same rectangular space envelope *BxH*. However, cross-sections can differ not only for these properties but also for the main sizes of the cross-sections. The dimensions of the envelope are, therefore, another parameter, which cannot be neglected. A simple envelope, which can be described by just one dimension, is the square. The most simple rectangular cross-sections to which structures can be compared on a reference basis and then selected is a square cross-section. The reasons for the choice of a square as a reference section are:

- the square can be changed into different proportions along the width and the depth into a rectangle, which is the envelope of any generic shape.
- the square belongs to the class of the rectangular shape. Rectangles meet a design requirement in less space than all other shapes.

The square reference section is identified by:

B_o, H_o : width and height

A_o = area of reference section

I_o = second moment of area of reference section

Z_{Do} = section modulus of the reference section

r_{go} = radius of gyration of the reference section

Note that for the reference section

$A = A_{Do} = A_o$ $I = I_{Do} = I_o$ $Z = Z_{Do} = Z_o$ $\psi_A = \psi_I = \psi_Z = 1$

Differences in sizes between envelopes of cross-section are described by two linear multiplicators, u and v, which specify the relative change in width and height of the reference and a generic shape envelope. They are introduced as:

$$\begin{cases} u = \dfrac{B}{B_o} = \dfrac{b}{b_o} \\ v = \dfrac{H}{H_o} = \dfrac{h}{h_o} \end{cases} \tag{3.10}$$

where $B_o = H_o = \sqrt{A_{Do}}$. Note that for hollow or open sections, the multiplicators are applied also to the internal dimensions as $u = b/b_o$ and $v = h/h_o$.

In general, the geometric quantities of a cross-section can be provided by two separate features: shape and envelope. While ψ_A, ψ_I, ψ_Z describe the contribution of the shape to the envelope, u and v quantify the contribution of the envelope sizes with respect to the reference square. This is shown in Figure 3.1.

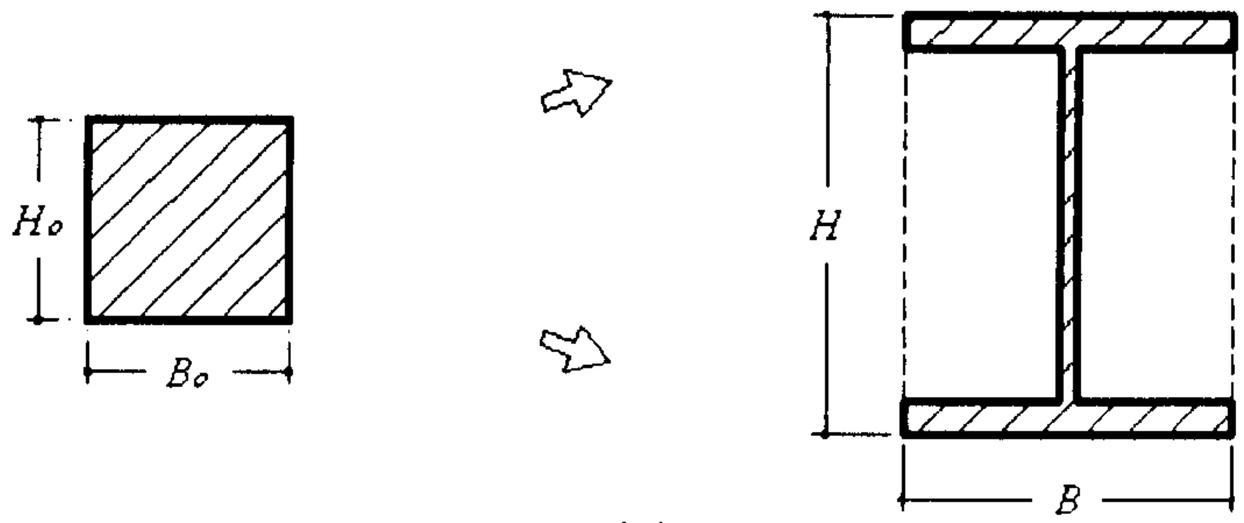

Figure 3.1 (a) The reference and a generic section. (b) u and v describe changes in the envelope size, i.e. envelope contribution. The transformers ψ_I, ψ_Z and ψ_A provide the shape contribution to the structural envelope.

3.5 THE NEW PARAMETERS IN THE EQUATIONS OF THE DESIGN CASES

The shape transformers are now used to rewrite the equations of structural mechanics presented in Section 3.3 for the design requirements.

3.5.1 Objective function

By replacing the area as function of ψ_A and the envelope dimensions, the objective function given by equation (3.1) is rewritten as:

$$\underbrace{\frac{m}{L}}_{F} = \underbrace{\rho}_{M}\ \underbrace{\psi_A}_{S}\ \underbrace{BH}_{A_D} \tag{3.11}$$

F is the functional requirement. The variables are:

Material property, M: ρ Shape property, S: ψ_A Area envelope, A_D: BH

3.5.2 Tensile load design

Replacing the area, *A*, of equation (3.2) with the expression of ψ_A, given in (3.8) as a function of *B* and *H* of the envelope, gives the tensile load:

$$P = \sigma_y{}^t \psi_A BH \tag{3.12}$$

P is the functional requirement. The variables are:

Material property, M: $\sigma_y{}^t$ Shape property, S: ψ_A Area envelope, A_D: BH

3.5.3 Bending stiffness design

If the second moment of area I in (3.3) is substituted with expression (3.8) , where I_D is function of the width *B* and of the depth *H* of the cross-sectional envelope, i.e. $I_D=1/12BH^3$, the bending stiffness of a cross-section is given by:

$$\frac{kL^3}{c_1} = E\psi_I BH^3/12 \tag{3.13}$$

the variables are:

Material property, M: E Shape property, S: ψ_I I Envelope, I_D: $BH^3/12$

3.5.4 Strength design

By substituting ψ_Z in equation (3.4) and Z_D as a function of the envelope dimensions *B* and *H*, i.e. $Z_D = 1/6BH^2$, the failure moment requirement in strength design is given by:

$$M_y = \sigma_y \psi_Z BH^2 / 6 \tag{3.14}$$

the variables are:

Material property: σ_y Shape property: ψ_Z Z Envelope, Z_D: $BH^2/6$

3.5.5 Compression load design

Yield design. Substituting the expression of the shape transformer ψ_A, given in (3.8), as a function of B and H, gives the load which causes yield in a short and thick strut:

$$P = \sigma_y{}^c \psi_A BH \tag{3.15}$$

the variables are:

Material property: $\sigma_y{}^c$ Shape property: ψ_A A Envelope, A_D: BH

Euler's buckling design. Analogous to bending stiffness design, the stiffness requirement for a slender strut under compressive load is:

$$\frac{P_{crit}}{n^2\pi^2} L^2 = E\psi_I BH^3 / 12 \tag{3.16}$$

the variables are:

Material property: E Shape property: ψ_I I Envelope, I_D: $BH^3/12$

Since E and ψ_I are the properties which describe the flexural and compressive stiffness, the name "*stiffness design*" is used in this work for both beam and slender struts.

Compression stress failure design.

The Rankine Gordon formula is used for struts of any slenderness. The aim is to replace in equation (3.7) the general expression of area and radius of gyration with the new design parameters. The steps are:

- from equation (3.8) , the area and the radius of gyration of a generic section are:

$$A = \psi_A A_D \tag{3.17}$$

$$r_g{}^2 = \lambda_I r_{gD}{}^2 \tag{3.18}$$

- The radius of gyration r_{gD} in (3.18) can be expressed as a function of the multiplicator of the heights, ν, and of the area A_D. For a given material and compressive load, $P/\sigma_y = A = \psi_A A_D$ is the area requirement of a section. There are an infinite number of solutions which satisfy the requirement. Among these, a solution is the square envelope where $A_{Do} = A/\psi_A$ and, consequently, $A_{Do} = A_D$. From equation (3.10) $\nu = H/\sqrt{A_{Do}} = H/\sqrt{A_D}$, and the radius of gyration of the envelope can be written as:

$$r_{gD}{}^2 = \frac{H^2}{12} = \frac{\nu^2}{12} A_D \tag{3.19}$$

- Combining equations (3.17) with (3.19) to eliminate A_D and replacing r_{gD} in equation (3.18), gives

$$r_g{}^2 = \underbrace{A}_{requirement} \quad \underbrace{z\nu^2}_{Envelope,D} \quad \underbrace{\frac{\lambda_I}{\psi_A}}_{Shape,S} \tag{3.20}$$

Equation (3.20) is split into three groups and has the desired effect of separating the contributions of shape, *S*, and envelope, *D*, for a given area requirement. ψ_A, λ_I, and ν are the dimensionless parameters which the designer can control to select the shape properties and the height ratio between a generic envelope and its square envelope (for $\nu>1$ $H>B$, for $\nu<1$ $H<B$).

- Finally, substituting (3.20) in equation (3.7) gives:

$$\frac{P}{A} = \frac{\sigma_y}{1 + \mu \dfrac{L^2}{Az\nu^2 \lambda_I / \psi_A}} \tag{3.21}$$

This expression will be used in Chapter 6 to derive the value of the minimum area which prevents failure in compressive struts of variable length. In equation (3.21) the area, A, is an implicit function of P and L, and the failure stress P/A is dependent on:
Material properties: μ , σ_y Design parameters: ψ_I and λ_I Envelope: ν

Equations from (3.11) to (3.16) and (3.21) will be used to model the mass-efficiency of engineering structures in the following Chapters.

3.6 DESIGN SCENARIO

In Section 3.5, the theory of the shape transformers has permitted the objective function, equation (3.11), and the design requirements, equations (3.12) to (3.16), to be express as a product of material, M, and geometry, $G=SxG_D$, so that

$$F = MxG = MxSxG_D \tag{3.22}$$

where

F	are the functional requirements specified by the problem
$G_D = f[B,H;u,v]$	describes the geometric quantities of the envelope $D(BxH)$
$S = S[\psi_A,\psi_I,\psi_Z]$	are the shape properties of the cross-section
$M = M[\rho,E,\sigma_y]$	are the material properties

In this section the different options of the parameters, D, S and M, which can be varied in a design application are described. For each option, the design scenario specifies the variables which affect the structural performance. If the performance p of a structure is measured by mass efficiency, then p is a function $f()$ of at least four parameters

$$p = f(F,D,S,M) \tag{3.23}$$

Since F is generally the design input. D, S and M are generally the design variables. In the selection process, the best solution often involves a compromise between these three variables as shown in Figure 3.1.

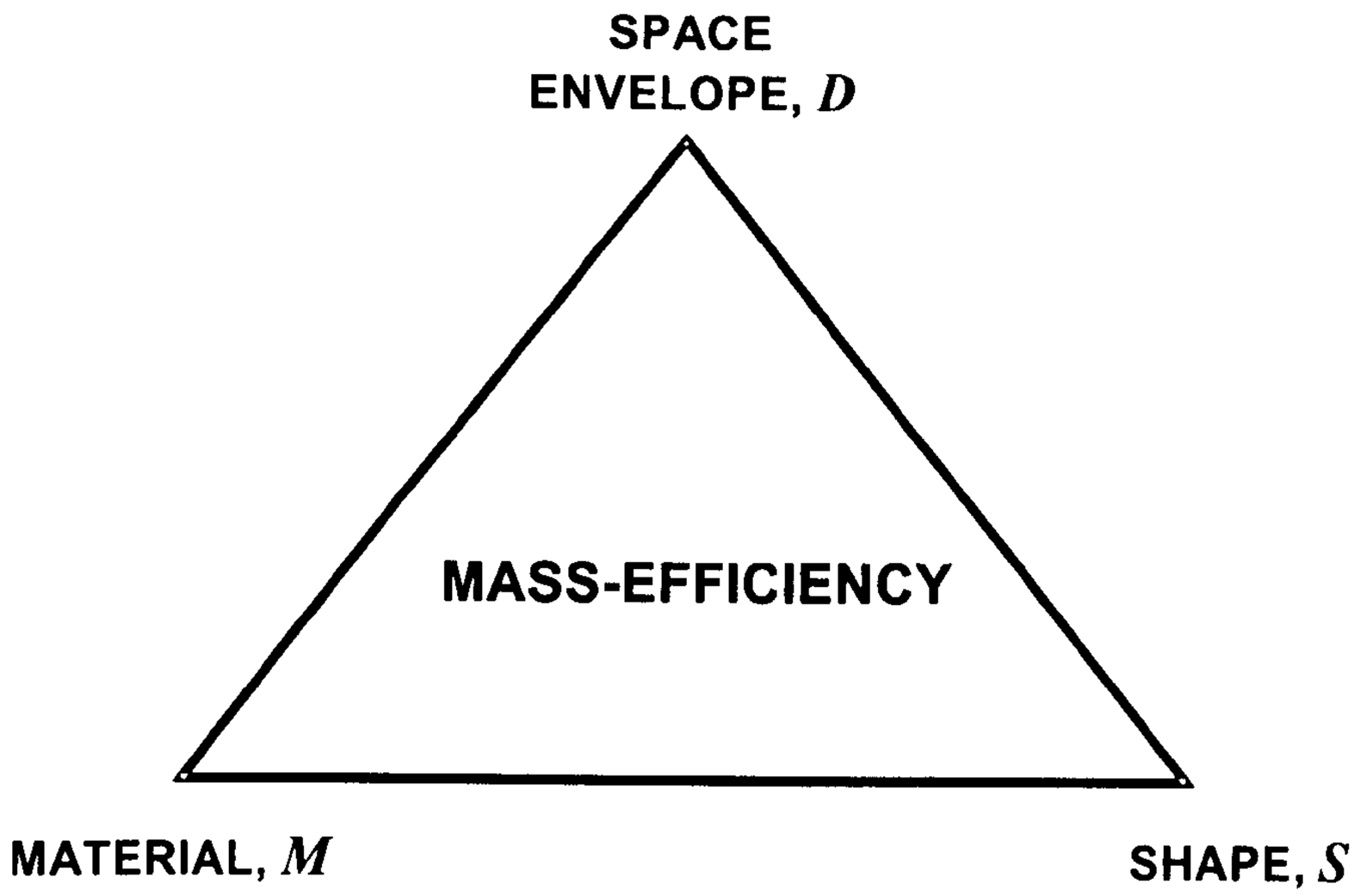

Figure 3.1 **M**aterial properties, **S**hape properties and **D**imensions of the envelope describe the structural performance of a cross-section.

In addition to the functional requirement *F*, the design variables must be compatible with the design constraints such as geometric constraints, material availability or shape availability. Figure 3.2 illustrates a range of cases where different cross-sections meet the functional requirement *F*. Since there are one or more variables, the performances are different. For example, Figure 3.2a shows that for a given material and shape (in this case the diamond family) the height and width of the cross-sectional envelope are changed whilst meeting the same design requirement, and consequently changes in the variable *D* occur. Figure 3.2b illustrates that for a given shape, both the material *M* and the dimensions of the envelope *D* can be varied to meet F. Figure 3.2c indicates that for a given material, changes in the variable *S* usually cause a variation in the envelope. Figure 3.2d and Figure 3.2e display other possible changes of the design variables. It may be the case that in a particular design application there is a restriction on the design parameters *D, S* and *M* that can be varied.

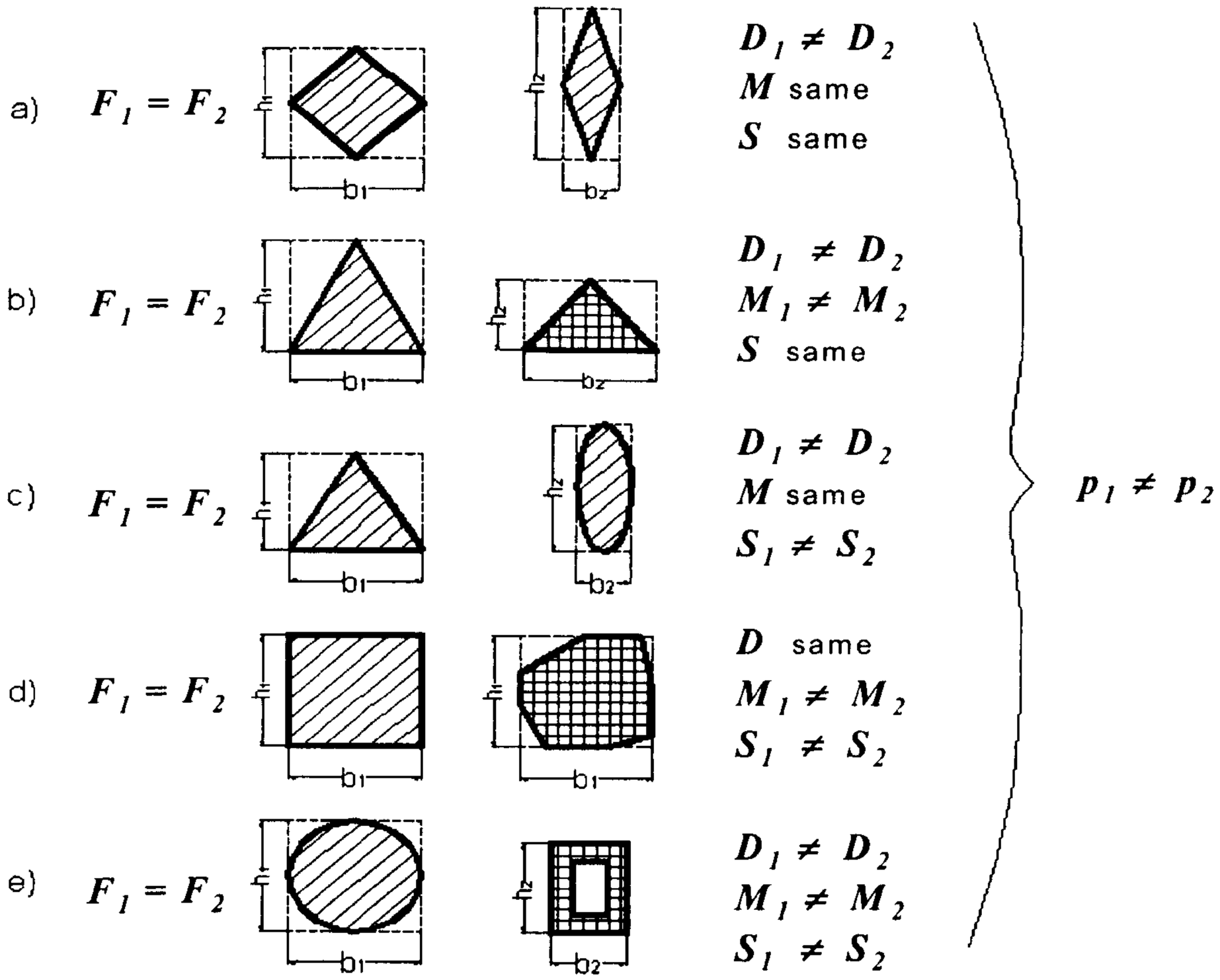

Figure 3.2 How the variables can affect the performance of the structures meeting a functional requirement: a) cross-sectional envelope variations, b) variations in material and envelope c) changes in shape and envelope d) material and shape vary in the same envelope e) all the variables change.

Table 3.1 summarises the different options of the parameters. The cases are illustrated in the cases of Figure 3.6. Whereas in each of the conditions the functional requirement remains the same, the other parameters *D*, *S* and *M* in equation (3.23) can be fixed or varied. Therefore the structural performance is a function of the free design variables. For example, in selection condition 1 the structures differ only for the dimensions of the cross-sectional envelope *D* as one material *M* and one shape *S* are available. In condition 2 the selection occurs among structures of the same shape *S* but different for material *M* and cross section envelope dimensions *D*. Conditions 3, 4 and 5 consider other permutations of selection criteria. Selection conditions 1 and 2 are examined in Chapter 4, condition 3 in Chapter 5 and Chapter 6 illustrates the alternatives provided by 4 and 5.

Selection condition		FUNCTIONAL REQUIREMENT *F*	CROSS SECTION GEOMETRY		MATERIAL *M* (ρ, E, σ_y)	Structural performance *p= f(D,S,M)*	Chapter
			ENVELOPE *D* (B,H)	SHAPE *S* (ψ_A, ψ_I, ψ_Z,)			
1	Cross section Envelope	Stiffness or Strength	**Variable**	Fixed	Fixed	$p=f(\boldsymbol{D})$	4
2	Cross section Envelope & Material	Stiffness or Strength	**Variable**	Fixed	**Variable**	$p=f(\boldsymbol{D, M})$	4
3	Cross section Envelope & Shape	Stiffness or Strength	**Variable**	**Variable**	Fixed	$p=f(\boldsymbol{D, S})$	5
4	Shape & Material	Stiffness or Strength	Fixed	**Variable**	**Variable**	$p=f(\boldsymbol{S, M})$	6
5	Cross section Envelope & Shape & Material	Stiffness or Strength	**Variable**	**Variable**	**Variable**	$p=f(\boldsymbol{D, S, M})$	6

Table 3.1 Conditions for stiffness and strength design.

3.7 SUMMARY

The rectangular envelope and the shape within the envelope have been identified as the constituent elements of a cross-section. This concept has been used to define dimensionless design parameters which model the geometric quantities of a cross-section. A cross-section is specified by the envelope, the material properties and the shape properties. The shape transformers are the shape properties of the envelope derived in analogy to the material properties. The envelope efficiency parameter describes how efficiently the shape fills the envelope. Expressions and ranges of the design parameters have been provided to tackle different selection tasks. The parameters have been substituted in the equations of mechanics for different design cases. These equations will be used to model the mass-efficiency in the following Chapters for different permutations of the selectable variables.

CHAPTER 4

MATERIAL SELECTION

4.1 INTRODUCTION

Two complementary approaches for modelling the mass-efficiency of structures for any scaling conditions are presented. One approach is the **performance criterion**, while the other is the **performance index**. In this Chapter, the theory of shape transformers is used to examine the first two selection conditions, 1 and 2, of the design scenarios given in Table 3.5 and illustrated in Figures 3.6a) and b). In condition 1 the only parameter under the control of the designer is the envelope, *D*, while in condition 2 the material, *M*, and *D* are the variables. In both cases *S* is fixed and, hence, the cross-sections have the same shape properties. The solid rectangle is chosen as the shape of the structural elements. Since for rectangular cross-sections the shape fills completely the envelope, the shape properties are unity. The analysis is carried out for stiffness design and strength design and is based on the assumption that materials are homogenous and isotropic, obey Hooke's law and have Young's modulus *E* and yield strength σ_y which is the same in tension and compression.

Five main parts constitute the framework of the Chapter:

- The aim of the first part is to define the set of **feasible solutions in the design space** for cross-sections which meet a functional requirement. Since in structural design **geometrical constraints** generally restrict the space which a cross-section can occupy, examples of constraints and their effects on magnitude and direction of scaling of the sections are illustrated.
- The second and third parts describe the approaches for selecting light structures in stiffness and strength design. Both **approaches** present an **analytical** derivation and a **graphical** visualisation. The first is the "**performance criterion**" which uses the "**combined selection graph**" for the conditions 1 and 2 of Table 3.5. The second is the "**performance index**" which permits the selection of the best material when *D* and *M* are variables. The graphical representation of this approach is given by the "**material regimes chart**".
- In the fourth part the approaches are compared. **Relationships** and limits of applicability are investigated firstly **analytically** and then **graphically** by the use of material charts in normal and logarithmic scale respectively for the performance criterion and the performance index.
- The Chapter concludes with an **application** of both the approaches to a design case in order to demonstrate the theory.

4.2 THE FEASIBLE SOLUTIONS IN THE DESIGN SPACE

4.2.1 Curves of design requirement and objective function

Functional requirement. The functional requirement is a relation described by the design specifications, the geometric and the material variables. There are a large number of feasible structures which satisfy the requirement in the design space. All these solutions belong to a curve whose points specifies the envelope of the cross-sections. For example, in bending stiffness design, for a given material and cross-section, the requirement, k, of a structural member is expressed by equation (3.13). Since $\psi_I=1$ for rectangular cross-section, the stiffness requirement is given by:

$$\frac{12kL^3}{c_1} = BH^3E \tag{4.1}$$

Equation (4.1) can be represented by a curve of constant stiffness, k, in a graph, B versus H, of the design space, i.e. $H = \underbrace{\left(\frac{12kL^3}{c_1}\right)^{1/3}}_{const}\left(\frac{1}{BE}\right)^{1/3}$. Figure 4.1 illustrates curves obtained using equation (4.1) for a given stiffness k= 280*10^{6}N/m. The structure is assumed to be a cantilever with length L=5m and c_1=3. The variables are the height, H, and width, B, which are related to the design space, and the material properties of the structure. As can been seen in Figure 4.1, for each material, steel with E_{st} = 210GPa and aluminium with and E_{al} = 79GPa, there is a set of infinite solutions, which satisfy the input k (note that these data are purely for illustration and the resulting physical dimensions are often impractical). Since from equation (4.1) $H=f(1/BE)$, the material property E and the design specifications determines a relation between the sizes of the envelope B and H. For a given material, this relation is represented by a curve of feasible structures, as shown in Figure 4.1. Materials with high E, for example steel, determine feasible solutions curves which subtend less space, whereas feasible cross-sections with lower Young's Modulus, i.e. aluminium, are described by a curve which subtends more space.

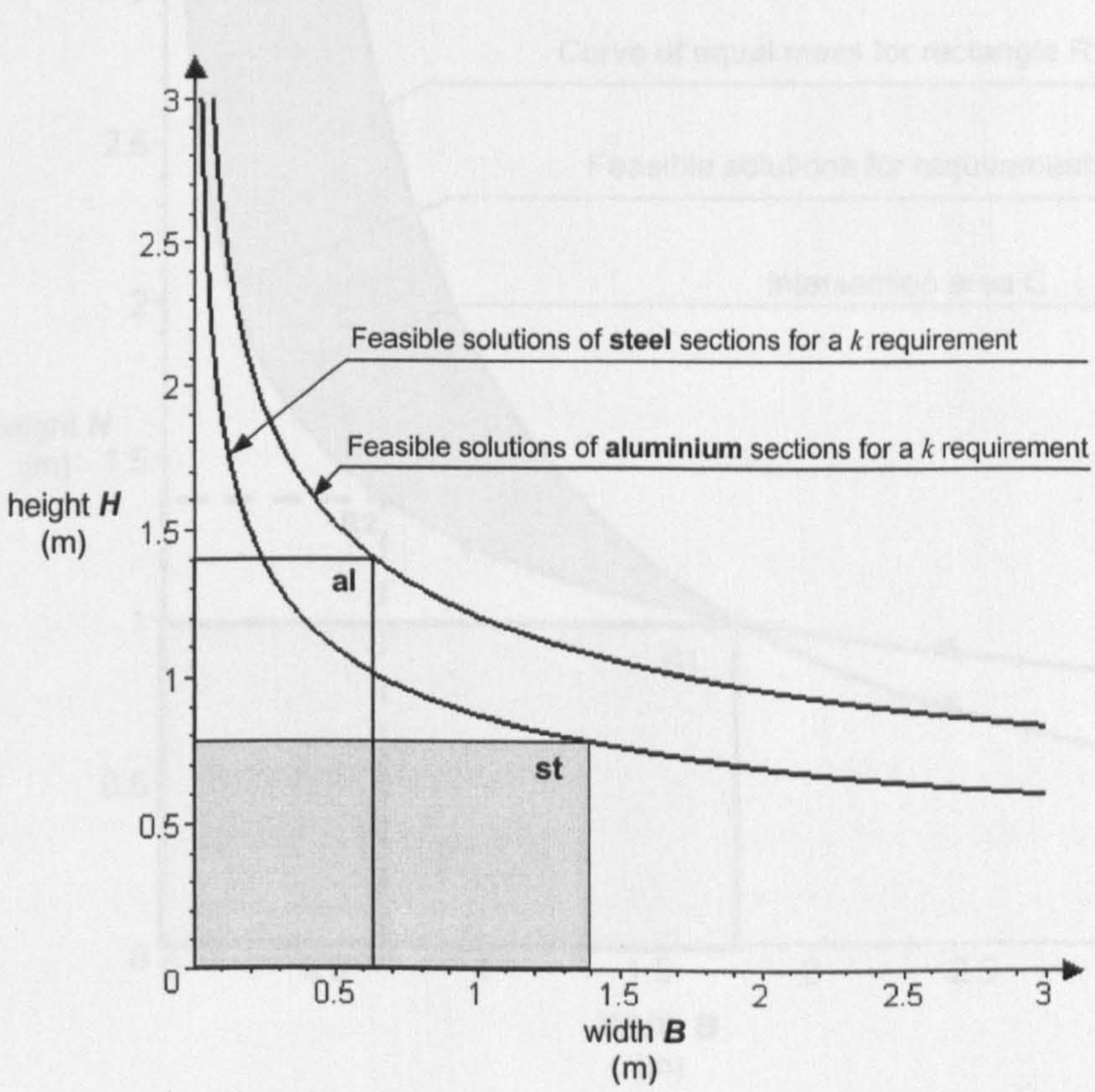

Figure 4.1 Stiffness requirement, k=280*10^{6}N/m, for steel, st, and aluminium, al, of rectangular cross-sections.

Objective function. For a given material, rectangular cross-section and set of design requirements, the expression of the mass m is a function of the width *B* and of the depth *H* of the cross-sectional envelope, and from equation (3.11) is given by:

$$\frac{m}{L} = BH\rho \tag{4.2}$$

Figure 4.2 illustrates curves obtained using equations (4.2) and (4.1), where the only variables are the height and width of an aluminium (ρ_{al}=2.9 Mg/m^3) cantilever with length *L*=5m and c_1=3, i.e. the same case of Figure 4.1. Curves m-R1 and k-R1 represent all rectangular cross-sections of equal mass, m=25.7 Mg, and equal stiffness, k= 280*10^{6}N/m, respectively. Each curve corresponds to the mass and the stiffness of rectangle R1. Rectangle R2 has the same stiffness and has lower mass than rectangle R1. Compared to the envelope R1 all the rectangles under the curve m-R1 have lower mass. Envelopes above curve k-R1 are stiffer. The shaded area C in Figure 4.2 represents solutions for all possible rectangles that are both stiffer and lighter than rectangle R1.

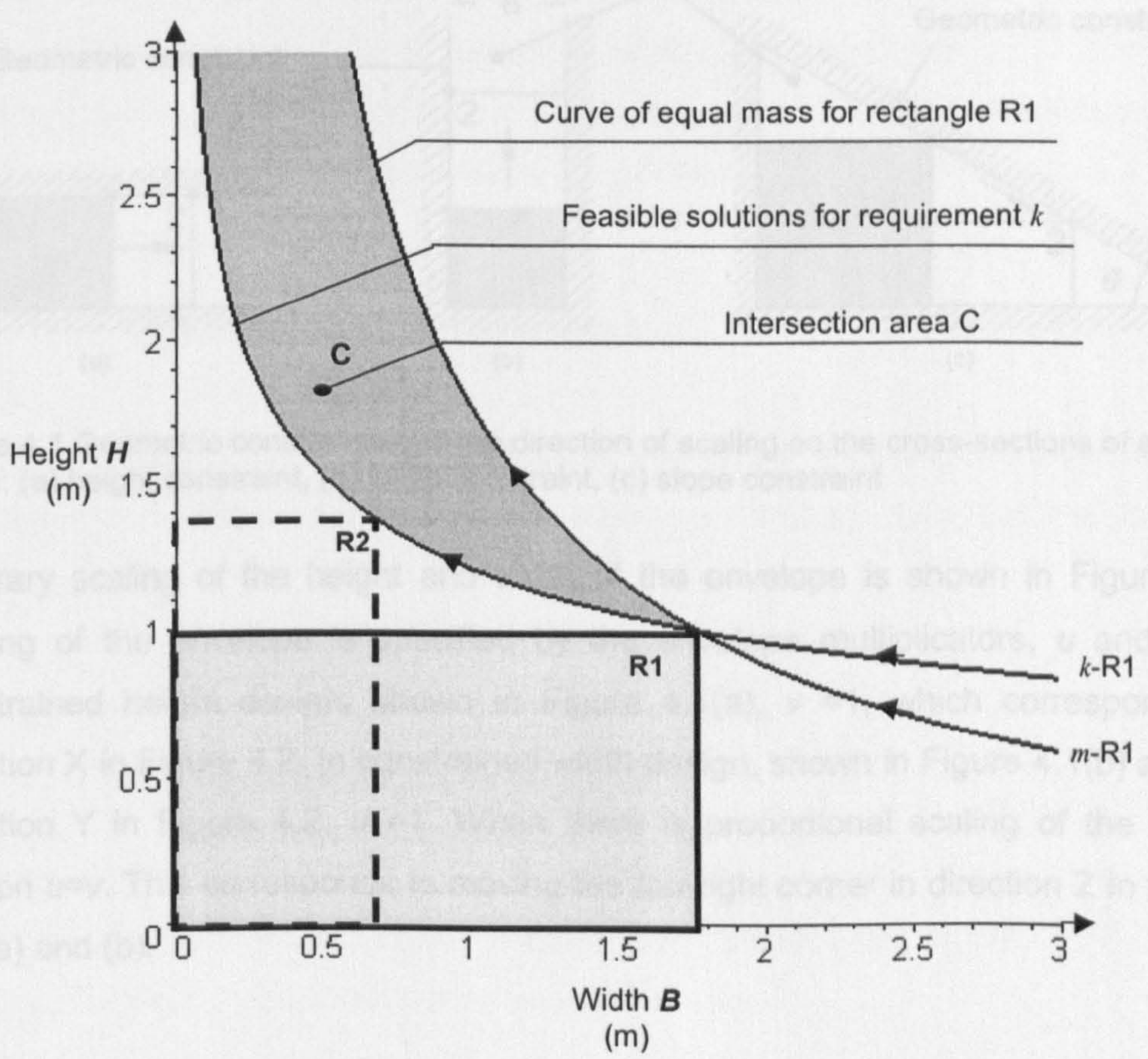

Figure 4.2 Curves of equal stiffness k-R1 and mass m-R1.

4.2.2 Geometrical constraints

In structural design it is very common that designers have to take into account spatial limitations. For example, height and width constraints are shown in Figure 4.1(a) and (b). Height constraints are common in floor structures and width constraints are common in wall structures. A slope constraint is shown in Figure 4.1 (c). This type of constraint is quite common in highly integrated structures such as cars and aircraft. Figure 4.1 shows examples where geometric constraints limit one or both of the envelope dimensions of different cross-sectional shapes. In these cases structures are forced to fit within a limited space and then to be scaled in a certain direction. For example, a height constraint, Figure 4.1(a), forces the cross sections to be scaled horizontally. A width constraint, Figure 4.1(b), imposes a vertical scaling direction. Figure 4.1(c) illustrates the effect of a sloped constraint on both the height and width of the shape envelopes.

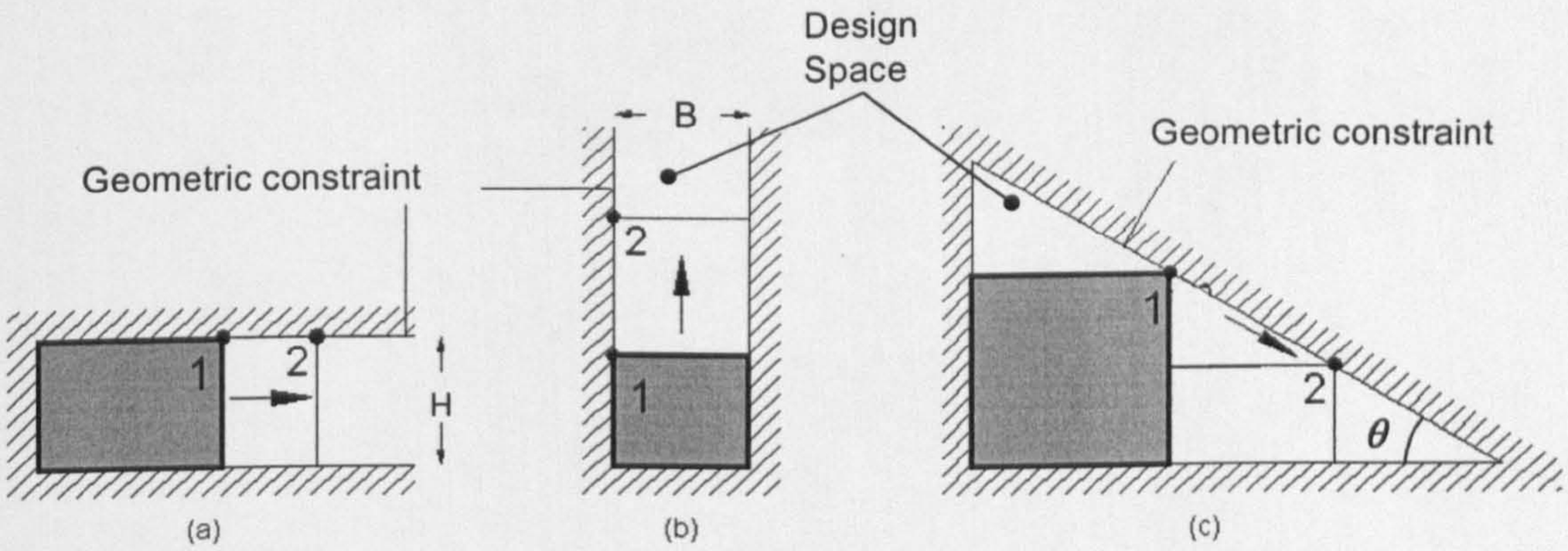

Figure 4.1 Geometric constraints and the direction of scaling on the cross-sections of a beam: (a) height constraint, (b) width constraint, (c) slope constraint

Arbitrary scaling of the height and width of the envelope is shown in Figure 4.2. Scaling of the envelope is specified by the envelope multiplicators, *u* and *v*. In constrained height design, shown in Figure 4.1(a), *v* =1, which corresponds to direction X in Figure 4.2. In constrained width design, shown in Figure 4.1(b) and for direction Y in Figure 4.2, *u* =1. When there is proportional scaling of the cross-section *u=v*. This corresponds to moving the top-right corner in direction Z in Figure 4.2 (a) and (b).

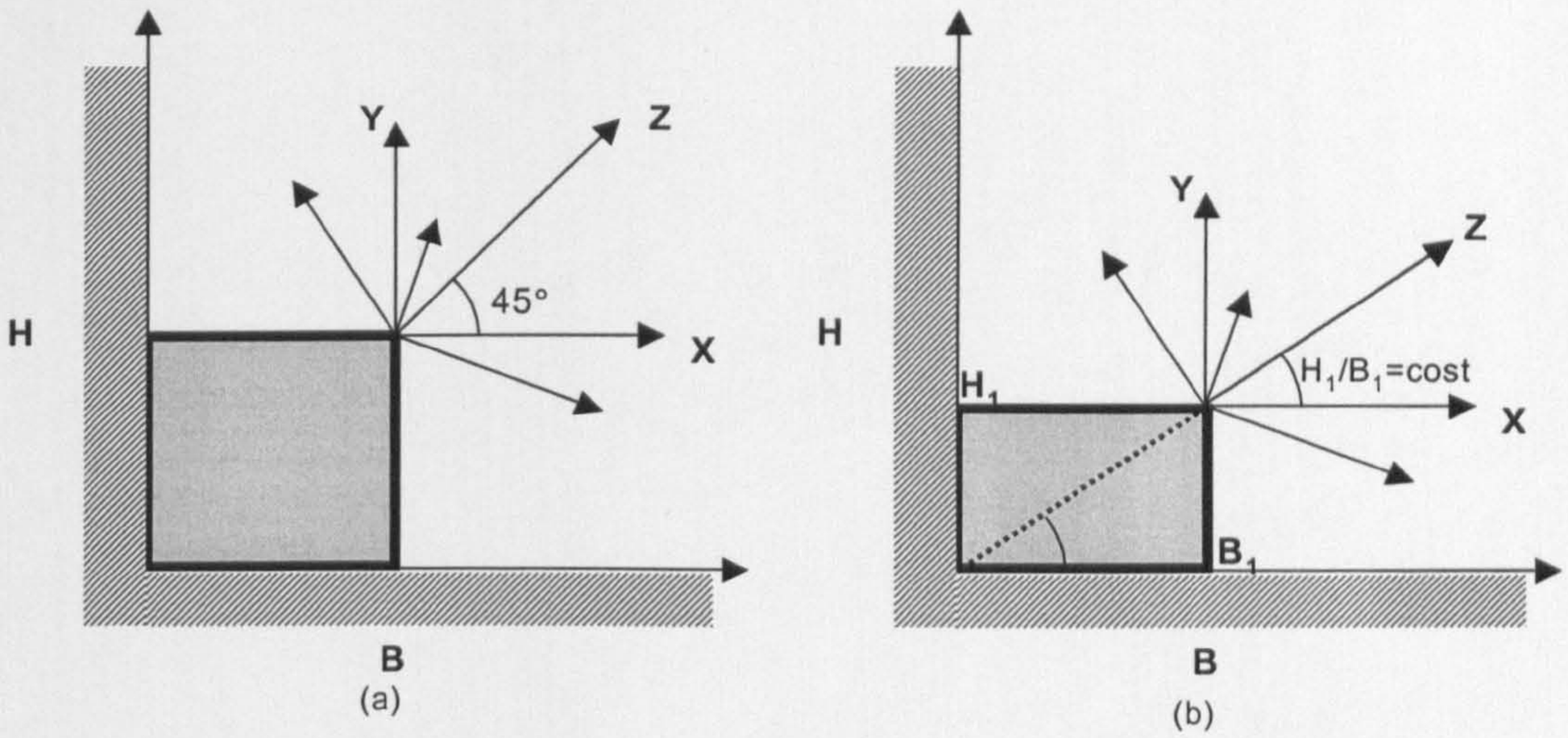

Figure 4.2 Arbitrary direction of scaling of square, (a), and rectangular, (b), cross-section: **Z**) Proportional scaling H_1/B_1 = const (u=v) **X**) Horizontal scaling H_1 = const (v =1), **Y**) Vertical scaling B_1 = const (u =1)

Geometrical constraints generally restrict the magnitude and direction of scaling of the cross-sections and, therefore, must be considered in the selection of low-mass structures. Two approaches to selection which can cope with any geometrical constraint, such as those illustrated in Figure 4.1, are presented in this Chapter: the performance criterion in Section 4.3 and the performance index in Section 4.4.

4.3 THE PERFORMANCE CRITERION

The performance criterion can be defined as the ratio of the design requirement and the objective function. If mass is the objective function, then the performance criterion, $\tilde{p}$, is given by:

$$\tilde{p} = \frac{requirement}{mass} \tag{4.3}$$

Equation 4.3 permits all the selection conditions of the design scenario shown in Table 3.5 for a given stiffness, strength and tensile load requirement. In this Chapter, the performance criterion is used to examine:

constraint, such as those illustrated in Figure 4.1, are presented in this Chapter: the performance criterion in Section 4.3 and the performance index in Section 4.4.

4.3 THE PERFORMANCE CRITERION

The performance criterion can be defined as the ratio of the design requirement and the objective function. If mass is the objective function, then the performance criterion, $\tilde{p}$, is given by:

$$\tilde{p} = \frac{requirement}{mass} \tag{4.3}$$

Equation 4.3 permits all the selection conditions of the design scenario shown in Table 3.5 for a given stiffness, strength and tensile load requirement. In this Chapter, the performance criterion is used to examine:

- Tensile load design for the case where *M, S* and *D* are active. This is illustrated in Section 4.3.1. Note that since all the variables are considered active, this case will not be investigated in the following Chapters.
- Bending stiffness and strength design for conditions 1, where *D* is the only variable, and 2, where *D* and *M* are variables. Since *S* is fixed, all the candidate cross-sections have the same shape properties as shown in Figures 3.6a) and 3.6b). In order to avoid repetition, Section 4.3.2 illustrates condition 1 for stiffness design and Section 4.3.3 deals with condition 2 for strength design.

4.3.1 Tensile load design

For a given tensile load requirement, *P*, from equations (3.12) and (3.11) the performance criterion, $\tilde{p}$, for ties of the same length, *L*, is given by

$$\tilde{p} = \frac{P}{m} = \frac{\sigma_y{}^{t}\psi_A BH}{\rho\psi_A BHL} \tag{4.4}$$

After rearranging expression (4.4), the performance, p, defined as the inverse of the mass, is given by:

$$p = \frac{1}{m} = \underbrace{\left[\frac{1}{PL}\right]}_{F} \underbrace{\left[\frac{\sigma_y{}^{t}}{\rho}\right]}_{M} \tag{4.5}$$

The second member of equation (4.5) is a product of two factors: *M* refers to the material properties of the envelope and *F* contains the load requirement and the length, *L*. Since the shape transformer, ψ_A, is the same for the design requirement and objective function, the variable *S* is not relevant in considering the performance. The shape property, ψ_A, and the envelope *D* have no effect on the mass of a structure in tensile load design, thus, σ_y/ρ is the criterion of selection.

4.3.2 Stiffness design

In stiffness design the performance criterion, $\tilde{p}$, is given by the ratio of equation (3.13) and (3.11):

$$\tilde{p} = \frac{k}{m} = \frac{c_1}{12L^4} \frac{E}{\rho} \frac{\psi_I}{\psi_A} H^2 \tag{4.6}$$

then the performance *p* is given by:

$$p = \frac{1}{m} = \underbrace{\left[\frac{c_1}{12kL^4}\right]}_{F} \underbrace{\left[\frac{\psi_I}{\psi_A}\right]}_{S=const} \underbrace{\left[\frac{E}{\rho}\right]}_{M} \underbrace{\left[H^2\right]}_{D=f(M)} \tag{4.7}$$

The second member of equation (4.7) can be factorised into four groups: *F* collects the constant parameters of the problem and the stiffness requirement, *S* are the shape properties which are constant, while the variables are the material properties, *M*, and the envelope sizes, *D*.

In bending stiffness design, both the equations (3.13) and (4.7) must be generally considered in a selection task. As explained for Figure 4.1, the height of a rectangular envelope, *D*, which satisfies the stiffness requirement is a function, $H=f(1/BE)$, of the material. Since the height of the envelope, D, in equation (4.7) must be a solution of the stiffness requirement, equation (3.13), the variable *D* is not generally separable from *M*. Consequently, E/ρ cannot be considered as the only criterion of selection.

This is shown in the next Section with a graph which combines the stiffness requirement, equation (3.13), and the performance, equation (4.7).

Combined graph for envelope selection

Figure 4.1 shows a graphical solution of the stiffness requirement and the performance criterion for condition 1 of Table 3.5, where the only variable is *D*. Equations (3.13) and (4.7) are plotted on the right and left side of the graph respectively. The data are for a steel (ρ=7.9 Mg/m^3, E=210 GPa) cantilever with length L=5m and c_1=3 which must meet a stiffness requirement, k= 600*10^{6}N/m. (These data are purely for illustration. The physical dimensions are impractical).

Since the material is fixed, the performance of the cross-sections depends on the sizes of the envelopes, *D*. R_1, R_2, and R_3 are three cross-sections with equal stiffness and same shape properties, *S*, which in this case are chosen to be $\psi_A=\psi_I=1$. The performance of R_1, R_2, and R_3 are p_1, p_2 and p_3. p_1 is greater than p_3. However, the rectangle R_2 is lighter then the rectangle R_1. This shows that variation of the sizes of the envelope, *D*, can provide opposite results for cross-sections with the same shape and material properties. It is evident that since there is only one curve, which satisfies the stiffness requirement, the only possible scaling of a cross section is along the curve k. Simple horizontal scaling, *v=1*, vertical scaling, *u=1* and proportional scaling, *u/v*= constant, are not feasible for condition 1 of Table 3.5.

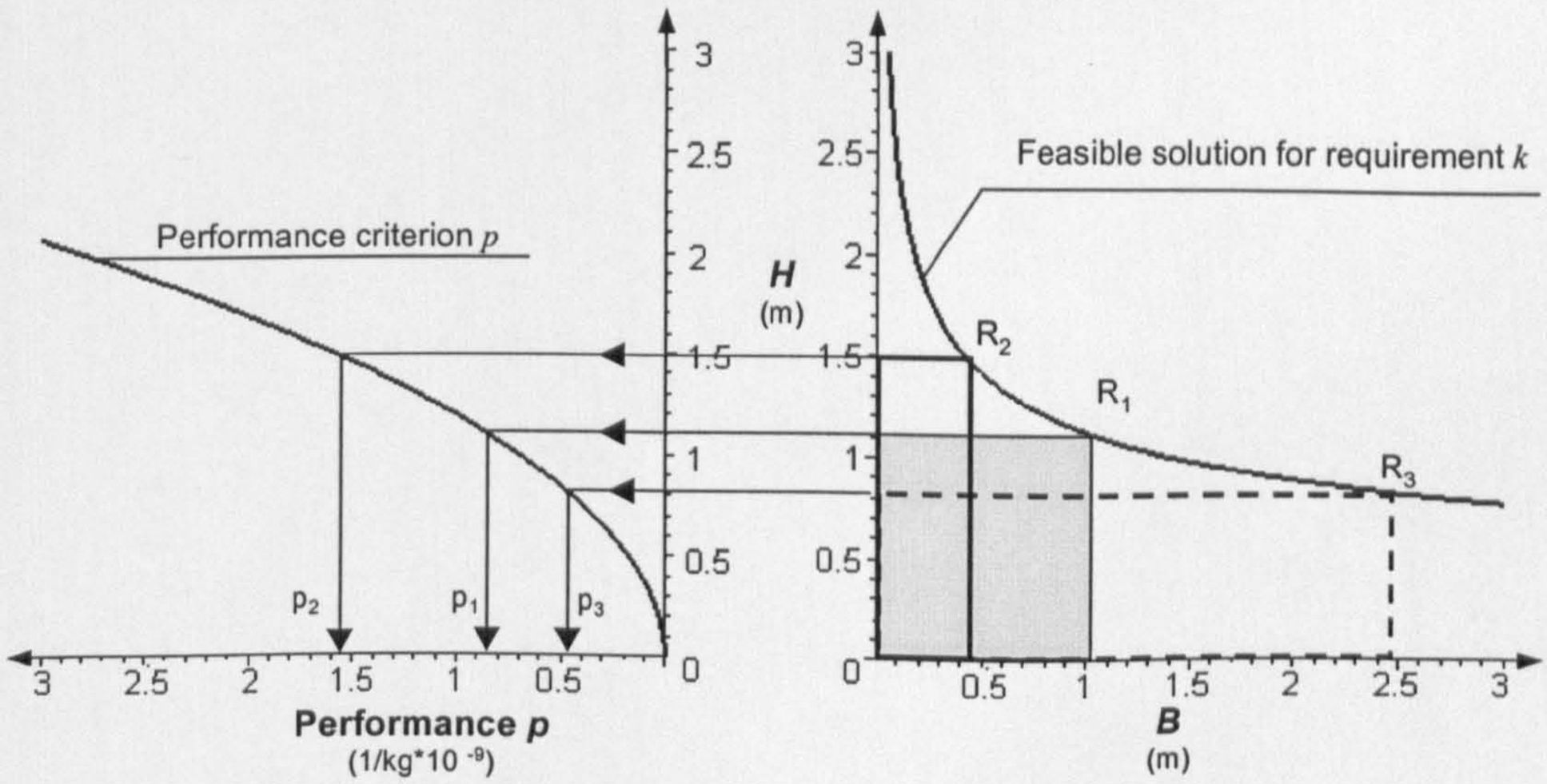

Figure 4.1 Combined selection graph for *D* variable in stiffness design

Combined graph for material and envelope selection

In selection condition 2 of Table 3.5, both *D* and *M* are variables. The functional requirement, equation (3.14), and the selection criterion, equation (4.9), differ for each material and, therefore, are described by two curves in both sides of Figure 4.1. The structural component has *L*=1.5m and the candidate materials of rectangular cross-sections are aluminium (ρ=2.9 Mg/m^3, σ_y =20 MPa) and steel (ρ=7.9 Mg/m^3, σ_y =280 MPa). The failure moment requirement is M_y = 15*10^{6}Nm. (These data are purely for illustration)

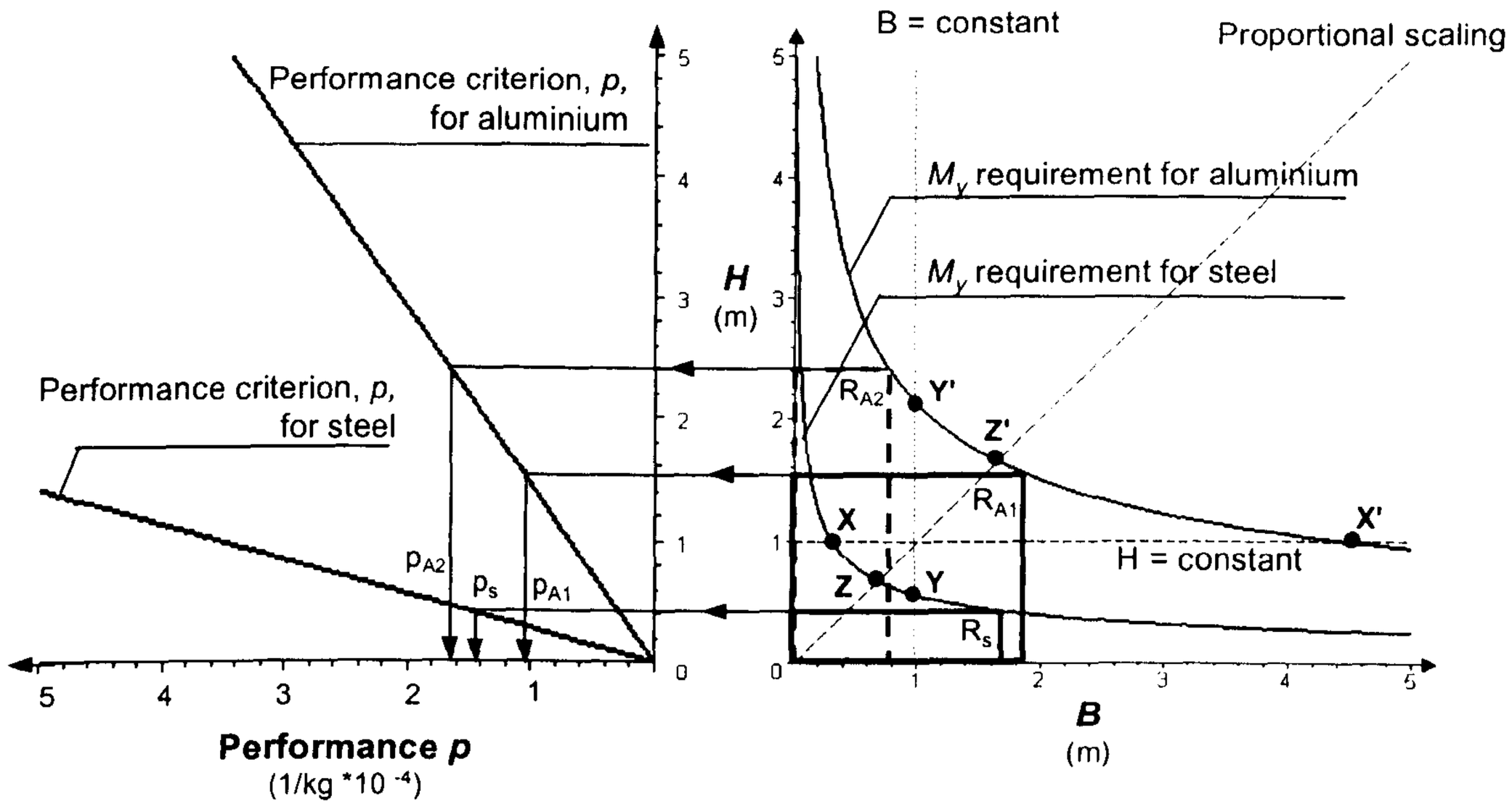

Figure 4.1 Combined selection graph for *D* and *M* variables in strength design.

The space subtended by the requirement curves shows that materials with high σ_y, for example steel, needs less space to meet the requirement, thus providing a space advantage. In Figure 4.1, three rectangles are considered: R_S for steel and R_{A1} and R_{A2} for aluminium. The performance p_S is greater than p_{A1} but worse than p_{A2}. This illustrates that when M and D are variables, σ_y/ρ cannot generally be separated to determine the relative performance because the height in equation (4.9), is a function $H=f(\sigma_y)$ of the material. In contrast to condition 1 of Table 3.5, in selection condition 2 *M* is variable and, therefore, scaling can occur from all the points of each M_y requirement curve. Horizontal (from point X to X'), vertical (from Y to Y') and proportional scaling (from Z to Z') are feasible. In the following Section, it will be shown that only in these three scaling directions *D* and *M* are separable and there is no need to consider both the equations of the stiffness requirement and the performance criterion for selection.

4.4 THE PERFORMANCE INDEX

A performance index is a combination of material properties which permits the selection of the best material, M, in a particular application. In the previous Section, the performance criterion method showed that material and envelope are generally variables that are not separable and for this reason they must be selected together. However, when the dimensions of the space envelope are scaled in certain directions, such as those marked X, Y and Z in Figure 4.1, D does not depend on M and the material becomes the only variable to be selected. Therefore, knowing the scaling direction a priori allows the performance index to be used for selecting the only variable M.

4.4.1 Stiffness design: general solution E^q/ρ for any arbitrary scaling

In stiffness design, the ratios E/ρ, $E^{1/2}/\rho$ and $E^{1/3}/\rho$ are performance indices which lead to the selection of the best material respectively for constrained height, proportional scaling and constrained width [note that these indices have been identified by other authors (Crane, F.A.A and Charles, J.A., 1984; Ashby. M.F. 1989) as reported in Chapter 2]. From this, it can be seen that the direction of scaling affects the power to which E is raised. As selection condition 2 in Table 3.5 shows, the performance, $p=f(M,D)$, is a function of the free variables M and D. However, if the direction of scaling has been set in advance, such as in horizontal, proportional or vertical scaling, the exponent, q, of the Young's modulus E is an expression of the variable D. Therefore, the aim of the following analysis is finding a general function $q=f(D)$ in order to derive a general expression of the performance index for arbitrary scaling.

Analysis

From equation (3.11), the ratio of the masses of the reference structure m_o and a generic structure m of the same length L and cross-sectional shape, is

$$\frac{m_o}{m} = \frac{\rho_o}{\rho}\frac{A_o}{A} \tag{4.10}$$

As maximising the performance index minimises the mass, using the multiplicators u and v in equations (4.10), the ratio of the performance for the structures is

$$\frac{p}{p_o} = \frac{m_o}{m} = \frac{\rho_o}{\rho}\frac{1}{uv} \tag{4.11}$$

Expressions for u and v in terms of the design requirement are now sought. For stiffness design, equation (3.13), both structures are required to meet the same stiffness requirement, $k=k_o$, where

$$E_o I_o = IE \tag{4.12}$$

and

$$\frac{E_o}{E} = \frac{I}{I_o} \tag{4.13}$$

The ratio of the second moments of area of the two structures can also be stated in terms of multipliers u and v, so that

$$\frac{I}{I_o} = uv^3 \tag{4.14}$$

When the height of the two structures is constrained $v=1$, and u is

$$u = \frac{I}{I_o} \tag{4.15}$$

Alternatively when the width is constrained $u=1$, and v is given by

$$v = \left(\frac{I}{I_0}\right)^{\frac{1}{3}} \tag{4.16}$$

The performance indices for constrained height ($v=1$) and width ($u=1$) follow from equations (4.11), (4.13), (4.15) and (4.16), so that with

v=1 :
$$\frac{p}{p_o} = \frac{\rho_o}{\rho}\frac{I_o}{I} = \frac{\rho_o}{\rho}\frac{E}{E_o} \tag{4.17}$$

u=1 :
$$\frac{p}{p_o} = \frac{\rho_o}{\rho}\left(\frac{I_o}{I}\right)^{1/3} = \frac{\rho_o}{\rho}\left(\frac{E}{E_o}\right)^{1/3} \tag{4.18}$$

For arbitrary scaling conditions $u \neq 1$ and $v \neq 1$, a solution is sought such that,

$$\frac{p}{p_o} = \frac{\rho_o}{\rho}\left(\frac{E}{E_o}\right)^q \tag{4.19}$$

where q is yet to be determined.

For these conditions:

$$\begin{cases} u = \left(\dfrac{I}{I_o}\right)^{\alpha} \\ v = \left(\dfrac{I}{I_o}\right)^{\beta} \end{cases} \tag{4.20}$$

and using expression (4.20), equation (4.14) is rewritten as

$$\frac{I}{I_o} = uv^3 = \left(\frac{I}{I_o}\right)^{\alpha+3\beta} \tag{4.21a}$$

and

$$\alpha + 3\beta = 1 \tag{4.21b}$$

From equation (4.20) the exponents α and β are

$$\begin{cases} \alpha = \lg_{\left(\frac{I}{I_o}\right)} u = \lg_{\left(uv^3\right)} u \\ \beta = \lg_{\left(\frac{I}{I_o}\right)} v = \lg_{\left(uv^3\right)} v \end{cases} \tag{4.22}$$

The ratio of the performance indices p/p_o follows from equation (4.11) using equations (4.20) through (4.22), so that

$$\frac{p}{p_o} = \frac{\rho_o}{\rho}\left(\frac{I_o}{I}\right)^q = \frac{\rho_o}{\rho}\left(\frac{E}{E_o}\right)^q \tag{4.23}$$

where q

$$q = \log_{(uv^3)} uv = \frac{\ln uv}{\ln uv^3} \tag{4.24}$$

Equation (4.23) permits the performance indices for arbitrarily scaled cross sections with the same shape properties to be compared. In particular the exponent q represents a parameter that describes the scaling of the dimensions of the cross-sectional envelopes of structures using different materials. This is because each material, as it has been explained in Sections 4.3.2 and 4.3.3, requires a different space to meet the functional requirement k, described by equation (3.13).

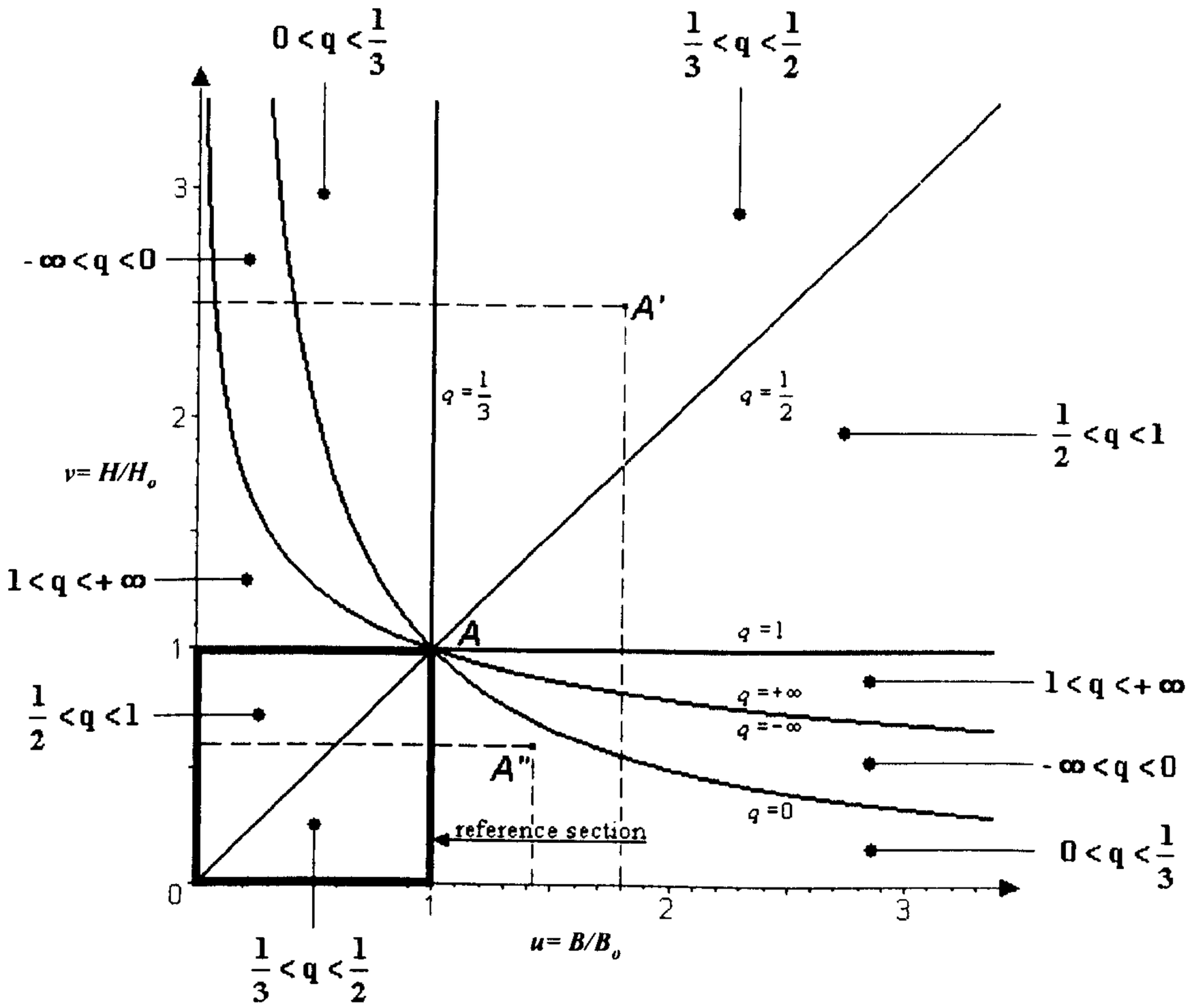

Figure 4.1 Solutions of the scaling parameter q for all directions of scaling in stiffness design. A: reference section; A': 1/3 <q< 1/2; A": 0 <q< 1/3.

Figure 4.1 shows a plot of results for $q=f(u,v)$. These results are consistent with the previous values of $q=1/3$, $q=1/2$, $q=1$ for constrained width, proportional scaling and constrained height respectively. The figure shows that for two curves $uv^3=1$ and $uv=1$, q is unbounded (i.e. $q = \pm \infty$) and zero respectively. These results give an indication about the relative importance of Young's modulus and density. When q approaches zero the density is more important in comparison to Young's modulus. In contrast when q approaches infinity, Young's modulus is relatively more important compared to the density. This immediately shows that the direction of scaling has a very important effect on material selection. Furthermore, Figure 4.1 shows examples of arbitrary scaled rectangular sections of different materials. If the reference structure A of unit dimensions according to the stiffness requirement, is rescaled so that u=1.8, v=2.5, point A moves to point A' and $1/2<q<1$. Alternatively, if point A moves to point A", then also $0<q<1/3$. As well as regions defined by $1/2<q<1$ and $0<q<1/3$, distinct regions for other ranges of q are shown.

In the next Section, useful ranges of q where one material provides lower mass compared to others are presented. These ranges of q are used to produce the limiting regimes chart.

Limiting material regimes for material and envelope selection

The limiting material regimes refer to regions of the design space, B vs H, where the material properties, M, contained in a structural envelope provide a relatively better performance for specific ranges of the scaling conditions, q. The general solution to the performance index, equations (4.23) and (4.24), enables a comparison to be made between the performance of different materials for any direction of scaling. In stiffness design the performance index p for arbitrary scaling, with the aim of minimising mass, is expressed by

$$p = \frac{E^q}{\rho} \tag{4.25}$$

where q is a function of the multipliers u and v.

Examples of a full range of solutions for this performance index for three materials: aluminium, steel and glass fibre reinforced plastic (GFRP), are shown in Figure 4.1.

The performance index has been plotted as a function of the scaling parameter q using values of E and ρ given in Table 3.2.

When the direction of scaling is known in a design task, q can be calculated from equation (4.24) and the relative performance of different materials can be immediately determined from Figure 4.1. The intersection points of two curves in Figure 4.1 represent values of the scaling parameter q where both materials perform equally. Thus when q, for example, is greater than 1.025, steel cross-sections have a better performance index than Aluminium and also GFRP cross-sections. When the scaling parameter q is less than 0.49, all GFRP rectangular cross-sections provide the best performance compared to aluminium and steel.

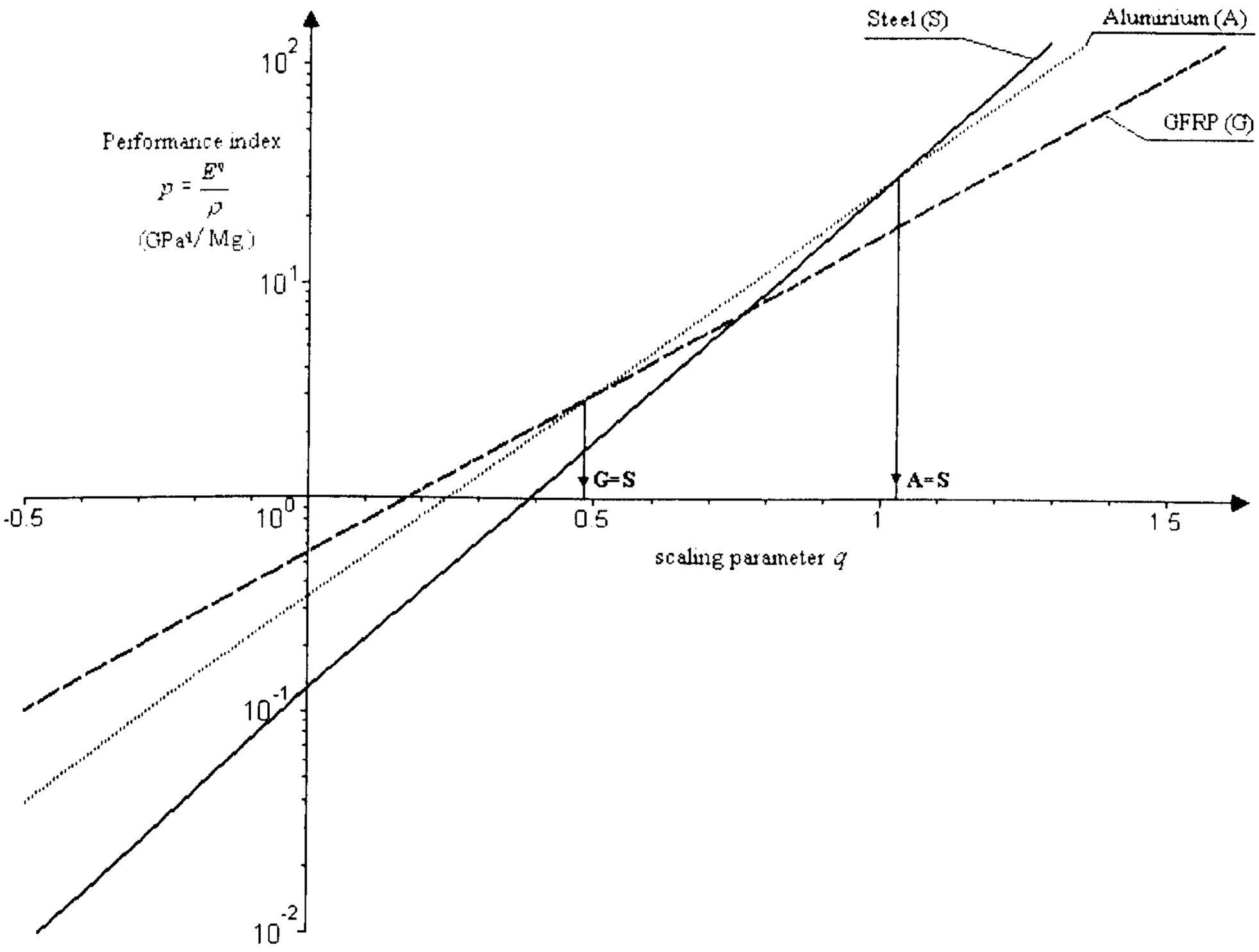

Figure 4.1 Performance of three materials for a range of values of q in stiffness design

The parameter q is the scaling parameter. Variations in v from variation in u, for a given value of q can be found by inverting equation (4.24) so that

$$v = u^{\frac{(1-q)}{(3q-1)}} \tag{4.26}$$

Curves of special q values for which two materials have the same performance index can be plotted using (4.26). These special values of q, obtained from Figure 4.1, are plotted in Figure 4.2. Figure 4.2 is the **limiting material regimes** chart which maps regions where the performance of one material is relatively better compared to the others for any arbitrary scaling. For example in stiffness design all the rectangular cross-sections manufactured from Aluminium provide the best performance index in the region where $0.49<q<1.025$. Alternatively, all cross-sections scaled so that they lie in the GFRP region provide minimum mass compared to steel and aluminium. In general, materials with high Young's modulus, such as steel, perform relatively better for high values of q.

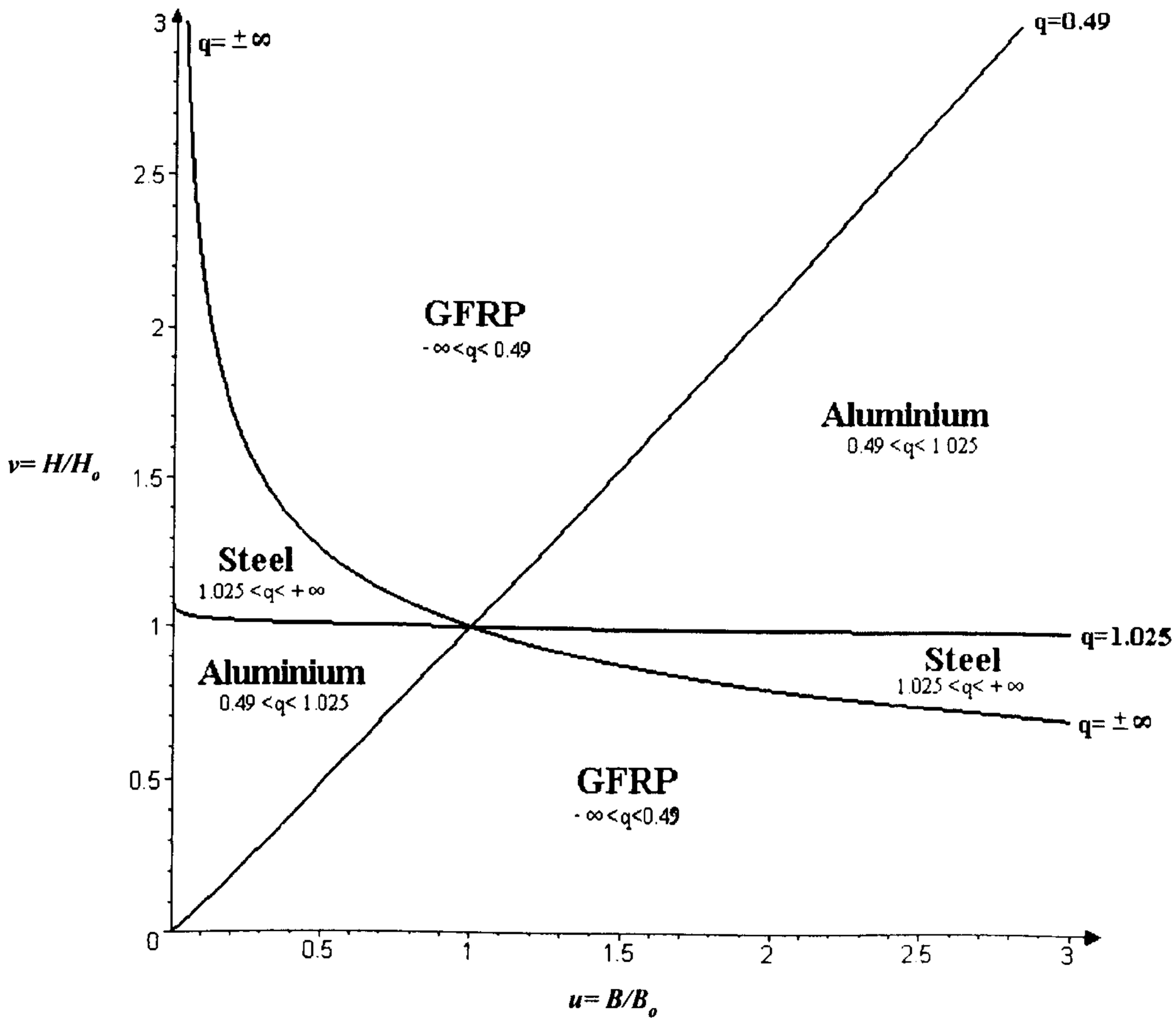

Figure 4.2 Limiting material regimes for Steel, Aluminium, GFRP in stiffness design

In Section 4.8, an example of design application, where the limiting material regimes shown in Figure 4.2 are used without the need of any calculation, is presented.

4.4.2 Strength design: general solution σ^q/ρ for any arbitrary scaling

The procedure to derive the general solution of the performance index for strength design is entirely analogous to the stiffness case. For this reason, it is reported in Appendix B. The general solution for the selection of the material properties of arbitrarily scaled envelopes is given by:

$$\frac{p}{p_o} = \frac{\rho_o}{\rho}\left(\frac{Z_o}{Z}\right)^q = \frac{\rho_o}{\rho}\left(\frac{\sigma_y}{\sigma_{yo}}\right)^q \tag{4.27}$$

where q is given by:

$$q = \log_{(uv^2)} uv = \frac{\ln uv}{\ln uv^2} \tag{4.28}$$

For a failure moment requirement, equation (4.27) allows the relative performance index for arbitrarily scaled structures of the same shape, *S*, and different material to be compared. The exponent $q=f(u,v)$ describes the scaling of the dimensions of the envelopes containing different materials. In Figure 4.1, the performance index is plotted as a function of the scaling parameter *q*. A full range of solutions is shown for arbitrary scaling of a square section. For $uv^2=1$ *q* is unbounded (i.e. $q = \pm \infty$). For vertical, proportional and horizontal scaling of the square reference, $q=1/2$, $q=2/3$, $q=1$ respectively. For arbitrary scaling, *q* has different values. For example, if the reference structure A of unit dimensions, according to the requirement, is rescaled to E, then $-\infty<q<1/2$. Alternatively, if point A moves to C, then $2/3<q<1$. Figure 4.1 is analogous to Figure 4.1 and the features outlined for a stiffness requirement are applicable to strength design.

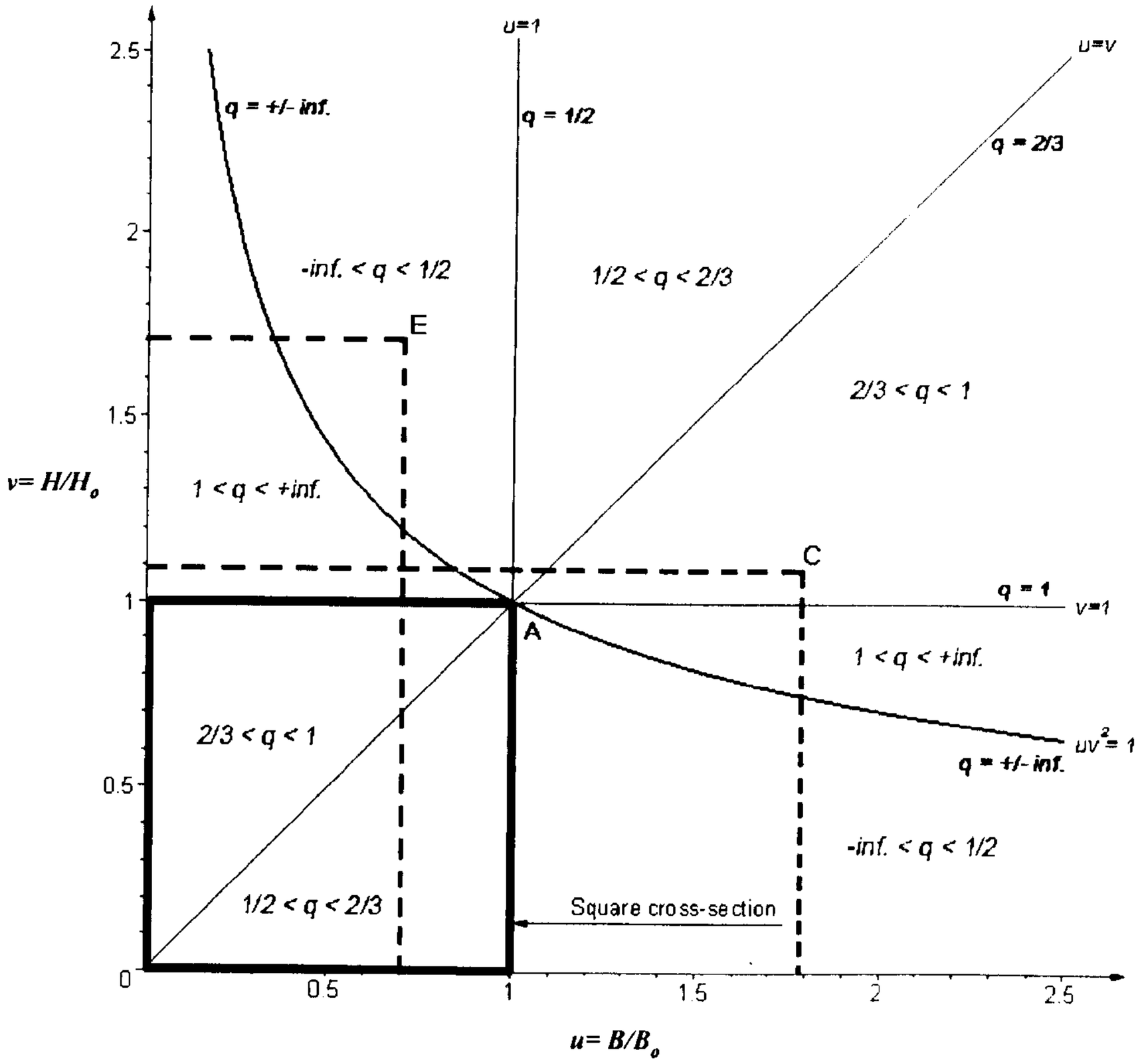

Figure 4.1 Solutions of the scaling parameter q for all directions of scaling in strength design. A: square section; C: 2/3 <q< 1; E: -inf. <q< 1/2;

Limiting material regimes for material and envelope selection

The material regimes for strength design are similar to Figure 4.2 although the relevant material property is σ_y, rather than E, in addition to ρ. An example of material regimes for strength design will be illustrated in Chapter 8 for a natural structure, where S and M are variable.

4.5 COMPARISON OF PERFORMANCE CRITERION AND PERFORMANCE INDEX

The performance criterion and the performance index are two approaches to the selection of the best structure for a design application. The aim of this Section is to explain the relationship, the applicability limits and the advantages of the approaches.

4.5.1 Relationship

The performance index enables the selection of the best material for an envelope which is scaled in any arbitrary direction with respect to a reference section. In order to make a proper comparison of the approaches, the performance criterion has to be expressed in term of relative performance of a structure, p, to the reference, p_o. From equations (4.7) and (4.9) the ratio of the performance for rectangular cross-sections is:

for stiffness design $$\frac{p}{p_o} = \frac{\rho_o}{\rho}\frac{E}{E_o}\frac{A_o}{A}\frac{I}{I_o} = \frac{\rho_o}{\rho}\frac{E}{E_o}\frac{H^2}{H_o^2} = \frac{\rho_o}{\rho}\frac{E}{E_o}v^2$$

for strength design $$\frac{p}{p_o} = \frac{\rho_o}{\rho}\frac{\sigma_y}{\sigma_{yo}}\frac{A_o}{A}\frac{Z}{Z_o} = \frac{\rho_o}{\rho}\frac{\sigma_y}{\sigma_{yo}}\frac{H}{H_o} = \frac{\rho_o}{\rho}\frac{\sigma_y}{\sigma_{yo}}v$$

Comparing the approaches gives:

Design	Performance criterion	Performance index
Stiffness	$\frac{p}{p_o} = \underbrace{\frac{\rho_o}{\rho}\frac{E}{E_o}}_{M}\ \underbrace{v^2}_{D}$	$\frac{p}{p_o} = \underbrace{\frac{\rho_o}{\rho}\left(\frac{E}{E_o}\right)}_{M}^{\underbrace{q}_{D}}$
Strength	$\frac{p}{p_o} = \underbrace{\frac{\rho_o}{\rho}\frac{\sigma_y}{\sigma_{yo}}}_{M}\ \underbrace{v}_{D}$	$\frac{p}{p_o} = \underbrace{\frac{\rho_o}{\rho}\left(\frac{\sigma_y}{\sigma_{yo}}\right)}_{M}^{\underbrace{q}_{D}}$

As can be seen, the differences are not in the material domain, M, but in the geometric domain of the space envelope D. The relation of the D factors are:

	Performance criterion		Performance index
Stiffness	$\frac{I}{I_o}\frac{A_o}{A} = \frac{uv^3}{uv} = v^2$	$\Leftrightarrow$	$q = \frac{\ln uv}{\ln uv^3}$
Strength	$\frac{Z}{Z_o}\frac{A_o}{A} = \frac{uv^2}{uv} = v$	$\Leftrightarrow$	$q = \frac{\ln uv}{\ln uv^2}$

While in the performance criterion the ratios $I/I_o * A_o/A$ is a factor which multiplies E/E_o, in the performance index the terms I/I_o and A/A_o compare at the exponent of

E/E_o as $q = \frac{\ln uv}{\ln uv^3} = \log_{uv^3} uv = \log_{\frac{I}{I_o}} \frac{A}{A_o}$. Since in stiffness design the cross-sections have the same stiffness, then $k/k_o = EI/E_oI_o = 1$. Therefore, substituting $E/E_o = I_o/I$ in the performance criterion and in the performance index, gives :

	Performance criterion		Performance index
Stiffness	$\frac{p}{p_o} = \frac{\rho_o}{\rho}\frac{A_o}{A}$	$\Leftrightarrow$	$\frac{p_o}{p} = \frac{\rho_o}{\rho}\left(\frac{I}{I_o}\right)^{-\log_{\frac{I}{I_o}}\frac{A}{A_o}} = \frac{\rho_o}{\rho}\left(\frac{I}{I_o}\right)^{\log_{\frac{I}{I_o}}\frac{A_o}{A}} = \frac{\rho_o}{\rho}\frac{A_o}{A}$

As expected, the performance criterion and index are two approaches which give the same results.

4.5.2 Limitations of performance criterion and index

- **Performance index**. Although in stiffness design $EI = EI_o$ and, hence, q becomes the power of the ratio of the Young's Modulus, q is not an attribute of the material properties. q describes the relative change of the envelopes, whose space sizes is determined by E in order to meet the stiffness requirement. For this reason, the performance index, E^q/ρ, can be applied only if M and D are variables.
- **Performance criterion**. In contrast, the performance criterion is more general and can be applied also to the case where the variable is only D, as has been shown in Figure 4.1.

There are conditions where the performance criterion is more suitable than the performance index:

- **Unknown direction of scaling:** when the direction of scaling in unknown at the beginning of a design task, the power of the performance index cannot be calculated. Therefore, it might be better to refer to the expression of the performance criterion, where ***M* and *D*** cannot be separated and **must be selected together**. As shown in Figure 4.1, since the envelope sizes must be a solution of the requirement curve, there are cases where a material M_1 provides a better performance than a material M_2 and other cases which present opposite results. Therefore, when the direction of scaling is unknown, it is not generally possible to consider E/ρ as the selection criterion. E/ρ can be considered the

selection criterion only if two cross-sections, *C* and C_o, have the same radius of gyration, $r_g = r_{go} = \sqrt{I/A}$, because in such a case $I_o/A_o = I/A$ and $p/p_o = \rho_o/\rho * E/E_o$.

- **Specified direction of scaling**: when the direction of scaling is known from the design, the scaling factor *q* becomes a constant and **the only variable to be selected is *M***. The reason for this is that since $I/I_o = uv^3$ is a function of two multiplicators, u and v, the number of variables can be decreased to one when scaling conditions are imposed:

Horizontal	$v=1$	$\frac{I}{I_o} = u$	the only variable to be isolated is u	$u = \frac{I}{I_o}$	$q = 1$
Vertical	$u=1$	$\frac{I}{I_o} = v^3$	the only variable to be isolated is v	$v = \left(\frac{I}{I_o}\right)^{1/3}$	$q = \frac{1}{3}$
Proportional	$u=v$	$\frac{I}{I_o} = \left(\frac{A}{A_o}\right)^2$	the only variable to be isolated is A	$\frac{A}{A_o} = \left(\frac{I}{I_o}\right)^{1/2}$	$q = \frac{1}{2}$

It is important to highlight that q =1 and q =1/3 refer to physical design spaces and they can be directly used as a performance measure for height and width constraint respectively. On the other hand, q = 1/2 is not related to any physical constraint which impose a scaling direction to the sections. As explained in Chapter 2, $E^{1/2}/\rho$ is not the best index which maximises the performance of a cross-section unless there is a reason to scale proportionally. An example of such a reason is when an equiaxed cross-section is subjected to bending from any direction.

4.6 MATERIAL CHARTS

The mass, m, and the design requirement, F, of a cross-section $C(m,F)$ can be displayed on a chart where the material properties of m, i.e. ρ, and of F, such as E *and* σ_y are on the horizontal and vertical axes respectively. The theory of the shape transformers has shown in Section 3.5 that the mass and the functional requirement of a cross-section $C(m,F)$ can be expressed by a product $MxSxG_D$, i.e. $C(\underbrace{MxSxG_D}_{m}, \underbrace{MxSxG_D}_{F})$.This Section considers the graphical selection of the best *M* which minimises the mass per unit length of a component. For a given *S*, the mass and the functional requirement of a cross-section, *C*, can be represented by the following co-ordinates in the case of *D* fixed and *D* variable:

D fixed	*D* variable
$C\left(\frac{m}{SxG_D}=M \;,\; \frac{F}{SxG_D}=M\right)$	$C\left(\frac{m}{S}=MxG_D \;,\; \frac{F}{S}=MxG_D\right)$

Note that the fixed parameters are on the left-hand side of each equation and the variables to be selected are on the right hand side.

4.6.1 Normal scale material charts for the performance criterion

The **performance criterion** can be used with the chart in Figure 4.1, where E is plotted against ρ **on normal axes**. M and D are variables. The following observations can be made about the relative positions of materials on the chart.

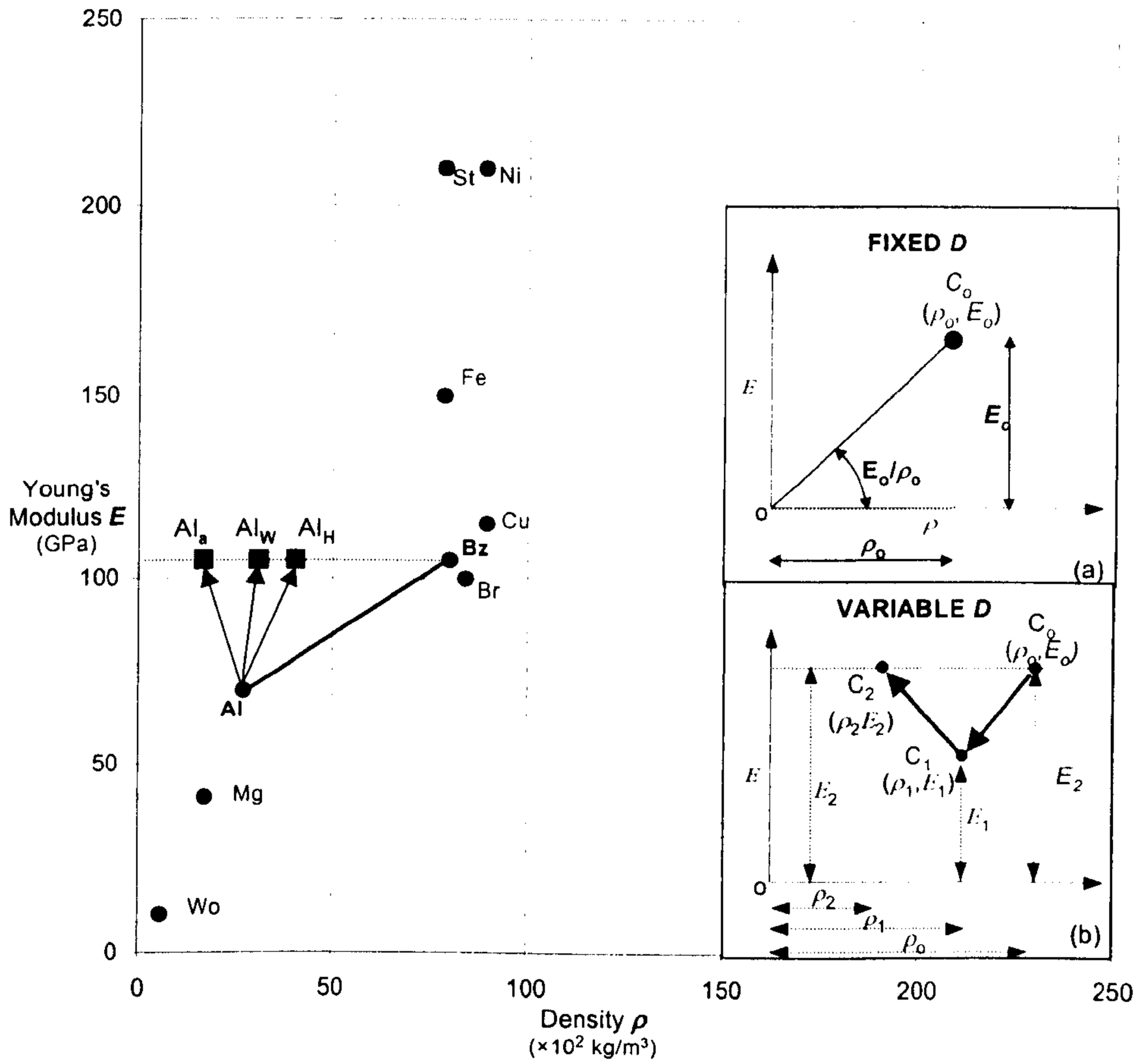

Figure 4.1 Normal scale material chart E-ρ for stiffness design. (Data from Table below)

Material	graph notation	ρ (×10² kg/m³)	E (GPa)	Material	graph notation)	ρ (GPa)	E (GPa)
Aluminium	**Al**	27.1	70	Iron	**Fe**	78.7	150
Brass	**Br**	84	100	Magnesium	**Mg**	17.4	41
Bronze	**Bz**	80	105	Nickel	**Ni**	88.9	210
Copper	**Cu**	89.4	115	Steel	**St**	78.5	210
GFRP	**Gf**	18	30	Wood; Ash	**Wo**	6.0	10

- ***D* fixed.** The properties of a cross-section are $C\left(\frac{m}{SxG_D}=M,\frac{k}{SxG_D}=M\right)$.

  Therefore, the co-ordinates *(ρ, E)*, i.e. mass and stiffness of C, specify the points of each material in the chart (4.11). Envelopes with the same stiffness lie on a horizontal line. This means that a stiffness requirement is satisfied only if two envelopes contain materials with the same Young's modulus. For a fixed envelope, the performance criterion takes the form E/ρ and is the slope of the line linking each point and the origin, O, as shown on the right box (a) of Figure 4.1 for a cross-section $C_o(m_o\rightarrow \rho_o, k_o\rightarrow E_o)$.

- ***D* variable.** The properties of a cross-section are $C\left(\frac{m}{S}=MxG_D,\frac{k}{S}=MxG_D\right)$. For a given S two cross-sections $C_o(M_o,S,D_o)$ and $C_1(M_1, S, D_1)$ with $D_o = D_1$ constant are considered. If *D* can vary, then C_1, in Figure 4.1 b), can be scaled according to the stiffness requirement to C_2 (M_2,S,D_2) with $D_2\neq D_1$ and $M_2=M_1$, i.e. C_2 (M_1,S,D_2). Combining equations (4.13) and (4.14), C_o and C_2 meet the same stiffness, i.e. $k_o=k_2$, for the following condition:

$$\frac{k_2}{k_o}=\frac{E_2I_2}{E_oI_o}=\frac{E_1}{E_o}uv^3=1 \qquad (4.29)$$

Consequently if a value of *u* is chosen, equation (4.29) can be used to determine the appropriate value of *v* that satisfies the stiffness requirement. The box (b) of Figure 4.1 shows an example. $C_o(\rho_o, E_o)$ and $C_1(\rho_1, E_1)$ represent the cross-section with same envelope sizes, $D_o=D_1$, but with different stiffness, $k_o\neq k_1$. If C_1 is scaled to C_2 according to equation (4.29) in order to meet the requirement, $k_o=k_2$, then the position of C_1 moves along the arrow C_1C_2 to the co-ordinate C_2 (ρ_2, E_2) given by

$$\begin{cases}E_2=uv^3E_1\\ \rho_2=uv\rho_1\end{cases} \qquad (4.30)$$

In general for **arbitrary scaling** of the envelope, D_o, of a cross-section $C_o(\rho_o,E_o)$, **both** the multiplicator ***u* and *v*** must be used in equation (4.30) **to display the mass and stiffness** of C_2 $(m_2\rightarrow\rho_2,\ k_2\rightarrow E_2)$ in Figure 4.1. For example, according to equation (4.29), the effect of an arbitrary scaling with u= 0.4 and v=1.5 of an aluminium section, Al, is shown by Al_a(16.8, 105) in Figure 4.1.

However, for three scaling conditions, which are **horizontal, vertical and proportional**, **the mass and the stiffness**, i.e. the position, of C_2 on the chart can be **determined without knowing** the specific values of ***u* or *v***. This is because imposing a scaling condition, allows *u* and/or *v* in equations (4.29) to be determined directly by E_o/E_1 as shown in the Table below.

Prescribed scaling		Derived condition from (4.29)	C_2 (ρ_2, E_2) from (4.30)	
Horizontal scaling	$v=1$	$u= E_o/E_1$	$m_2 \rightarrow \rho_2 = \rho_1(E_o/E_1)$	$k_2 \rightarrow E_2 = E_o$
Vertical scaling	$u=1$	$v=(E_o/E_1)^{1/3}$	$m_2 \rightarrow \rho_2 = \rho_1(E_o/E_1)^{1/3}$	$k_2 \rightarrow E_2 = E_o$
Proportional scaling	$u=v$	$u=v=(E_o/E_1)^{1/4}$	$m_2 \rightarrow \rho_2 = \rho_1(E_o/E_1)^{1/2}$	$k_2 \rightarrow E_2 = E_o$

Two examples of aluminium envelopes, Al_W and Al_H, respectively for horizontal and vertical scaling are considered. Al_W and Al_H have the same stiffness of a bronze envelope and, consequently, lie on the horizontal line shown in Figure 4.1. The co-ordinates of the aluminium envelopes, derived from the above Table, are: Al_W (31, 105) for width constraint and Al_H (40.6, 105) for height constraint. Al_w and Al_H are lighter then the bronze envelope, Br, and, for this reason, according to the slope E/ρ, i.e. the performance criterion, they are shown on the left of Br in Figure 4.1.

4.6.2 Log scale material charts for the performance index

Since the range of material properties is very large, **logarithmic scale axes** are usually adopted to display all the materials as shown in Figure 4.1(a), where *log E* is plotted against $log\rho$. Therefore, taking logs of the general solution of **performance index,** $p = E^q/\rho$, gives:

$$\log E = \frac{1}{q}\log \rho + \frac{1}{q}\log p \tag{4.31}$$

From Figure 4.1 the following observations can be drawn:

- The power, *q*, indicates a scaling condition. $1/q$ is the slope of a line which can be used for the selection of the best material. Materials which lie on the same line perform equally. Since 1 and 1/3 are the powers which provide the most significant criteria, selection guide lines of slope 1 and 1/3 are reported on the left bottom of the Figure 4.1(a). In Section 4.4.1 the values of *q*, which provides the same performance for cross-sections of Aluminium, Steel and GFRP, were derived and are shown in Figure 4.1(a).

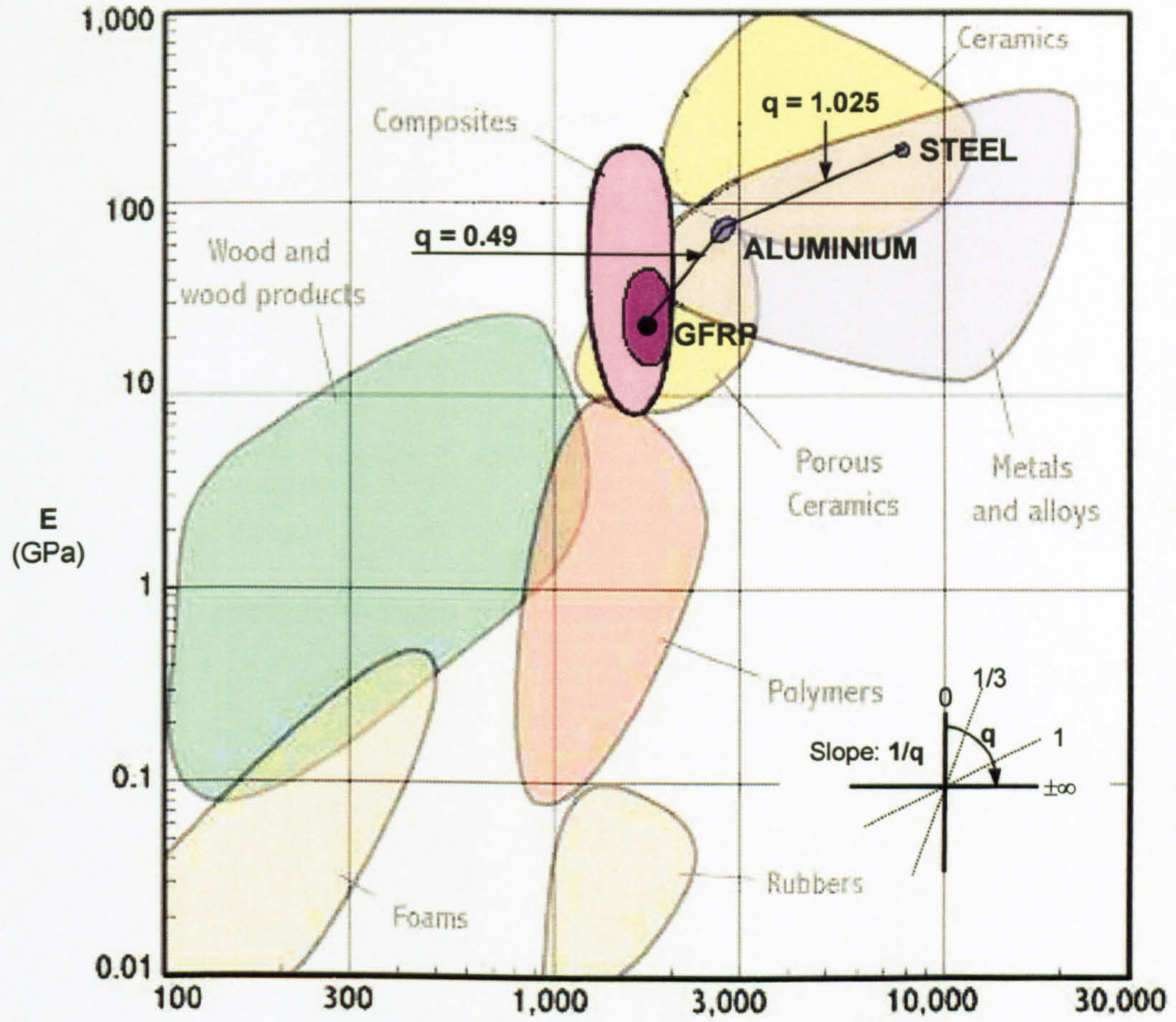

Figure 4.1 (a) Log-log scale material chart E - ρ for stiffness design.

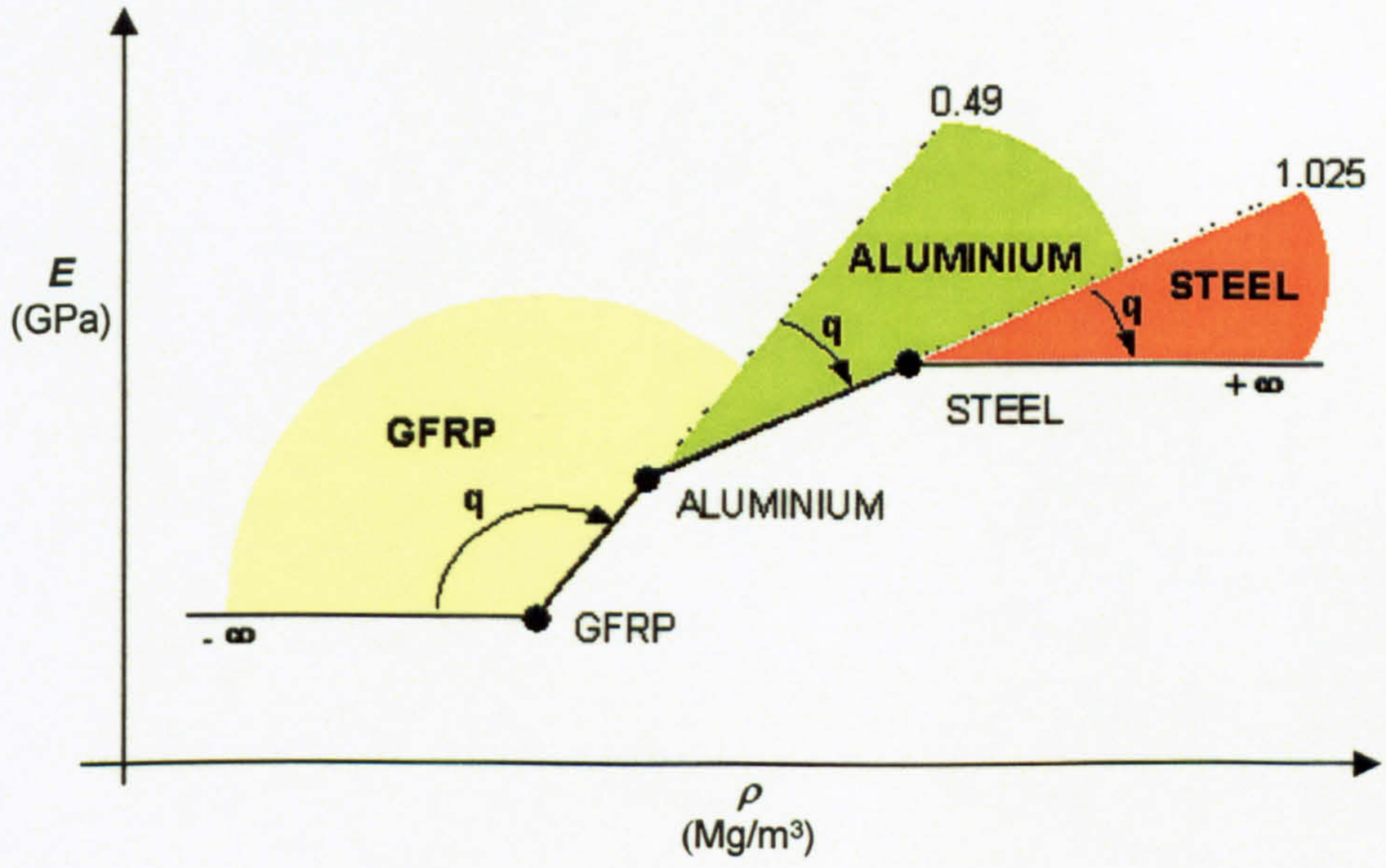

Figure 4.12 (b). A zoom of Figure 4.12(a) to show the best material for ranges of q.

- The ranges of q where one material performs better than another are shown in Figure 4.1(b). This is an enlarge view of Figure 4.1(a). This shows that the sizes of the envelope containing a material can provide better or worse performance with respect to the relative scaling of the sections.

4.6.3 Improved version of the material regimes map.

As explained in Chapter 2, the guidelines of slope 1/q in Figure 4.1 allows the selection of the best structure within the material domain. However, for arbitrary scaling it is always necessary to know how the envelopes are scaled. This limit is overcome by the material regimes chart which brings the selection in the context of the design space and, hence, both M and D can be simultaneously selected. A more comprehensive version of the earlier limiting material chart, shown in Figure 4.2, is illustrated in Figure 4.1 for four materials.

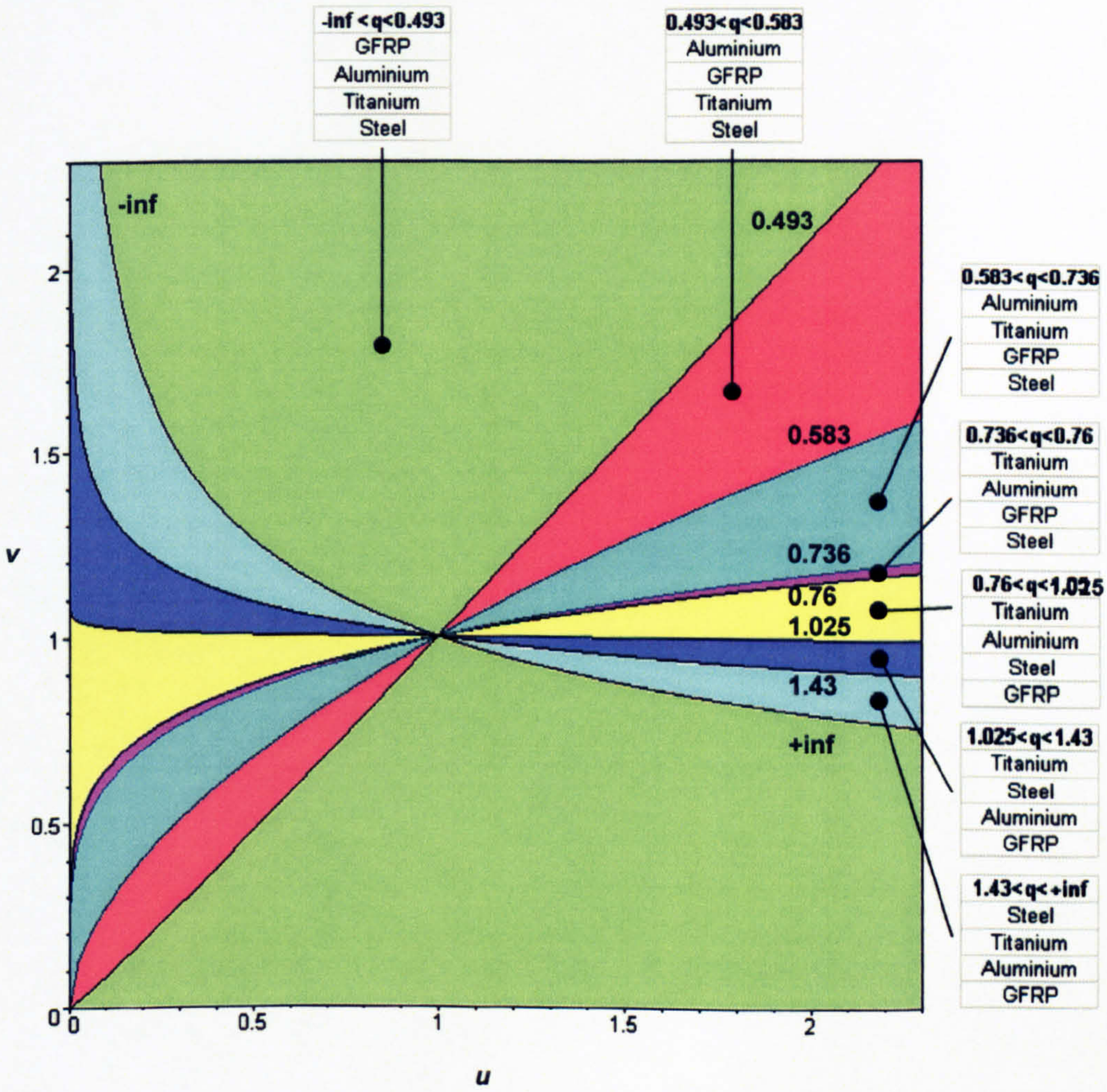

Figure 4.1 Example of limiting material implemented for four materials. Each colour corresponds to a material-ranking region defined by q ranges.

The improved version of the limiting material charts shown in Figure 4.1 has been created by using the plot of the performance index, $p=E^q/\rho$, for steel, aluminium, titanium and GFRP as a function of q. An example of this plot is shown in Figure 4.1 for three materials. From the plot of $p=E^q/\rho$ for steel, aluminium, titanium and GFRP, values of q where two materials have the same performance can be determined and ranking of materials for different ranges of q can be specified. Equation (4.26) has been used to plot in Figure 4.1 the curves of q of equal performance for steel, aluminium, titanium and GFRP. The ranking of the candidate materials from the best (top) to the worst (bottom) is shown for each coloured region. The ranking indicates how material compete in the design space for any scaling condition, q. Superimposing the stiffness curves, equation (3.13), for each material on the map shown in Figure 4.1 permits the whole design space to be explored. During a selection task, a group of available materials can be pre-selected and, using equations (4.25) and (4.26), a computerised implementation could be adopted to plot the material regimes.

4.7 MATERIAL TABLES

The general solution of the performance index can also be used to produce Tables of q for specific materials and angles of slope constraints for stiffness and strength design. These Tables can be used by designers to directly compare the performance of different cross-sections and materials for a particular application. Table 4.1 presents, as an example, values of q for two materials for a given stiffness requirement. An aluminium square section is chosen as reference section and the sloped constraint lies on its top right vertex. For a given sloped constraint, θ, such as that shown in Figure 4.1(c), the values of q in Table 4.1 can be used in equation (4.25) to assess the relative performance.

θ sloped constraint angle	**0°**	**10°**	**20°**	**30°**	**40°**	**50°**	**60°**	**70°**	**80°**	**90°**
q for steel and aluminium	1	1.25	1.54	1.85	2.18	2.56	3.03	3.69	4.88	1/3

Table 4.1 q values to be inserted in the performance index E^q/ρ to select the best material for a given sloped constraint angle. Note that the reference section is the aluminium square (Data: steel E=210 GPa ρ=7.9Mg/m^3, aluminium E=79 GPa ρ =2.9 Mg/m^3)

4.8 APPLICATIONS

The following application has the purposes of demonstrating the theory and showing how the method can be applied. (The data used are purely for illustration).

4.8.1 Design case

A design case study has been carried out using both selection charts: the combined graph, shown in Figure 4.1, and the limiting material regimes chart, shown in Figure 4.2. The final results are the same and are confirmed by the numerical calculations presented in Tables 4.3 and 4.4. The example is a 4-metre cantilever that must support an end load of 1000 N with an allowable end deflection, δ, of 3.2 cm. This is illustrated in Figure 4.1. Steel and aluminium are the candidate materials and these are assumed to be available in rectangular shapes. The design data are summarised in Table 4.2. Two design constraints are examined. First a height constraint is imposed, and second a sloped constraint with θ=16.6° and q = 1.44. These conditions are shown in Figure 4.1 (a) and (b).

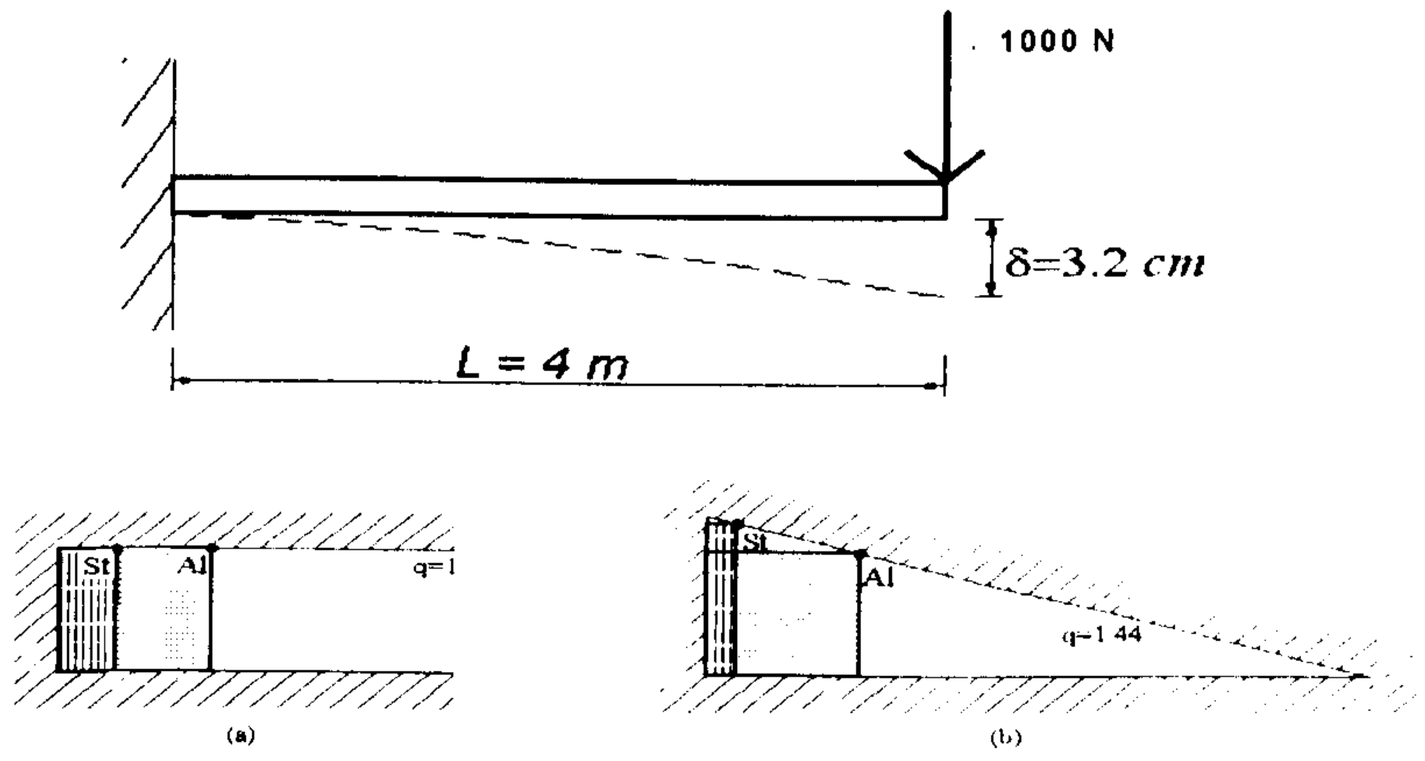

Figure 4.1 The cantilever and its cross-sections in two different constrained conditions: (a) height constraint·(q=1), (b) sloped constraint with θ=16.6° q=1.44).

Limiting material regimes graph

Figure 4.1 illustrates that, for steel and aluminium when q > 1.025, steel performed better than aluminium. The limiting regimes for the two materials are again illustrated in Figure 4.1 and Figure 4.2. In the first case, there is a height constraint, q =1 and a steel rectangular cross section, that provides the same stiffness, lies within the region where aluminium is better. Therefore aluminium provides lower mass. In the second case there is a sloped constraint, Figure 4.1(b). The same aluminium section 1x1m is compared with a steel rectangular cross-section. The sloped constraint

dictates the direction of scaling. Figure 4.2 illustrates that this constraint intersects the region where steel performs better than aluminium. This is in contrast to the first case, the steel cross-section has lower mass than aluminium.

Combined performance graph

The combined performance graphs for the two constraints q = 1 and 1.44, are illustrated in Figure 4.3 and Figure 4.4 respectively. For a horizontal constraint the graphical solution shown in Figure 4.3 demonstrates that the performance of the aluminium cross section is marginally better than steel. The numerical results in Table 4.2 show that the mass saving using aluminium is just 2%. When there is a sloped constraint, this leads to steel providing minimum mass. Table 4.3 shows that a remarkable mass saving of 33% is achieved.

This result demonstrates that geometric constraints can have a very important influence on what is an optimal material. Using the performance indices E/ρ, $E^{1/2}/\rho$ and $E^{1/3}/\rho$ always indicates that aluminium is better than steel. However, the design example shows that when there is a sloping height constraint with θ=16.6°, steel can be better than aluminium.

	Young's Modulus	Density	Load	Deflection	Stiffness requirement	Length	Boundary condition
	E	ρ	W	δ	k	L	c_1
	GPa	Mg/m^3	N	m	N/m	m	
Aluminium	79	2.9	1000	0.0324	30859	4	3
Steel	210	7.9	1000	0.0324	30859	4	3

Table 4.1 Design data for case study.

	Width	Height	Width multiplicator	Height multiplicator	Power q	Stiffness	Perform. index	Mass	Mass saving
	B	H	u	v	q	k	$p=\frac{E^q}{\rho}$	m	
	m	m				N/m		Mg	
Aluminium	1.00	1.00			1.00	30859	27.2	11.60	2%
Steel	0.376	1.00	0.376	1.00	1.00	30859	26.5	11.89	

Table 4.2 Numerical results for height constraint (q =1)

	Width	Height	Width multiplicator	Height multiplicator	Power q	Stiffness	Perform. index	Mass	Mass saving
	B	H	u	v	q	k	$p=\frac{E^q}{\rho}$	m	
	m	m				N/m		Mg	
Aluminium	1.00	1.00			1.44	30859	186.3	11.60	
Steel	0.197	1.24	0.197	1.24	1.44	30859	279.6	7.731	33%

Table 4.3 Numerical results for sloped constraint (q=1.44)

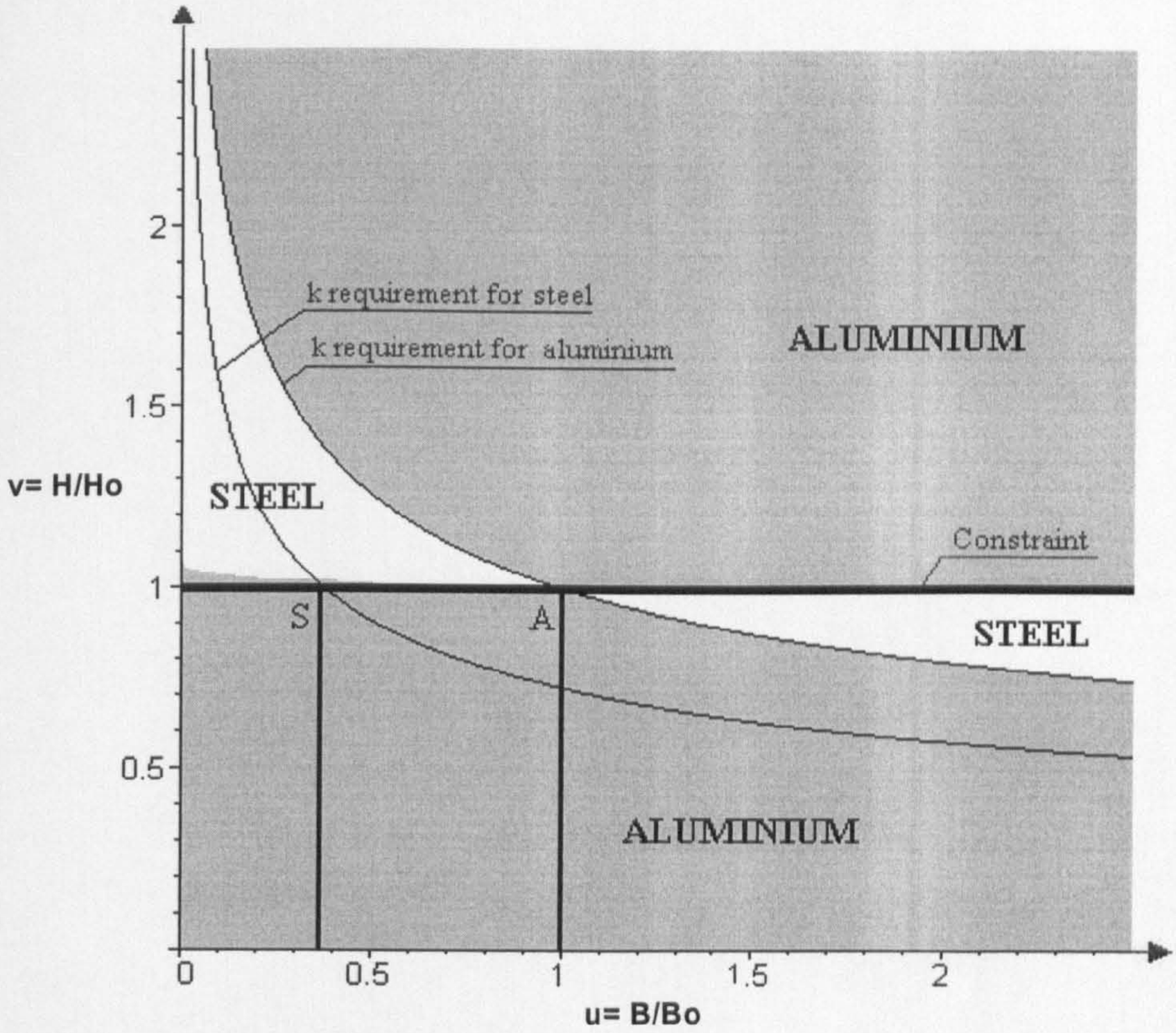

Figure 4.1 Limiting material regimes graph for a horizontal constraint (q=1)

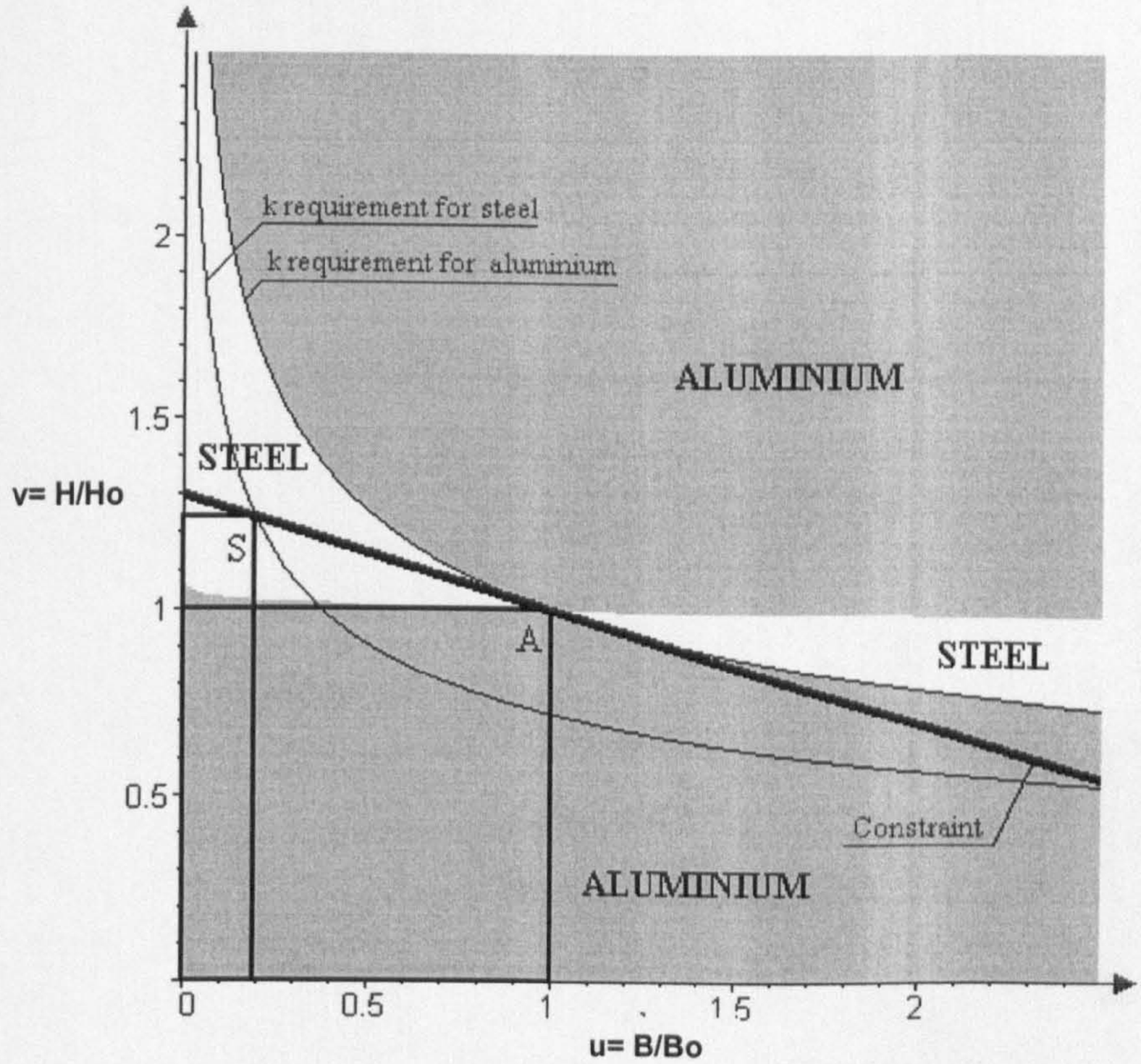

Figure 4.2 Limiting material regimes graph for a sloped constraint (q=1.44).

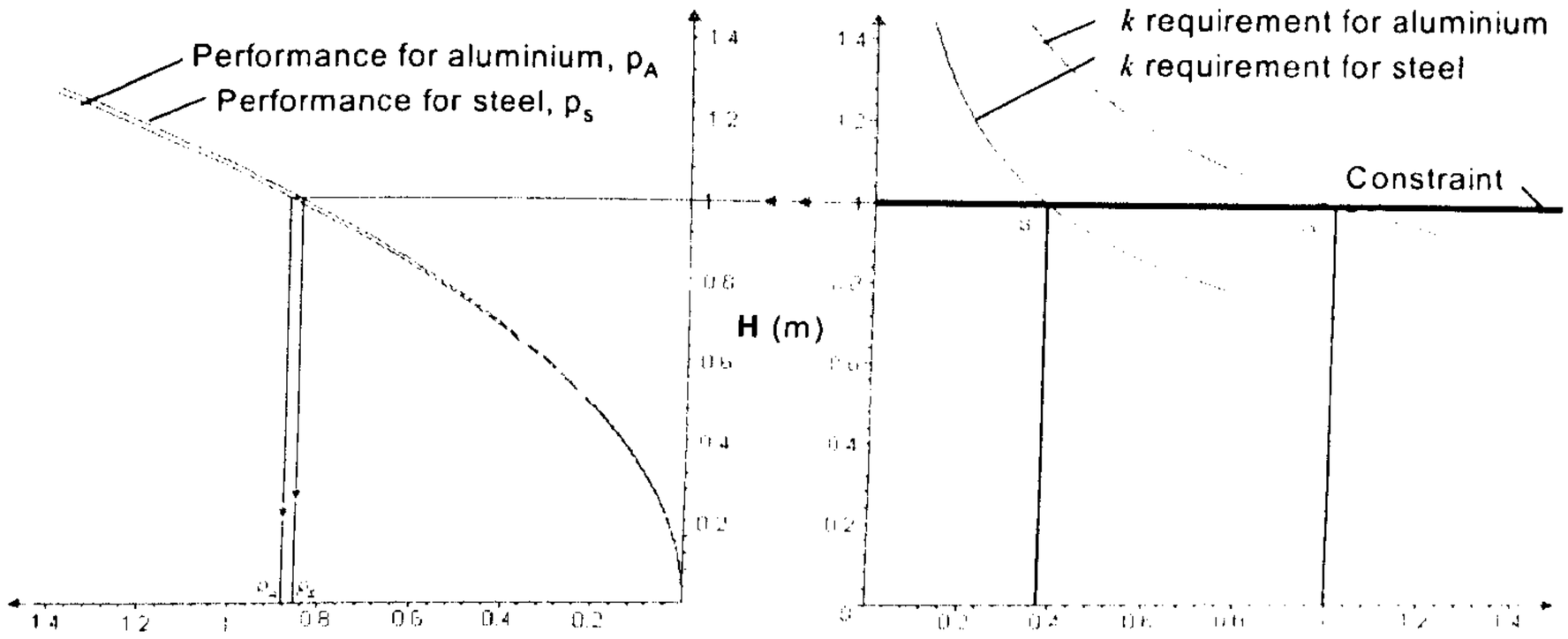

Figure 4.3 Combined graph for a horizontal constraint (q =1).

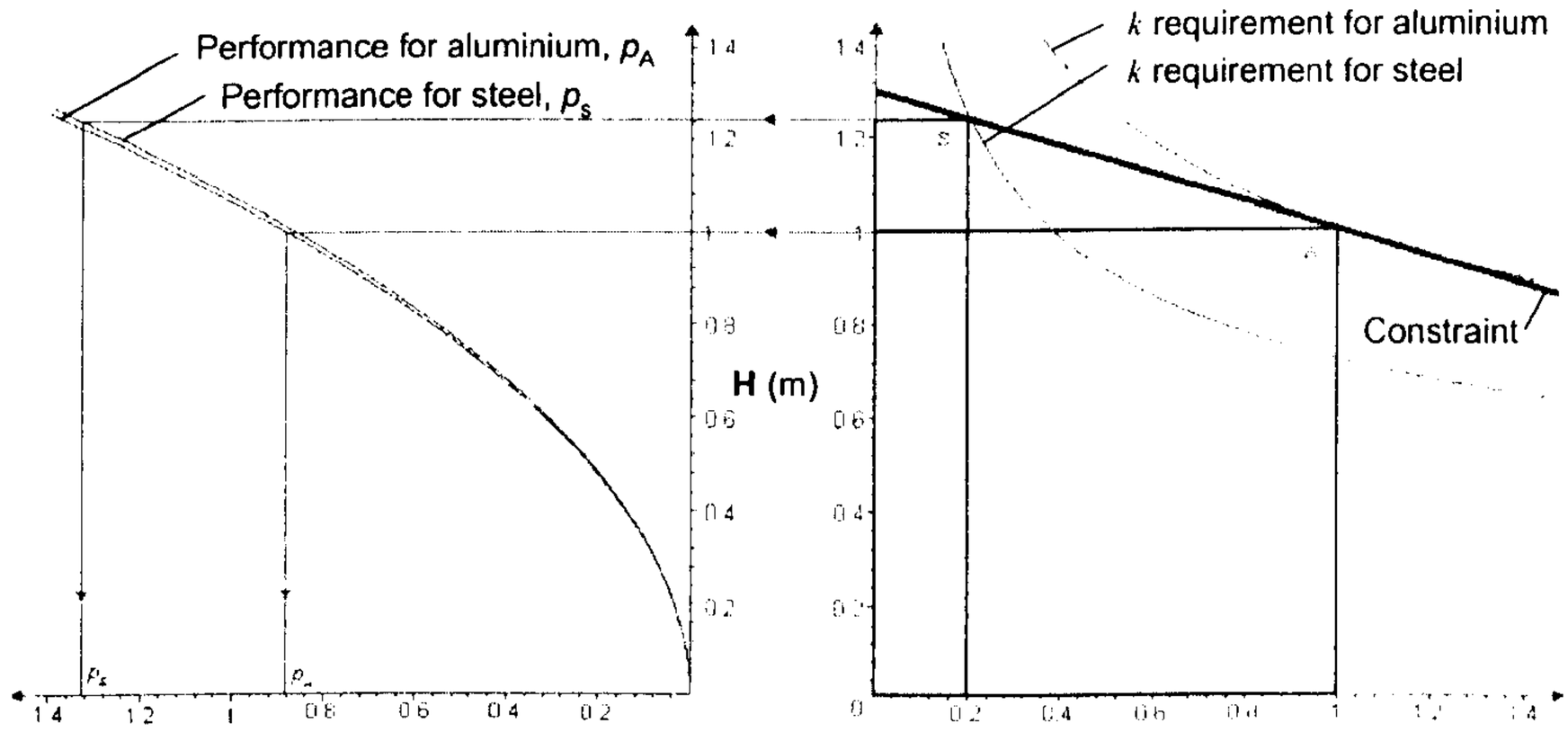

Figure 4.4 Combined graph for a sloped constraint with θ=16.6° (q=1.44).

4.9 SUMMARY

In this Chapter, the mass-efficiency of sections with a prescribed shape has been modelled. General expressions of the performance criterion and of the performance index have been given for stiffness and strength design and can be applied for any arbitrary direction of scaling. The approaches have been examined and it has been shown that when the direction of scaling is known, the performance criterion is the performance index given by a combination of material properties. The approaches have been explored graphically. Different types of design charts have been introduced to facilitate understanding. Combined graphs, material regime maps and material charts in normal and logarithmic scale, can help the designer in a selection task. Material, M, and shape, S, properties determine the sizes of the envelope, D, for cross-sections satisfying a design requirement. When geometrical constraints impose a particular direction of scaling to the envelope, D, this can have an important influence on what is the best material.

CHAPTER 5

SELECTION OF CROSS-SECTION SHAPES

5.1 INTRODUCTION

The performance criterion and the performance index are used in this Chapter to examine the case where the structures differ for the variables envelope, *D*, and shape, *S*, as shown in Figure 3.6c). This corresponds to selection condition 3 of the design scenarios in Table 3.5. Stiffness and strength are the design requirements considered in the analysis. In this Chapter, the material *M* is a fixed parameter and it is assumed to be homogenous and isotropic. In addition it is assumed that the material obeys Hooke's law and has Young's modulus *E* and yield strength σ_y which is the same in tension and compression.

This Chapter is divided into five parts:

- In the first part, the **feasible solutions** which satisfy the functional requirement **in the design space** are illustrated for structures which differ for the shape *S*. Examples of **geometrical constraints** applied to cross-sectional shapes in the design space are illustrated. The purpose is to show how spatial restrictions rule the magnitude and the direction of scaling of the structural envelopes, *D*.
- In the second and third parts, the performance criterion and the performance index are used to derive analytical expressions of the performance of different cross-sections and to illustrate graphically the process of selection. The performance criterion uses the **"combined selection graph"** to elucidate the

effect of envelope variations on the efficiency in the case of solid shapes for a stiffness requirement and hollow shapes for strength design. The general solution of the **"performance index"** for the variable *S* is derived to enable the selection of the best shape for any arbitrary direction of scaling. A **shape regimes chart** is developed in analogy to the material regimes chart in Chapter 4.

- The fourth part starts with a brief summary of the relationship and the features of the approaches. Then, the performance criterion is used to produce the **envelope efficiency map**, which plots on natural axes the shape properties (ψ_A, ψ_I). The performance index, on the other hand, is employed to select low-mass cross-section shapes in a logarithmic scale chart.
- The last section considers the envelope efficiency map and the limiting shape regimes graph. The envelope efficiency map is used to derive geometric conditions to optimise the dimensions of different cross-sectional shapes. The limiting shape regimes graph is applied with the performance index in a design application to show the effect of geometrical constraints on the efficiency of structures.

5.2 FEASIBLE CROSS-SECTIONS IN THE DESIGN SPACE

5.2.1 Curves of the functional requirement

Chapter 4 showed that the functional requirement is a relation satisfied by an infinite number of cross-sections. A requirement curve describes an infinite number of feasible solutions (*BxH*) of the envelope, *D*. In addition, each material, *M*, identifies a unique curve which subtends a unique space. When the property variable is *S*, rather than *M*, the cross-sections differ for the shape transformers. In this case, the bending stiffness requirement, *k*, of structures, expressed by equation (3.13), is rearranged as:

$$\frac{12kL^3}{c_1 E} = \psi_I BH^3 \tag{5.1}$$

where the left hand side contains the specifications of the problems, and the variables, *D* and *S*, are on the right.

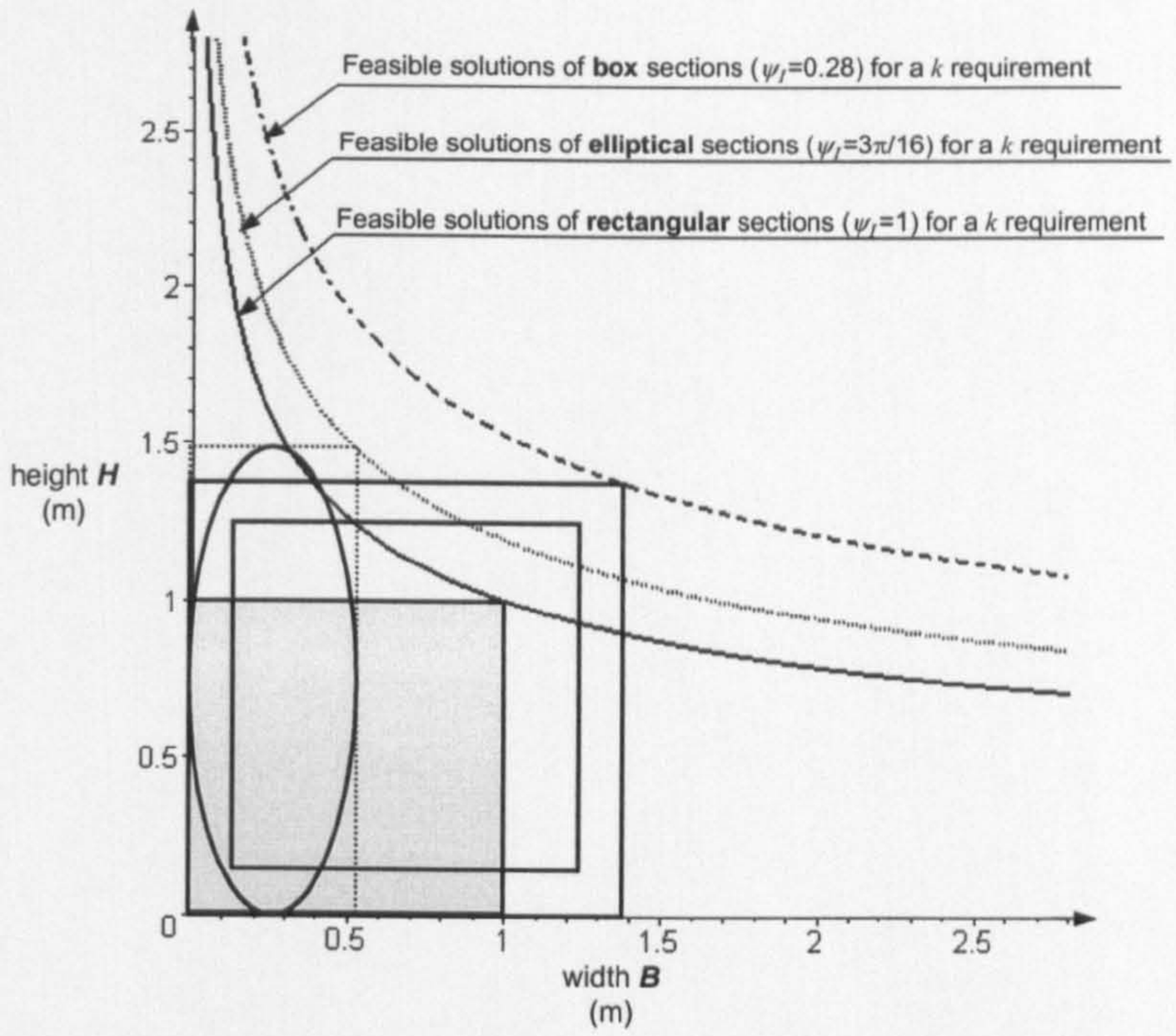

Figure 5.1 Stiffness requirement, *k*, for square, ellipse and box cross-sections of the same material, i.e. steel.

Figure 5.1 illustrates curves obtained using equation (5.1). The curves are the feasible solutions of three different steel cross-sections (ρ=7.9 Mg/m^3, E=210 GPa) of equal stiffness k=420*10^6 Nm of a cantilever of length, L=5m. From Table 3.3, the shape properties (ψ_A, ψ_I) of the envelopes are respectively: S_1(1,1) for rectangular cross-sections, S_2(π/4, 3π/16) for elliptical cross-sections, S_3(0.15, 0.28) for the box sections shown in Figure 5.1. The shape property, ψ_I, identifies a requirement curves of the envelopes, *BxH*, in the same way as the material property, *E*, satisfies the requirement in Figure 4.1 when *M* is variable. This shows that the effect of the material properties on the space subtended by the curves of the feasible cross-sections is analogous to the effect produced by the shape transformers.

5.2.2 Constrained cross-sectional shapes

For a given design requirement, such as stiffness or moment failure, solutions for a cross-section in the design space are represented by a curve, e.g. Figure 5.1. A unique space is determined by the properties contained in the envelope. Geometrical constraints restrict the space of cross-sections. The constraints must also be taken into account in the case where the variable property is the shape, *S*, rather than the material, *M*.

As explained in Chapter 4, in any field of engineering it is common to deal with height, width and slope constraints, such as those shown in Figure 5.1, when selecting the lightest shape for a structure. In Figure 5.1(a) and (b) one dimension of the envelope is fixed respectively by a height and width constraint which impose the sections to be horizontally and vertically scaled. Figure 5.1(c) shows a slope constraint which limits the magnitude and direction of scaling at an angle θ.

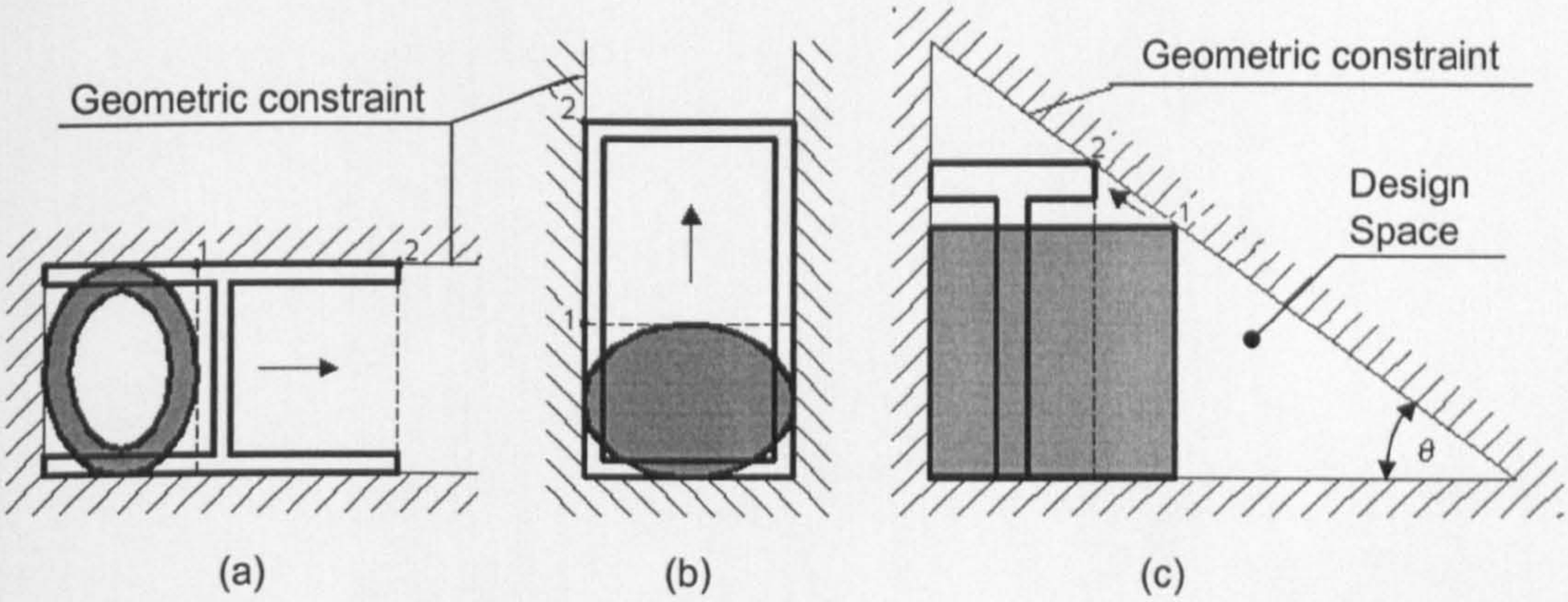

Figure 5.1 Geometric constraints and the direction of scaling on cross-sections of different shapes: (a) height constraint, (b) width constraint, (c) slope constraint

In general, arbitrary scaling of envelopes for different shapes, *S*, is shown in Figure 5.3. The multiplicators, *u* and *v*, are employed to describe the scaling of different cross-sections. They assume particular values for constraints of the height, *v* =1 (direction X in Figure 5.3), of the width, *u* =1 (direction Y in Figure 5.3), and for proportional scaling, u=v, (direction Z in Figure 5.3).

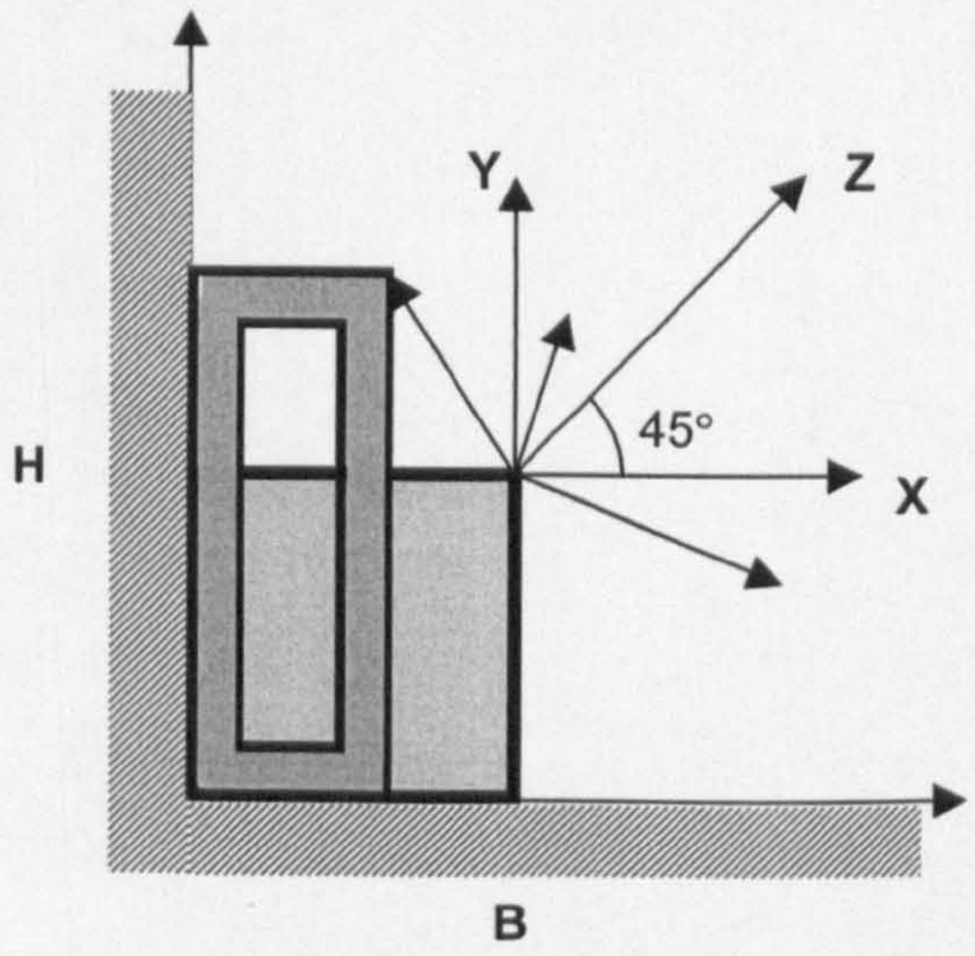

Figure 5.2 Arbitrary direction of scaling of square: X) Horizontal scaling: *v* =1, Y) Vertical scaling: *u* =1, Z) Proportional scaling: *u=v*

For any geometric constraint, the selection of the best shape, which minimises the mass of a structure, can be carried out with two complementary approaches: the performance criterion, which is presented in Section 5.3, and the performance index whose expression is derived in Section 5.4.

5.3 THE PERFORMANCE CRITERION

The ratio of the requirement to the objective function is the definition of the performance criterion as described in Chapter 4. Since the objective function is the mass, maximising the performance minimises the mass of a structure.

The performance criterion is used in this Chapter for the selection condition 3 of Table 3.5, where the variables of a design case are *D* and *S*. Since *M* is fixed, all the structures are made of the same material. The performance criterion uses the combined graph to illustrate solutions for stiffness and strength requirements. However, in order to avoid repetition, the combined graph considers the case of solid shapes in stiffness design and hollow shapes for strength design. It is evident that the observations drawn for the stiffness of solid shapes can be extended to hollow sections for strength and vice versa. Because of the analogy between material, *M*, and shape, *S*, properties, the format presented here is similar to that described in Section 4.3 for material selection.

5.3.1 Stiffness design

If the parameters envelope, *D*, and shape, *S*, are both variable in a design application, the performance criterion, $\tilde{p}$, in stiffness design, is given by the ratio of equations (3.13) and (3.11):

$$\tilde{p} = \frac{k}{m} = \frac{c_1}{12L^4} \ \frac{E}{\rho} \ \frac{\psi_I}{\psi_A} \ H^2 \tag{5.2}$$

and since $\lambda_I = \psi_I / \psi_A$, as defined by equation (3.9), the performance , p, is

$$p = \frac{1}{m} = \underbrace{\left[\frac{c_1}{12kL^4}\right]}_{F} \ \underbrace{\left[\frac{E}{\rho}\right]}_{M=const} \ \underbrace{[\lambda_I]}_{S} \ \underbrace{[H^2]}_{D=f(S)} \tag{5.3}$$

The second member of equation (5.3) has four factors. In this case, the variables are *S* and *D*, whereas the material parameters are fixed. *F* represents the functional requirements.

The groups of parameters in (5.3) are not independent because in stiffness design, both the equations (3.13) and (5.3) must be generally considered for the selection. In a similar way with Figure 4.1, in Figure 5.1 the height of the envelopes, *D*, are function, $H=f(1/B\psi_I)$ (see equation (5.1)), of the shape properties and are solutions of the stiffness requirement curve. Therefore, the variable $D=f(S)$ is not generally separable from *S* and λ_I cannot be considered as the only criterion. This is shown in the next Section with the selection-combined graph.

Combined selection graph for solid shapes

Figure 5.1 gives a graphical solution to the optimal cross-section selection where *D* and *S* are the design variables. On the right hand side, curves of constant stiffness k, equation (5.1), for different solid cross-sectional shapes are illustrated. On the left hand side, the performance criterion given by equation (5.3) is displayed. The data used in Figure 5.4 are for a steel (ρ=7.9 Mg/m^3, E=210 GPa) cantilever, c_1=3, of length L=5m which has an end load and which has to meet a stiffness requirement k=420*10^6 N/m.

Of all the cross sections, the rectangle is the shape that completely occupies the available space and, therefore, it provides a spatial benefit. No other shape can meet the stiffness requirement for the same dimensions (width and height) of the envelope. If the design goal is **to minimise space** rather than mass, then **the best shape is the rectangle.**

The performance of shapes is dependent on the dimensions of the space envelope *D*. For example, three different envelopes are shown in Figure 5.4, one for a rectangle, R, and the other for two ellipses, E_1 and E_2. The performance of ellipse E_1 is better than for the rectangle R. However, the opposite result can be obtained if E_2 is compared with R. In addition, Figure 5.4 shows that the scaling of the envelope is possible from any point of a curve to another because $D=f(S)$. For arbitrary scaling of the envelopes sizes both multiplicators, *u* and *v*, are unknown because $u \neq v \neq 1$. X, Y, Z are three particular scaling conditions which corresponds to horizontal, vertical

and proportional. Imposing scaling conditions, X, Y or Z, to the envelopes gives u=1,v=1 and u=v respectively.

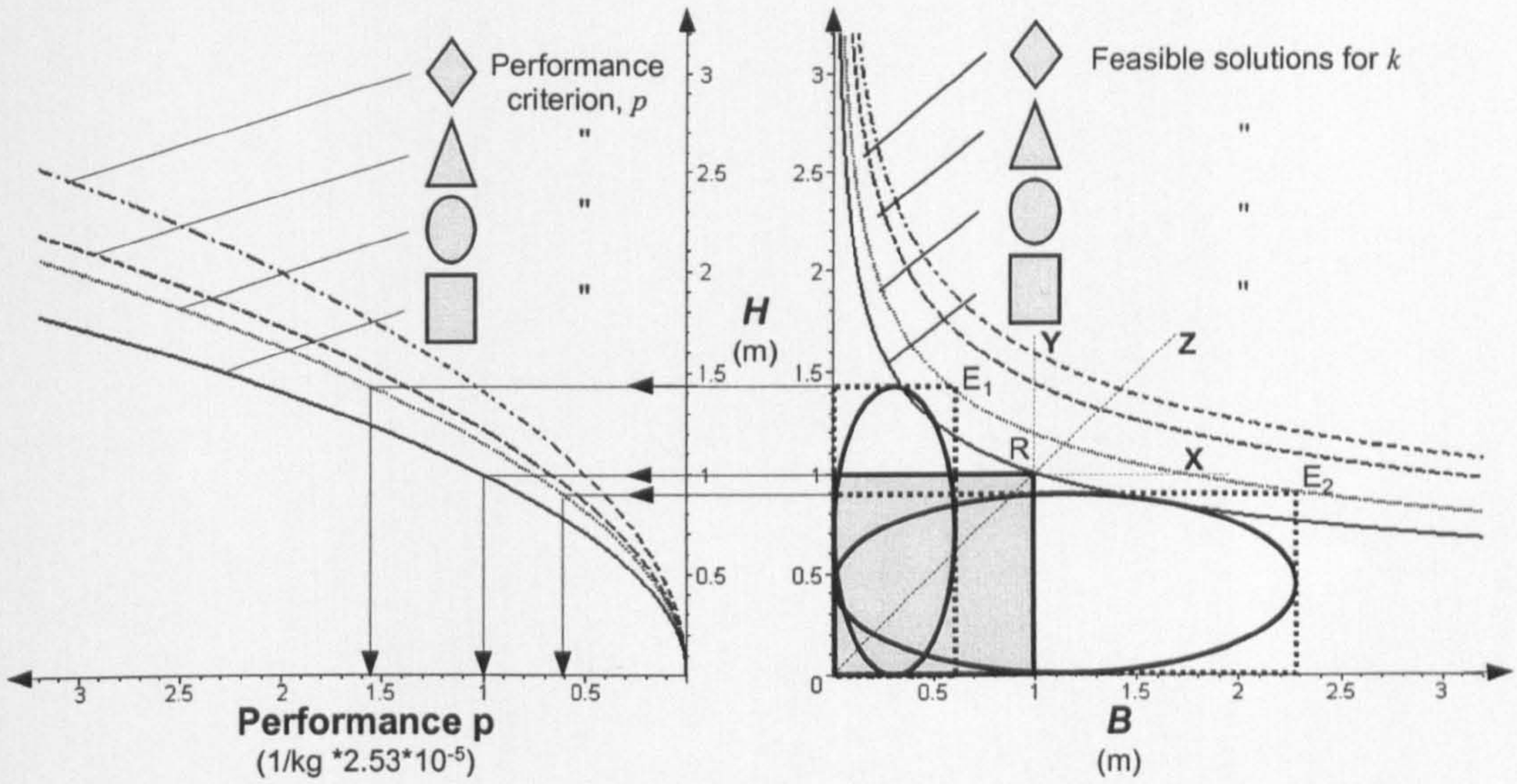

Figure 5.1 Combined graph for *D* and *S* variables for solid sections in stiffness design. (The data are for illustration).

5.3.2 Strength design

In strength design, the selection criterion for cross-sections where *D* and *S* are variables, is given by the ratio of equations (3.14) and (3.11):

$$\frac{M_y}{m} = \frac{1}{L}\frac{\sigma_y}{\rho}\frac{\psi_Z}{\psi_A}\frac{H}{6} \tag{5.4}$$

and the performance, p, is given by:

$$p = \frac{1}{m} = \underbrace{\left[\frac{1}{6LM_y}\right]}_{F}\ \underbrace{\left[\frac{\sigma_y}{\rho}\right]}_{M=const}\ \underbrace{[\lambda_Z]}_{S}\ \underbrace{[H]}_{D=f(S)} \tag{5.5}$$

There are four groups of parameter in expression (5.5). *F* represents the functional requirement and the boundary conditions parameters of the problem, shape properties, *S*, and envelope sizes, *D*, are variable. The material parameters, *M*, are fixed.

As with stiffness design, the factors in (5.5) are not independent. Both the equation of the strength requirement (3.14) and the equation of the performance criterion (5.5) must be considered. According to equation (5.5), the height of the envelope, D, is a function of the shape transformer, i.e. $H=f(1/B\psi_Z)$, and therefore λ_Z cannot be generally considered as the criterion of selection.

Combined graph for hollow shape selection

The earlier results for solid sections in stiffness design is extended to consider hollow shapes for a strength requirement. As with Figure 5.4, Figure 5.5 shows curves for the failure moment M_y (equation 3.14) and performance of both solid and hollow sections (equation 5.5). The data used in Figure 5.4 is for a steel (ρ=7.9 Mg/m^3, σ_y=280 MPa) cantilever, c_1=3, of length L=5m which has an end load and which has to meet a moment failure M_y=46.6*10^6 Nm.

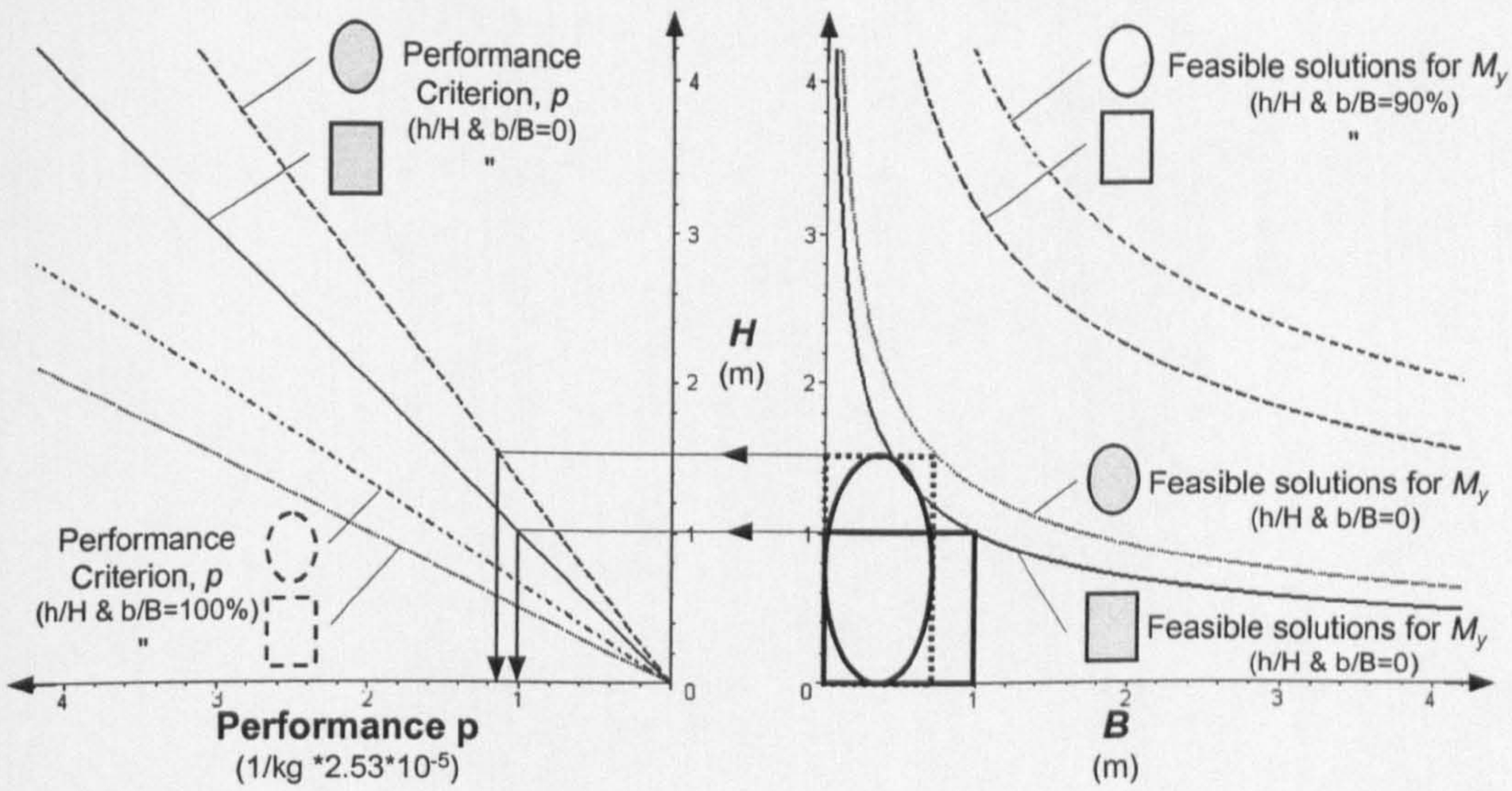

Figure 5.1 Combined graph for D and M variables for solid and hollow sections in strength design. (The data are purely for illustration).

Solid shapes generally require less space but have lower λ_Z. Figure 5.1 shows that as b/B and h/H ($0<b/B<1$, $0<h/H<1$) increase, the strength requirement curves of hollow cross-sections move upwards from curves provided by their respective solid shapes (b/B=0, h/H=0) to a theoretical limit where $h=H$ and/or $b=B$ and the thicknesses reduce to 0. Since these limit conditions cannot be visualised in the design space, a feasible limit of the strength curves has been plotted for b/B=90%, h/H=90% on the right of Figure 5.5. In contrast, the performance criterion for the

values h=H and/or b=B, i.e. no thickness, (for b/B=100%, h/H=100%) can be represented by limiting curves on the left of Figure 5.5. This is because the values of λ_Z have a finite range as shown in Table 3.4. For a given design requirement, there are limits to the heights of the envelopes due to buckling. These are investigated in Section 6.7.

5.4 THE PERFORMANCE INDEX

The cross-section is conceived as an envelope containing material and shape properties. The shape properties, S, of a section, called shape transformers, have been defined in Chapter 3 as geometrical quantities of the shape with respect to its surrounding envelope, D. Chapter 4 has illustrated the general solution of the performance index E^q/ρ where M and D are variable. This Section uses the analogy between material and shape to derive an expression of the performance index p= $f(S,D)$ where S, rather than M, is the variable property.

5.4.1 Modelling the geometric properties

In order to derive the general solution of the performance index for the variable S, the relevant geometric quantities are firstly modelled for each design context. This is carried out for the variables D and S as follows:

- ***D***: the multiplicators, u and v, relate the envelope sizes of the square reference and a generic section. The relations, in terms of area, second moment of area and section modulus between the reference and a generic shape envelope are:

$$\begin{cases} \dfrac{A_D}{A_o} = uv \\ \dfrac{I_D}{I_o} = uv^3 \\ \dfrac{Z_D}{Z_o} = uv^2 \end{cases} \tag{5.6}$$

- ***S***: the shape transformers ψ_A, ψ_I, and ψ_Z link the geometric quantities, *G*, of a shape and its envelope, i.e. $S=G/G_D$. The definitions in 3.4.2, are here repeated for clarity:

$$\begin{cases} \psi_A = \dfrac{A}{A_D} \\ \psi_I = \dfrac{I}{I_D} \\ \psi_Z = \dfrac{Z}{Z_D} \end{cases} \tag{5.7}$$

- ***D* and *S***: the relations between a generic cross-section and the reference are:

$$\begin{cases} \dfrac{A}{A_o} = \dfrac{A}{A_D}\dfrac{A_D}{A_o} = \psi_A uv \\ \dfrac{I}{I_o} = \dfrac{I}{I_D}\dfrac{I_D}{I_o} = \psi_I uv^3 \\ \dfrac{Z}{Z_o} = \dfrac{Z}{Z_D}\dfrac{Z_D}{Z_o} = \psi_Z uv^2 \end{cases} \tag{5.8}$$

These expressions are used to derive a general expression of the performance index for arbitrary scaling of the cross-sectional shapes for a stiffness and strength requirement.

5.4.2 Stiffness design: general solution $\psi_I{}^q/\psi_A$ for any arbitrary scaling

Selection condition 3 of Table 3.5 shows that the performance index, *p=f(S,D)*, is a function of the variables *S* and *D*. However, if the direction of scaling is known, the performance index can be seen as a combination of only shape properties, *p=f(S)*, which enables the selection of the best shape for a particular application. Analogous to 4.4.1, this Section illustrates the derivation of a general performance index for any arbitrary scaling.

Analysis

For two structures of the same length and material, the ratio of their masses, *m* (for the generic case) and m_o (for the reference case) is:

$$\frac{m}{m_o} = \frac{\rho}{\rho_o}\frac{A}{A_o} = \psi_A uv \tag{5.9}$$

Maximising the performance index minimises the mass. Therefore from (5.8), the ratio of the performance indices of a generic structure relative to the reference structure is:

$$\frac{p}{p_o} = \frac{m_o}{m} = \frac{1}{\psi_A uv} \tag{5.10}$$

For bending stiffness design, the generic and the reference structures are required to meet the same stiffness requirement, where:

$$E_o I_o = IE \tag{5.11}$$

From (5.8) the ratio of the stiffness of the two structures of the same material (E=E_o) can also be stated in terms of multipliers, u and v, and geometric transformer, ψ_I , so that:

$$\frac{I}{I_o} = \psi_I uv^3 \tag{5.12}$$

Performance index for a height constraint.

When the height of the two structures is constrained v=*1*, and u is:

$$u = \frac{I}{I_o}\frac{1}{\psi_I} \tag{5.13}$$

and from (5.10) the ratio of the performance indices is:

$$\frac{p}{p_o} = \frac{\psi_I}{\psi_A} = \lambda_I \tag{5.14}$$

Equation (5.14) is comparable to the performance index E/ρ for the case where the material M is variable.

Performance index for a width constraint.

When the width is constrained *u=1*, and *v* is given by:

$$v = \left(\frac{I}{I_o} \frac{1}{\psi_I} \right)^{1/3} \tag{5.15}$$

and from (5.10) the ratio of the performance indices is:

$$\frac{p}{p_o} = \frac{\psi_I^{1/3}}{\psi_A} \tag{5.16}$$

Equation (5.16) permits the selection of the best shape, *S*, for a width constraint in the same way that $E^{1/3}/\rho$ is the performance index for selecting the best material, *M*.

General solution of the performance index for arbitrary scaling.

For $u \neq 1$ and $v \neq 1$, a general solution is sought. The ratio of the performance indices can be written as:

$$\frac{p}{p_o} = \frac{\psi_I^{q}}{\psi_A} \tag{5.17}$$

where *q* is an expression which is yet to be determined, but known to be $q=1$ for constrained height and $q=1/3$ for constrained width.

For generic *u* and *v*:

$$u = \left(\frac{1}{\psi_I} \right)^{\alpha}$$
$$v = \left(\frac{1}{\psi_I} \right)^{\beta} \tag{5.18}$$

and using expressions (5.18) in equation (5.12) gives:

$$\psi_I uv^3 = \left(\frac{1}{\psi_I}\right)^{\alpha+3\beta} \tag{5.19a}$$

and

$$\alpha + 3\beta = 1 \tag{5.19b}$$

From equation (5.18), the exponents α and β are:

$$\begin{cases} \alpha = \lg_{\left(\frac{1}{\psi_I}\right)} u = \lg_{(uv^3)} u \\ \beta = \lg_{\left(\frac{1}{\psi_I}\right)} v = \lg_{(uv^3)} v \end{cases} \tag{5.20}$$

The ratio of the performance indices p/p_o follows from equation (5.10) using equations (5.18) through (5.20), so that:

$$\frac{p}{p_o} = \frac{{\psi_I}^q}{\psi_A} \tag{5.21}$$

where q:

$$q = \log_{(uv^3)} uv = \frac{\ln uv}{\ln uv^3} \tag{5.22}$$

Equation (5.21) allows the relative performance index for arbitrarily scaled structures of different cross-sectional shapes to be compared. The exponent q represents a parameter that describes the scaling of the dimensions of the cross-sectional envelopes due to changes of the shape S. In particular, it is a function of u and v, which are the scaling factors of the width and the height of the section envelopes. It is evident that the general solution of the performance index for condition 3 of Table 3.5, takes the form of the function $p=f(S,D)$.

In Figure 5.1, regions for the scaling parameter $q=f(u,v)$ have been plotted. Values of $q=1/3$, $q=1/2$, $q=1$ are for constrained width, proportional scaling and constrained height respectively. Shapes with values of ψ_I near to 1, such as hollow rectangles,

perform relatively better for high values of q. In contrast, when q approaches zero the value of the area, ψ_A, is more important than the value of the second moment of area, ψ_I. This confirms that the direction of scaling has a very important effect not only on the material selection but also on the shape selection. Figure 5.6 shows two examples of arbitrarily scaled envelopes. If the reference structure A, for instance, has a cross-section of unit dimensions, and, according to the stiffness requirement, is rescaled with $u=B/B_o=b/b_o$ and $v=H/H_o=h/h_o$ so that point A of the shape envelope moves to point A', then $1/3<q<1/2$. Distinct regions for other ranges of q are shown.

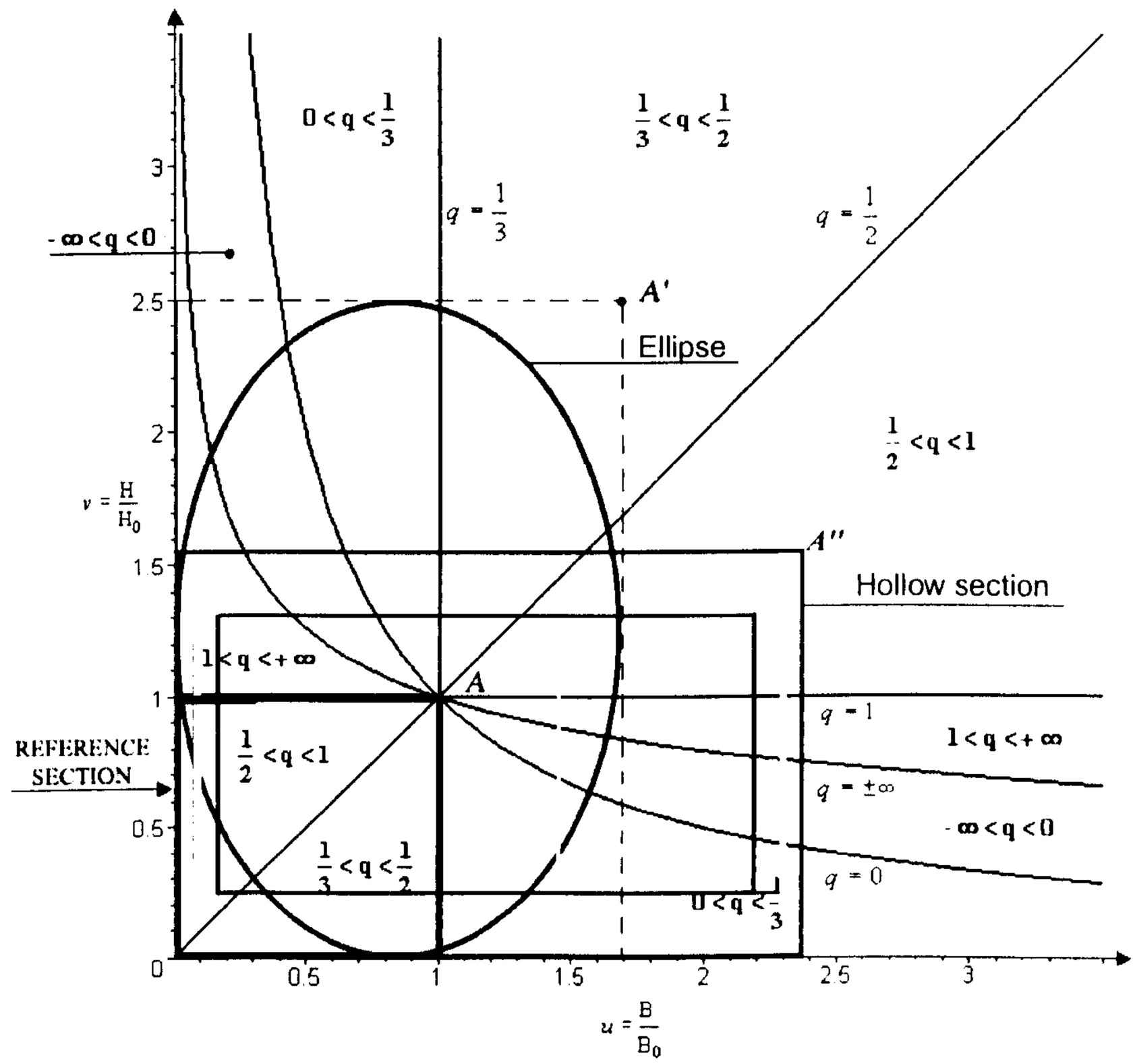

Figure 5.1 How scaling affects the scaling parameter q. Cross-section A': $1/3 < q < 1/2$, Cross-section A'': $1/2 < q < 1$

Limiting shape regimes

In this Section, the general solution of the performance index, equation (5.21), is used to provide a performance map, which can help the designer in the selection of

light shapes for any scaling condition. This is similar to the chart of the limiting material regimes presented in Chapter 4.

Whilst the performance index E^q/ρ gives the selection of the best material for structures whose cross-sections have a fixed shape, ${\psi_I}^q/\psi_A$ governs the selection where $p=f(S,D)$ for a given stiffness requirement, k. This analogy exists because for a given design requirement, cross-sectional envelopes experience dimensional variations in accordance with their values of shape, ψ_I, and/or material, E, properties.

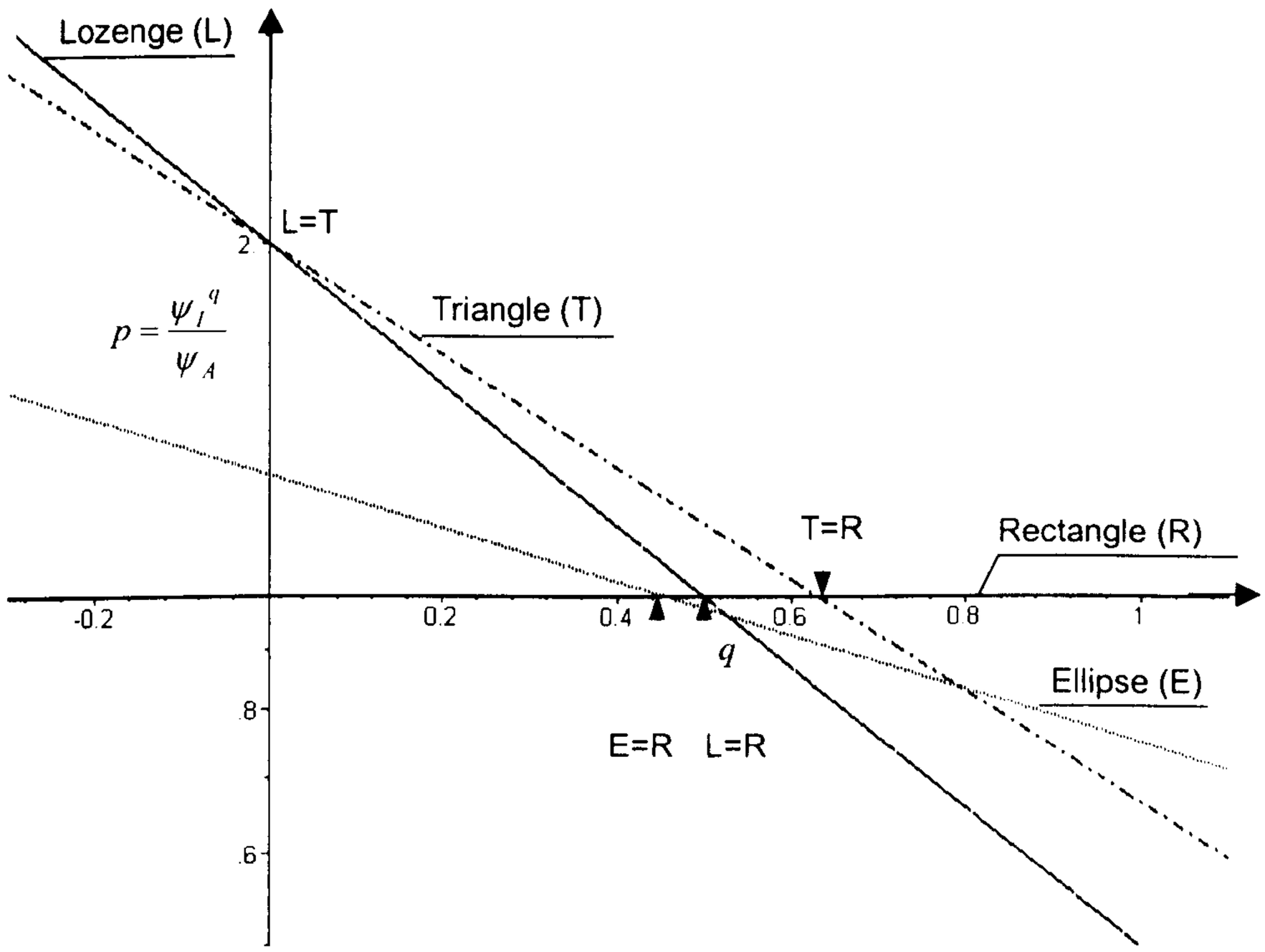

Figure 5.1 Performance index as a function of the scaling parameter q for four shapes.

Examples of a full range of solutions for equation (5.21) are shown in Figure 5.1 for four solid shapes: lozenge, triangle, ellipse and rectangle. The performance index has been plotted as a function of the scaling parameter q using values of ψ_I and ψ_A given in Table 3.3. Since the rectangle is the envelope of any shape and the shape properties are unity, the curve for p as a function of the scaling parameter, q, in Figure 5.1 is a horizontal line with p=1 for all q. The intersection points among the four lines represent values of q where two shapes perform equally. For values of the

scaling parameter q less than 0, a lozenge provides better performance, whereas for positive q less than 0.631 triangular cross-sections are better. Rectangular cross-sections are lighter for q greater than 0.631.

The scaling parameter for the shapes is q. The variation in v as a function of u and q can be found by inverting equation (5.22) so that:

$$v = u^{\frac{(1-q)}{(3q-1)}} \tag{5.23}$$

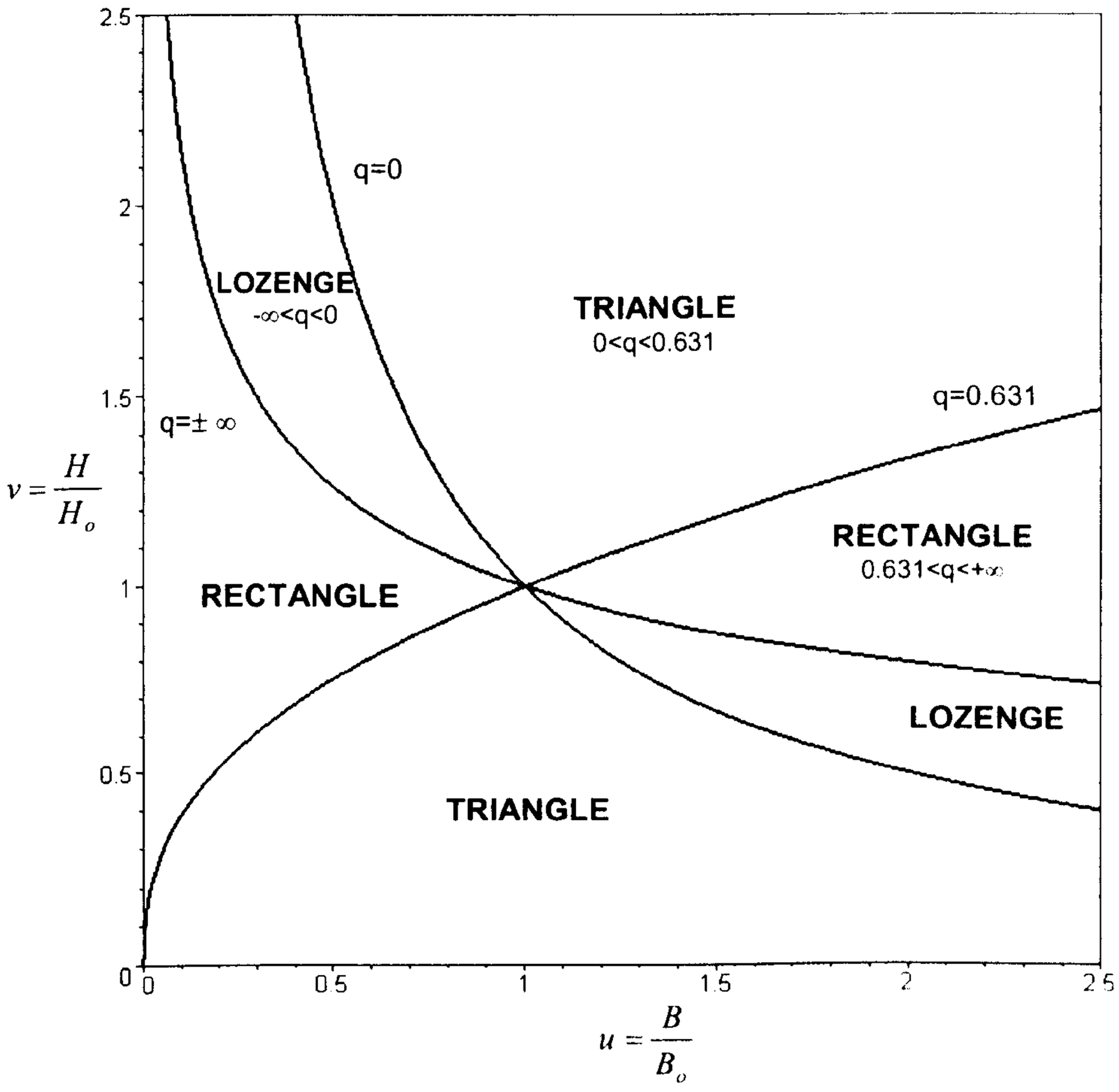

Figure 5.2 Example of limiting shape regimes for rectangle, triangle and lozenge.

Using equation (5.23), curves of special values of q for which two shapes have the same performance index (see Figure 5.7) are plotted on the design space in Figure 5.8, which is called the **limiting shape regimes chart**. Ranges where one shape provides better performance compared to others are shown in the design space u, v.

In Section 5.8.2 the limiting shape regimes is used in a design application to compare the rectangle with I-sections.

5.4.3 Strength design: general solution $\psi_Z{}^q/\psi_A$ for any arbitrary scaling

The derivation of the performance index for strength design is analogous to the stiffness case. For this reason it is shown in Appendix C.

$$\frac{p}{p_o} = \frac{\psi_Z{}^q}{\psi_A} \tag{5.24}$$

where q:

$$q = \log_{(uv^2)} uv = \frac{\ln uv}{\ln uv^2} \tag{5.25}$$

Equation (5.24) is the relative performance index for arbitrarily scaled structural envelopes of different shapes for a failure moment requirement. The exponent $q=f(u,v)$ describes the scaling of the envelopes sizes, which is determined by the shape properties.

In Figure 5.9 the performance index is plotted as a function of the scaling parameter q. A full range of solutions is shown for arbitrary scaling of a square section. For $uv^2=1$, q is unbounded (i.e. $q = \pm \infty$). For vertical, proportional and horizontal scaling of the square reference, $q=1/2$, $q=2/3$, $q=1$ respectively. Depending on the direction of scaling, q can have any value between $-\infty$ and $+\infty$. For example, for a particular strength requirement, if the reference structure A of unit dimensions is rescaled to B with $u=B/B_o=b/b_o$ and $v=H/H_o=h/h_o$, then $-\infty<q<1/2$. Alternatively, if point A moves to C, then $1/2<q<2/3$. Similar considerations to Figure 5.1 for stiffness design can be drawn also to Figure 5.1 for a strength requirement.

Limiting shape regimes

An example of shape regimes for strength design will be illustrated in Chapter 9 for a natural structure, where S and M are variable.

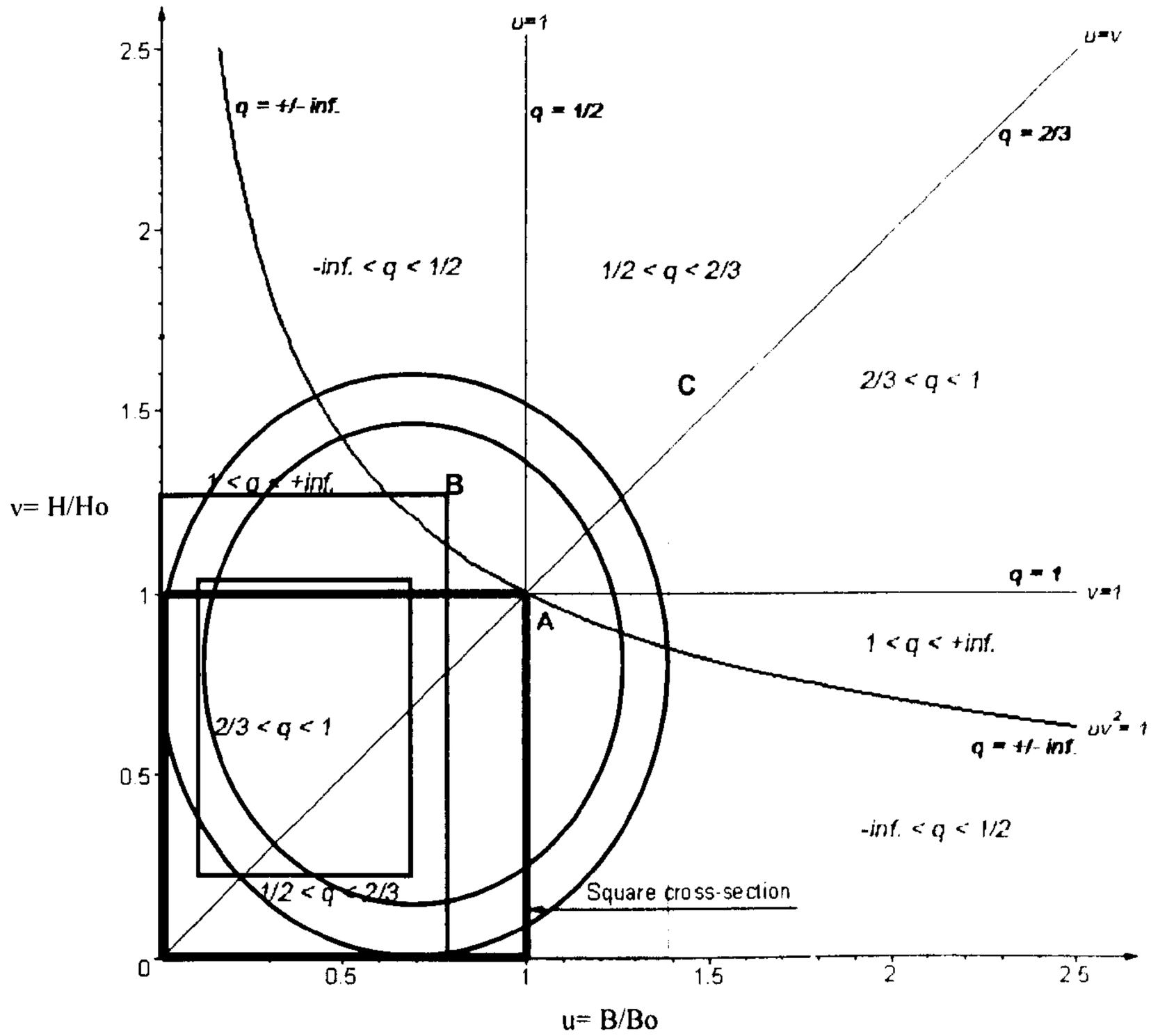

Figure 5.1 Solutions of the scaling parameter *q* for all directions of scaling in strength design.
A: square section; B: -∞ <*q*< 1/2; C: 1/2 <*q*< 2/3.

5.5 COMPARISON OF PERFORMANCE CRITERION AND PERFORMANCE INDEX

The comments given in Chapter 4 for the comparison of performance criterion and performance index can be applied to the case where *S* is the variable. This Section gives a brief summary of the relationship of the two approaches.

The relative performance of a structure, p, to the reference, p_o. can be expressed by the performance criterion (equation (5.3) for stiffness and equation (5.5) for strength) and the performance index. For *M* fixed and *S* variable, the expressions are:

	(Section 5.3) Performance criterion	(Section 5.4) Performance index
Design		
Stiffness	$\frac{p}{p_o} = \frac{\psi_I}{\psi_A} \quad v^2 = \underbrace{[\lambda_I]}_{S} \quad \underbrace{[v^2]}_{D}$	$\frac{p}{p_o} = \underbrace{\frac{1}{\psi_A}}_{S} \underbrace{\psi_I^{\,q}}_{D}$

Strength $\frac{p}{p_o} = \frac{\psi_Z}{\psi_A} \quad v = \lambda_Z \quad v$ $\qquad \frac{p}{p_o} = \frac{1}{\underbrace{\psi_A}_{S}} \underbrace{\psi_Z}_{D}^{q}$

In the case where *S* is the variable, the above expressions differ for how the group *D* is expressed. As it could be expected, although the equations describe the structural performance in different forms, they are mathematical identities. The reason for this is that in the performance criterion the term $v^2 = (I_D/I_o)/(A_D/A_o)$ is in the performance index the exponent of a logarithm $q = \frac{\ln uv}{\ln uv^3} = \log_{uv^3} uv = \log_{\frac{I_D}{I_o}} \frac{A_D}{A_o}$.

When the **direction of scaling** is **unknown,** the variables ***D* and *S*** are **not separable** since S define a relation between the height and the width of the envelope D. From the above expressions of the performance criterion, it is evident that the only conditions that allow separation of the variables for an unknown direction of scaling is when two sections have the same ratio I/A, or Z/A.

The **performance criterion** expression **is** the **performance index** when the direction of scaling is known a priori. The reason for this is that the constraints are applied to the envelope sizes, *D*, and not to the properties, *M* and *S*, of the cross-sections. **In specified conditions of scaling** such as those with *H*=const, *B*= const, and *H/B*=const, *q* has a definite value and the selection is given by just a combination of shape properties. In horizontal and vertical scaling, *q* is respectively 1/3 and 1/2 for stiffness, and 1/2 and 1 for strength design. These scaling conditions are imposed by geometrical constraints. The proportional scaling condition, where *q* is 1/2 for stiffness and 2/3 for strength, is not imposed by any particular spatial restrictions. The index $\psi_I{}^{0.5}/\psi_A$ is appropriate when bending is applied to both axes x-x and y-y of a cross-section.

5.6 SHAPE CHARTS

Chapter 4 has shown that the mass, m, and the design requirement, F, of a cross-section $C(\underbrace{MxSxG_D}_{m} , \underbrace{MxSxG_D}_{F})$ can be displayed on a material chart to select the best *M* for a cross-section with *D* fixed and *D* variable. Since shape properties have

been defined in analogy with the material properties, shape charts in normal and logarithmic scales can be produced in a similar way to the material chart. The shape transformers of m, i.e. ψ_A, and of F, i.e. ψ_I for stiffness and ψ_Z for strength, are displayed on shape charts for selecting the lightest cross-section in any scaling condition. This Section presents the graphical selection of the best *S* which minimises the mass of a unit length component. The properties of a cross-section, *C*, in term of mass and functional requirement are given by the following co-ordinates in the case of *D* fixed and *D* variable:

D fixed	*D* variable
$C\left(\frac{m}{MxG_D}=S\ ,\ \frac{F}{MxG_D}=S\right)$	$C\left(\frac{m}{M}=SxG_D\ ,\ \frac{F}{M}=SxG_D\right)$

5.6.1 Envelope efficiency map for the performance criterion

Stiffness design. In Figure 5.10 the **performance criterion,** given by equation (5.2) is used for the case where *M* is constant and *S* is variable. The shape transformer ψ_I is plotted against ψ_A **on normal scale axes**, using the expressions presented in Table 3.4 for a range of typical cross-sections. The values of ψ_A and ψ_I are on the axes and is between 0 and 1. On the right top of the graph, there is the case where the envelope, *BxH*, is filled as both shape transformers are unity. The chart is the **envelope efficiency map** which is analogous to the material charts. It can be used for the case where the space envelope *D* is fixed or variable.

***D* fixed** (i.e. the ratio of the sizes *B* and *H* is fixed). The shape properties of a cross-section $C\left(\frac{m}{MxG_D}=S\ ,\ \frac{F}{MxG_D}=S\right)$ are the co-ordinates of each point in the map (5.10). Within the range of ψ_I plotted as a function of ψ_A there are two limiting curves, curves 1 and 2. These curves have been plotted using expressions in Tables 3.3 and 3.4. Within curves 1 and 2 exist all geometric cross-sectional shapes that partially fill the envelope defined by *B* and *H*. Furthermore, there are no cross-sectional shapes within the envelope *BxH* that are outside the boundaries defined by the curves 1 and 2. Curve 1 represents the conditions where the upper and lower outside surfaces of the beam are occupied by material. This is the case of an I-beam with an infinitely thin vertical web with the dimensions *B-b* tending to zero (see Table 3.3) or a layered system

with the centre filled with material of very low Young's modulus relative to the outside material. Curve 2 represents a rather idealised case of an I-section beam turned on its side (e.g. a H section). The outer sides of the *H* are infinitely thin (with the dimension b tending to zero) with the centre cross member increasing with thickness with increasing ψ_I and ψ_A. It should be noted that for both curves 1 and 2 the rectangular design space coincides with the envelope surrounding the extremities of the shape. In Figure 5.1 when $\psi_I = \psi_A = \lambda_I = 1$ the rectangular envelope is completely filled. When $\lambda_I = 1$ and $\psi_I = \psi_A < 1$, the envelope *BxH* is filled in direct proportion to the shape transformers, ψ_I and ψ_A. This is illustrated by cross-sections placed on the diagonal line in Figure 5.1.

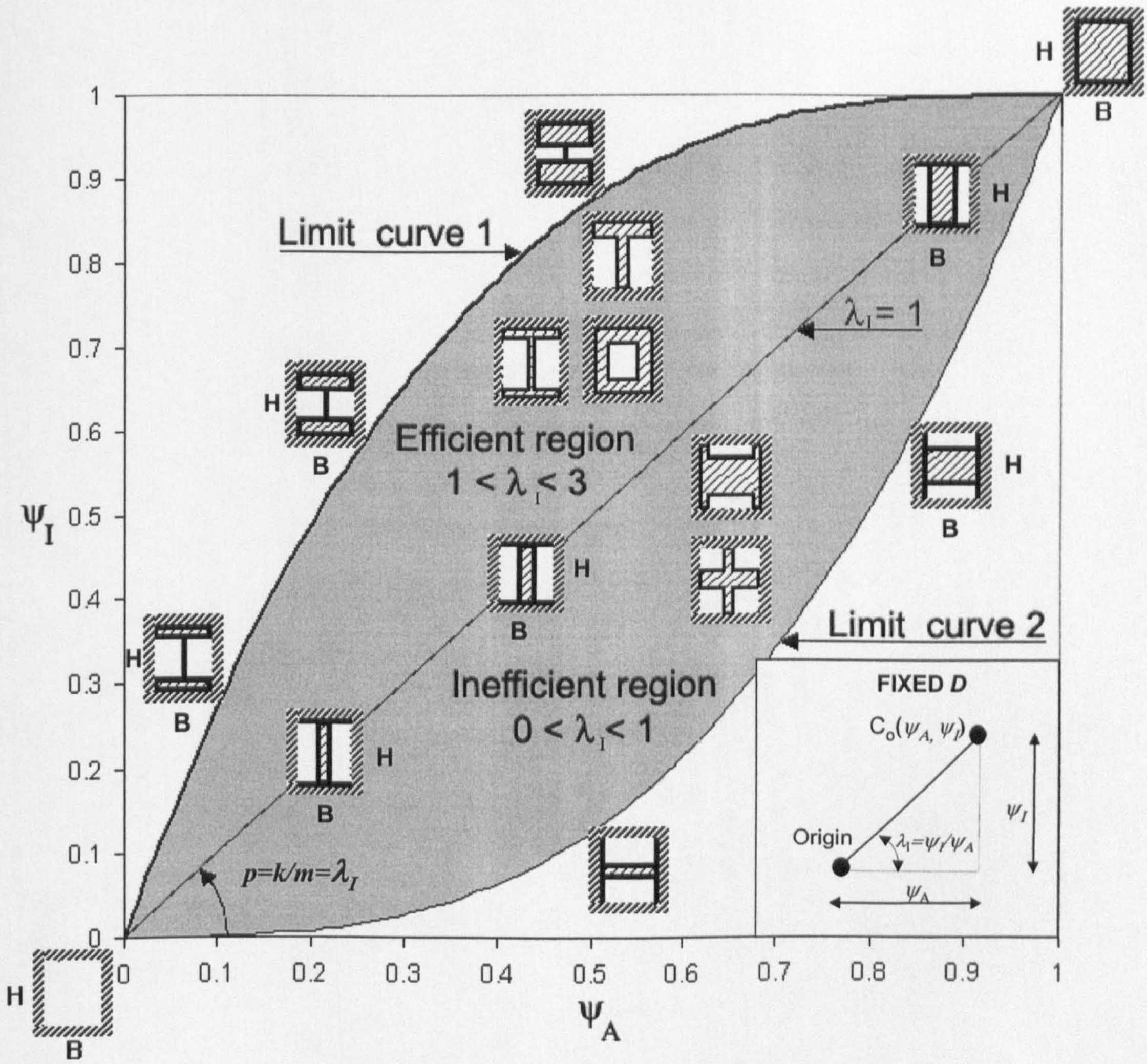

Figure 5.1 Envelope efficiency map for stiffness design in normal scale. (Data from the Table 3.3 and 3.4)

The domain between curves 1 and 2 can be split into two regions, namely **efficient and inefficient regions**. Cross-sectional shapes where material is away from the neutral axis lie in the efficient region, where $1< \lambda_I <3$. Examples of shapes that lie in the efficient region are I and T sections. Hollow rectangular sections also lie in the efficient region. A number of shapes are illustrated in Figure 5.1. When the majority of material is near to the neutral axis, $0< \lambda_I <1$, the cross-sectional shapes lie in the inefficient region. Examples of cross-sectional shapes that occupy the inefficient region are shown in Figure 5.1.

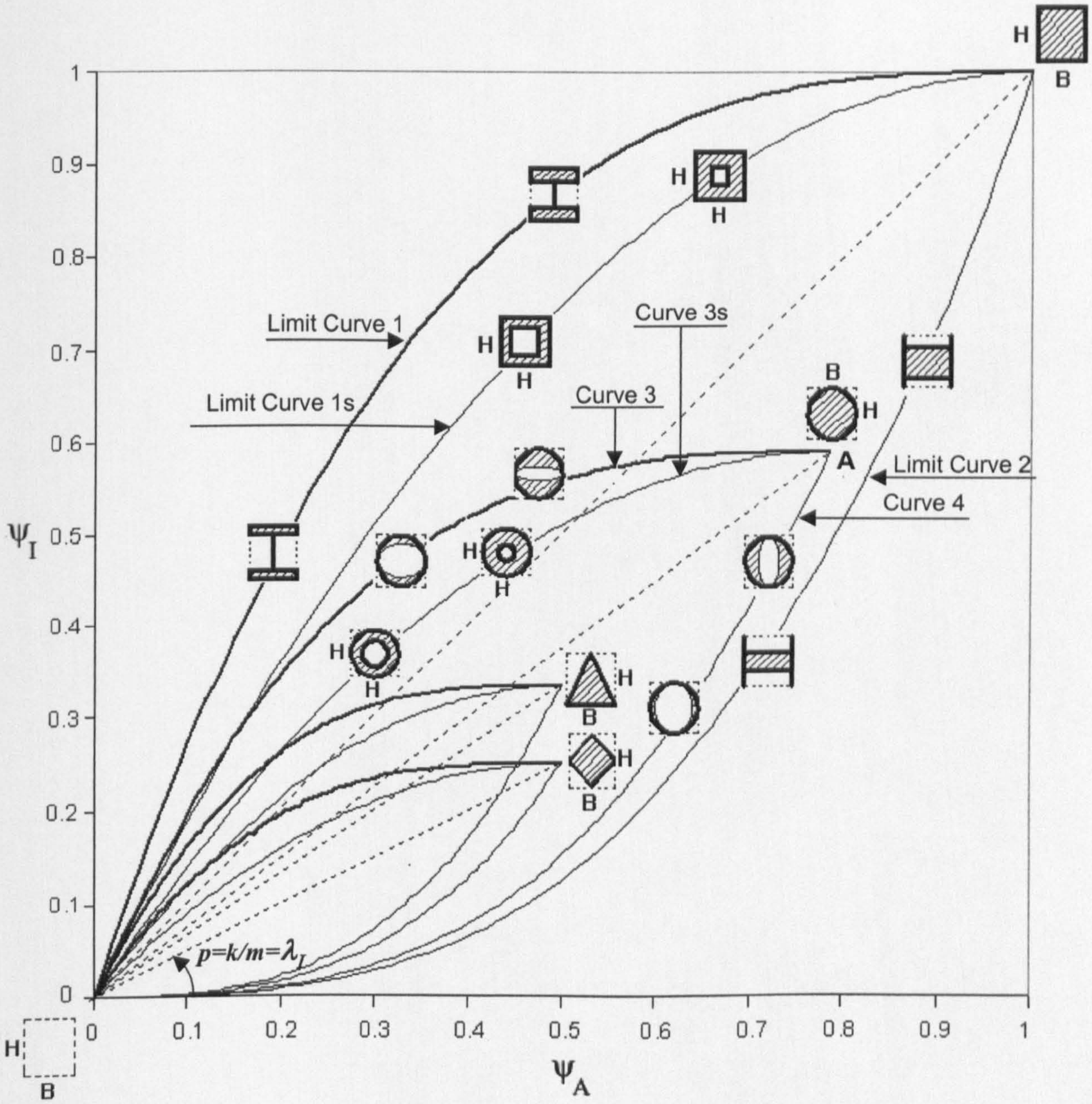

Figure 5.2 An envelope efficiency map for different classes of shapes. The shape domain of the rectangle encloses any other domains (ellipse, triangle, lozenge).

In Figure 5.2, the equivalent curves for curves 1 and 2 in Figure 5.1 are shown for different classes of shape. For elliptical cross-sections, values of ψ_A and ψ_I are less than unity, with their maximums at $\pi/4$ and $3\pi/16$ respectively for the solid shape, as shown in Table 3.3. These maximum values are shown in Figure 5.2 at point A. Curve 3 is the limiting curve for all elliptical shapes that are hollow, but with material close to the top and bottom of the outer surfaces. When the material is on the outer side edges the efficiency of the beam in bending is described by curve 4. When the envelope is square, rather than rectangular, $B=H$, the limiting curves in the envelope efficiency map move from curves 1 and 3 for rectangular and elliptical shapes to curves 1s and 3s respectively. Since the domain within the limiting curves is reduced, the range of λ_I is also reduced as shown in Table 3.4. For example, for rectangular sections the efficient region is when $1<\lambda_I<3$, whereas for square sections $1<\lambda_I<2$. Similar to curves 1 to 4, curves are illustrated for triangular and lozenge shaped cross-sections. It is emphasised that none of these shapes has a performance or efficiency that lies outside the boundary described by curves 1 and 2. As with the efficient and inefficient regions defined for rectangular shapes, each domain for each shape class can be sub-divided into two regions. For example, a triangle has an efficient section when $2/3<\lambda_I<2$, and an inefficient section when $0<\lambda_I<2/3$.

***D* variable** (i.e. the ratio of the sizes, *B* and *H*, is variable). The co-ordinates of scaled cross-sections are given by $C\left(\frac{m}{M}=SxG_D\ ,\ \frac{F}{M}=SxG_D\right)$. Six cross-sections of the same material, C_o, C_1, C_2, C_H, C_V, C_p, are considered for the scaling of the cross-section. C_o is a rectangular cross-section with $S_o(\psi_A=1, \psi_I=1)$ and sizes of the envelope, D_o, B_o and H_o. The position of the rectangle C_o on the envelope efficiency map is shown in Figure 5.3. $C_1(MxS_1xD_1)$ is an I section with infinitely thin vertical web that lies on curve 1 as shown in Figure 5.1. C_1 has M, $D_o=D_1$, and $S_1(\psi_{A1}=0.43, \psi_{I1}=0.81)$. C_o and C_1 are not scaled whereas C_2 is an arbitrarily scaled cross-section derived from C_1, i.e. C_2 (M,S_1,D_2), and C_H, C_V, C_p are horizontally, vertically and proportionally scaled cross-sections derived from C_1. C_o and C_1 are not on the same horizontal line because C_1 cannot provide the same stiffness of C_o, $k_o=k_1$ as shown in Figure 5.3. However, if the cross-section C_1 is scaled to C_2 with $D_1\neq D_2$, i.e. $C_2(M,S_1,D_2)$, the stiffness k_o, provided by C_o can be made to be the same as that for C_2, i.e. k_2

= k_o. From equation (5.12) the cross-sections meet the same requirement for the condition:

$$k_2 / k_o = uv^3 \psi_{I1} = 1 \tag{5.26}$$

For a given value of *u,* equation (5.26) can be used to determine the value of *v* to satisfy a stiffness requirement, which is represented by a horizontal line, ψ_I=1, in Figure 5.3. For example, C_2 is an arbitrarily scaled envelope given for *u*=0.4 and *v*=1.45. When the cross-section, C_1, is scaled to meet the stiffness requirement ψ_I = 1, then C_1 in Figure 5.3 moves along the arrow C_1C_2 according to equation (5.26) to the co-ordinate C_2 (ψ_{A2}, ψ_{I2}) given by:

$$\begin{cases} \psi_{I2} = uv^3 \psi_{I1} \\ \psi_{A2} = uv\psi_{A1} \end{cases} \tag{5.27}$$

Expressions (5.27) gives for C_2 the following co-ordinate C_2(0.25,1).

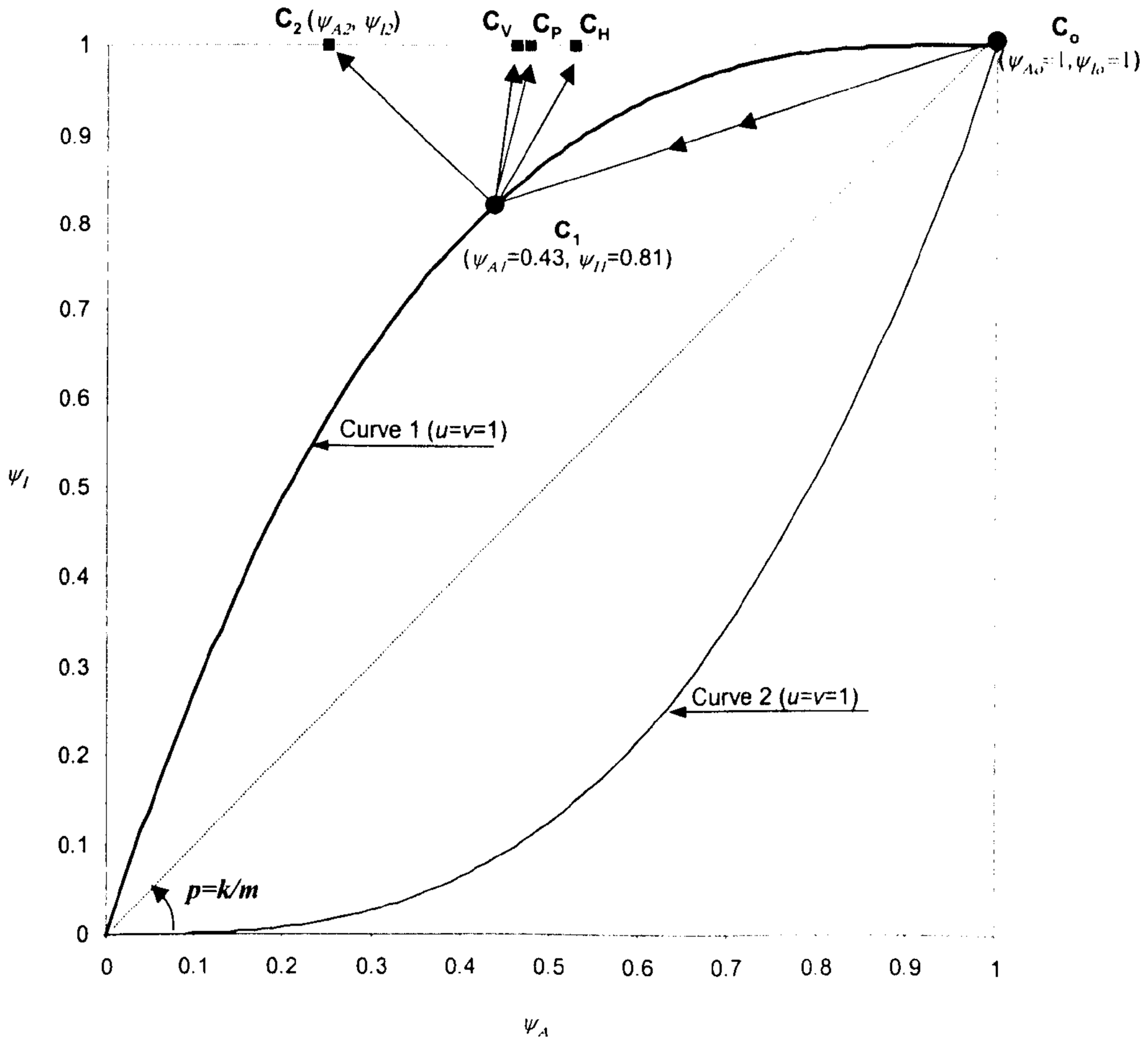

Figure 5.3 The effect of scaling on the envelope efficiency map.

In contrast with arbitrary scaling, for three scaling conditions, the mass and the stiffness, i.e. the position, of C_H (**horizontal scaling**), C_V (**vertical scaling**), C_p (**proportional scaling**) on the chart can be directly determined only by the **shape properties without** using ***u*** and ***v*** from equations (5.27). Imposing a prescribed condition of scaling in equation (5.26) and replacing the unknown parameter in (5.27) gives the following co-ordinate for C_2 :

Prescribed scaling		Derived condition from (5.26)	C_2 (ψ_{A2}, ψ_{I2}) from (5.27)	
Horizontal scaling	$v=1$	$u=1/\psi_{II}$	$m_2 \rightarrow \psi_{A2}\cdot\psi_{A1}(1/\psi_{II})$	$k_2 \rightarrow \psi_{I2}\cdot\psi_{I0}$
Vertical scaling	$u=1$	$v=(1/\psi_{II})^{1/3}$	$m_2 \rightarrow \psi_{A2}\cdot\psi_{A1}(1/\psi_{II})^{1/3}$	$k_2 \rightarrow \psi_{I2}\cdot\psi_{I0}$
Proportional scaling	$u=v$	$u=v=(1/\psi_{II})^{1/44}$	$m_2 \rightarrow \psi_{A2}\ \psi_{A1}(1/\psi_{II})^{1/2}$	$k_2 \rightarrow \psi_{I2}\cdot\psi_{I0}$

Therefore, using the third column of the above Table gives the following shape properties, shown in Figure 5.3:

for C_H S (0.52,1) for C_p S (0.47,1) for C_V S (0.46,1)

Strength design

- ***D* fixed.** Figure 5.4 illustrates the envelope efficiency map for the shape class of rectangles in strength design. This time, the performance criterion, equation (5.4), has been plotted for a fixed envelope *D* **on normal scale axes**. The expressions of ψ_Z and ψ_A are given in Table 3.4 and their values are between 0 and 1. (Note that $\psi_Z \neq \psi_I$ and $\lambda_Z \neq \lambda_I$ because, as explained in chapter 3, the expressions of Z in Table 3.2 are approximate).The parameter λ_Z is the slope of each point in the graph and indicates how efficiently the area is utilised in a given envelope *BxH* for a strength requirement. As can be seen, the extent of the shape domain is smaller than the envelope efficiency domain for stiffness. The reason for this is that the expressions of λ_Z given in Table 3.4 are a function of the square of the ratio *h/H* rather than the cube as for λ_I.

In Figure 5.5 the performance of other classes of shapes are displayed for a fixed envelope *D*. This graph resembles Figure 5.2. The differences are in the expression of λ_Z, hence the shape domain of the rectangle does not fully contain the ellipse class domain.

The considerations carried out for fixed and variable *D* in stiffness design are similarly applicable for the case of strength design. For this reason, the case of *D* variable is not examined. Examples of application of the envelope efficiency map are given in Section 5.8.

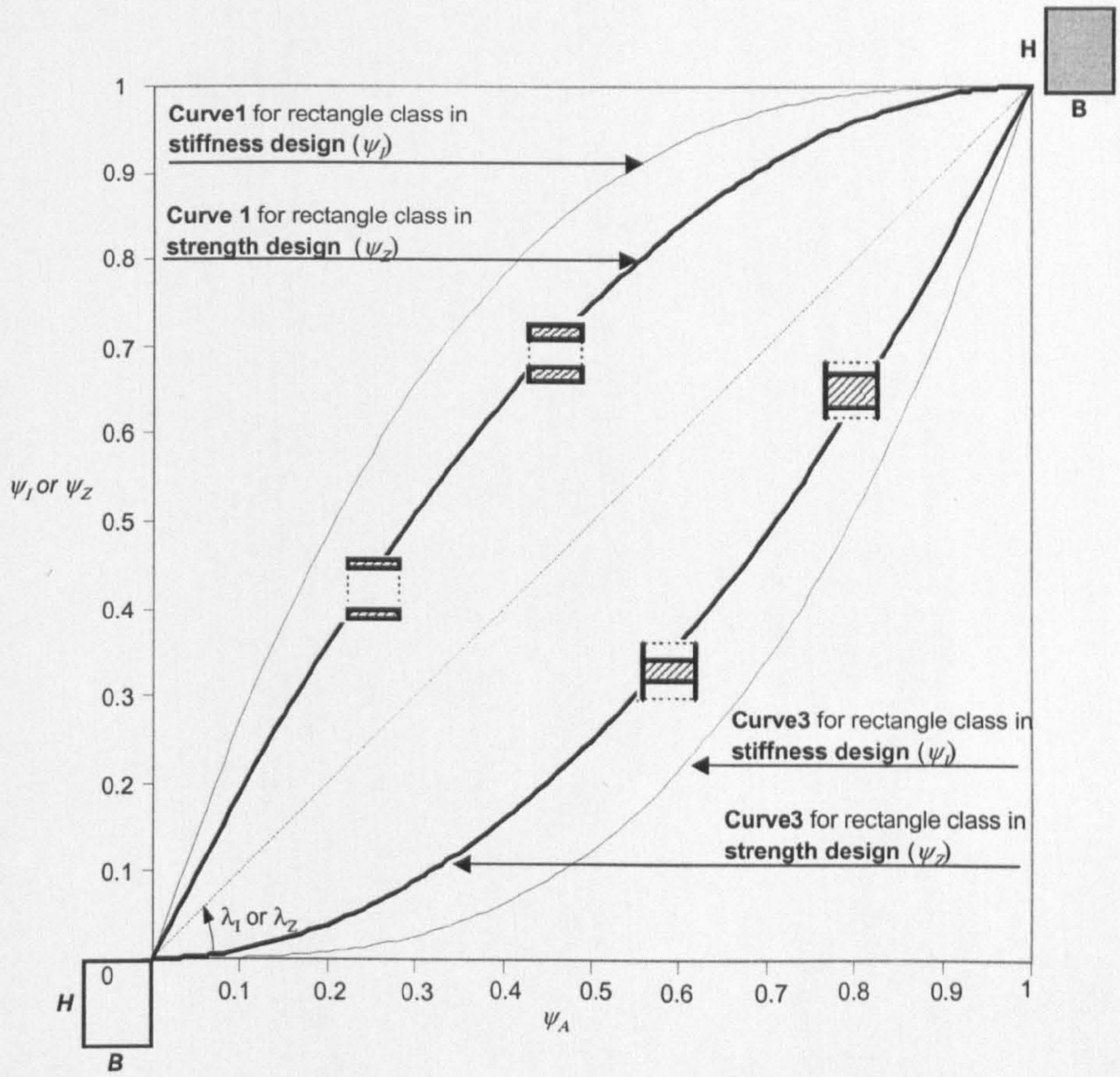

Figure 5.4 Efficiency domains of the rectangle class for stiffness design and strength design

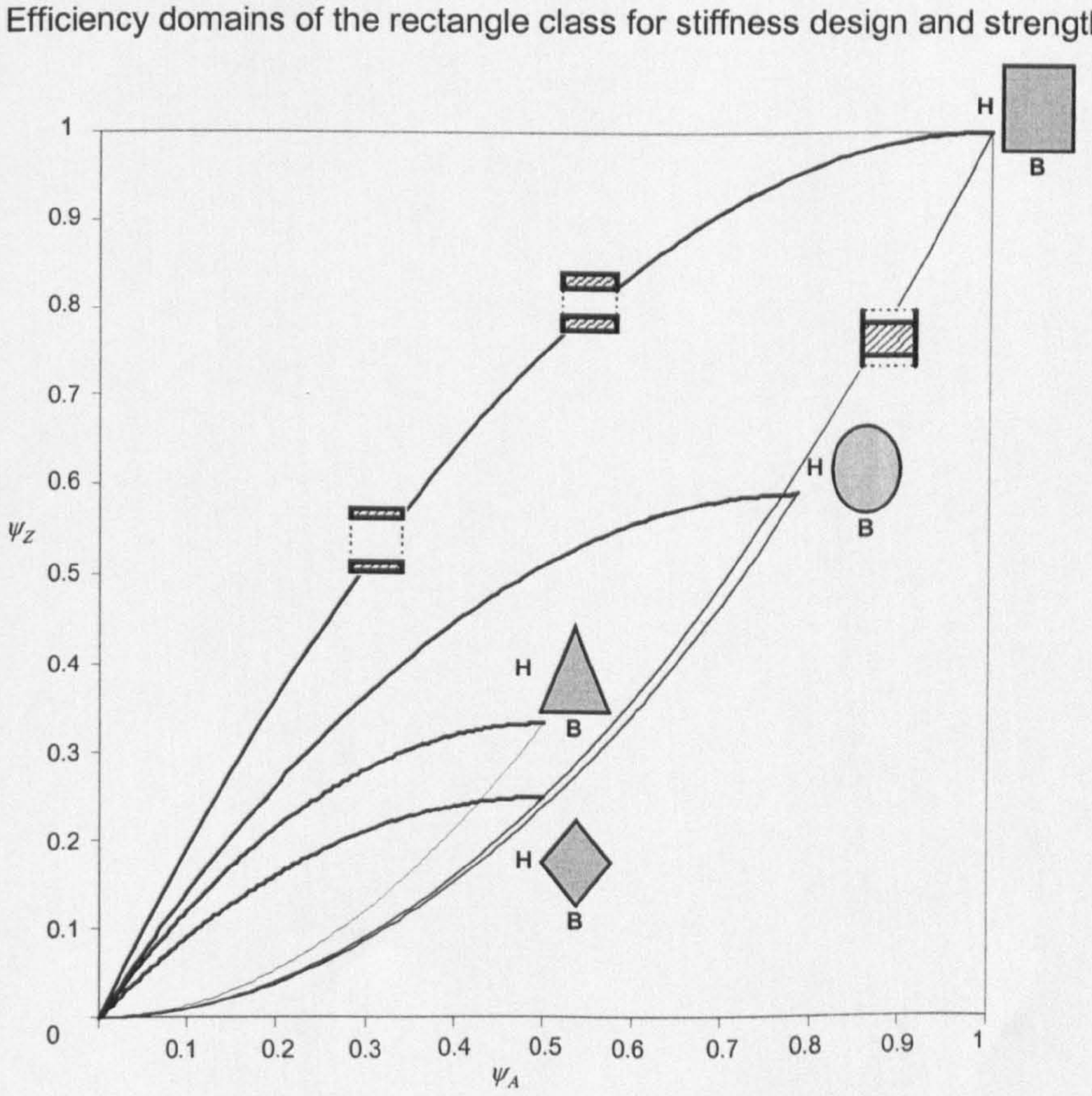

Figure 5.5 Existence shape domains for four shape classes in strength design.

5.6.2 Log scale shape charts for the performance index

In Figure 5.1 (a), the shape properties, $(\psi_I\ \psi_A)$, are displayed in **logarithmic scale axes** for the **performance index,** $p = \psi_I^q/\psi_A$, whose log expression is given by:

$$\log\psi_I = \frac{1}{q}\log\psi_A + \frac{1}{q}\log p \tag{5.28}$$

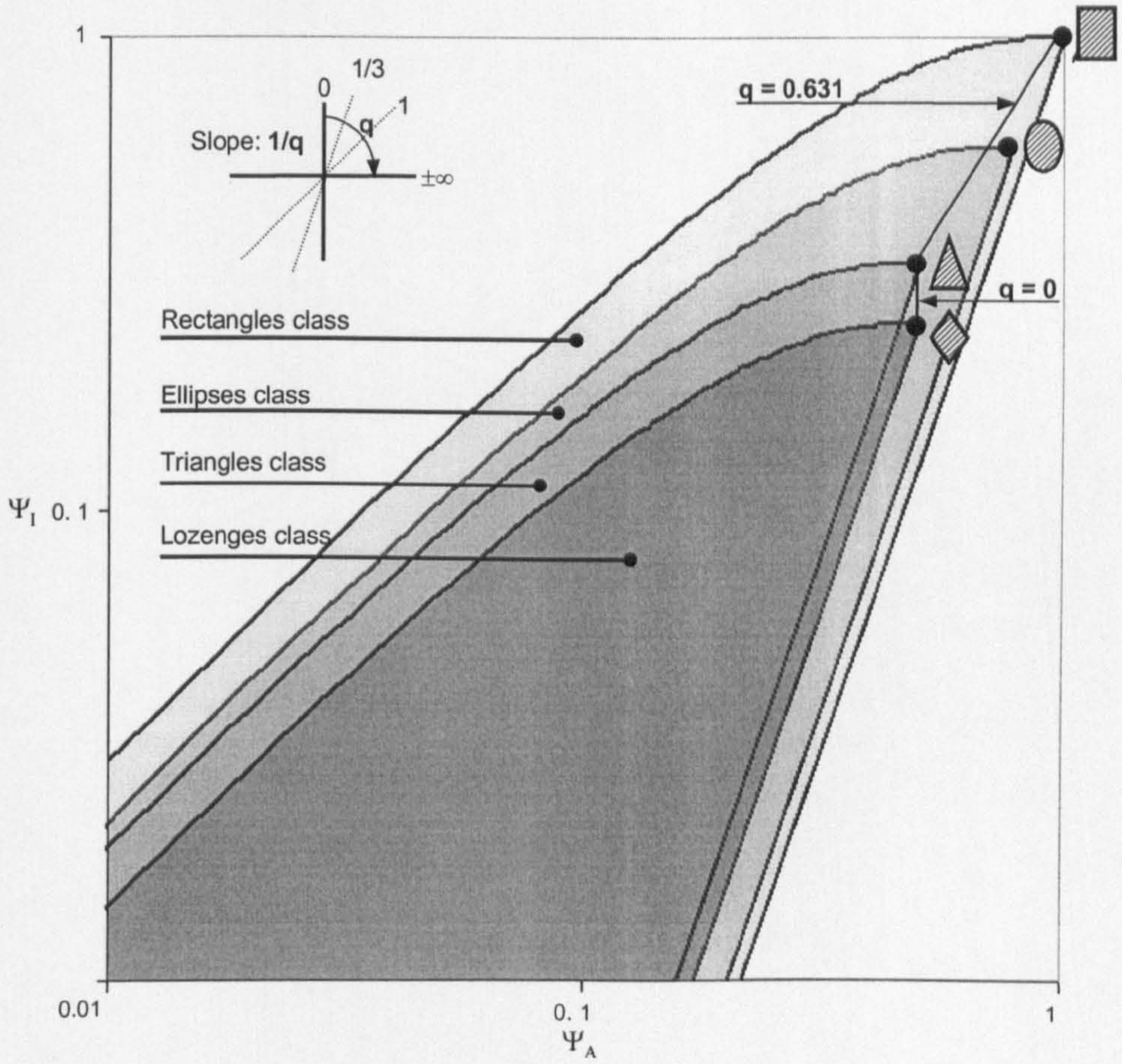

Figure 5.1(a) Log-log scale shape chart $\psi_I - \psi_A$ for stiffness design.

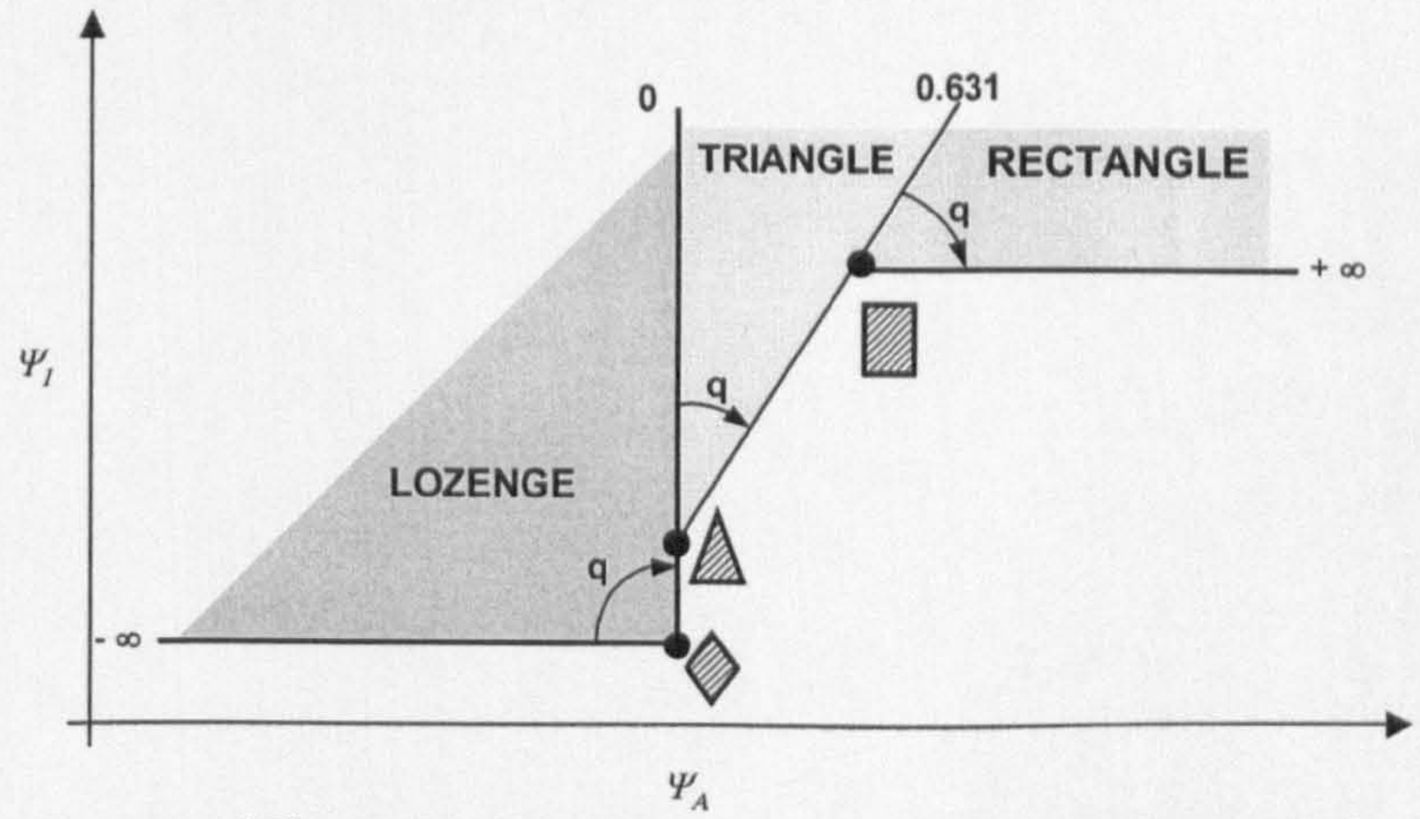

Figure 5.15(b). A zoom of Figure 5.15(a) to show the best shape for ranges of q.

- As with Figure 4.12, the following observation can be made from Figure 5.1. Four classes of rectangle, ellipse, triangle and lozenge are illustrated. Each class contains shapes derived from the solid shapes. The powers of q=1 and q=1/3, of the performance index are the guidelines for the selection of the best shapes for the case of width and height constraint in stiffness design. The values of q where two cross-sectional shapes provide the same mass have been shown in Figure 5.1, and are represented in Figure 5.1 as the line connecting two couples of shape properties (ψ_I, ψ_A).
- Figure 5.15(b) shows ranges of q where one shape, such as the lozenge, the triangle or the rectangle, is lighter compared to the others. For example, for $-\infty<q<0$ the lozenge is lighter than the triangle and rectangle. If the scaling of the cross-sections is such that $0<q<0.631$, then the triangle has the lowest mass. However, for $0.631<q<+\infty$ the rectangle has the best performance. This confirms that the scaling of the structural envelopes containing different shape properties has a large effect on the selection of the best shapes for a given design requirement.

5.6.3 Improved version of the shape regimes map

The logarithmic shape charts illustrated in Figure 5.1 plot the shape properties and superimposes selection guidelines. However, geometrical constraints are usually applied to the structural envelopes in the design space. Therefore, for a generic slope constraint it could be more useful to settle the selection in the context of the design space rather than in the shape domain. Analogous to Figure 4.13, Figure 5.1 shows an example of the improved limiting shape regimes for four shapes where the selection occurs in the design context. Using Figure 5.1, values of q where two shapes have the same performance can be determined and ranking of shapes for different ranges of q can be specified. Equation (5.23) has been used to plot the curves of q, in Figure 5.1. The ranking of the candidate shapes from the best (top) to the worst (bottom) is shown for each coloured region. The ranking indicates how different shapes compete in the design space for any scaling condition, q. This procedure can be used to implement a computerised selection to help designers in the selection of the best shapes when D is variable.

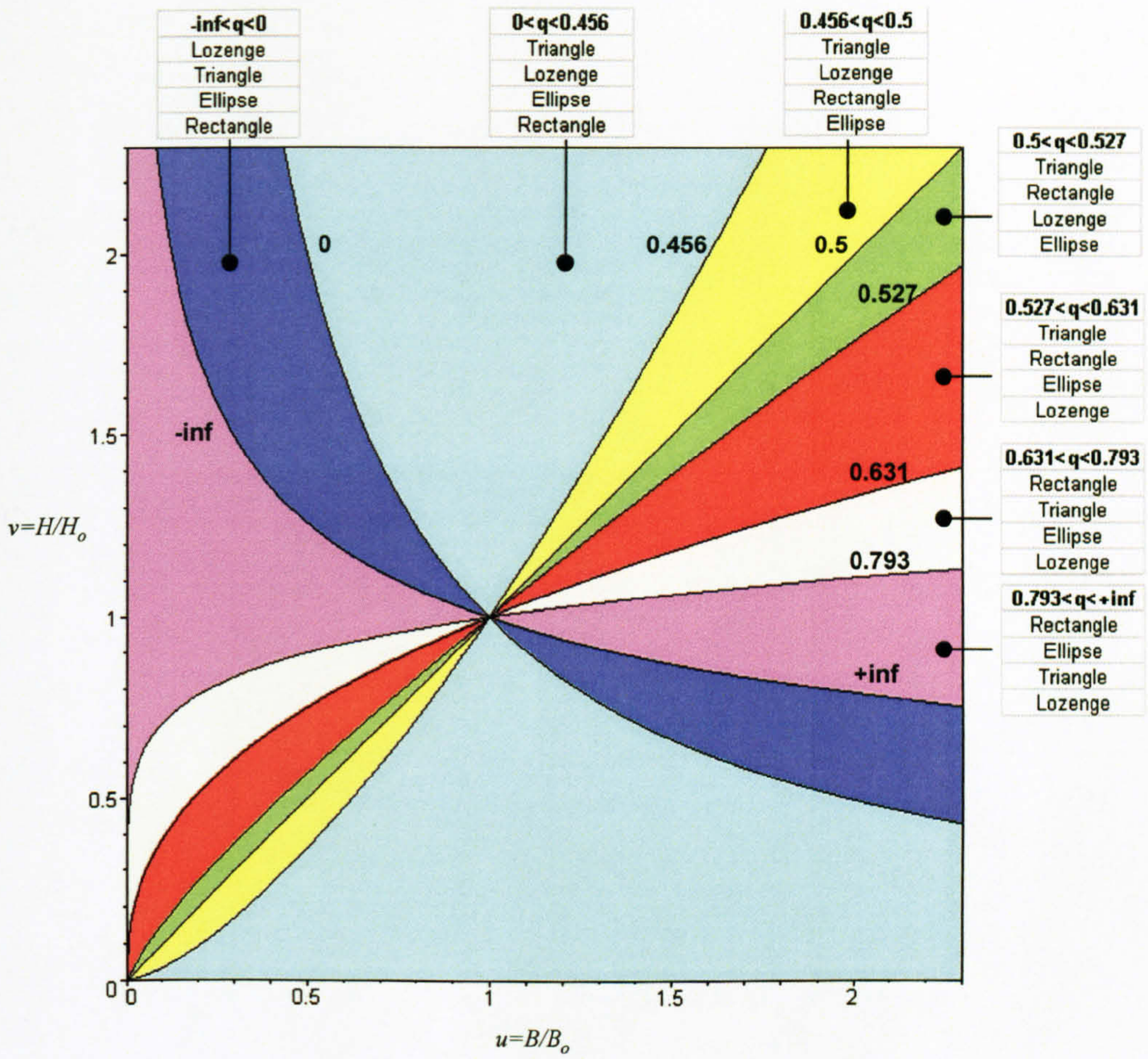

Figure 5.1 Example of limiting regimes shapes implemented for four shapes. Each colour corresponds to a shape-ranking region defined by ranges of q.

5.7 SHAPE TABLES

In Chapter 4, the performance index E^q/ρ was used to produce an example of a design Table of q for two materials and angles of the slope constraint. In a similar way, the index ψ_I^q/ψ_A can be used to produce Tables of q to select the best shape, S, for a given angle θ of constraint, such as that shown in Figure 5.2 (c). An example is given in Table 5.1 for stiffness design. The values of q are to be used in equation (5.23) to compare the performance of three shapes with the reference section.

θ slope constraint angle	0°	10°	20°	30°	40°	50°	60°	70°	80°	90
q for										
ELLIPSE	1	-	-	-	-	-1.41	-2.55	-3.89	-6.15	1/3
TRIANGLE	1	-	-	-	-	-	-5.25	-1.31	-2.44	1/3
LOZENGE	1	-	-	-	-	-	-	-0.80	-1.72	1/3

Table 5.1 q values to be inserted in the performance index $\psi_I{}^q/\psi_A$ to select the lightest shape for a given sloped constraint angle

5.8 APPLICATIONS

This Section describes two applications. The first involves an exploration of the envelope efficiency map. Conditions for optimising the thickness of shapes with the same envelope are derived. In the second application, the limiting shape regimes chart is used for a design problem which consists of determining the best performance of a cantilever subjected to an end load.

5.8.1 Geometric conditions for optimising stiffness and mass

The shape transformers ψ_A and ψ_I represent, for a given material, the relative mass and stiffness of a cross-section respectively. Therefore, optimisation of the mass for a given stiffness (related to ψ_I) means changing the geometric transformer ψ_A. Similarly, improving the stiffness for a given mass involves retaining ψ_A at a constant value and increasing ψ_I. The geometric conditions that arise for a given stiffness and mass requirement are explored.

Minimisation of mass

The envelope efficiency map shown in Figure 5.1 illustrates efficient and inefficient regions for cross-section shapes that are bounded by the envelope *B* and *H*. For a given stiffness requirement, e.g. ψ_I=0.7, minimisation of the mass requires lower values of ψ_A. An example is shown in Figure 5.1 for I section beams and hollow box-sections. The best path for minimising the mass for a given stiffness is from point R to A. It has already been shown that in bending stiffness design there are no possible solutions for values of ψ_A less than that at point A in Figure 5.1. At intermediate values of ψ_A between points R and A there are many shapes that can meet the stiffness requirement. Furthermore, if ψ_I=0.7 represents the desired minimum stiffness, the cross-sectional shapes that lie in the shaded area above points R and A, and the limit curve 1 also provide an efficiency, λ_I, greater than the point R in Figure 5.1.

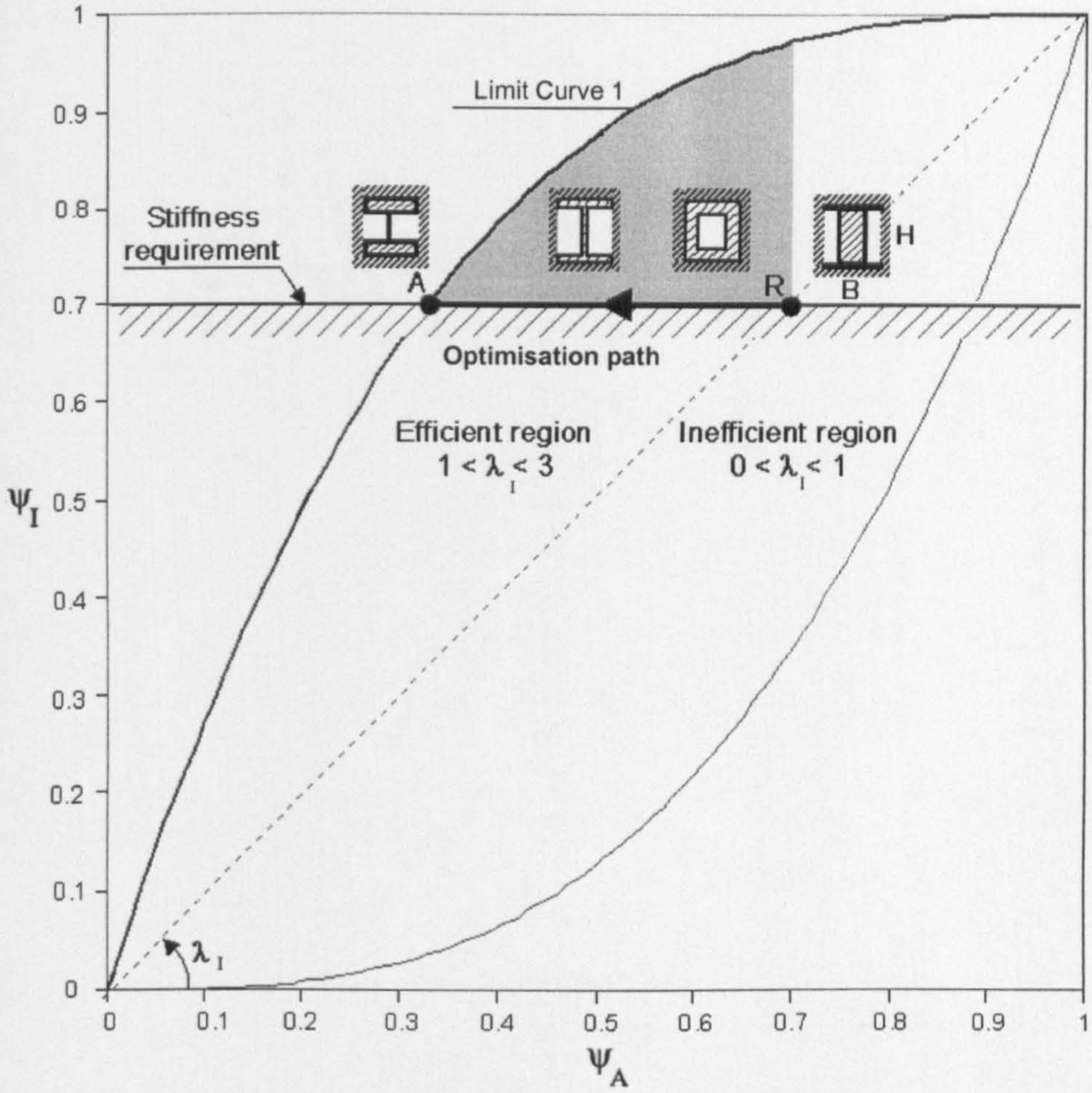

Figure 5.1 The shaded area above the stiffness line refer to selectable shapes. However for a given design space *BxH*, the best optimisation path is from A to R.

Further examples of minimisation of mass for a given stiffness requirement are illustrated in Figure 5.2. One design case is to consider reducing the mass of a solid circular section. Values of ψ_I and ψ_A for this section correspond to point E in Figure 5.2. For a given stiffness (e.g. ψ_I=0.59) minimising mass requires exploring shapes that lie along the path E to ERI. There are many shapes that occupy the design space BxH. For simplicity H and I sections that lie along the path E to ER I are considered. Along the line E-W-ERI the rectangular section equivalent to the solid elliptical section that yields ψ_I=0.59 has the dimensions (from the expressions of ψ_I in Table 3.3) which satisfy:

$$\frac{b}{B}\left(\frac{h}{H}\right)^3 = 0.411 \tag{5.29}$$

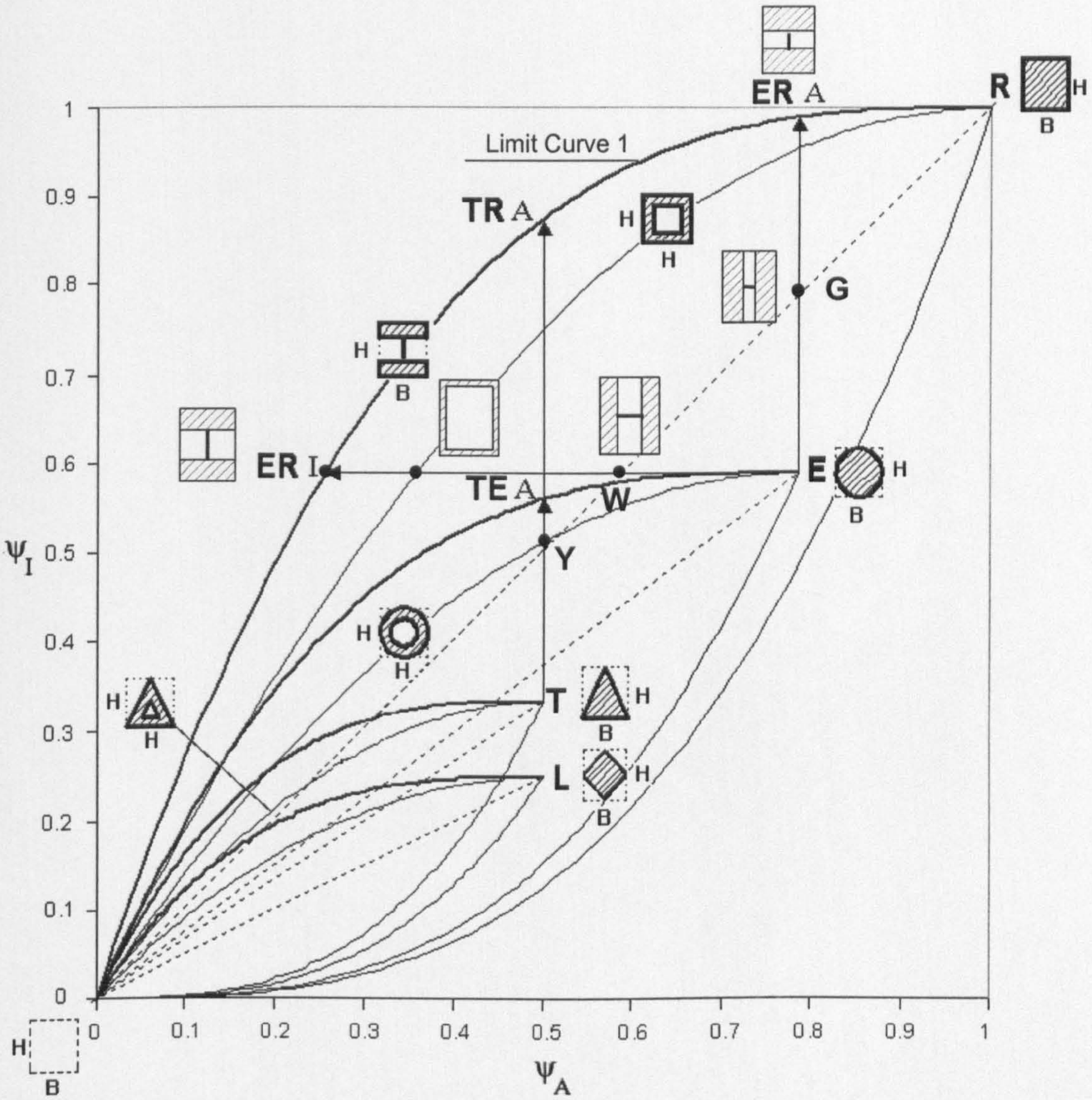

Figure 5.2 Optimisation paths for given ψ_I and ψ_A for minimising mass and maximising stiffness.

This is also illustrated in Table 5.1. When *b*=0 and *h*<*H* the idealised I-section with ψ_I=0.59 lies on curve 1 in Figure 5.2. The corresponding values of *h/H* for this condition is 0.743 as shown in Table 5.2. The variation of the thickness, i.e. the ratio b/B and h/H, for box and I sections that lie along path W to ERI is given by equation (5.29) and is shown in Figure 5.3.

Geometric conditions to select and optimise hollow sections	ψ_I requirement of solid shape 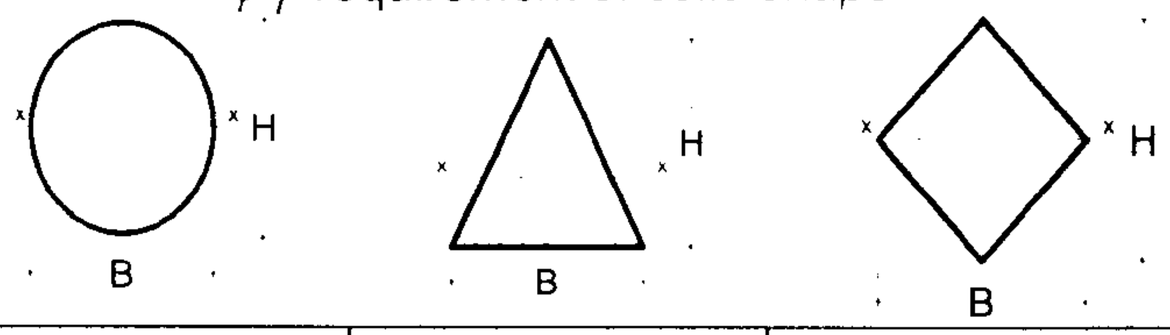		
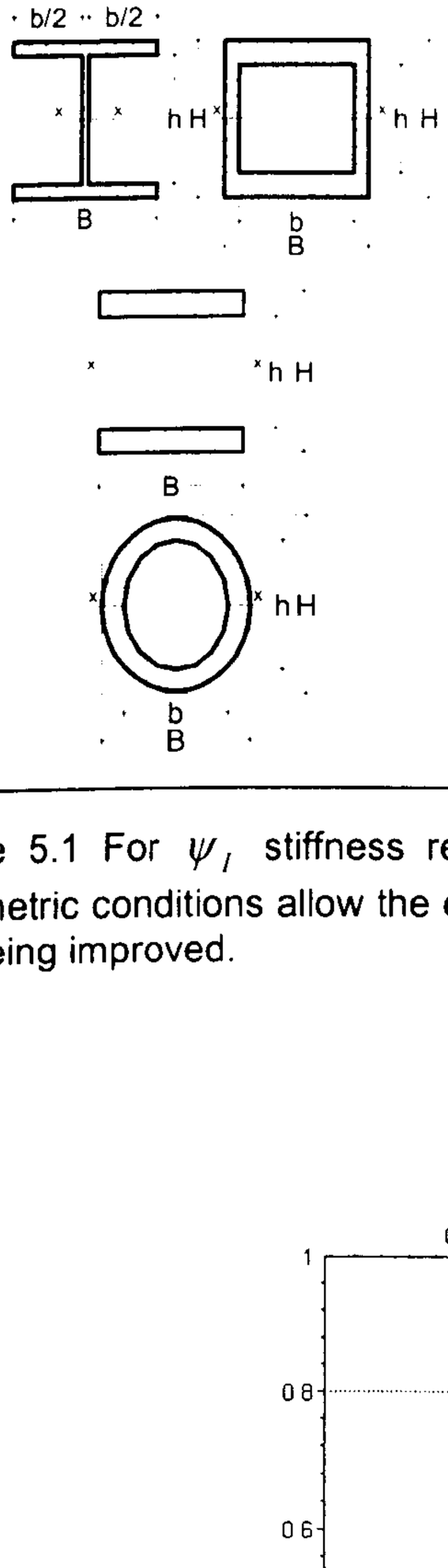	$\frac{b}{B}\left(\frac{h}{H}\right)^3 = 0.411$	$\frac{b}{B}\left(\frac{h}{H}\right)^3 = 0.67$	$\frac{b}{B}\left(\frac{h}{H}\right)^3 = 0.75$
	$\frac{h}{H} = 0.743$	$\frac{h}{H} = 0.874$	$\frac{h}{H} = 0.909$
		$\frac{b}{B}\left(\frac{h}{H}\right)^3 = 0.433$	$\frac{b}{B}\left(\frac{h}{H}\right)^3 = 0.575$

Table 5.1 For ψ_I stiffness requirement (i.e. solid section on the first row), the above geometric conditions allow the efficiency of hollow sections (first column) in a fixed space to be being improved.

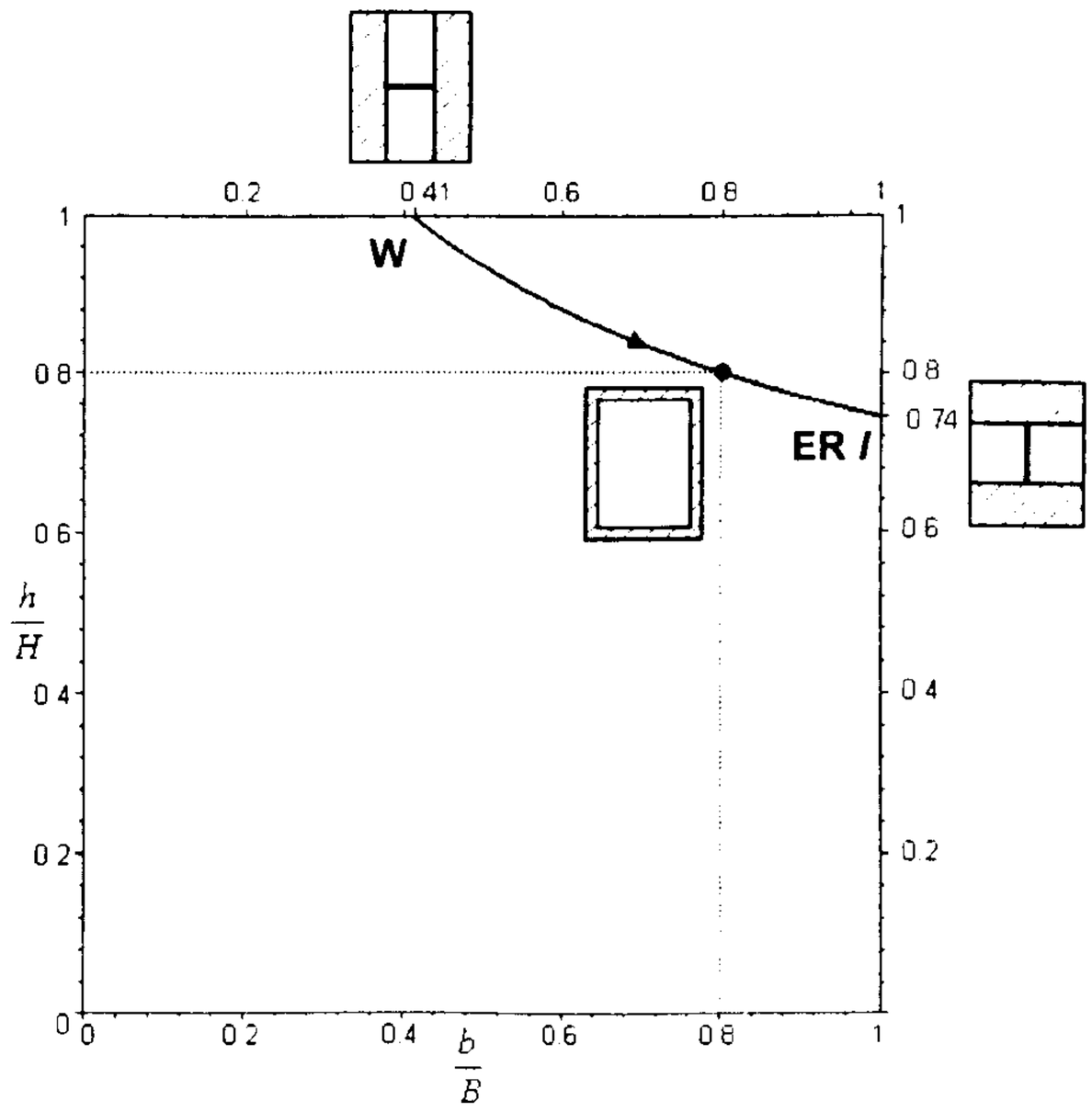

Figure 5.3 Variation of beams dimensions for a given ψ_I=3/16π =0.59

Maximising stiffness

For a given mass, the bending stiffness can be increased by moving along a vertical line on the envelope efficiency map. Several examples are shown in Figure 5.2. By moving along the line E-G-ERA in Figure 5.2 with $\psi_A = \pi/4$, various shapes with the same envelope sizes can be chosen that improve the stiffness. Again for simplicity box and I-sections are examined. As shown in Table 5.1 those sections that provide the same ψ_A as for an elliptical solid section have dimensions that satisfy:

$$\frac{b}{B}\frac{h}{H} = 0.215 \tag{5.30}$$

The idealised I-section with b=0 and $\psi_A = \pi/4$ lies on curve 1 in Figure 5.2 at point ER *A*. The corresponding value of *h/H* is 0.215 (see Table 5.1). The variation of the ratios of *b/B* and *h/H* that corresponds to the path G to ERA is given by equation (5.30) and is shown in Figure 5.1.

Geometric conditions to select and optimise hollow sections	ψ_A requirement of solid shape 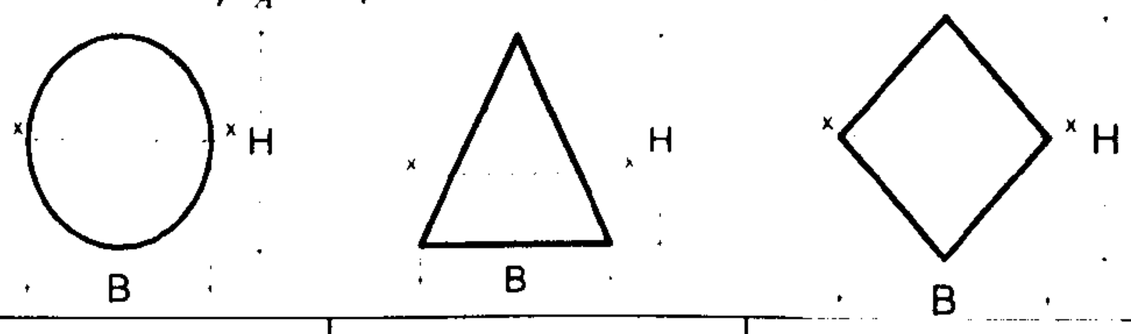		
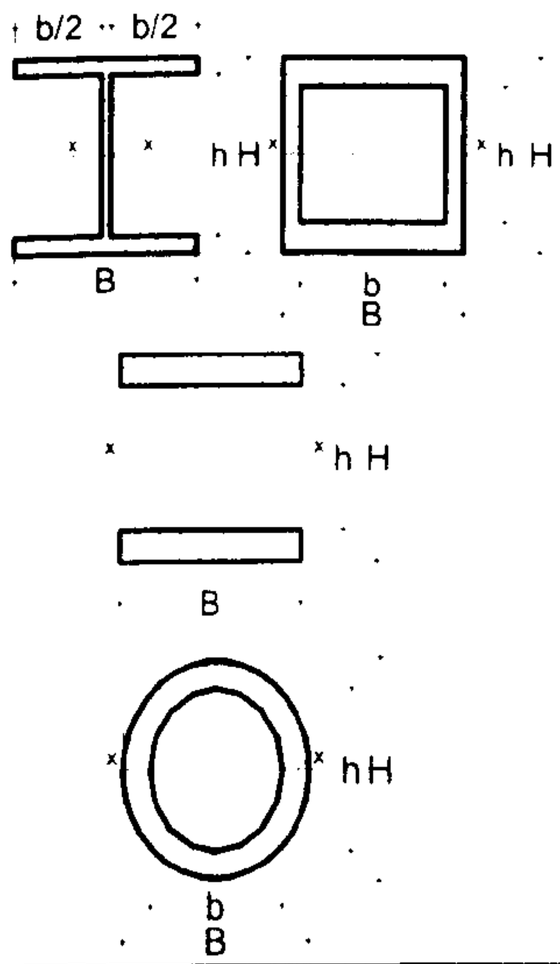	$\frac{b}{B}\frac{h}{H} = 0.215$ $\frac{h}{H} = 0.215$	$\frac{b}{B}\frac{h}{H} = 0.5$ $\frac{h}{H} = 0.5$ $\frac{b}{B}\frac{h}{H} = 0.363$	$\frac{b}{B}\frac{h}{H} = 0.5$ $\frac{h}{H} = 0.5$ $\frac{b}{B}\frac{h}{H} = 0.363$

Table 5.1 For a ψ_A requirement (solid section on the first row), the above geometric conditions allow the efficiency of hollow sections (first column) in a fixed envelope to be improved.

This example can be extended to consider other shapes in a rectangular design space *BxH*. Point T in Figure 5.2 represents the best performance for a solid triangular cross-section ψ_A=0.5 and ψ_I=1/3 (see Table 5.3). Assuming a given mass with ψ_A=0.5, the solid triangle can be replaced by a more efficient shape, such as a hollow ellipse, at point TEA, or even better, an idealised box or I-section at TRA. The geometric conditions for equivalent rectangular shapes for solid ellipse, triangular and lozenge sections are shown in Table 5.1.

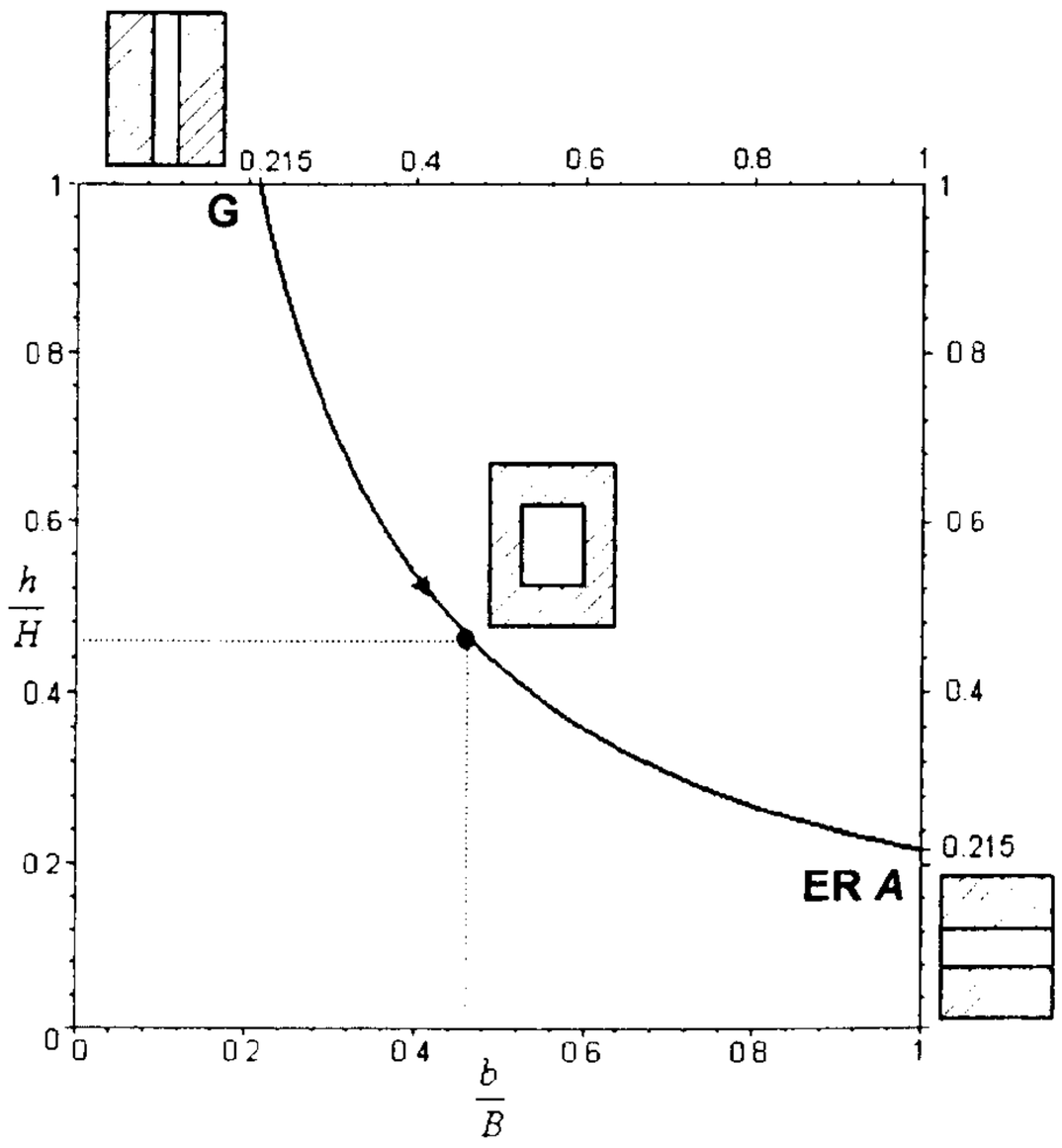

Figure 5.1 Variation of beams dimensions for a given $\psi_A=\pi/4=0.785$

5.8.2 Design case study

The case study of a cantilever beam subjected to an end load presented in Section 4.8 for *M* variable is presented here when *S* is variable. The example is a 4-metre cantilever that must support an end load of 1000 N with an allowable end deflection, δ, of 3.2 cm. This is illustrated in Figure 5.1. An aluminium solid rectangular section and an I-section are considered since these are common cross-sectional shapes. In the analysis the Young's Modulus, *E*, is 79 GPa and the density, ρ, is 2.9 Mg/m^3. An aluminium square section is chosen as the reference section. Two constraints which intersect the corner of the aluminium square section, chosen as the reference, are

examined. First where there is steep slope with θ=42.3°. This corresponds to a value of q = -0.21. The second is a shallow constraint with θ=6.8° where there is a severe restriction on height but less restriction on width. Here q = 4.81.

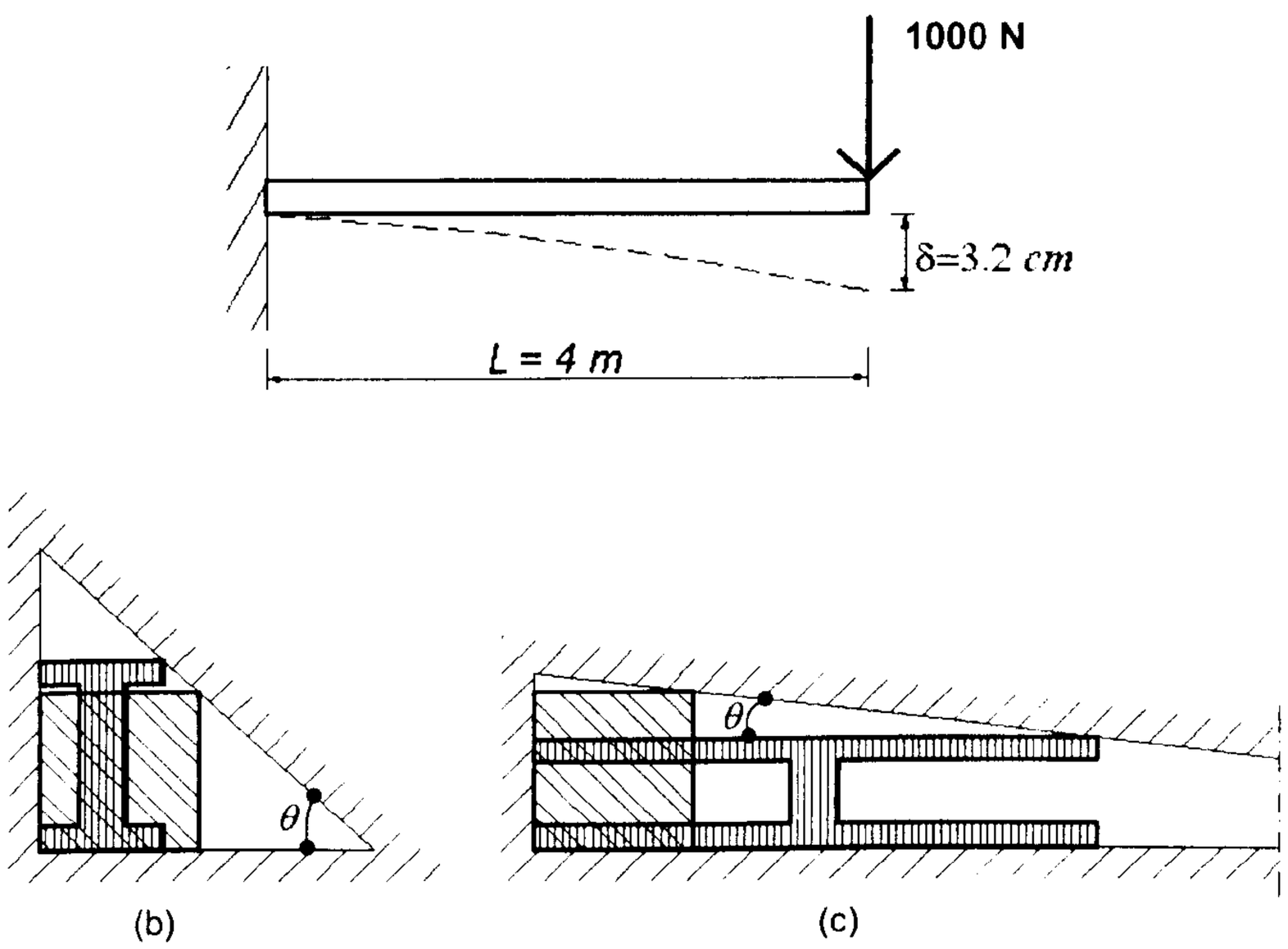

Figure 5.1 The cantilever (a) and its cross-sections in two different constrained conditions: (b) steep sloped constraint with θ=42.3°. (q=-0.21), (c) shallow sloped constraint with θ=6.8° (q=4.81).

Limiting shape regimes graph

The limiting regimes for the two shapes and two design constraints are illustrated in Figure 5.1 and Figure 5.2, where all regions in grey indicate that all I-sections provide the lightest structure, while in the narrow white region only solid rectangle cross-sections give the lightest structures.

When there are narrow limits, Figure 5.1 illustrates there are four solutions R1, R2, I1 and I2, where the stiffness requirement curves intersect the constraint line. Points I1 and I2 lie in the regions where the I-sections provide the best performance compared to the reference section R1.

In the second constraint case, Figure 5.2 shows four solutions R1, R2, I1 and I2. Whereas point I1 lies in the region where the I-sections are lighter, I2 is located where the square reference, R1, provides the best performance. Therefore, in this case the section, R1, performs better than the I-section in providing minimum mass for the same bending stiffness. In Table 5.1 and Table 5.2, numerical calculations validate the results.

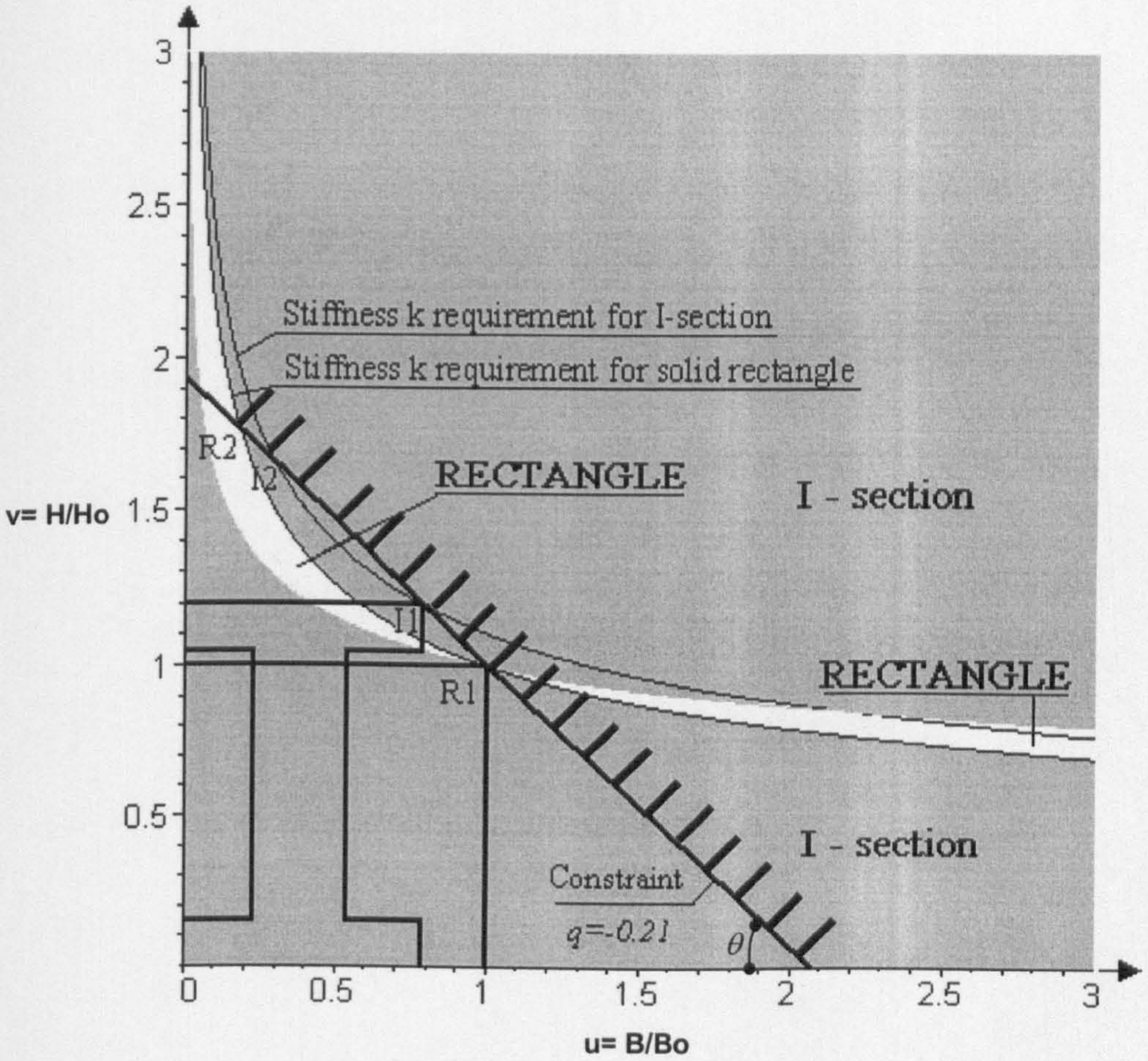

Figure 5.1 Limiting shape regimes graph for the steep constraint with θ=42.3°.

	ψ_A	ψ_I	B	H	$H\text{-}h = B\text{-}b$	u	v	q	k	$p=\frac{\psi_I}{\psi_A}^q$	m	Mass saving
			m	m	m				N/m		Mg	
Rectangle	1.00	1.00	1.00	1.00		1		-0.21	30859	1.00	11.6	
I-section I1	0.54	0.74	0.78	1.20	0.30	1.20	0.78	-0.21	30859	1.98	5.85	50%

Table 5.1 Numerical results for steep constraint with θ=42.3° (q= -0.21)

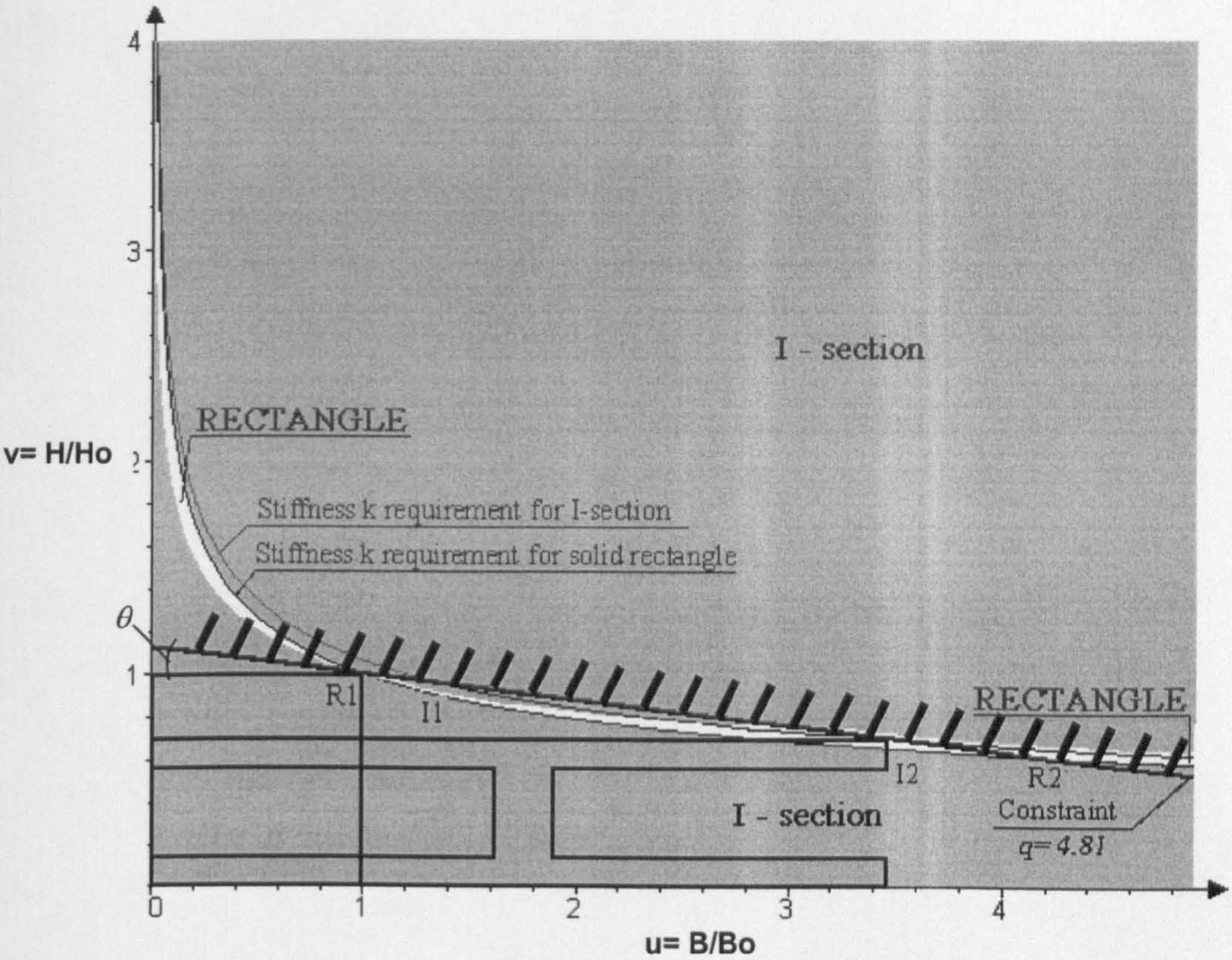

Figure 5.2 Limiting shape regimes graph for shallow constraint with θ=6.8°.

	ψ_A	ψ_I	B	H	$H\text{-}h = B\text{-}b$	u	v	q	k	$p=\frac{\psi_I^{\,q}}{\psi_A}$	m	Mass saving
			m	m	m				N/m		Mg	
Rectangle	1.00	1.00	1.00	1.00		1		4.81	30859	1.00	11.6	
I-section I2	0.48	0.83	3.52	0.70	0.30	0.70	3.52	4.81	30859	0.85	13.6	-17%

Table 5.2 Numerical results for shallow constraint with θ=6.8° (q= 4.81)

5.9 SUMMARY

This Chapter has examined the selection of cross-sectional shapes for a given material and functional requirement. The shape transformers have been used to derive a general solution of performance index and criterion for arbitrary scaling of the cross-sections. These two approaches have been explored analytically and graphically. Different design charts have been presented to gain insight. The envelope efficiency map has been produced in analogy to the material chart for stiffness and strength design. While material properties are displayed on material charts, it has been shown that shape properties can be plotted for different classes of shapes on the envelope efficiency map. The charts have been examined and have been used to tackle different design applications.

CHAPTER 6

CO-SELECTION OF MATERIAL AND SHAPE PROPERTIES

6.1 INTRODUCTION

In this Chapter the theory of the shape transformers is applied to the case where both material, *M*, and shape, *S*, are design variables. The Chapter consists of the following three parts:

- The first part examines the **co-selection of *M* and *S***. This corresponds to conditions 4 and 5 in Table 3.5, illustrated respectively in Figures 3.6d) and 3.6e). In contrast to condition 5, condition 4 considers cross-sections with the same envelope, *D*, and different material, *M*, and shape, *S*, properties. For this reason, the **interchangeability condition of material and shape properties** is introduced. The performance criterion and performance index are used to show the co-selection of material and shape in normal and logarithmic **material charts**.
- The second part uses the envelope efficiency map to explore the **practical limits to the shape transformers** due to the limitations of the manufacturing processes of currently available standard cross-sections.
- The last section considers the role of material and shape properties for the **design of compressive struts**. The cases presented in Chapter 3 for yield design, Euler's compressive design and compression stress failure are analysed. Expressions of performance and minimum mass are given.

6.2 INTERCHANGEABILITY OF M AND S IN THE DESIGN SPACE

Condition 4 of Table 3.5, shown in Figure 3.6(d), describes the co-selection of material and shape properties in a given envelope. In order to examine this, a condition for interchanging the product of the material properties, *M*, and the shape properties, *S*, of a cross-section is derived.

In Chapter 3, the theory of the shape transformer has shown that the design requirements can be expressed as a product $F = G_D x S x M$, i.e. equation (3.22). When two cross-sections, C_1 and C_2, satisfy a given functional requirement F, then $F_1 = F_2$ and from equation (3.22):

$$\underbrace{G_{D1} x S_1 x M_1}_{C_1} = \underbrace{G_{D2} x S_2 x M_2}_{C_2} \tag{6.1}$$

where $G_D = f[B, H]$, $S = S[\psi_A, \psi_I, \psi_Z]$ and $M = M[\rho, E, \sigma_y]$

If *D* is fixed as in Figure 3.6d, then $D_1 = D_2$ and from equation (6.1) **the spatial interchangeability condition** is given by:

$$S_1 x M_1 = S_2 x M_2 \tag{6.2}$$

Equation (6.2) shows that for a given functional requirement, $F = F_1 = F_2$, the product of the material and shape properties, $S_1 x M_1$, for a cross-section C_1 can be exchanged with $S_2 x M_2$ for C_2 without any variation of the envelope size, *D*.

For given envelope $D = D_1 = D_2$, materials M_1 and M_2 and shape S_1, the spatial interchangeability, equation (6.2), applied to the equations of the design cases given in Section 3.5, gives the following shape transformers for S_2

$$\psi_{A2} = \frac{\rho_1}{\rho_2} \psi_{A1}$$ for given mass, *m*, and length, *L* , from equation (3.11) (6.3)

$$\psi_{A2} = \frac{\sigma^t_{y1}}{\sigma^t_{y2}} \psi_{A1}$$ for a given tensile load, *P*, from equation (3.12) (6.4)

$$\psi_{I2} = \frac{E_1}{E_2} \psi_{I1}$$ for given stiffness, *k*, and length *L* , from equation (3.13) (6.5)

$$\psi_{Z2} = \frac{\sigma_{y1}}{\sigma_{y2}} \psi_{Z1}$$ for a given moment failure, M_y, from equation (3.14) (6.6)

The effect of the spatial interchangeability conditions on the space occupied by the curves of the functional requirement are now examined.

The curves of functional requirement and mass

Two cross-sections C_1 and C_2 are considered. C_1 has material properties $M_1(\rho_1, E_1)$ and shape transformers $S_1(\psi_{A1}, \psi_{I1})$. C_2 has $M_2(\rho_2, E_2)$ and $S_2(\psi_{A2}, \psi_{I2})$. For a given design requirement, there are an infinite number of solutions, *BxH*, of the envelope D_1 for C_1 and an infinite number of solutions, *BxH*, of the envelope D_2 for C_2. For example in stiffness design, from equation (3.13) the feasible solutions, *BxH*, for C_1 and C_2 belong to the following curves *H=f(B)*:

$$\begin{cases} H = \left(\dfrac{12kL^3}{c_1} \dfrac{1}{E_1} \dfrac{1}{\psi_{I1}} \dfrac{1}{B} \right)^{1/3} \\ H = \left(\dfrac{12kL^3}{c_1} \dfrac{1}{E_2} \dfrac{1}{\psi_{I2}} \dfrac{1}{B} \right)^{1/3} \end{cases} \tag{6.7}$$

In a similar way, in strength design the requirement, equation (3.14), is described by the curves:

$$\begin{cases} H = \left(6M_y \dfrac{1}{\sigma_{y1}} \dfrac{1}{\psi_{Z1}} \dfrac{1}{B} \right)^{1/2} \\ H = \left(6M_y \dfrac{1}{\sigma_{y2}} \dfrac{1}{\psi_{Z2}} \dfrac{1}{B} \right)^{1/2} \end{cases} \tag{6.8}$$

Curves of equal masses for C_1 and C_2 are given by:

$$\begin{cases} H = \dfrac{m}{L} \dfrac{1}{\rho_1} \dfrac{1}{\psi_{A1}} \dfrac{1}{B} \\ H = \dfrac{m}{L} \dfrac{1}{\rho_2} \dfrac{1}{\psi_{A2}} \dfrac{1}{B} \end{cases} \tag{6.9}$$

Equations (6.7) and (6.9) are plotted in Figure 6.1 and Figure 6.2 for a cantilever with length L=5m, c_1=3. The rectangular sections are out of aluminium M_{al}(ρ=2.71 Mg/m^3, E=70 GPa) and S_{al}(ψ_A=1, ψ_I=1) and copper with M_{cu} (ρ= 8.94 Mg/m^3, E=115 GPa) and S_{cu}(ψ_A=1, ψ_I=1). The stiffness requirement is k=200*10^6 N/m in Figure 6.1 and the mass requirement is m = 20 Mg in Figure 6.2. Since the shape properties of rectangles are unity, the space occupied by the solid cross-sections is minimised.

However, copper envelopes occupy less space since E and ρ are higher. If shape properties other than those of the rectangle are selected for copper sections, then the requirement curves for k shows that more space is required.

Examples of the effect of the interchangeability conditions, equations (6.5) and (6.3), on the requirement curves are shown respectively in Figure 6.1 and Figure 6.2. For example, using equation (6.5), the shape transformer ψ_I of a shaped copper is ψ_{I2}=0.608 and applying ψ_{I2} on the rectangular envelope D_{cu} allows the stiffness requirement curve of the shaped copper in Figure 6.1 to be superimposed to the requirement curve of the aluminium rectangular section. In a similar way, equation (6.3) has been used to derive the shape transformer ψ_{A2}=0.303 which is applied to a rectangular copper D_{cu}. The effect of this is shown in Figure 6.2. The curve which describes the mass requirement for the shaped copper is superimposed to that for the rectangular aluminium.

The interchangeability conditions for S and M are necessary to analyse selection condition 4 of Table 3.5. This is shown in the following Section with the performance criterion.

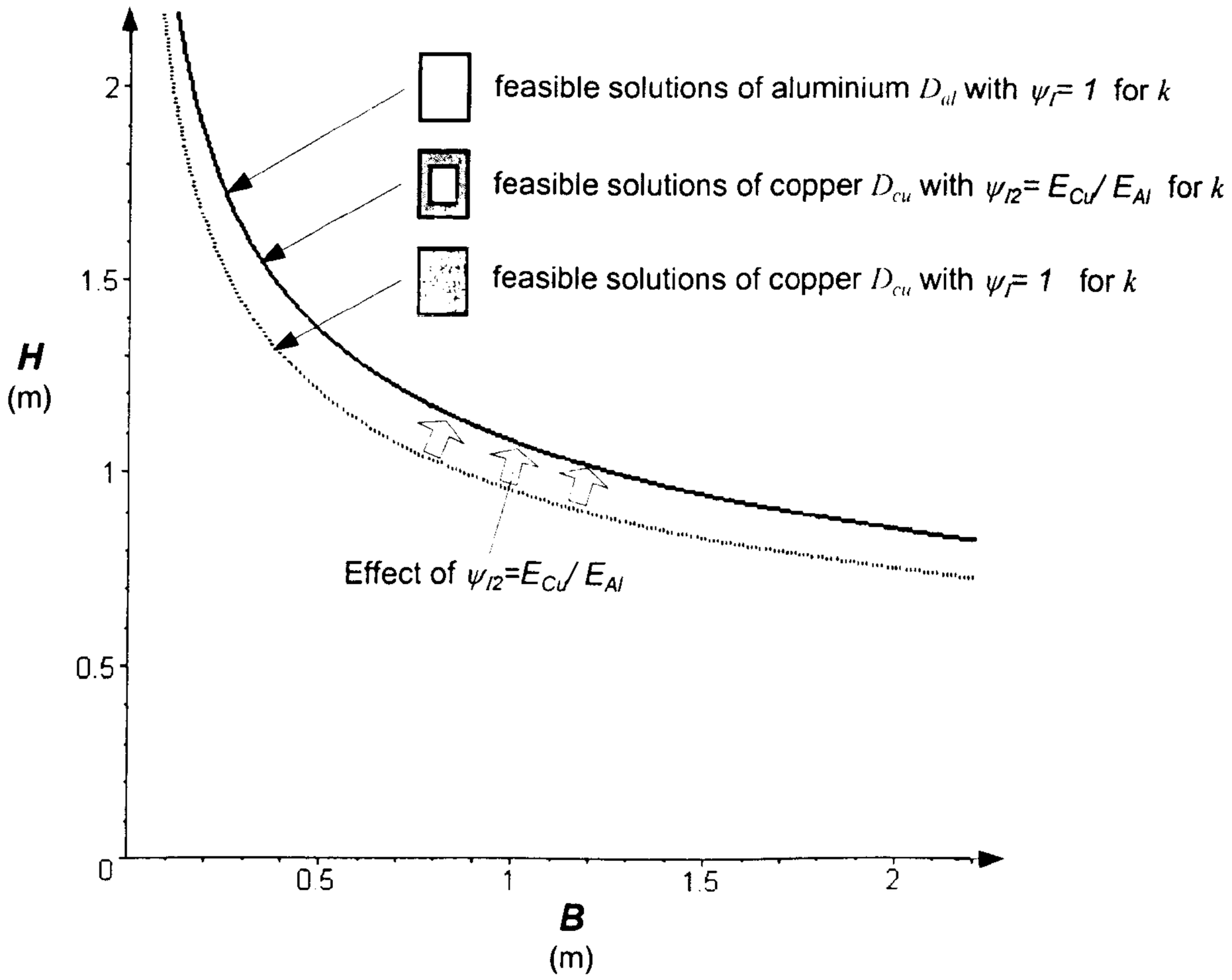

Figure 6.1 Feasible solutions for aluminium and copper envelopes in stiffness design (k=200*10^6 N/m).

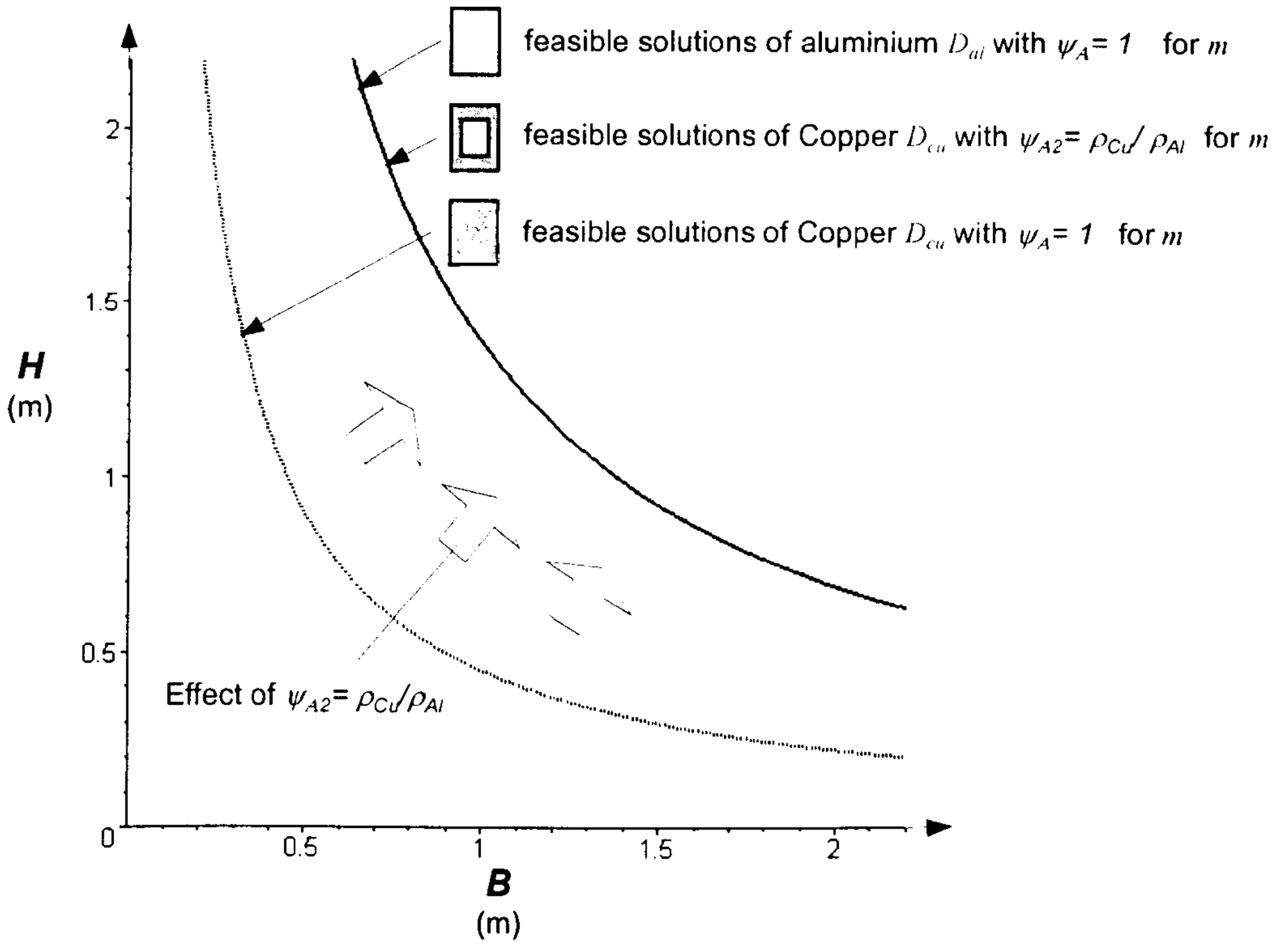

Figure 6.2 Curves of equal mass (m=20 Mg) for aluminium and copper envelopes.

6.3 PERFORMANCE CRITERION

From the general expression of the performance criterion, p , i.e. ratio between stiffness, equation (3.13), and mass, equation (3.11), the performance, p, for structural envelopes, D, with M and S variables, is given by:

$$p = \frac{1}{m} = \underbrace{\left[\frac{c_1}{12kL^4}\right]}_{F} \underbrace{\left[\frac{E}{\rho}\right]}_{M} \underbrace{[\lambda_I]}_{S} \underbrace{[H^2]}_{D=f(M,S)} \qquad \text{for stiffness design} \qquad (6.10)$$

$$p = \frac{1}{m} = \underbrace{\left[\frac{1}{6M_y}\right]}_{F} \underbrace{\frac{\sigma_y}{\rho}}_{M} \underbrace{[\lambda_Z]}_{S} \underbrace{H}_{D=f(M,S)} \qquad \text{for strength design} \qquad (6.11)$$

In stiffness design, the performance, equation (6.10), and the requirement, equation (6.7), allow conditions 4 and 5 of Table 3.5 to be examined. The spatial interchangeability condition introduced in Section 6.2 is now used to examine condition 4 of Table 3.5 in the following two cases:

- **One active interchangeability condition.** For a given stiffness, $\psi_{I2} = \frac{E_1}{E_2}\psi_{I1}$

permits the curves of the requirement to be superimposed. Figure 6.1 shows an example for aluminium envelopes, D_{al}, and copper envelopes D_{cu} with the same stiffness k=20*10^{6}N/m. The properties of D_{al} are M_{al}(ρ=2.71 Mg/m^3, E=70 GPa) and S_{al}(ψ_A=1, ψ_{I1}=1). For D_{cu}, the properties are M_{cu} (ρ=8.94 Mg/m^3, E=115 GPa) and S_{cu} (ψ_A= 0.374, ψ_{I2}=0.608). For the copper envelope, ψ_{I2} has been derived using equation (6.5), while ψ_A is the shape transformer for hollow rectangle with $b/B=h/H$ given in Table 3.3. If the envelope is fixed, i.e. $D_{cu}=D_{al}$ (condition 4 of Table 3.5), Al≡Cu in Figure 6.1 and the cross-sections have a different performance, $p_{cu} > p_{al}$.

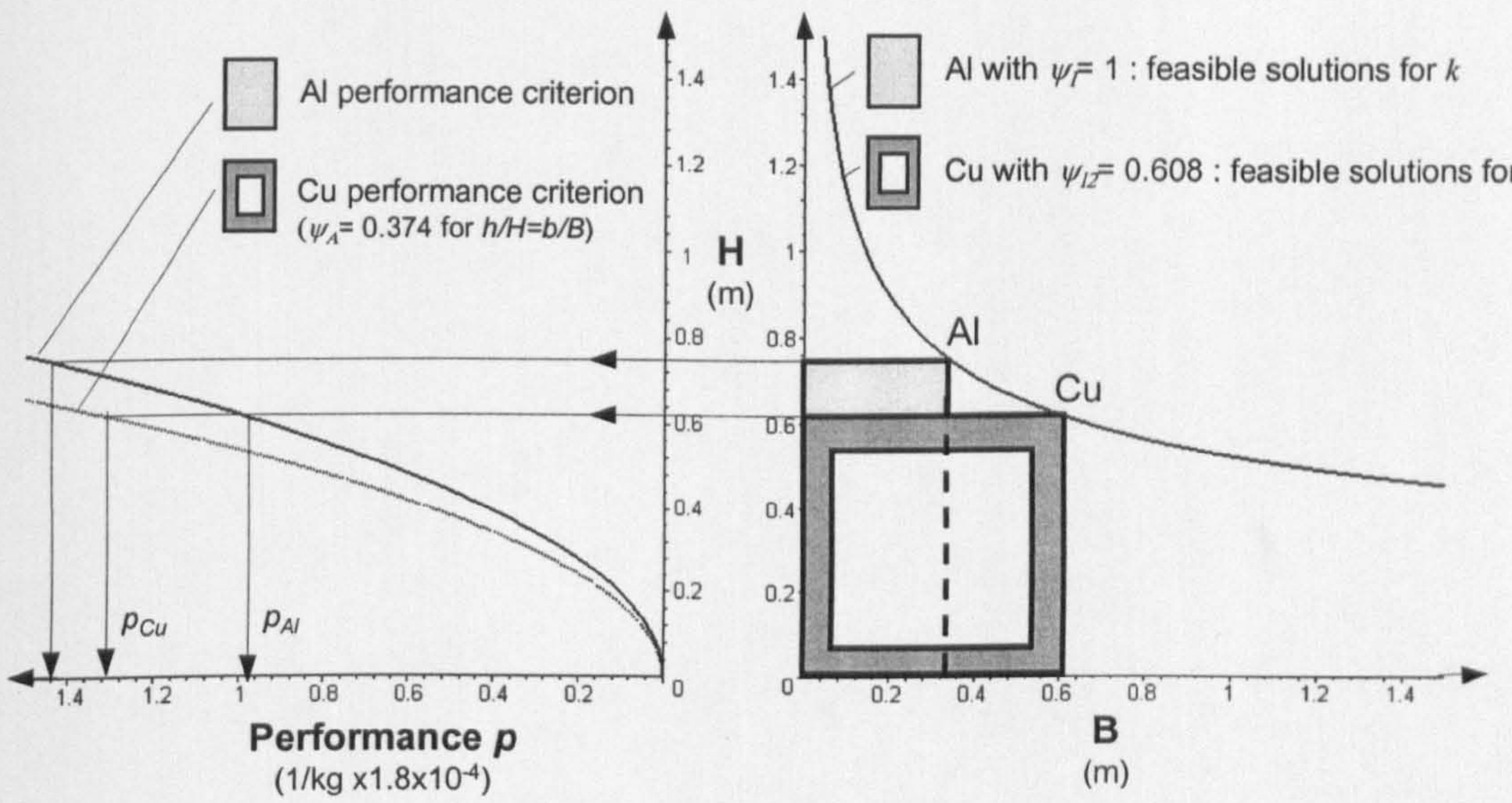

Figure 6.1 Two performance curves and one stiffness requirement curve. For Al ≡ Cu , i.e. condition 4 of Table 3.5, $p_{Cu}>p_{Al}$.

- **Two active interchangeability conditions.** $\psi_{I2} = \frac{E_1}{E_2}\psi_{I1}$ and $\psi_{A2} = \frac{\rho_1}{\rho_2}\psi_{A1}$

permit the curves of constant mass and constant stiffness to be superimposed. Figure 6.2 shows that the aluminium rectangular envelope, D_{al}, and copper, D_{cu}, with S_{cu} (ψ_{A2}= 0.303, ψ_{I2}= 0.608) given by equations (6.3) and (6.5), are described by one requirement curve and one performance curve. In contrast to the previous case, if D is fixed, i.e. $D_{al}=D_{cu}$ (condition 4 of Table 3.5), Al≡Cu in Figure 6.2 and the cross-sections have the same stiffness and same performance, i.e. same mass.

It is important to note that when the design requirement is specified by the spatial interchangeability conditions, then horizontal, vertical and proportional scaling are not feasible because there is only a unique requirement curve. Although the shape properties are different, this case is similar to condition 1 of Table 3.5 illustrated in Figure 4.5.

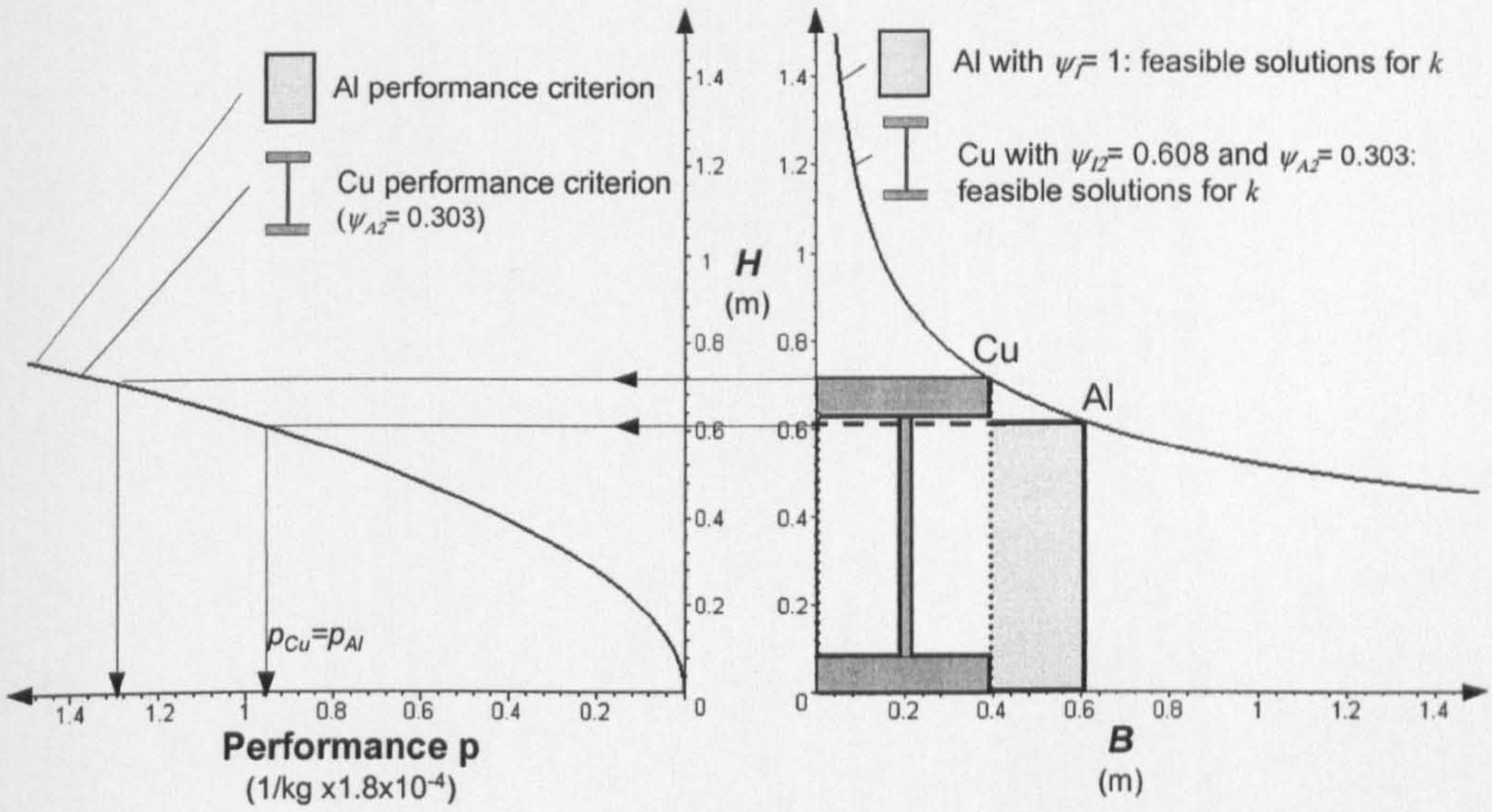

Figure 6.2 One performance curve and one stiffness requirement curve. For Al ≡ Cu, condition 4 of Table 3.5, $p_{Al}=p_{Cu}$.

6.4 PERFORMANCE INDEX

The performance index can be adopted for condition 5 of Table 3.5 where *M*, *S* and *D* are variables. However, for condition 4, where *D* is fixed and *u=v=1*, there is no solution for the performance index because *q=f(u,v)* is unbounded.

The derivation of the general expression of the performance index for arbitrary scaling is analogous to those in Chapters 4 and 5. For this reason it is not examined in detail here. The only differences are the following conditions to impose to *u* and *v*:

$$\begin{cases} u = \left(\dfrac{E_o}{E} \dfrac{1}{\psi_I} \right)^{\alpha} \\ v = \left(\dfrac{E_o}{E} \dfrac{1}{\psi_I} \right)^{\beta} \end{cases} \quad \text{for stiffness design} \tag{6.12}$$

$$\begin{cases} u = \left(\dfrac{\sigma_{y_o}}{\sigma_y} \dfrac{1}{\psi_Z} \right)^{\alpha} \\ v = \left(\dfrac{\sigma_{y_o}}{\sigma_y} \dfrac{1}{\psi_Z} \right)^{\beta} \end{cases} \quad \text{for strength design} \tag{6.13}$$

6.4.1 Stiffness design: $(E\psi_I)^q/\rho\psi_A$ for any arbitrary direction of scaling

For a stiffness requirement the general expression of the performance index is given by:

$$p = \frac{(E\psi_I)^q}{\rho\psi_A} \tag{6.14}$$

where $q = \ln uv / \ln uv^3$ and u and v are a function of $f(E, E_o, \psi_I)$ given by (6.12).

6.4.2 Strength design: $(E\psi_I)^q/\rho\psi_A$ for any arbitrary scaling

In strength design, the performance index is:

$$p = \frac{(\sigma_y \psi_Z)^q}{\rho\psi_A} \tag{6.15}$$

where $q = \ln uv / \ln uv^2$ and u and v are function $f(\sigma_y, \sigma_{yo}, \psi_Z)$ given by (6.13).

6.5 CO-SELECTION OF MATERIAL AND SHAPE

Graphical charts and tables can be used to co-select material and shapes. This Section illustrates first the graphical selection using material charts in normal and logarithmic scales for the conditions 4, i.e. fixed envelope, and 5, i.e. variable envelope of Table 3.5. Finally, the use of tables for M and S variable is considered.

Chapters 4 and 5, have shown how the theory of shape transformers is used to display the mass, m, and the design requirement, F, of a cross-section $C(\underbrace{MxSxG_D}_{m}, \underbrace{MxSxG_D}_{F})$ on material and shape charts. In a similar way, the graphical co-selection of M and S can be illustrated by superimposing, the envelope

efficiency map, i.e. shape chart, to a material chart. In such a case, the co-ordinate of a cross-section, *C*, for the cases where D is fixed or variable, are:

D fixed	*D* variable
$C\left(\frac{m}{G_D}=MxS\ ,\ \frac{F}{G_D}=MxS\right)$	$C\ (\ m=MxSxG_D\ ,\ F=MxSxG_D\ )$

6.5.1 Normal scale material charts

When *M* and *S* are variables, the performance of a cross-section C(m,k) is represented in a normal scale chart by the performance criterion, $p=k/m$. From equation (6.10), if the envelope is fixed, then $p=k/m=E\lambda/\rho$. The performance, p, is the slope of the line connecting each point on a material chart and the origin. This is shown in Figure 6.1. In the following, two cases of selection are examined for a fixed envelope, *D*, and for a variable *D*.

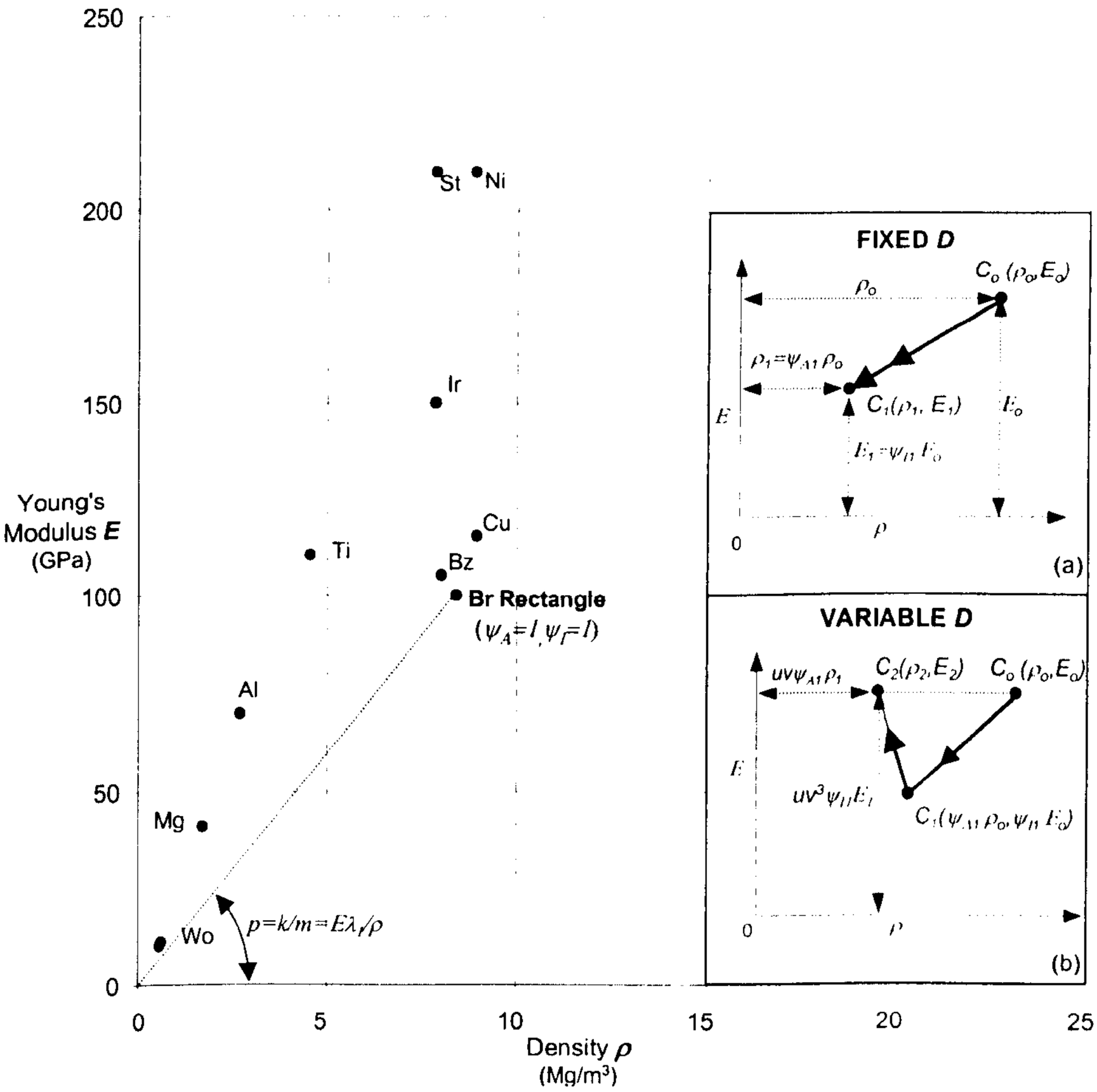

Figure 6.1 Normal scale material chart E - ρ for stiffness design.

- **Fixed envelope *D*.**

  The mass, m_o, and the stiffness, k_o, of a rectangular cross-section, C_o($\underbrace{M_o x S_o x G_{D_o}}_{m_o}$, $\underbrace{M_o x S_o x G_{D_o}}_{ko}$), with material properties M_o (ρ_o, E_o), shape properties S_1(ψ_{Ao}=1, ψ_{Io}=1) and envelope D_o (B,H) is illustrated in Figure 6.1a) by the co-ordinate C_o(ρ_o, E_o). For a cross-section C_1($\underbrace{M_1 x S_1 x G_{D_1}}_{m_1}$, $\underbrace{M_1 x S_1 x G_{D_1}}_{k_1}$) with envelope, D_o=D_1, and material, M_1=M_o, but different shape properties S_1(ψ_{A1}, ψ_{I1})≠ S_1(1,1), m_1 and k_1 are identified by C_1($M_o x S_1$, $M_o x S_1$), so that:

$$\begin{cases} m_1 \rightarrow \rho_1 = \psi_{A1}\rho_o \\ k_1 \rightarrow E_1 = \psi_{I1}E_o \end{cases} \quad \text{for stiffness} \tag{6.16}$$

As explained in Chapter 5 with the envelope efficiency map, shaping a rectangular cross-section has the effect of decreasing the stiffness and the mass according to the values of the shape transformers (0<ψ_A<1, 0<ψ_I<1). Therefore, since the envelope is fixed, i.e. D_1=D_o, any value of the shape properties S_2 does not permit the stiffness, k_1, of the cross-section C_1 to be the same stiffness, k_o, of the rectangle C_o. This means that C_1 cannot lie on the horizontal line, k_o , E_o, of C_1 as shown in Figure 6.1a).

The material chart is used to display material properties, *M*, as the envelope efficiency map is used to plot shape properties, *S*. **Superimposing** the effect of **the two charts** shows the benefit of shaping a material, i.e. MxS, for a prescribed envelope, D. Using the expressions of the shape transformers given in Table 3.3, the mass, $m_1 = \psi_{A1}\rho_1$, and the stiffness, $k_1 = \psi_{I1}E_1$, have been plotted in Figure 6.2 for bronze M(ρ =7.8 Mg/m^3, E=115 GPa) and aluminium M(ρ =2.9 Mg/m^3, E=70 GPa). Bronze cross-sections between A and B provide the same stiffness as that of the aluminium rectangular cross-section. However, only bronze cross-sections in the efficient region between A and C are lighter.

It is evident that other efficiency domains of different shape classes can be superimposed. For example, the shape class of the elliptical cross-sections is shown for bronze in Figure 6.2. The advantage of this graphical superimposition is that all the ranges of material, *M*, and shape, *S*, properties can be displayed on one chart to compare different shaped materials, MxS.

In a similar way in strength design, for a given moment failure, M_y, m_1 and M_{y1} of a cross-section C_1 are displayed by:

$$\begin{cases} m_1 \rightarrow \rho_1 = \psi_{A1}\rho_o \\ M_{y1} \rightarrow \sigma_{y1} = \psi_{Z1}\sigma_{yo} \end{cases} \quad \text{for strength} \tag{6.17}$$

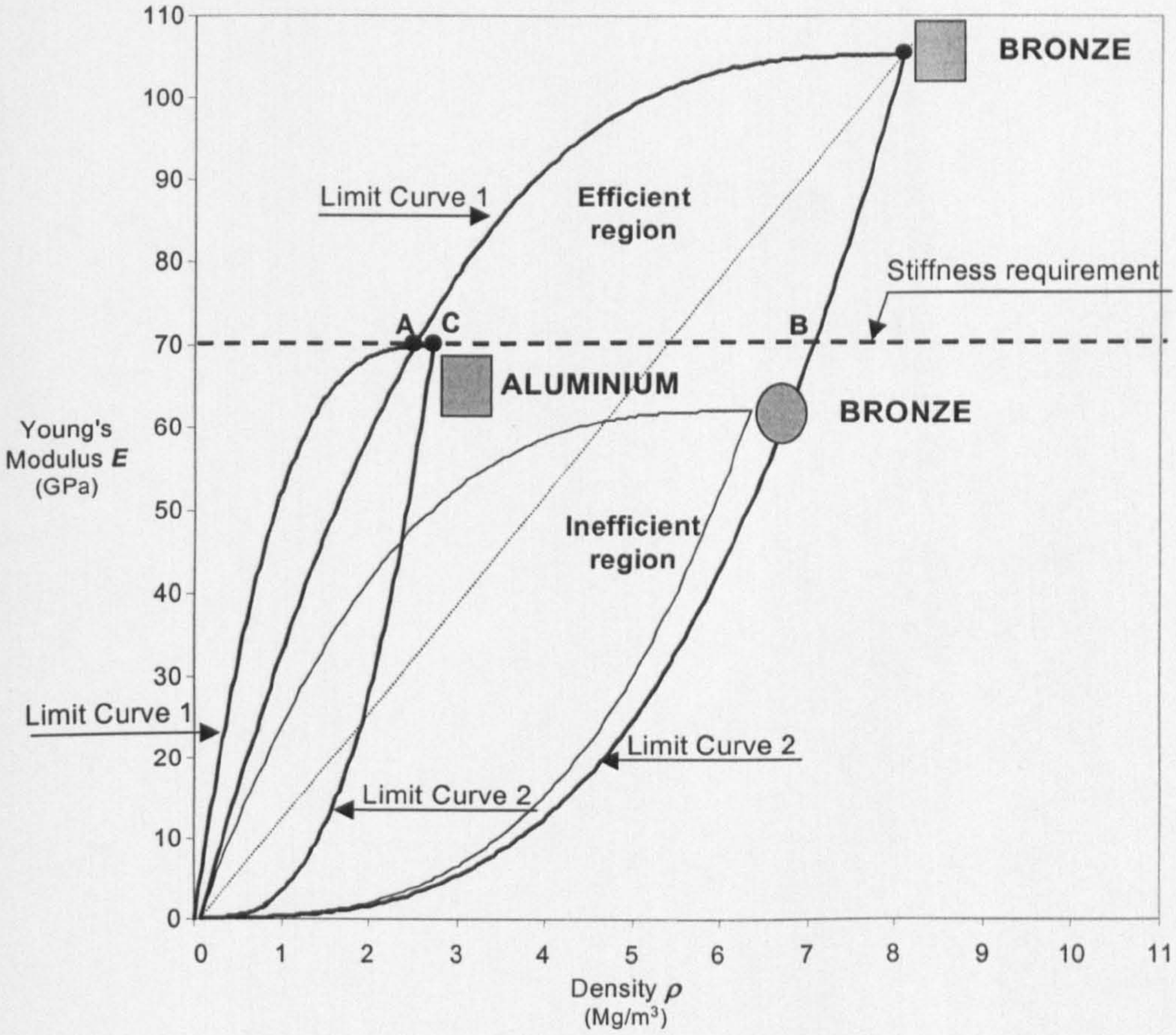

Figure 6.2 Co-selection of material, *M*, and shape, *S*, properties normal scale material chart E - ρ for stiffness design. (Note that *D* is fixed)

- **Variable *D*.**

  Arbitrary scaling

In the case of *D* fixed, Figure 6.1a) shows that two cross-sections $C_1(m_1, k_1)$ and $C_1(m_o, k_o)$ with $M_1 = M_o$ and $S_1 \neq S_o$ have different stiffness $k_1 \neq k_o$. C_1 is now arbitrarily scaled to $C_2(\underbrace{M_2 x S_2 x G_{D2}}_{m_2}, \underbrace{M_2 x S_2 x G_{D2}}_{k_2})$ with $D_2 \neq D_1$, $M_2 = M_1 = M_o$ and $S_2 = S_1$, i.e. $(\underbrace{M_o x S_1 x G_{D2}}_{m_2}, \underbrace{M_o x S_1 x G_{D2}}_{k_2})$ as shown in Figure 6.1b). C_2 has the same stiffness of C_1, i.e. $k_2 = k_1$, if u and v satisfy the condition:

$$k_2 / k_o = uv^3 \psi_{I1} = 1 \tag{6.18}$$

For a given ψ_{I2} and u, the value of v which satisfies equation (6.18) gives the following mass, m_2, and stiffness, k_2, of $C_2(m_2, k_2)$:

$$\begin{cases} m_2 \rightarrow \rho_2 = uv\psi_{A1}\rho_o \\ k_2 \rightarrow E_2 = E_o \end{cases} \quad \text{for stiffness} \tag{6.19}$$

Equation (6.19) shows that the shape properties and also the multiplicator u and v specify the co-ordinates of $C_2(m_2, k_2)$. Figure 6.1b) illustrates the effect of scaling the envelope D_1 to D_2 with respect to the stiffness requirement, $k_2=k_o$, equation (6.18). This time the cross-sections C_2 and C_o lie on the same horizontal line representing the stiffness k_o.

Proportional, vertical and horizontal scaling

As explained in Chapters 4 and 5, when the direction of scaling of the envelope, D, is prescribed in advance, then u and v can be expressed as a function of the shape transformers. Therefore, in contrast to arbitrary scaling, there is no need to know both the values of u and v. For instance, for horizontal, vertical and proportional scaling, the co-ordinate of $C_2(m_2, k_2)$, given by equation (6.19) does not depend on u and v and are given by:

Prescribed scaling		Derived condition from (6.18)	C_2 (ρ_2,E_2) from (6.19)	
Horizontal scaling	$v=1$	$u= 1/\psi_{I1}$	$m_2 \rightarrow \rho_2 = \rho_o \psi_{A1} (1/\psi_{I1})^{1/3}$	$k_2 \rightarrow E_2 = E_o$
Vertical scaling	$u=1$	$v=(1/\psi_{I1})^{1/3}$	$m_2 \rightarrow \rho_2 = \rho_o \psi_{A1} (1/\psi_{I1})$	$k_2 \rightarrow E_2 = E_o$
Proportional scaling	$u=v$	$u=v=(1/\psi_{I1})^{1/4}$	$m_2 \rightarrow \rho_2 = \rho_o \psi_{A1} (1/\psi_{I1})^{1/2}$	$k_2 \rightarrow E_2 = E_o$

In a similar way, the previous arguments apply for a failure moment requirement, M_y. The co-ordinate of a cross-section $C_3(m_3, M_{y3})$ are given by:

$$\begin{cases} m_3 \rightarrow \rho_3 = uv\psi_{A2}\rho_1 \\ M_{y3} \rightarrow \sigma_{y3} = \sigma_{y1} \end{cases} \quad \text{for strength} \tag{6.20}$$

6.5.2 Logarithmic scale material charts.

The general expression of the **performance index**, $p = (E\psi_I)^q / \rho\psi_A$, can be used for the selection in **a logarithmic scale ρ-E chart.** In order to display the position and thus the performance of a cross-section C(m,k), with respect to its mass, m, and stiffness, k, the **performance index** is rearranged as:

$$\log E\psi_I = \frac{1}{q}\log \rho\psi_A + \frac{1}{q}\log p \qquad (6.21)$$

The material chart shown in Figure (4.12) displays the material properties, *M*. The shape chart illustrated in Figure (5.15) plots the shape transformers, *S*. Superimposing the shape chart, Figure (5.15), on the material chart, Figure (4.12), permits the selection with the performance index, equation (6.21). One advantage of the logarithmic chart is that the slopes $1/q$ can be used as guide lines to compare scaled cross-sections. As in Chapters 4 and 5, q=1, q=1/2 and q=1/3 are used to select among cross-sections which are horizontally, proportionally and vertically scaled respectively. The following cases are examined.

- ***D* fixed.**

  As with Figure 6.2, cross-sections with the same envelope, *D(B,H)*, are displayed in Figure 6.1 by co-ordinates C($\underbrace{\psi_A\rho}_{m}$, $\underbrace{\psi_I E}_{k}$). In this case, the performance index, as explained in Section 6.4, cannot be used because u=v=*1* and q=*ln(uv)/ln(uv^3)* is unbounded. Therefore, for *D* fixed the performance is given by the performance criterion, p=k/m.

- ***D* variable.**

  For a given stiffness, two cross-sections C_1 and C_2 with different material, $M_1 \neq M_2$, shape, $S_1 \neq S_2$, and envelope $D_1 \neq D_2$, are considered. This is illustrated in Figure 3.6e) and corresponds to condition 5 of Table 3.5. The performance indices of C_1 and C_2 are: $p_1 = (E_1\psi_{I1})^q / \rho_1\psi_{A1}$ and $p_2 = (E_2\psi_{I2})^q / \rho_{12}\psi_{A2}$.

  C_1 is a rectangular steel cross-section and is shown by St in Figure 6.1. The guidelines $1/q$ are now used to compare the performance of C_1 to C_2. For a

given q, i.e. for a given condition of scaling, the cross-section C_2 has equal performance to C_1 if it lies on the same guideline. The cross-sections above or below the line have better or worse performance index. An example of a steel rectangular cross-section competing with other cross-sections is shown in Figure 6.1 for a height constraint, q=1.

Figure 6.1 shows the limiting curves of the rectangle shape class for steel, st, aluminium, al, and lead, pb. As with Figure 6.2, other classes of shapes can be superimposed. For example, the limiting curves of elliptical cross-sections are shown for aluminium. A computerised version of the graph could be implemented for the whole range of material and shape properties. For each material the limiting curves for different class of shapes can be superimposed in order to help in the selection of the best *S* and *M* properties for cross-sections scaled in different directions.

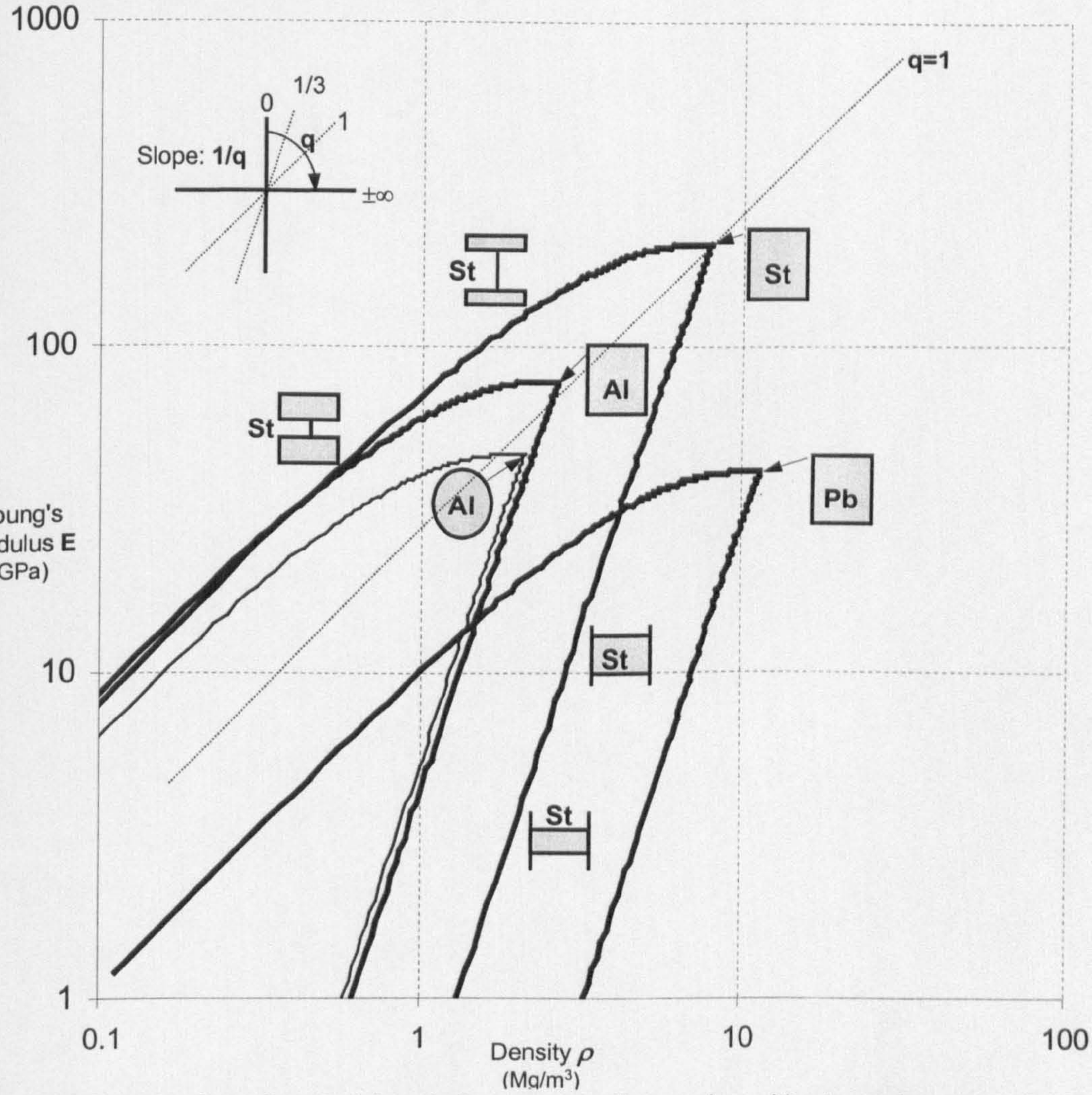

Figure 6.1 Co-selection of material and shape properties on logarithmic scale material chart E - ρ for stiffness design

6.5.3 Material and shape tables

From the expression of q, it is possible to produce tables of q for specific materials, shapes and angles of slope constraint. These tables can be used by designers to directly compare the performance of different cross-sections and materials for a particular application. Table 6.1 presents, as an example, values of q for two materials and two shapes. An aluminium square is chosen as a reference section and the sloped constraint lies on its top right vertex. For a given sloped constraint θ, such as that shown in Figure 5.2(c), the values of q in Table 6.1 can be used in equation (6.14) to assess the relative performance.

θ sloped constraint angle		0°	10°	20°	30°	40°	50°	60°	70°	80°	90
	q for										
AL	Reference	q^*	q^*	q^*	q^*	q^*	q^*	q^*	q^*	q^*	q^*
	Ellipse	1	-	-	-	-	-1.41	-2.55	-3.89	-6.15	1/3
STEEL	Rectangle	1	1.25	1.54	1.85	2.18	2.56	3.03	3.69	4.88	1/3
	Ellipse	1	1.38	1.97	2.68	3.46	4.33	5.39	6.85	9.46	1/3

Table 6.1 For a given sloped constraint angle, θ, the value q of a generic section replaces q^* for the reference. '-' denotes no solution in the design space.

6.6 EFFICIENCY LIMITS FOR PRACTICAL CROSS-SECTIONAL SHAPES

This Section explores the limits to the envelope efficiency parameter λ_I for practical steel cross-sections currently available in the market. Standard cross-sections generally have different envelope sizes and shapes. The envelope and shape of the cross-sections both contribute to the structural performance. In general, the higher the height of D and the value of λ_I, the better is the efficiency. The ranges of the envelope efficiency parameter, λ_I, given in Table 3.4 are, therefore, an effective means to select efficient shape properties. The higher λ_I, the lighter is the shape for a given envelope. However, there are limits to the values of λ_I. These limits are generally imposed by current manufacturing constraints and buckling.

The envelope efficiency map is used here to examine the limits of λ_I due to manufacturing constraints. These limits are related only to the contribution of the shape properties and, therefore, they cannot be used to compare directly the structural performance.

The shape properties, ψ_A and ψ_I, of steel cross-sections available in the market are shown on the envelope efficiency map in Figure 6.1. The structures considered are I-shapes of different typologies (IPE, HEA, HEB, INP), C shapes (UPN), tubes and boxes (the symbols IPE, HEA, HEB, INP and UPN correspond to the cross-sectional shapes shown at the bottom of Figure 6.1). The data for these improved sections are not very scattered but they group together close to the limit curve 1. The efficiency of I-sections cannot achieve the efficiency of an idealised I-section with web thickness (B-b)=0. Hollow circular sections (or tubes) lie on a curve that lies within the limit curve 3 for circular sections. Circular sections with a very small wall thickness are generally impracticable to manufacture.

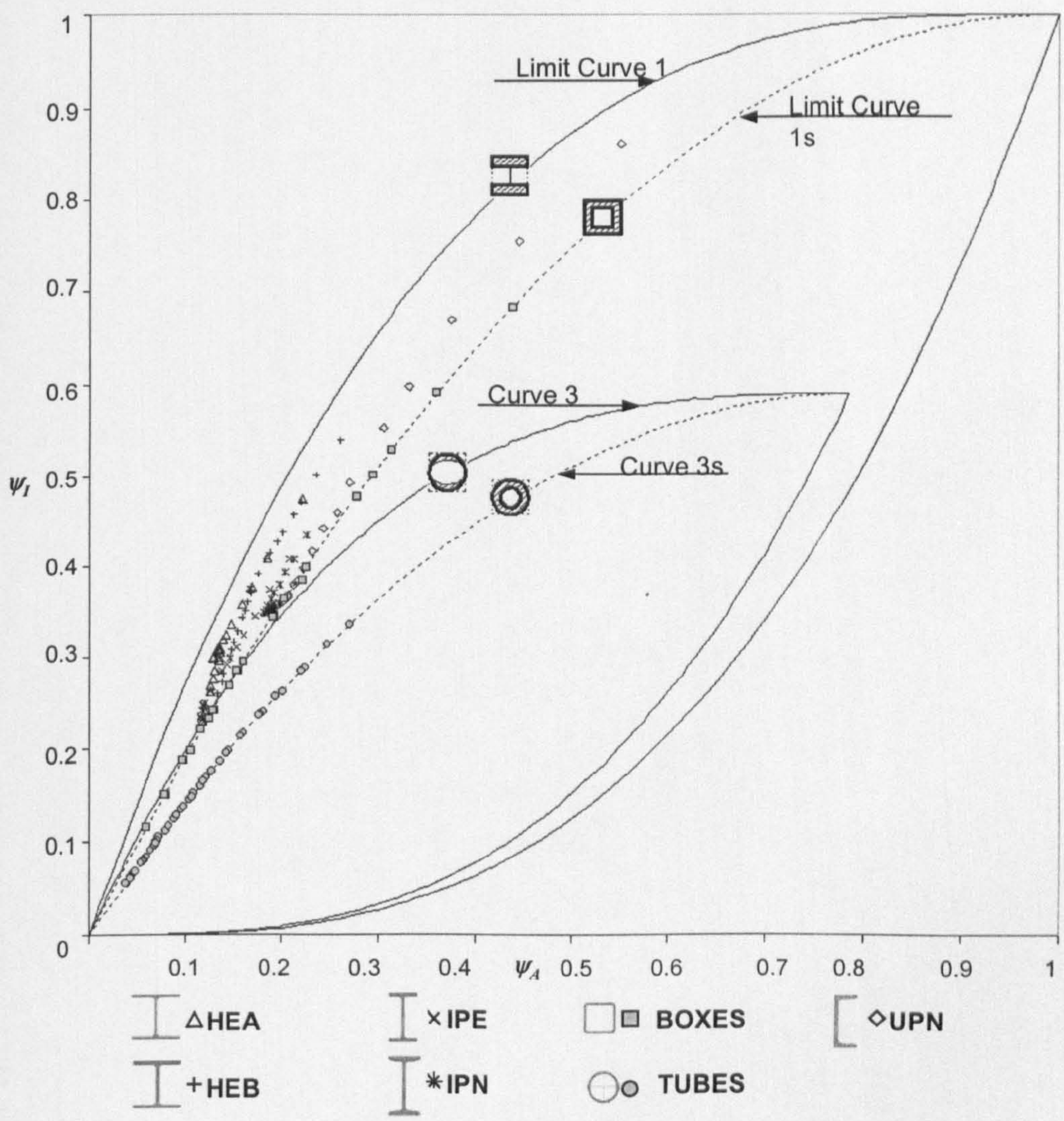

Figure 6.1 Plot of the shape transformers for steel cross-sections available in the market. (Data source: EURONORM EU 53-62; 19-57;5679-73).

The empirical limits of λ_I for the various shapes in stiffness design are: 2.32 for HEA, 2.25 for HEB, 2.08 for IPE, 1.92 for IPN, 1.82 for UPN, 1.94 for square tubes and 1.46 for circular tubes. It should be noted that these limits refer only to the shape properties of sections since the contribution of the envelope sizes to the stiffness of the cross-section is not considered on the envelope efficiency map, Figure 6.1.

6.7 COMPRESSION LOAD DESIGN

In this Section the performance of compressive struts is examined for the three design cases where *M* and *S* are variable. As described in Chapter 3, short thick struts, long slender columns and real compressive members of any slenderness are considered. The performance criterion is used with the combined graph to illustrate the case of slender columns of constant length with very small geometric imperfections. For short thick struts and real struts (i.e. struts which can have any slenderness) direct expressions of minimum-mass are derived. These expressions of minimum mass are used in Chapter 8 for modelling the efficiency of compressive members of variable length for different structural forms.

6.7.1 Compression yield design

Columns with low slenderness, L/r_g, collapse under compression because the load induces yield in the cross-sectional shape. If buckling is not a failure mode in the compressive member, then from equation (3.15) the minimum area, A, to prevent collapse is given by:

$$A = \psi_A A_D = \psi_A BH = \frac{P}{\sigma_y^c} \tag{6.22}$$

From equation (6.22) it is evident that for a given material, σ_y^c, and load, *P*, the minimum area, *A*, is not dependent on the shape properties ψ_A. Therefore, it is not necessary to select in advance the shape of a section to determine the value of the minimum area. However, the shape transformer ψ_A and σ_y^c determine the space occupied by the shape within the structural envelope as $A_D = BH = P/\psi_A \sigma_y^c$.

6.7.2 Compression Euler's buckling design

For a given P_{crit} which induces elastic buckling in a slender column, the performance criterion, p□, from equations (3.11) and (3.16) is given by:

$$\tilde{p} = \frac{P_{crit}}{m} = \frac{n^2\pi^2}{12L^2} \frac{E}{\rho} \frac{\psi_I}{\psi_A} H^2 \tag{6.23}$$

then the performance is:

$$p = \frac{1}{m} = \underbrace{\left[\frac{n^2\pi^2}{12L^2P_{crit}}\right]}_{F} \underbrace{\left[\frac{E}{\rho}\right]}_{M} \underbrace{[\lambda_I]}_{S} \underbrace{[H^2]}_{D=f(M,S)} \tag{6.24}$$

The second member of equation (6.24) contains four groups. The functional requirement, *F*, gathers the constant parameters. *M* and *S* collect the material and shape properties respectively, while *D* is the envelope contribution. *M* and *S* specify the space occupied by the curves of functional requirement given by equation (3.16). Therefore, the factor *D=f(S,M)* is not generally independent from the material and shape properties because both the equations of the requirement, (3.16), and of the performance, (6.24), have to be considered in a selection task. Only if the direction of scaling is imposed a priori, the performance criterion has the same expressions of the performance index as for bending stiffness design illustrated in Chapters 4 and 5.

Buckling limits for the sizes of a structural envelope

This Section derives the limits to the sizes of a structural envelope for a slender strut under elastic buckling. For a given length, L, and support conditions, the maximum compressive stress for slender struts is given by the proportional limit stress of the material which from (3.6) is

$$\sigma_y^c = \left(\frac{n\pi}{L}\right)^2 E r_g^{\,2} \tag{6.25}$$

If the radius of gyration, r_g, in the expression (6.25) is expressed in terms of the shape transformers as $r_g^{\,2} = \frac{\psi_I}{\psi_A}\frac{H^2}{12} = \lambda_I \frac{H^2}{12}$, then the limit height, H_{lim}, of the envelope is given by:

$$H_{\lim} = \underbrace{\frac{\sqrt{12}L}{n\pi}}_{const} \underbrace{\left(\frac{\sigma_y^c}{E}\right)^{0.5}}_{M} \underbrace{\left(\frac{1}{\lambda_I}\right)^{0.5}}_{S} \tag{6.26}$$

Expression (6.26), shows that for a given length *L*, the limit to the height of a structural envelope is a function of the material properties, σ_y^c and *E*, and shape properties, ψ_A and ψ_I. H_{lim} can be of practical use in constrained design applications because it defines the range of the permitted heights for the structural envelopes. For example, Figure 6.1 uses the combined graph to show the range of the envelope not subjected to buckling for aluminium and steel. The performance criterion and the stiffness requirement, given by equations (3.16) and (6.23) respectively, are plotted on the left and right hand side of Figure 6.1. The stiffness requirement for a pin jointed strut (*n=1*) of length *L*=5m is $k=340*10^6$ N/m. The cross-sections have material properties Al(ρ=2.71 Mg/m^3, *E*=70 GPa, σ_y^c=20 MPa) St(ρ=7.9, *E*=210, σ_y^c=300) and shape properties Al(ψ_A=0.5, ψ_I =0.6) St(ψ_A=0.25, ψ_I =0.55). Equation (6.26) is used to mark the cut-off for the feasible envelopes of the requirement curve, *k*. These are points C and D in Figure 6.1 for aluminium and steel respectively. The dashed style line represents envelopes which would buckle.

It is interesting to note that material and also shape properties determine the limits to the sizes of the envelopes subjected to Euler buckling failure. This is because *M* and *S* determine the space required by the set of feasible cross-sections to satisfy the design requirement.

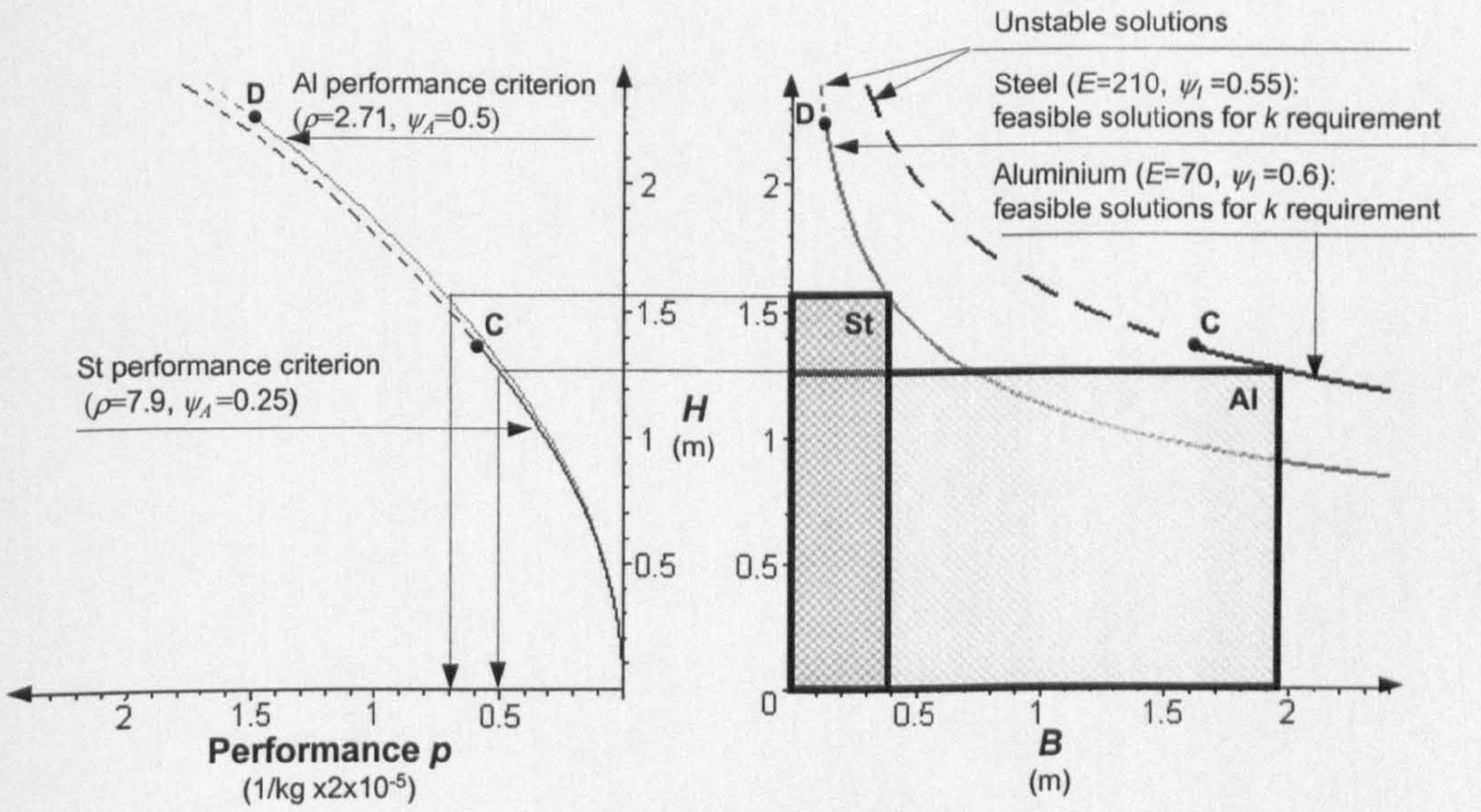

Figure 6.1 Limits to the height of the envelopes due to buckling.

6.7.3 Compression stress failure design

As explained in Chapter 3 the Rankine Gordon formula is a suitable formula to model the failure of actual struts with material and production imperfections. Although the formula does not have a physical meaning because it is derived by considering the interaction of yield and buckling failure modes, it gives an accurate estimation of the compressive failure stress. It can be used for dimensioning struts of any slenderness ratio, material and shape at the stage of conceptual design.

Solving equation (3.21) for a positive A, gives the minimum area, which prevents failure of compressive members of length, L, under a load P, and which is given by:

$$A = 0.5\frac{P\lambda_I z v + \sqrt{P\lambda_I z\left(P\lambda_I z v^2 + 4\sigma_y^c \psi_A \mu L^2\right)}}{z\lambda_I v \sigma_y^c} \tag{6.27}$$

where z=1/12 and $\mu = \sigma_y^c / \pi^2 E$.

For a given length and compressive force, the parameters in control of the designer in equation (6.27) are: material (σ_y and E), shape (λ_I and ψ_A), and envelope, v. The contribution of the shape and the contribution of the envelope are separated. Shape transformers and envelope multiplicators are dimensionless parameters and the ranges are specified in Table 3.3 and 3.4. They can be used to minimise the mass of a strut at the conceptual stage of design. An example is shown in Chapter 8, where the expression (6.27) is used to explore the interaction between the selection of cross-sectional shapes and alternative structural forms.

6.8 SUMMARY

This Chapter has used the theory of shape transformers to analyse the role of material and shape properties. Firstly, the co-selection of material and shape has been examined analytically with the performance criterion and performance index. The selection of material and shape has been explored graphically with normal and logarithmic material charts for cases where the envelope is fixed and scaled. The limits to the shape properties have been investigated for standard cross-sections. Finally, the shape transformers have been used to analyse the design of compressive structural members and to derive the buckling limits to the height of a cross-section.

CHAPTER 7

STRUCTURED LAYERED SYSTEMS AND PLASTIC BENDING

7.1 INTRODUCTION

This Chapter extends the theory of shape transformers to consider structured layered systems and plastic bending design. The Chapter consists of two sections:

- The first part investigates **structured layered systems.** The **structuring** and the **layering** of material are identified as two ways of shaping a cross-section. The shape transformers are used to show that any cross-section can be considered as a structured material arranged in layers within an envelope. General expressions are given for the properties and the performance of a structured layered system. The envelope efficiency map and material chart are used to visualise systems containing layers with different shape and material properties.
- In the second part, **plastic bending design** is examined. An analogy is used to consider a rigid plastic cross-section as a layered system which contains elastic material and plastic material. **Plastic shape transformers** are defined for the plastic case. Plastic bending is analysed in terms of geometric properties. **Envelope efficiency maps** are developed in two and **three dimensions**.

7.2 STRUCTURED LAYERED SYSTEMS

Structured layered cross-sections are shown in Figure 7.1. These systems can be adopted in engineering to achieve high performance. Structured systems can also be found in nature, such as the microstructures of the stem of some plants and the cuttlefish. Figure 7.1a) illustrates a structured cross-section containing a number of identical shaped cells. Figure 7.1b) shows the effect of shaping the structured cross-section of Figure 7.1a). The systems shown in Figure 7.1c) and d) are shaped in layers containing different shapes and materials respectively. Figure 7.1e) and f) illustrate combinations of layers filled with different materials and structured with different shapes.

The cross-sections in Figure 7.1 show that structuring and layering are two ways of shaping materials. In the following analysis, the shape transformers are used to describe how structuring and layering determine the properties and the performance of a structured multi-layered system.

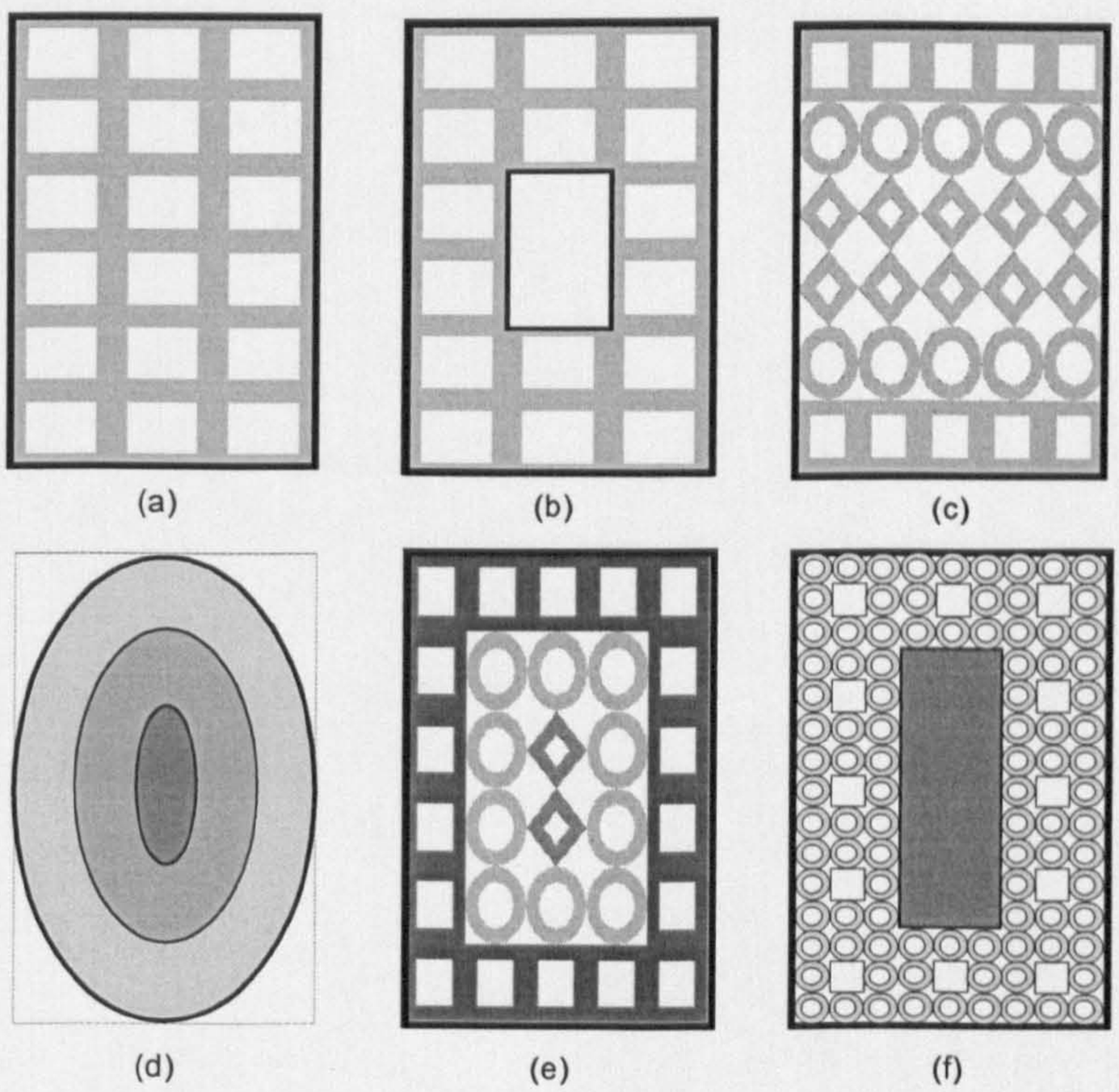

Figure 7.1 Examples of structured systems.

7.2.1 Structuring

Structuring involves shaping a material into a cell. The assembly of shaped cells makes a structured system as shown in Figure 7.1a). Any cell can be considered as a cross-section which is part of the system. There can be hierarchical levels of structuring. For example, Figure 7.1a) shows the effect of a first level of structuring. A further level of structuring the system is achieved by structuring each single cell.

Analysis

The theory of the shape transformers, S, illustrated in Chapter 3, showed that a geometric quantity, G, of a cross-section can be expressed as a product of the geometric quantity, G_D, of a rectangular envelope, and a shape transformer, S, so that $G=G_D x S$. This means that applying S_1 to a geometric quantity, G_o, of a rectangular cross-section, $C_o\ (M_o,S_o,G_D)$, with $G_o=G_D$ and $S_o=1$, has the effect of "transforming" G_o in $G_1=G_o x S_1=G_D x S_1$ so that the cross-section C_o is "transformed" into $C_1(M_o,S_1,G_D)$.

The cross-section C_o shown in Figure 7.1 is considered. The cross-section $C_o(M_o,S_o,G_D)$ with $G_o=S_o x G_D=G_D$,consists of n equal rectangular cells $C_{oi}(M_{oi},S_{oi},G_{Doi})$ with $G_{oi}=S_{oi} x G_{Doi}=G_{Doi}$. The cells C_{oi} are cross-sections symmetric about the axis x-x of C_o. For this reason, a geometric quantity, $G_D=G_o$, of the system C_o is the sum of the geometric quantity $G_{Doi}=G_{oi}$, of each cell, C_{oi}, and G_o is given by:

$$G_o = G_D = \sum_{i=1}^{n} G_{oi} = nG_{oi} = nG_{Doi} \tag{7.1}$$

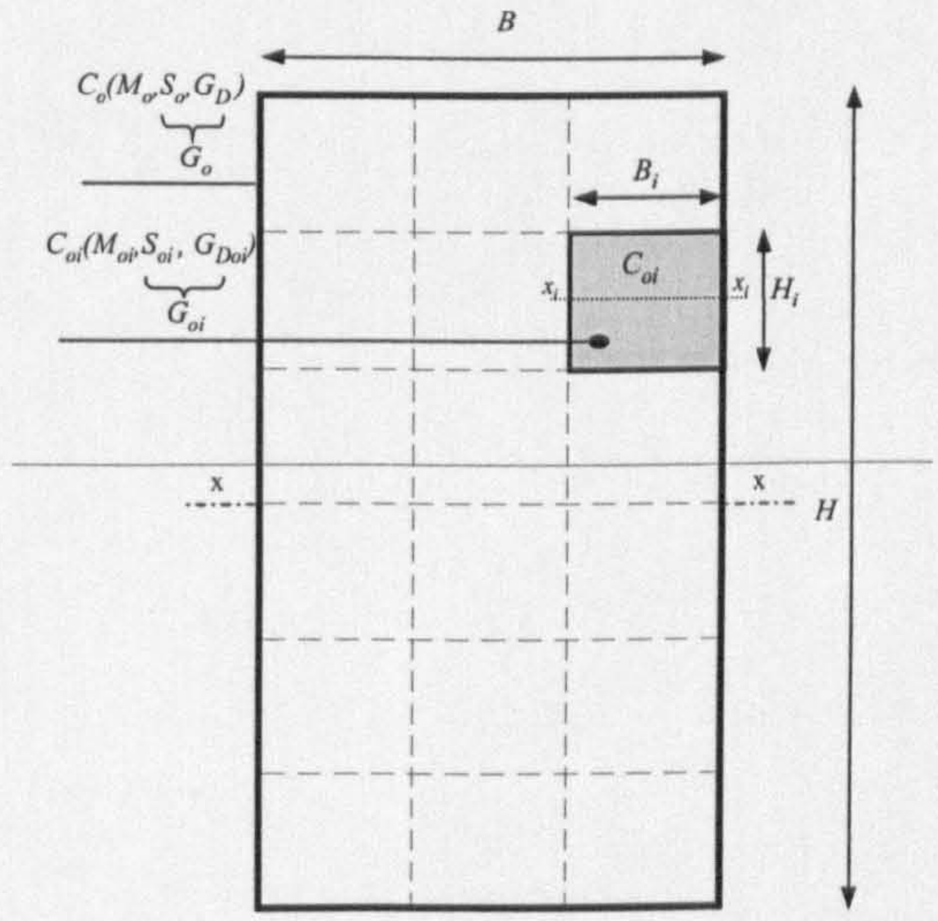

Figure 7.1 A structured cross-section $C_o\ (M_o,.S_o,\ G_{Do})$ consisting of n cells $C_{oi}(M_{oi},\ S_{oi},\ G_{Doi})$

First level of structuring, S^1

If S^j is a level which structures the system C_o, S^1 is the first level of structuring applied to C_o. S^1 describes the shape properties of cells with shapes symmetric respect to the cell axis x_i-x_i, as in Figure 7.1. S^1 is applied to each cell C_{oi} so that the geometric quantity G_{Doi} is transformed into S^1xG_{Doi}. Structuring a cross-section C_o with S^1, i.e. giving a shape S^1 to each cell, transforms the cross-section C_o in a structured system C_1 (M,G_1). The geometric quantity G_1 of C_1 is given by replacing G_{Doi} with S^1xG_{Doi} in equation (7.1), such that:

$$G_1 = nS^1G_{Doi} = S^1G_D = S^1G_o \tag{7.2}$$

From the definition of shape transformer, $S=G/G_D$, the shape property S_1 for C_1 is

$$S_1 = \frac{G_1}{G_D} \tag{7.3}$$

Rearranging equation (7.2) and combining it with equation (7.3) gives for C_1 (M, S_1, G_D) the following shape property S_1

$$S_1 = S^1 \tag{7.4}$$

Equation (7.4) shows that structuring a cross-section, C_o, with a number of cells, n, with symmetric shape, has the same effect as shaping C_o with $S_1 = S^1$. This means that structuring is a way of shaping material. Examples of structuring the cross-section C_o (M_o,S_o,G_D) in Figure 7.1 are shown in Figure 7.2. The structured cross-sections, C_1, have envelope $D(B$=3 units, H=6 units). Figure 7.2a) to d) show structured cross-sections consisting of n cells, C_{oi}, with $S_i(\psi_A$=0.51, ψ_I=0.76) and different sizes, D_{oi}. If C_o in Figure 7.1 has only one cell $C_{oi}=C_o$, then **structuring is shaping** the material in the envelope D. This is shown in Figure 7.2e) for a hollow shaped cross-section with $S(\psi_A$=0.51, ψ_I=0.76). All the cross-sections C_1, Figure 7.2a) to e), have the same A and I. (Note that ψ_A and ψ_I are derived using Table 3.3 with $h/H=b/B=h_i/H_i=b_i/B_i$=0.7). Another example is given in Figure 7.2f) to i) for ellipse shapes. The shape transformers of ellipse ($\psi_A=\pi/4$, $\psi_I=3/16\pi$) have been used to shape each cell with the result of structuring the cross-section C_o in Figure 7.1. Area, A, and second moment of area, I, of the structured cross-sections, Figure 7.2f) to i), and the shaped section in Figure 7.2l), are equal.

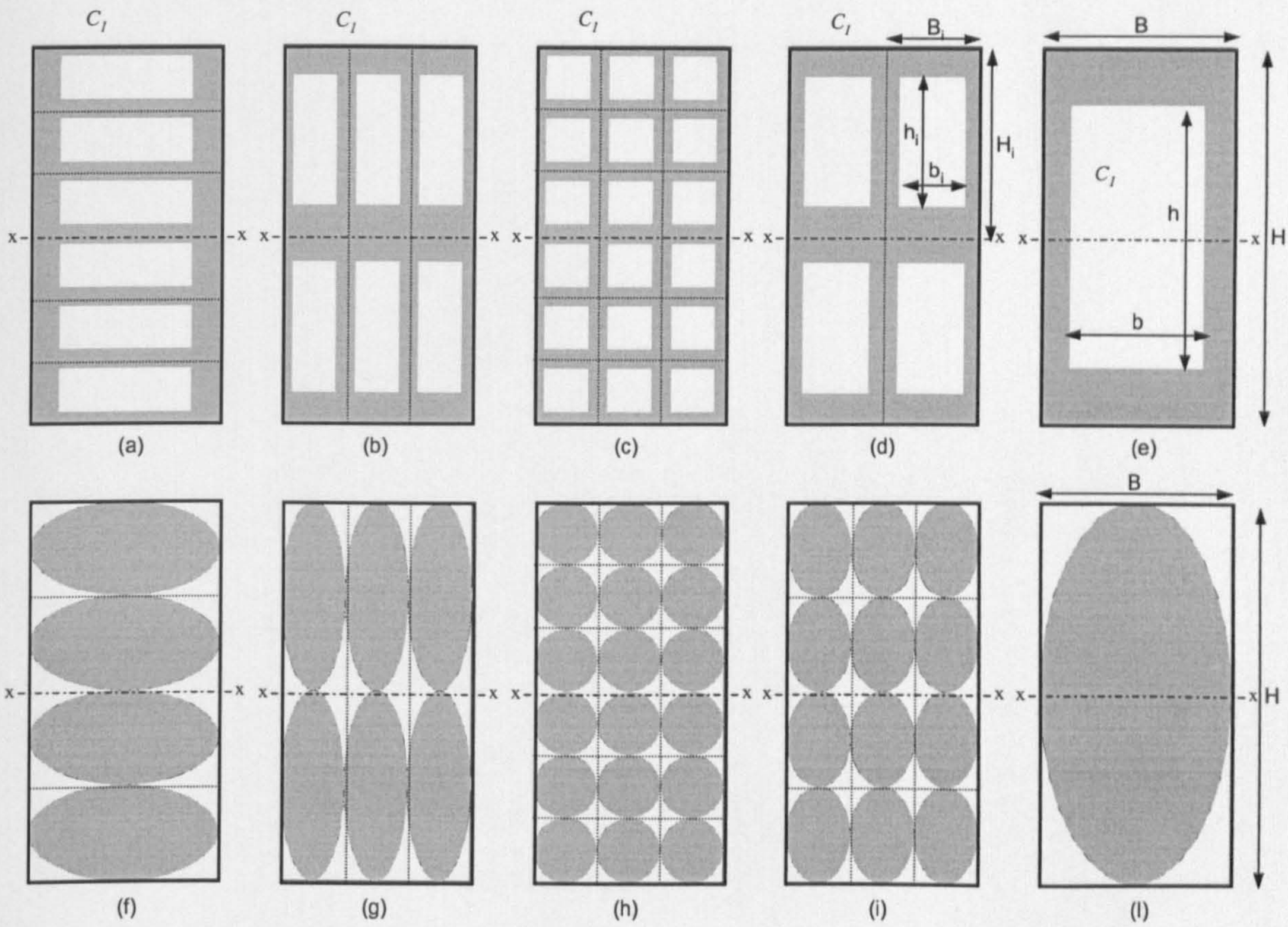

Figure 7.2 Equal geometric quantities, A, I and Z for structured cross-sections, a) to d) and f) to l), and shaped cross-section, e) and l).

Second level of structuring, S^2

If shape transformers, S^2, are applied to the geometric quantities, G_1, of the cross-sections, C_1, shown in Figure 7.2, then there is a second level of structuring applied to C_o. In this case the structured cross-section, C_2, derived from C_1 (M,G_1) has the geometric quantities G_2 given by

$$G_2 = S^2 x G_1 \tag{7.5}$$

Substituting equation (7.2) in (7.5) gives:

$$G_2 = S^2 x G_1 = S^2 x S^1 x G_D \tag{7.6}$$

Using the definition of shape transformer, $S_2=G_2/G_D$, makes it possible to derive from equation (7.6) the following shape properties for the cross-section C_2 (M,S_2,G_D)

$$S_2 = S^2 x S^1 \tag{7.7}$$

Figure 7.3a) shows an example of a level of structuring applied to the cross-cross-section C_1 shown in Figure 7.2c), i.e. a second level of structuring applied to C_o in

Figure 7.1. This level of structuring consists in giving a shape to each cell, C_{oi} ($D_{oi}(B_o$=1, H_{oi}=1)), of C_1 ($D(B$=3, H=6)) with the shape transformers $S^2(\psi_A$=0.878, ψ_I=0.985) (values given by $h/H=b/B$=0.35 using Table 3.3 for each cell, C_{oi}). The steps of structuring are summarised as follows:

level of structuring	Shape transformer applied	Cross-section	Shape properties
0	$S^o(\psi_A$=1, ψ_I=1)	C_o	$S_o(\psi_A$=1, ψ_I=1)
1st	$S^1(\psi_A$=0.51, ψ_I=0.76)	C_1	$S_1(\psi_A$=0.51, ψ_I=0.76)
2nd	$S^2(\psi_A$=0.878, ψ_I=0.985)	C_2	$S_2=S^1 S^2(\psi_A$=0.448, ψ_I=0.749)

The structured cross-section C_1 in Figure 7.2c) is shaped with the shape transformers $S^2(\psi_A$=0.878, ψ_I=0.985) in Figure 7.3b). Figure 7.3c) shows the shaping of the cross-section C_o, Figure 7.1, with shape transformers $S_2=S^1S^2(\psi_A$=0.448, ψ_I=0.749) (values given by h/H=0.675 and b/B=0.819 using Table 3.3 for C_o). According to equation (7.7) all the structured cross-sections, C_2, shown in Figure 7.3 have shape properties $S_2=S^1S^2(\psi_A$=0.448, ψ_I=0.749) and, consequently, since D is fixed, have the same geometric quantities, area and second moment of area. Despite the equality of the geometric quantities, it is important to note that an advantage of structuring is that it increases the resistance to local buckling of the cross-sections. For example, if the cross-sections in Figure 7.3 are subjected to compressive internal forces acting along the height, H, then the structured systems in Figure 7.3a) and b), have more resistance to buckling load than the shaped section in Figure 7.3c). The reason for this is that the internal height, h, of the structured cross-sections, i.e. the buckling length, is reduced.

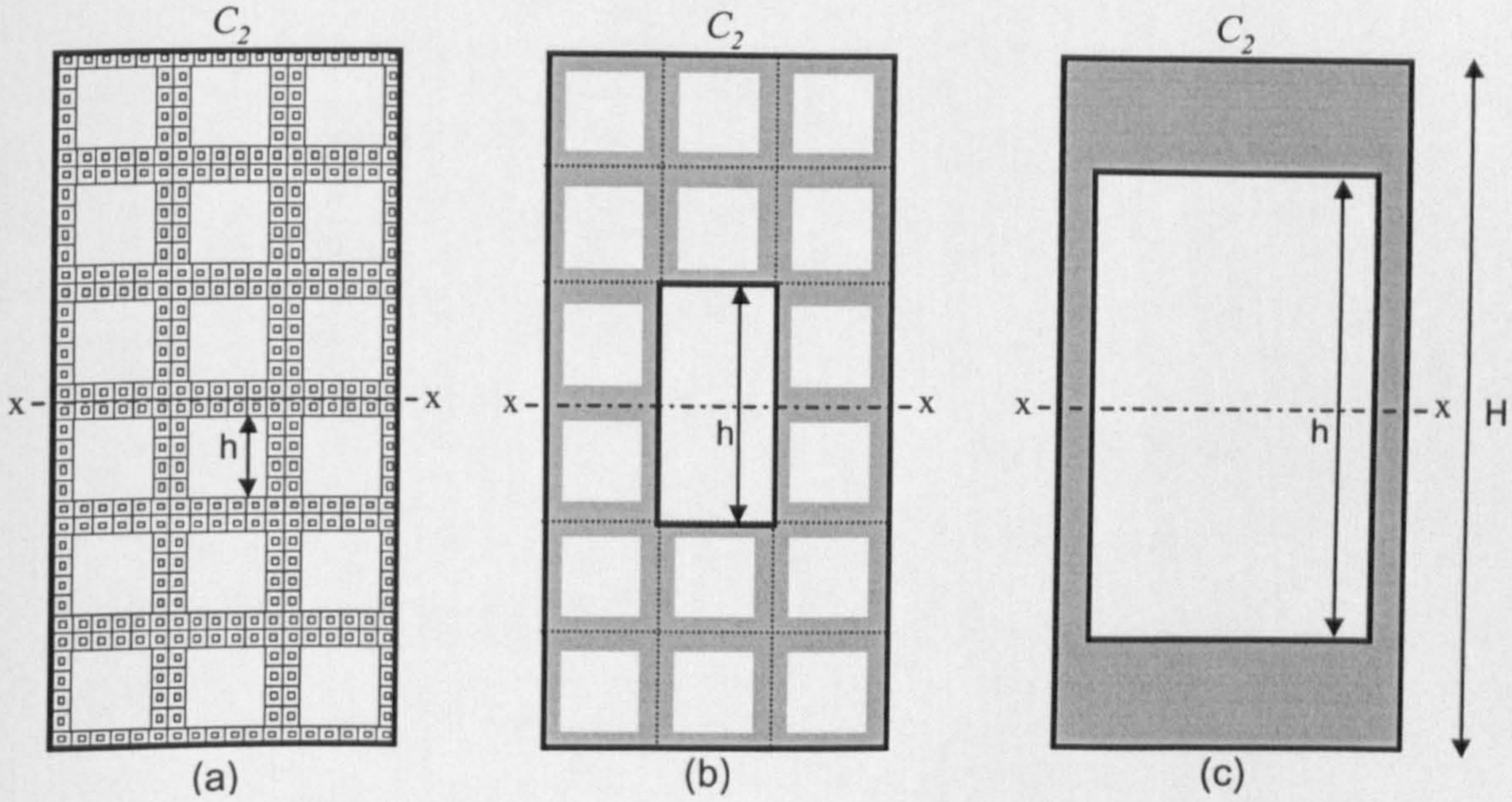

Figure 7.3 a) Two levels of structuring applied to C_o in Figure 7.2. b) Shaping C_1 in Figure 7.3c). c) Shaping C_0 in Figure 7.2. All the cross-sections have same A and I.

t level of structuring, S^t

Structuring the cross-section C_2 in Figure 7.3a) with a third level S^3 gives a cross-section C_3. Applying S^3 to C_2 gives that a geometric quantity of C_3 is $G_3 = S^3 x G_2$ and from equation (7.6) $G_3 = S^1 x S^2 x S^3 x G_D$. Although infinite levels of structuring can be pursued, there are limits due to economical reason and manufacturing constraints. In general, after t levels of structuring, S^t, a geometric quantity G_t, of a cross-section, C_t, is given by

$$G_t = S^1 x S^2 x S^3 x ... x S^t x G_D = \prod_{j=1}^{t} S^j x G_D \qquad (7.8)$$

and using the definition of shape transformer, $S_t = G_t / G_D$, in equation (7.8), gives the following S_t for a structured system $C(M, S_t, G_D)$:

$$\boxed{S_t = \frac{G_t}{G_D} = \prod_{j=1}^{t} S^j} \qquad (7.9)$$

Properties and performance of a structured system

The properties describing the objective function and the functional requirement for a structured cross-section are derived using equation (3.22), i.e. $F = MxG = MxSxG_D$. Replacing equation (7.9) in equation (3.22) gives for $C(M, S_t, G_D)$:

$$F = MxS_t xG_D = Mx \prod_{j=1}^{t} S^j xG_D \qquad (7.10)$$

As in Chapters 4, 5, and 6, the mass, m, and the design requirement, F, for a structured system, C, with given envelope, D, and material, M, can be expressed from equation (7.10) by the following co-ordinates:

$$\boxed{C\left(\frac{m}{MxG_D} = \prod_{j=1}^{t} S^j \;,\; \frac{F}{MxG_D} = \prod_{j=1}^{t} S^j \right)} \qquad (7.11)$$

In stiffness design, the performance of the system is given by the performance criterion, $p = F/m = k/m$:

$$\boxed{p = \frac{E}{\rho} x \prod_{j=1}^{t} \lambda_{li}^{j}} \qquad (7.12)$$

The mass and the functional requirement of C can be represented on the envelope efficiency map and on the material chart. An example will be given in Section 7.2.3.

7.2.2 Layering

Multilayered systems are structures which contain different combinations of materials and/or shapes placed in layers. Examples of layered systems are shown in Figure 7.1. Layering is produced by nesting cross-sections which are symmetric to the neutral axis. Each nested cross-section has an envelope with different sizes and different materials and/or shapes. For example, Figure 7.1a) and d) illustrate systems with 3 nested cross-sections C_1, C_2, C_3. Each cross-section has different envelopes D_1, D_2, D_3 containing shape properties $S_1 \neq S_2 \neq S_3$ and the same material $M_1=M_2=M_3$. In Figure 7.1b) and e), the materials contained in the envelopes of the nested cross-section are different, i.e. $M_1 \neq M_2 \neq M_3$. Figure 7.1c) and f) show that the envelopes $D_1 \neq D_2 \neq D_3$ contain different material and also shape properties, i.e. $S_1 \neq S_2 \neq S_3$ and $M_1 \neq M_2 \neq M_3$.

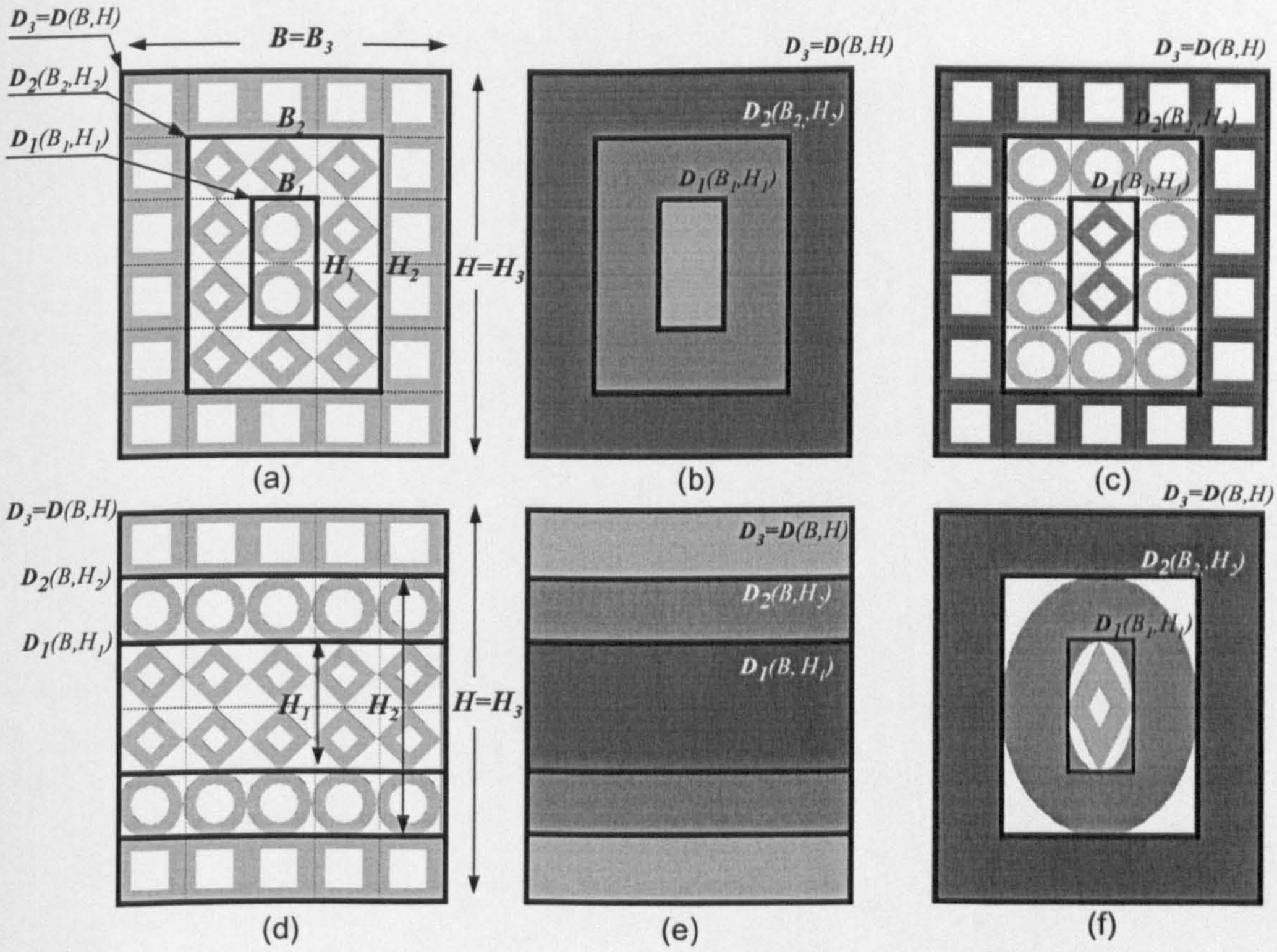

Figure 7.1 Structured layered systems using different material and shape properties.

Shape transformers for layered system.

As defined in Chapter 3, the shape transformers are the shape properties of the envelope describing the sizes of a cross-section. In the systems shown in Figure 7.1, nesting the cross-sections produces layers, i.e. envelopes D_i, which always have different sizes. It is important, therefore, to consider how the inner envelopes are scaled relative to the envelope D of the system C. In a similar way to the scaling of the sizes of a cross-section described in the previous Chapters, scaling of the layers can be in any arbitrary, vertical, horizontal and proportional direction.

Table 7.1 shows the shape transformers for a multilayered system for different scaling of the layers. These shape transformers, $S=G_{Di}/G_D$, describe the geometric properties of the inner layer (dark colour) which can contain either material or shape properties different from the outer layer (light colour). The shape transformers for the outer layer are given in Table 3.3.

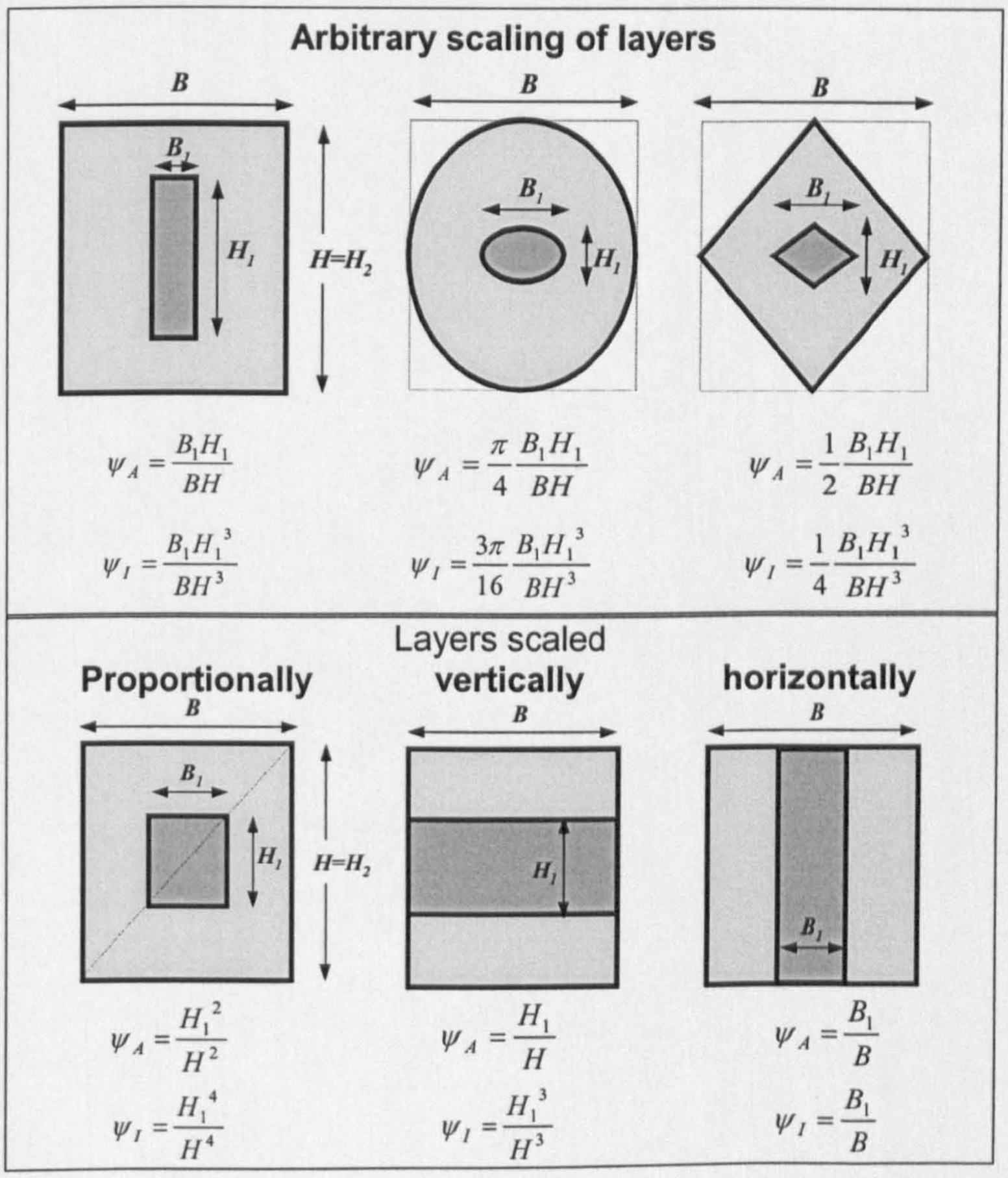

Table 7.1 Shape transformers, $G_{Di}/G_{D,}$ for multilayered system.

The shape transformers of Table 7.1 complete the list of shape transformers for standard cross-sections given in Table 3.3. The reason for having Table 7.1 is that standard cross-section can be considered as "multilayered" system with the outer layer filled with a material and with air in the inner layer. Air is not a material and does not contribute to the geometric properties of the system. Consequently, the shape transformers in Table 7.1 for standard cross-sections are nil and only Table 3.3 is necessary. In addition, it is important to note that the condition where the outer layer is air and material inside, is unfeasible because it produces a scaling of the envelope of the system. This is in contrast with the definition of shape transformers which measure the shape properties and not the scaling of a cross-section.

7.2.3 Layering and structuring material

Shaping involves layering and structuring materials. Any of the systems shown in Figure 7.1 involve layering and structuring. General expressions of the properties which describe the mass and the functional requirement of a system which is structured, i.e. aggregation of shaped cells, and layered, i.e. nesting of cross-sections with different M and/or S, are now derived.

Properties and performance of structured layered systems

A structured layered cross-section, C, such as in Figure 7.1c), is considered. C consists of 3 nested cross-section C_i with envelope D_i, material, M_i, and shape properties, $S_i=S_i=\Pi S^j$ (equation (7.9)). The material properties, M_i, and shape properties, ΠS^j, contained in each envelope are placed in symmetric layers within the system. The mass and functional requirement of each cross-section, C_i, of a system C of unit length are given by:

$$m_i = M_i x \prod_{j=1}^{t} S_i^j x G_{Di} \tag{7.13}$$

$$F_i = M_i x \prod_{j=1}^{t} S_i^j x G_{Di} \tag{7.14}$$

Each cross-section C_i is placed symmetrically within another. Therefore, the geometric quantities of the layered system are the sum of the geometric quantities of

each cross-section C_i. The total mass, m, and requirement, F, of the system C containing n nested cross-sections, C_i, are:

$$m = \sum_{i=1}^{n} M_i x \prod_{j=1}^{t} S_i^j x G_{Di} \tag{7.15}$$

$$F = \sum_{i=1}^{n} M_i x \prod_{j=1}^{t} S_i^j x G_{Di} \tag{7.16}$$

The properties which describe the mass and the functional requirement of a layered structured system C with M and S variable, are derived by normalising the equation (3.22), i.e. $F = MxG = MxSxG_D$, with respect to G_D and are given by:

$$C\left(\frac{m}{G_D} = \sum_{i=1}^{n} M_i x \prod_{j=1}^{t} S_i^j x \underbrace{\frac{G_{Di}}{G_D}}_{\textit{Shape transformer}}, \frac{F}{G_D} = \sum_{i=1}^{n} M_i x \prod_{j=1}^{t} S_i^j x \underbrace{\frac{G_{Di}}{G_D}}_{\textit{Shape transformer}}\right) \tag{7.17}$$

Where n is the number of the nested cross-sections C_i with envelope D_i, material properties M_i and shape properties $\Pi\, S_i^j$. t is the number of structuring, S_i^j, for each nested cross-section C_i. The factor G_{Di}/G_D relates the envelope, D_i, of an inner nested cross-section, C_i, to the envelope, D, of the system, C. Consequently, G_{Di}/G_D is the shape transformer for multi-layered systems given in Table 7.1.

As explained, layering and structuring are two features of shaping. Both determine the shape properties of a system. They are effectively the same thing since a structured cross-section such as those in Figure 7.1a) and Figure 7.3a) can be considered as horizontally or vertically scaled layers where both the material and shape properties of the nested cross-sections are equal. Therefore, **layering** has to be included in the shape properties of the system $S_i = \Pi\, S_i^j$ **as another level**, t, **of structuring**.

From equation (7.17), the mass, m and the stiffness, k, of a layered structured system C in stiffness design, are given by

$$C\left(\frac{m}{A_D} = \sum_{i=1}^{n} \rho_i x \prod_{j=1}^{t} \psi_{Ai}^j, \frac{k}{I_D} = \sum_{i=1}^{n} E_i x \prod_{j=1}^{t} \psi_{Ii}^j\right) \tag{7.18}$$

and the performance, $p=k/m$, is given by:

$$p = \sum_{i=1}^{n} \frac{E_i}{\rho_i} x \prod_{j=1}^{t} \lambda_{Ii}^{j} \tag{7.19}$$

In the next Section, expressions (7.18) and (7.19) will be used to represent on graphical maps the properties and performance of different structured systems.

7.2.4 Maps for multilayered structured systems

The envelope efficiency map and the material chart are used to visualise the properties and the performance of structured layered systems in relationship to layer location. The systems have layers which are proportionally, vertically and horizontally scaled as shown in Figure 7.1. This Section examines for bending stiffness design the following systems:

- Layered systems using shapes [Figure 7.1a), b), c)]. The envelope efficiency map is used to represent the properties, mass and stiffness, and performance.
- Layered systems using materials [Figure 7.1d), e), f)]. The properties and the performance are plotted on the material chart.

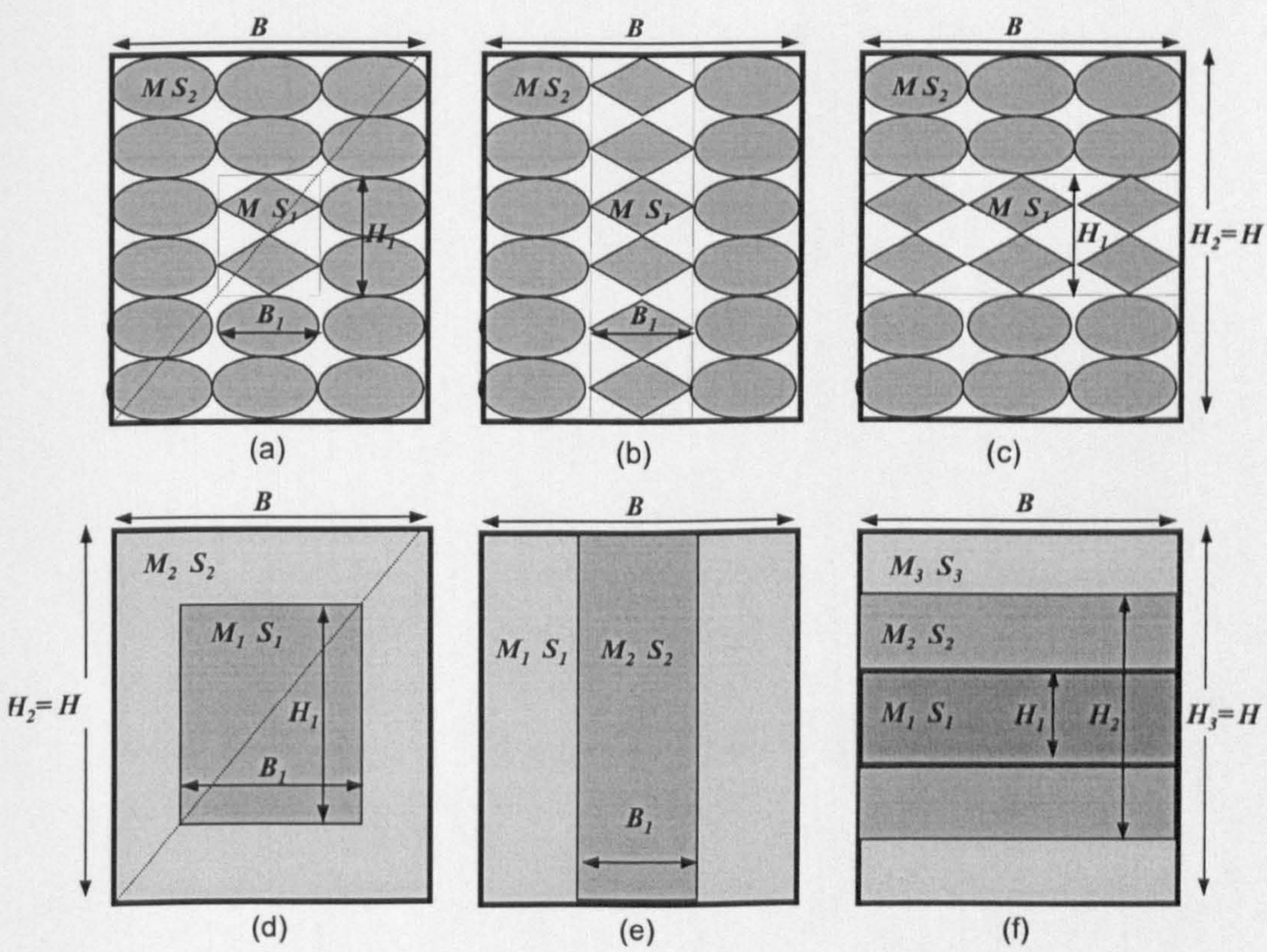

Figure 7.1 Layered systems with different scaling of the inner envelope.

Layered system using shapes

A system *C* containing layers with two shapes, ellipse and lozenge, is considered. The shape properties are: ellipse ($\psi_{A1}=\pi/4$, $\psi_{I1}=3\pi/16$), lozenge ($\psi_{A2}=1/2$, $\psi_{I2}=1/4$). From equation (7.18), the properties describing the mass and the stiffness of the system, *C*, with material properties $M(\rho,E)$ are given by the co-ordinates:

$$C\left(\frac{m}{MxG_D}=\sum_{i=1}^{n}\prod_{j=1}^{t}S_i^j\ ,\ \frac{F}{MxG_D}=\sum_{i=1}^{n}\prod_{j=1}^{t}S_i^j\right) \tag{7.20}$$

Using the expressions of ψ_A, ψ_I, λ_I in Tables 3.3 and 7.1, the properties of *C* with arbitrarily scaled layers are:

$$\frac{m}{\rho A_D}=\psi_{A1}^2\ \underbrace{\psi_{A1}^1}_{\frac{B_1H_1}{BH}}+\psi_{A2}^2\ \underbrace{\psi_{A2}^1}_{1-\frac{B_1H_1}{BH}} \tag{7.21}$$

$$\frac{k}{EI_D}=\psi_{I1}^2\ \underbrace{\psi_{I1}^1}_{\frac{B_1H_1^3}{BH^3}}+\psi_{I2}^2\ \underbrace{\psi_{I2}^1}_{1-\frac{B_1H_1^3}{BH^3}} \tag{7.22}$$

and the performance from equation (7.19) is:

$$p=\frac{k}{m}=\lambda_{I1}^2\lambda_{I1}^1+\lambda_{I2}^2\lambda_{I2}^1 \tag{7.23}$$

Equations (7.21) and (7.22) are plotted in Figure 7.1 for proportional, i.e. $H/B=H_1/B_1$, vertical, i.e. $B=B_1$, and horizontal, $H=H_1$, scaling of the layers. Point L and E represent the properties of solid shapes or structured systems with n cells containing the same shape properties of lozenge and ellipse. Curves 1 and 2 represent the combination of layers shown in Figure 7.1c), i.e. layers vertically scaled. Curves 3 and 4 describe the properties of systems with proportional scaling of the layers as in Figure 7.1a). System with layers with variable width and same height, Figure 7.1b), are represented by line 5. Curves 1 and 2 in Figure 7.1 represent symmetric layered systems with ellipse shapes on the upper and lower surfaces (Curve 1), or with lozenge on the upper and lower surface (Curve 2). As explained in the previous Chapters, all the possible multilayered systems lie within the domain bounded by the limiting curves 1 and 2. Curves 3 and 4 describe respectively the properties of systems with ellipses on the outer and inner layer. The systems described by line 5 can have lozenges either at the outer or inner layers.

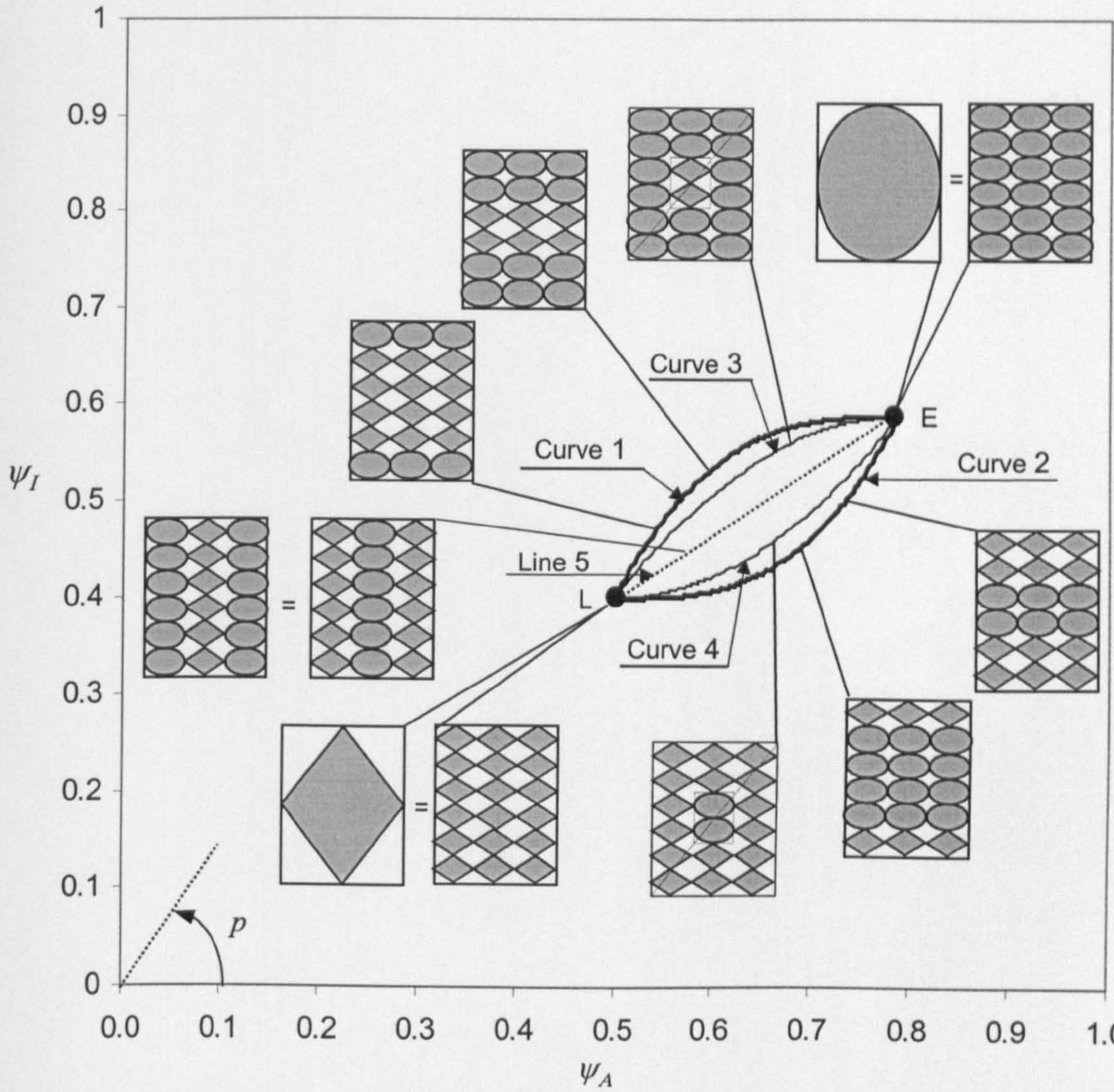

Figure 7.1 Efficiency map for structured layered system using structured lozenges and ellipses.

Layered system using materials

The systems in Figure 7.1d), e) and f) are combinations of proportionally, vertically and horizontally scaled layers filled with two or three materials. The relationship between layer location and the properties of these systems are examined.

a) Two materials

A multilayered system which contains two materials, a titanium alloy IMI 834 and a titanium metal matrix composite Ti-6A1-4V, is considered. The material properties are for Ti-6A1-4V M_1(ρ_1=4.38 Mg/m^3, E_1= 204 GPa and) Ti-834 M_2 (ρ_2=4.57 Mg/m^3, E_2= 114 GPa) and the shape properties are given in Tables 7.1 and 3.3. From

equations (7.18) and (7.19), the mass, stiffness and performance of the system with two arbitrarily scaled layers are given by:

$$\frac{m}{A_D} = \underbrace{\psi^1_{A1}}_{\frac{B_1H_1}{BH}}\rho_1 + \underbrace{\psi^1_{A2}}_{1-\frac{B_1H_1}{BH}}\rho_2 \tag{7.24}$$

$$\frac{k}{I_D} = \underbrace{\psi^1_{I1}}_{\frac{B_1H_1^3}{BH^3}}E_1 + \underbrace{\psi^1_{I2}}_{1-\frac{B_1H_1^3}{BH^3}}E_2 \tag{7.25}$$

$$p = \frac{k}{m} = \frac{E_1}{\rho_1}\lambda^1_{I1} + \frac{E_2}{\rho_2}\lambda^1_{I2} \tag{7.26}$$

Note that when $\psi^1{}_{A1} = \psi^1{}_{I1} = \lambda^1{}_{I1} = 1$, then $\psi^1{}_{A2} = \psi^1{}_{I2} = \lambda^1{}_{I2} = 0$ and the layered system is all Ti-MMC. Similarly when $\psi^1{}_{A1} = \psi^1{}_{I1} = \lambda^1{}_{I1} = 0$, then the layered system is all Ti-834 because $\psi^1{}_{A2} = \psi^1{}_{I2} = \lambda^1{}_{I2} = 1$. These extreme values are illustrated in Figure 7.1. Curves 1 and 2 describe the combinations of vertically scaled layers. Curves 3 and 4 corresponds to proportional scaling of the layers as in Figure 7.1d), while line 5 illustrates layers horizontally scaled, Figure 7.1e). Curves 1 and 2 in Figure 7.1 represent symmetric layered systems with Ti-MMC on the upper and lower surfaces (Curve 2), or with Ti-834 on the upper and lower surface (Curve 1). All the possible multilayered systems lie within the domain bounded by the limiting curves1 and 2. Curves 3 and 4 are for proportionally scaled layers with all Ti-834 on the outer and inner layer respectively.

The flexural stiffness of the same planar multilayered systems considered in Figure 7.1 have been recently examined by Smith and Partridge (1999). The results of their analysis is shown in Figure 7.2. They showed that all the possible layered materials, symmetric and asymmetric, based on the two-material systems Ti-MMC and Ti 834 are located in a domain defined by the curves 1 and 2 shown in Figure 7.2.

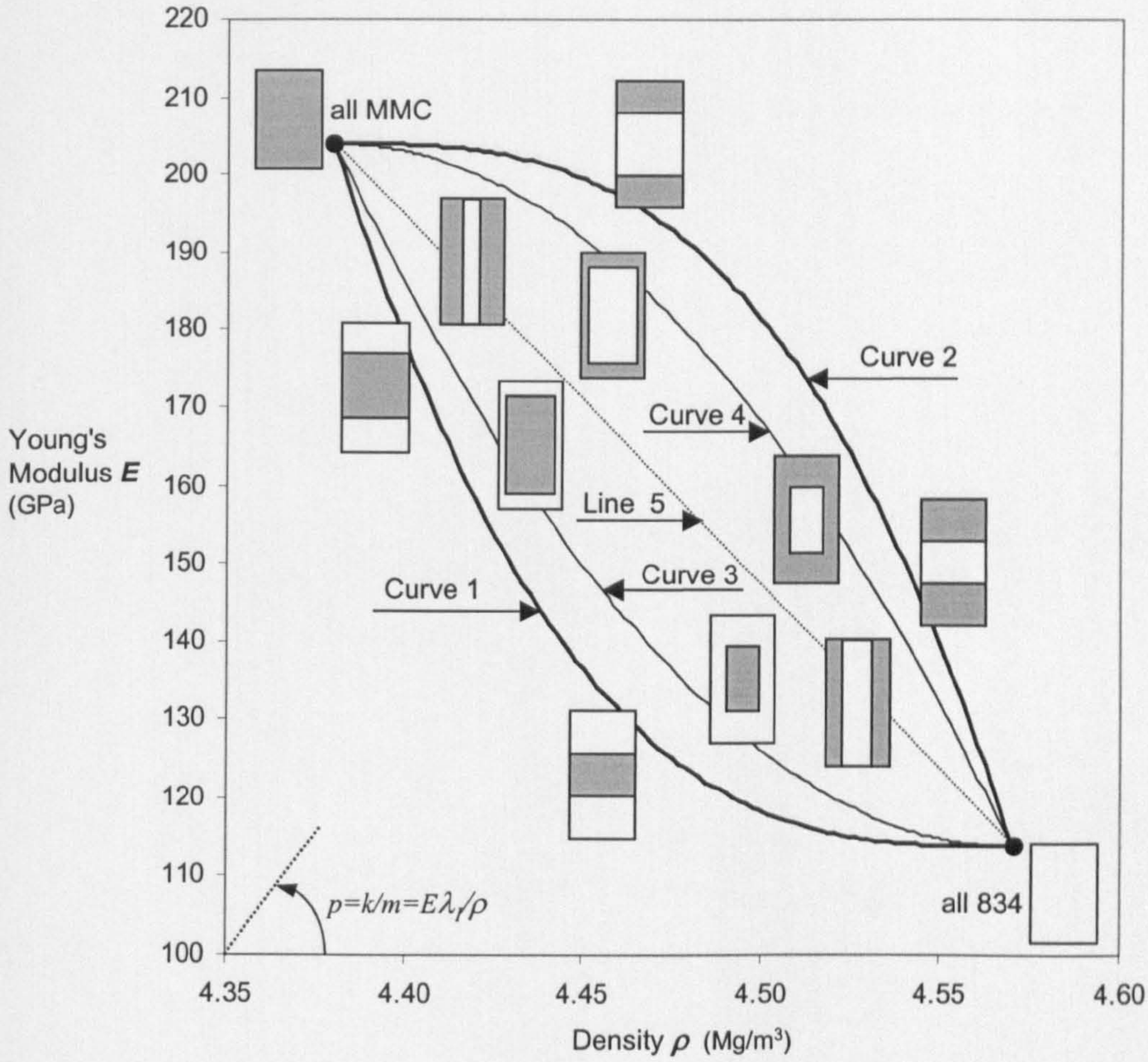

Figure 7.1 Efficiency map for material layered system using Ti-MMC and Ti-834.

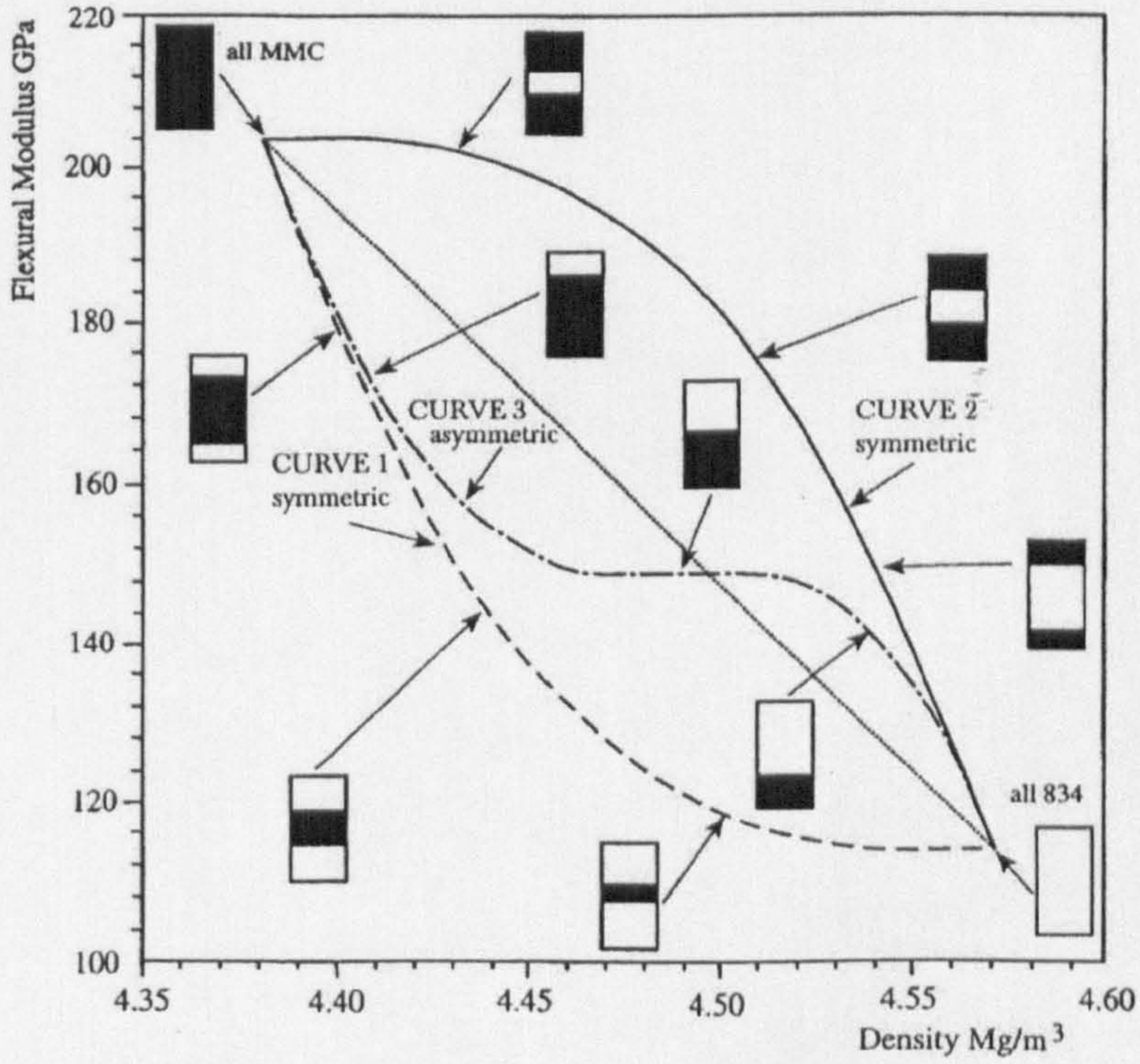

Figure 7.2 Flexural stiffness of two- and three-layer system using Ti-MMC and Ti-834 (Smith, D.J. and Partridge, P.G., 1999).

b) Three materials

A combination of vertically scaled layers for three materials, lead, Pb, aluminium, Al, and steel, St, is considered. This is shown in Figure 7.1f). The material properties are: Al(ρ_1= 2.71Mg/m^3, E_1=79GPa), Pb M_2(ρ_2=11.3Mg/m^3, E_2= 41GPa) and St(ρ_3=7.85Mg/m^3, E_3=210GPa). The shape properties are given in Tables 7.1 and 3.3. From equations (7.18) and (7.19), mass, stiffness and performance of the systems are:

$$\frac{m}{A_D} = \underbrace{\psi_{A1}^1}_{\frac{H_1}{H}} \rho_1 + \underbrace{\psi_{A2}^2}_{1-\frac{H_1}{H_2}} \underbrace{\psi_{A2}^1}_{\frac{H_2}{H}} \rho_2 + \underbrace{\psi_{A3}^1}_{1-\frac{H_2}{H}} \rho_3 \tag{7.27}$$

$$\frac{k}{I_D} = \underbrace{\psi_{I1}^1}_{\frac{H_1^3}{H^3}} E_1 + \underbrace{\psi_{I2}^2}_{1-\frac{H_1^3}{H_2^3}} \underbrace{\psi_{I2}^1}_{\frac{H_2^3}{H^3}} E_2 + \underbrace{\psi_{I3}^1}_{1-\frac{H_2^3}{H^3}} E_3 \tag{7.28}$$

$$p = \frac{k}{m} = \frac{E_1}{\rho_1}\lambda_{I1}^1 + \frac{E_2}{\rho_2}\lambda_{I2}^2\lambda_{I2}^1 + \frac{E_3}{\rho_3}\lambda_{I3}^1 \tag{7.29}$$

Equations (7.27) and (7.28) have been plotted in Figure 7.3 for all the possible combinations of two materials, i.e. Al-St, St-Pb, Pb-Al. The points, St, Al and Pb represent the case where the envelope of the system is fully filled with one material. Curves 1 and 2 are the same curves of Figure 7.1 but for a layer combination with steel and aluminium. Curve 3 and 4 represent the layered system for steel and lead while curves 5 and 6 for lead and aluminium layers. All the possible layer combinations using together three materials, i.e. aluminium, steel and lead, are located within the "main domain" bordered by the limit curves 1, 3 and 5. The reason for this is that when a third material such as lead is introduced into a system with Al and St, e.g. point C_2 on curve 1, layers of steel or aluminium are removed and replaced with layers of lead which have lower Young's modulus and higher density. The result is that the performance is decreased and point C_2 move right towards C_3 insight the main domain 1-3-5. In a similar way, this can be applied for systems lying on curves 3 and 5. Adding a third material layer to a two-material layered system has the effect of changing the performance. The performance of the system moves from the limit curves which describe a two vertically scaled layers system to a point which is included in the main domain.

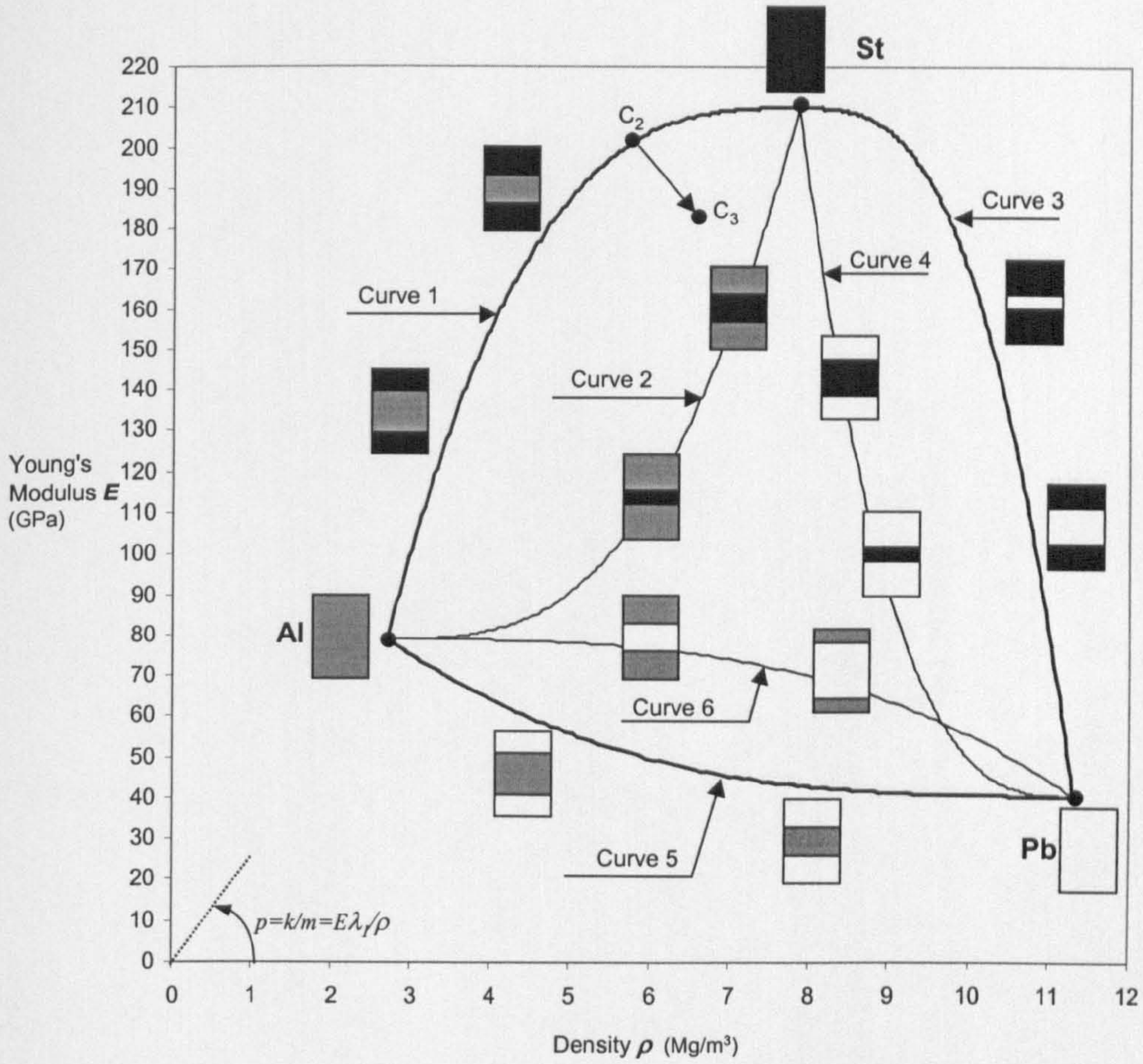

Figure 7.3 Efficiency map for a combination of three material layers using Al, Pb, and St.

7.3 PLASTICITY IN BENDING

The plastic deformation of engineering components is examined using plastic analysis. This Section uses the shape transformers to discuss the case of bending involving plastic deformation.

The plastic bending analysis is based on the following assumptions (Dowling, N.E., 1993):

i) Pure bending is applied and shear stresses are negligible.

ii) The material is elastic perfectly plastic.

iii) Young's modulus, E, and yield stress, σ_y, are the same for tension and compression.

iv) Bending occurs in the plane of symmetry of the beam.

v) Plane cross-sections remain plane during deformation.

The stress-strain relationship of the material is shown in Figure 7.1. In the elastic region, between the origin and C_e, there is a linear variation of the strain from the neutral axis with greatest stresses at the extreme fibres of the section. The furthest fibres reach the yield stress, σ_y, and strain, ε_o, at C_e. Beyond the initial yield point, between C_e and C_p, the deformation increases, but the stress cannot exceed σ_y, as shown in Figure 7.1. As a result, the core of the cross-section, C_{e-p}, is elastic and the extreme fibres, which have overcome ε_o, become plastic. The fully plastic moment is reached in C_p when any longitudinal fibre of the beam, half in compression and half in tension, is at the yield point σ_y.

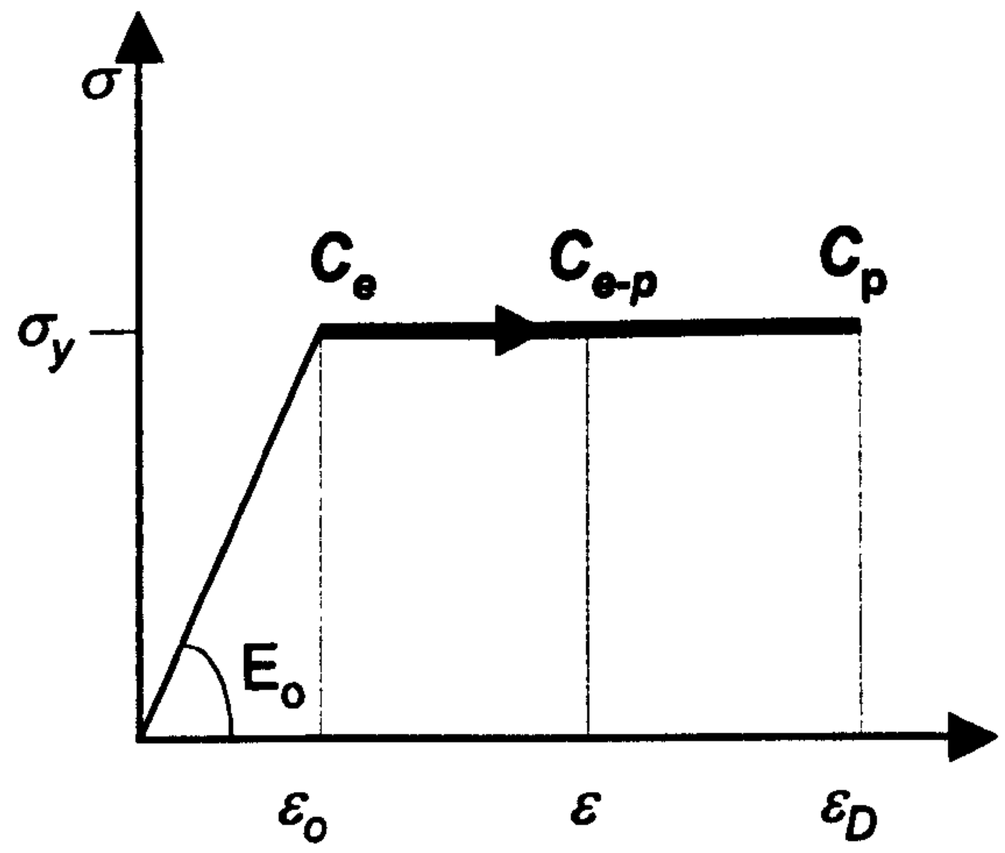

Figure 7.1 Stress-strain relationship for elastic plastic material.

7.3.1 The analogy between an elastic-plastic envelope and a sandwich section

In the plastic range between C_e and C_p of Figure 7.1, the cross-sections have material under two different stress regimes. In the core of the section, the material behaves elastically while material stressed at the same yield point is located at the extreme fibres. Figure 7.1 shows that it is possible to consider the cross-section, $C_{e\text{-}p}$, as a sandwich section, i.e. a vertically scaled layers system, made of two "fictitious materials": elastic in the centre and plastic at the ends.

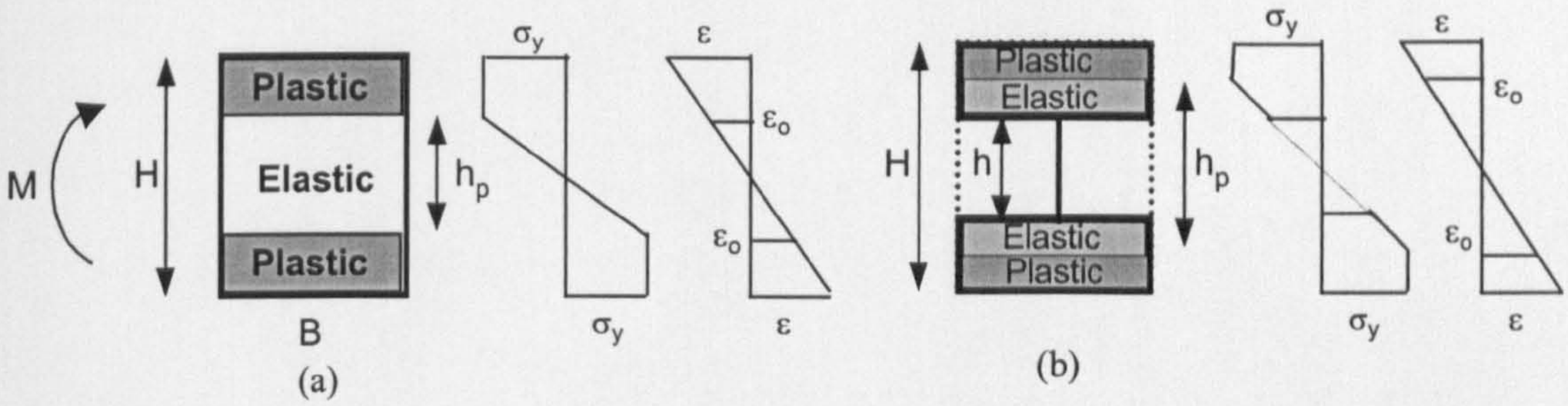

Figure 7.1. a) Fictitious rectangular section made of elastic and plastic material. b) I-section with infinitesimal web thickness in the elastic-plastic zone.

The assumption v) of the plastic analysis specifies that the section must remain plane after the deformation. This results in a linear variation of the strain from the neutral axis, which is expressed as:

$$\frac{\varepsilon_o}{\varepsilon} = \frac{h_p}{H} \tag{7.30}$$

where ε_o is the deformation of the yield fibre nearest to the neutral axis, i.e. $\varepsilon_o = \sigma_y / E_o$ (point C_e in Figure 7.1), and ε is the strain in the horizontal direction at the furthest point of the envelope, i.e. $\varepsilon = \sigma_y / E$ (point $C_{e\text{-}p}$ in Figure 7.1).

Since $\varepsilon_o / \varepsilon = E_o / E = h_p / H$ the relation in terms of deformation, or Young's modulus can be expressed in terms of geometric dimensions: elastic zone height to envelope height ratio. This expression will be used in the next Section to define the shape transformers for plastic bending for cross-sections of the rectangular class.

7.3.2 The shape transformers for the plastic case

In this Section plastic shape transformers are defined for cross-sections of the rectangular class. The following symbols are introduced to identify the elastic structural envelope, C_e, from the elastic-plastic section, $C_{e\text{-}p}$, in Figure 7.1.

For a section, C_e, in the elastic region

A_e = area of the section, C_e A_D = area of the envelope *BxH*

Z_e = section modulus of section, C_e Z_D = section modulus of the envelope

Note that Z_e is the elastic section modulus for strength design, i.e. $Z=M_y/\sigma_y$ with σ_y the yield stress at the furthest point from the neutral axis of the section.

For the section, $C_{e\text{-}p}$, in the elastic-plastic region.

A_p = area of the plastic part of the section, $C_{e\text{-}p}$

Z_p = section modulus of the plastic part of the section, $C_{e\text{-}p}$

Z_e = section modulus of the elastic part section, $C_{e\text{-}p}$

Note that the total section modulus of the section $C_{e\text{-}p}$ is given by Z_p+Z_e

The **plastic shape transformers** are defined as:

$$\begin{cases} \psi_A{}^P = \dfrac{A_p}{A_D} \\ \psi_Z{}^P = \dfrac{Z_p + Z_e}{Z_D} = \dfrac{Z_p}{Z_D} + \psi_Z{}^e \end{cases} \tag{7.31}$$

For the fully plastic rectangular envelope, the shape transformers are:

$$A_p = A_D \rightarrow \psi_A{}^P = 1$$

$$Z_p = 1.5 Z_D \rightarrow \psi_Z{}^P = 1.5$$

From the analogy illustrated in the previous Section, the plastic shape transformer of the area is:

$$\psi_A{}^P = 1 - \frac{h_p}{H} = 1 - \frac{\varepsilon_o}{\varepsilon} \tag{7.32}$$

Plastic range from C_e to C_p

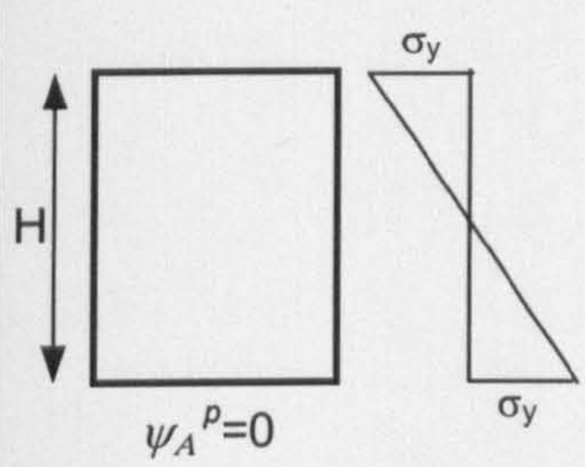

ELASTIC ENVELOPE, C_e

Geometric quantities

$$A^p = 0\,,\; Z_p = 0$$

$$Z_e + Z_p = Z_e$$

Shape transformers

$$\psi_A{}^p = 0$$

$$\psi_Z{}^p = 1$$

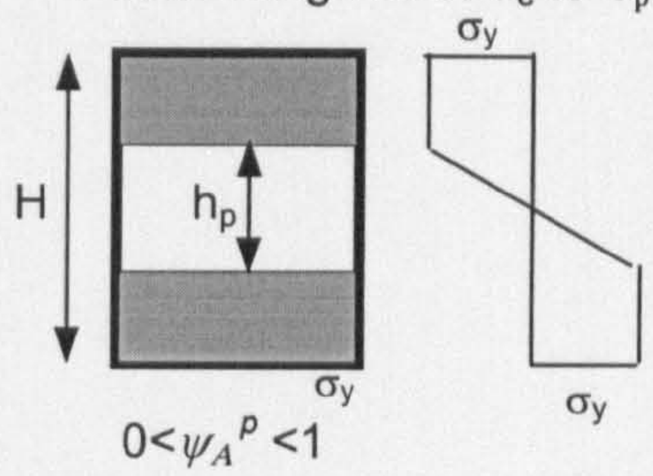

ELASTIC-PLASTIC ENVELOPE, $C_{e\text{-}p}$

Geometric quantities

$$A^p = B(H - h_p)$$

$$Z_e + Z_p = \frac{B}{4}\left(H^2 - \frac{h_p{}^2}{3}\right)$$

Shape transformers

$$\psi_A{}^p = 1 - \frac{h_p}{H}$$

$$\psi_Z{}^p = \frac{1}{2}\left(3 - \left(\frac{h_p}{H}\right)^2\right)$$

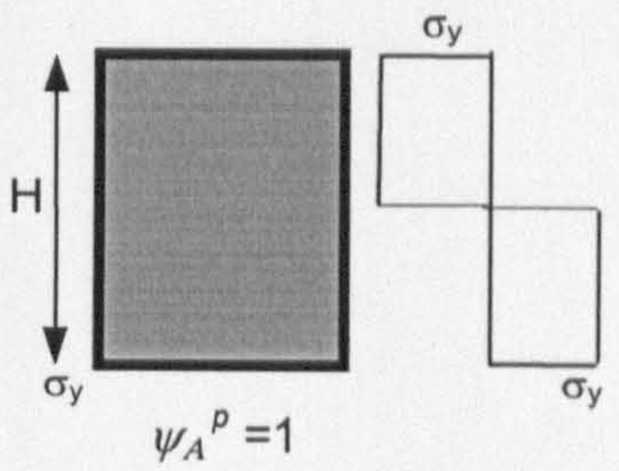

FULLY PLASTIC ENVELOPE, $C_{e\,p}$

Geometric quantities

$$A_p = BH$$

$$Z_e + Z_p = \frac{BH^2}{4}$$

Shape transformers

$$\psi_A{}^p = 1$$

$$\psi_Z{}^p = 1.5$$

Plastic range from C_e to C_p

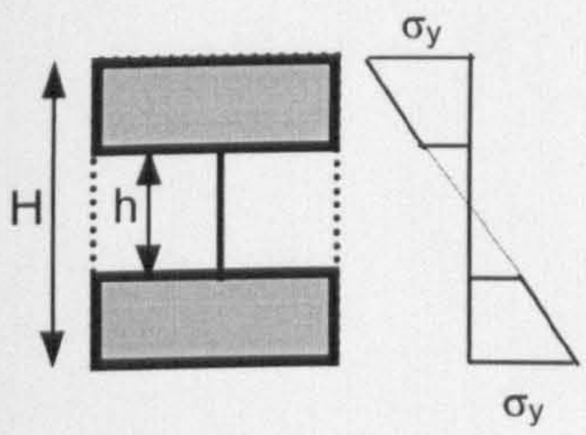

ELASTIC C_e

Geometric quantities

$$A^p = 0\,,\; Z_p = 0$$

$$Z_e + Z_p = Z_e$$

Shape transformers

$$\psi_A{}^p = 0$$

$$\psi_Z{}^p = \psi_Z{}^e$$

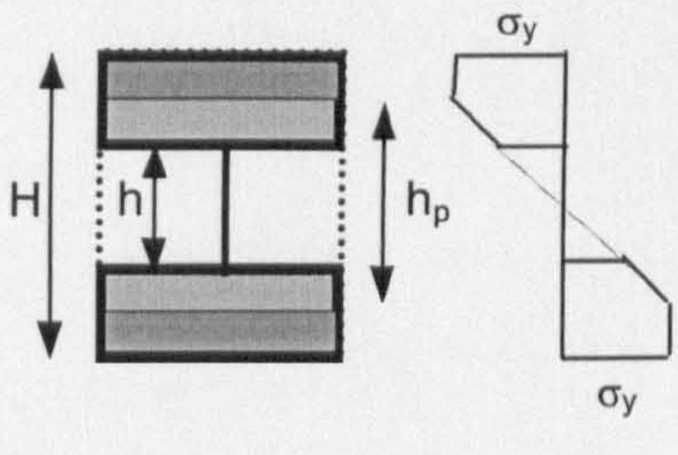

ELASTIC-PLASTIC $C_{e\text{-}p}$

Geometric quantities

$$A^p = B(H - h_p)$$

$$Z_e + Z_p = \frac{B}{12}\left(3H^2 - h_p{}^2 - 2h^2\right)$$

Shape transformers

$$\psi_A{}^p = 1 - \frac{h_p}{H}$$

$$\psi_Z{}^p = \frac{1}{2}\left(3 - \left(\frac{h_p}{H}\right)^2 - 2\left(\frac{h}{H}\right)^2\right)$$

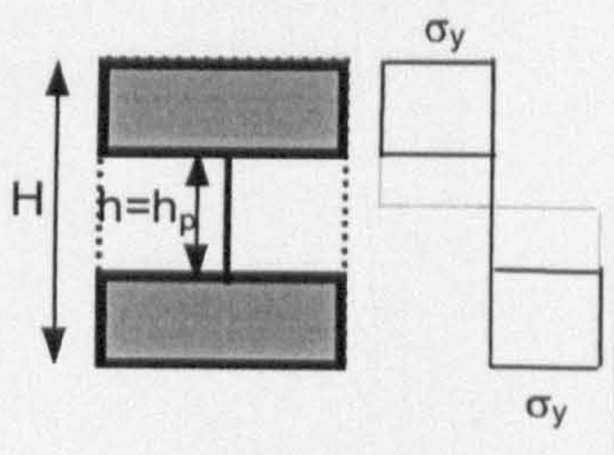

FULLY PLASTIC C_p

Geometric quantities

$$A^p = B(H - h)$$

$$Z_e + Z_p = \frac{B(H^2 - h^2)}{4}$$

Shape transformers

$$\psi_A{}^p = \psi_A{}^e$$

$$\psi_Z{}^p = 1.5\psi_Z{}^e$$

Table 7.1 Shape transformers and geometric quantities for rectangular cross-section (top) and I section (bottom) in plastic bending.

Expressions of the shape transformers $\psi_A{}^p$ and $\psi_Z{}^p$ are shown in Table 7.1. They are for the cross-sections that belong to the rectangle class, such as rectangle and I-section. Expressions of $\psi_Z{}^e = Z/Z_D$ and $\psi_A{}^e = A/A_D$ are given in Table 3.3. The ranges of ratio of the elastic shape transformers to the plastic shape transformers are:

$$\begin{cases} 0 \le \dfrac{\psi_A{}^p}{\psi_A{}^e} \le 1 \\ 0 \le \dfrac{\psi_Z{}^p}{\psi_Z{}^e} \le 1.5 \end{cases} \tag{7.33}$$

7.3.3 The envelope map for plastic bending

Expressions of $\psi_Z{}^p$ and $\psi_A{}^p$, given in Table 7.1, and of $\psi_Z{}^e$ and $\psi_A{}^e$ given in Table 3.3 are used to plot the curves in Figure 7.1 which is divided into lower and upper parts.

In the lower part of Figure 7.1, within the range 0 to 1 defined by $\psi_Z{}^e$ and $\psi_A{}^e$, there are the limiting curves, curves 1e and 2e, for elastic cross-sections. As shown in Chapter 5, the curves 1e and 2e define the elastic domain of all the geometric cross-sectional shapes that partially fill the envelope in strength design.

Curves 3 and 4 define the existence domain of all the shapes which are in the elastic-plastic region. The limit curve 1e for elastic shapes with infinitesimal web thickness becomes curve 3 when the material is completely plastic. For example, plastic deformation in the outer fibres of an I-section, at position G in Figure 7.1, moves G to upwards until all the elastic cross-sectional area becomes fully plastic in H. Similarly, the fully elastic section at C moves to D when plasticity starts in the section shown at C. For a complete elastic rectangular envelope at A, the elastic-plastic behaviour moves position A to B.

The shape transformer $\psi_Z{}^p$ increases with $\psi_A{}^p$. In order to show the range of $\psi_A{}^p$, $\psi_Z{}^p$ is plotted as a function of $\psi_A{}^p$ on the axis A*-A of the upper part of Figure 7.1, for a rectangular cross-section. The curves 1p and 2p are within the ranges

$1<\psi_Z{}^p<1.5$ and $0<\psi_A{}^p<1$. For the elastic rectangle, $\psi_A{}^e$ is unity and $\psi_A{}^p$ is zero. This is represented in the lower part by A and at the origin of the upper part by A*. Curves 1p and 2p indicate the plasticity path. Curve 1 describes how the section modulus of the plastic part of a cross-section increases with the plastic area (dark grey) in the outer fibres of a rectangular envelope of elastic material (light grey). Curve 2p has been plotted in a similar way to the elastic efficiency map. However, curve 2p does not have a physical meaning because it illustrates envelopes containing one material with an unrealistic stress distribution, i.e. plastic zone in the core and elastic behaviour in the outer fibres. In order to achieve this distribution, a loading condition must be applied to the beam that cannot be normally applied in practice. (This is feasible, however, for two layered system containing two materials with the material 1 in the outer sides with $\sigma_{y1} >> \sigma_{y2}$ of the material 2 in the middle).

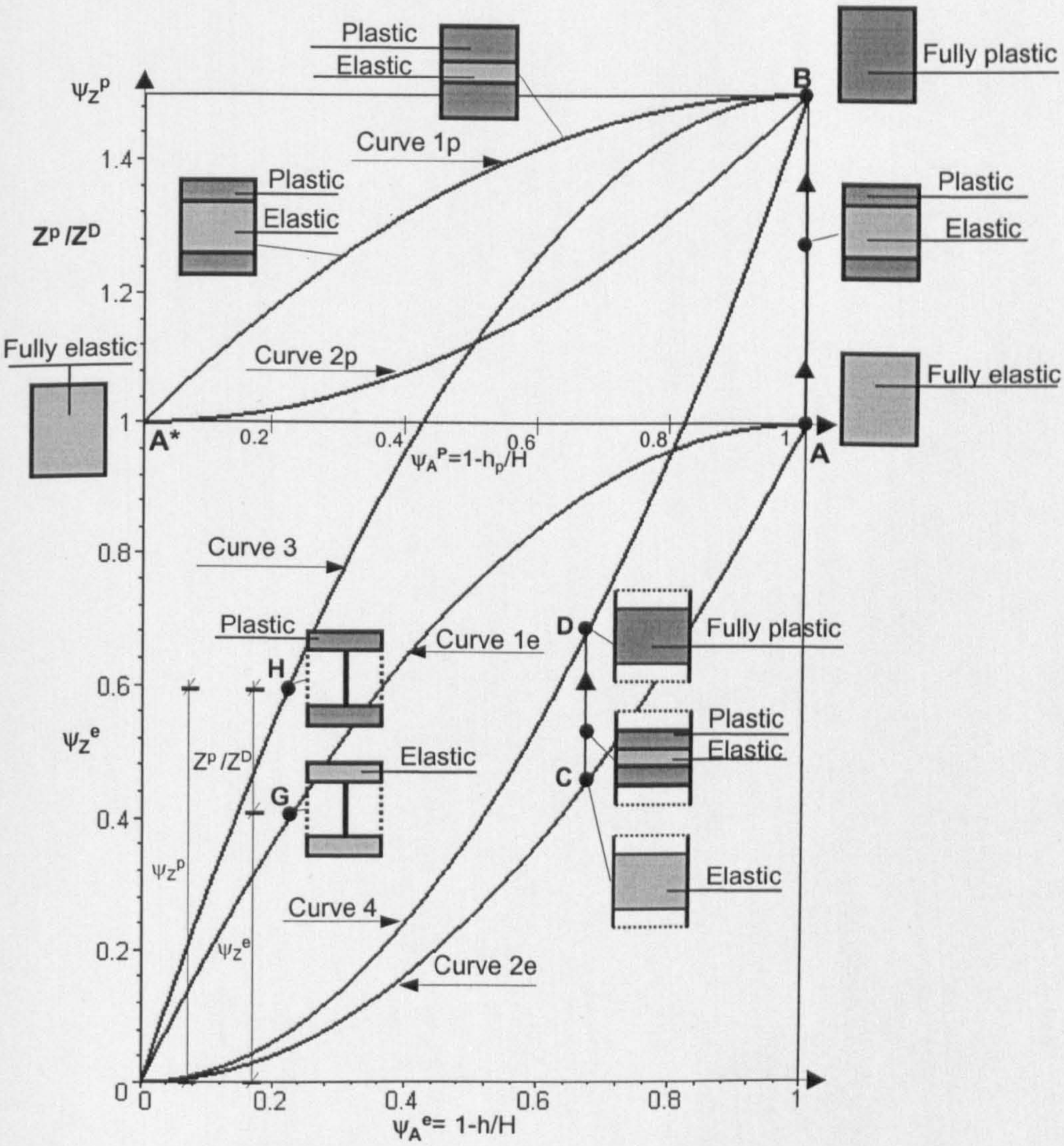

Figure 7.1 Plasticity map for elastic-plastic envelopes.

7.3.4 Three dimensional envelope map for plastic bending

The lower and upper parts have been distinguished in Figure 7.1 in order to plot the variation of $\psi_Z{}^p$ as a function of $\psi_A{}^e$ and also $\psi_A{}^p$. A three dimensional graph makes it possible to plot $\psi_Z{}^p$ on two distinct axes $\psi_A{}^e$ and $\psi_A{}^p$. Figure 7.1 shows two three-dimensional maps where $\psi_Z{}^p$ is plotted as a function of both the shape transformers, elastic $\psi_A{}^e$ and plastic $\psi_A{}^p$. The maps have been produced using expressions in Table 7.1, 3.3 and 3.4.

The expressions of the plastic shape transformers, equations (7.31), define the volume in Figure 7.1a) and b). The volume is bounded by three planes which contain all the shapes of the rectangle class in the elastic and plastic zone. The features of these planes are:

- On the plane $\psi_A{}^e$-$\psi_Z{}^e$ of Figure 7.1a), the curves 1e and 2e describe the efficiency map for strength design when there is material in the elastic region. For a given elastic area, the strength of a structural envelope is increased by moving along a vertical line, such as from point C to E. The vertical line is the optimisation path which has been explained in Chapter 5 for stiffness design.
- On the plane $\psi_A{}^p$-$\psi_Z{}^p$, the increase of the plastic area, described by $\psi_Z{}^p$, on the outer fibres of the cross-section is shown in Figure 7.1a). The plasticity paths, i.e. curves 1p and 2p, on the upper part of Figure 7.1 are now shown for different values of $\psi_A{}^e$ in Figure 7.1a). For a rectangular cross-section with $\psi_A{}^e$=1 A and B are the ending and starting points of both curves 1p and 2p. On the contrary, for cross-sections with $0<\psi_A{}^e<1$, this does not occur. For example for $\psi_A{}^e$=0.7 in Figure 7.1a), the plasticity path, curve 1p, of the cross-section at E, becomes curve EF. In Figure 7.1b) the plasticity path for the rectangle, i.e. curve 2p, becomes for the cross-section at C curve CD. The reason for this is that $\psi_A{}^e$=1 describes only the properties of the rectangle, point A in Figure 7.1a), while each value of $\psi_A{}^e$ within $0<\psi_A{}^e<1$ describes different cross-sections at points from C to E, as it has been explained in Section 5.8.1.
- On the plane where $\psi_A{}^e - \psi_A{}^p$ of Figure 7.1, the curves 3 and 4 of Figure 7.1 are plotted. On this plane there are all the cross-sections with a fully plastic area.

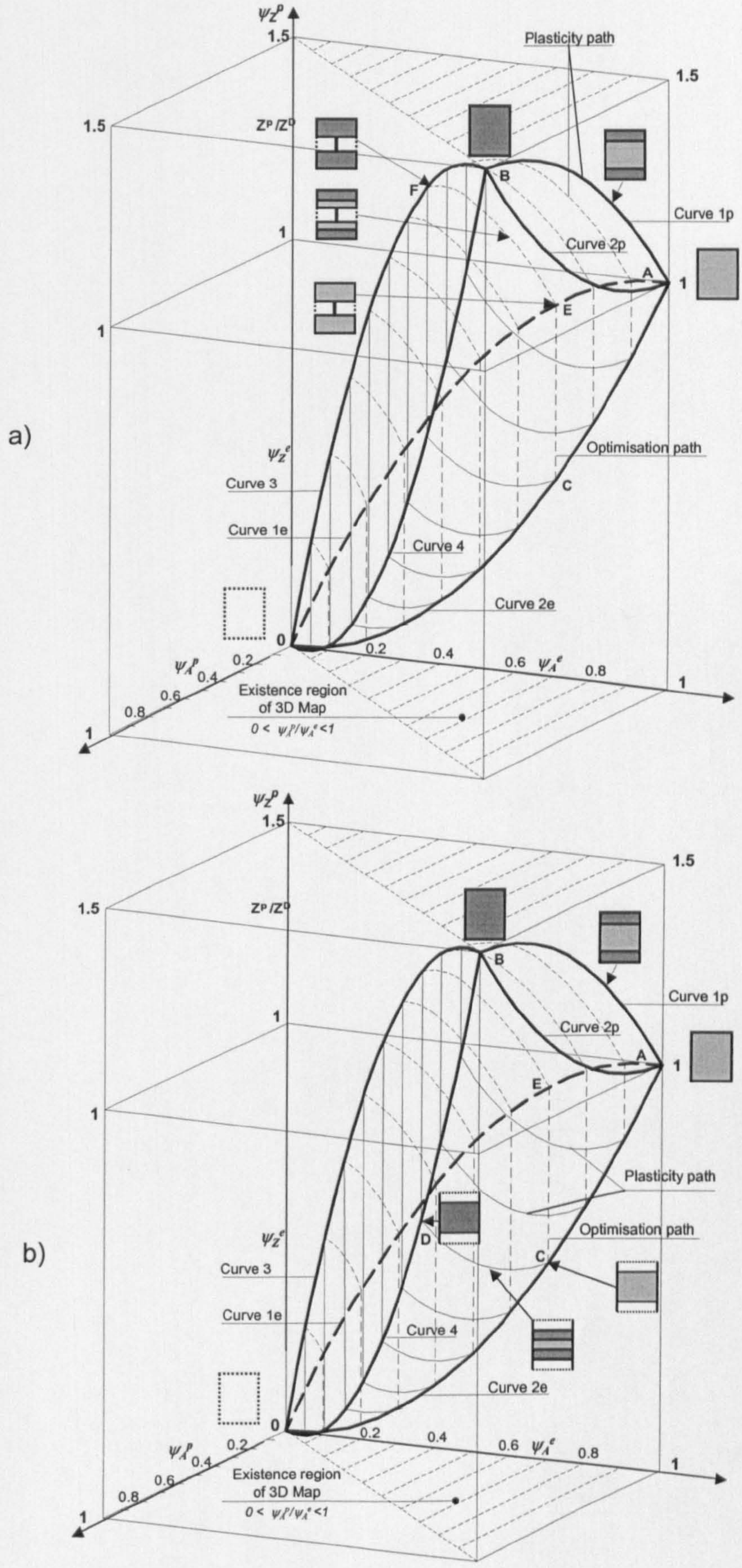

Figure 7.1 3D envelope maps for plastic bending.

One advantage of applying the theory of the shape transformers to plastic bending is that the problem can be treated in terms of geometric properties of the shapes. In contrast, common analysis (Dowling, N.E. 1993) examines plastic deformation in the domain of loading, i.e. applied moment, against strain. The 3D envelope map for plastic bending illustrates all the cross-sections of the rectangle domain which can be in the elastic and elastic-plastic region. The use of the shape transformers to produce the envelope map for plastic bending can provide a user-friendly visualisation of the results and, therefore, give a better understanding of the design problem.

Plastic design methods are used in practice to design single members and structural systems in several areas of engineering. For example, in civil construction, steel frameworks are designed to exploit the plastic behaviour of the material shaped in different cross-sections. The analysis of plastic bending reported in this section can be extended to examine the potential level of ductility of different classes of shapes. The use of shape transformers in plastic design permits the cross-sectional shape with the best level of ductility to be selected for a given application.

7.4 SUMMARY

Structuring and layering have been identified as two features of shaping a material. Both these aspects are described by the shape transformers which specify the shape properties of a system. This permits general expressions describing the properties of any structured layered system to be derived. Standard cross-sections are simple cases of layered systems where one layer is filled with air. The envelope efficiency map and material chart have been used to visualise the performance of combinations of layers using different materials and structured shapes.

An analogy between an elastic-plastic envelope and a sandwich section has been used to extend the theory to the case of plastic bending. Plastic shape transformers have been defined. A three dimensional map has shown that the plastic bending case can be treated in terms of geometric properties of the shapes to provide a better understanding of the design problem.

CHAPTER 8

STRUCTURAL FORM SELECTION

8.1 INTRODUCTION

Chapters 4, 5, 6 and 7 have considered the optimisation of a cross-section by selection of design attributes. This Chapter examines the optimisation of structural form by selection of the geometric variables of a structure. In this work, two structural forms are considered:

1. a continuous element with tapering of the cross-sectional shape along the length
2. frameworks which are constituted of more structural members.

The Chapter consists of the following:

- In the first part, parametric expressions for the mass of structural forms are modelled. The functions of mass are provided for three cases:
  - i) different **tapering** of a cantilever beam.
  - ii) pin-jointed **frames**, where **yield** governs the design of struts.
  - iii) pin-jointed **frameworks** where the constituent elements suffer failure either due to **buckling** or yield according the their slenderness.
- The second part presents the optimum conceptual design for three applications:
  - i) Tapered cantilever beam and truss cantilever. Traditional design charts are used to compare the mass of **alternative structural concepts**.
  - ii) Pin-jointed structures for yield design. This application is an **industrial case** developed in consultation with a bulk materials handling company in U.K. A new **nested performance chart** is used to plot the mass function for frames with more than two design variables. (The explanation of the concept of the nested performance chart is reported in the Appendix D).
  - iii) Pin-jointed frameworks with buckling considered. The shape transformers are used to explore the **interaction between the selection of** the optimum overall **form and** the optimum **cross-sectional shapes**.

8.2 THE FUNCTIONS OF MASS FOR STRUCTURAL FORMS

This Section provides the mass as a function of geometric variables, *g.v.*, for structural form. These functions are used to produce design charts for the selection of alternative structural concepts. In this Chapter, the geometrical variables, *g.v.*, which describe variation in the form of a structure are:

1. The tapering for cantilever beams (Section 8.2.1).
2. The angles between members and the lengths of elements of pin-jointed structures (Sections 8.2.2 and 8.2.3).

8.2.1 Tapered cantilever beam in strength design

Tapered beams, as shown in Figure 8.1, are considered for the optimum design of an end load cantilever in strength design. It is assumed that:

a) The maximum allowable stress, σ_y, is the same in tension and compression.
b) The weight required to support shear loads is negligible.
c) The self-weight of the structure is not considered.
d) Buckling is not considered in the parts of the component in compression.

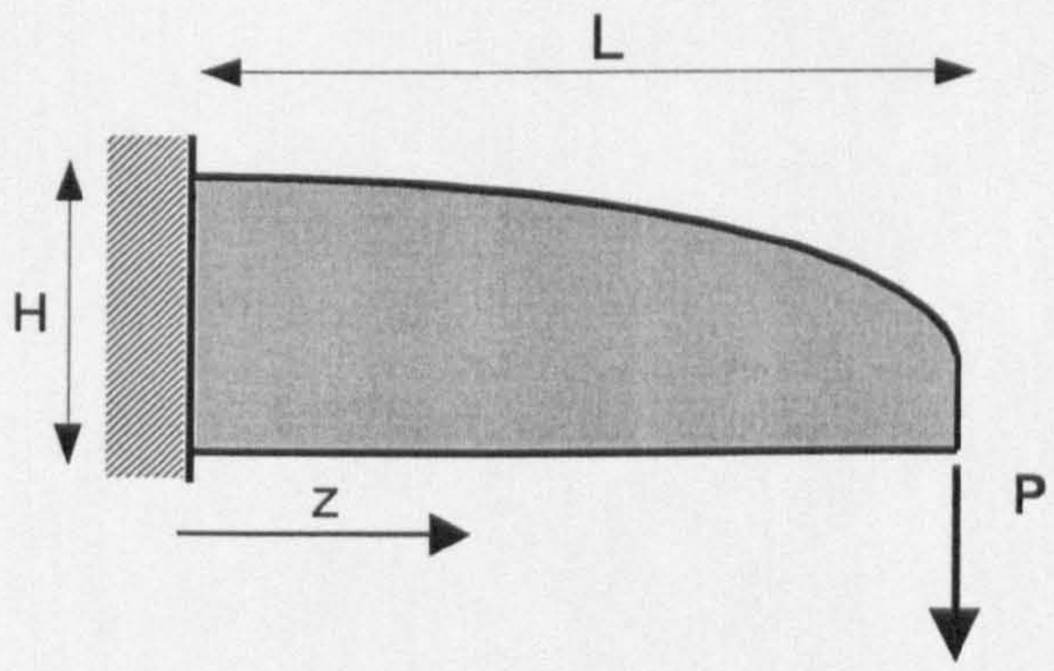

Figure 8.1 Cantilever beam with non uniform cross-section along the longitudinal axis.

The mass of the cantilever beam shown in Figure 8.1 is given by

$$m = \rho \int_0^L A(z)dz \tag{8.1}$$

where ρ is the density of the material, and $A(z)$ is the cross-sectional area varying along the longitudinal axis z.

To derive a function of the mass, the area of the beam is replaced with the functional requirements: strength of the material and bending load. In general, the stress σ is related to the geometry with the section modulus Z in any cross-section at distance point, z, from the free end of the cantilever as follows:

$$\sigma = \frac{M(z)}{Z(z)} \tag{8.2}$$

If y_{max} is the distance of the furthest fibres from the neutral axis, the section modulus Z at any point, z, of the beam from the general expression of I, i.e. $I = \int_A y^2 dA$, is:

$$Z(z) = \frac{1}{y_{\max}(z)} \int_A y^2(z) dA(z) \tag{8.3}$$

Combining equation (8.3) and (8.2) to isolate the area and then substituting in equation (8.1), gives the following function of the mass for a given moment M_y which causes yield, σ_y, in the cross-section at the support:

$$m = \frac{\rho M_y}{\sigma_y} \int_0^L f(z) dz \tag{8.4}$$

where $f(z)$ is a function, $f(z)$, which depends on the cross-sectional shape and the tapering of the cross-sections.

If the moment increases linearly with H/L, as in Figure 8.1, then the mass, m, can be expressed as a dimensionless function given by:

$$\boxed{\frac{m}{M_y \rho / \sigma_y} = f(L/H)} \tag{8.5}$$

where f is a function which depends on the tapering of the cross-sections along the longitudinal axis. Equation (8.5) will be used in Section 8.4 to produce design charts which enables comparison of the mass of tapered cantilevers and different truss cantilevers.

8.2.2 Pin-jointed frame in yield design

A function of the mass is derived for pin-jointed frameworks, such as those shown in Figure 8.1. The following assumptions have been considered:

a) The constituent members have uniform cross-section along their length.

b) The weight of the pin-joints between members is neglected.

c) The self-weight of the structure is disregarded.

d) The structures are considered statically determinate externally and internally. The equations of equilibrium are sufficient to derive the reactions and the internal forces from external loads. Therefore, the stiffnesses of the elements at a joint, described by geometric and material properties, can be ignored to determine the internal forces.

e) The maximum allowable stress, σ_y, is the same in tension and compression.

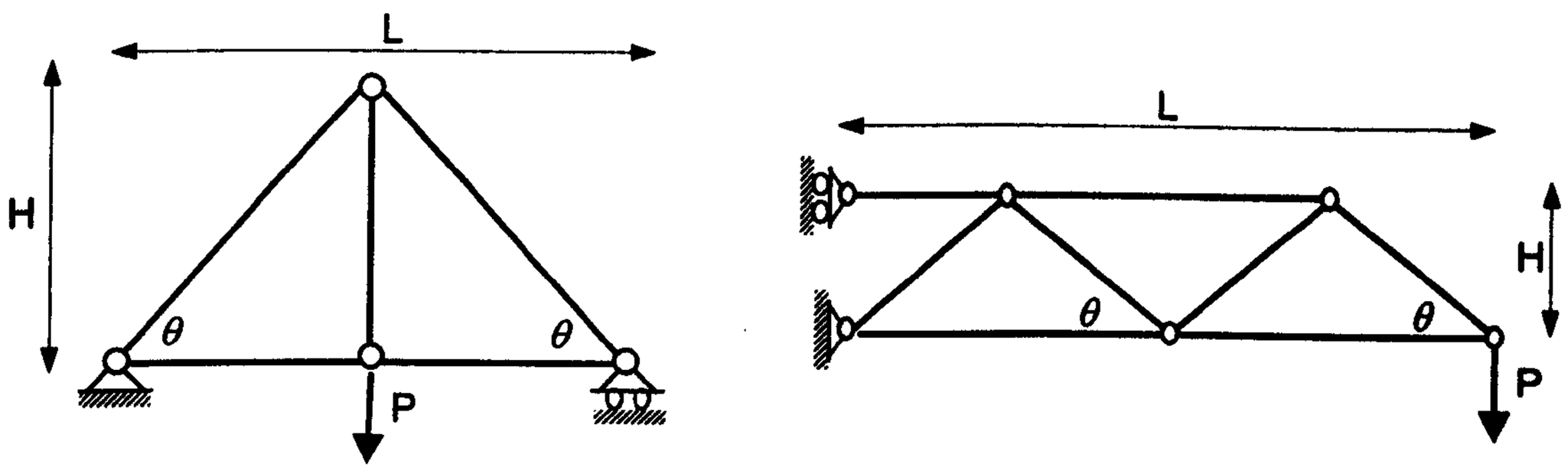

Figure 8.1 Pin-jointed structures.

For a pin-jointed structure consisting of n members made from a single type of material, the length of a typical member i is L_i, its area is A_i and the volume is A_iL_i. The total mass, m, of the structure is the objective function to be minimised and the mass is given by:

$$m = \rho \sum_{i=1}^{n} A_i L_i \tag{8.6}$$

Compression and tension members are included in equation (8.6) so that:

$$m = \rho \sum_{i=1}^{n} \left(A_i^t L_i^t + A_i^c L_i^c \right) \tag{8.7}$$

where A_i^c, L_i^c and A_i^t, L_i^t are the cross-sectional areas and lengths of the compression and tension elements of the structure respectively.

Since buckling is neglected for yield design, the variables A_i^c and A_i^t of each member of the structure are substituted in equation (8.7) by the load requirement and material yield stress. As shown in Chapter 4, for tension members, the minimum area, A_i^t, does not depend on the cross-sectional shape and it is given by:

$$A_i^t = \frac{P_i^t}{\sigma_y} \tag{8.8}$$

where P_i^t is the internal force in tension elements and σ_y is the yield tensile stress.

For compressive members, the minimum area, A_c, does not depend on the cross-sectional shape and it is given by:

$$A_i^c = \frac{P_i^c}{\sigma_y} \tag{8.9}$$

where P_i^c is the internal force in each compression member and σ_y is the yield compression stress.

Substituting equations (8.8) and (8.9) in (8.7), the mass is:

$$m = \frac{\rho}{\sigma_y} \sum_{i=1}^{n} \left(P_i^t L_i^t + P_i^c L_i^c \right) \tag{8.10a}$$

In equation (8.10a), it can be seen that only the yield stress influences the mass for given internal forces and lengths of the elements. If *g.v.* are the geometric variables, such as the overall height H of a structure or the angle θ between members in Figure 8.1, which determine spatial variations of a structural form, then the internal forces, P_i^t and P_i^c, and the length, L_i^c and L_i^t, of each member, can be expressed as function of *g.v.* and equation (8.10a) is re-written as:

$$m = \frac{\rho}{\sigma_y} \sum_{i=1}^{n} \left(P_i^t(g.v.) L_i^t(g.v.) + P_i^c(g.v.) L_i^c(g.v.) \right) \qquad (8.10b)$$

The values of *g.v.* which minimise the mass, i.e. equation (8.10b), determine the form of an optimum pin-jointed structure, i.e. the optimum arrangement of the members in a structural layout. Since the geometric and material properties of the cross-sections of the constituent elements are not included in equation (8.10b), there is no interaction between the selection of the geometric variables, *g.v.*, of the form and the selection of the geometric variables of a cross-section, D and S.

8.2.3 Pin-jointed frame with buckling included

The optimum design of pin-jointed structures, Figure 8.1, which can buckle is examined. The same assumptions made in Section 8.2.2 are considered. The Rankine-Gordon formula presented in Chapter 3 is used to derive an expression of the minimum area for compressive members which, in practice, collapse for material breakdown at buckling loads less than the Euler predictions. From equation (6.52), the minimum area, A_c, for strut elements of any length, L^c, is given by:

$$A^c = 0.5 \frac{P^c \lambda_I z v + \sqrt{P^c \lambda_I z \left(P^c \lambda_I z v^2 + 4 \sigma_y \psi_A \mu L^{c^2} \right)}}{z \lambda_I v \sigma_y} \qquad (8.11)$$

where z=1/12 and $\mu = \dfrac{\sigma_y}{\pi^2 E}$.

Expression (8.11) shows that when buckling is involved, it is necessary to consider material properties, σ_y and E, geometric properties, λ_I, ψ_A, λ_I, v, L, and also the load intensity, P^c.

Substituting equations (8.11) and (8.8) in (8.7), gives the mass of a pin-jointed structure which can collapse either by buckling or yield:

$$m = \frac{\rho}{\sigma_y} \sum_{i=1}^{n} \left(P_i^t L_i^t + \frac{P_i^c \lambda_I z v + \sqrt{P_i^c \lambda_I z \left(P_i^c \lambda_I z v^2 + 4 \sigma_y \psi_A \mu L_i^{c^2} \right)}}{2 z \lambda_I v} L_i^c \right) \qquad (8.12a)$$

Equation (8.12a) shows that to minimise the structural mass of a framework it is essential that tensile and compressive member forces, material and geometric properties of the cross-sections, i.e. contribution from the shape properties and envelope, and the lengths of the elements should be taken into account.

As with equation (8.10b), if the internal forces, P_i^t and P_i^c, and the length, L_i^c and L_i^t, of each member are expressed in function of design geometric variables, *g.v.*, the equation (8.12a) is re-written as:

$$m = \frac{\rho}{\sigma_y} \sum_{i=1}^{n} \left(P_i^t(g.v.) L_i^t(g.v.) + \frac{P_i^c(g.v.)\lambda_I z v + \sqrt{P_i^c(g.v.)\lambda_I z \left(P_i^c(g.v.)\lambda_I z v^2 + 4\sigma_y \psi_A \mu L_i^{c2}(g.v.) \right)}}{2z\lambda_I v} L_i^c(g.v.) \right) \quad (8.12b)$$

The optimum values of *g.v.* which minimise equation (8.12b) describe the form of a minimum mass pin-jointed frame. The optimum values of *g.v.* take into account the interaction between the geometric variables of a cross-section, i.e. D and S, and the variables, *g.v.*, which determine the optimum overall form, i.e. the spatial variation between structural members.

The use of λ_I, ψ_A and v at the early stage allows the designer to quickly pre-select efficiency, shape properties, and the size ratio of the envelopes without determining real dimensions of the cross-sections. The range of the dimensionless values of λ_I and ψ_A are given in Tables 3.3 and 3.4. In Section (8.3.3) a case study will show the effects of the interaction between cross-sections selection and form selection for different structural designs.

8.3 APPLICATIONS

The aim of this Section is to apply the functions of mass provided in Section (8.2) to three structural design cases. The applications use design charts to compare the mass of different structural forms.

- The first case uses equation (8.5) and equation (8.10b) for the optimum design of different cantilever beam and truss cantilever. Traditional charts are produced for the selection of alternative structural form.
- The second is an industrial case developed in consultation with a bulk materials handling company, who manufacture structures and machinery for excavation

and handling of materials. In this case, in addition to traditional charts, a new nested performance chart is used to visualise performance trends for pin-jointed frames with four variables. A detailed explanation of the nested performance chart is reported in the Appendix D.

- The third application considers large-scale structures, common in areas such as bridge and crane design. In this case the function of the mass given by equation (8.12b) for frame whose structural members can collapse for yield or buckling failure is applied. The results are visualised through traditional charts, which show the interaction between cross-section selection and form selection.

Methodological approach

Each application uses a methodology which consists of the following steps:

1. Identifying a **benchmark structure** for a given load condition. The benchmark defines the optimum design of a structural form for a particular load. Although the benchmark can be a non-practical structure, it has two purposes:
   a) to act as a reference for the mass comparison among different structures which can be put into perspective,
   b) to show that there is not a great benefit in pursuing further optimisation when a structural form gets close to the mass of the benchmark.
2. Proposing alternative **candidate structures** from experience and/or creativity which meet the loading conditions and specifying the possible operational geometric constraints.
3. Using the results of Section (8.2) to modelling the **mass** of the structures **as a function of geometric variables**.
4. Finding **optimum values** of the geometric variables which minimise the mass of candidate structures.
5. Using **charts to map performance trends**.
6. Providing **insight**.

8.3.1 Cantilever beam

The case study is a cantilever beam subjected to an end load P, as in Figure 8.1.

Benchmark.

As a benchmark a cantilever developed by Michell (1904) is chosen. Figure 8.1 shows the Michell structure for a cantilever with an end load *P*. Michell (1904) showed that this structure has the minimum mass possible for the given boundary conditions. The reason for this is that all the elements meeting at a joint are orthogonal (i.e. intersect at 90 degrees). It is assumed that the compressive elements (continuous lines in Figure 8.1) do not buckle and the cantilever withstands the load without exceeding the yield stress of the material, σ_y.

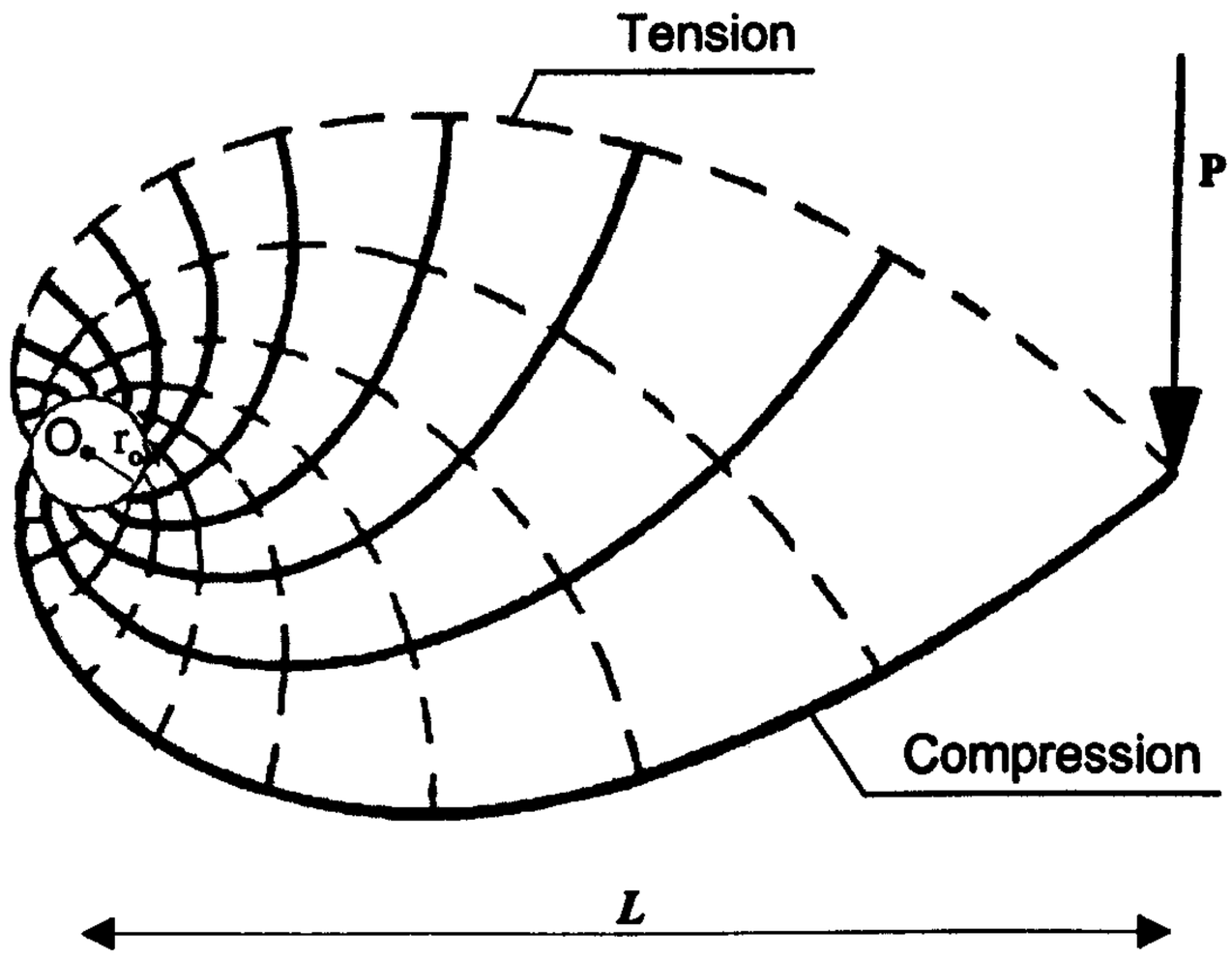

Figure 8.1 Michell structure for a cantilever with an end load

Michell (1904) showed that the mass of orthogonal spirals encircling the origin O, as shown in Figure 8.1, subjected to a moment M_y=P*L with a fixed support in the circle of radius r_o and centre O is given by

$$m = M_y \frac{\rho}{\sigma_y} 2\log\left(\frac{L}{r_o}\right) \tag{8.13}$$

If it is assumed that the radius of the circular support, which has no rotation, is r_o=$L/10$, then the mass of the Michell cantilever is:

$$m = 2M_y \frac{\rho}{\sigma_y} \tag{8.14}$$

Expression (8.14) gives the minimum mass benchmark that can be achieved for a cantilever beam. The mass of other practical candidates structures subjected to the same loading conditions, can be compared with the Michell structure.

Candidate structures

Two groups of different structural forms for a cantilever with an end load are chosen:

1. Different single cantilevers such as a uniform cross-section beam, a fully stressed linear tapered width beam, a fully stressed parabolic tapered beam, a fully stressed tapered width sandwich structure which contain a foam core *h*, as shown in Figure 8.2.
2. Different frame cantilevers: cable stay and truss, as shown in Figure 8.3.

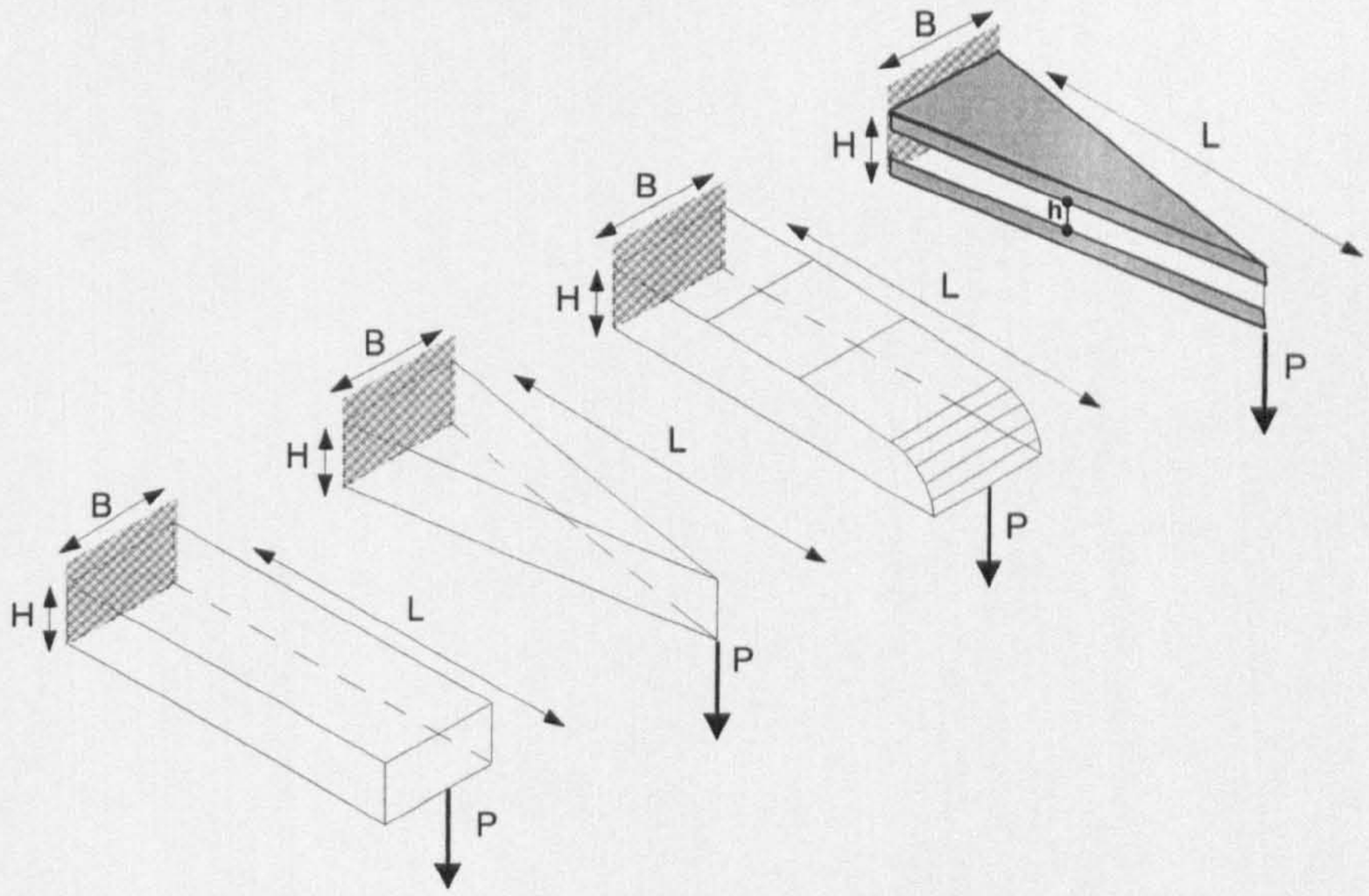

Figure 8.2 Single tapered cantilever beams.

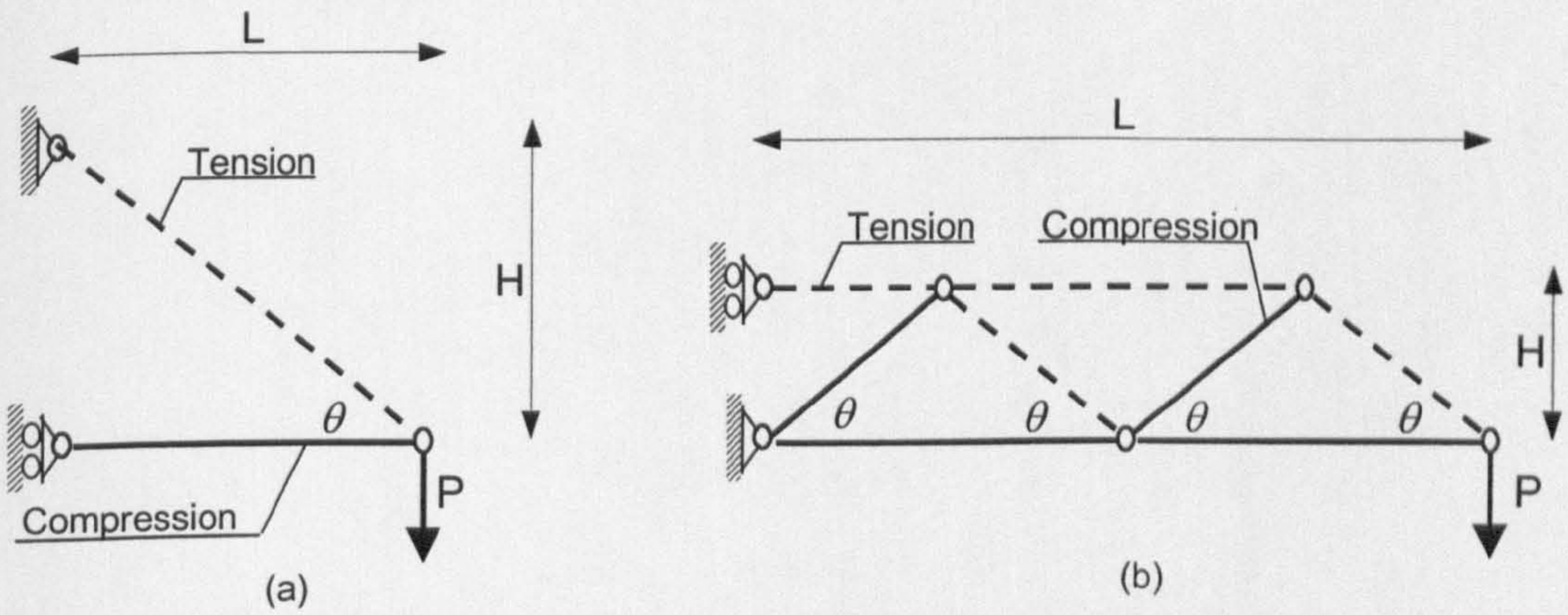

Figure 8.3 a) Cable stay structure. b) Truss structure

Functions of mass

The procedure illustrated in Section 8.2.1 and the equations of equilibrium are used to derive the mass of the tapered cantilever beams shown in Figure 8.2. For a given

M_y and material, equation (8.5) is used to write the mass of the following structural forms:

1a	Uniform cross-section beam	$\frac{m}{M_y\rho/\sigma_y}=\frac{6L}{H}$
1b	Fully stressed tapered (linear) width beam	$\frac{m}{M_y\rho/\sigma_y}=\frac{3L}{H}$
1c	Fully stressed tapered (parabolic) depth beam	$\frac{m}{M_y\rho/\sigma_y}=\frac{4L}{H}$
1d	Fully stressed tapered (linear) width sandwich beam. For the sandwich beam shown in Figure 8.3, it has been assumed that only the skin equilibrates $M_y=P.L$ and determines the mass	$\frac{m}{M_y\rho/\sigma_y}=\frac{L}{H}$

The internal forces of the frame structures in Figure 8.3 are calculated by the static analysis. The internal forces $P_i=f(\theta)$ and the length $L_i=f(\theta)$ of each member are expressed as a function of the geometric variable, θ (with $\theta=\cot^{-1}(L/H)$), and are replaced in equation (8.10b). For a given M_y and material, the expressions of the mass are given by:

2a	Cable stay structure in Figure 8.3)	$\frac{m}{M_y\rho/\sigma_y}=\left(\frac{\cos^2\theta+1}{\sin\theta\cos\theta}\right)$
2b	Truss structure in Figure 8.3)	$\frac{m}{M_y\rho/\sigma_y}=\left(\frac{4\cos^2\theta+1}{\cos\theta\sin\theta}\right)$

Optimum values.

Solving the derivative of the function of mass, $m=f(\theta)$, for the frame cantilever, 2a and 2b, and equalising to zero, gives the minimum values of θ. The minimum values of θ and their respective values of mass are given by:

2a	cable stay:	$\theta_{opt}=54.7^o$	$\left(\frac{L}{H}\right)_{opt}=\sqrt{2}/2$	$\frac{m}{M_y\rho/\sigma_y}\cong 2.82$
2b	truss:	$\theta_{opt}=29.2^o$	$\left(\frac{L}{H}\right)_{opt}=4\sqrt{5}/5$	$\frac{m}{M_y\rho/\sigma_y}\cong 4.47$

Design charts and Insights

Figure 8.4 shows how the mass of the four cantilever beams, 1a, 1b, 1c, 1d compare with the mass of the Michell structure. The following observations can be

drawn. First, the height to length ratio L/H has a critical effect on mass (note that it is unusual to have beams with L/H<1, i.e. height larger than the length). Second, a beam of uniform cross section is very inefficient. Third, when tapering a beam, it is more efficient to taper width than depth. The reason for this is that the tapered depth beam is losing the benefit of depth in section. Fourth, the sandwich beam is the most efficient compared to the Michell.

Figure 8.5 shows the mass trends of the trusses, 2a, 2b, compared to Michell. The results show that the truss structure is more efficient than the cable stay for values of L/H greater than 2, i.e. θ=27° in Figure 8.3. However, the cable stay is more efficient than the truss cantilever for values of L/H less than this value, e.g. θ<27°. The reason for this is that when L/H is large the cable stay has a very inefficient shallow angle. However, when L/H is large, e.g. θ<27°, the truss structure has the disadvantage that it has long lengths of the members which could be unstable.

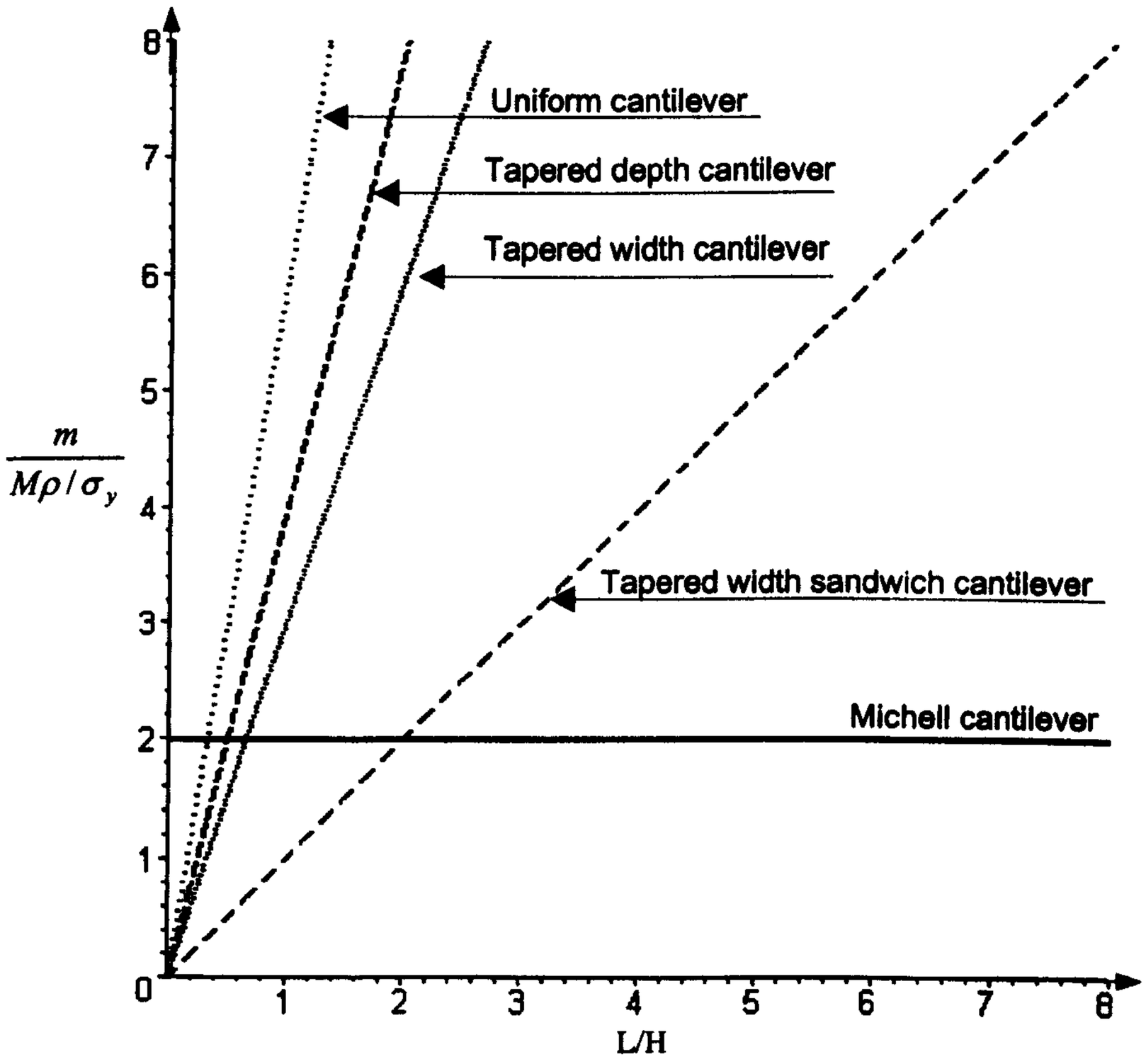

Figure 8.4 Mass of cantilever beam compared to the Michell structure

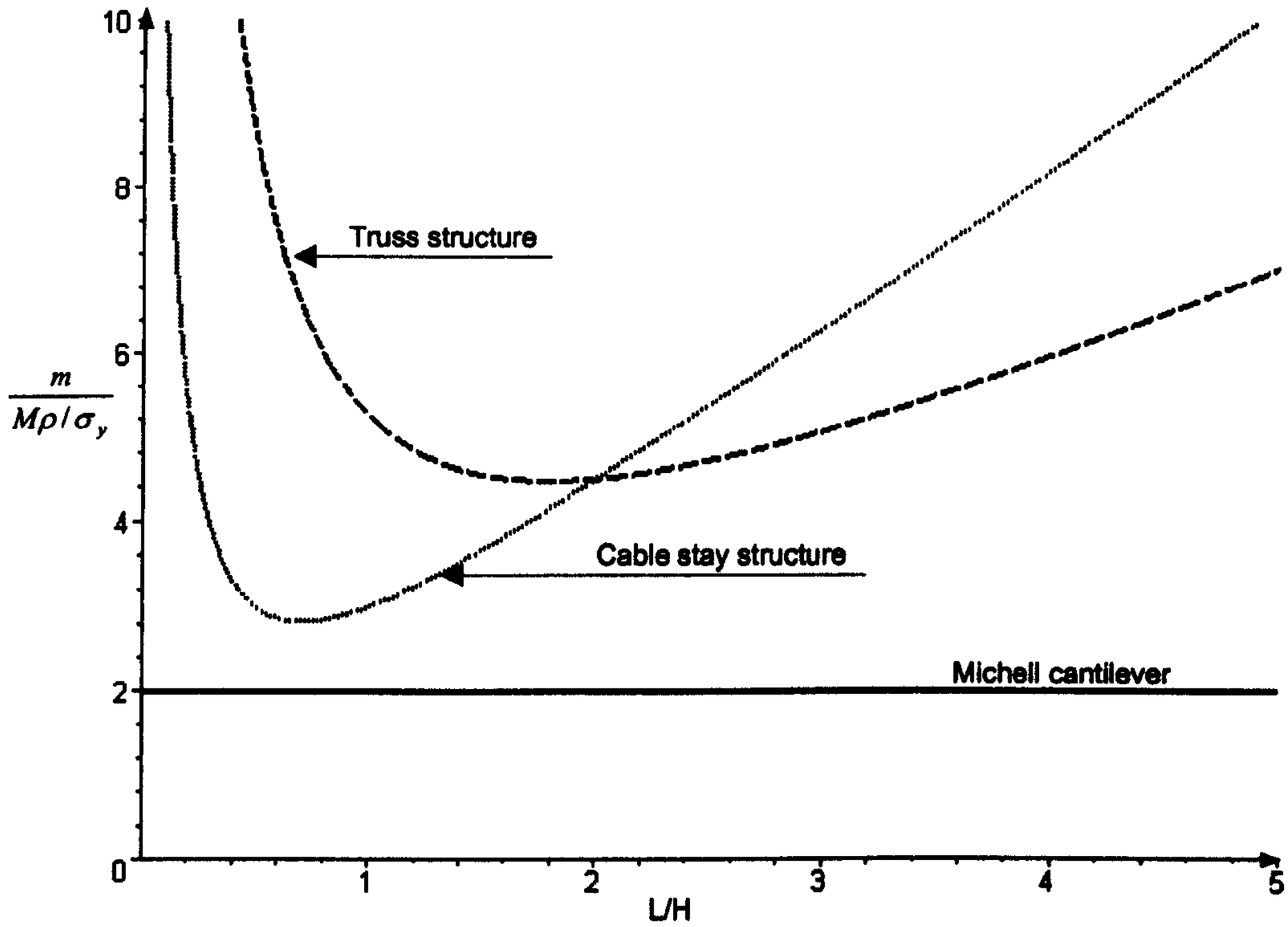

Figure 8.5 The mass of cables stay and truss cantilevers compared to the Michell structure

The charts of this case study have shown that the relative mass of different structural forms can be compared. The charts help designers to explore how the mass of alternative structures is influenced by a given set of geometric variables.

8.3.2 Industrial case: pin-jointed frame yield design

A design application developed in consultation with an industrial company is presented in this Section. Strachan and Henshaw, nowadays Metso, is a company specialised in designing and manufacturing machinery for stacking, blending and reclaiming of bulk materials. Typical examples of these structures are shown in Figure 8.1 and Figure 8.2. The main purpose of this design study is to explore different structural forms which could improve the mass efficiency of these machines at the early stage of design. The performance of alternative structural concepts has been modelled through the expressions presented in Section (8.2). Traditional charts have been used to gain insight and a nested performance chart (the details of the nested performance chart are illustrated in the Appendix D) have been employed to explore the whole design space and to reveal performance pattern.

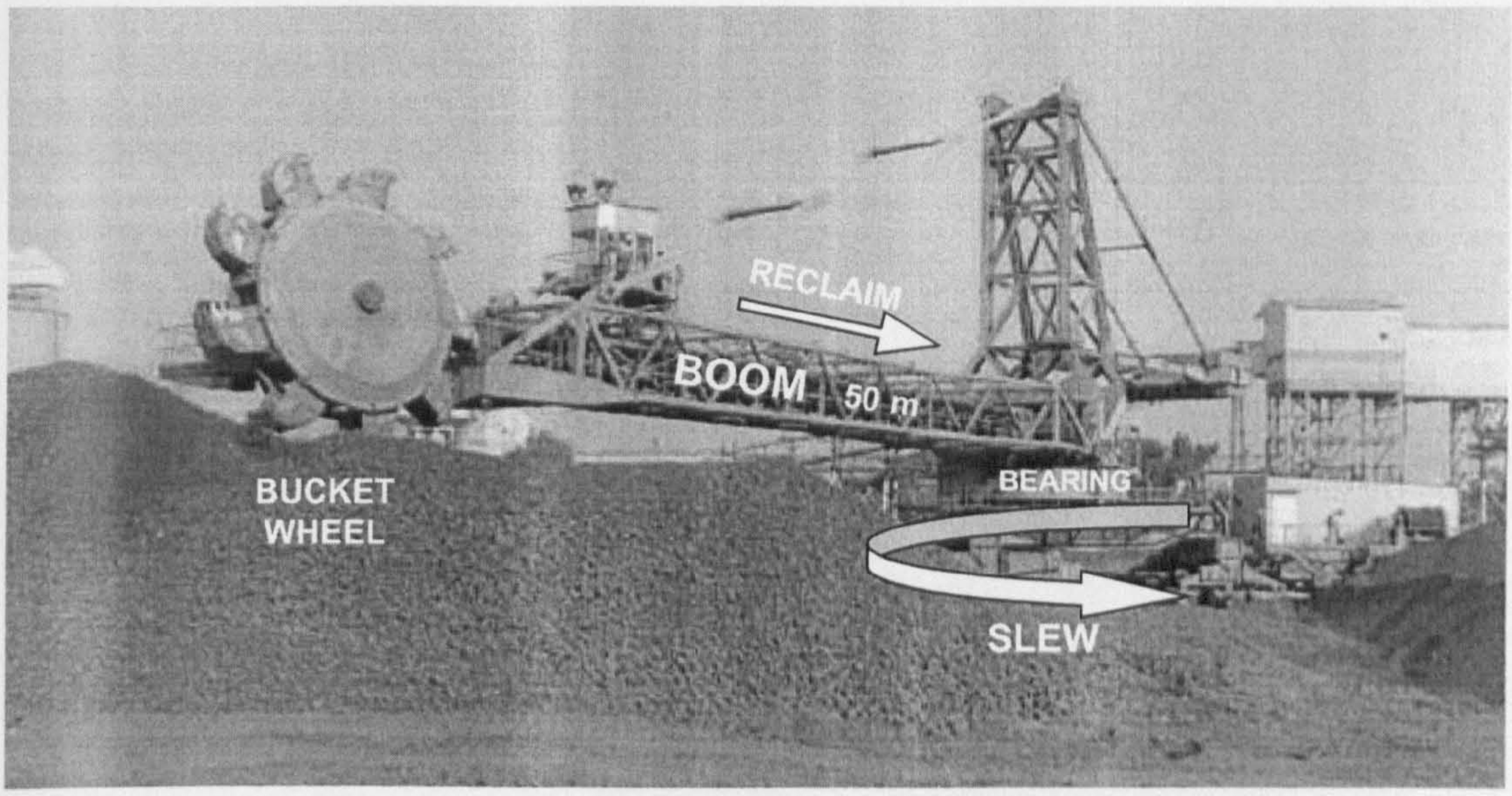

Figure 8.1 Handling machine for material reclaiming.

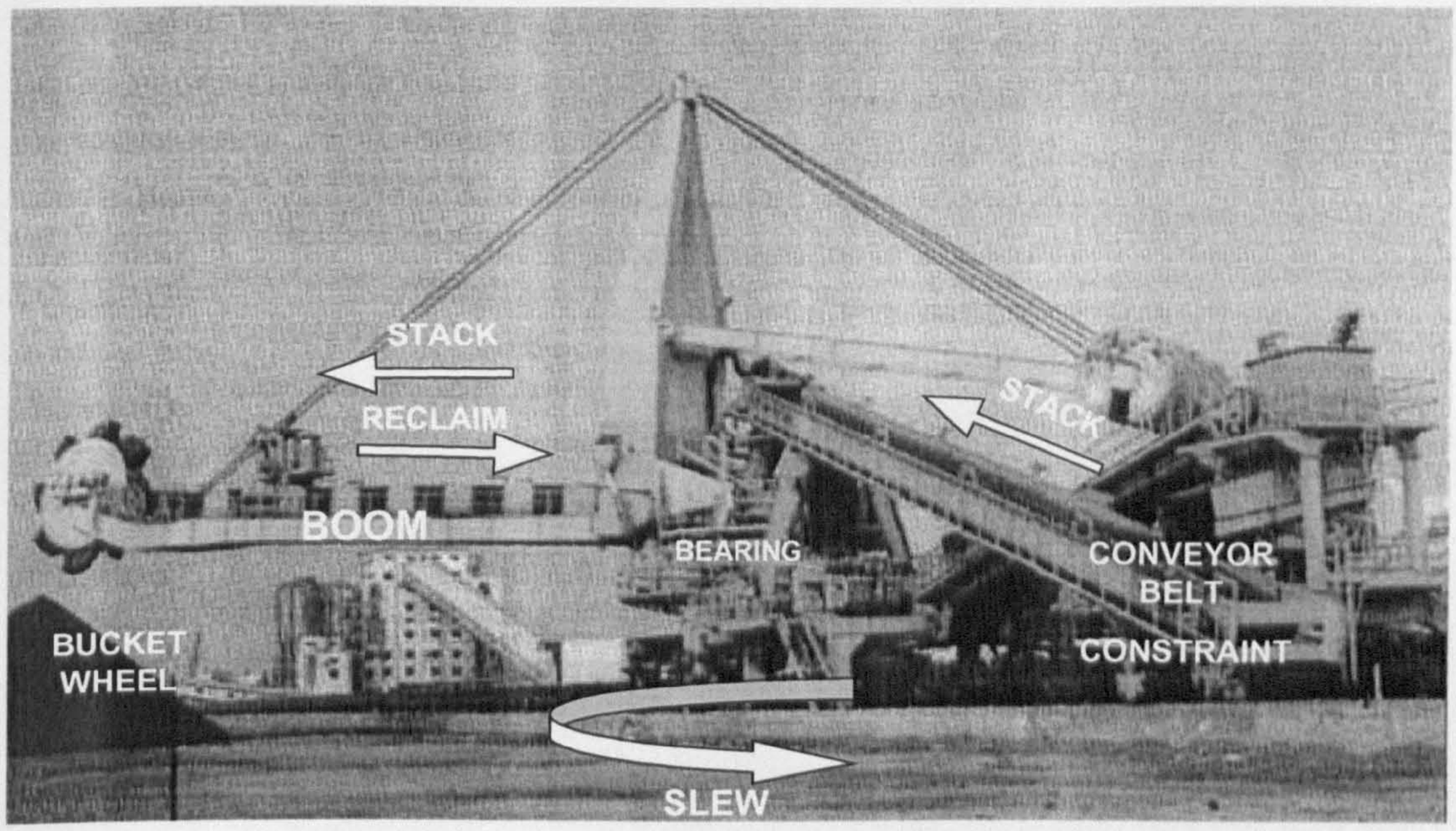

Figure 8.2 Handling machine for reclaiming and stacking of bulk raw material.

Description of the machines. The machines are specialised in moving bulk raw material from their source to the ultimate point of use via railways, ships and conveying systems. The installations range from 300 to 6000 tonnes per hour with boom lengths up to 65 metres and bucket wheel diameter up to 10 metres as shown in Figure 8.1. The main mass of the structure can slew on an axial bearing in order to form parallel piles on each side of the railway track. Two set of machines have been generally manufactured. In the case of the machine shown in Figure 8.1, the material is reclaimed in one direction from the bucket wheel to the central support. This machine is called a reclaimer. Figure 8.2 shows a machine which can move

material in both directions: reclaiming from right to left and stacking in opposite direction from a convey belt placed on the left hand side. These machines are called stackers and reclaimers.

Objectives

In general, the design of the handling machines shown in Figure 8.1 and Figure 8.2, have the following objectives:

1. **Minimise the cost of the structure.** The importance of the mass is very much influenced by the scale of the structure. Material handling machinery are very large weighing up to several hundred tons. In general, the cost of a structure can be broken into the following main parts: design costs, material costs, manufacturing costs (machining, welding etc), assembly and transportation costs. In the case of a very large structure, the mass has a very strong influence on the cost. The reason for this is that a very large structure has a large inherent material cost and the mechanical parts require a large amount of machining and welds. In addition, a large mechanical system tends to attract a large amount of transportation costs. With heavy machinery, for every kg reduction in mass, there is not only a material cost saving but there is also a saving in machining, welding and transportation costs. The close relationship between mass and cost for very heavy machinery means that there is a strong incentive for designers to spend time and effort in **minimising** the **mass of the structure.**
2. **Minimise the cost of the axial bearing.** Since the cost of the bearing depends on the applied force, the second objective is **minimising the reaction** at the central support.

The **reaction**, R, and structural **mass**, m, are the **two objective functions** to minimise. This is because variables which minimise the mass can be different than the variables which minimise the reaction. To be consistent with the unit of measures for reaction (Newton) and mass (Kg), the mass-performance is expressed in terms of structural weight, $W=m*g$ (Newton), where g is the gravitational constant. The total reaction, R, at the central support is given by the sum of the applied load, $Load$, and the weight, W, of the structure to support it. Therefore, the total reaction is:

$$R = Load + W \tag{8.15}$$

Design conditions.

The form of the structures is influenced by the function performed by the machines. The machines can be specialised in only material reclaiming or both reclaiming and stacking of material. These conditions specify two different designs which have been examined:

1. **Unconstrained Design - U.D.** (Figure 8.1): Since the machinery reclaims material only in one direction, the form of the structure can use the whole design space without any geometrical limitations.
2. **Constrained Design - C.D.** (Figure 8.2): A convey belt is located on the counterbalance side to allow the stacking. The convey system restricts the design space. Consequently the form of the structure cannot occupy the space where there is the conveyor belt as shown in Figure 8.1.

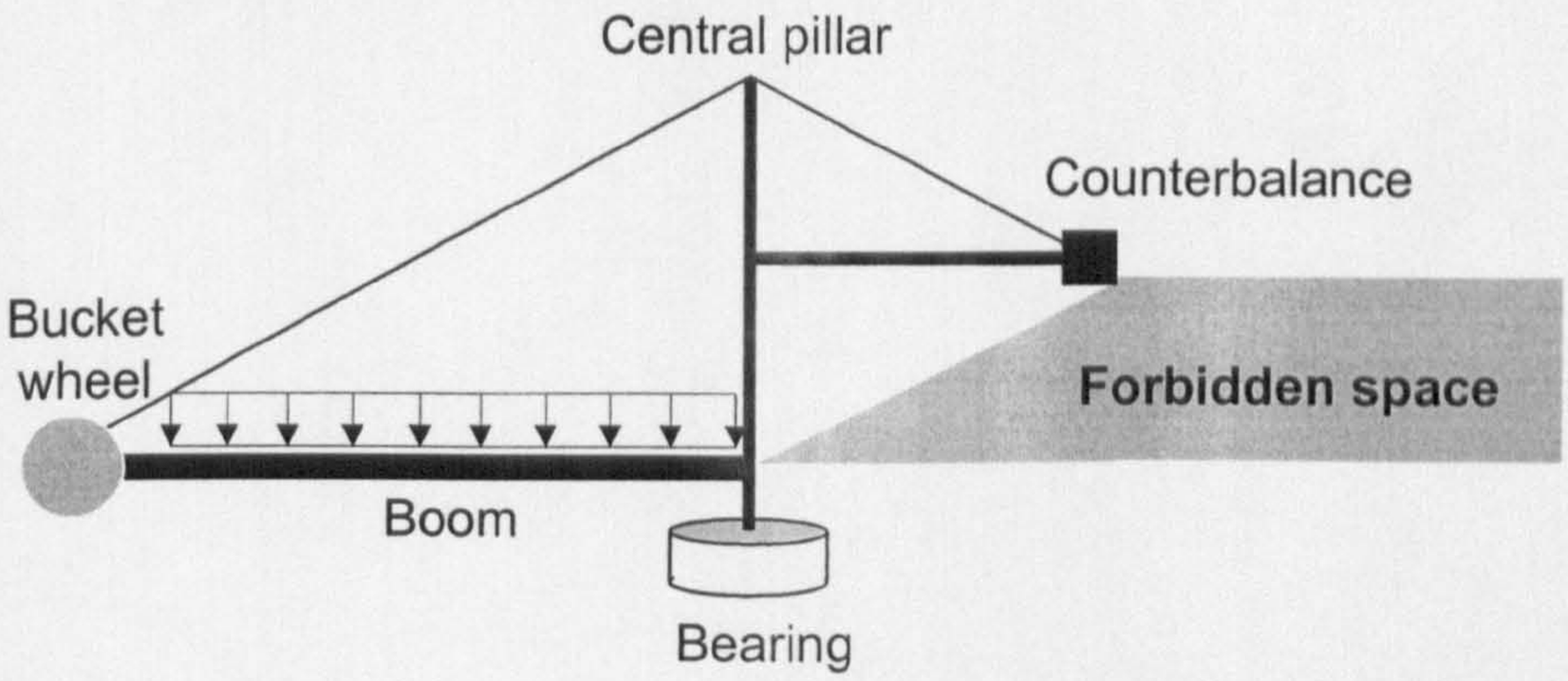

Figure 8.1 The structure cannot occupy the space where the conveyor belt is located, i.e. shadow region.

Industrial demands

The following requirements were specified by the company:

- **Visualise the whole design space.** There is a need to know the trends of the mass. Mapping the functions of mass in the whole design space allows the geometrical constraints to the variables for any design conditions to be applied.
- **Negotiate geometrical constraints.** Since the operational constraints are negotiable at the beginning of design, the performance charts should be easy to understand and should help to find an agreement among the members of a multidisciplinary team.

- **Understand efficient features and patterns.** Structural designers seek beneficial structural features. Exploring performance patterns can help to gain useful insights for the development of new structural layouts.

Analysis of the structural systems

Loading conditions. There are two main loads considered at the early stages for these material handling structures. On one side, the left hand boom in Figure 8.1, there is a uniformly static loading that represents the moving raw material. On the other side, a counterbalance is arranged to keep the centre of gravity well within the diameter of the central support, the bearing ring, which is located under the vertical pillar in Figure 8.1 and Figure 8.2.

Benchmark.

As a benchmark for a double cantilever in unconstrained design, a framework derived from a Michell structure is presented first. Figure 8.11a) shows the Michell structure for a simply supported and centrally loaded framework. This structure is the lightest form for this load case (Michell, 1904). Figure 8.11b) shows the same Michell structure where the central point load and reaction are inverted (support in the central position and point loads at the end). Figure 8.11c) shows the nesting of the inverted Michell structure shown in Figure 8.11b). The end point loads are replaced by a uniformly distributed load carried by infinite number of ties (semicircle). In yield design this theoretical structure is the lightest for this load case.

The performance of the derived Michell structures can be calculated for an infinite number of ties and struts and is given by:

$$W = PL\frac{\rho g}{\sigma_y} \tag{8.16}$$

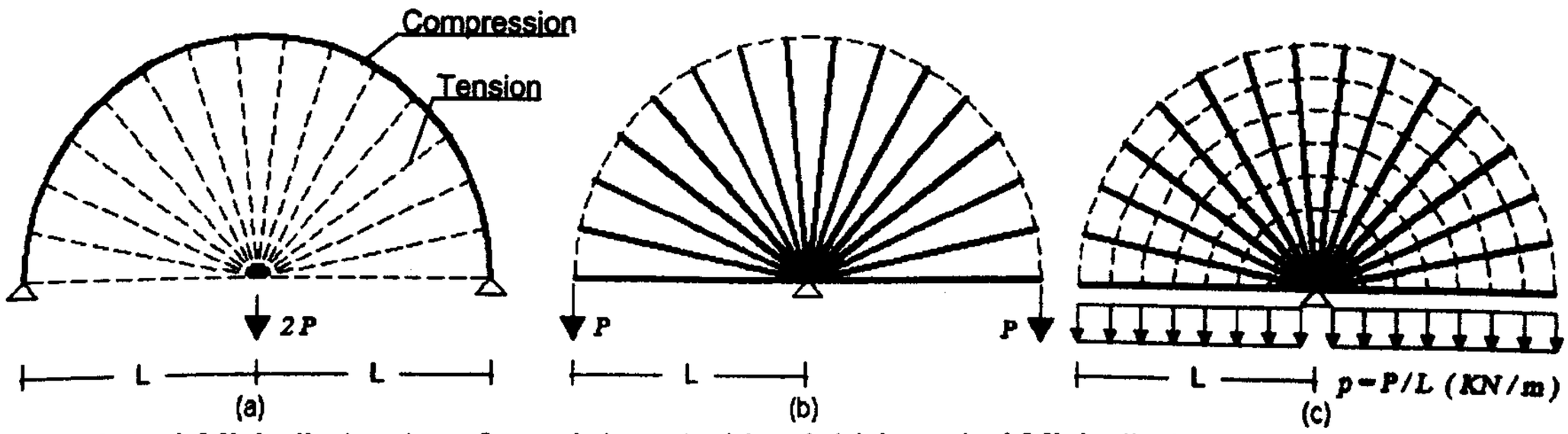

Figure 8.1 a) Michell structure for point central load, b) Inverted Michell structure for end point loads c) Michell derived structure for uniform load = Benchmark.

Candidate structures

U. D. A series of candidate structures shown in Figure 8.2 are proposed for unconstrained design. These alternative structural forms are called derived Web, Parallel and Convergent structures. There are two reasons for selecting these forms. First, structures with ties and struts rather than beams are generally preferred because the under-stressed material in cross-sections subjected to bending is redundant. Second, the form of the web structure with a finite number n of ties, is very close to derived Michell structure with $n\rightarrow\infty$, Figure 8.2c), and therefore could provide a good performance. Third, the variable β for Parallel and Convergent structure, common in bridge design, enables the benefit of the variation of height, H, to be taken into account.

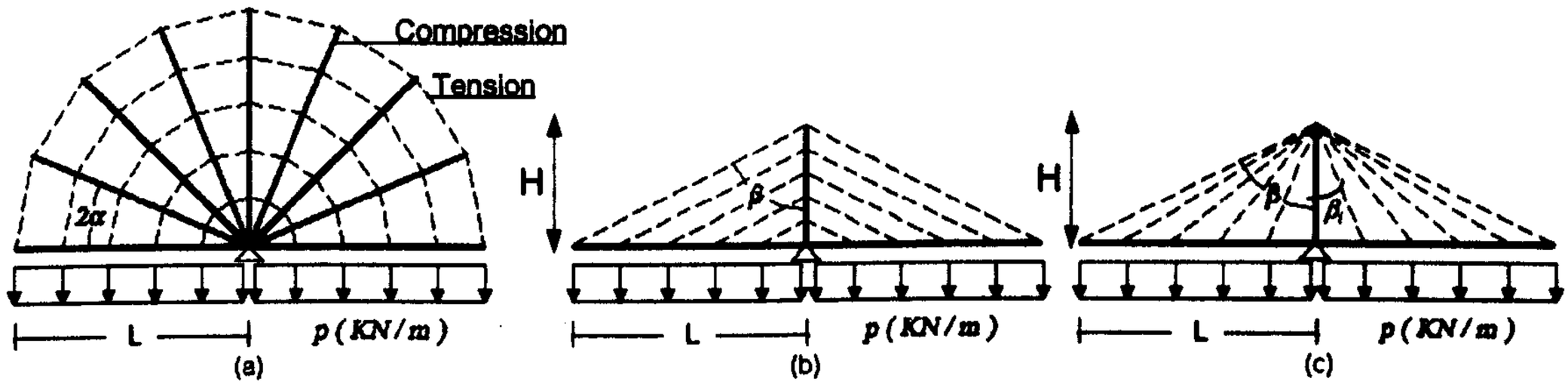

Figure 8.2 Three different structural forms for U.D.: a) Web structure, b) Parallel structure, c) Convergent structure.

C.D. For constrained design, Figure 8.3 shows a structural form, called lozenge frame, for constrained design. The reasons for this form are: i) the lozenge does not have the central pillar subjected to significant bending moment as the structure in Figure 8.1, ii) the lozenge structure is derived from the parallel structure in Figure 8.2b) where the right boom forms an angle θ with the horizontal, Figure 8.3a). The angle θ describes the forbidden space of the constrained structure shown in Figure 8.1.

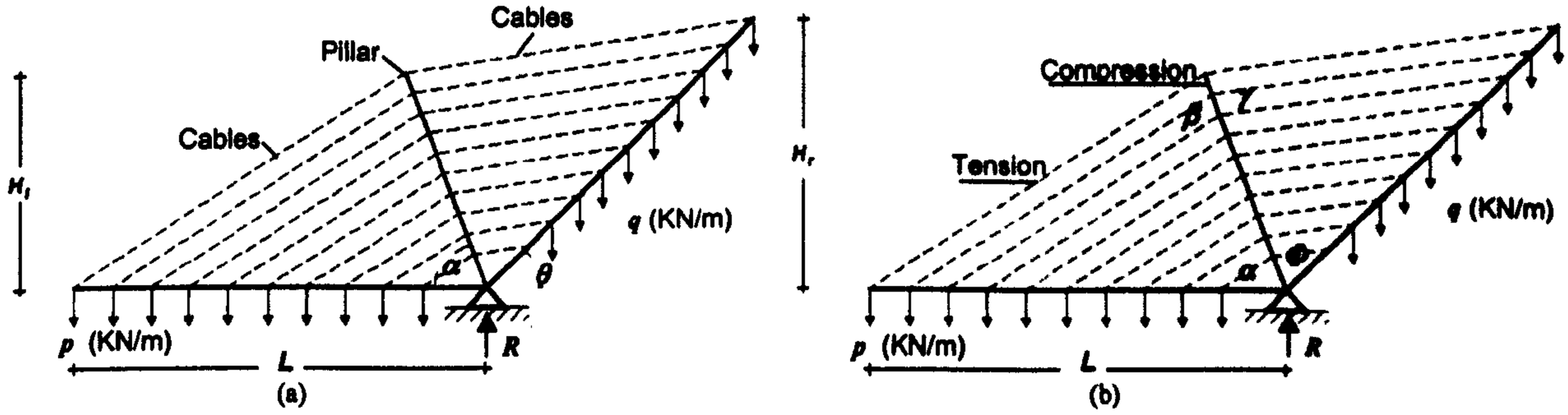

Figure 8.3 Lozenge frame for C.D. with 2 set of four design variables. (Note *L* is fixed)

Although only one set of variables could be sufficient to determine the minimum mass for the lozenge frame, two different sets of four variables, shown in Figure 8.3, are considered. In Figure 8.3a) the variables are: two heights, H_l and H_r, and two angles, α and θ. In Figure 8.3b), the variables are four angles: α, β, γ and θ. The length, L, of the boom is given. There are two reasons for two sets of variables.

1) Designers from industrial collaborators suggest to produce selection chart where the geometric variables can be easy to handle. These variables are the heights of pillar and right boom and two angles at the base of the central pillar. However, as it will be shown later, the structure with four angle variables enables performance patterns to be explored more clearly.
2) The results obtained with the different groups of variables, Figure 8.3a) and b), can be compared in other to check their validity.

Functions of mass

The frames have been assumed to be statically determinate, have structural members with uniform cross-sections along the length and are subjected to axial load. However, the pin-jointed frames in Figure 8.3 are statically indeterminate and have a uniform load which cause bending moment in each span. The following desired effects can be obtained if a high number of ties is considered:

- The bending moment in each span between ties is very low compared to the compression load and, therefore, can be neglected. The boom is therefore subjected only to axial loading.
- The boom can be considered as a continuous beam with a number n of supports, i.e. ties, at distance L/n. For $n>7$ the reaction at the supports, i.e. the magnitude of the internal force carried by the ties, can be approximately computed as half the uniform load between each span with exception to the end tie opposite to the central support. With this assumption at the early design, the stiffness of the members at each joint of the boom can be disregarded.

As a consequence of these assumptions, static analysis and trigonometry can used to derive the internal forces, P_i, and lengths, L_i, in each member of the lozenge frame as a function of the four variables. The expression (8.12b) is used to model the mass of structures for yield design.

Unconstrained design.

In unconstrained design, the beams on the right and left sides of Figure 8.2 are horizontal and have equal lengths. Consequently, the uniform load on the right, p, and left, q, beams are equal because for rotation equilibrium $qL=pL$. In addition the $Load$ does not depend on the geometric variable β for the parallel and convergent. Therefore, the reaction, $R = Load + W$ with $Load=2pL$, depends only on the structural weights, W. Equation (8.12b) gives the following weights function:

- for the web frame

$$W = 2pL^2 \frac{\rho g}{\sigma_y} \frac{\pi}{\alpha} \tan\alpha \frac{1}{n^2} \sum_{i=1}^{n} i \tag{8.17}$$

- for the parallel frame

$$W = 2pL^2 \frac{\rho g}{\sigma_y} \frac{1}{n^2} \sum_{i=1}^{n} i \left(\frac{2}{\tan\beta} + 2\tan\beta + \frac{2}{\sin\beta\cos\beta} \right) \tag{8.18}$$

- for the convergent frame

$$W = 2pL^2 \frac{\rho g}{\sigma_y} \left[\frac{2}{\tan\beta} + \frac{1}{n^2} \left(\frac{2}{n} \tan\beta \sum_{i=1}^{n} i^2 + 2 \sum_{i=1}^{n} \frac{i}{\sin\beta_i \cos\beta_i} \right) \right] \tag{8.19}$$

where $\beta = \tan^{-1}(L/H)$, $\beta_i = \tan^{-1}(L/(nH))$, n is the number of ties and σ_y is the yield stress.

Constrained design

Figure 8.3a) shows that θ can vary. The length of the right boom is a function of θ, i.e. $H_r/\sin\theta$, and, therefore, the applied load $q=f(\theta)$ varies with θ to assure the rotation equilibrium of the system. In contrast to U.D., the $Load=f(\theta)$ is not constant and it is $Load = pL + pL^2 \tan\theta / H_r$.

Two heights - two angles.

Using equation (8.10b) and (8.15) for the lozenge frame shown in Figure 8.3a) with design variables: two heights, H_l and H_r, two angles, α and θ, gives the reaction, R:

$$R = \underbrace{pL + \frac{pL^2 \tan\vartheta}{H_r}}_{Load} + \underbrace{pL \frac{\rho g}{\sigma_y} \frac{1}{n^2} \sum_{i=1}^{n} i \left(\frac{H_l}{\sin\beta^2} + \frac{L}{\tan\beta} + \frac{H_l \sin(\beta+\gamma-\vartheta)}{\sin\alpha \sin\beta \sin(\alpha-\gamma+\vartheta)} + \frac{L\cos(\vartheta-\gamma)}{\sin\gamma\cos\vartheta} + \frac{L\sin\vartheta}{H_r \sin\gamma} \left((H_l - H_r)^2 + \left(\frac{H_l}{\tan\alpha} + \frac{H_r}{\tan\vartheta} \right)^2 \right)^{0.5} \right)}_{\text{Structure weight, } W}$$

where:

$$\beta = -\tan^{-1}\left(\frac{H_l \tan\alpha}{H_l - L\tan\alpha} \right) \qquad \gamma = -\sin^{-1}\left(H_l \sin(\alpha+\vartheta) \Big/ \sin\alpha \left((H_l - H_r)^2 + \left(\frac{H_l}{\tan\alpha} + \frac{H_r}{\tan\vartheta} \right)^2 \right)^{0.5} \right)$$

Four angles.

From equations (8.10b) and (8.15), the reaction function for the structure shown in Figure 8.3b) with four angle variables: α, β, γ and Φ, is given by:

$$R = \underbrace{pL - pL\frac{\sin(\gamma+\Phi)}{\sin\gamma}\frac{\sin\beta}{\cos(\alpha+\Phi)\sin(\alpha+\beta)}}_{Load} + \underbrace{p\frac{L^2\rho g}{\sigma_y}\frac{1}{n^2}\sum_{i=1}^{n} i\left(-\frac{1}{\tan(\alpha+\beta)} - \frac{\cos(\gamma-\alpha)}{\cos(\alpha+\Phi)\sin(\gamma+\Phi)} + \frac{\sin(\gamma+\beta)}{\sin\gamma\sin\beta} + \frac{\sin\alpha}{\sin(\alpha+\beta)\sin\beta} + \frac{\sin\Phi}{\sin\gamma\sin(\gamma+\Phi)}\right.}_{\text{Structure weight, } W}$$

Data

The following data have been suggested by the industry and have been considered:

Length of the boom L=50m

Uniform load: p = 50 KN/m

Material: steel with ρ= 7900 kg/m^3, σ_y= 300 MPa, E=210*10^3 MPa.

Optimum values.

Unconstrained design

The optimum values for frames shown in Figure 8.2 with a number of ties n =10 for each beam, are:

	Structure weight W_{min} (KN)	H(W_{min}) (m)	Applied Load 2P (KN)	Reaction (KN)
Michell (infinite ties & struts)	101	50	5000	5101
Web (n=10 ties & struts)	112	50	5000	5112
Convergent	160	81	5000	5160
Parallel	142	50	5000	5142

It is evident that for any value of the variable H the load is constant, $Load=2pL$= 5000 KN. Therefore, variations in the reaction, R, are determined only by the weight of the structure.

It is worthy to note that the structure shown in Figure 8.1 and currently designed by industrial collaborators for the same geometric and loading conditions, provides:

Structure weight W=565 KN Applied $Load$: 5000KN Reaction R= 5565KN

All the candidate structures for U.D. provide a better structure weight for yield design. The reason is that the effect of ties has a large benefit on the mass of the frames. However, the web structure, Figure 8.2a) is the best for yield design because it is derived from the optimum Michell layout.

Constrained design

Two systems of partial derivatives for the reaction R and for the structure weight W with respect to each variable are solved with a mathematical software, i.e. Maple. The minimum values of R and W for the lozenge frame with 10 number of ties for each beam are:

- For the **best** reaction, **R**:

W_{min} (KN)	$H(W_{min})$ (m)	Applied Load (KN)	**Reaction** (KN)
167	104	3098	**3265**

- For the **best** structure weight, **W**:

W_{min} (KN)	$H(W_{min})$ (m)	Applied Load (KN)	Reaction (KN)
112	44.7	6658	6769

Figure 8.4a) and b) shows the optimum structures for the two objective functions in C.D: minimum structure weight, W and minimum reaction, R. The structure which provides the minimum reaction has a large height, whereas the best structure has the struts of the same length and equal angles between the struts. In such a case, the lozenge layout assumes the form of a web structure with one central strut and two lateral beams.

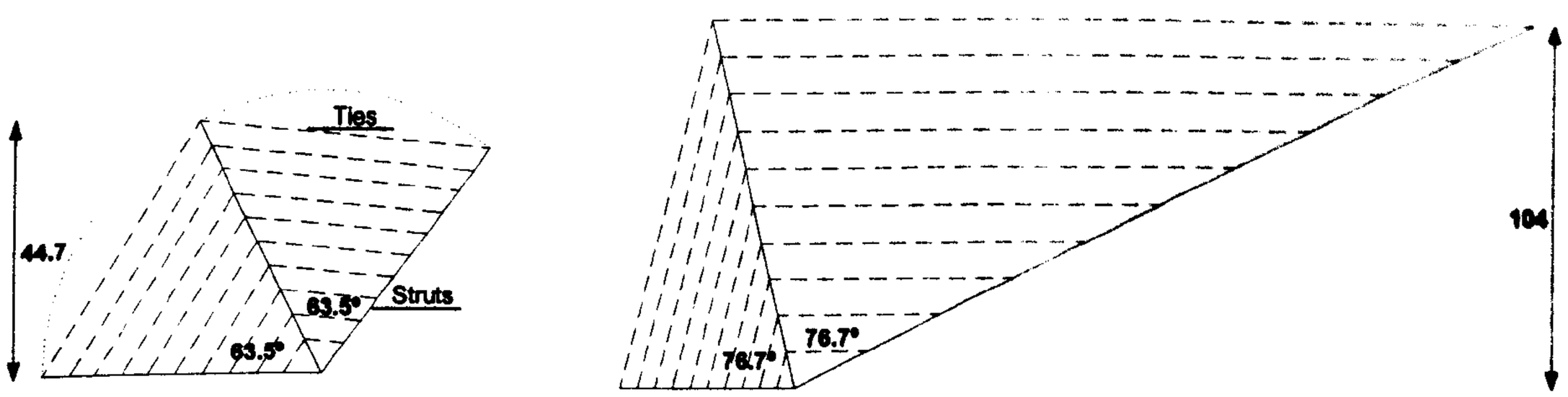

Figure 8.4 Constrained design. a) Lozenge frame for minimum structure weight. b) Lozenge frame for minimum reaction

Design charts

Traditional charts and Insights for U.D.

Figure 8.5 shows the structural weights for frames which can exploit the whole design space. Equations (8.16), (8.17), (8.18) and (8.19) have been used to plot the functions of mass for convergent and parallel frames with the height, H, variable and n=10 for each beam.

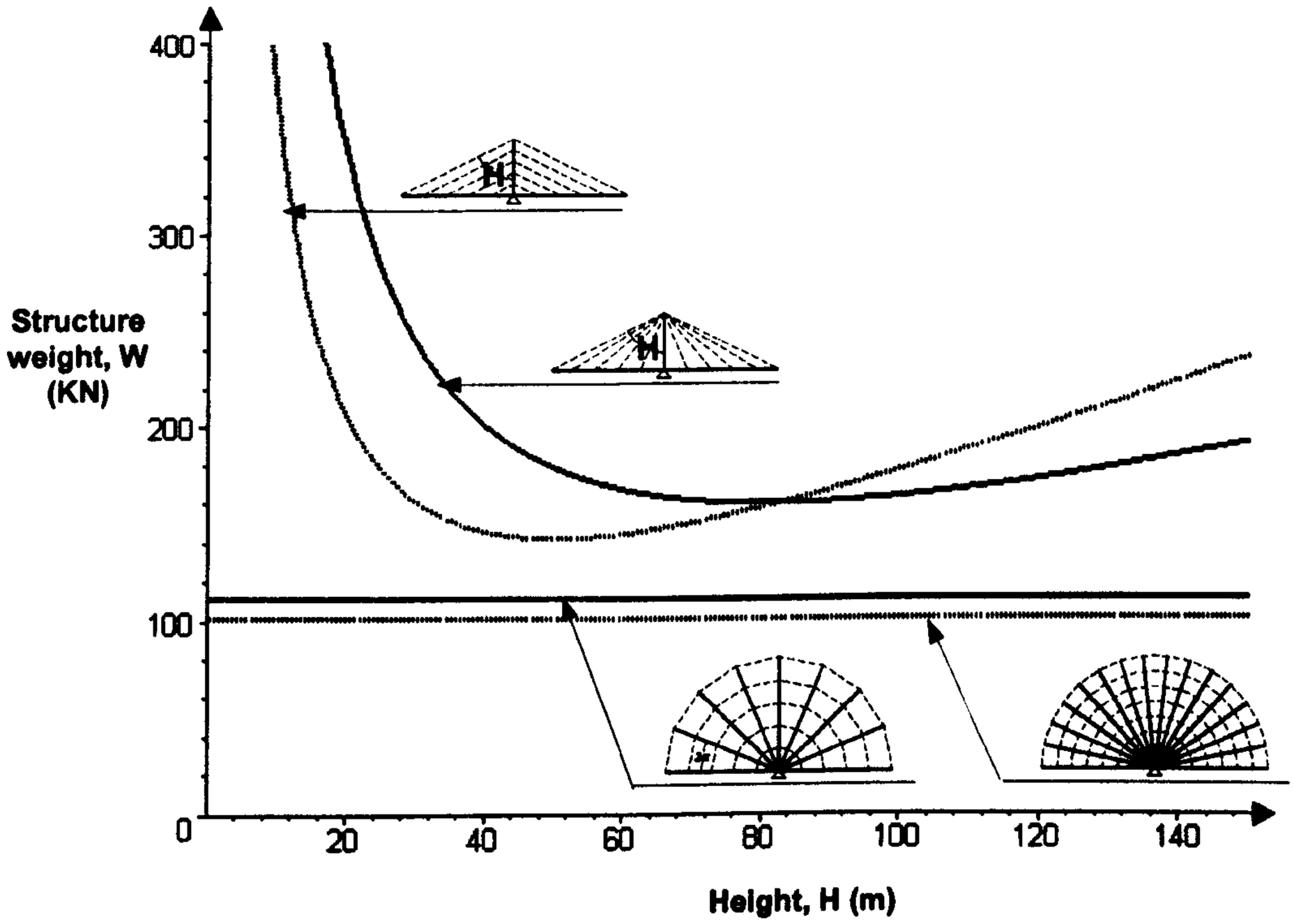

Figure 8.5 Performance trends for structures in U.D with one variable, *H*.

The minimum structural weight is given by the web frame. 10 ties yields the performance of the web to be closed to the derived Michell's layout with infinite ties. The performances of parallel and convergent frameworks with ten ties are quite close. The convergent is less sensitive to height variation. However, the parallel performs better for low height such as H< 80m.

Nested performance charts and Insights for C.D.

Both versions of the nested performance chart, illustrated in the Appendix D, have been developed for the lozenge frame of Figure 8.3a) and Figure 8.3b). As examples, both versions are presented here for the structure in Figure 8.3a) whose variables were suggested by the designers of the industrial collaborators. In order to avoid repetition, the nested chart for the lozenge in Figure 8.3b) is not provided. However, the performance patterns derived by inspecting the chart with the set of four angle variables, i.e. lozenge in Figure 8.3b), are reported.

Version I - two variables discretised. Figure 8.6 shows the nested chart for the structure weight of the frame where two design variables, H_l and H_r, are discretised,

as example, into three values. The variables α and θ are plotted on traditional two-variable performance charts within each box of the matrix. Each sub chart shows contours of equal structure weight with variation of 5 KN from one contour to the other. In the top right-hand corner of each sub-chart a ranking is given from 1st to 9th which ranks the peak performance within each chart. Figure 8.6 also illustrates a path from the worst peak performance to the best peak performance. This chart is more helpful than having separate design charts because an individual chart is clearly put into context. The layout helps because it shows how charts are related to each other in the overall scheme

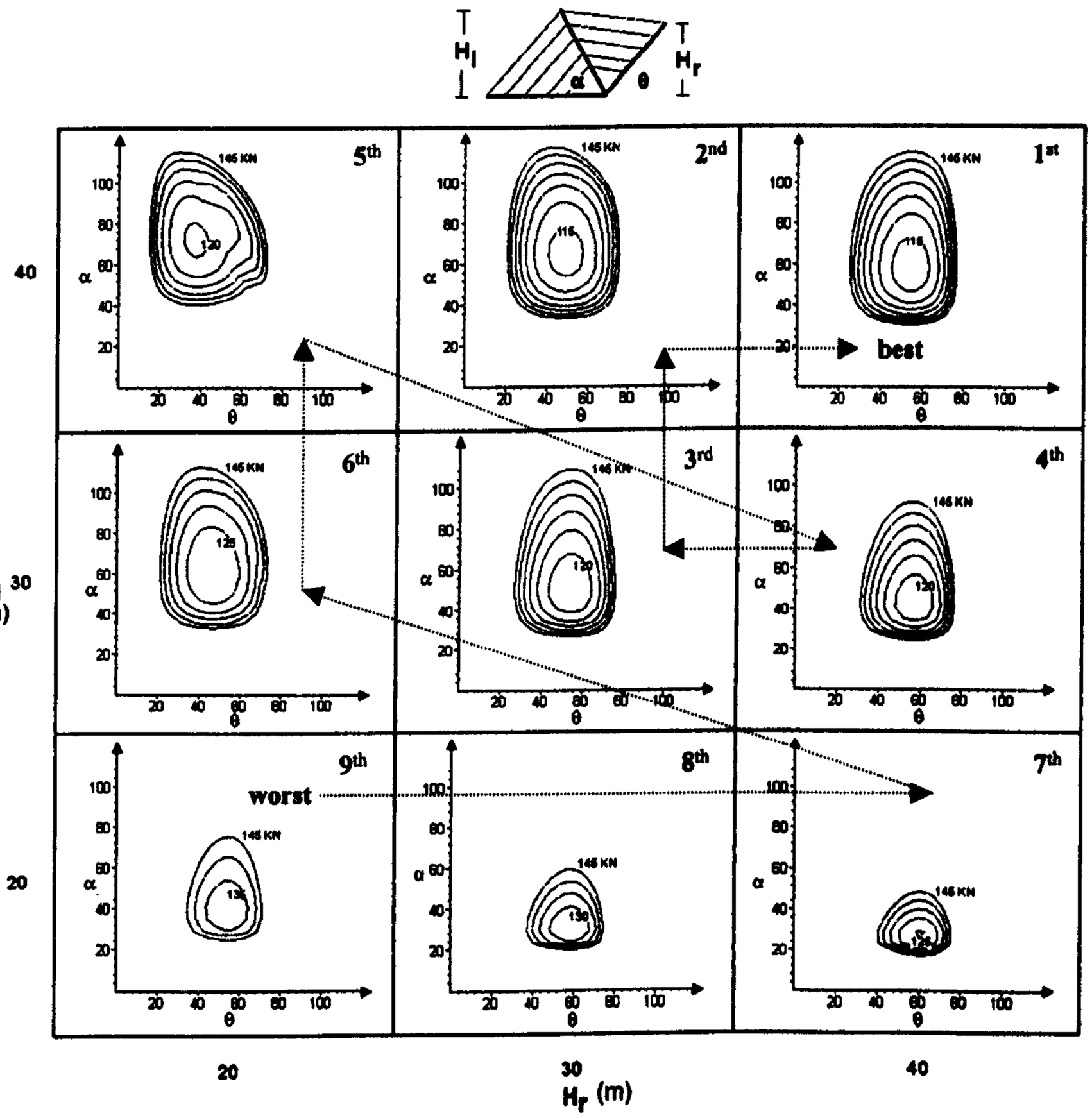

Figure 8.6 Version I of nested performance chart for two discretised heights and two continuos angles variables

By scanning the chart, it is possible to observe performance trends. For example, the following observations can be made for the discretisation mesh from 20m to 40m heights:

i) The best peak performance is achieved when the heights H_l and H_r are maximised.

ii) The bottom row and the left column illustrate that the worst performance are when at least one height is constrained to the lowest value.

iii) There is a great weight penalty when H_l is constrained in height.

iv) Each column shows that increase in H_l produces a larger depth of performance contours along α. Therefore, the performance is more sensitive to variation of α.

v) Each row shows that increases in H_r makes the position of the optimum point move towards decreasing values of α. On the contrary, the position of the optimum point along θ is not particularly sensitive to the increase of H_l in each column.

It is important to note that beginning and end values of the discretised variables and the increment between two consecutive values have to be carefully calibrated in order to have more accurate performance trends. This will be evident with the version II of the nested performance chart.

- **Version II: one variable at optimum value.** Figure 8.7 shows the second version of the nested performance chart where three design variables H_l, H_r and θ are discretised and α is the variable. In order to see the finer detail, the range of the discretised variable has been increased for both the objective functions: reaction and structural weight. 125 boxes are displayed on the chart. In this case, the graph in each cell is a single colour (or shade) which indicates the optimum value of α for that particular combination of discrete variables. This chart can sometimes be more convenient than the previous nested performance charts because there is a direct indication of performance through the colour of the box. The chart gives a straightforward visual representation of performance trends throughout the whole design space. One drawback is that the exact value of the optimum angle α is not shown. As with the previous nested performance charts, the chart of Figure 8.7 can be used to make the following observations for the discretisation mesh indicated:

1. For R, the reaction objective
   - Maximising both the heights minimised the reaction.
   - The best reaction is achieved for low angles θ from 40° to 80°
2. For W, the structure weight objective:

- The best peak performance is achieved when H_l and H_r have similar values close to 40m and for $\theta = 50°$. (This is in contrast with observation i) of version I because here the range of height has been increased)
- H_l has a more significant impact on the performance.

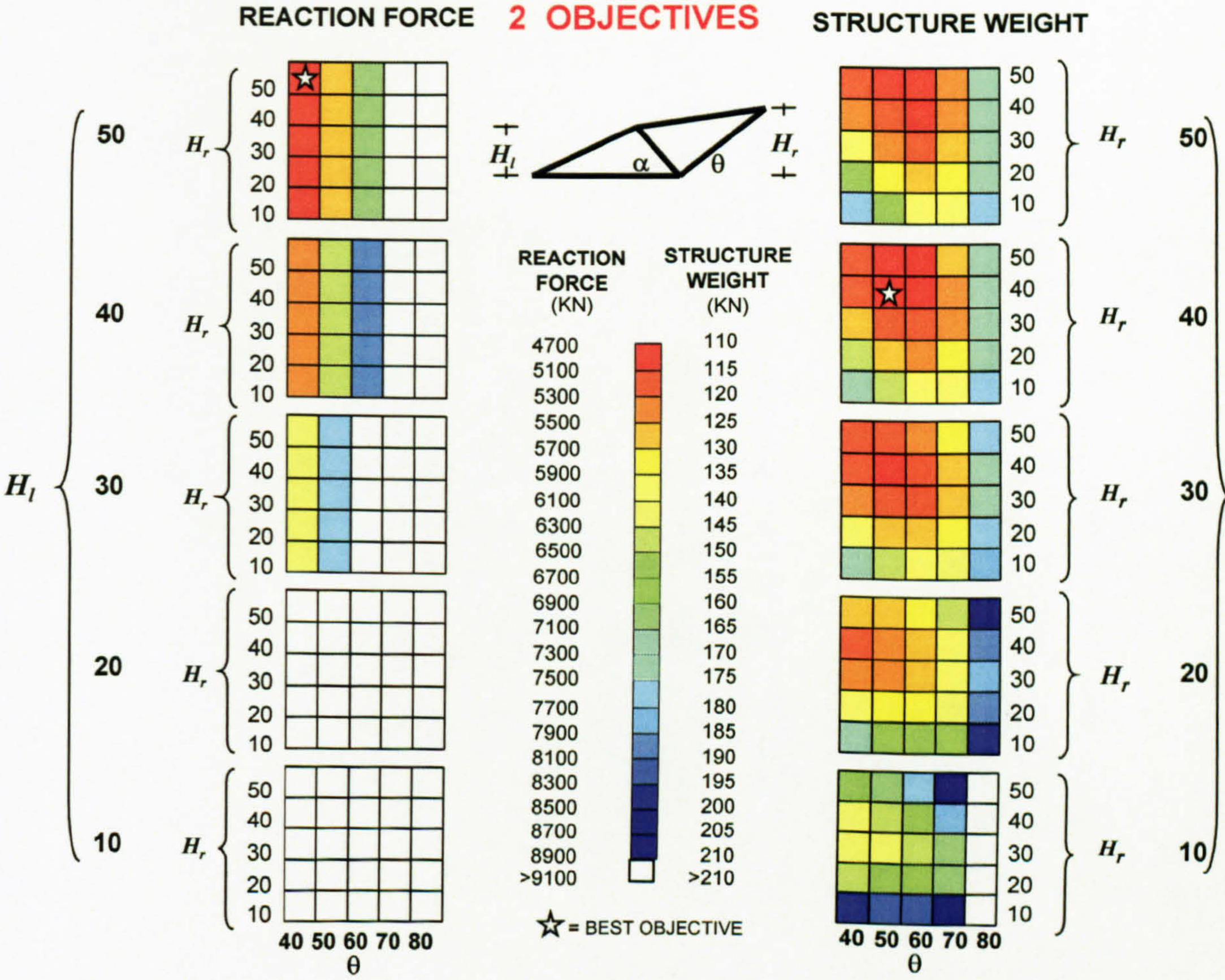

Figure 8.7 Version II of nested performance chart for three variables discretised, H_l, H_r, θ.

Exploring performance patterns.

Figure 8.6 and Figure 8.7 has been presented here to show examples of the nested performance chart. For the industrial case study, the set of four angle variables for the lozenge frame shown in Figure 8.3b) have been used to discover performance patterns. These patterns were not easily discovered with the lozenge with two heights and two angles. The results of the patterns discovered with the four angle variables lozenge frame are summarised here.

1. **Structural weight patterns.** The steps for minimising the structural weight of a lozenge structure are shown in Figure 8.8. For a given set of parameter, the

optimisation ruling law and the best value of the variable are reported at the top of each picture. For example, step (a) in Figure 8.8 shows that for a given length, L, of the boom and angle α, the optimum length of the member, c, lays on a semicircle with radius = L. Analogously in step (b) for a given f and angle Φ, the optimum length of the member c is for c=f. Step (c) is a combination of (a) and (b). As can be seen in step (d), the form of the lozenge frame is optimised if the structural members are progressively rearranged as the web structure shown in Figure 8.4a). This is because the web structure in constrained design is derived by the optimum Michell's layout for unconstrained design.

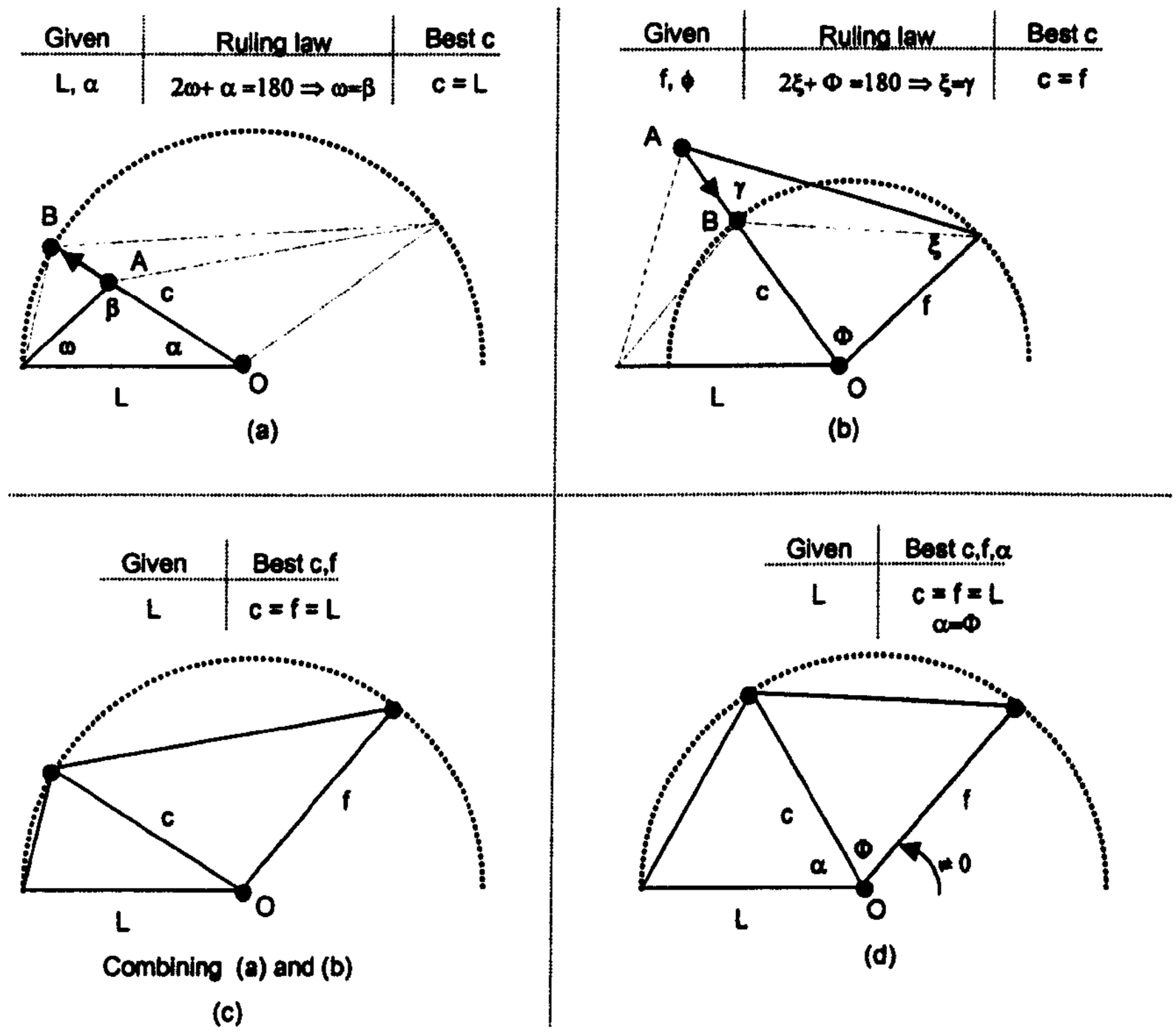

Figure 8.8 Optimisation patterns for minimising the structural weight of a lozenge structure.

2. **Reaction patterns.** Increasing the arm of the moment given by the counterbalance load on the right beam of the lozenge frame minimises the reaction. Therefore, in C.D. higher heights benefit the reaction towards the optimum structures shown in Figure 8.4b) where H_{opt}=104m.

3. **Trade off for R and W.** Figure 8.9a) shows that the two objectives, reaction and weight structures, are optimised for layouts with contrasting forms. Therefore, for an available height inferior to boom length the best trade off structure is when H_l=H_r and point A shown in Figure 8.9b) reaches B. In such a case, the best position of C is when the angles α and ω are equal as in Figure 8.9c).

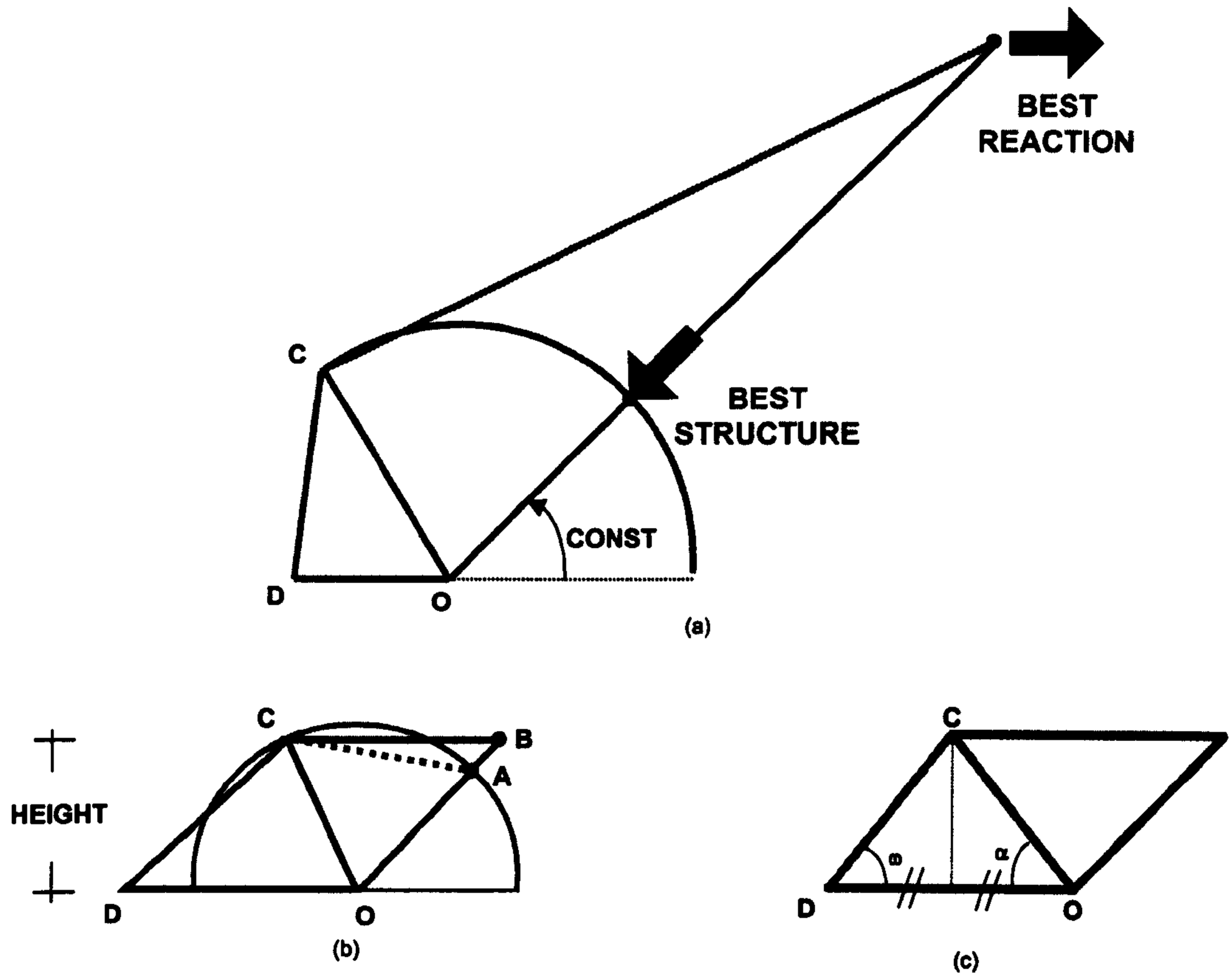

Figure 8.9 Best trade off for multi-objective optimisation.

The use of the nested performance chart in this Section has permitted patterns of performance to be explored for a structural form designed for yield. Although the effect of buckling has not been included, these patterns can be still used as a starting point for the conception of a structural form. Section 8.3.3 shows an application where the theory of the shape transformer is used to include buckling at the early stage of design.

8.3.3 Large scale structures: pin-jointed frame compressive failure design

The selection of large-scale structural forms is common in many areas of design, such as mechanical, civil and aerospace engineering. The most crucial factor in determining the mass-efficiency of a structure is the overall structural form which is usually selected at the early stage of design. Since in the previous applications different structural concepts were modelled for yield design, the analysis was focused only on the structural benefits provided by optimal forms. However,

mechanical instability is one of the main issues of structural design and it can be important in the selection of efficient forms. In order to include the effect of buckling of compressive members, the geometric properties of the cross-section have to be considered. The selection of cross-sectional shape is, therefore, a prerequisite for a proper selection of structural form. This Section uses the shape transformer, i.e. equation (8.12b) to model the efficiency of different structural forms which can fail either by buckling or yielding. The result of this application can be applied to the industrial case, Section 8.3.2, for unconstrained yield design.

The case study is a double horizontal cantilever subjected to uniform load and a central pillar. Three different structural topologies are shown in Figure 8.2. Frameworks subjected to this type of load condition are used in material handling equipment, as illustrated for unconstrained design in Section 8.3.2, and bridges. The performances, expressed in term of structural weight, $W=mg$ with gravity, g, are considered for two conditions. Firstly, when buckling does not govern the design of compressive members, i.e. yield design. Secondly, when there is an interaction between selection of structural form and selection of cross-sections of compressive elements, i.e. compressive failure design.

Benchmark.

The Michell structure shown in Figure 8.11c) is chosen as benchmark, although buckling is not taken into account.

Candidate structures

The same candidate structures for the unconstrained design of the industrial application, Figure 8.2, are considered.

Functions of weight

The structural weight function for yield design is given by equation (8.10b). While the function of mass for compressive failure design is given by equation (8.12b) where the shape transformers, the envelope efficiency parameter, and a scaling factor are integrated to model the structural efficiency of each compressive member. Their dimensionless values are selected from the allowable ranges given in Tables 3.3 and 3.4 to describe the geometrical properties of the cross-sections.

Data

The same data used for unconstrained design in Section 8.3.2 are purposely adopted for this application: n = 10 for each horizontal beam, L=50m, load p = 50 KN/m, steel ρ= 7900 kg/m^3, σ_y= 300 MPa, E=210*10^3 MPa.

Optimum values.

Yield design. The minimum weights and the optimum values of β are:

	W_{min} (KN)	$\beta(W_{min})$	
Derived Michell	101	-	
Web	112	-	
Convergent	160	58°	which corresponds to H=81 m in Section 8.3.2
Parallel	142	45°	which corresponds to H=50m in Section 8.3.2

Compressive failure design.

The shape contribution given in Tables 3.3 and 3.4 and the envelope contribution are used to specify the geometric properties of the compressive member of three cross-sections. These values inserted in equation (8.12b) for the three frameworks shown in Figure 8.2, give the following results:

- For **solid circular cross-sections** where the shape contribution is given by ψ_A=**π/4** and $\lambda = 3/4$, the envelope contribution is v = **1**, the minimum weights and the optimum values of β are:

	W_{min}(KN)	$\beta(W_{min})$
Web	886	-
Convergent	1876	62°
Parallel	298	55°

- For **hollow circular cross-sections**, the envelope contribution is v = **1** and the shape contribution is chosen to be ψ_A=**0.25** and $\lambda = 2$. The minimum weights and the optimum values of β are:

	W_{min}(KN)	$\beta(W_{min})$
Web	470	-
Convergent	882	58°
Parallel	184	51°

- For **hollow rectangular cross-sections** where the shape contribution is selected to be ψ_A **= 0.25** and λ =2, the envelope contribution to be ***v* = 0.55,** minimum weights and the optimum values of β are given by:

	W_{min}(KN)	$\beta(W_{min})$
Web	640	-
Convergent	1300	61°
Parallel	232	53°

These results show that for the case of unconstrained design in Section 8.3.2, a proper selection of the cross-sectional shapes and envelope contribution fulfil the benefit of an efficient structural form when buckling is included.

Design charts and Insights

The three structures, web, parallel and convergent are plotted for the case of yield design in Figure 8.1 and the three cases of compressive failure design in Figures 8.21, 8.22 and Figure 8.4 respectively. The data are the same as for unconstrained design in the application presented in Section 8.3.2.

Figure 8.20 illustrates that for yield design the structure weight does not depend on the cross-section and designer can select directly an optimum structural form. The charts shown in Figure 8.2, Figure 8.3 and Figure 8.4 illustrate that all the structures require more material, i.e. higher mass, to prevent buckling (i.e. compare results with Figure 8.1). Nevertheless, by changing the cross-section reductions in weight can be achieved. For example, hollow sections perform better than solid cross-sections. Therefore, the selection of the best structural form depends on the cross-sections of the compressive members.

The number of compressive members is such that the web is not the most efficient as in Figure 8.1. However, the convergent frame performs worse because the central pillar has to support a constant compressive force along its whole length. This feature does not occur in the parallel frame which provides the minimum weight and shows a performance trend less sensitive to variation in β.

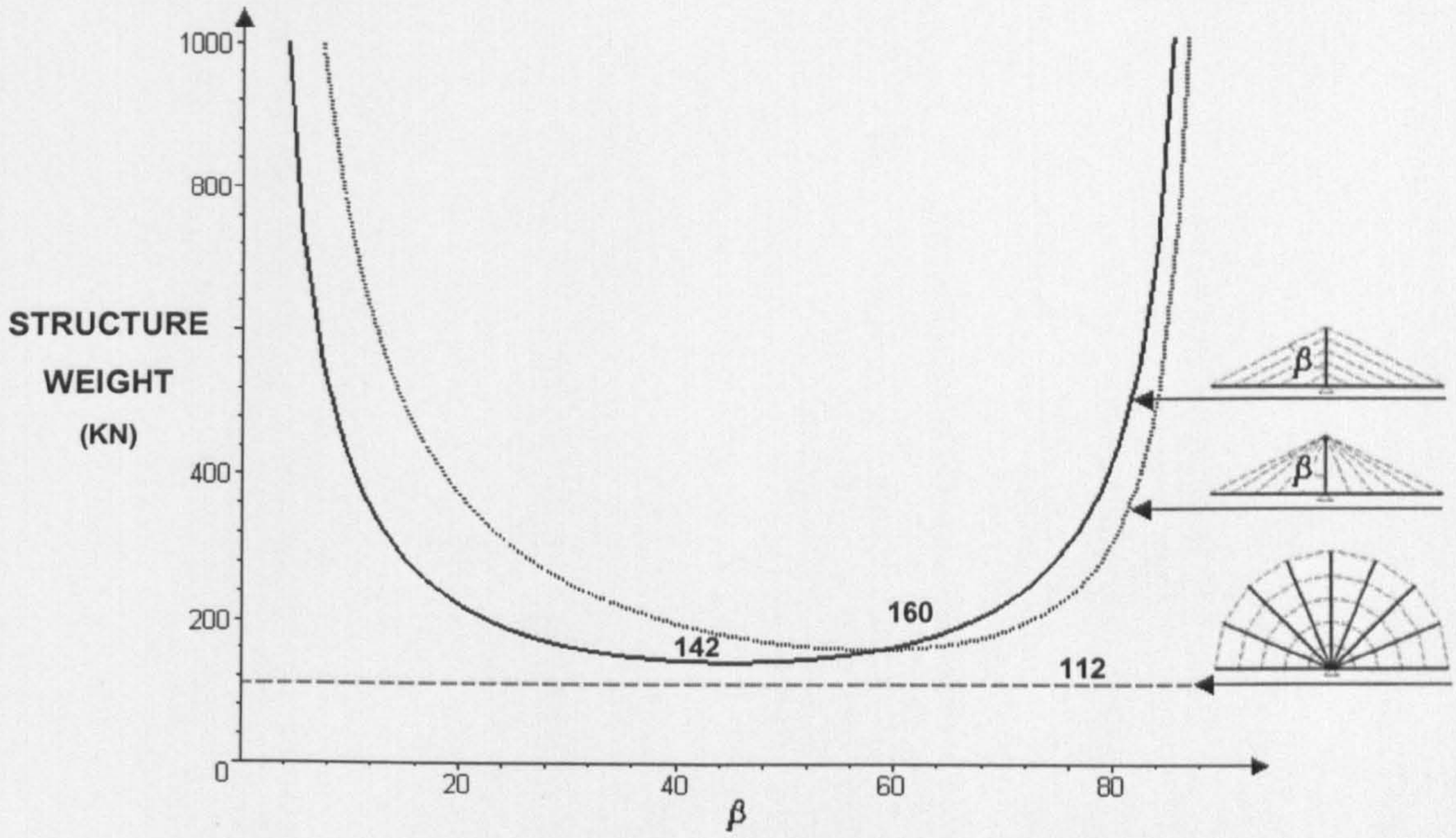

Figure 8.1 No interaction between the structural form and the cross-sections of its members

SHAPE: $\psi_A = \pi/4$ $\lambda = 3/4$

ENVELOPE: v=1

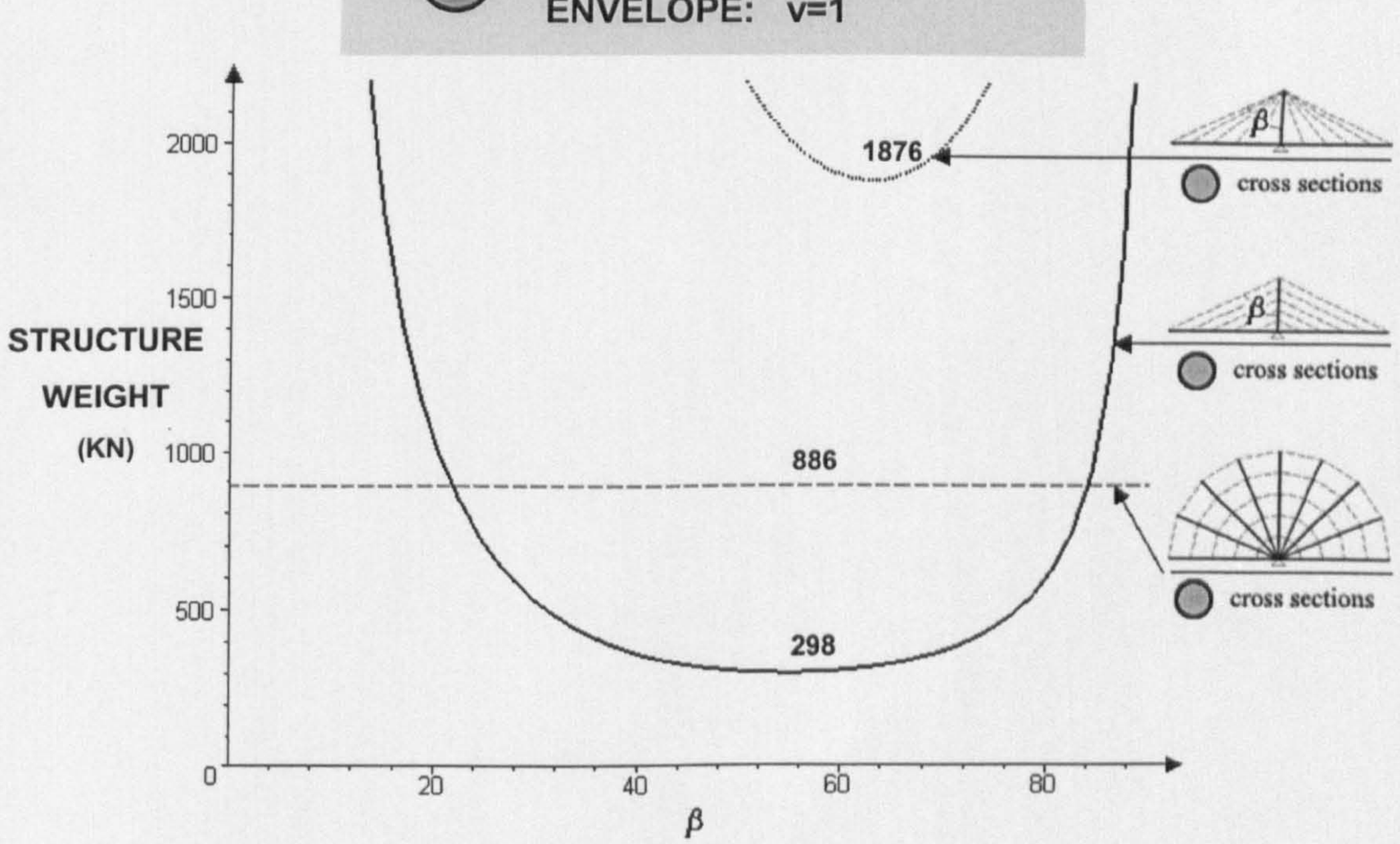

Figure 8.2 The structural form interacts with the solid circular cross sections of its compressive members.

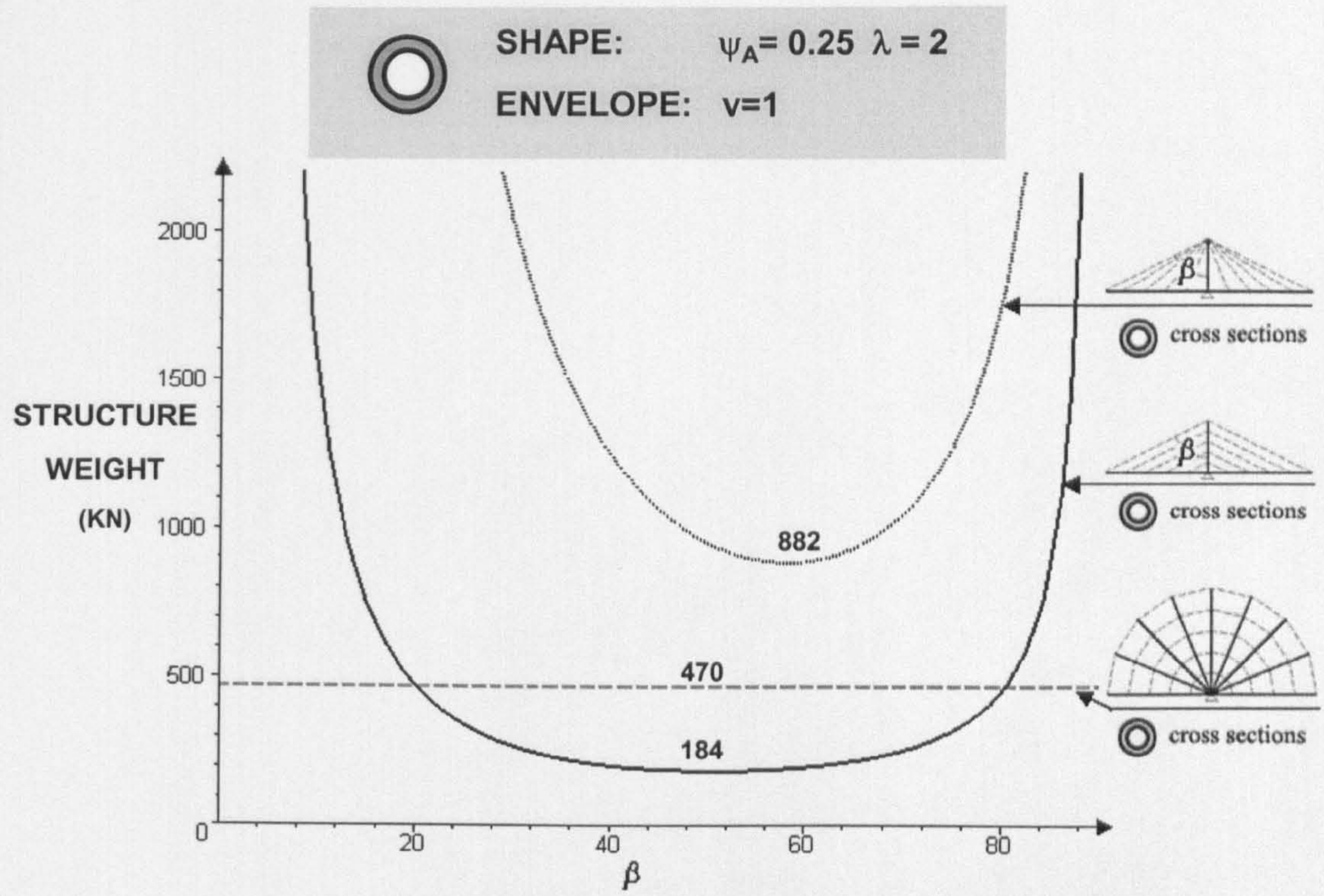

Figure 8.3 The structural form interacts with the hollow circular cross sections of its compressive members

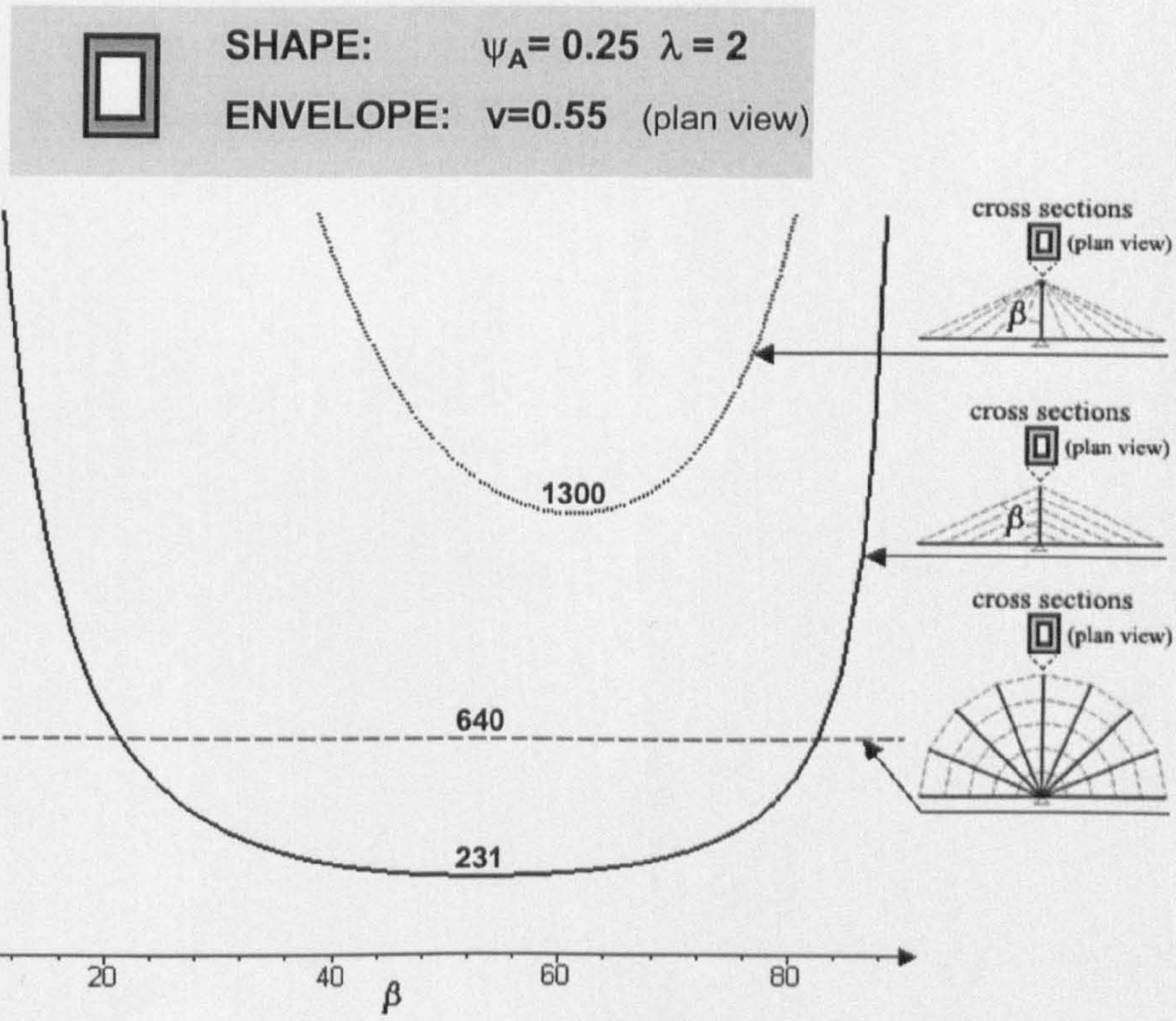

Figure 8.4 The structural form interacts with the hollow rectangular cross sections of its compressive members

8.4 SUMMARY

The mass of different structural forms has been modelled in this Chapter. The mass for tapered structural elements and pin-jointed frames have been given for yield design. Unlike to previous methods of form selection for the early stage, the theory of shape transformers has included buckling. The geometric properties of arbitrary scaled cross-sections have been included in parametric equations of performance. This permits the production of design charts which show the interaction of form selection with cross-sectional shape selection in order to provide insight and understanding to the designer. For systems with more than two variables the nested performance chart has been introduced to give a visual representation of performance trends throughout the whole design space. Design applications have been carried out. These applications have applied the functions of mass for yield and compressive failure design for different structural topologies. In addition the applications show the benefits of the nested performance chart for optimising the form of a structure with multiple objectives.

CHAPTER 9

MODELLING THE EFFICIENCY OF NATURAL STRUCTURES USING SHAPE TRANSFORMERS: CASE STUDY OF A TREE BRANCH

9.1 INTRODUCTION

So far the theory of the shape transformers has been applied to man made engineering systems. This Chapter considers a natural system: a tree branch. In this Chapter the theory of the shape transformers is applied to the mass-efficiency of a large branch which has grown adaptively into an optimal cross-sectional shape.

There are two parts to this Chapter:

- First, the methodology of analysing the tree as a structural system is illustrated. The main loading conditions experienced by a tree during its life and the mechanism of growth are elucidated. (A review of the optimal structural features which a tree develops adaptively is reported in the Appendix E together with a survey of the similarities between trees and engineering structures).
- In the second part, the shape transformers are applied to a case study. The mass-efficiency of a modified horizontal branch of a tree is modelled. There are two aims of this Section. The first is to compare the efficiencies of the modified branch-section and a common circular branch in terms of mass and occupied space. The second is to estimate the differences in efficiency given by the combination of geometric and material properties of the branch and of a circular steel cross-section.

9.2 METHODOLOGY

The main function of a tree is to develop a canopy of leaves to capture sunlight. In order to support the foliage layer, the tree builds a structure using the least amount of bio-material. The competition with other plants is one factor that encourages the tree to grow toward the source of natural light. However, the tree builds a structure also downwards, underneath the soil, to perform a variety of vital functions, such as uptake of water and the provision of a structural foundation.

The tree can be considered as a system made up of constituent parts, i.e. structural subsystems, as shown in Figure 9.1. For example, the foundation structure is the structural subsystem which anchors the tree to the soil. Another structural sub-system is the primary structure which grows vertically in elevation to support the branching system, i.e. secondary structure. The branches grow laterally and upwardly from the main support to carry the widest surface of leaves, the foliage canopy. The interfaces between the foundation, primary and secondary structures, constitute the structural joints, which connect all the different load-carrying elements. Finally wood is the constituent micro-structured material.

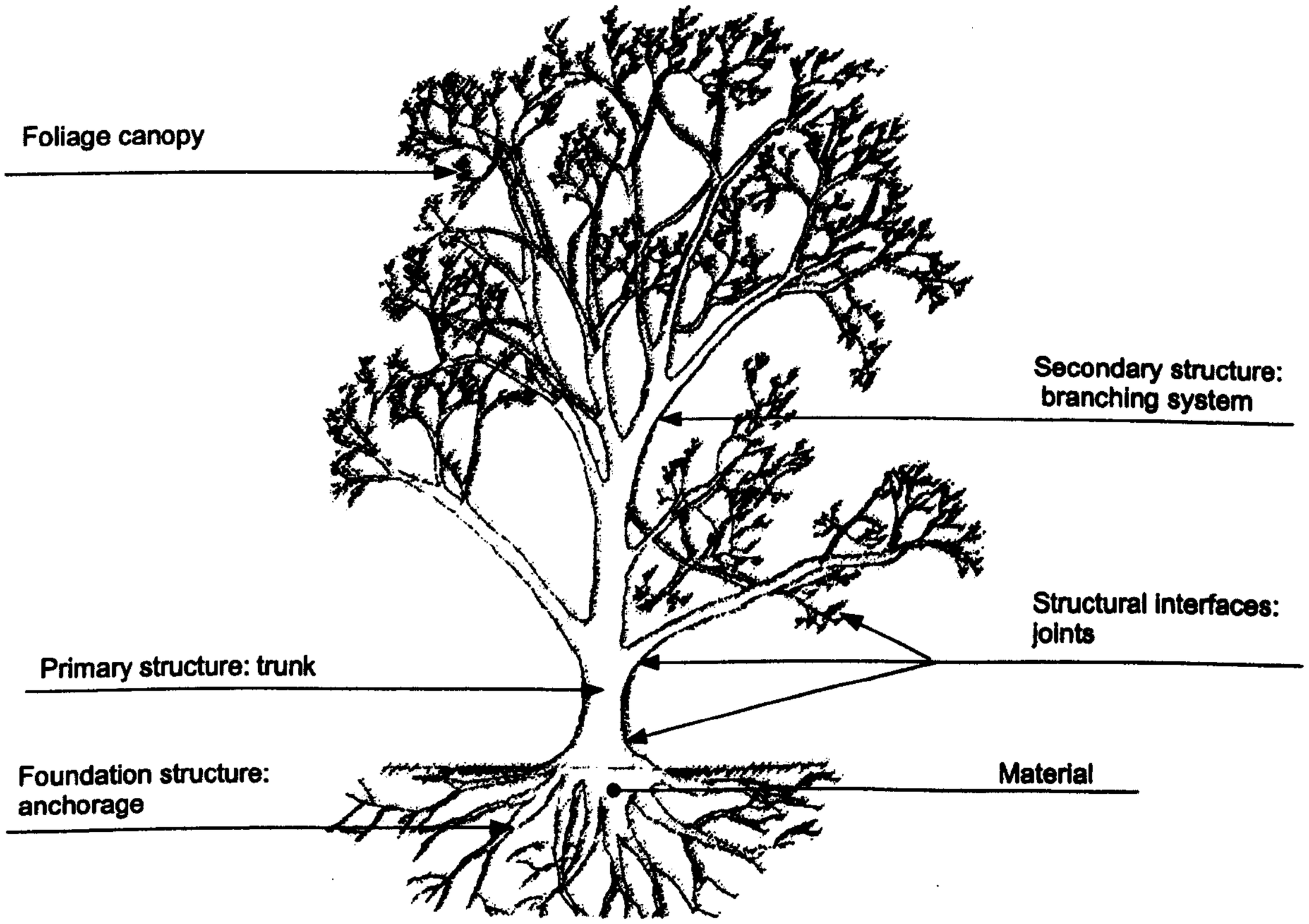

Figure 9.1 The constituent elements of a tree.

9.3 LOADING CONDITIONS

Of the external loads experienced by the tree during its life, the wind is one of the most significant. Under the action of the aerodynamic force of the **wind** on the leaf canopy, the main trunk and each structural element act as a cantilever. The wind loading is approximately given by (Bedford, A. and Fowler, W., 2002):

$$F_w = 0.5\,\rho\,C_d\,A_f\,v_w^2 \qquad (9.1)$$

where ρ = air density (kg/m^3), C_d =drag coefficient, A_f = frontal area (m^2), v_w = wind velocity (m/sec^2).

Since the wind velocity increases from the ground upward, the tree experiences an increased loading as the tree increases size. The aerodynamic forces usually come from all directions and produce bending moments which have the highest values at the junctions between the different structural elements. The largest bending moment experienced by the tree occurs at the foundation-trunk joint.

The **self-weight** of the tree is another important source of loading. Self-weight exerts compressive forces in the trunk if the trunk is vertical. However, self-weight produces bending moments in any section of the trunk or branches which are not vertical. As a free-standing cantilever fixed at the base, the tree can buckle under its own weight. The critical Euler load is given by equation (3.16).

9.4 ADAPTIVE GROWTH

Most of the efficient features employed by the tree occur by adaptive growth (Horn, H,S, 1973, Mattheck C., 1989,1991). This is because the tree develops a structure in response to mechanical loading. Therefore, the structure of a tree is generally sufficiently strong to withstand the forces encountered during its history.

Trees undergo structural adaptation by *reinforcing* regions exposed to higher stresses, especially compressive static stresses. Since wood is placed faster in areas where higher stresses occur, the structural benefit is that the stress concentration is reduced and the use of living material is optimised during the growth.

The natural adaptive response has the effect of producing optimal developmental and morphological changes in the overall form. Optimisation of form occurs in the longitudinal and transversal shape of each constituent element and in their junctions. A detailed survey of these optimal structural features and their application in engineering is reported in the Appendix E. In the next Section the mass-efficiency of a modified horizontal branch developed adaptively is examined. The general solution of the performance index for arbitrarily scaled cross-section in strength design is applied.

9.5 CASE STUDY ON ADAPTIVE GROWTH

Figure 9.1 shows an example of a branch with a horizontal connection with the trunk on a pine tree. This branch is actually a secondary trunk. The tree is located at Cotham Park in the city of Bristol, UK. The advantage of the secondary trunk is that it greatly increases the size of the leaf canopy of the tree. The secondary trunk requires a very strong joint with the main trunk. This has been achieved by the adaptive growth of the branch into a highly modified and efficient cross-section. The joint has been transformed from a circular section into a roughly rectangular section with a width to depth ratio of 3:1, as shown in Figure 9.2. This transformation has increased the bending strength by a factor of approximately nine times. Without the adaptive growth the tree could not support such a secondary trunk.

In Chapters 4 and 5 the performance index has been applied to arbitrarily scaled cross-sections in stiffness design. This application illustrates an example of the performance index in strength design. The shape transformers for the modified cross-sectional shape shown in Figure 9.2 are used to analyse the mass-efficiency and to produce the shape regimes graphs for the failure moment requirement of the branch. Two cases are considered:

1. The first considers cross-sections with the same material properties, i.e. wood. The modified branch-section and a common circular branch are compared, in terms of mass and also space efficiency, for different scaling of the envelopes.
2. The second compares cross-sections with different material and shape properties for different envelope scaling. The mass-efficiency of the natural system is referenced to a man-made cantilever with a circular steel cross-section

(a)

(b)

(c)

(d)

Figure 9.1 a) The tree in Cotham Park (Bristol). b) & c)The branch of the tree d) A bottom-up view of the branch.

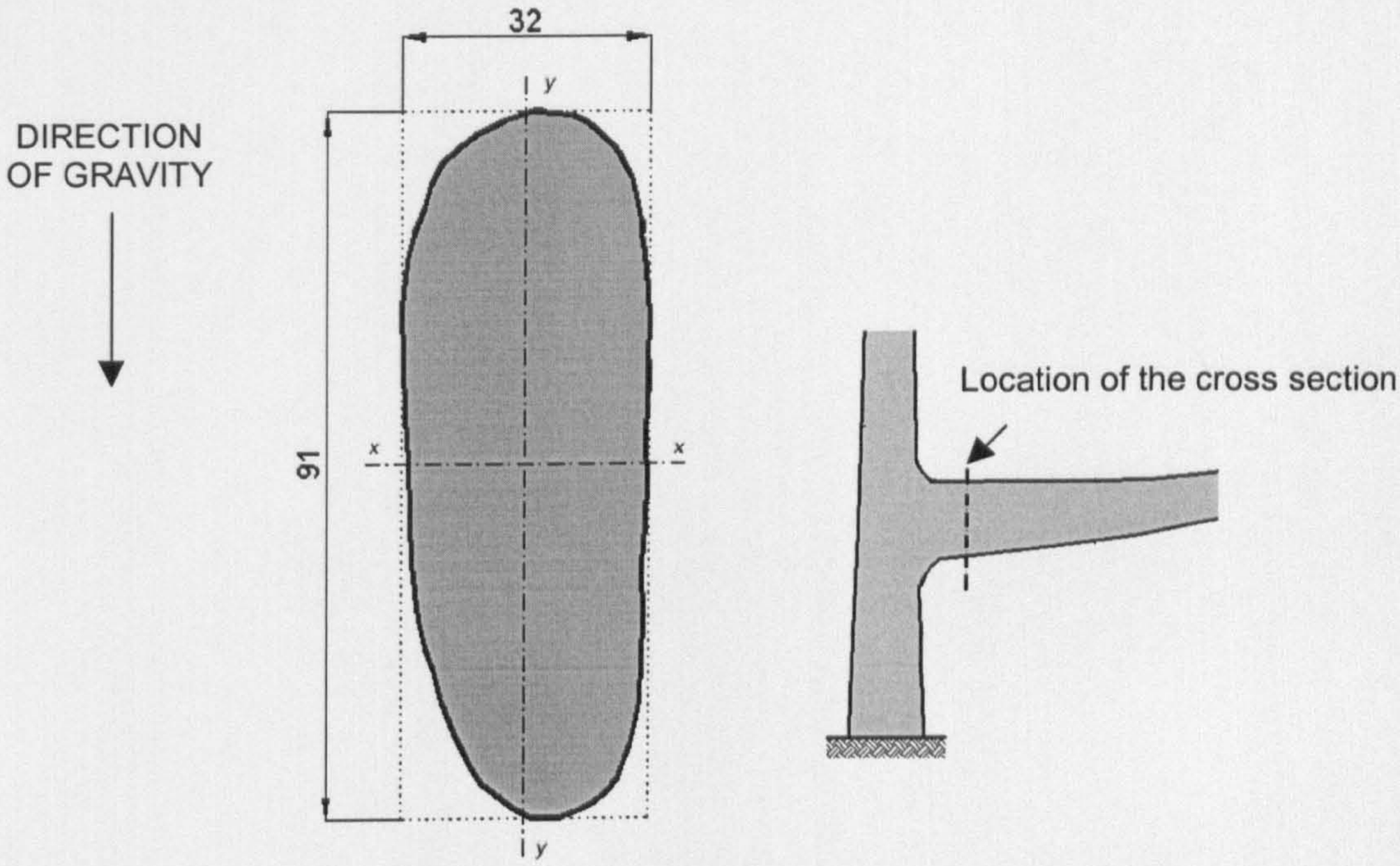

Figure 9.2 Actual branch cross-sectional-shape at the joint with the main trunk (measurements in cm).

9.5.1 Analysis of the branch cross-section

The branch shown in Figure 9.1a) can be modelled schematically as a cantilever, which is built-in at the main trunk. The cross-section at the beginning of the branch, shown in Figure 9.2, supports the bending moment, which in this case is mainly due to self-weight of the branch.

The dimensions and the shape of the cross-section of the tree have been carefully measured. A detailed survey has permitted a series of separate drawings to be produced and then assembled together. The overall drawing of the cross-section has been scanned and a computer software (i.e. Autocad) has been used to calculate the geometric quantities of the cross-section shown in Figure 9.2. The material properties and the geometric quantities are given in Tables 9.1 and 9.2 respectively.

Material	σ_y (MPa)	ρ (Mg/m^3)
Wood	100	0.59
Steel	400	7.9

Table 9.1 Materials properties.

Shape envelope width	B	0.32	m
Shape envelope depth	H	0.91	m
Perimeter	$2p$	2.12	m
Area	A	24.43	m^2
Section Modulus along xx	Z	0.0306	m^4
Shape transformer of Area	ψ_A	0.84	
Shape transformer of Section Modulus	ψ_Z	0.693	

Table 9.2 Geometric quantities of the branch section shown in Figure 9.2

Performance index

For a given failure moment, the performance index p for the arbitrary scaled cross-sections shown in Figure 9.1, is given by equation (6.12), which is:

$$p = \frac{(\sigma_y \psi_Z)^q}{\rho \psi_A} \tag{9.2}$$

with the scaling parameter $q = \ln uv / \ln uv^2$, u and v are the envelope multiplicators.

Equation (9.2) is used to analyse the mass-efficiency of the cross-sections in Figure 9.1 for the moment requirement $M_y = \sigma_y Z = 3.06 * 10^6$ N.m of the branch cross-section shown in Figure 9.2. The branch cross-section and the circular cross-section are considered for different relatively scaling of their envelopes. The branch cross-section is chosen as a reference. The shape properties of the cross-sections are given in Tables 3.3 and 9.2.

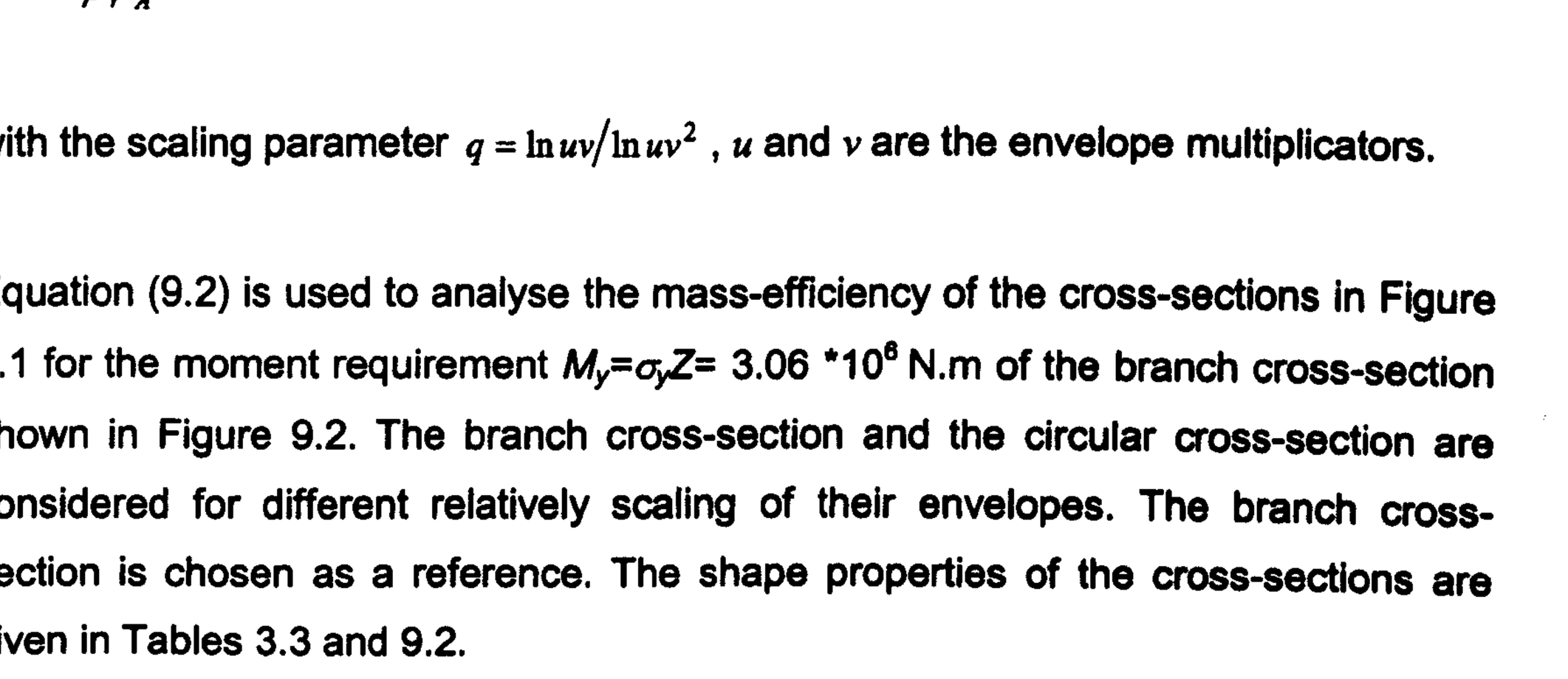

Figure 9.1 Arbitrary scaling of two cross-sections.

9.5.2 Actual branch compared to a wood circular section

The branch cross-section shown in Figure 9.2 is compared to a wood circular solid section, which belong to the shape class of the ellipse. Since the performance index is used to analyse the mass-efficiency, both the cross-sections in Figure 9.1 can be arbitrarily scaled in any direction according to the failure moment requirement.

Equation (9.2) is plotted as a function of the scaling parameter, q, in Figure 9.1. As explained in Chapters 4 and 5, the intersection point of the performance curves of two cross-sections, i.e. the actual branch and the ellipse, represents a special value of the scaling parameter q where both the cross-sections perform equally. When q is greater than 0.42 the scaling between the branch section and the ellipse is such that the actual branch has a better performance index than the ellipse. Alternatively for q<0.42 ellipses are lighter. The value of q for the scaling between the circular and the branch cross-sections shown in Figure 9.1 is q=2.81, as illustrated in Table 9.3.

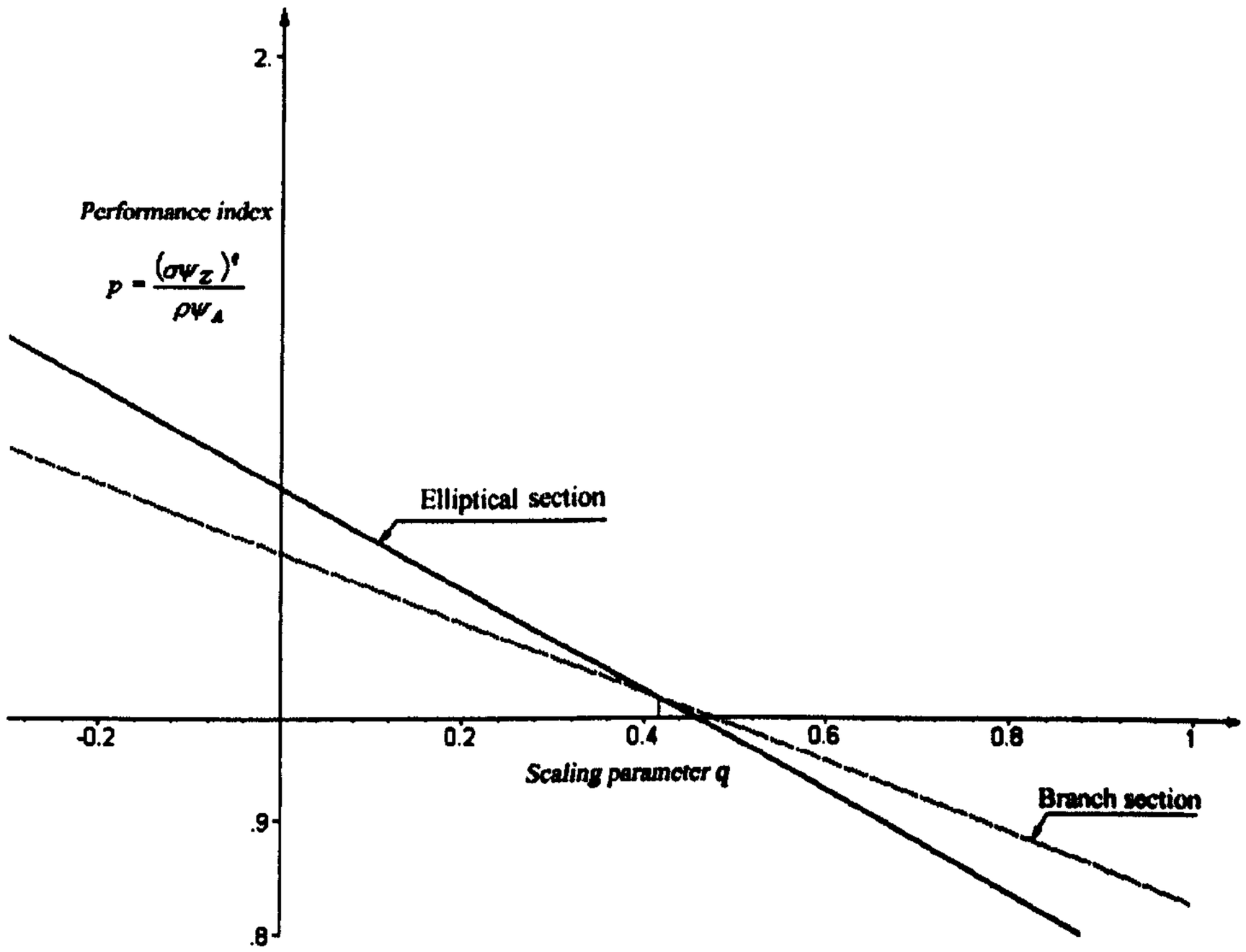

Figure 9.1 Performance of elliptical cross-sections and branch section for a range of q.

In Figure 9.2 the failure moment requirement is plotted for the branch section and ellipse together with the boundary curve of q=0.42. Since the real branch section is chosen as the reference section, points of q unbounded define its failure moment requirement. In a similar way to Chapters 4 and 5, the outcome from Figure 9.1 is used to map the limiting shape regime in Figure 9.2. The special q curve and q

unbounded set the boundaries of the grey region, called the branch section region, where ellipses are less efficient. Consequently among the ellipse shape class, a circular (sub class) section is heavier than the real branch.

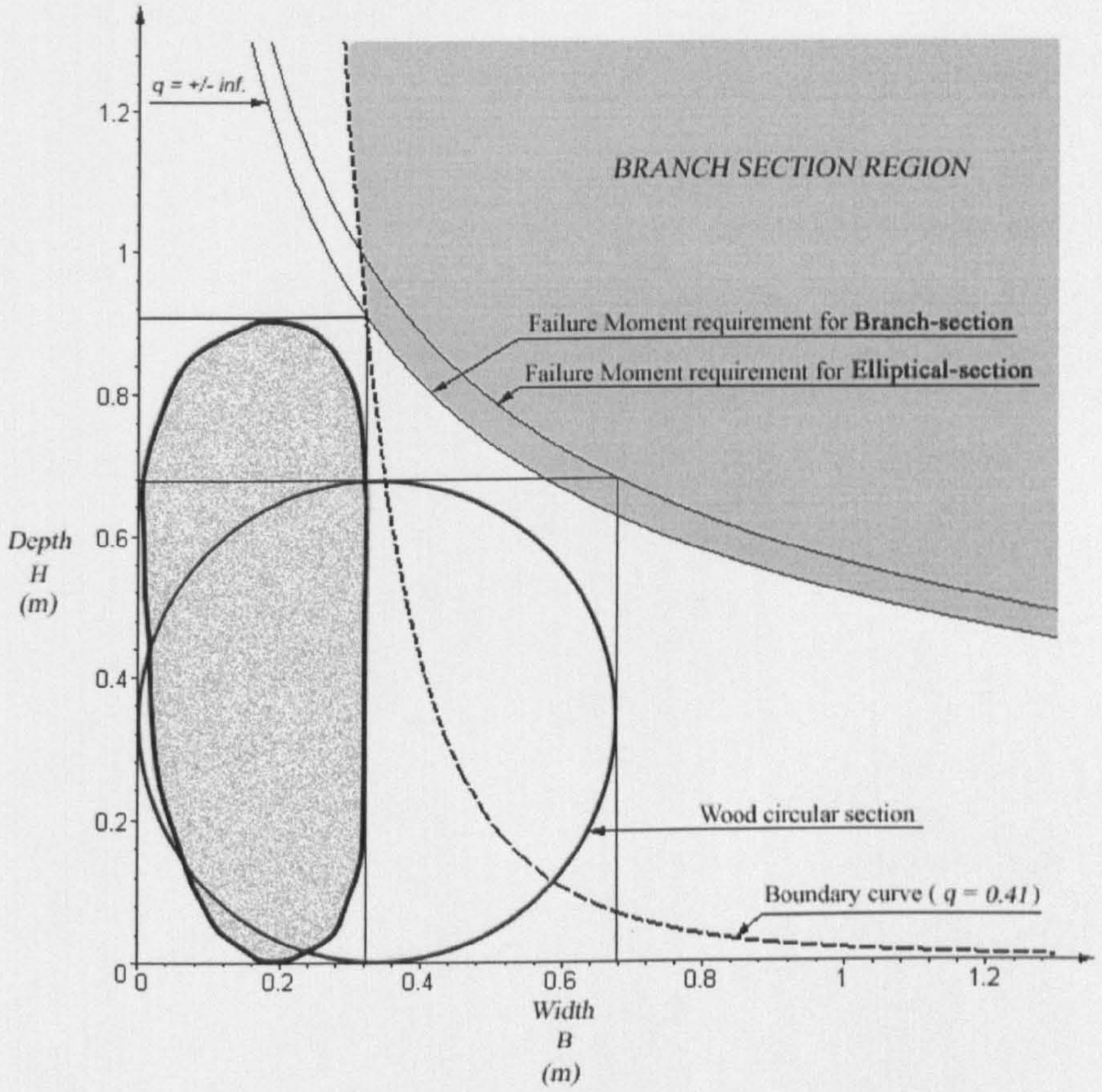

Figure 9.2 Limiting shape regimes

The performance indices, as shown in Table 9.1, allow the mass saving to be quantified as a percentage (32%) of the real branch compared to a common round section. In addition, the analysis gives information about the space efficiency. The diameter required by a circular branch (68 cm) exceeds the dimensions of the main trunk (65 cm) of the tree shown in Figure 9.1. Therefore, a circular branch would be unable to fit in the main trunk.

MATERIAL	SHAPE	Width B	Height H	Failure moment $M_y=\sigma_y Z$	Width multiplicator u	Height multiplicator v	Power of p q	Performance index $p=\frac{(\sigma_y \psi_Z)^q}{\rho \psi_A}$	Mass saving
		m	m	N.m *10^6					
Wood	circle	0.68	0.68	3.06	0.472	1.342	2.81	203511.5	
Wood	branch	0.32	0.91	3.06	0.472	1.342	2.81	300401.2	32%

Table 9.1 Comparison between the branch section and a wood circular section.

9.5.3 Actual branch compared to a steel circular section

The branch cross-section shown in Figure 9.2 is now compared to a cross-section with different material and shape properties, i.e. a steel circular cross-section, for different scaling of the envelopes. Comparing natural and man-made systems helps to understand the performance improvement added by the wood properties. The macro-shape and the microstructure of wood accomplish an excellent cocktail of efficiency.

Figure 9.1 shows the performance index curve of the real branch and arbitrarily scaled steel elliptical sections. For the special value q= -6.99 the two structures perform equally well. In Figure 9.2 the q unbounded and the q special value border the limiting shape and material regimes for the two structures. In the grey branch section region, defined for q>-6.99, steel elliptical structures are heavier. Lighter steel structures can be found for very large widths, not shown in Figure 9.2. The value of q for the scaling of the circular steel cross-section and the branch section is 0.38, as shown in Table 9.4.

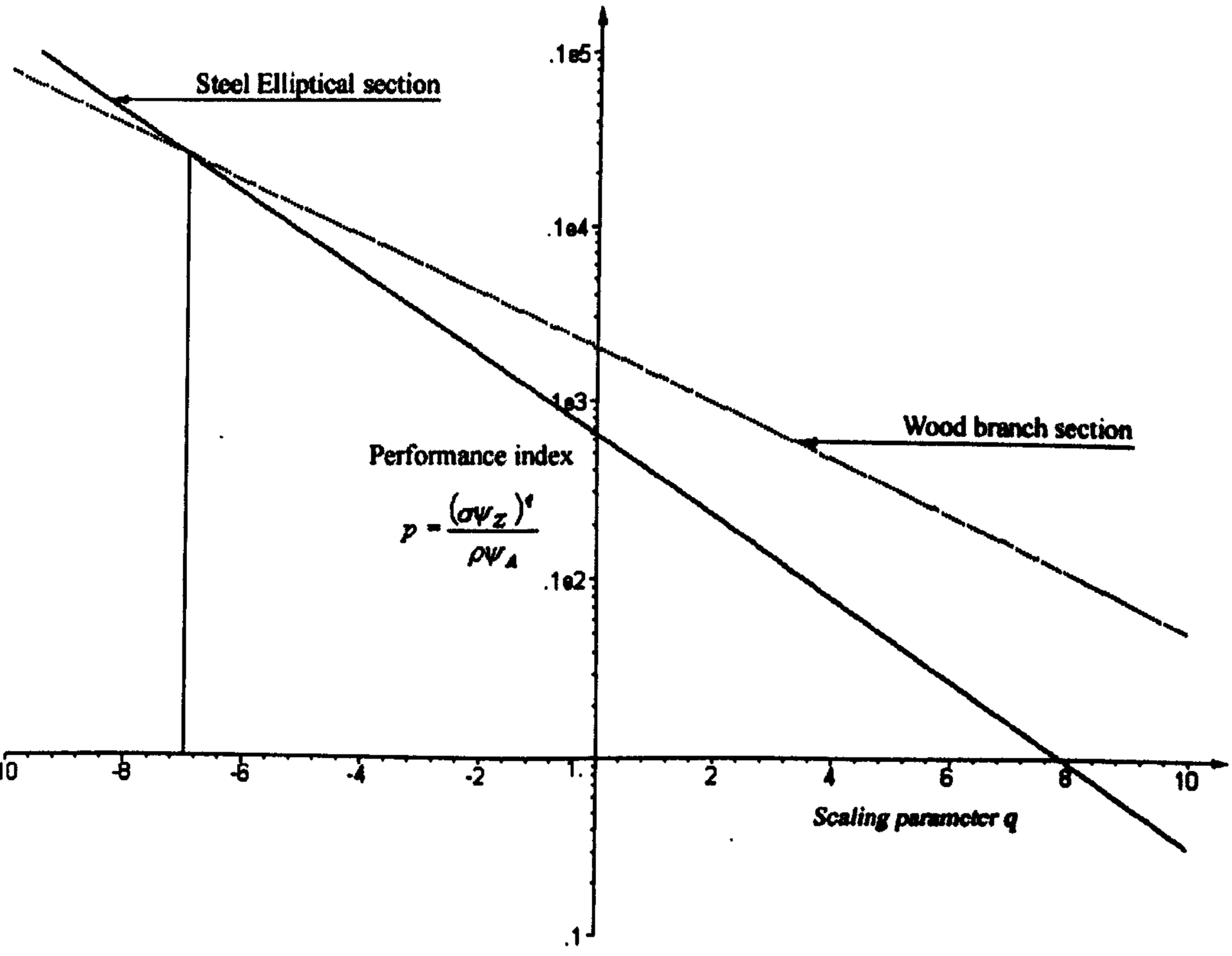

Figure 9.1 Performance of steel elliptical shape and branch section for a range of q

Among the elliptical steel cross-sections, the rounded shaft of 43cm diameter enables material to be compacted in less space but it demands 87% more mass than the real branch (see Table 9.1). Therefore, not only the steel circular section, but the whole range of man made structures, represented in Figure 9.2, have a worse performance. It is evident that the natural system joins together geometric and material properties in a profitable way.

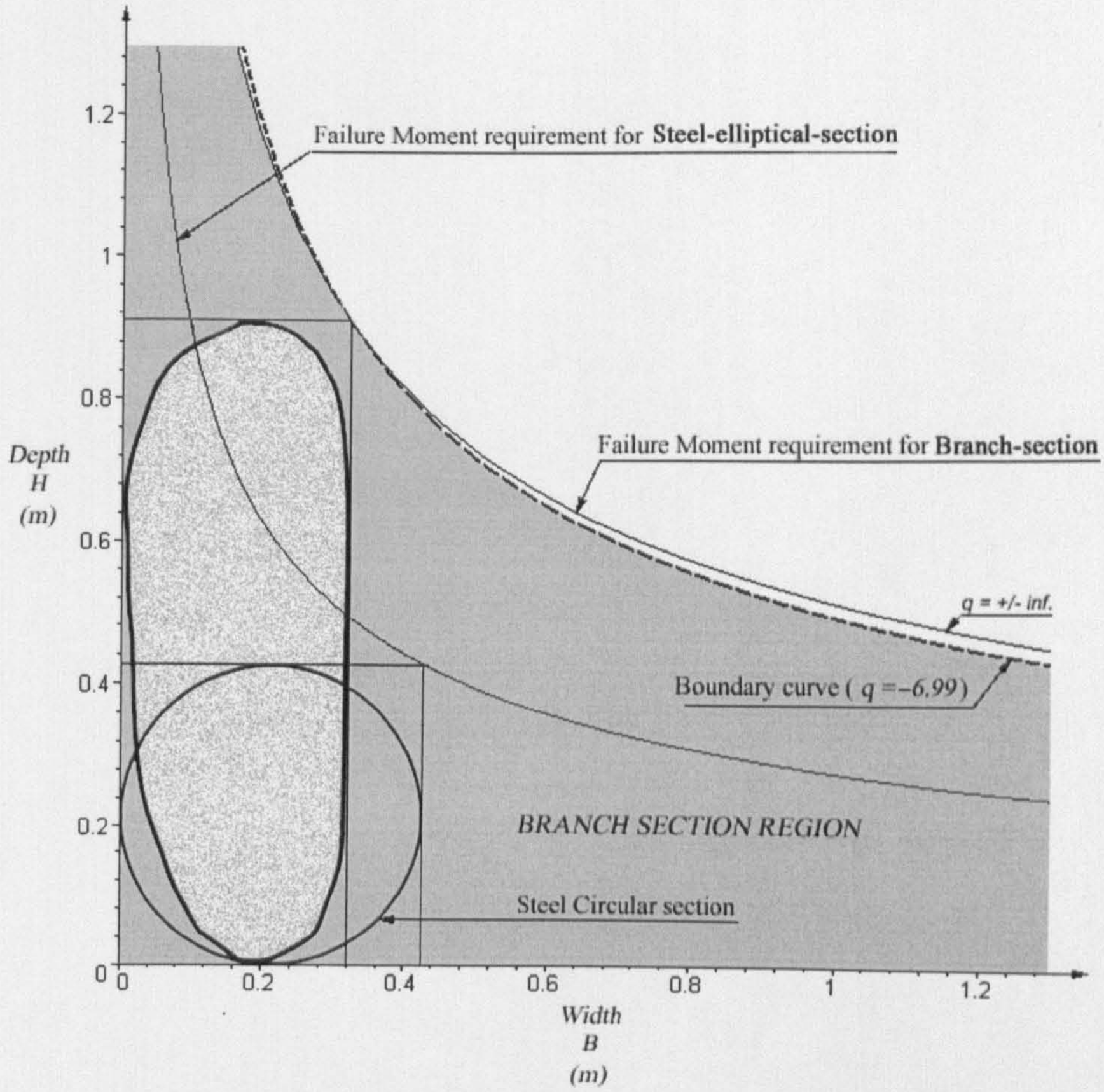

Figure 9.2 Limiting shape and material regimes

MATERIAL	SHAPE	Width	Height	Failure moment	Width multiplicator	Height multiplicator	Power of performance index	Performance index $p=\frac{(\sigma_y \psi_Z)^q}{\rho \psi_A}$	Mass saving
		B	*H*	$M_y=\sigma_y Z$	*u*	*v*	*q*		
		m	*m*	*N.m *10^6*					
Steel	circle	0.43	0.43	3.06	0.75	2.13	0.38	1.30	
Wood (pine)	branch	0.32	0.91	3.06	0.75	2.13	0.38	10.19	87%

Table 9.1 Comparison between the branch section and a steel shaft.

9.6 SUMMARY

In this Chapter the shape transformers and the performance index have been used to investigate the structural efficiency of a horizontal branch. The cross-sectional shape of the tree has been developed efficiently by adaptive growth in response to the mechanical loading. Performance maps enables comparison between a wood branch and a set of man-made cantilever for a given moment requirement. This has shown that trees achieve high structural efficiency from both material, i.e. microstructure, and shape perspectives.

CHAPTER 10

CONCLUDING REMARKS AND FUTURE WORK

10.1 INTRODUCTION

Design involves making choices among a range of alternative solutions. Experience, creativity and also intuition can be used to select the best solutions. However, when a systematic procedure of selection is established, this can make selection more efficient and reliable and can provide insight to designers. In structural design, selection must be made amongst a very broad number of materials, cross-sections and structural forms. Systematic procedures of selection can help designers in the selection of the best combination of these variables.

This thesis has presented a new theory for modelling the mass-efficiency of structures. The theory has been used to produce a method for the selection of material, shape and structural forms for conceptual design. It can be of particular interest in different fields of engineering to a variety of parties such as designers, educators, students and manufacturers.

This Chapter presents two sections.

- The first discusses the main contributions of the research in terms of analysis and visualisation of the performance information.
- The second proposes directions for further development of the research.

10.2 RESEARCH CONTRIBUTIONS

The central part of the thesis involves the definition of the shape transformer. The **shape transformers**, S, are **dimensionless** attributes which relate the geometric quantities, G, of a cross-section to the geometric properties of the rectangular envelope, G_D, specified by the main sizes of the cross-section, i.e. $S=G/G_D$. The shape transformers give the **shape properties** to a rectangular envelope. Shape transformers have been used to define **classes of shapes** in a similar way to which there are classes of material. Applying a shape transformer, S, to the geometric quantity G_D of a rectangular envelope "transforms" the geometric quantity G_D into $G=SxG_D$. Shape properties, S, and material properties, M, are separated by the contribution of the sizes, D, of a cross-section, so that the functional requirement, F, and the objective function are expressed as $F=MxG=MxSxG_D$.

The research contributions, which are mainly derived by applying the theory, can be sorted into two groups. The first contributions are concerned with general analytical solutions for the mass-efficiency of structures. The second involves new types of selection charts.

10.2.1 Analysis

1. The **general expressions of the performance index** for arbitrary scaling of the cross-section in stiffness and strength design are respectively $(E\psi_I)^q/\rho\psi_A$ with $q=ln(uv)/ln(uv^3)$ and $(\sigma\psi_Z)^q/\rho\psi_A$ with $q=ln(uv)/ln(uv^2)$. Since u and v are the scaling multiplicator function of material and shape properties, the performance index compares the mass efficiency of cross-sections with different M and S. A summary of the indices for the selection of the material and shape properties in different scaling condition is shown in Tables 10.1 and 10.2:
2. The **performance criterion** is the ratio of the functional requirement and the objective function, $p=F/m$. It can be applied in any scaling condition and also for cross-sections which differ only for their sizes.
3. The **relation** between the performance criterion and the performance index have been explored. It has been shown that the two approaches differ only for how the term describing the envelope, D, is expressed.

Properties Selection	Bending stiffness requirement				
	D Fixed	D scaled			
		Horizontally	Vertically	Proportionally	Arbitrarily
Material	E/ρ	E/ρ	$E^{1/3}/\rho$	$E^{1/2}/\rho$	E^{q}/ρ
Shape	λ_I/ρ	λ_I/ρ	$\psi_I^{1/3}/\psi_A$	$\psi_I^{1/2}/\psi_A = \lambda_I/\psi_A$	ψ_I^{q}/ψ_A
Material and shape	$E\lambda_I/\rho$	$E\lambda_I/\rho$	$(E\psi_I)^{1/3}/\rho\psi_A$	$(E\psi_I)^{1/2}/\rho\psi_A$	$(E\psi_I)^{q}/\rho\psi_A$

Table 10.1 Performance index for the selection of the properties in bending stiffness design

Properties Selection	Strength requirement				
	D Fixed	D scaled			
		Horizontally	Vertically	Proportionally	Arbitrarily
Material	σ/ρ	σ/ρ	$\sigma^{1/2}/\rho$	$\sigma^{2/3}/\rho$	σ^{q}/ρ
Shape	λ_Z/ρ	λ_Z/ρ	$\psi_Z^{1/2}/\psi_A$	$\psi_Z^{2/3}/\psi_A = \lambda_Z/\psi_A$	ψ_Z^{q}/ψ_A
Material and shape	$\sigma\lambda_Z/\rho$	$\sigma\lambda_Z/\rho$	$(\sigma\psi_Z)^{1/2}/\rho\psi_A$	$(\sigma\psi_Z)^{2/3}/\rho\psi_A$	$(\sigma\psi_Z)^{q}/\rho\psi_A$

Table 10.2 Performance index for the selection of the properties in strength design

4. The expressions of the shape transformer have been used to derive geometric conditions for **optimising** the **internal geometry of the shapes**, such as thickness. The geometric conditions describe the optimisation path and have been defined so that they minimise mass and maximise stiffness.

5. The **interchangeability conditions** have shown that if the sizes of two cross-sections C_1 and C_2 are equal, i.e. $D_1=D_2$, the product M_1xS_1 can be interchanged with M_2xS_2. Therefore, for given materials, 1 and 2, and shape properties of a cross-section 1, the shape transformers for the section 2 are:

for given mass	for given stiffness	for given strength
$\psi_{A2} = \rho_1\psi_{A1}/\rho_2$	$\psi_{I2} = E_1\psi_{I1}/E_2$	$\psi_{Z2} = \sigma_1\psi_{Z1}/\sigma_2$

6. **Structuring** and **layering** are two ways of shaping materials. Structuring involves shaping material in a cell so that assembling cells symmetrically around the neutral axis produces a structured system. Layering consists of nesting cross-sections with different material and/or shape properties.
   a) **Structuring**. Different levels of structuring can be applied to a cross-section. The shape property which relates the geometric quantity, G, of a structured

system after t levels of structuring and the geometric quantity of the system, G_D, is given by

$$S_t = \frac{G_t}{G_D} = \prod_{j=1}^{t} S^j$$

where S^j is the shape transformer applied at a level j of structuring.

b) **Layering**. Shape transformers have been defined for systems with layers scaled in arbitrary, proportional, vertical and horizontal directions. Any system can be considered as a structured layered system. A standard cross-section of homogenous material is a layered system where one component is air.

c) **Structured layered system**. The properties, mass and functional requirement, and the performance of a structured layered system, C, in stiffness design are given:

$$\frac{m}{A_D} = \sum_{i=1}^{n} \rho_i x \prod_{j=1}^{t} \psi_{Ai}^{j}$$

$$\frac{k}{I_D} = \sum_{i=1}^{n} E_i x \prod_{j=1}^{t} \psi_{Ii}^{j}$$

$$p = \sum_{i=1}^{n} \frac{E_i}{\rho_i} x \prod_{j=1}^{t} \lambda_{Ii}^{j}$$

where n is the number of nested cross-sections, i.e. layers.

7. In the **plastic bending case**, the analogy between an elastic-plastic envelope, with elastic core and plastic extreme fibres, and a sandwich section has made it possible to define the shape transformers for the plastic case. The plastic shape transformers, $\psi_A{}^p, \psi_Z{}^p$, for the class of rectangles are reported in Table 10.3 together with the general shape transformers, $\psi_A{}^e, \psi_Z{}^e$, for elastic bending.

Elastic bending	Plastic bending
$\begin{cases} \psi_A{}^e = \dfrac{A}{A_D} \\ \psi_Z{}^e = \dfrac{Z}{Z_D} \end{cases}$	$\begin{cases} \psi_A{}^p = \dfrac{A_p}{A_D} \\ \psi_Z{}^p = \dfrac{Z_p}{Z_D} + \psi_Z{}^e \end{cases}$

Table 10.3 Shape transformers for elastic and plastic case. (A and Z for a cross-section, A_D and Z_D for the envelope, A_p and Z_p for plastic region in the envelope).

8. The **limits to the sizes** of a cross-section for a slender strut under elastic buckling **depend on the material and the shape properties**. The H limits are given by:

$$H_{\lim} = \underbrace{\frac{\sqrt{12}nL}{\pi}}_{const} \underbrace{\left(\frac{\sigma_y}{E}\right)^{0.5}}_{M} \underbrace{\left(\frac{1}{\lambda_I}\right)^{0.5}}_{S}$$

9. The shape transformers have been used to explore the **interaction of cross-sectional shape selection and form selection** at the preliminary stage of design. The expression of the **area to prevent failure either by buckling or yield** for compressive members is:

$$A^c = 0.5\frac{P^c\lambda_I z\nu + \sqrt{P^c\lambda_I z\left(P^c\lambda_I z\nu^2 + 4\sigma_y\psi_\lambda\mu L^{c^2}\right)}}{z\lambda_I\nu\sigma_y}$$

10. The study of the **optimal structural features of tree** (in Appendix E) has shown that horizontal branches develop **deep sections** by growing **non-concentric rings**. There are two reasons. Firstly, when the branch becomes a significant size, the self-weight is the dominant load which acts downwards and thus the regions of the branches where the highest compressive stresses occur are at on the underside of the branch. Secondly, the compression strength of wood is lower than the tensile stress due to the thin wall of the microstructured cells. Consequently, the tree reinforces the base of the branch by growing more cells far from the neutral axis.

10.2.2 Visualisation

1. The **combined graph** has been used to plot together the performance criterion and the functional requirement for any scaling of the cross-sections. This illustrates that the mass-efficiency of a cross-section depends on material, shape properties and sizes of the envelope.
2. The **material and shape regimes graphs**, introduced with the performance index, has shown the selection of the best material and/or shape properties in the geometric domain rather than in the material domain. The advantage of this is that any kind of geometrical constraints can be shown in the design space. An **improved version** of the map shows the ranking of the properties of material or

shape or combination for regions of the design space. The ranking classifies the properties of the envelopes which belong to a certain region.

3. The shape transformers have been plotted on the **envelope efficiency map** to permit the selection of shapes from different classes and for any scaling conditions of the envelopes. The map has been explored in natural and logarithmic scale. The map is analogous to the material charts which plot the material attributes. Each class of shapes is within two limiting curves. A feature of the limiting curves of the rectangle class is that only for a stiffness requirement all other shapes are contained.

4. Since the material charts and the efficiency envelope map plot material and shape properties of a cross-section with fixed sizes, superimposing the two charts, i.e. MxS, enable the **selection of material and shape** to be **integrated in one stage**. The **guidelines** are used in the logarithmic scale material chart to assist the designer in the **co-selection of material and shape properties** for horizontal, vertical and proportional scaling. Conversely to these particular scaling conditions, when the direction of scaling is not specified the multiplicators, u and v, must be considered to estimate q and to establish the position of a cross-section on the chart.

5. The **envelope efficiency map** and the **material chart** have been used to display the mass and the functional requirement of **structured layered systems**. The maps have explored the properties of systems with layers containing different shape or material and scaled in any direction.

6. Two-dimensional and **three-dimensional maps** have been shown that the **plastic bending** case can be discussed in the geometric domain rather than in the loading domain. The shapes of the rectangular class in the elastic and plastic domain are enclosed in a definite volume defined by the ranges of the shape transformers.

7. **The envelope map** has been used to investigate the limits of the shape properties due to **manufacturing constraints** of standard steel cross-section. The limits to the shape transformers could have been plotted because the envelope sizes have been disregarded. On the other hand, the combined graph has been applied for exploring the limits of the envelope sizes which prevent Euler's buckling.

8. The **nested performance chart** is a sub-matrix of two variables chart which permits performance trends to be displayed **for** systems with **more** than three **variables**. It has shown the utility to explore patterns of performance for multi-objective optimisation problems.
9. **Design charts** have shown the effect of the **interaction between cross-sectional shapes and form** for the selection of alternative pin-jointed structures at the **early stage of design**.

10.3 FUTURE WORK

There are two types of suggestions for further research. The first is more general and deals with the application of the theory to other topics of engineering which are not necessarily related to structural design. The second concerns with structural design and optimisation.

1. **Application of the shape transformers to other engineering fields.**
   The shape transformer are a means for comparing the geometric quantities of cross-sectional shapes. The definition of a shape transformer is associated to a geometric quantity. In this thesis, they have been defined for five geometric quantities such as area, second moment of area, section modulus, plastic area and plastic section modulus (actually, the linear multiplicator, u and v, can be thought as length transformers). When a geometric quantity is involved in an engineering problem different from structural design, it could be possible to define a shape transformer. Shape transformer for the perimeter and for the volume could be defined. One possible application is the selection of the optimum cross-sectional shapes for fluids pumps. Appropriate shape transformers could be defined to compare the flow rate for different cross-sectional shapes of the pumps. There are possible applications in the fields of heat engineering. When the criterion of selection for an engineering component is the ratio of the heat generated throughout the object and the loss through its surface, shape transformers could be defined to compare the alternative forms of the object. The object can be considered in a three-dimensional envelope and

changes in sizes of the 3D envelope could be assessed by the multiplicators of depth, width and length.

2. **Application of the shape transformers to structural optimisation.**

i) This thesis has considered tension, bending and compression and has defined the shape transformers using formulas for area, second moment of area and section modulus of the cross-sections. Other mechanisms of transfer load which can be examined are **torsion** and **shear**. However, for torsion and shear, closed-form solutions are not always possible. Therefore, approximate formulas for the relevant geometric quantities, such as, for example the torsional moment of area, could be adopted.

ii) The **plastic bending** case has been examined for the shape class of the rectangle. The analytical approach and the development of the three dimensional map can be extended to **other classes of shapes** such as elliptical, triangular and lozenge shapes. In such a case, it would be possible to show the effect of the plastic shape transformer on the material charts.

iii) The concept of a two dimensional envelope enclosing the shape of a cross-section could be extend to **three dimensions**. A rectangular prism, $BxHxL$, can be the **envelope** of a structural member. The tapering of the longitudinal profile, which has been examined in Chapter 8, could be expressed in terms of shape transformers. Differences in sizes of an element could be assessed by three linear multiplicators for the width, $u=B/B_0$, depth, $v=H/H_0$, and length, $w=L/L_0$, of the 3D envelope. Consequently, the **material charts** could be used to display the effect of **"forming" a material in three dimensions**.

iv) The **design charts** and the **performance map** have been produced using mathematical and graphical packages without any automatic procedures. The next step is to **implement** the procedures of the charts and of the performance maps as **computer software**. For example, the improved version of the material and shape regimes graph and the envelope efficiency map could be implemented. The **co-selection** of material and shape, could be implemented in a software for material selection similar to that developed in Cambridge (Cebon and Ashby, 1991). A computerised implementation of the **nested performance charts** would facilitate performance patterns to be discovered for different structural forms. In such a case, an **archive of structural forms** could be populated with more complex structures. Geometric **rules for optimising a**

topology could be associated to each structural form of the archive, in a similar way to the lozenge frame.

v) In this work, the optimal structural features of a tree have been investigated. The **study of other natural systems** could be very useful to understand how nature optimises a system to perform a number of functions. The principles can be transferred to engineering.

vi) Adaptive structures and multifunctional joints have been identified as features of a tree which are under exploited in engineering. Multi-functionality and adaptation to loading are routes to optimisation. It could be interesting to develop a methodology for **preliminary design of shape-adaptable structures** using shape transformers. The starting point could be comparing the mass-efficiency of an adaptive component and a standard structure which performs the same function. The standard structure has two parts with a rigid connection to allow movement while the adaptable structure consist of one component with flexibility spread over a region. Design indices of performance and shape transformers could be developed for comparing the mass-efficiency of traditional structures with flexible structures.

APPENDIX A

MATERIAL INDICES FOR HORIZONTAL, VERTICAL AND PROPORTIONAL SCALING

A.1 Procedure

Although from the literature it appears that indices for selecting materials were known in the 1960' (Shanley, 1960), a standard procedure was developed lately (Ashby, M.F., 1989). The steps for deriving an index for material selection are:

- Describing the objective function and the design requirement with equations.
- Identifying the variables in term of material and geometric properties in the objective function and in the design requirement.
- Using the equations of the design requirement to eliminate the free variables in the objective function.
- Grouping the remaining variables, such as material and some aspects of the geometry, and the constants of the problem to express the objective function as a product, *FxGxM*, of the functional requirement, *F*, the geometry, *G*, and the material, *M*.
- Isolating the group of the variables, i.e. the material properties, from the constant parameters to derive the index for material selection.

In this Appendix A, an example for a simply supported centrally loaded beam with rectangular cross-section is considered. The procedure to derive an index for the selection of the material which minimises the mass of the beam for a given stiffness is reported.

Objective function

The objective is to minimise the mass of a beam of given length, L, density, ρ, and cross-sectional area, A. The objective function is the mass of the beam given by:

$$m = \rho AL = \rho BHL \tag{A.1}$$

where B and H are the sizes of a rectangular cross-section.

Functional requirement

The bending stiffness, k, for a simply supported beam designed to deflect less than δ under a central point load P, is the functional requirement and is given by:

$$k = \frac{P}{\delta} \tag{A.2}$$

From the elasticity's theory, the stiffness of the beam can be expressed in terms of material and geometric properties of the beam as:

$$k = c_1 \frac{EI}{L^3} \tag{A.3}$$

where c_1 is a constant which depends on the details of the load and boundary conditions.

The general expression of the second moment of area of a cross-section is

$$I = \int_A y^2 dA \tag{A.4}$$

For a solid cross sectional area with two symmetric axes, the second moment of area can be written as

$$I = zBH^3 = zH^2 A \tag{A.5}$$

where z is a constant of the cross-sectional shape.

Substituting equation (A.5) in (A.3), gives the following expressions of the design requirement:

$$k = zc_1 \frac{EBH^3}{L^3} = zc_1 \frac{EH^2 A}{L^3} \tag{A.6}$$

In order to derive an index for selecting the material which minimises the mass of a beam, it is necessary that the free variables of the functional requirement, equation (A.6), are replaced in the objective function. In equation (A.6), the area, *A*, the height, *H*, or the width, *B* of a cross-section can be considered free variables. Each of these parameters is variable for three scaling conditions of the cross-section: proportional, vertical, horizontal. Vertical and horizontal scaling are generally imposed by geometrical constraints.

- **Proportional scaling.** If the value of the area is variable, then the ratio of the sizes, *H/B*, of the cross-section is fixed. The cross-sections are relatively proportionally scaled.
- **Vertical scaling.** If the height is variable and the width is fixed, then the cross-sections are vertically scaled.
- **Horizontal scaling.** When the width is free and the height is constrained, there is a horizontal scaling of the cross-sections.

A.2 Proportional scaling

The variable is the value of the area of the cross-section. If the cross section is assumed to be an equiaxed shape (circle, square, etc.), the term H^2 of the second moment of area in (A.6) is replaced by *A* because equation (A.5) is written as:

$$I = zA^2 \tag{A.7}$$

Combining equation (A.7) with (A.3), the free variable is given by:

$$A = \underbrace{\left(\frac{kL^3}{c_1 z}\right)^{0.5}}_{const} \underbrace{\left(\frac{1}{E}\right)^{0.5}}_{Material} \tag{A.8}$$

The first group in equation (A.8) collects the constant parameters of the problem. The second group is the material property of the functional requirement. For different materials, the cross-sections are proportionally scaled because the Young's Modulus determines the value of the area, and then the sizes, of the cross-section.

Replacing equation (A.8) in (A.1), gives the mass of a beam for a given stiffness, *k*:

$$m = \underbrace{\left(kL^5/c_1 z\right)^{0.5}}_{Const} \underbrace{\rho/E^{0.5}}_{Material} \tag{A.9}$$

Maximising the index $E^{0.5}/\rho$ minimises the mass of proportionally scaled sections.

A.3 Horizontal scaling

When different materials are considered, a height constraint has the effect of imposing horizontal scaling to the cross-sections. Since the height, *H*, is a constant parameter, then the width, *B*, is the variable. From equation (A.6), the width, *B*, is given by:

$$B = \underbrace{\frac{kL^3}{c_1 z H^3}}_{const} \quad \underbrace{\frac{1}{E}}_{Material} \tag{A.10}$$

For different materials, the value of *B* is determined by the material property of the functional requirement, which is the Young's Modulus in bending stiffness design.

Substituting equation (A.10) in (A.1), the mass of the beam is given by

$$m = \underbrace{kL^4/c_1 z H^2}_{Const} \quad \underbrace{\rho/E}_{Material} \tag{A.11}$$

Maximising the index E/ρ gives the best material for horizontal scaling.

A.4 Vertical scaling

Vertical scaling is imposed by a constraint on the width of cross-sections. Therefore, *B* is fixed and the variable is *H*. From equation (A.6) the height, *H*, is given by:

$$H = \underbrace{\left(\frac{L^3 k}{c_1 z B}\right)^{1/3}}_{const} \quad \underbrace{\left(\frac{1}{E}\right)^{1/3}}_{Material} \tag{A.12}$$

For different materials, the height of a cross-section is determined by the value of the Young's Modulus.

Replacing equation (A.12) in (A.1), the mass of the beam is given by

$$m = \underbrace{\left(kL^6 B^2/c_1 z\right)^{1/3}}_{Const} \quad \underbrace{\rho/E^{1/3}}_{Material} \tag{A.13}$$

The highest index $E^{1/3}/\rho$ gives the material which minimises the mass of cross-sections which are vertically scaled.

APPENDIX B

GENERAL SOLUTION σ^q/ρ FOR ARBITRARY SCALING IN STRENGTH DESIGN

The procedure to derive the general solution of the performance index for strength design is entirely analogous to the stiffness case, given in Section 4.4.1.

In strength design, the design input is the failure moment requirement, given by equation (3.14). Rectangular cross-sections have $\psi_A = \psi_z = 1$ and meet the same requirement, $M_{yo} = M_y$, such that:

$$\sigma_{yo} Z_o = \sigma_y Z \tag{B.1}$$

The ratio of the failure moment of the structures can also be stated in terms of multipliers *u* and *v*, so that:

$$\frac{Z}{Z_o} = uv^2 \tag{B.2}$$

Performance index for height constraint.

When the height of the two sections is constant, *v=1* and *u* from (B.2) is given by:

$$u = \frac{Z}{Z_o} \tag{B.3}$$

and from equation (4.11) the ratio of the performance index are:

$$\frac{p}{p_o} = \frac{\rho_o}{\rho} \frac{\sigma_y}{\sigma_{yo}} \tag{B.4}$$

Performance Index for width constraint.

When two sections have same width, *u=1* and *v* from (B.2) is given by:

$$v = \left(\frac{Z}{Z_o} \right)^{\frac{1}{2}} \tag{B.5}$$

and from equation (4.11) the ratio of the performance index are:

$$\frac{p}{p_o}=\frac{\rho_o}{\rho}\left(\frac{\sigma_y}{\sigma_{yo}}\right)^{\frac{1}{2}} \tag{B.6}$$

Performance index for arbitrarily scaling

For arbitrarily scaling $u\neq1$ and $v\neq1$, a general solution is sought such that:

$$\frac{p}{p_o}=\frac{\rho_o}{\rho}\left(\frac{\sigma_y}{\sigma_{yo}}\right)^{q} \tag{B.7}$$

where q is yet to be determined.

For these conditions:

$$\begin{cases} u=\left(\dfrac{Z}{Z_o}\right)^{\alpha} \\ v=\left(\dfrac{Z}{Z_o}\right)^{\beta} \end{cases} \tag{B.8}$$

rewriting equation (B.2) gives:

$$uv^2=\left(\frac{Z}{Z_o}\right)^{\alpha+2\beta} \tag{B.9a}$$

and

$$\alpha+2\beta=1 \tag{B.9b}$$

From equation (B.8) the exponents α and β are:

$$\begin{cases} \alpha=\lg_{\left(\frac{Z}{Z_o}\right)}u=\lg_{(uv^2)}u \\ \beta=\lg_{\left(\frac{Z}{Z_o}\right)}v=\lg_{(uv^2)}v \end{cases} \tag{B.10}$$

The ratio of the performance indices p/p_o follows from equation (4.11) using equations (B.8) through (B.10), so that:

$$\frac{p}{p_o}=\frac{\rho_o}{\rho}\left(\frac{Z_o}{Z}\right)^{q}=\frac{\rho_o}{\rho}\left(\frac{\sigma_y}{\sigma_{yo}}\right)^{q} \tag{B.11}$$

where $q=\log_{(uv^2)}uv=\dfrac{\ln uv}{\ln uv^2}$ (B.12)

APPENDIX C

GENERAL SOLUTION $\psi_Z{}^q/\psi_A$ FOR ARBITRARY SCALING IN STRENGTH DESIGN

The failure moment is the design requirement, given by equation (3.14), and the relevant shape transformer is ψ_Z. In strength design, the generic and the reference cross-sections meet the failure moment requirement, $M_{yo}=M_y$, such that:

$$\frac{Z}{Z_o}=\frac{\sigma_o}{\sigma}=1 \qquad \text{(C.1)}$$

Since the structure are made out of the same material, $\sigma=\sigma_o$. The multipliers, u and v, and the geometric transformer ψ_Z are used through (5.8) to rewrite (C.1) as:

$$\frac{Z}{Z_o}=\psi_Z u v^2 \qquad \text{(C.2)}$$

Performance index for height constraint.

For a height constraint the two structures are scaled so that $v=1$, and u from (C.2) is:

$$u=\frac{Z}{Z_o}\frac{1}{\psi_Z} \qquad \text{(C.3)}$$

and the ratio of the performance indices from (5.10) is:

$$\frac{p}{p_o}=\frac{\psi_Z}{\psi_A}=\lambda_Z \qquad \text{(C.4)}$$

λ_Z is the performance index for S *in the* same way as σ/ρ is the performance index for M variable.

Performance index for width constraint.

When the width is constrained $u=1$, and v from (C.2) is given by:

$$v=\left(\frac{Z}{Z_o}\frac{1}{\psi_Z}\right)^{1/2} \qquad \text{(C.5)}$$

and from (5.10) the ratio of the performance indices is:

$$\frac{p}{p_o} = \frac{\psi_Z{}^{1/2}}{\psi_A} \tag{C.6}$$

Equation (C.6) leads to the selection of the best shape for a width constraint. Similarly, $\sigma^{1/2}/\rho$ is the performance index for selecting the best material.

General solution of the performance index for arbitrary scaling.

For arbitrary scaling $u \neq 1$ and $v \neq 1$. The ratio of the performance indices can be written as:

$$\frac{p}{p_o} = \frac{\psi_Z{}^q}{\psi_A} \tag{C.7}$$

where q is an expression which is to be determined.

For generic u and v:

$$u = \left(\frac{1}{\psi_Z}\right)^{\alpha}$$
$$v = \left(\frac{1}{\psi_Z}\right)^{\beta} \tag{C.8}$$

and using expressions (C.8), equation (C.2) is rewritten as:

$$uv^2 = \left(\frac{1}{\psi_Z}\right)^{\alpha+2\beta} \tag{C.9a}$$

with: $\alpha + 2\beta = 1$ (C.9b)

From equation (C.8), the exponents α and β are:

$$\begin{cases} \alpha = \lg_{\left(\frac{1}{\psi_Z}\right)} u = \lg_{(uv^2)} u \\ \beta = \lg_{\left(\frac{1}{\psi_Z}\right)} v = \lg_{(uv^2)} v \end{cases} \tag{C.10}$$

The ratio of the performance index p/p_o follows from equation (5.10) using equations (C.8) through (C.10), so that:

$$\frac{p}{p_o} = \frac{\psi_Z{}^q}{\psi_A} \tag{C.11}$$

where $q = \log_{(uv^2)} uv = \dfrac{\ln uv}{\ln uv^2}$ (C.12)

APPENDIX D

NESTED PERFORMANCE CHARTS

D.1 INTRODUCTION

This Appendix illustrates a new performance chart, which is called **nested performance chart**, for structural systems with more than two design variables. First, traditional charts with one or two variable are presented.

D.1.1 Performance charts

Physical equations are generally used to model the performance of structural forms. However, it is generally not possible for engineering designers to optimise and select design variables by just inspecting the equations of the performance function because the equations are usually complicated and difficult to interpret directly.

One approach to finding the optimum values of the design variables to satisfy the performance function is to use a computational search programme. However, such methods have some *disadvantages* as reported in Chapter 2. Another approach to finding optimum values of the design variables is to produce *performance charts*. The equations can be interpreted and understood if the performance function is plotted against the design variables. These charts enable designers to visualise how the performance changes as a particular design variable is changed. The performance charts, therefore, can be used to select and optimise each design variable. More importantly, they give a clear visual representation of performance trends for all or a large part of the design space. The designers can use the charts to identify a range of low mass designs and also to gain insight into why certain

structural features are advantageous. The charts can also be shown to team members who are not experts in structural engineering to illustrate how performance is affected by changes in design parameters. When this is done, performance charts help the whole team to come to an agreement about which concept has the best overall performance.

Traditional performance charts generally only contain one or two variables. However, engineering systems often involve more than two important design variables. In order to graphically represent the performance of the system as a function of more than two design variables, it is usually necessary to produce a large number of separate performance charts. These can be difficult to interpret because the designer must understand the relationship between all the separate charts.

In the next two sections, traditional charts, which contain one or two variables, and a new performance chart, called a nested performance chart, which is able to plot more than two design variables, are presented.

D.2 TRADITIONAL CHARTS

This Section examines the advantages and the drawbacks of the traditional charts used to visualise the mass of a structure with more variables. As example, the mass m=f(x,y,z,w) of a structure with four variables x,y,z,w, is considered.

D.2.1 One-variable performance charts

Figure D.1 shows a traditional one-variable performance chart for the variable x, for the case when the other variables, y, z and w are fixed. The chart shows the mass, m, of a structure in the range 0<x<100. The chart makes it possible for the designer to make the observations on performance trends. For example, the minimum mass is achieved at x=*50*, the mass increases significantly for small values of *x* and does not vary much when 30<x<*80*.

Whilst the performance chart shown in Figure D.1 is useful because shows performance trends and not only optimum point solutions, it has a drawback in that three design variables are fixed. In order to visualise the performance of the whole

design space (i.e. different permutations of all variables) it is necessary to produce a large set of design charts for a number of discrete settings of all the variables. The number of design charts, *N*, required to cover the whole design space is given by:

$$N = d^n \tag{7.1}$$

where *n* is the number of variables and *d* is the number of discrete levels for each variable.

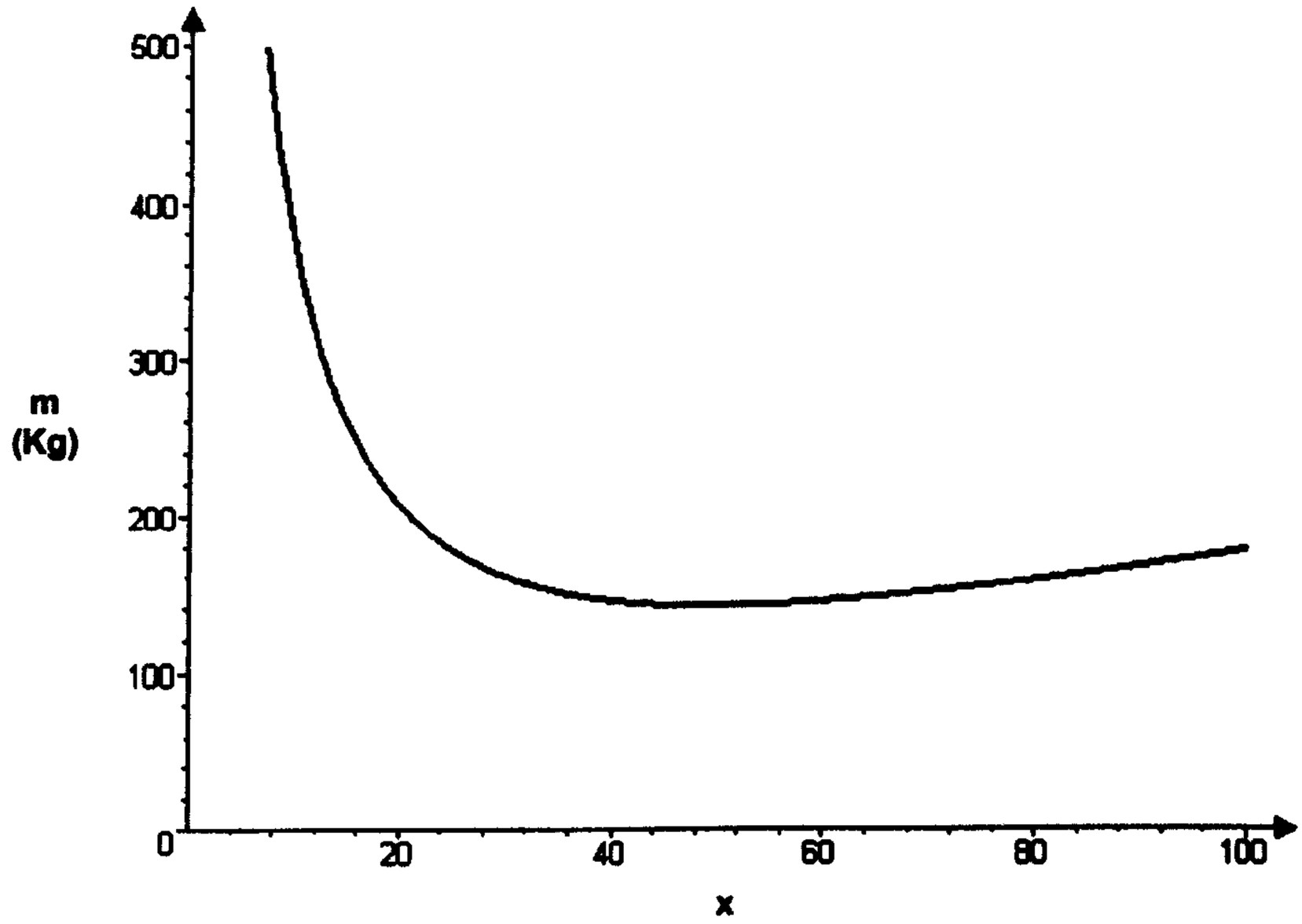

Figure D.1 Performance function, m, of a structure with one active design variable, x.

For example, if design charts were produced for three discrete values of each design variable then it would be necessary to produce $3^4 = 81$ charts in total to cover all the different permutations of values of the discrete variables. Such a large number of design charts makes it difficult for the designer to view the design space and gain insight.

D.2.2 Two-variable performance chart

Figure D.1 shows a type of traditional performance chart which plots performance as a function of two design variables x and y. In this case the variables z and w are fixed. The structural performance is plotted with lines of constant mass which are analogous to height contour lines on a geographic map. The lowest mass occur in the trough of the contours.

As with the one variable performance chart, it is necessary for the designer to produce separate design charts in order to view the whole design space. For the case of *n* design variables, the number of design charts, *N*, required to cover the whole design space is given by:

$$N = d^{(n-2)} \qquad (7.2)$$

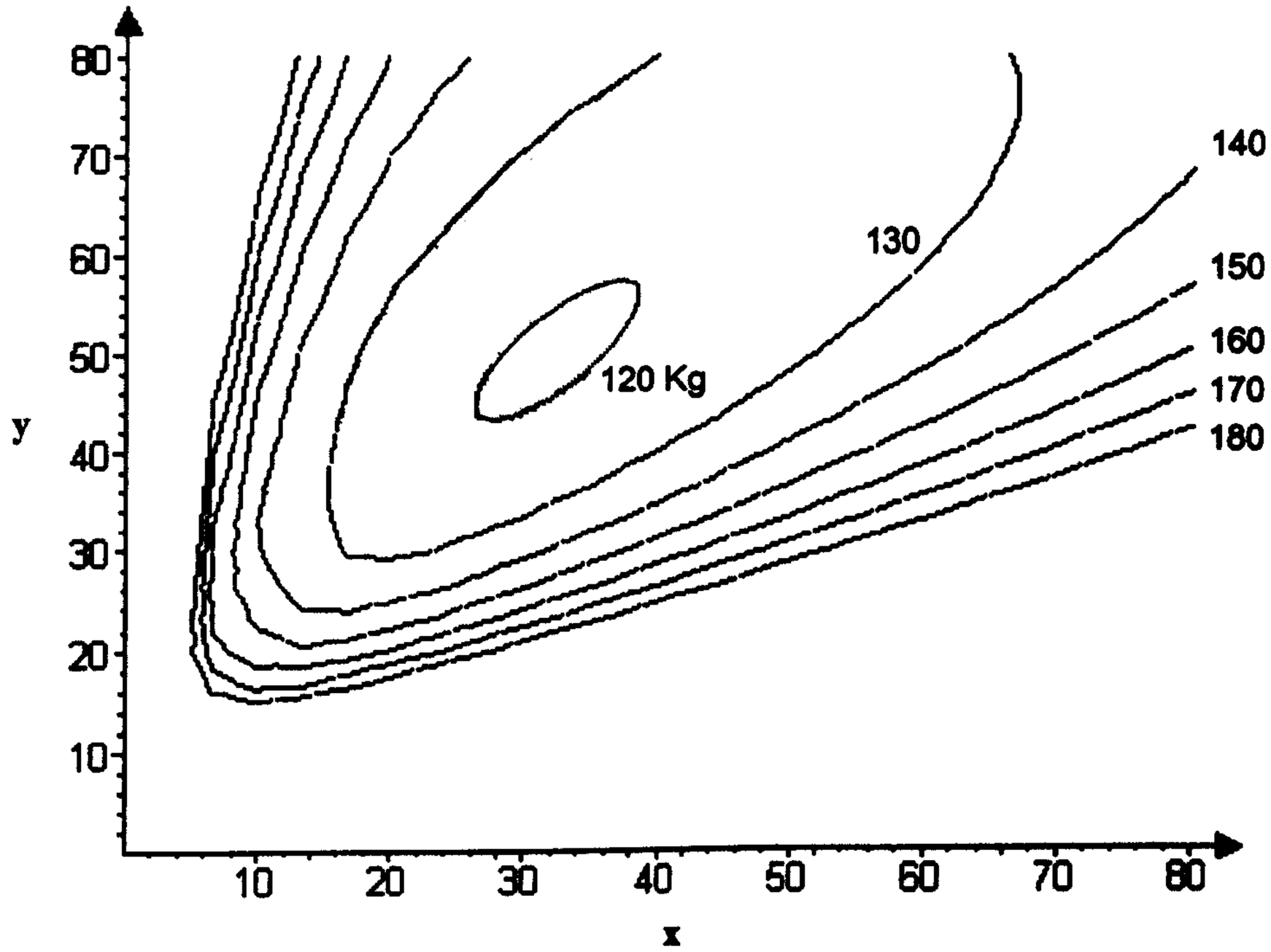

Figure D.1 Performance function, m, of a structure with two active design variable, x and y.

If design charts were produced for three discrete values of four design variables then it would be necessary to produce $3^{(4-2)} = 9$ charts. Even though this is a significant improvement on the number of charts required for single-variable performance charts, there are still a significant number of charts. It is difficult to interpret nine separate performance charts because the designer must understand the relationship between all the separate charts.

D.2.3 Three-variable performance charts

It is possible to produce three dimensional performance charts which contain three-dimensional shells of constant performance plotted on a three-axes graph. However, such charts are very difficult to understand and it can be very difficult to read off the values of the design variables from the axes for a particular level of performance.

D.3 NESTED PERFORMANCE CHARTS

The nested performance chart can be developed in two versions.

VERSION I: two variables discretised. The first version consists of a sub-matrix of charts as shown in Figure D.1.

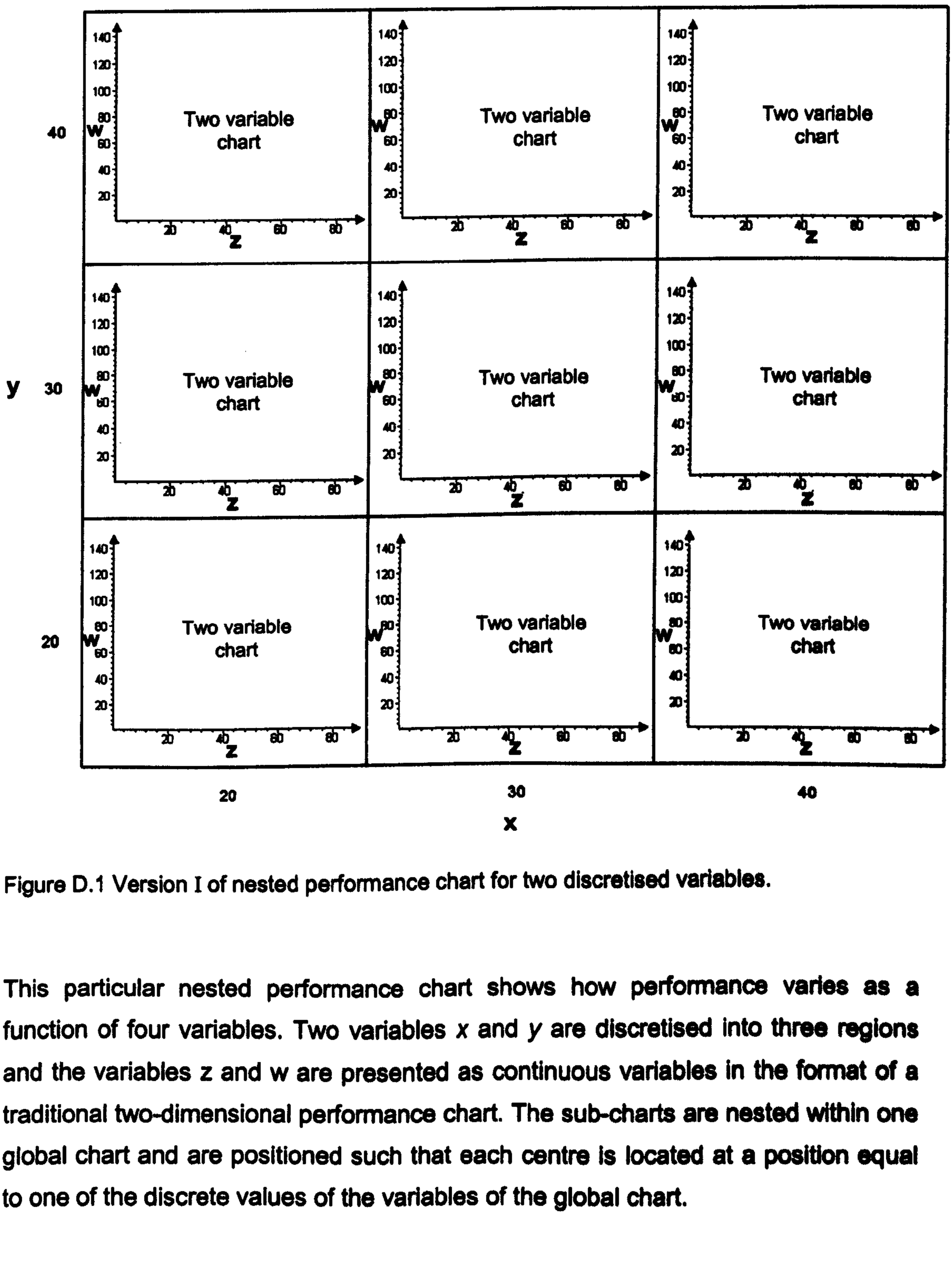

Figure D.1 Version I of nested performance chart for two discretised variables.

This particular nested performance chart shows how performance varies as a function of four variables. Two variables *x* and *y* are discretised into three regions and the variables z and w are presented as continuous variables in the format of a traditional two-dimensional performance chart. The sub-charts are nested within one global chart and are positioned such that each centre is located at a position equal to one of the discrete values of the variables of the global chart.

The nested performance chart is more helpful than having separate design charts because an individual chart is clearly put into context. The layout helps because it shows how charts are related to each other in the overall scheme. One limitation of nested performance charts is that at least two design variables must be discretised. This means that the charts do not generally reveal the exact optimum values of the design variables. However, the charts enable the designer to quickly identify the approximate values of the optimum design variables. If the designer needs to identify the exact optimum values of the design variables, then they can produce more refined nested charts in the appropriate areas.

VERSION II: three variables discretised. Figure D.2 shows the second version of the nested performance chart where three design variables are discretised. x, y and z are discretised and w is the variable. 27 boxes are displayed on the chart. However, in this case the graph in each cell is a single colour (or shade) which indicates the performance for the optimum value of w and for that particular combination of discrete variables. The darker the colour, the lower the mass and vice versa. This chart can sometimes be more convenient than the previous nested performance charts because there is a direct indication of performance through the colour of the box.

These charts give a straightforward visual representation of performance trends throughout the whole design space. The method could be extended in principle to more than four design variables if there are nests within nests. In such a case, it would be necessary to have a computerised implementation of the concept.

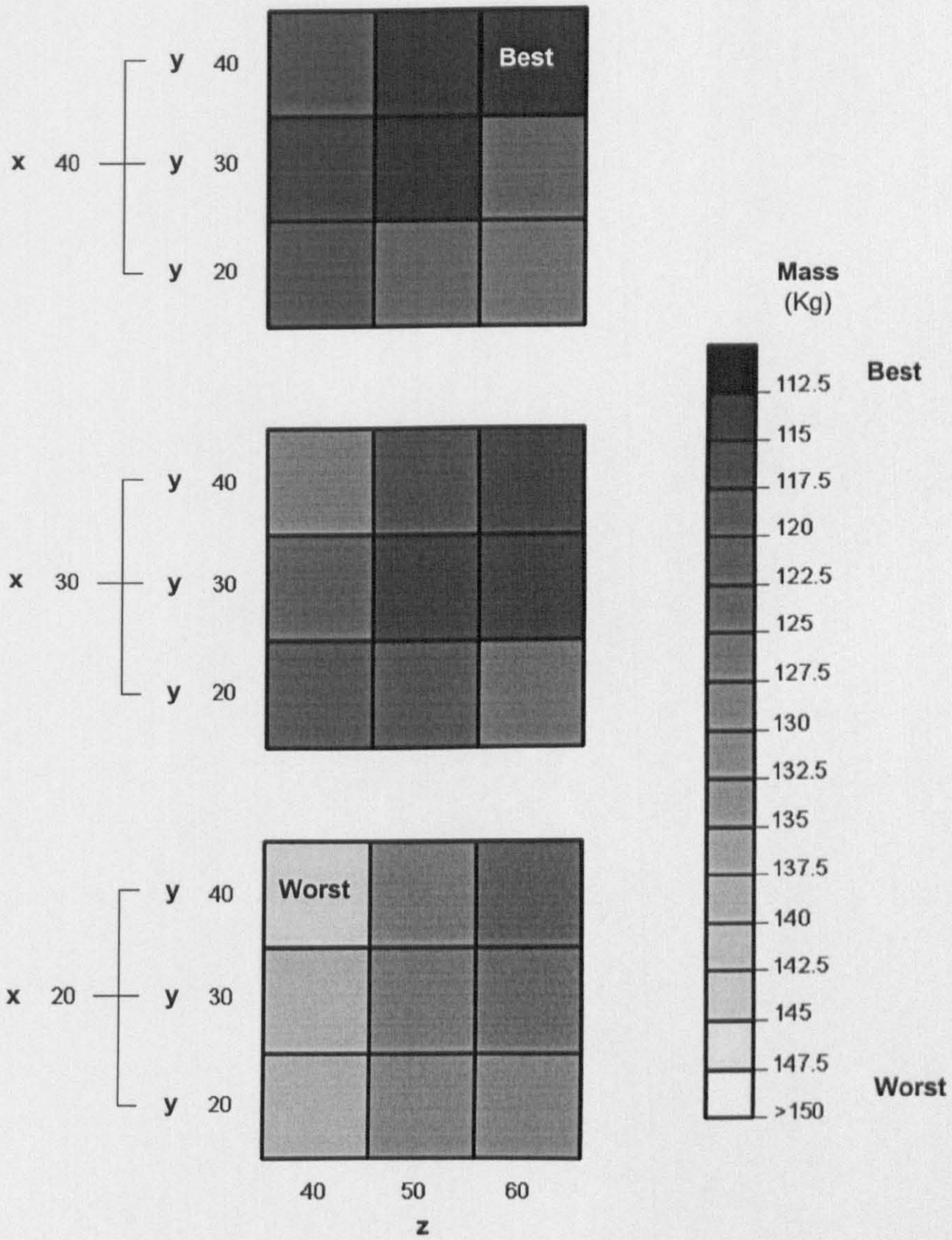

Figure D.2 Version II of nested performance chart for three discretised variables

APPENDIX E

OPTIMAL STRUCTURAL FEATURES OF TREES AND THEIR APPLICATION IN ENGINEERING

E.1 INTRODUCTION

This Appendix complements Chapter 9. There are two parts:

- In the first, the optimal structural features which trees develop by adaptive growth are examined. The methodology illustrated in Chapter 9 is used to investigate the structural features. The analysis starts with the general level, i.e. the overall form, proceeds to each structural zone of the tree and concludes with the material level.
- The second part draws parallels and similarities between trees and engineering structures. The aim is to offer understanding which can be instructive in many areas of design.

E.1.1 Glossary

Leeward:	sheltered from the wind.
Windward:	exposed to wind.
Tap root:	a deep vertical root directly under the trunk.
Sinker root:	a deep vertical root which comes from a lateral root.

E.2 OPTIMAL STRUCTURAL FEATURES

E.2.1 Overall form

There are several optimal features in the form of the tree:

- **Hierarchical structure.** The tree develops a hierarchical structure to support a large foliage canopy. Each structural element has a precise function and position within the tree. Each part resists the forces transmitted by the subordinate elements and transfers its own load on the elements which precede it in the hierarchical scale. Hierarchical structures are tolerant to damage and can present optimally decreasing sizes of elements at each hierarchical level according to the magnitude of applied forces.
- **Flexibility.** A flexible structure can adjust its form when loaded, thus reducing the severity of load. A flexible structure also improves toughness.

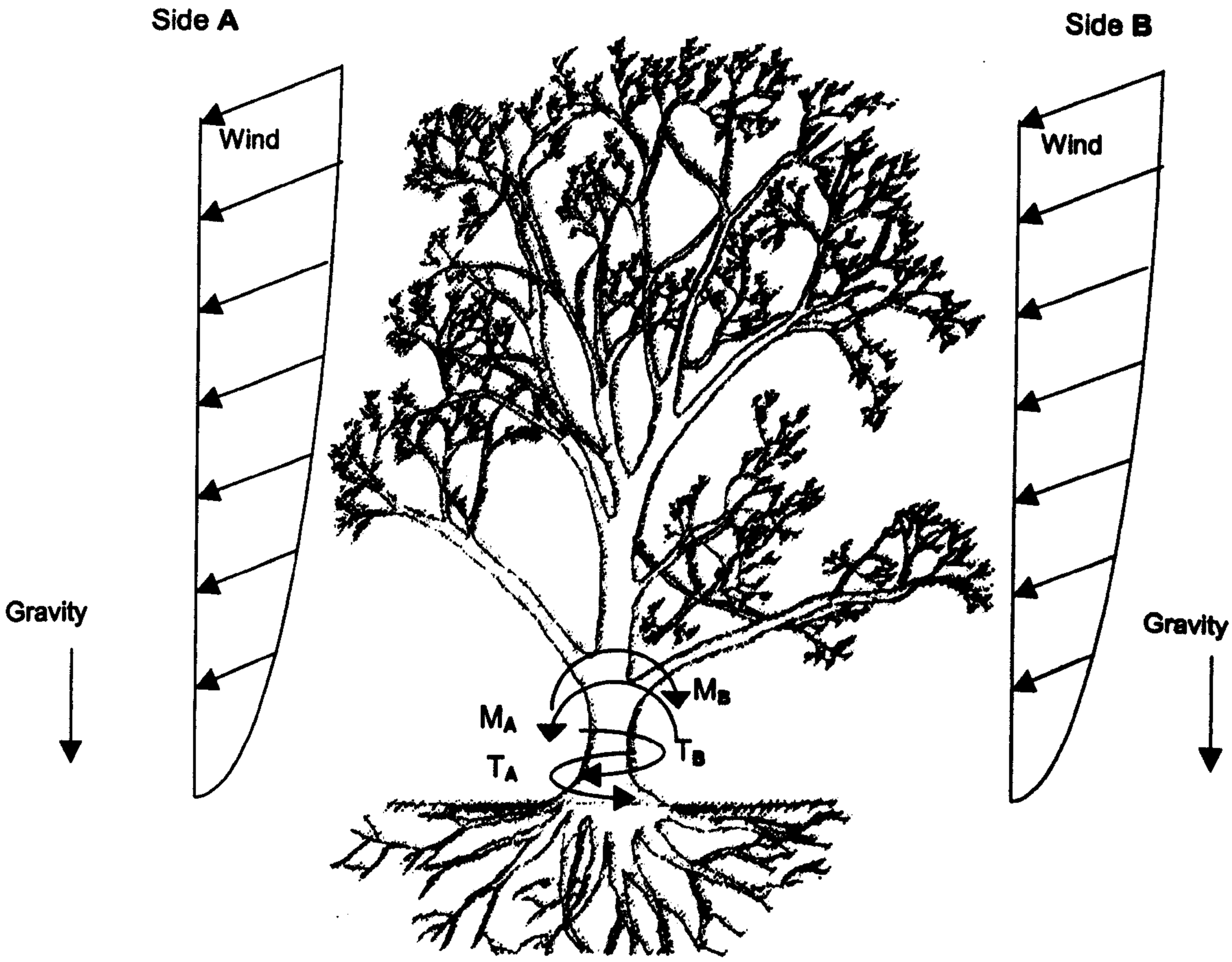

Figure E.1 The balanced form enables the bending, M, induced by the self weight, and the torsion, T, caused by the wind, to be nearly equal and opposite.

- **Convergent form.** The lateral branches, which assume an equilibrium position at a given angle to gravity, converge into one vertical support. Since the compression forces are concentrated into the trunk and transmitted into the soil, one foundation structure is required
- **Balanced forces**. The secondary structure presents a balanced distribution of its elements around the main support. The benefit of developing a balanced form is shown Figure E.1. Self-weight on each side of the tree induces roughly equal but opposite bending moments on the trunk. The action of the wind on the canopy on each side of the tree induces roughly equal and opposite torsion moments.
- **Optimised proportions**. The tree grows in height in relation to the trunk diameter. The self-weight increases with the volumes of the dimensions whereas the buckling load increases only with the area. If a tree, during its growth, should increase the dimensions of its structure proportionally, then it would eventually fail under its own weight. The tree, on the contrary, perceives the increased stresses due to self-weight and responds by growing the dimensions of the trunk faster than the height. However, the diameter of the trunk appears to be over designed if only the self-weight is considered (McMahon, T. A., 1973). This is because the tree optimises the proportions of its form also in response to the stimuli induced by the wind.

E.2.2 Foundation structure: anchorage

The foundation structure provides the anchorage of the tree to the ground. The forces induced by external loads and self-weight at the base must be transferred into the soil. The soil and roots prevent the tree from uprooting under wind action. Whereas the number, direction, sizes and shapes of the roots are developed in response to the applied forces, the soil cannot show any adaptive response. The components, which resist the turning moment (Coutts, M. P., 1983a, 1983b, 1986), are shown in Figure E.1. The most significant is the resistance offered by the windward roots in tension. Another important factor is the weight of the root-soil plate, while the resistance of the soil and of the compressive leeward roots have a marginal contribution.

- **Stiff root system**. The tree builds a stiff root system in two ways. In the first case, shallow lateral roots are developed only horizontally and are attached to a tap root, which is a deep root growing directly under the trunk. In the second, deep sinkers grow downward from the lateral roots at some distance from the axis of the trunk (Coutts, M. P., 1986).
- **Orientated distribution of roots**. The number and the position of the roots are important factors for an efficient anchorage. For example, a symmetric distribution of roots is appropriate if the wind comes from any direction. However, the tree can adapt to an unidirectional wind (Coutts, M. P., 1983a). In this scenario, the tree allocates roots in the direction of rocking (particularly on the lee side) because it promotes a more efficient anchorage. On the contrary roots perpendicular to the direction of wind offer little resistance to uprooting because they are subject to torsion.

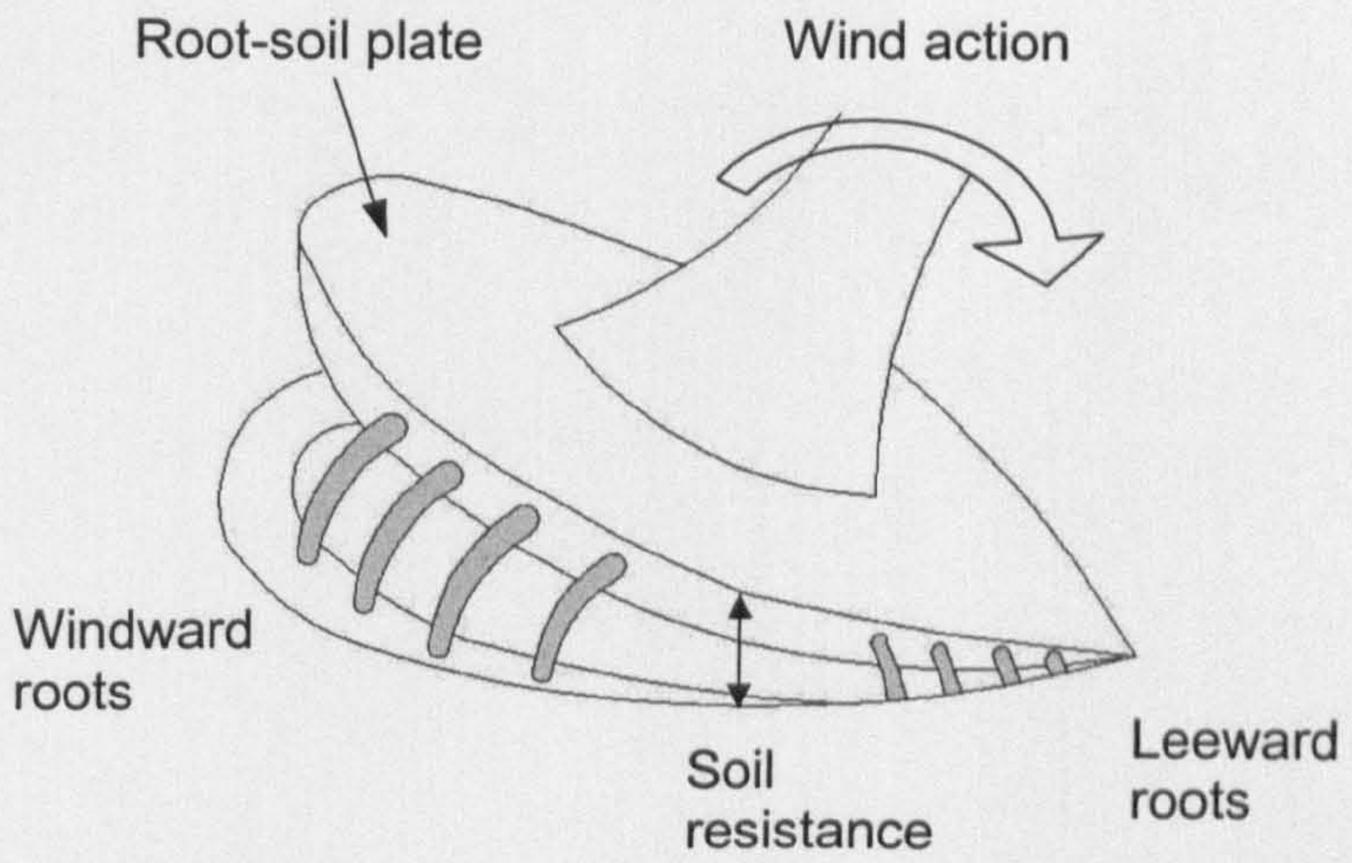

Figure E.1 Foundation structure: the components of the anchorage system.

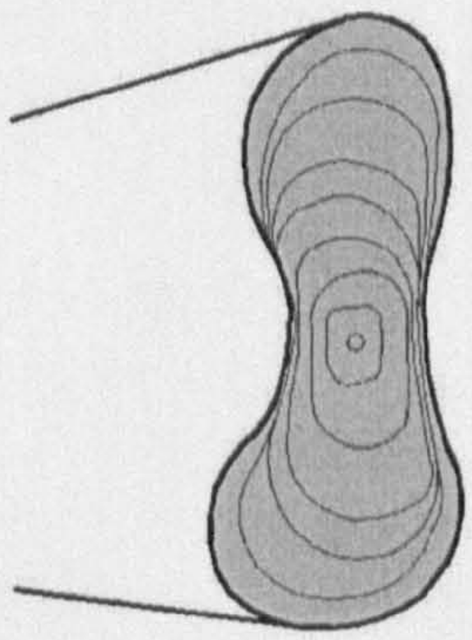

Figure E.2 Foundation structure: the modified shape of a shallow root under a regime of repeated strain.

- **Optimised shape of roots.** The shape and the sizes of the roots are also developed by adaptive growth. When a weak root is repeatedly swayed back and forth, the tree develops an optimised shape (Wood, C. J., 1995), as shown in Figure E.2. The repeated loading regime induces compressive and tensile stresses which grow from the centre to the outer fibres of the root along the direction of bending. However, the loading regime is alternate and compressive stress occurs in both the regions at the top and at the bottom of the root. Consequently, new material is equally added in these areas.

.

E.2.3 Foundation-primary structure interface

The joint between primary structure and root system experiences a very large bending moment induced by wind action. The trunk transmits tension and compression forces to the windward and leeward sides of the anchorage respectively.

- **Reinforced joint.** Since a high concentration of stresses occur at the base of the trunk, the tree is stimulated to increase the strength of its structure by growing wood cells at the interface of the foundation with the primary structure. As a result, the tree enlarges the base of the trunk relative to the rest of the trunk.

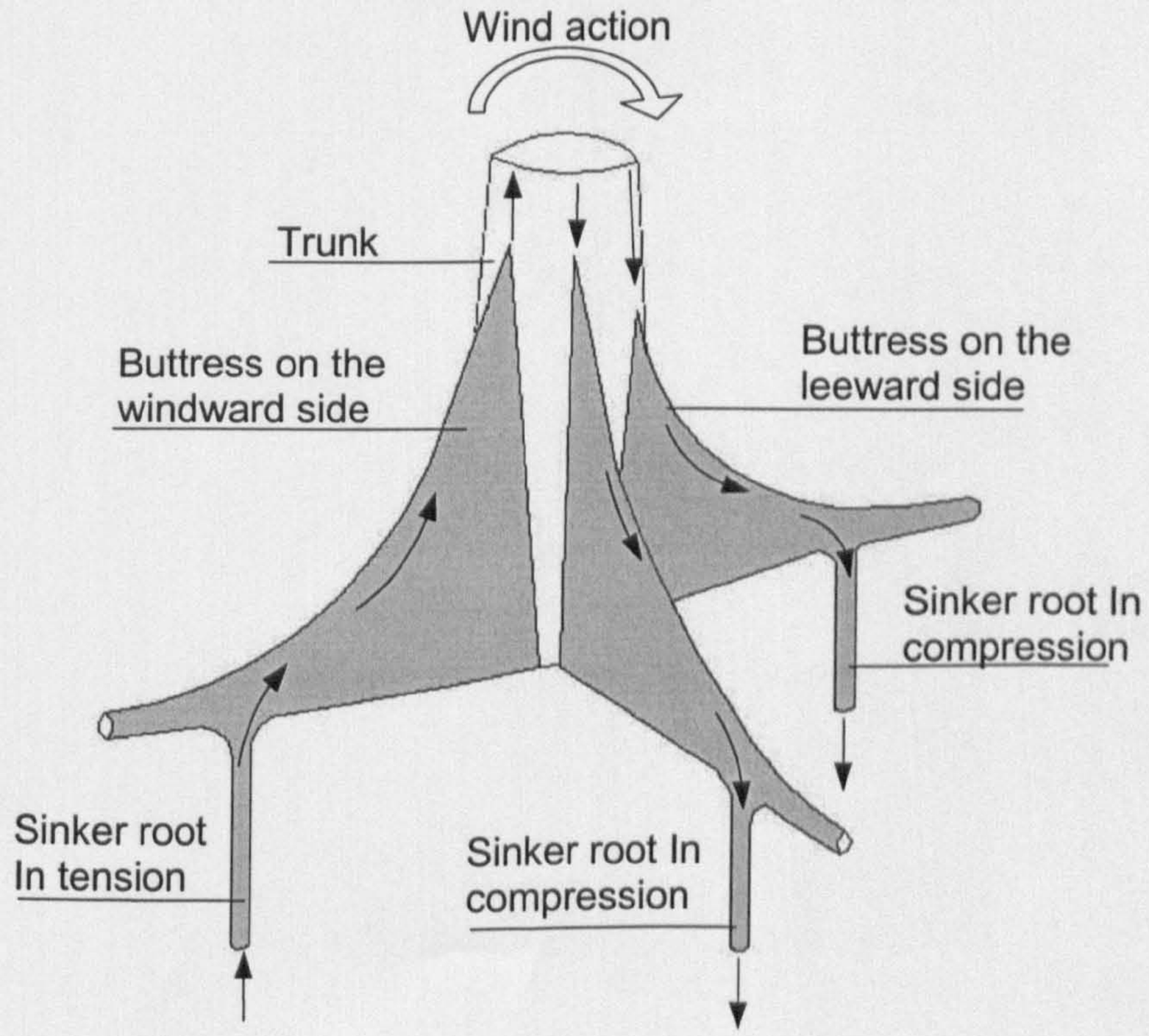

Figure E.1 Trunk-foundation interface: the buttress system strengthens the junction.

- **Buttress**. In tropical rainforests, trees minimise the use of living material by developing a system of buttresses (Coutts, M. P., 1983, Ennos, A. R., 1995). The sinker roots brace the trunk like angle brackets to constitute the buttresses, as shown in Figure E.1. This occurs because new wood is added along the force flow to reduce the stress level. At this junction, the force flow proceeds from the trunk towards the windward and leeward sinkers which transmit tension and compression forces into the soil. The function of the buttress is, therefore, to prevent the fracture of lateral roots.

E.2.4 Primary structure: trunk

Efficient features in the primary structure are tapering and pre-stressing of the trunk.

- **Tapered trunk.** The tapering of the trunk occurs by adaptive growth to the applied forces. The direction and magnitude of self-weight and wind loading determine the types of internal forces which occur in the trunk. Firstly, the compressive load due to self-weight is vertical and induces axial stress uniformly distributed in each section of the trunk. Secondly, the bending load, due to wind loading, causes an uneven distribution of tensile and compressive stress at the windward and leeward sides of the trunk respectively. While multidirectional wind produces maximum compressive and tensile stresses at the extremities of a cross-section all around its periphery, the highest stresses induced by a unidirectional wind occur only in the one direction of bending. In this case, the tree responds by growing extra cells in areas of highest stresses as shown in Figure E.1a and Figure E.1b. These cells produce annual growth rings, which are concentric in the trunk. Over a period of time the net result of the growth rings is to produce a tapered trunk as shown in Figure E.1c. One advantage of tapering the trunk is that the tree can grow faster by having little redundant material.

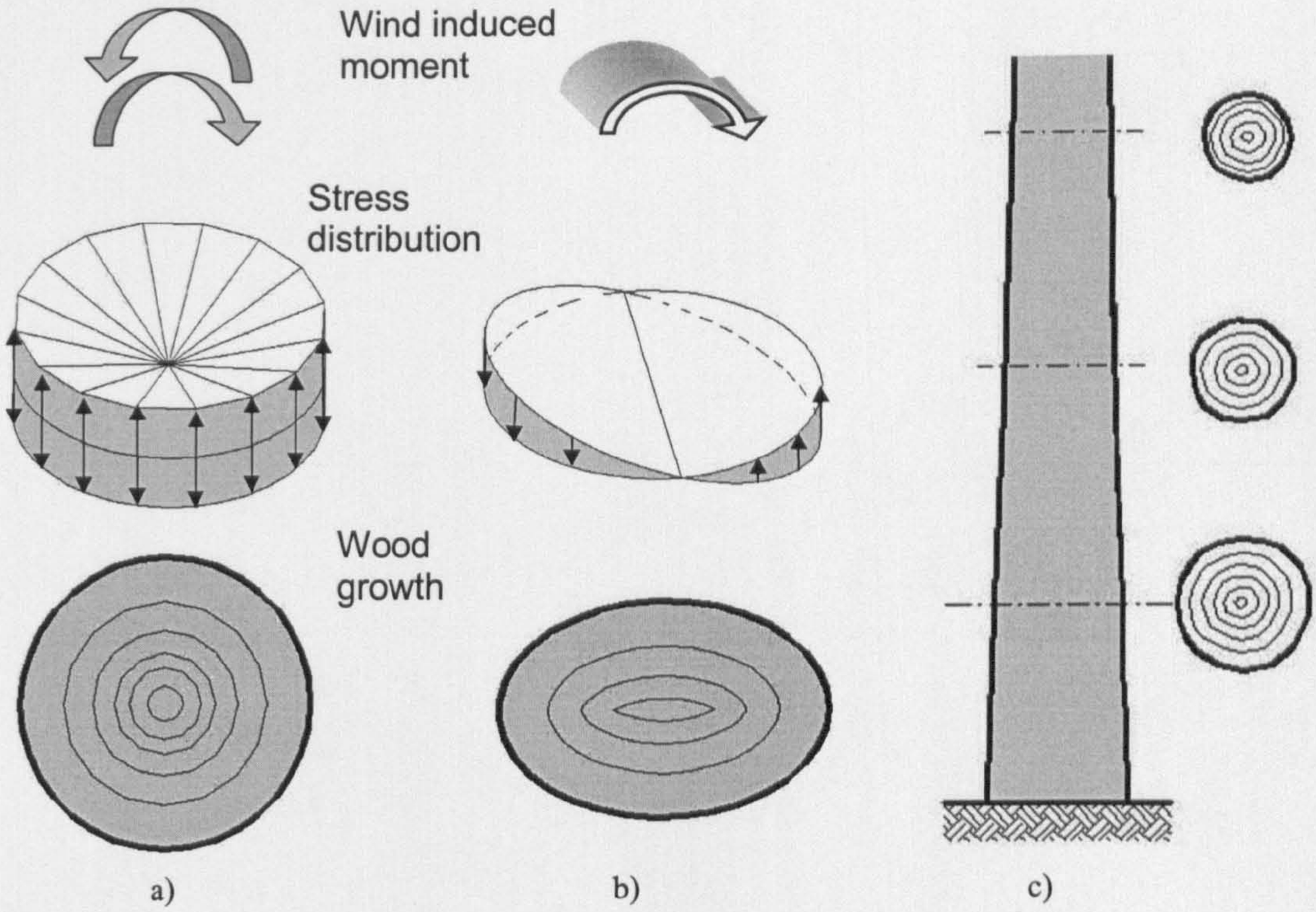

Figure E.1 **a)** Multidirectional wind. **b)** Unidirectional wind. **c)** Tapered trunk in the case of multidirectional wind.

- **Preloading**. Tree trunks have preloading in their outer fibres, which causes residual tensile stresses in these areas as shown in Figure E.1a. When the tree is subjected to aerodynamic loading, bending stresses are superimposed on the residual stress as shown in Figure E.1b. This is a beneficial feature because it means that when the trunk is subjected to bending moments, the compressive stresses are less than the tensile stresses in magnitude. Since the compressive strength of wood is lower than the tensile strength, the preloading significantly improves the strength of the tree.

The maximum tensile stress in bending *is given by*

$$\sigma^t = \sigma_p + M_y / Z \qquad \text{(E.1)}$$

where σ_p is the tensile prestress, M is the maximum bending moment, y is the distance to the neutral axis, I is the second moment of area

The maximum compressive stress in bending is given by

$$\sigma^c = \sigma_p - M_y/Z \qquad \text{(E.2)}$$

The above equations show how the maximum compressive bending stress is reduced by tensile preloading. A typical value of pre-load stress is σ_p = 27 MPa [Gordon, J.E., 1978].

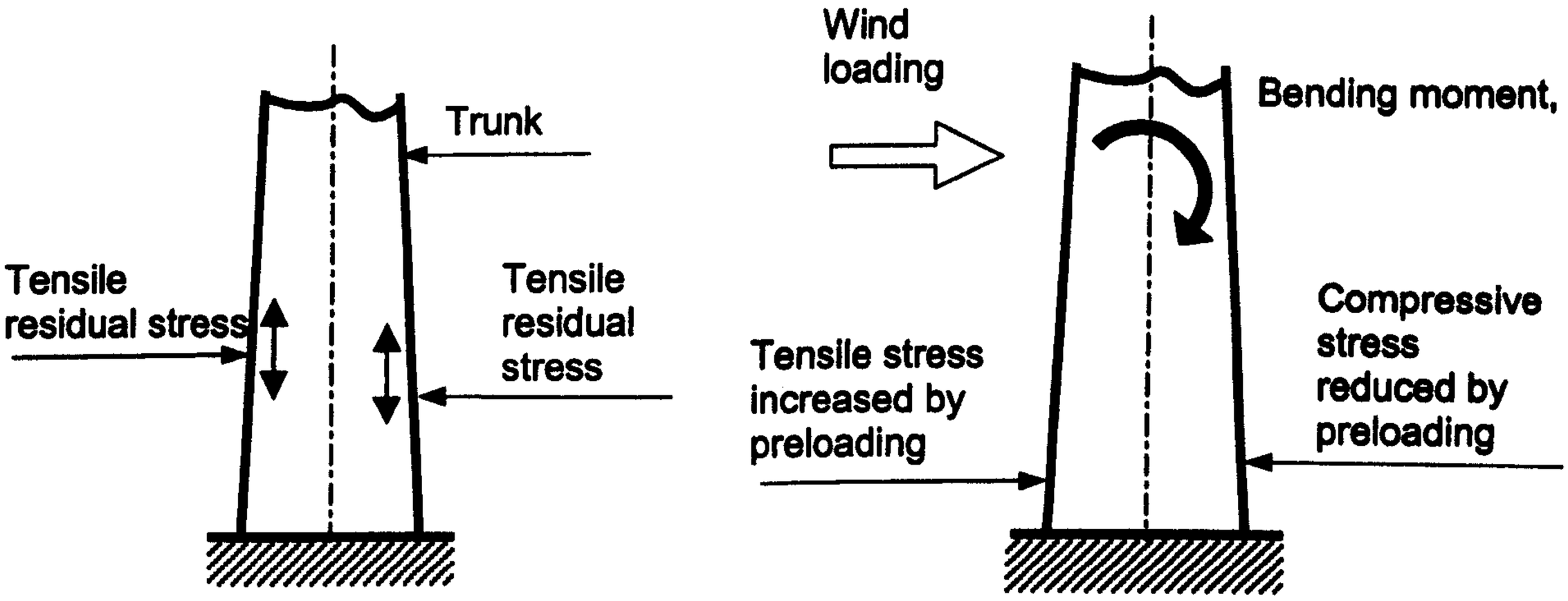

Figure E.1 Stresses in outer fibres with no wind loading (a) and high wind loading (b)

E.2.5 Primary-secondary structure interface

The trunk-branch junctions must provide a strong support for the branches. Strength is produced by reinforcement of material.

- **Reinforced joint.** At branch joints, branches experience the highest value of bending moment induced by self-weight and wind loading. The tree is stimulated to strengthen the underside of the junction, where there is high concentration of compressive stress, as shown in Figure E.1 and Figure E.1. This optimal feature has been discussed in more detail in the case study reported in Chapter 9.

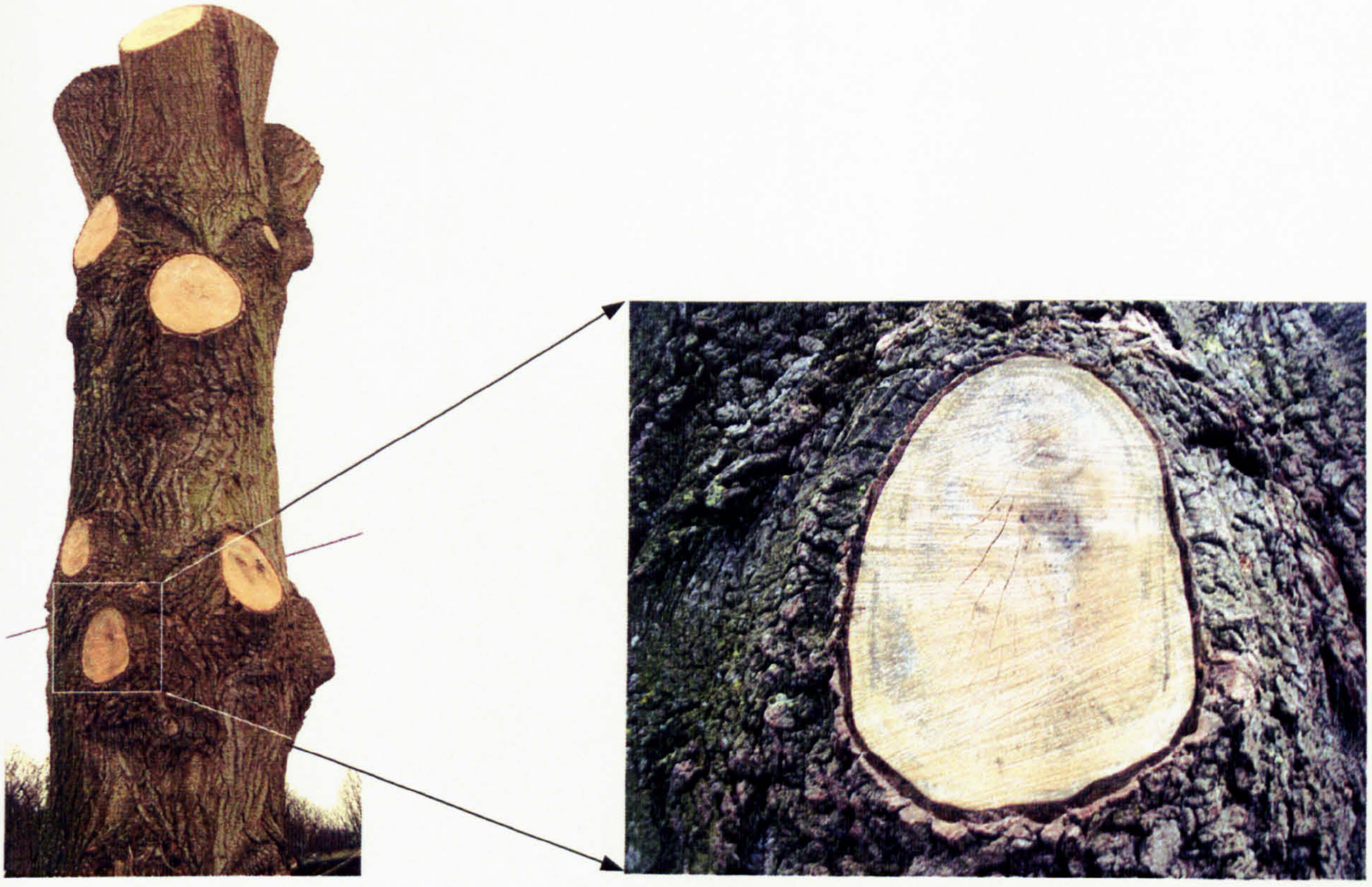

Figure E.1 Wood growth at the reinforced junction of the branches with the trunk.

E.2.6 Secondary structure: branching system

The tree achieves an efficient use of material in the secondary structure by growing tapered branches and deep sections as shown in Figure E.1.

- **Tapered branches.** The dimensions of the branches along the longitudinal profile are modified in response to the magnitude of the applied loads.
- **Deep sections.** In the case of a horizontal branch, bending loads come from two sources. Firstly, bending loads are provided in nearly all directions due to the wind loading. Secondly, bending loads due to self-weight are produced in the downward direction of the branch. In the case of wind, as the branch is scaled up, the wind loading increases with the square of the dimensions and the induced bending moment at the branch junction with the third power. Since the section modulus of the branch increases with the cube, the branch does not need to change in shape in order to cope with wind loading. However, in the case of self-weight loading, as the branch is scaled up, the self-weight increases with the cube of the increase in scale and the bending moment at the branch-

trunk joint increases with the fourth power. During the growth of a horizontal branch, self-weight becomes more and more dominant, thus highest stresses are at the top and bottom of the branch. Since the compression strength of wood is lower than the tensile stress, the branch is reinforced faster in regions of compression and the tree grows more cells at the base of the branch. As a consequence, the growth rings are not concentric as for the trunk. In addition for large branches, the branch becomes rectangular in section shape.

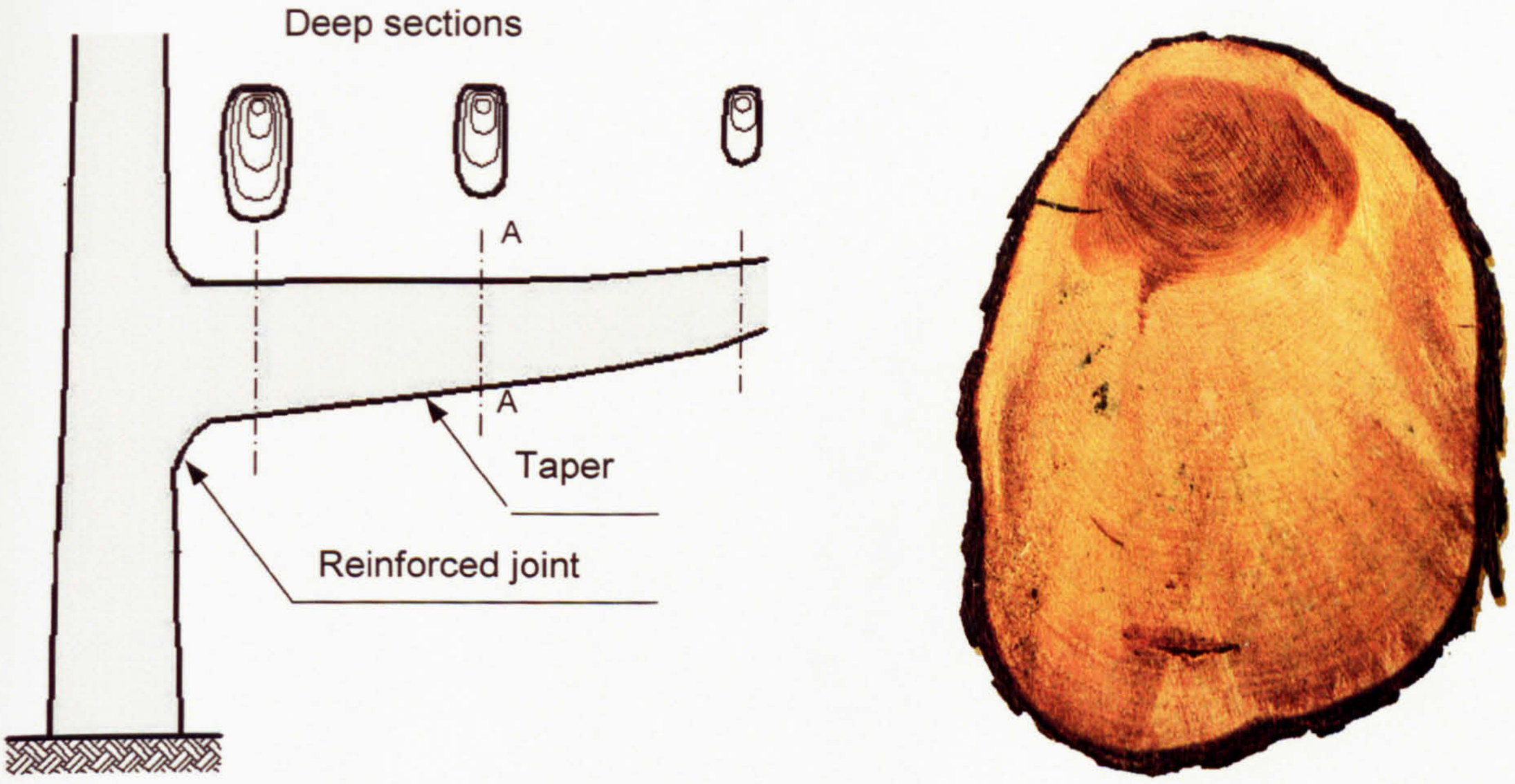

Figure E.1 Tapering of the branch and sample of deep section at A-A.

E.2.7 Secondary structure-foliage canopy interface

The node of the twig with the leaf has two main functions. Firstly, the upper side of the leaf must be kept outward in order to capture the sunlight and, thus, wind-bending moments must be withstood. Secondly, the drag forces, which are transferred by the leaf to the tree and then to the root, have to be minimised in order to reduce the uprooting of the tree.

- **Multipurpose leaf joint.** This junction presents a groove along the length of the upper side of the leaf stem (Vogel S., 1998), as shown in Figure E.1. The structural benefit of this groove is that the leaf can easily twist in order to reduce the wind drag, without losing resistance to bending.

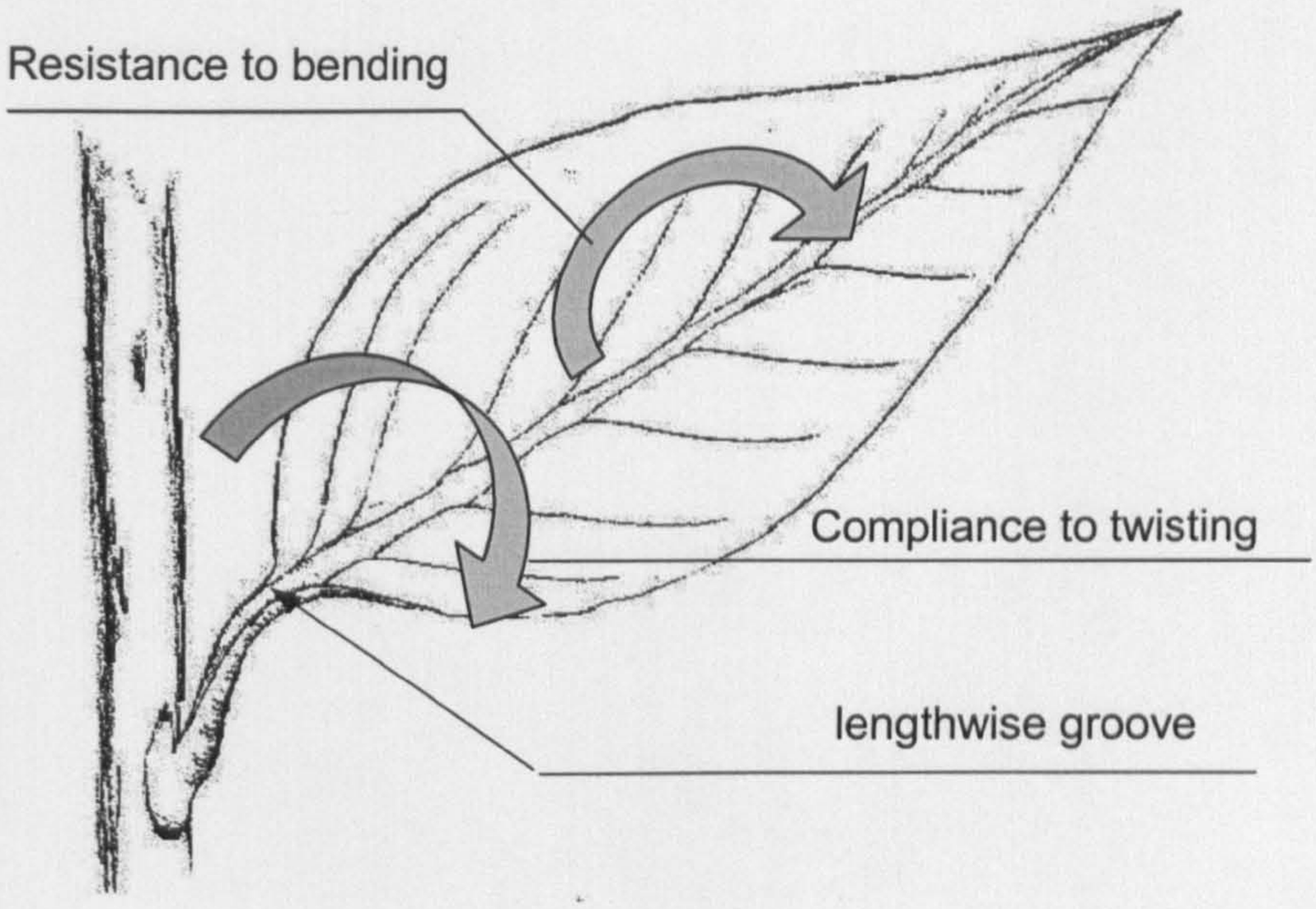

Figure E.1 The structural joint of leaf.

E.3 OPTIMAL MATERIAL FEATURES

E.3.1 Basic material

Wood is made up of tiny cells which have rigid walls. The main structural component of the cell wall in wood is cellulose. Cellulose is a high molecular weight, long, linear polymer of the simple common sugar, glucose. Glucose is synthesised in the leaves of trees and other plants by the action of sunlight on water and carbon dioxide, with the aid of the green catalyst, chlorophyll. Some of the mechanical properties of cellulose are shown in Table E.1 together with the common engineering materials GFRP, aluminium and steel (Ashby, M.F., *et al*, 1994). The table shows that a single cellulose fibre has an extremely high strength to weight ratio.

	Density ρ Mg/m^3	Young'sModulus E GPa	Yield Strength σ_y MPa
Single cellulose fibre	1.500	100	1000
GFRP	1.800	30	150-600
Aluminium	2.800	73	100-600
Steel	7.850	207	500-1400

Table E.1 Mechanical properties of cellulose and common engineering materials

E.3.2 Micro-structure

Wood has a prismatic cellular structure as shown in Figure E.1. Some woods such as palm and bamboo have a hexagonal microstructure [Gibson L.J. *et al.*, 1995], but other trees have five sided or four sided cells. Individual cells typically have a size of the order of 100 μm. This means that individual cells are very small compared to the global size of the trunk or branch.

The cells are the microscopic living cells of the wood. The cells are joined end to end so that a grain structure runs parallel to the stem or trunk. The alignment of plant cells is important because the grain structure is parallel with the direction of bending stresses.

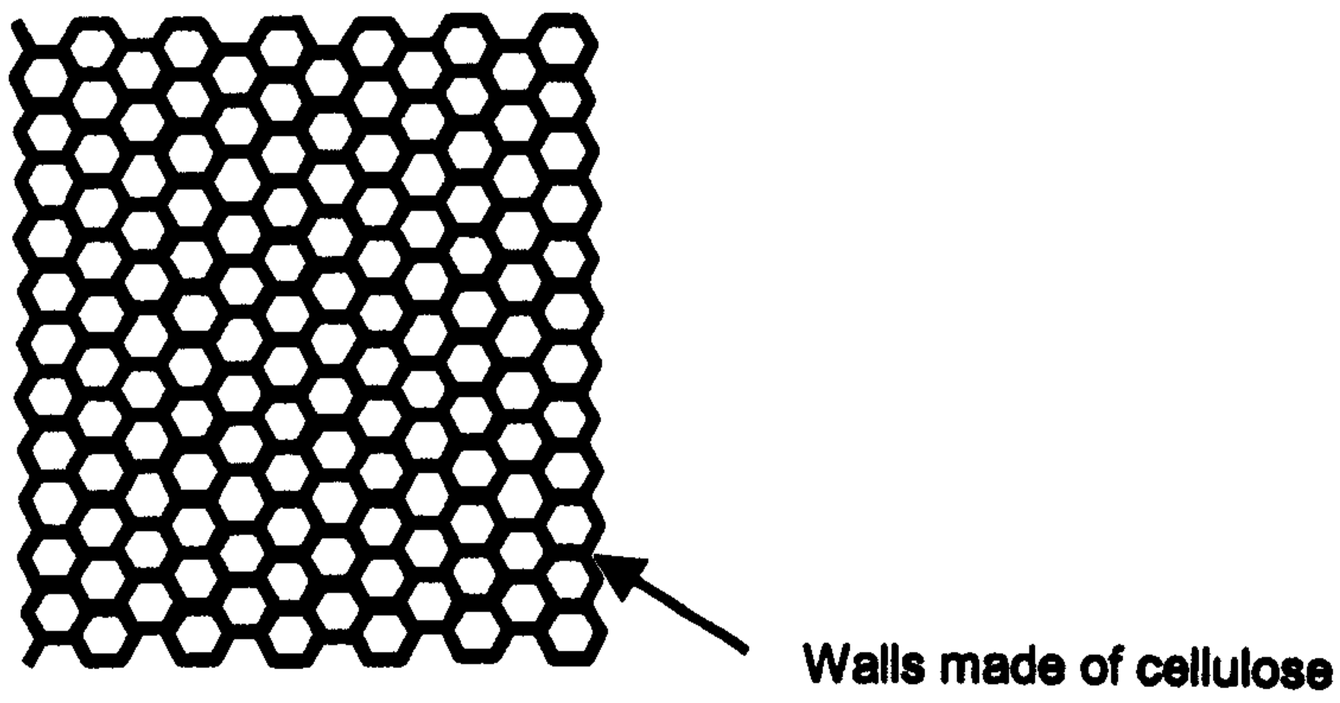

Figure E.1 Cellular structure of wood

The micro-structure of wood has a number of advantages:

- it reduces the density of the material thus placing material further away from the neutral axis, so increasing the structural efficiency.
- it can help improve resistance against global buckling by reducing the slenderness ratio.
- it can make the material tougher by introducing discontinuities.
- it can provide other functions such as water take-up in wood.

If dry wood were made from solid cellulose, it would have a density of about 1500 kg/m^3. In practice, all types of dry wood have a lower density due to the cellular structure. Woods have a wide range of densities from about 150 kg/m^3 for balsa wood to 1000 kg/m^3 for lignum. The tensile strength of wood along the grain range is

from 40 to 100 MPa, and it is roughly threefold the compression strength. This is because the thin cell walls of the microstructure can buckle under axial load. This is the main factor which induces the trees to reinforce the region subjected to high compressive stress.

	Specific density ρ Mg/m^3	Young's modulus E GPa	Yield strength σ_y MPa
Lignum	1.0	25	145
Ash	0.7	18	110
Oak	0.65	12	100
Pine	0.6	11	80
Fir	0.45	10	70
Spruce	0.3	8	50
Balsa	0.15	5	25

Table E.1 Material properties

E.4 SIMILARITIES WITH ENGINEERING STRUCTURES

Since natural and human structures are subjected to the same physical laws, it is not surprising that most of the features employed by a tree are already used in engineering structures. Engineers have learnt to design structures which resembles those exploited by nature from the beginning of time. Efficient structural features already used in engineering are:

- **Structural hierarchy**. A good rule for design a structure is to organise the elements in hierarchical scale. In this structural arrangement, superfluous parts are eliminated and each constituent element is employed for one specific function, which is to resist one internal force. Since the material can be used to its limit, the element sizes are decreased and a weight reduction of the overall structure is achieved.
- **Balanced forces**. In bridges and crane structures, the symmetry of geometry and/or forces produces balanced forms, as shown in Figure E.1.
- **Convergent form**. In the case of ship rigging, since the horizontal beams converge to the same vertical support, only one mast is required. The convergent form shown in Figure E.2 is balanced.

- **Reinforced joint**. The reinforcement of joints is quite common in structural design. For example, Figure E.3 and Figure E.4 show two structural joints: a foundation junction where the rib and the holding-down bolts act as the buttresses and the sinker root respectively, and a column-beam connection strengthened by stiffener and haunch.
- **Shaped sections**. Although the I section shown in Figure E.5 does not match the elegance of the I shaped root of Figure E.2, it is widely and successfully used in engineering structures for economical reasons.
- **Tapered elements**. Adjusting the longitudinal profiles to the internal forces induced by the applied load, is another way to improve structural efficiency. Figure E.6 shows examples of tapering profiles in the case of column, cantilever and beam structures.
- **Prestressing.** Prestressing is extensively used for prefabricated structures as shown in Figure E.7. Whereas the tree prestresses wood in all directions of the trunk section to increase the weaker compressive strength, engineers usually combine two materials, such as steel and concrete, to achieves prestressing in the only direction of bending. The technology employed for concrete structures, such as cable stay for bridges, large roofs for buildings, geotechnics works and offshore structures, is also applied to masonry and composite material.

There are some features of trees which are not commonly used by engineers. Multipurpose joints, microstructure and adaptive structures need more understanding and research to be applying to engineering cases.

E.5 SUMMARY

Trees have a large number of optimal structural features. Since the structure of a tree develops in an adaptive way, features are well optimised for the particular environment of an individual tree. Among the structural features examined in this Appendix, the non-eccentric growth of the ring, which causes efficient shaping of the cross-sections in horizontal branch, has been explained. Analogies with engineering structures have been discussed in order to gain understanding which can stimulate innovative solutions in many areas of design.

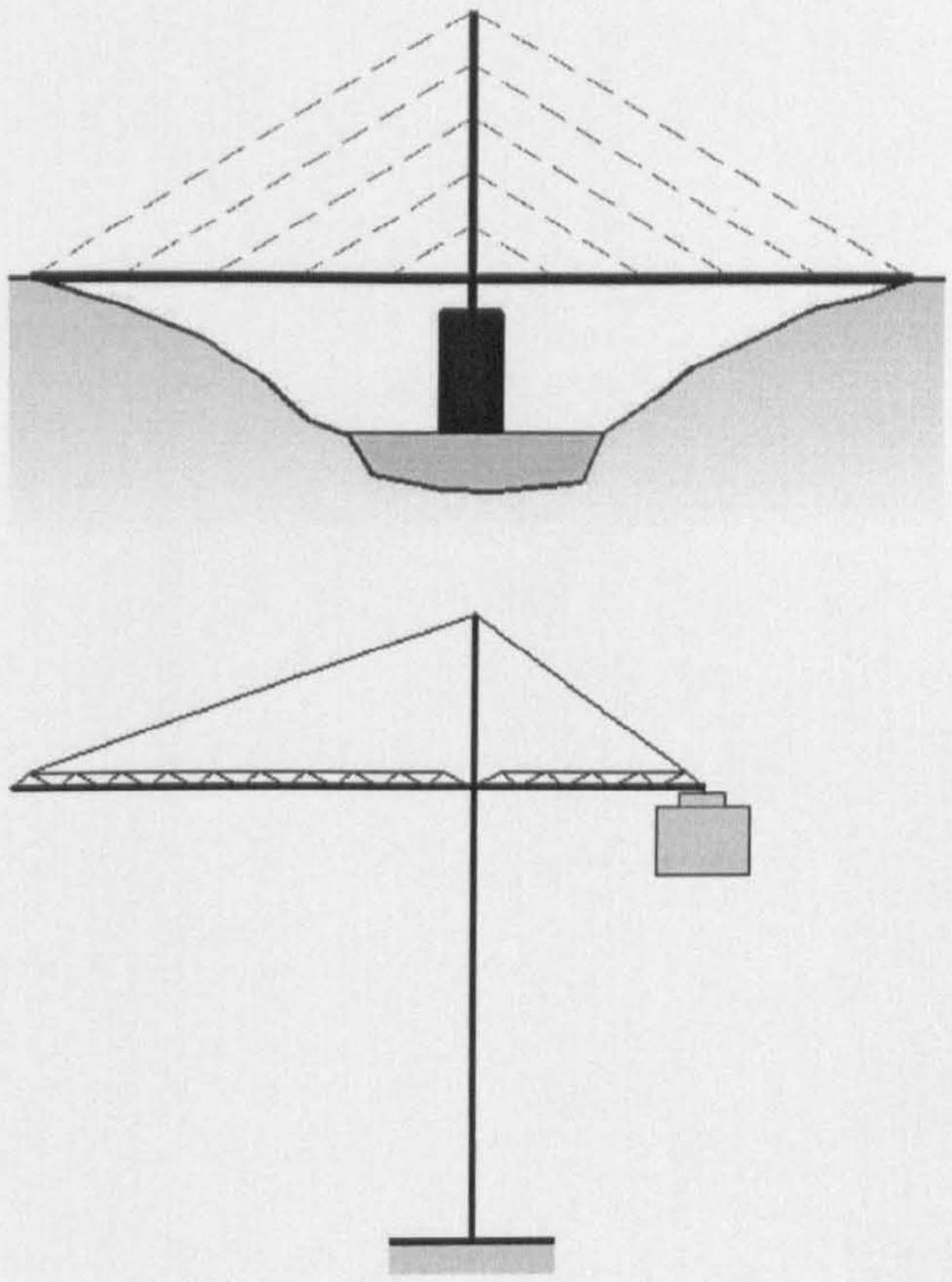

Figure E.1 Balanced form in bridge and material handling structures

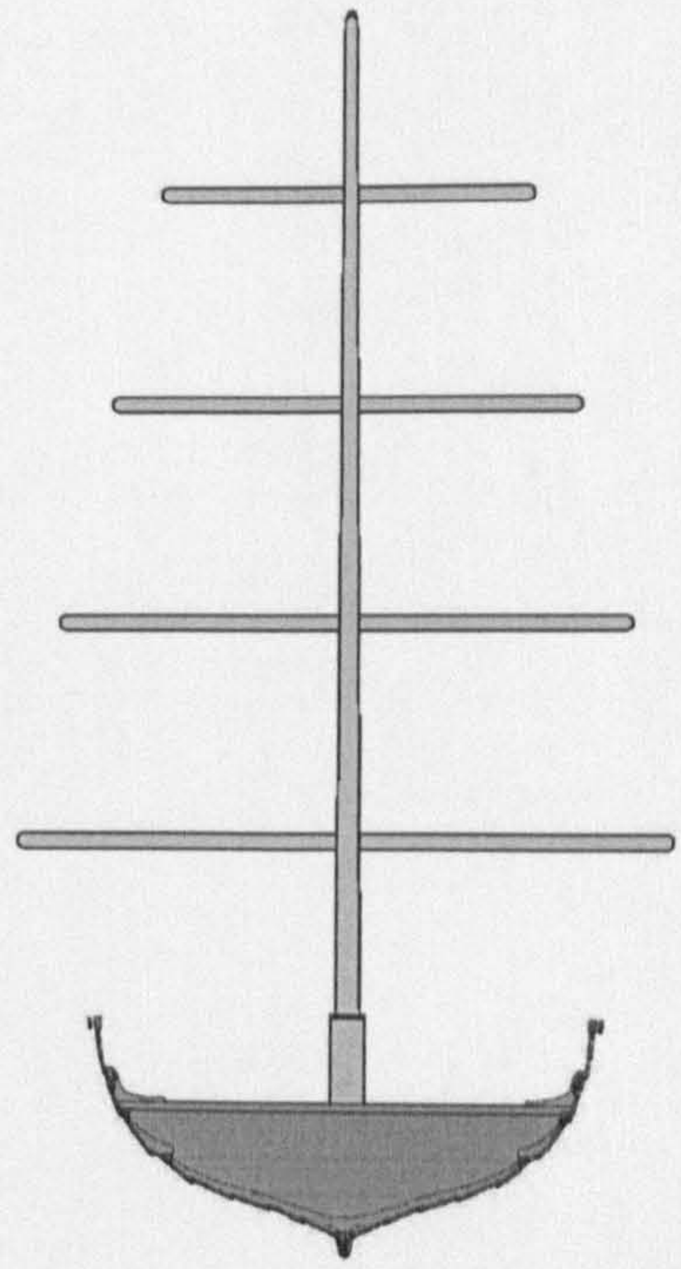

Figure E.2 Convergent form in ships

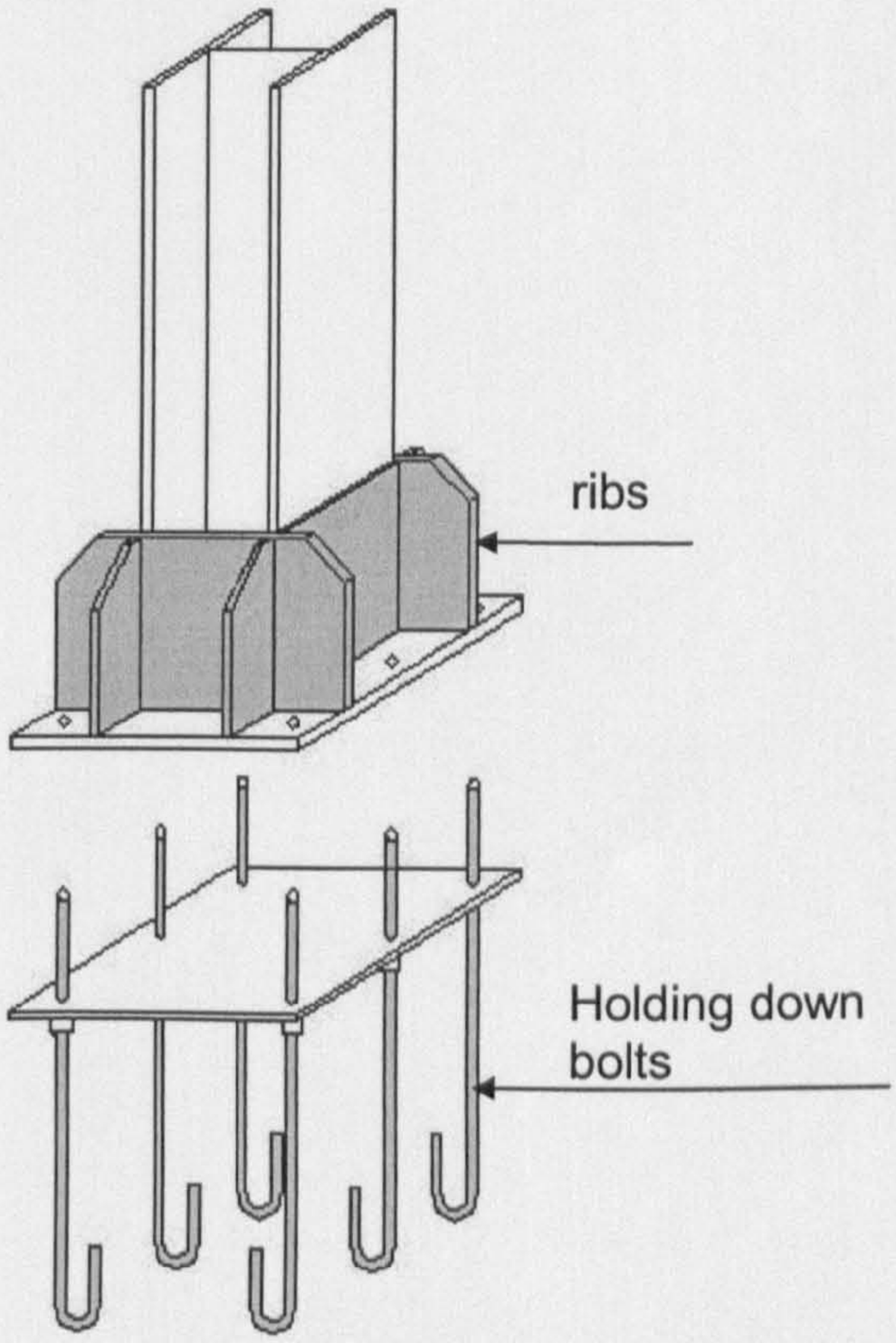

Figure E.3 Foundation joint

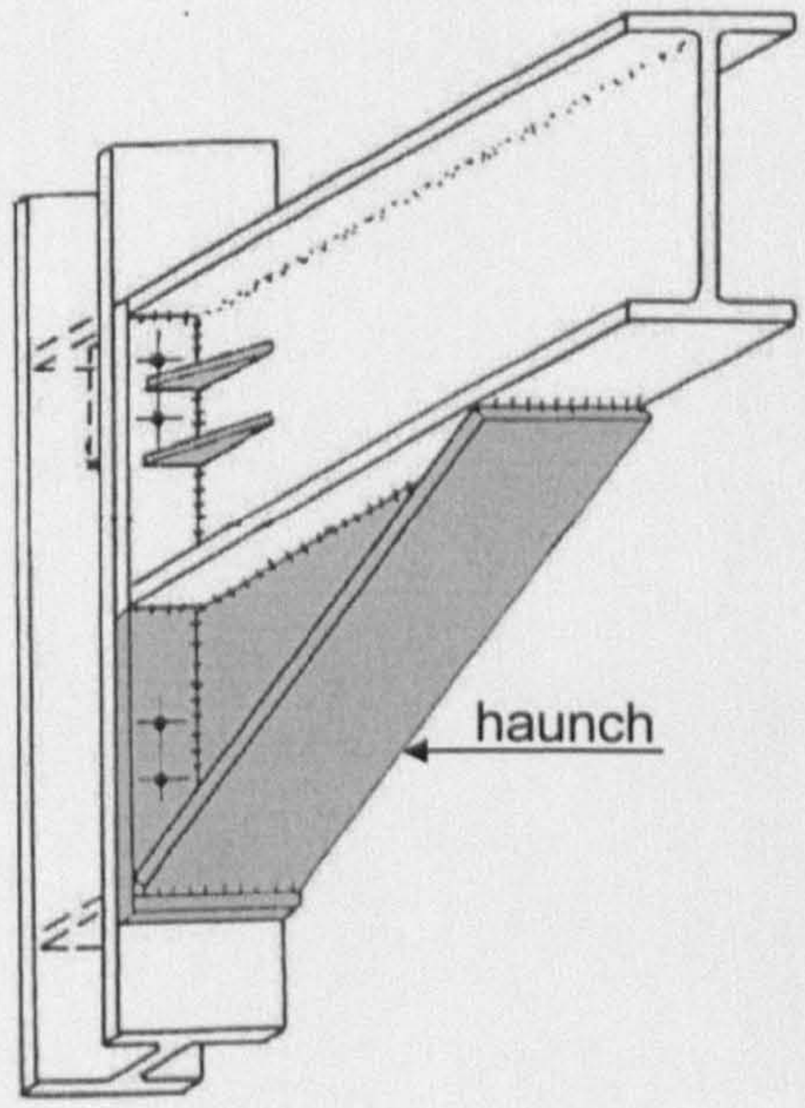

Figure E.4 Column beam joint

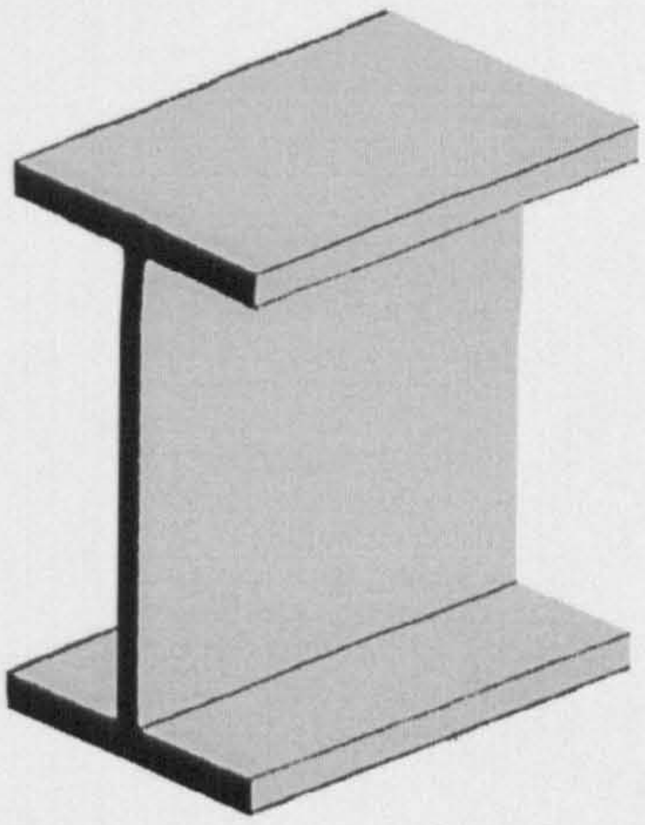

Figure E.5 I section

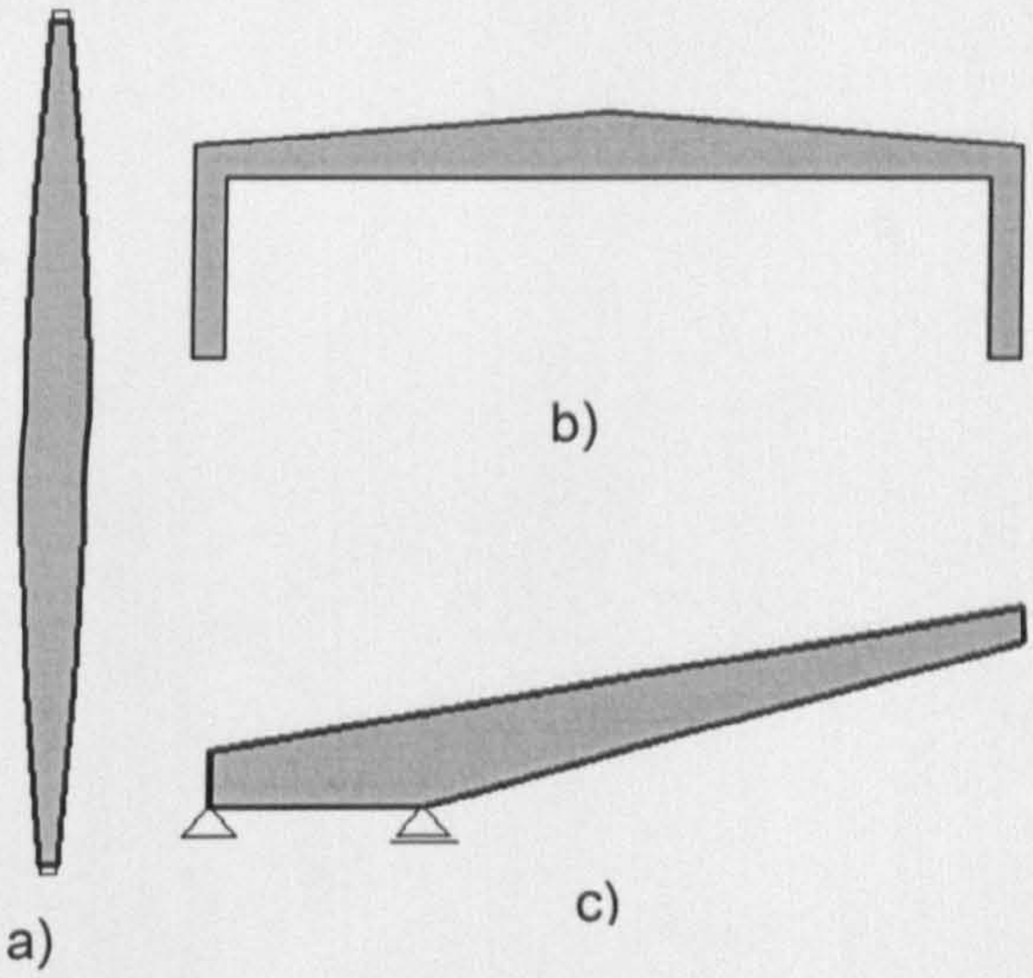

Figure E.6 Tapered forms: a) column, b) portal, c) cantilever

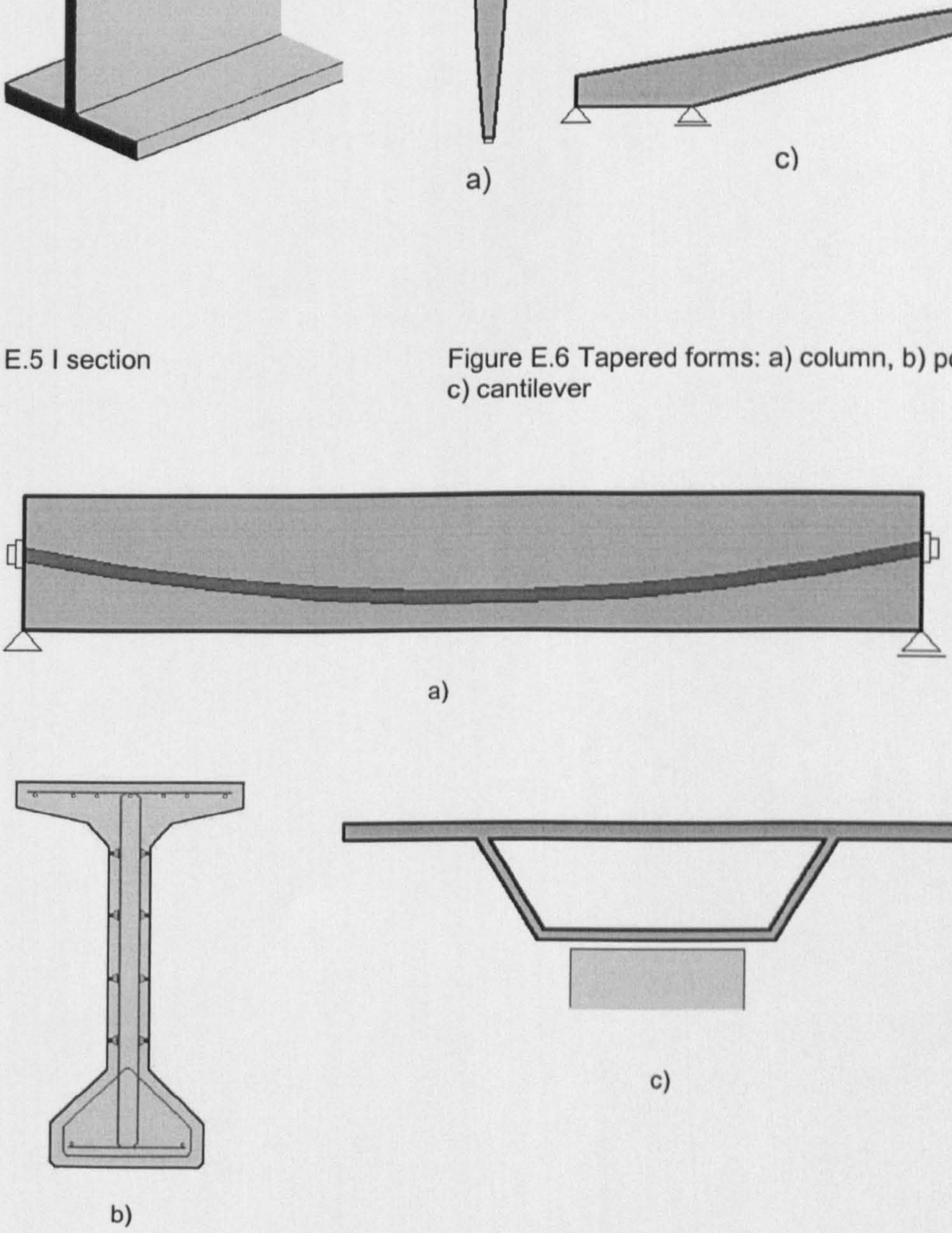

Figure E.7 a) Pre-tensioned beam, b) I section, c) deck bridge section

REFERENCES

Arora, J. S. (1989) *Introduction to optimum design*, McGraw Hill International

Ashby, M. F. (1989) Materials selection in conceptual design. *Material Science and Technology*, Vol. 5, pp. 517 - 525.

Ashby, M. F. (1991) Materials and shape. *Acta Metall. Mater.*, 39(6), pp.1025 - 1039.

Ashby, M. F. (1992) *Materials Selection in Mechanical Design*, 1st ed., Pergamon Press, Oxford.

Ashby, M. F. (1999) *Materials Selection in Mechanical Design*, 2nd ed, Pergamon Press, Oxford.

Ashby, M. F., L.J. Gibson, U. *Wegst and R.* Olive (1994) The mechanical properties of natural materials, *Proc. R. Soc. Lond.* A 540, pp. 123 140

Asimow, M. (1962) *Introduction to design*, Englewood Cliffs, Prentice-Hall, Inc.

Bedford, A. and Fowler, W. (1999) *Statics: engineering mechanics*. Addison Wesley.

Bedford, A. and Fowler, W. (2002) Engineering mechanics: statics & dynamics. Upper Saddle River, N.J. : Prentice Hall.

Birmingham R. W., (1994) A graphical exploration of the interaction of material and form in structural design. PhD thesis, Department of Marine Technology, University of Newcastle, UK.

Briand, C. H., Amy, D. D., Wilson ,K. A., and Woods, H. E. (1998) Allometry of axis length, diameter and taper in the devil's walking stick, *American Journal of Botany*, 85(9), pp. 1201–1206.

Burgess S. C., (1998a) The ranking of efficiency of structural layouts using form factor. Part 1: Design for Stiffness, *Proc. Instn Mech. Engrs, Part C, Journal of Mechanical Engineering Science,* Vol 212, pp. 117-128.

Burgess S. C., (1998b) The ranking of efficiency of structural layouts using form factor. Part 2: Design for Strength, *Proc. Instn Mech. Engrs, Part C, Journal of Mechanical Engineering Science,* Vol 212, pp. 129-140.

Burgess, S. C. (2000a) Shape factors and material indices for dimensionally constrained structures. Part1: beams. *Proc. Instn Mech. Engrs, Part C, Journal of Mechanical Engineering Science,* Vol. 214, pp 371-379.

Burgess, S. C. (2000b) Shape factors and material indices for dimensionally constrained structures. Part2: shaft. *Proc. Instn Mech. Engrs, Part C, Journal of Mechanical Engineering Science,* vol. 214, pp 381-388.

Caldwell, J.B. and Woodhead R.G., (1973) Ship structures: some possibilities for improvement, *North East Cost Institution - Institution Engineers & shipbuilders - Transaction* , vol 89, pp. 101 - 120

Caldwell, J.B., Caldwell, P.S., and Severn, R.T (1983) Sea born structures, *Engineering structures, Development in the 20th century*, The university of Bristol Press.

Case, J., Chilever, L., Ross C.T.F. (1999) *Strength of materials and structures.* Arnold, London

Chan A.S.L., (1960) *The Design of Michell Optimum Structures* , The college of aeronautics Cranfield. Report No 142

Chan H.S.Y., (1963) *Optimum Michell Frameworks for Three Parallel forces,* The college of aeronautics Cranfield Report No 167

Chapman, C., Saitou, K., and Jakiela M.J., (1993) Genetic algorithm as an approach to configuration and topology Design, *ASME proceedings, Advanced in design automation.* Vol 65-1, pp. 485-498.

Chu, N. D., Xie, Y.M., Hira, A., Steven, G.P. (1997), On various aspects of evolutionary structural optimization for problems with stiffness constraints. *Finite elements in Analysis and Design,* 24, pp. 197-212.

Coutts M.P. and Grace J.. (1995) *Wind and trees*. Cambridge University Press

Coutts, M. P., (1983a) Root architecture and tree stability, *Plant and soil*, 71, pp. 171-188.

Coutts, M. P., (1983b), Development of the structural root system in Sitka spruce. *Forestry*, 59, pp. 1-16.

Coutts, M. P., (1986), Components of tree stability in Sitka spruce on peatygley soil. *Forestry*, 59, pp. 173-197.

Cox, H.L and Smith, H.E. (1943) *Structure of minimum weight*, Aeronautical Research committee, Report and memoranda N. 1923

Cox, H.L. (1965) *The design of structures of least weight*. Pergamon Press, Oxford

Crane, F.A.A and Charles, J.A., (1984) *Selection and use of engineering materials*. Butterworth-Heinemann, Oxford

Cross, N. (2000) *Engineering design methods: strategies for product design*, John Wiley & Sons Ltd, Baffins, Chichester.

Dieter, G. E. (2000) *Engineering design: a materials and processing approach*, McGraw-Hill International

Dowling, N.E. (1993) *Mechanical behaviour of materials: Engineering methods for deformation, fracture and fatigue*, Prentice-Hall International, Inc. New Jersey

Duffy, A.H.B. and Legler, S., (1999) Rationalising past designs for reuse, *ICED 99* International Conference on Engineering Design, Munich, pp. 377-380

Engel, H. (1967) *Structure systems*, Deutsche Verlags-Anstalt, Stuggart.

Engesser, F. (1889), *Ueber die Knickfesrigkeit Gerader Stäbe*. Zeitschrift für Architektur und Ingenieurwesen, Vol 35, N 4 Hannover (reported in: Timoshenko, 1953)

Ennos, A. R., (1995) Development of buttress in rainforest trees: the influence of mechanical stress. In *Wind and trees*, Cambridge University Press.

Fogg, G.E.: (1970) *The growth of plants*, G.E, Fogg - Harmondsworth, Penguin.

French, M.J. (1988) *Invention and evolution: design in nature and engineering* Cambridge University Press

Galileo, G. (1638) *Discorsi e dimostrazioni matematiche intorno a due nuove scienze attenenti alla meccanica & I movimenti locali*, in "Opere" di Galileo Galilei, Franz Brunetti. UTET, 1980

Gere, J. M. (1996) *Mechanics of materials* James M. Gere, Stephen P. Timoshenko. PWS Publishing Company Boston.

Gibson L.J. (1984), Optimization of stiffness in sandwich beams with rigid foams cores, *Materials Science and Engineering, Elsevier Sequoia*, 67, pp. 125-135.

Gibson, L. J. and Ashby, M. F. (1997) *Cellular Solids: Structure and Properties,* Cambridge University Press.

Gibson, L.J., Ashby, M. F., Karam G.N., Wegst, U. and Sherliff, R., (1995), The mechanical properties of natural materials. II. Microstructures for mechanical efficiency, *Proc. R. Soc. Lond.* A 450, pp. 141 162.

Gordon, J. E. (1988) *The science of structures and material*, Scientific American Books.

Gordon, J.E. (1978), Structures or why things don't fall down. Penguin books.

Haftka, R.I.T. (1992) *Elements of structural optimization* Dordrecht, Kluwer Academic, London

Hemp, W.S. (1958) *The theory of structural design*, The college of aeronautics Cranfield Report No 115.

Hemp, W.S. (1973) *Optimum structures, Clarendon press, Oxford.*

Hill, R.(1998) *The mathematical theory of plasticity*. Oxford Clarendon Press.

Holland, J. H., (1975) *Adaptation in Natural and Artificial Systems*, University of Michigan Press, Ann Arbor, Michigan.

Horn, H. S. (1971) *The adaptive geometry of trees, Princeton University Press, Princeton.*

Huang, J.S. and Gibson, L.J. (1995) Microstructural Design of Cellular Materials: Honeycomb Beams and Plates, *Acta Metallurgica et Materialia*, Elsevier Science, 43, 1643-1650.

Jasinski, F. (1895), Noch ein Wort zu den Knickfragen, Schweizerische Bauzeitung, Vol 25, N 25 (reported in Timoshenko, 1953).

Karman, T. (1956) *Collected woks of Theodore von Karman*, Butterworths Scientific Publications, London.

King, D. A. (1991) Tree allometry, leaf size and adult tree size in oldgrowth forests of western Oregon, *Tree Physiology* 9, pp. 369-381.

Kirkpatrick, S., Gerlatt, C. D. J., and Vecchi, M.P., (1983) Optimization by Simulated Annealing, *Science*, 220, pp. 671-680.

Lakes, R. (1993) Material with structural hierarchy. *Nature*. Vol. 361, pp 511-515

Lyndon, R.F. (1989) *Plant development: the cellular basis,* Unwin Hyman, London.

Macdonald, A. J. (2001) *Structure & Architecture,* Architecture Press, Oxford.

Majid, K. I. (1974) *Optimum design of structures*. Newnes-Butterworths, London

Maksymowych, R. (1973) *Analysis of leaf development*. Developmental and cell biology series. Cambridge University Press,

Mattheck, C. (1991) *Trees: the mechanical design*, Springer-Verlag,Berlin.

Mattheck, C., (1989), Engineering components grow like trees, Kernforschungszentrum Karlsruhe, 67,1661-86.

Maxwell, J. C. (1995) The *scientific letters and papers* of James Clerk Maxwell, *(1862-1873)*. Cambridge University Press.

McMahon, T. A. (1973) *Size and shape in biology*, *Science* 179, pp. 1201-1204

Meiser, V. (1995), *Computational Science Education Project*, electronic book from U.S. Department of Energy, Vanderbilt University, Nashville, Web sites http://csep1.phy.ornl.gov/csep.html

Meriam, J.L.(1998) *Engineering mechanics,* New York, Chichester, Wiley

Michell, A. G. M. (1904) The limits of economy of material in frame-structures. *Phil. Mag.*, 8, pp. 589-597.

Morey, P.R. (1973) *How trees grow*. Edward Arnold London.

Mosbrugger, V. (1990) *The tree habit in land plants*, , *Springer-Verlag, Berlin*

Nha, C. D., Xie, Y.M., Hira A., Steven G.P. (1997) On various aspects of evolutionary structural optimization for problems with stiffness constraints, *Finite Element in Analysis and Design*, Elsevier Science, pp. 197-212

Niklas, K.J. (1992) *Plant biomechanics: an engineering approach to plant form and function*. The University of Chicago Press, Chicago.

Niklas, K.J. (1997a) Mechanical properties of black locust (Robinia pseudoacacia L.) wood. Size- and age-dependent variations in sap- and heartwood, *Annals of Botany 79: 265–272.*

Niklas, K.J. (1997b) *The Evolutionary Biology of Plants*, University of Chicago Press.

Pahl, G and Beitz, W. (1996) *Engineering design :a systematic approach*, Luciënne Blessing, and Frank Bauert, edited by Ken Wallace, Springer, London.

Parkhouse, J.G, (1984) Structuring a process of Material Dilution, *Proc. 3rd Int. Conf. On Space Structures*, H. Nooshin. Elsevier Applied Science Publishers, pp. 367 374

Parkhouse, J.G. and Sepangi, H.R., (1993) Macromaterials, *Conference proceedings E. FN Spon, Garas Armer and Clarke*, London, pp. 3-13.

Parkhouse, J.G., (1987) Damage accumulation in structures, *Reliability Engineering*, Elsevier Applied Science Publishers Ltd , 17, 97-109

Petroski, H. (1994) *Design paradigms: case histories of error and judgement in engineering,* Cambridge University Press

Prager, W. (1958) *On a problem of optimal design*, Tech. Rep. Div. Appl. Math., Brown University, Providence, Rhode Island, 38.

Qing, L., Steven G.P., Querin, O.M. and Xie Y.M., (2000) Evolutionary shape optimization for stress minimization, *Computational Mechanics*, Springer-Verlag Berlin, pp. 129-139.

Qing, L., Steven, G.P., Querin, O.M. and Xie, Y.M., (1999) evolutionary shape optimisation for stress minimisation, *Mechanics Research communications*, *Elsevier Science Ltd*, Vol 26, n. 6, pp. 657-664.

Rozvany, G.I.N., (1976) *Optimal design of flexural systems: beams, grillages, slabs, plates and shells*, Pergamon International Library

Schwefel, H.P. (1995) *Evolution and Optimum Searching*, Wiley Interscience, John Wiley & Sons, New York.

Shanley, F. R. (1946) The column paradox, *Journal of the Aeronautical Sciences*, Vol 13, N 12.

Shanley, F. R. (1960) *Weight-strength Analysis of Aircraft Structures*, 2nd ed. New York, Dover

Shea, K., (2001) An approach to multi-objective optimization for parametric synthesis, Design method for performance and sustainability, *ICED 01, International conference on Engineering Design,* Glasgow, pp. 03-210

Shea, K., Cagan, J., Fenves, S. J., (1997) A shape annealing approach to optimal truss design with dynamic grouping of members. *ASME Journal of Mechanical Design,* Boston, Vol.119, (3), pp. 388-394,

Shelley, A., Ethenier and Vogel S., (2000) Reorientation of daffodil flowers in wind: Drag reduction and torsional flexibility, *American Journal of Botany*, 87(1), pp 29-32

Sigmund, O and Pederson, P. (1996) *Topology optimization*, Department of Solid Mechanics, Technical University of Denmark, Web site: http://www.topopt.dtu.dk/

Smith, D.J, Partridge P.G., (1999) Flexural stiffness envelopes for planar multilayered systems containing two dissimilar materials. *Proc. Instn Mech. Engrs, Part L, Journal of Material and Design*, Vol. 213, pp 381-388.

Starling, A.C. and Shea, K. (2002) A clock grammar: the use of parallel grammar in performance-based mechanical synthesis, *Design Theory and methodology, ASME DETC 2002, Montreal.*

Steven, G.P., Li Qing and Xie, Y.M., (2000) Evolutionary topology and shape design for general physical field problem, *Computational Mechanics*, Springer-Verlag Berlin, 129-139.

Steven, G.P., Li Qing and Xie, Y.M., (2001) Topology and Shape Structural Optimization that Minimizes Maximum Stress and Maximizes Stiffness, *Computers and Structures*, Elsevier Science Ltd.

Stokes, A., Fitter, A.H., Coutts, M. P., (1995) Responses to young trees to wind: effects on roots growth. In *Wind and trees*, Cambridge University Press.

Suppapitnarm, A., (2001) Conceptual design of bicycle frame by multi-objective optimisation, PhD thesis, Engineering Design Centre, Cambridge.

Timoshenko, S. P. (1953) *History of strength of materials* New York London McGraw-Hill.

Torroja, E. (1958) The structures of Eduardo Torroja :an autobiography of engineering accomplishment by Eduardo Torroja, Mario Salvadori. New York, F.W. Dodge

Vogel, S., (1998) *Cats' paws and catapults: mechanical worlds of nature and people.* Penguins books

Wagner, H. (1929) Remarks on airplane struts and girders under compressive and bending stresses; Index Values, NACA TN N 500

Weaver, P. and Ashby, M. F. (1996) Material limits for shape efficiency. *Journal of Engineering design*, , 7(2), pp.129-150.

Weaver, P. and Ashby, M. F. (1997) The Optimal Selection of Material and Section-Shape. *Progress in Material Science*, 41, pp.61-128.

Wood, C. J., (1995) Understanding wind forces on trees. In *Wind and trees*, Cambridge University Press.

Xie, Y.M. and Steven, G.P. (1993) A simple evolutionary procedure for structural optimisation. *Computer & Structures,* 49, pp. 885-896

Xie, Y.M., Steven G.P., (1996) Evolutionary structural Optimization for dynamic problems, *Computers and Structures*, Elsevier Science, Vol. 58 N6, pp.1067-1073.

Young, W.G. and Roark, R.J, (1989) *Formula for stress and strain*, New York, McGraw Hill.

GLOSSARY

Scaling of the cross-sections	is described by the relative changes in width and height of the cross-sections.
Combined selection graph	is a selection chart which displays on the right hand side the equation of the functional requirement and on the left hand side the performance.
Constraints	are restrictions to the design space. They can be applied to the sizes of a cross-section or to the overall form of a structure.
Design space	is the space which a designer can use to locate a structure.
Envelope	is the rectangle described by the main sizes of a cross-section.
Envelope efficiency map	is a design chart for the selection of the shape properties of a cross-section. It is analogous to the material chart.
Limiting regimes graph	is a design chart which maps the regions of the design space where the performance of a material or a shape is better compared to the others.
Nested performance chart	is a design chart which displays the performance trends of a structure with more than three variables.
Shape transformers	are the shape properties of a cross-section. They are defined for a geometric quantity, such as the area and the second moment of area. They relate the geometric quantity of a cross-section and the geometric quantity of the rectangular envelope.
Space interchangeability condition	is a condition to exchange the product of material and shape properties without altering the main dimensions of the cross-section.